

中美地震小区划讨论会会议录

PROCEEDINGS OF THE

JOINT U.S.-P.R.C.

MICROZONATION WORKSHOP

1981年9月11—16日

中国 哈尔滨



中美地震小区划讨论会会议录

1981年9月11—16日

中国 哈尔滨

Any opinions, findings, conclusions
or recommendations expressed in this
publication are those of the author(s)
and do not necessarily reflect the views
of the National Science Foundation.

中国国家地震局 主办
美国国家科学基金会

中国科学院工程力学研究所筹备

i.a.a

中国科学院工程力学研究所印刷

1.6

中美地震小区划讨论会

目 录

	页次
一、综合报告	
地震烈度的含意、用途和局限性.....	1—1
胡聿贤	
关于场地放大作用与土壤液化的地震小区划.....	2—1
谢里夫	
中国地震小区划现状及存在问题.....	3—1
章在墉	
小区划与土地利用规划.....	4—1
马 德	
公众政策中的地震危险性分析.....	5—1
威金斯	
二、地震小区划的地质研究	
1979年溧阳 6 级地震震中区工程地质特性研究.....	6—1
段光贤、王家钧、费涵昌	
地震小区划的地质研究.....	7—1
斯利蒙	
几次大地震烈度异常概况.....	8—1
陈达生	
地质条件对地震波影响的地震动危险区划图的编制.....	9—1
海 斯	
三、小区划的地球物理方法	
爆破模拟地震地面运动方法的探讨.....	10—1
张雪亮、黄树棠	

应用航空遥感技术研究唐山地震震害及小区划.....	11—1
邹学恭	
平均剪切模量在场地影响中的应用—唐山地震	
玉田低烈度异常区原因的探讨.....	12—1
刘曾武、董恩长、吕根盛	
王东强、魏培恒	
用于小区划的场地特征的地球物理技术.....	13—1
墨 菲 (由作者撤消)	
四、小区划的土动力学问题	
轻亚粘土的液化特性和现场判别.....	14—1
石兆吉、郁寿松	
土工结构抗震设计中的地基问题.....	15—1
汪闻韶	
土壤动力特性.....	16—1
石桥勳	
循环荷载作用下饱和砂土的液化破坏.....	17—1
刘颖、仝筠、齐心	
五、震害预测及小区划图的编制	
小区划的建筑规划与设计研究.....	18—1
拉戈里奥 王玛莎	
北京平原地震地面运动预测和区划.....	19—1
蒋溥、徐峰、王启明	
地震灾害与易损性分析.....	20—1
朱海之、王立功	
兰州市地震小区划.....	21—1
孙崇绍、陈丙午	
北京地区的地震活动性和小区划.....	22—1
周锡元、符圣聪、王广军	
六、场地反应与相互作用及其它	

场地反应与相互作用分析.....	23—1
雷斯曼尔	
土与结构接触面动力性状的初步研究 Not Published.	24—1
扶长生、俞载道 (由作者撤消)	
中国地震烈度衰减的区域特征.....	25—1
陈培善、金严、李文香	
不规则地形及不均匀地基土对地面运动及震害影响.....	26—1
陈丙午	
中国华北基岩最大加速度概率估计值.....	27—1
宋良玉、魏公毅	
地震危害与小区划的不确定性分析.....	28—1
基雷米杰安	

勘误表



**PROCEEDINGS OF THE
JOINT U.S.-P.R.C.
MICROZONATION WORKSHOP**

**HARBIN, CHINA
September 11—16, 1981**

**Workshop Sponsored by
National Science Foundation, U. S. A.
and
State Seismological Bureau, P. R. C.**

**Workshop Organized by
Institute of Engineering Mechanics
Academia Sinica**

Any opinions, findings, conclusions
or recommendations expressed in this
publication are those of the author(s)
and do not necessarily reflect the views
of the National Science Foundation.

Printed by
Institute of Engineering Mechanics
Academia Sinica
Harbin, China

CONTENTS

1 . General Reports	Page NO
Usage and Limitation of Earthquake Intensity	1 — 1
Hu Yuxian	
Microzonation with Respect to Site Amplification and Soil Liquefaction	2 — 1
Mehmet A. Sherif	
Status and Problems Arised in the Seismic Microzonation in China	3 — 1
Zhang Zaiyong	
Microzonation and Land Use Planning	4 — 1
George G. Mader	
Earthquake Risk Analysis in Public Policy	5 — 1
John H. Wiggins	
2 . Geological Consideration for Microzonation	
The Research of the Engineering Geological Features of the Epicentral Area of an Earthquake of Magnitude 6 in Liyang in 1979	6 — 1
Duan Guangxian, Wang Jiajun and Fei Hanchang	
Geologic Considerations for Earthquake Microzonation	7 — 1
David Burton Slemmons	
A Survey of Intensity Anomaly During Destructive Earthquakes	8 — 1
Chen Dasheng	

Construction of a Zoning Map of the Earthquake
Ground-Shaking Hazard which Shows the Effects
of Geology on Seismic Waves 9—1

Walter W. Hays

3 . Geophysical Technique for Microzonation

A Method of Simulating Earthquake Ground
Motion by Equivalent Blast Excitation10—1

Zhang Xueliang and Huang Shutang

Using Air Remote-Sensing Technique in Study of
Tangshan Earthquake Hazards and Hazard
Microzoning11—1

Zou Xuegong

Use of Average Weighted Shear Modulus in the
Study of Site Effect-Discussion on the Cause
of Low Intensity Anomaly in Yutian During
the Tangshan Earthquake12—1

Liu Zengwu, Dong Enchang, Lu Gensheng,

Wang Dongqiang and Wei Peiheng

Geophysical Techniques for Site Characterization
for Microzonation13—1

Vincent Murphy (Canceled by author)

4 . Soil Dynamics for Microzonation

Characteristics of Liquefaction of Clayey Silt and
it's Field Discrimination14—1

Shi Zhaoji and Yu Shousong

Foundation Problems in Aseismic Design of
Hydraulic Structures15—1

Wang Wenshao

Dynamic Soil Property16—1

Isao Ishibashi

Liquefaction Failure of Saturated Sandy Soil
Under Cyclic Loading17—1
Liu Ying, Tong Jun and Qi Xin

5 . Earthquake Damage Prediction and Construction of Microzoning Map

Architectural Planning and Design Considerations
of Microzonation18—1
Henry J. Lagorio and Marcy Wang

The Prediction and Zonation of Earthquake
Ground Motion in the Beijing Plain19—1
Jiang Pu, Xu Feng and Wang Qiming

Earthquake Hazards and Vulnerability Analysis20—1
Zhu Haizhi and Wang Ligong

The Seismic Microzoning of Lanzhou.....21—1
Sun Chongshao and Chen Bingwu

On the Seismic Activity and Microzonation
of the Beijing Area22—1
Zho Xiyuan, Fu Shengcong and Wang Guangjun

6 . Site Response, Interaction and Others

Site Response and Interaction Analysis23—1
John Lysmer

A Preliminary Study on the Dynamic Behavior
of the Soil-Structure Interface Not Published.....24—1
Fu Changsheng and Yu Zaidao (Canceled by authors)

The Regional Characteristics of Seismic
Intensity Attenuation in China25—1
Chen Peishan, Jin Yan and Li Wenxiang

Effects of Irregular Topography and Non-uniform Soil
Profiles on Earthquake Motion and Earthquake Damage26—1
Chen Bingwu

A Probabilistic Estimate of Maximum Accelration
in Rock in North China27—1
 Song Liangyu and Wei Gongyi
Seismic Hazard and Uncertainty
Analysis for Microzonation.....28—1
 Anne S. Kiremidjian

ERRATUM

USAGE AND LIMITATION OF EARTHQUAKE INTENSITY

Hu, Yuxian*

ABSTRACT

This paper describes at first two meanings and three uses of earthquake intensity ; discusses then the requirements related to earthquake intensity in structural design during various stages of progress of earthquake-resistant design; emphasizes the limitation of intensity used in current codes; and suggests to use in structural design the ground motion parameters without reference to earthquake intensity. Related results obtained and factors to be considered in microzonation are also discussed.

1. MEANING, USAGE AND NATURE OF EARTHQUAKE INTENSITY

Earthquake intensity is an old idea which may be traced back to 1783 when it was used as a means to describe the relative strength of earthquakes. It has been widely used since 19th century in Europe and America and many earthquake intensity scales have been suggested and used for its rating. Almost right from its beginning, two related but different meanings have been given to earthquake intensity: the direct and the indirect. By the direct meaning, intensity is a qualitative measure of the seriousness of the results of the earthquake on human feeling, ground disturbance, structural damage and object behavior; by the indirect meaning, it is a qualitative measure of the intensity of earthquake ground motion through the direct.

The usage of earthquake intensity falls generally into one of the following three groups. Firstly, it is used to direct the governmental or social aid to the damaged areas according to the severity given in the earthquake intensity distribution or the isoseismals drawn after a strong earthquake. Secondly, it is used to study the source mechanism of an earthquake and the tectonic activity of a district. Thirdly, it is used to group experience obtained for engineering structures under certain conditions and the requirements to be specified in design code for such conditions.

* Professor, Institute of Engineering Mechanics (IEM),
Academia Sinica

For almost 200 years, earthquake intensity remains to be a qualitative, global, rough and nonphysical rating rather than a quantitative, specific, accurate and physical quantity. In spite of the effort of many investigators trying to attach to intensity a physical quantity such as acceleration or velocity of ground motion, little results have been achieved and earthquake intensity remains a rough rating to be assessed according to intensity scale. It seems to the author that it will remain so for a long time. The reason is that there is a definite need for a qualitative and global rating to reflect the general trend of variation of damage or ground motion in the usage of intensity as mentioned above and there is no way to replace this simple rating in the near future.

2. ENGINEERING NEEDS OF EARTHQUAKE GROUND MOTION

The third way of using earthquake intensity is the engineering way which is the main interest of the present paper. The engineering need of earthquake intensity changes with the advance of the theory of earthquake-resistant design.

In its beginning period, perhaps before 1950, theory of earthquake-resistant design was in static stage where the effect of earthquake ground motion on structure was considered to be a static horizontal force, completely specified by a single parameter, such as the maximum horizontal acceleration of ground motion.

Response spectrum theory was initiated by professor G. W. Housner approximately in 1950. Since then, earthquake ground motion was treated as a vibrational process of certain spectrum, but this spectrum was considered unchanged in shape for different conditions in the early stage of response spectrum theory and number of independent parameter of earthquake ground motion remains to be only one.

This may be the reason that many seismic design codes before 1960 or so adopted earthquake intensity, an idea so popular then in Europe and America, as an index for zoning and design values of acceleration were given according to intensity. A typical example is the Soviet Union's code of 1957 in which seismic zonation, site effect and constructional measures were all specified through intensity.

But in the later stage of response spectrum theory, perhaps since 1960-70, it was suggested that the ground motion spectrum should vary in shape for different site conditions. Fig.1 shows the results of IEM published in 1965⁽⁴⁾ and of Seed, et al in 1974^(1,2), both showing clearly that the

softer the site, the larger the ordinates of the spectrum at longer periods with a difference of several times. Strong field evidence has been mentioned in literature to show the so-called selective damage which may be closely related to the variation of ground motion spectrum. Table 1 and Fig.2 show the results we obtained in the 1975 Haichang earthquake. Damage index I is a qualitative measure, coined by the author in 1970 during the field study of 1970 Tonghai earthquake to be used as a substitute for earthquake intensity⁽⁹⁾. $I = 0$ means no damage and $I = 1$ means complete collapse of all structures within a local area. Fig.2 was drawn from data given in Table 1. This set of data, based on a large amount of investigations in the field, shows clearly at least two facts as follows. (1) The intensity rating agrees roughly with damage of low masonry buildings, which seems to mean that intensity is rated primarily on the behavior of this kind of building, most popular in the shaken area. (2) The intensity rating has almost no relation with damage of brick smoke-stacks and site condition has a very strong influence on damage of long-period structure; the softer the site and/or the longer the epicentral distance, the greater is the damage index of long-period structure, similar as the result given in Fig.1. This result is readily accepted theoretically from wave propagation.

When theory of earthquake-resistant design advances to this stage, the requirement on ground motion undergoes a fundamental change. Earthquake motion is considered a physical quantity, no longer of only one, but of several independent parameters to control its vibrational characteristics, among which amplitude, spectrum and duration should not be ignored.

The importance of variation of spectral shape of ground motion has been recognized by several important design codes, such as the Chinese Code of 1974 and 1978, UBC and ATC-3 Model Code in the United States in approximately 1976, and the USSR draft code СНиП II-7 in 1979⁽¹⁰⁾, in which different spectral shapes are assigned to different site conditions in addition to independently varying ground accelerations.

In addition to peak values and spectral shape, duration of strong portion of ground motion is another important parameter controlling its effect on damage of structures. Data given in Table 2 show it clearly. Ground motions of the first 11 cases caused relatively slighter damage were of rather large peak accelerations of 0.3 - 0.7g in general and very short durations of 1 - 8 sec., while those of the last 7 cases caused comparatively heavier damage were of much smaller peak

accelerations of 0.04 - 0.2g and rather long durations of 20 - 60sec. The importance of duration is well known but not reflected yet in building codes because an easy and reasonable way of its consideration is still needed; for important structures like nuclear power plant, however, duration is considered in simulating input ground motions for dynamic analysis.

3. SITE CONDITIONS AND MICROZONATION

Microzonation idea was first used in USSR officially perhaps in 1957. By microzonation, it is meant that a subdivision of an area of the size of a county, a city or a complex construction site, usually in the same intensity zone from seismic zonation, is made by considering the effect of site conditions, such as local soil, ground water table, local topography and existence of faults. Seismicity is the main consideration in seismic zonation and not considered in microzonation according to the USSR idea though not so universally. The result of zonation is a zoning map of earthquake intensity, while the result of microzonation is a map of site intensity, intensity modified by considering effect of difference in site conditions.

Ground soil condition is now generally considered to have an important influence on ground motion and various schools seem to have agreed recently on its effect on spectral shape of ground motion. Table 3 shows the author's understanding of the international trend in code modification in this aspect. A common trend may be seen from Table 3 in the way of consideration of ground soil condition by modifying the shape of response spectrum instead of old way of adjusting the design earthquake intensity.

Main results obtained on earthquake ground motion and site effect by a research group, headed by the author from 1961 to 1978, in IEM are as follows (3-4, 6-9).

(1) Weak or potentially unstable ground may fail during a strong earthquake due to sand liquefaction, differential settlement, land slide, cracking or reduction of supporting capacity. To prevent the effect of ground failure on superstructure, a raise of design intensity or ground motion is neither effective nor economic, and site selection and foundation treatment should be a better recipe.

(2) Effect of ground soil condition on ground motion is to be considered by adjusting the shape of response

spectrum instead of adjusting the design intensity as used then in some countries, and a classification of ground soil conditions into 4 groups together with their corresponding design spectra was suggested on the basis of data available.

(3) Effect of faults should be differentiated. For causative faults, relative displacements across the fault may take place and result in ground failure. Site selection and special design of structures to accommodate this displacement are reasonable ways of considering its effect. Causative faults are found usually in epicentral area. For non-causative faults there is usually no risk of such ground failure and such faults may be treated as a ground soil problem with no additional adjustment of design earthquake intensity.

(4) Following the above-mentioned reasonings, a microzonation is not an adjustment of intensity to site intensity but a depicting of ground soil conditions by soil investigation with assistance of other in-situ tests and ground motion analyses. The term site intensity may be deleted from design code.

(5) In case that super-structural failure from ground failure can not be prevented, liquefaction of sand layers below foundation will accentuate damage of the super-structure through ground failure; but under conditions that there is a stable top soil layer of sufficient depth and strength to support the super-structure with no ground failure on surface, liquefaction of lower sand layer may prevent shear waves propagating into the structure and thus result in mitigating the damage to the super-structure.

(6) It is possible to compute the surface motion from input motion at bedrock and study the effect of ground soil condition on ground motion, considering the nonlinear property of soil.

(7) In structural design, ground motion parameters may be used without referring to earthquake intensity.

First 4 results were obtained and reported before 1972 and adopted in our current building code with some minor changes.

According our current code and current understanding, it is believed that following items should be considered in seismic microzonation.

(1) A map showing detailed seismicity of the region,

given the future probable earthquake magnitudes, locations and return periods or probabilities.

(2) Possibility and extent of ground failure during earthquakes expected in future.

(3) Possible values of various design parameters of ground motion, such as maximum or root-mean-square acceleration and velocity, response spectra and duration, if possible, with their coefficients of variation.

(4) Microzonation of ground soil conditions, with corresponding values of above-mentioned design parameters.

(5) Effects of other site conditions on ground motion and their microzonation.

4. CONTRADICTIONS BETWEEN EARTHQUAKE INTENSITY

AND GROUND MOTION PARAMETERS

Since 1960's, we have emphasized several times that earthquake damage to engineering structures may be introduced by quite different mechanism, namely structural vibration and foundation failure^(3,6-9). It is very important to distinguish one mechanism from the other because different measures should be taken to prevent or mitigate effectively the damage caused. Since earthquake intensity tries to combine, instead of distinguish, all factors or effects of all factors into a united single rating of global damage, an adoption of earthquake intensity idea, therefore, will be an obstacle to distinguish ground failure from structural vibration and easily result in adjusting the design intensity for seismically weak sites. In the current USSR seismic code, for example, the design intensity for structures on weak soils such as liquefiable sand layer should be increased by one grade. Such an increase of design intensity will result primarily in strengthening super-structure but is not effective at all in preventing the foundation from malfunctioning. The spectacular lesson of inclined and lying-on-ground apartment buildings in the well-known Niigata Earthquake is a definite proof of the ineffectiveness of the intensity adjusting recipe for weak foundations. This is one of the serious shortcomings of using earthquake intensity idea in seismic design of structures.

Another shortcoming introduced by earthquake intensity to structural design is the double-jumping of design peak

acceleration for change of intensity by one grade. A continuous change or a stepwise change of smaller quantity of design peak acceleration is more reasonable in providing a uniform factor of safety to the general trend of ground motion attenuation. The great inaccuracy in ground motion prediction, including the abnormalities in attenuation of intensity or ground motion, is not an excuse for preferring the double-jumping to a smaller step of changing the design parameters.

In contrary to the matter-of-accuracy nature of the second shortcoming of using earthquake intensity idea in designing, its third shortcoming is a contradiction in definition. This shortcoming or contradiction was pointed out in 1978 by the author in a discussion of the current Chinese seismic code⁽⁵⁾. As shown in Fig. 3, there are two parameters in our code⁽¹⁾ involved in the specified response spectra of ground motion $\alpha(\tau) = \beta(\tau) \cdot a/g$ in which a/g represents the specified maximum acceleration, changing only for different intensities, and $\beta(T)$ represents the response spectral shape, changing only for different site conditions. They are therefore independent parameters and here comes a contradiction in definition. For one and the same intensity, say VIII grade, $\alpha_{\max} = \beta_{\max} \cdot a/g = 0.45$ for all site conditions. For sites of different site conditions, if earthquake intensity is the same, total or global damage on each site should be nearly the same since earthquake intensity is defined as a rough measure of the global damage of a local area. But, on the other hand, according to our building code, as given in Fig. 3, the global damage on weak or soft sites of classification III will be much higher than that on stiff site of classification I, since the response spectrum on site III has much greater ordinates on the average than those on site I. This is a contradiction by definition. The fundamental cause of this contradiction lies in a mis-fitting of the persistent holding of the simple and global idea of earthquake intensity and the ever-stronger attack of multiple-parameters of the ground motion needed in the design code since a single parameter idea of earthquake intensity can never be consistent with an idea of multiple independent parameters of ground motion.

5. USING GROUND MOTION PARAMETERS IN DESIGN

A simple and straight-forward solution to the problem is to save earthquake intensity idea for uses such as drawing isoseismals to direct social or governmental aid to the damaged area and to study earthquake source mechanism but, on

the other hand, to adopt directly ground motion parameters without referring to earthquake intensity for structural design. A quite parallel example exists in wind-resistant design of structures which, even in our country, velocity of wind or pressure on structures are directly specified with no reference at all to wind grades although the later is very popularly used in public life and weather prediction.

In our current seismic codes, earthquake intensity is specified in three steps; it is the author's strong believing that other suitable physical quantities may be substituted with no trouble. Such an example is given in the following.

(1) ZONATION FOR CITY OR LAND-USE PLANNING

In our current practice, zonation is done according to earthquake intensity and the resulting intensity zoning map is used for city or land-use planning. For this usage of intensity zoning map, the predicted-earthquake map may be used as a convenient substitute. In the process of intensity zonation, a map showing the predicted earthquake epicenter zones has been completed and used as the basis of intensity zoning. The accuracy of intensity zoning is controlled by the accuracy of predicted-earthquake map, on which the possible epicenters together with the maximum magnitude of earthquakes expected within the coming 100 years, say, are given. This map should meet the needs of city and land-use planning.

(2) USING ACCELERATIONS FOR STRUCTURAL DESIGN

In our codes, design values of acceleration a or its equivalence α_{\max} are specified for various intensities as given in Fig. 3. The functional relation of intensity and acceleration is obtained from a set of data similar to Fig. 4, which shows the huge scattering in the relation between acceleration and intensity.

A very simple substitute for this usage of intensity is to draw on the map the acceleration values we are using now instead of intensity. This substitution sacrifices nothing at all but, on the contrary, makes one free from the shortcoming of a forced double-jumping change of design accelerations and leaves plenty of room for further addition of ground motion parameters such as duration.

(3) ACCUMULATION OF EXPERIENCE AND SPECIFICATION OF CONSTRUCTIONAL MEASURES

In our design codes, structures designed for different intensity zones require different constructional measures, such as structural materials and types, limitations on height of building and design details on the basis of experience and lessons accumulated from past strong earthquakes. It seems to the author that a combination of earthquake magnitude M and distance R is a convenient and better substitute of intensity for these purposes. There is no difficulties to re-organize our experience into this new frame of magnitude and distance; and, more important is the fact that experience in the new frame is more consistent with the up-to-date understanding on the subject because experience obtained from same intensity but of different combination of magnitude and distance may be quite different. For example, intensity of VIII from a very strong ($M = 8$) but distant ($R = 100\text{km}$) earthquake and that from a moderate ($M = 6$) and very close ($R = 0 - 10\text{km}$) earthquake will give totally different experiences owing to their great differences in ground motion characteristics, as have often been pointed out in the literature and identified so in the field.

Reasons against not referring to earthquake intensity in structural design may be grouped into two arguments, namely, the advantage of using intensity and the disadvantage of using directly ground motion parameters.

Considered as advantage of using intensity, simplicity, tradition and current code requirements are most commonly mentioned. It seems to the author that simplicity itself is not a merit, and tradition of using intensity was introduced into our engineering practice in 1955 when learning from the Soviet Union. As for current codes, they are guides for our present construction and should not be a barrier to improvement and advance. If a theory or a method matches better with facts, simplicity may yield, tradition **should be** overthrown and codes will be changed. Almost every change, correction, improvement, or revolution is accompanied with a break-through from some tradition, either in idea or in formality.

As disadvantage of using ground parameters, lack of strong motion data and great uncertainty in ground motion prediction seem to be on top of the list. Errors coming from lack of strong motion data have same effect on design ground motion parameters, either for the current method of assigning these parameters through earthquake intensity or directly with no reference to intensity, since intensity is eventually converted to these parameters through data similar to those

shown in Fig. 4. As for uncertainty in prediction, the greatest one seems to be the prediction of the time of occurrence, epicenter location and magnitude of future earthquake; uncertainties in estimating the attenuation, both of intensity and of ground motion, should be on the same level and much less than that of earthquake prediction, considering that an error of one grade in intensity means an error of 100 % in acceleration of ground motion.

REFERENCE

1. (1974), Seismic Design Code for Industrial, Office and Residential Buildings (TJ-74); revised (TJ-78), (1978), Beijing
2. Liu, Huixian: (1965), Some Remarks on Methods of Earthquake Response Analysis of Structures in Design Code, Res. Rept. IEM, Academia Sinica, V.2
3. Zhou, Xiyuan: (1965), Effects of Soil Conditions on Earthquake Response of Structures, Res. Rept. IEM, Academia Sinica, V.2
4. Chen, Dasheng: (1965), Data on Peak Acceleration and Acceleration Response Spectrum of Ground Motion, ditto, V.2
5. Hu, Yuxian: (1980), Contradiction of Intensity Idea and Adjustment of Shape of Response Spectrum in Chinese Seismic Design Codes, Earthquake Engineering and Engineering Vibrations, Sample Issue No.2
6. Hu, Yuxian and Zang, Zaiyong: (1979), Damage from the Haicheng Earthquake, Ch.2, Damage Distribution and Site Conditions
7. Hu, Yuxian; Sun, Pingshan; Zhang, Zaiyong; Tian, Qiwen: (1980), Effects of Site Conditions on Earthquake Damage and Ground motion, Earthquake Engineering and Engineering Vibrations, Sample Issue No.1
8. Ground Motion Division: (1976), Effect of Faults on Earthquake Intensity, Res. Rept. IEM, Academia Sinica
9. Res. Group of Tonghai Earthquake: (1973), Intensity Distribution and Site Effects of Tonghai Earthquake of 1973, Res. Rept. IEM, Academia Sinica
10. Поляков, С. В., Айзенберг, Я. М., Ойзерман, В. И.: /1979/, О Проекте новой главы СНиП II-7 "Строительство в сейсмических районах", Строительная механика и расчет сооружений, №.4
11. Housner, G. W. and Jennings, P. C.: (1973), Problems in Seismic Zoning, Proc. 5 WCEE
12. Seed, H. B., Ugas, C. and Lysmer, J.: (1974), Site-Dependant Spectra for Earthquake-Resistant Design, EERC Rept. 74-21, U. C. Berkeley
13. Borchardt, R. D. (ed): (1975), Studies for Seismic Zonation of the San Francisco Bay Region, Geological Survey Prof. Paper 941A

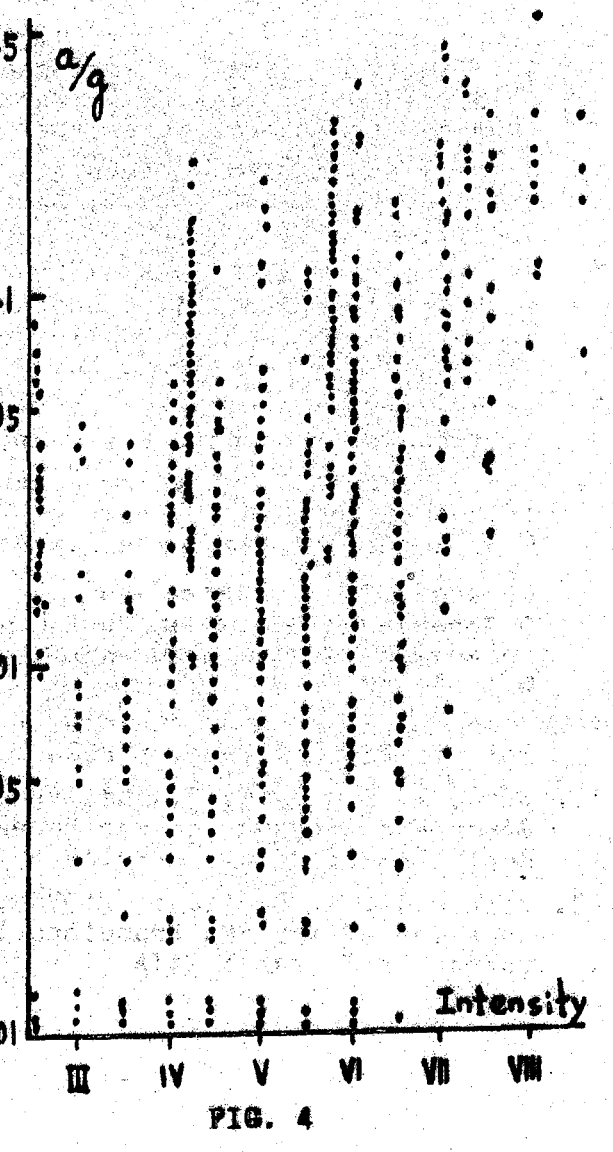
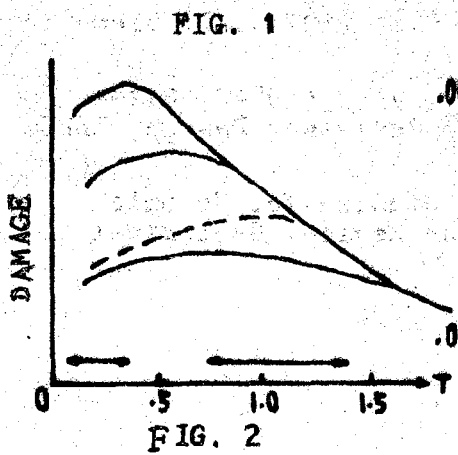
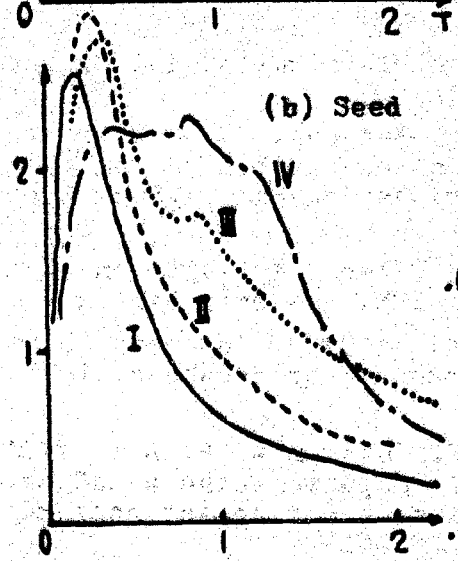
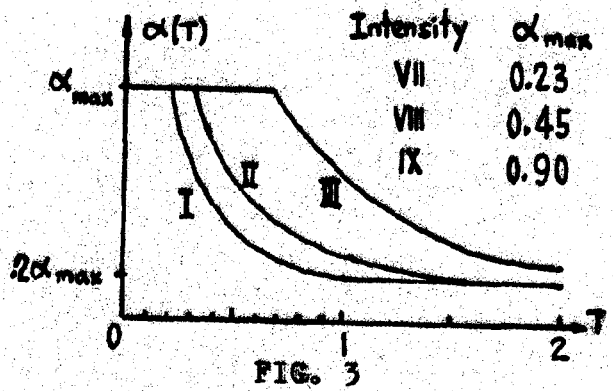
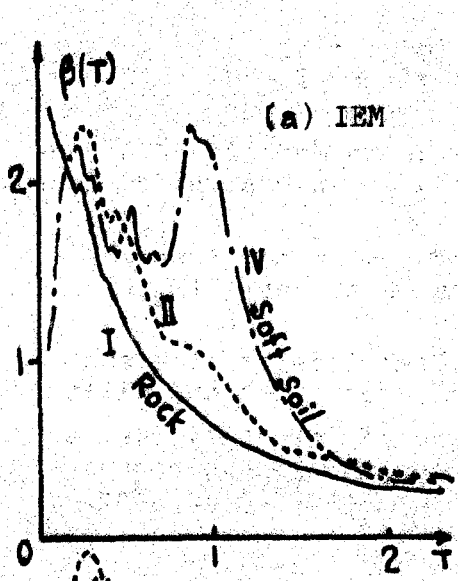


FIG. 1

FIG. 2

FIG. 3

FIG. 4

Table 1. Statistics of Damage of Smokestacks and Single-story Brick Buildings

NO.	CITY	I	SITE	SMOKESTACK		BRICK BLDG		DISTANCE KM
				NO.	DAMAGE INDEX	NO.	DAMAGE INDEX	
1	HAICHENG	IX	II	51	0.58	152	0.26	17
2	DASHIQIAO	IX	II	24	0.51	55	0.30	17
3	YINGKOU	VIII	III	34	0.51	189	0.15	38
4	TIANZHANGTAI	VIII	III	(3)	(0.78)	31	0.16	49
5	DAWA	VII	III	10	0.67	38	0.19	57
6	PANSHAN	VII	III	13	0.54	94	0.11	75
7	ANSHAN	VII	II	40	0.15	-	-	51
8	LIAOYANG	VII	II	93	0.28	93	0.09	80

Table 3. Development of Design Codes on Ground Motion

Country	Static theory	Response spectrum theory (Constant spectrum)	Response spectrum theory (Varying spectrum)
USSR	Intensity (Zonation, accelerate, constructural measures)		
	Effect of site conditions not considered	Effect of site conditions considered by adjusting intensity into site intensity	1979 Adjusting response spectrum according to 3 classes of site
China	1957, 1959 Same as USSR	1964 Draft Code, site intensity deleted, ground soil effect by adjusting spectrum. 4 classes of site	1964 Draft Code, site intensity deleted, ground soil effect by adjusting spectrum. 4 classes of site
USA	Acceleration following Japan	Intensity (Zonation, acceleration). Site effects not considered	Acceleration and velocity zonation. Site effect considered by adjusting spectrum

Table 2. Comparison of Intensity and Duration of Earthquake

DATE	EARTHQUAKE	STATION	M	DIST (KM)	INTENSITY I	a/g	DURATION (SEC)	REMARK
1964.11.14	Ibaraki-fu Bay, Japan	Tokaimura	5.1		V			I (Japan)=III
1967.11.11	East Hokkaido, Japan	Kushiro			VI			I (Japan)=IV
1967.11.19	Ibaraki-fu Bay, Japan	Tokaimura			V			I (Japan)=III
1972. 9. 4	Stone Canyon, USA	Melendy Ranch	4.7	0.1		0.69	2	No damage
1973.11. 4	Leukas, Greece	Leukas	6	25	VII	0.54	3	
1966. 8. 4	Matsushiro, Japan	Matsushiro	4.7	2	V	0.39	3	
1966. 4. 5	Matsushiro, Japan	Matsushiro	5.1	4	VI	0.42	4	
1957. 3.18	Port Hueneme, USA	Port Hueneme	4.7	7	VI	0.17	1-2	
1966. 6.28	Parkfield, USA	No.2	5.6	0.08	VII	0.50	2-8	Fault dist.
1971. 2. 9	San Fernando, USA	Pacoima	6.6		IX	1.25	7	
1965.12. 9	Mexico	Acapulco	6.8	60	VI	0.27	8	
1949. 4.13	Olympia, USA	Seattle	7.1	40	VIII	0.07	20-45	
1968. 5.16	Tokachi-oki, Japan	Hachinohe Muroran	7.9	179 310	VII-VIII VI	0.23	20-30	I (Japan)=V
1964. 6.12	Niigata, Japan	Niigata	7.7	38	VII-VIII	0.21	20-30	I (Japan)=IV
1940. 5.18	Imperial Valley, USA	El Centro	7.0	20	VIII	0.16	30	I (Japan)=V
1962. 5.11	Mexico	City Park	7.0	260	VI-VII	0.04	960	
1962. 5.19	Mexico	City Park	7.1	260	VI-VII	0.03	960	

MICROZONATION WITH RESPECT TO
SITE AMPLIFICATION AND SOIL LIQUEFACTION

by Mehmet A. Sherif¹

ABSTRACT

In this paper, the basic requirements for microzonation are identified and procedures for microzonation with respect to ground amplification and soil liquefaction are proposed and illustrated with practical examples. The Ratio Microzonation method which is proposed by the author and discussed in this paper, is a general procedure that could be used in microzonation with respect to ground amplification utilizing either microtremors or man made excitations as a source of ground disturbance. The application of the proposed procedure for microzonation with respect to soil liquefaction requires the knowledge of easily determinable soil properties which are discussed in this paper and the choice of design earthquake signature germane to the area under consideration.

1. Introduction and Definition

Microzonation is a process that involves incorporation of geologic, seismologic, and geotechnical concerns into land-use planning for earthquake effects so that engineers can design structures that will be less vulnerable to damage during major earthquakes. The term microzonation does not imply site-specific studies, but rather a more general and overall characterization of large parcels of land (ranging from a few to, say, 50 or 100 square kilometers). To be useful, microzonation should provide general guidelines relative to the types of structures that are most suited to an area, and it should also provide information on the relative damage potential of the structures already existing in a region. Combining the above two foci, microzonation provides a strategy for the development of land-use planning criteria for the establishment of new communities and the formulation of a systematic and informed decision-making process to assist in determining which existing structures should be strengthened in order to enhance their integrity and stability in the event of an earthquake.

Basic to any assessment of the likelihood of structural damage due to seismicity, however, is information about ground failure and ground amplification and the distribution of ground frequencies that may amplify

¹Professor of Civil Engineering and Adjunct Professor of Quaternary Research
University of Washington, Seattle, Washington, U.S.A.

the structural response. The ability to address these factors is among the basic and fundamental requirements for microzonation.

It would perhaps be wishful thinking to believe that we could predict the signature of the most damaging typical earthquake a region under consideration might experience so that we might use that ideal and most suitable earthquake signature as an input to our ground-amplification and response calculations. Unfortunately, Mother Nature is unpredictable and quite often it seems to produce in the same region seismic waves that are quite different in their intensity, frequency content, duration, and acceleration. Worse yet, most of the time we do not even have any record of seismicity of the region that we wish to microzone; and it is impractical to wait for a devastating earthquake to hit the area so that we may use the signature of that earthquake as an input into our microzonation scheme. Faced with all of the above difficulties, and in the absence of nature's willingness to accommodate our wishes, a microzonation technique leading to the assessment of site amplification through the utilization of natural microtremors may provide a reasonable and useful alternative.

Except in areas where the ground actually ruptures during an earthquake (in which case no viable analysis is possible), the strains generated in the ground by major earthquakes are small (considerably less than 1 percent). In view of this, it can be argued that the ground system can be considered, in general, to behave almost elastically. This being the case, it should be possible to use microtremor signals as a means of calculating relative ground amplification and frequency distribution without introducing unacceptable errors, provided that the non-stationary problems associated with microtremors are resolved.

It is generally accepted that microtremor signals are non-stationary; they vary as a function of time, and therefore cannot be used as viable tools for microzonation, and yet it has been shown that (Refs. 1, 2, 3, 4) if a certain procedure known as the ratio method is employed with care, microtremor data can be used for microzonation purposes, thus enabling the engineer to assess relative amplifications and frequency distributions within a candidate site (Ref. 3).

2. Basic Principles of the Ratio Method

The idea behind the Ratio Method is that at a given site where the seismic strains are small (less than 1%) the soil and sub-surface act upon seismic signals as a filter with nearly linear characteristics. Accordingly, the system through which seismic signals pass may be modeled as shown in Fig. 1, where the symbols $s(t)$, $f(t)$, $i(t)$, and $r(t)$ denote time-domain functions. Using the linear operation theory, the response function $r(f)$ can be defined by:

$$r(t) = s(t)*f(t)*i(t)* \quad (1)$$

where the symbol * denotes the mathematical process of convolution.

Also, if $S(f)$, $F(f)$, $I(f)$, and $R(f)$ are taken to represent frequency-domain functions corresponding to those time-domain functions shown in Fig. 1 [i.e., $s(t)$ and $S(f)$ are a Fourier transform pair], then the frequency-domain response $R(f)$ of the system can be defined by

$$R(f) = S(f) \times F(f) \times I(f) \quad (2)$$

where \times denotes multiplication, and $R(f)$ corresponds to the Fourier power spectrum.

Now, let us consider that we are operating at a given site two sets of three-component (NS, EW, and vertical) microseismic stations with exactly similar instruments except that one of the stations is left stationary (base station), while the other is transported from one location to the other (portable station). Moreover, imagine that the two stations (portable and base) were synchronized so that microseismic signals at both stations were recorded simultaneously on a magnetic tape and processed thereafter. The ratio of the power spectrum of the portable station to that of the base station can be expressed as:

$$\frac{R_p(f)}{R_b(f)} = \frac{S_p(f) \times F_p(f) \times I_p(f)}{S_b(f) \times F_b(f) \times I_b(f)} \quad (3)$$

Now, if the microtremor data were recorded at reasonably quiet hours and if the locations of the portable and base stations were reasonably close* the $S_p(f)$ in Eq. 1 will be the same as $S_b(f)$ (because the data from both stations are recorded at the same time), and $I_p(f) = I_b(f)$ (because the instruments at both stations are exactly identical). Therefore, Eq. 3 reduces to

$$\frac{R_p(f)}{R_b(f)} = \frac{F_p(f)}{F_b(f)} \quad (4)$$

*Varies with population density as well as with geologic setting. A certain amount of preliminary experimentation is necessary to determine the reasonable distance. (In general less than 5 miles.)

Thus, we note from Eq. 4 that the power spectral ratio at two locations yields a function which reflects solely the relative effect of site characteristics of the two stations. It must be noted here that Fourier power spectra are by definition equal to the squares of Fourier amplitudes, thus,

$$\frac{R_p(f)}{R_b(f)} = \frac{(X_p(f))^2}{(X_b(f))^2} \quad (5)$$

We therefore see that the square root of the power spectral ratio between the portable and base stations will yield a function which is a measure of the relative amplification between the two stations as a function of frequency. This function is known as the amplifications spectrum and is defined by

$$\text{Amplification Spectrum} = \sqrt{\frac{R_p(f)}{R_b(f)}} = \frac{X_p(f)}{X_b(f)} \quad (6)$$

It is seen from the above that the Ratio Method, if properly employed, provides a direct measure of relative amplification among different locations within the candidate site with respect to a fixed or permanent base station. Another attractive feature of the ratio technique is that the relationship expressed in Eq. 6 is almost stationary (Refs. 1, 2, 3, 4).

In view of the fact that the combined effects of NS, EW and vertical motions, rather than individual components, more profoundly influence the response and hence the safety of structures in an area, it is desirable that the amplification factors expressed in Eq. 6 be not individual but rather the resultant of the NS-EW and vertical spectral components, which is expressed as

$$C_R = (C_{NS}^2 + C_{EW}^2 + V_{vt}^2) \quad (7)$$

where C_{NS} , C_{EW} , and V_{vt} are the power spectra amplitudes of the north-south, east-west, and vertical triaxial components respectively.

3. Microzonation by the Ratio Method (Instrumentation and Practical Application)

Application of the Ratio Method in practice requires the utilization of two exactly identical three-dimensional microseismic measuring stations. One of the stations is placed in a permanent location and is designated as the base station; the other is moved from one location to the other within the area and is identified as the portable station. Figs. 2 and 3 are photographs of the base and portable stations, together with their associated components. Fig. 4 shows a block diagram identifying the various electronic components associated with the portable stations. The base station will be the same except for the absence of an oscilloscope. Our experience in Greece and in the U.S.A. has shown that a grid of a quarter of a mile regarding the location of portable stations appears to be reasonable for microzonation of rural and less populated areas. For cities or densely populated regions, however, a grid line of between 200 and 500 feet is recommended. Also, it is suggested that microseismic readings within cities and noisy regions be taken during quiet hours (say between 12 midnight and 5:00 a.m.). Furthermore, because of the high frequency content of microtremors it is recommended that a filter be used to cut off all frequencies above 10 Hz.

For data processing and analysis the following procedure is suggested:

1. To obtain statistically more representative power spectra for the portable and base stations, it is suggested that at least two power spectra be obtained for each of the NS, EW, and vertical components, as illustrated in Fig. 5.
2. From the above two power spectra for each component, obtain an average power spectra for each NS, EW, and vertical component. Smooth each average power spectrum twice.
3. Obtain the resultant power spectrum for each of the portable and permanent stations, using the average smoothed power spectrum for each NS, EW, and vertical component generated in Step 2 above and again smooth each of the resultant curves twice to eliminate minor and unimportant variations in frequency so that an engineering judgment can be made based on more significant information. An example of such a resultant is shown in Fig. 6.
4. From the resultant power spectrum obtained in Step 3 for each of the portable stations, prepare a table as shown in Fig. 7 indicating the distribution of predominant frequencies as a function of locations in the region, and plot the data as shown in Fig. 8.
5. Divide the resultant power spectrum of every portable station with the corresponding power spectrum of the permanent station to obtain relative amplification at each portable station. Fig. 9 shows a typical amplification curve.

3. Microzonation by the Ratio Method (Instrumentation and Practical Application)

Application of the Ratio Method in practice requires the utilization of two exactly identical three-dimensional microseismic measuring stations. One of the stations is placed in a permanent location and is designated as the base station; the other is moved from one location to the other within the area and is identified as the portable station. Figs. 2 and 3 are photographs of the base and portable stations, together with their associated components. Fig. 4 shows a block diagram identifying the various electronic components associated with the portable stations. The base station will be the same except for the absence of an oscilloscope. Our experience in Greece and in the U.S.A. has shown that a grid of a quarter of a mile regarding the location of portable stations appears to be reasonable for microzonation of rural and less populated areas. For cities or densely populated regions, however, a grid line of between 200 and 500 feet is recommended. Also, it is suggested that microseismic readings within cities and noisy regions be taken during quiet hours (say between 12 midnight and 5:00 a.m.). Furthermore, because of the high frequency content of microtremors it is recommended that a filter be used to cut off all frequencies above 10 Hz.

For data processing and analysis the following procedure is suggested:

1. To obtain statistically more representative power spectra for the portable and base stations, it is suggested that at least two power spectra be obtained for each of the NS, EW, and vertical components, as illustrated in Fig. 5.

2. From the above two power spectra for each component, obtain an average power spectra for each NS, EW, and vertical component. Smooth each average power spectrum twice.

3. Obtain the resultant power spectrum for each of the portable and permanent stations, using the average smoothed power spectrum for each NS, EW, and vertical component generated in Step 2 above and again smooth each of the resultant curves twice to eliminate minor and unimportant variations in frequency so that an engineering judgment can be made based on more significant information. An example of such a resultant is shown in Fig. 6.

4. From the resultant power spectrum obtained in Step 3 for each of the portable stations, prepare a table as shown in Fig. 7 indicating the distribution of predominant frequencies as a function of locations in the region, and plot the data as shown in Fig. 8.

5. Divide the resultant power spectrum of every portable station with the corresponding power spectrum of the permanent station to obtain relative amplification at each portable station. Fig. 9 shows a typical amplification curve.

6. From the data in steps 4 and 5, a final map may be prepared showing the average relative amplification and frequency distribution for the site of interest. An example of such a map is shown in Fig. 10. In this figure we note that the area in question has been divided essentially into three zones, I, II, and III, with respect to frequency distribution, and each zone has been further subdivided into smaller divisions reflecting differences in amplification factors in each of the above frequency domains. Such areas are labeled I_1 , I_2 , I_3 , II_1 , II_2 , II_3 , III_1 , and III_2 in Fig. 10.

The process used in the preceding data acquisition and processing is summarized in Fig. 11.

Since the primary objective of microzonation is to reduce damage to human life and property, it is essential that the site amplification and frequency distribution be translated into real-world terms in order to determine the seismic safety of existing structures and develop guidelines for the design of future structures in the microzoned area. In an effort to do this, and in the absence of better alternatives, a certain amount of averaging and engineering judgment has to be utilized. Within each of the zones in Fig. 10, we obtain the overall amplification-frequency curve by taking the average of the ratio curves for all the stations within that zone. An example of such an average amplification curve for Zone II_3 in Fig. 10 is shown in Fig. 12.

After having established the average characteristic amplification curve for each zone within the candidate site, the next necessary step involves the translation of amplifications into design accelerations. To do this, we should first establish the value of the maximum expected acceleration at the base station. The maximum anticipated accelerations at the base station can be obtained from historical seismicity in or near the area and the distance of the subject site from the nearest active fault line.

Assuming that an earthquake of magnitude 7.5 is likely to occur along a fault line 20 kilometers away from the site, it is expected, according to the data shown in Fig. 13, that the average ground acceleration level at the base station will be about 0.12g. Since the site in question does amplify the signals as indicated in Fig. 10, to obtain the design earthquake acceleration at various locations at the site the 0.12g station accelerations must therefore be multiplied by the frequency-dependent average amplification curves associated with each zone as expressed by Fig. 12 for Zone II_3 in Fig. 10.

Combining the above information with the empirical relationship expressed in Eq. 8, (Ref. 5) it should be possible to estimate the design accelerations to the number of building stories, as expressed in Fig. 14.

$$T = \frac{N}{T_0} \quad (8)$$

where T = period and N = number of stories.

It is evident that the type of information contained in Fig. 14 can be used for the design of future structures to be built at a given site. Furthermore, this information can also be used in assessing the safety of existing structures from a knowledge of their numbers of stories and the past acceleration level which they were designed to resist at the time of their construction.

It should be emphasized here that the above Ratio Method is not necessarily limited to the utilization of microtremors as a sole source for microzonation. Quite often, man generated signals using explosives or vibrations may prove to be an even more attractive signal source for microzonation.

4. Microzonation with Respect to Soil Liquefaction

Microzonation with respect to liquefaction can be carried out once the existence of liquefiable soil deposits in a region is established from preliminary soil investigations and if the geologists, seismologists, and engineers agree upon a typical earthquake acceleration time signature that may hit the area. In this paper, it is assumed that the design earthquake signature has already been agreed upon and is represented in Fig. 15.

By following the sequence of steps outlined in Fig. 16 the engineer should be able to evaluate whether or not liquefiable soil deposits exist in a region. Once the existence of liquefiable deposits is established, the next question to be asked is whether or not the soil will liquefy under the design earthquake signature shown in Fig. 15. The above question can be answered by following the procedure outlined below.

1. Determine the values of the in-situ natural and minimum void ratio e and e_{min} respectively and thereby obtain the value of the volume decrease potential $(e - e_{min})$. Then, either from Fig. 17 or from Eq. 9, obtain the value of α .

$$\alpha = 5.6(e - e_{min}) + 1 \quad (9)$$

2. Take 100 random grains of the soil and view them under a microscope and classify them according to the shape patterns shown in Fig. 18. Follow the procedure outlined in Table I and use Eq. 10 to determine the coefficient of sphericity ψ^* for the soil.

TABLE I

Sphericity Group, ψ_i	Number of Particles, N_i	$\psi_i \cdot N_i$
0.77	3	2.31
0.79	20	15.80
0.81	48	38.88
0.83	23	19.09
0.85	6	5.10
Total	100	81.18

From the data shown in Table I, the sphericity ψ is

$$\psi = \frac{\sum \psi_i \cdot N_i}{\sum N_i} = \frac{81.18}{100} = 0.812 \quad (10)$$

After having determined the values of volume-decrease potential $VDP = e - e_{min}$, the coefficient of uniformity $C_u = D_{60}/D_{10}$, the effective grain size D_{50} , and the sphericity ψ , obtain the value of C_1 from Eq. 11 (Ref. 6):

*It is recommended that at least three trials be made and the average of the three ψ 's be taken as representative.

$$C_1 = K\psi^{5.4} (e - e_{\min})^{2.25} \left(\frac{10.66}{C_u - 2.07C_u + 1.1} + 74 \right) \quad (11)$$

where K is a function of effective grain size and can be obtained from Fig. 19 for any value of D_{50} . Alternatively, the value of C_1 can be more easily determined from the nomograph proposed by the author (Ref. 6) which is shown in Fig. 20. It is interesting to note from Eq. 11 that the value of C_1 , and hence the liquefaction potential of the soil increases with increasing sphericity ψ and volume-decrease potential VDP and with decreasing uniformity coefficient C_u . This would mean that uniformity graded, loose round-particled fine sands are most susceptible to liquefaction.

3. From Fig. 15, identify the number of stress cycles, (considering each two zero crossings as one cycle) and show the values of the positive and negative shear stresses in each cycle, as shown in Fig. 21.

4. After having ascertained all the above information, follow the procedure outlined in Table II to determine whether the given soil will liquefy during the earthquake signal shown in Fig. 15.

The theoretical and experimental basis for the above procedure is contained in Refs. 6, 7, 8, 9 and 10. Reference 6 is appended to this paper to acquaint the reader with the basic principles involved in the above liquefaction assessment procedure.

REFERENCES

1. Sherif, M. A. and Bostrom, R.C., "A Microseismic Zoning Technique Employing a Base Station," Proceedings of the International Congress of the International Association of Engineering Geology, Paris, France, September, 1970.
2. Manfrida, J. Soil Amplification Studies Using Explosive Impulse. Master of Science Thesis in Civil Engineering, University of Washington, Seattle, Washington, 1977.
3. Sherif, M. A., "Microzonation of Thessaloniki, Using the Sherif-Bostrom (USA) Method," A Report to UNDP/UNESCO, Seismicity of the Balkan Region Project, August, 1973.
4. Sherif, M. A., Ishibashi, I. and Kearnes, J. K., "Microzonation by Amplification Ratio Technique," University of Washington Soil Engineering Research Report No. 13, May 1976.
5. Mattiesen, R. B. and Rojahn, C., Techniques for Seismic Zoning Structural Considerations. Proceedings of the International Conference on Microzonation for Safer Construction Research and Application, Seattle, 1972.
6. Sherif, M. A. and Ishibashi, I., "Soil Liquefaction during Earthquakes--University of Washington Research", University of Washington Soil Engineering Research Report No. 19, January 1980.
7. Sherif, M. A., Ishibashi, I., and Cheng, W. L., "Soil Liquefaction during Earthquakes--A New Theory," University of Washington Soil Engineering Research Report No. 20, October 1980.
8. Sherif, M. A. and Ishibashi, I., "A Rational Theory for Predicting Soil Liquefaction" Journal of Earthquake Engineering and Soil Dynamics, 1981 (in press).
9. Sherif, M. A., Ishibashi, I., and Tsuchiya, C., "Pore-Pressure Rise Mechanism and Soil Liquefaction," Soils and Foundations, Japanese Society of Soil Mechanics and Foundation Engineering, Vol. 17, No. 2, June 1977.
10. Sherif, M. A., Ishibashi, I., and Tsuchiya, C., "Pore-Pressure Prediction during Earthquake Loadings," Soils and Foundations, Japanese Society of Soil Mechanics and Foundation Engineering, Vol. 18, No. 4, December 1978.

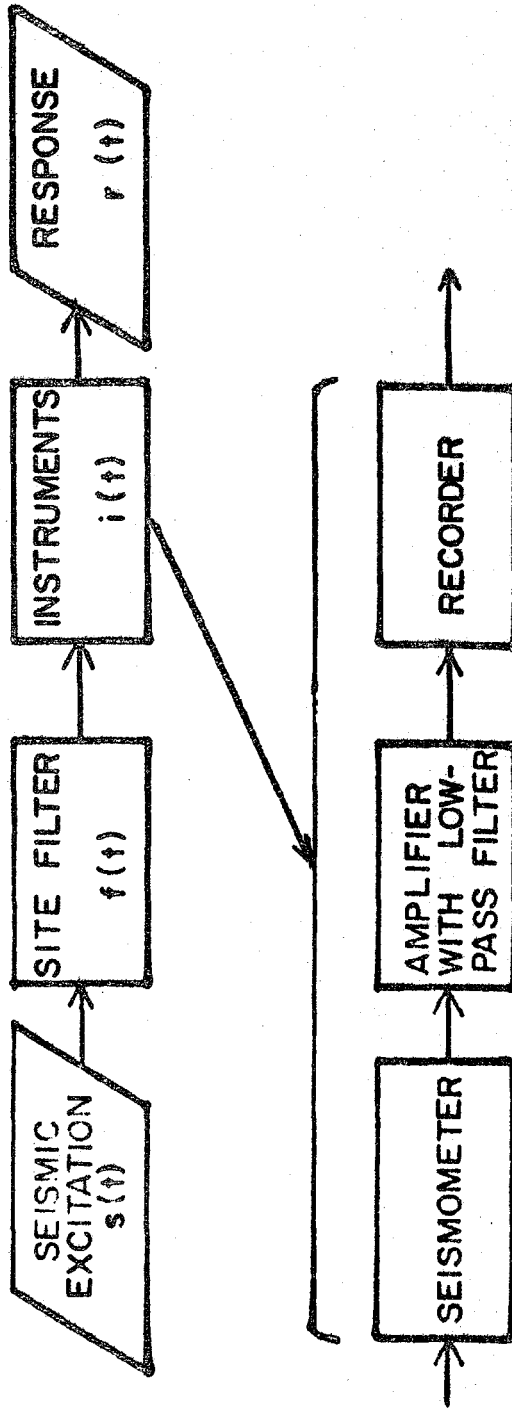


FIG. 1 SEISMIC INDUCED GROUND RESPONSE AND INSTRUMENTATION SCHEME

Reproduced from
best available copy.

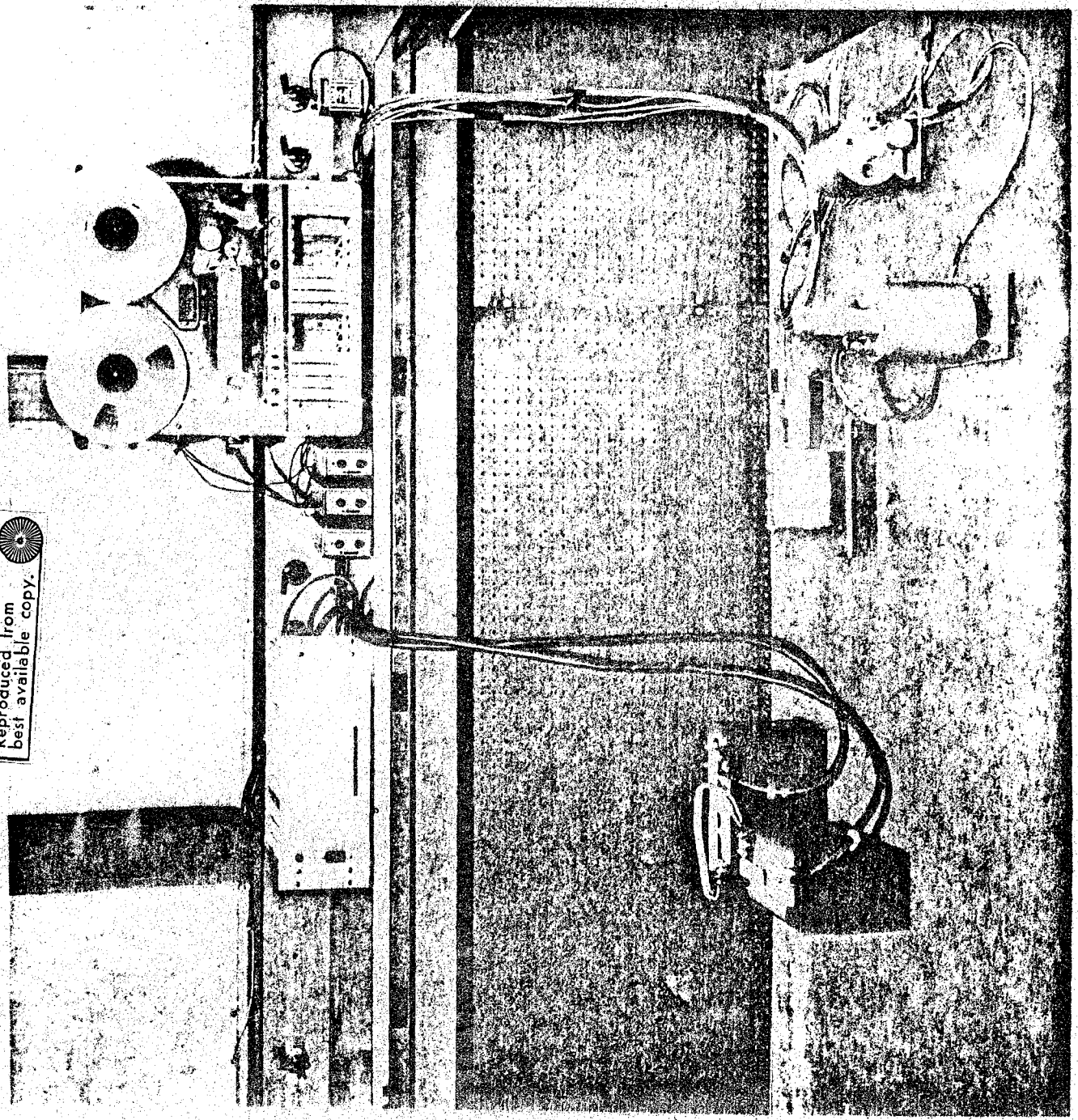


Fig. 2 Stationary Station Microzonation Data Monitoring System

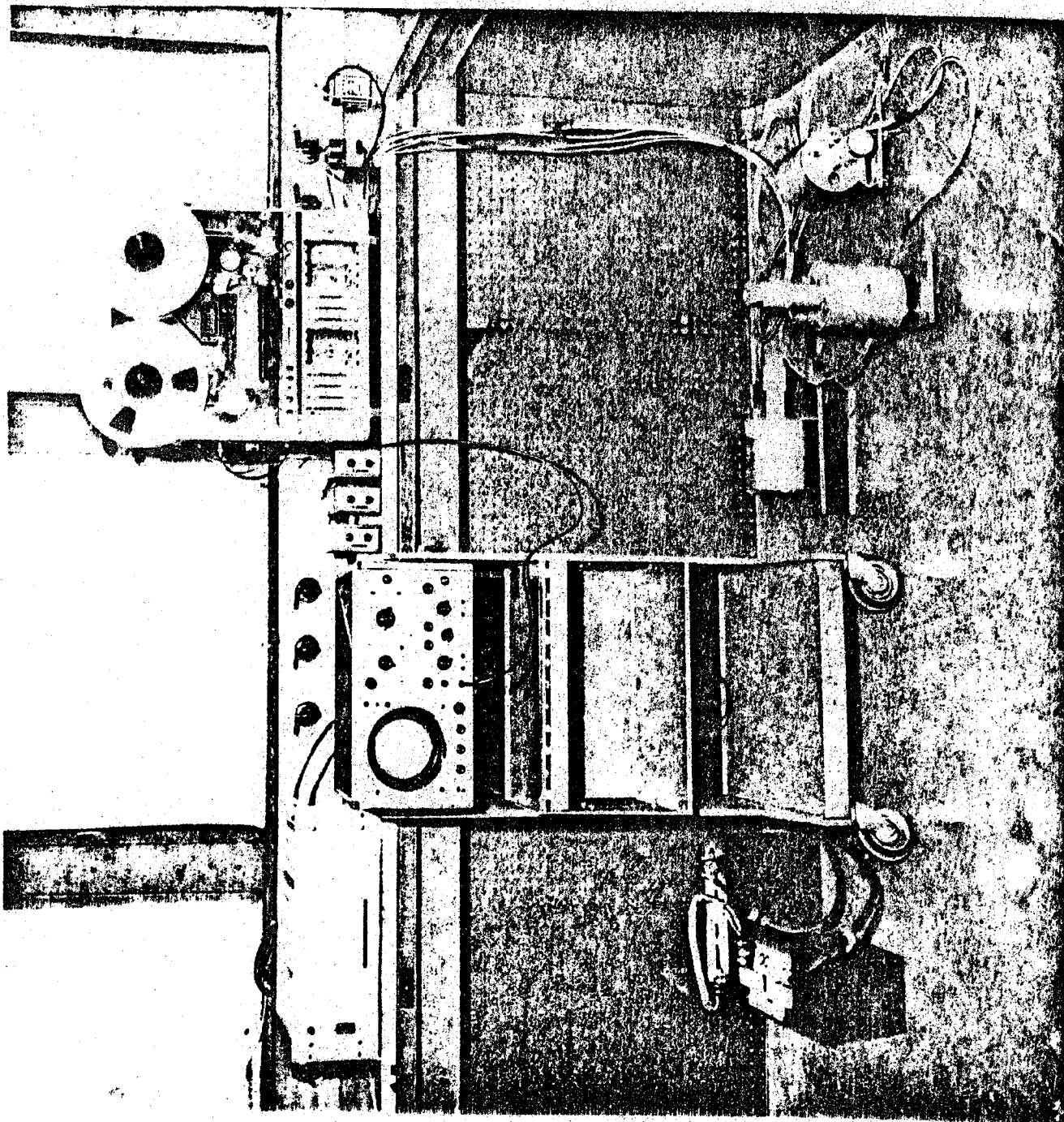


Fig. 3 Portable Station Microzonation Data Monitoring System

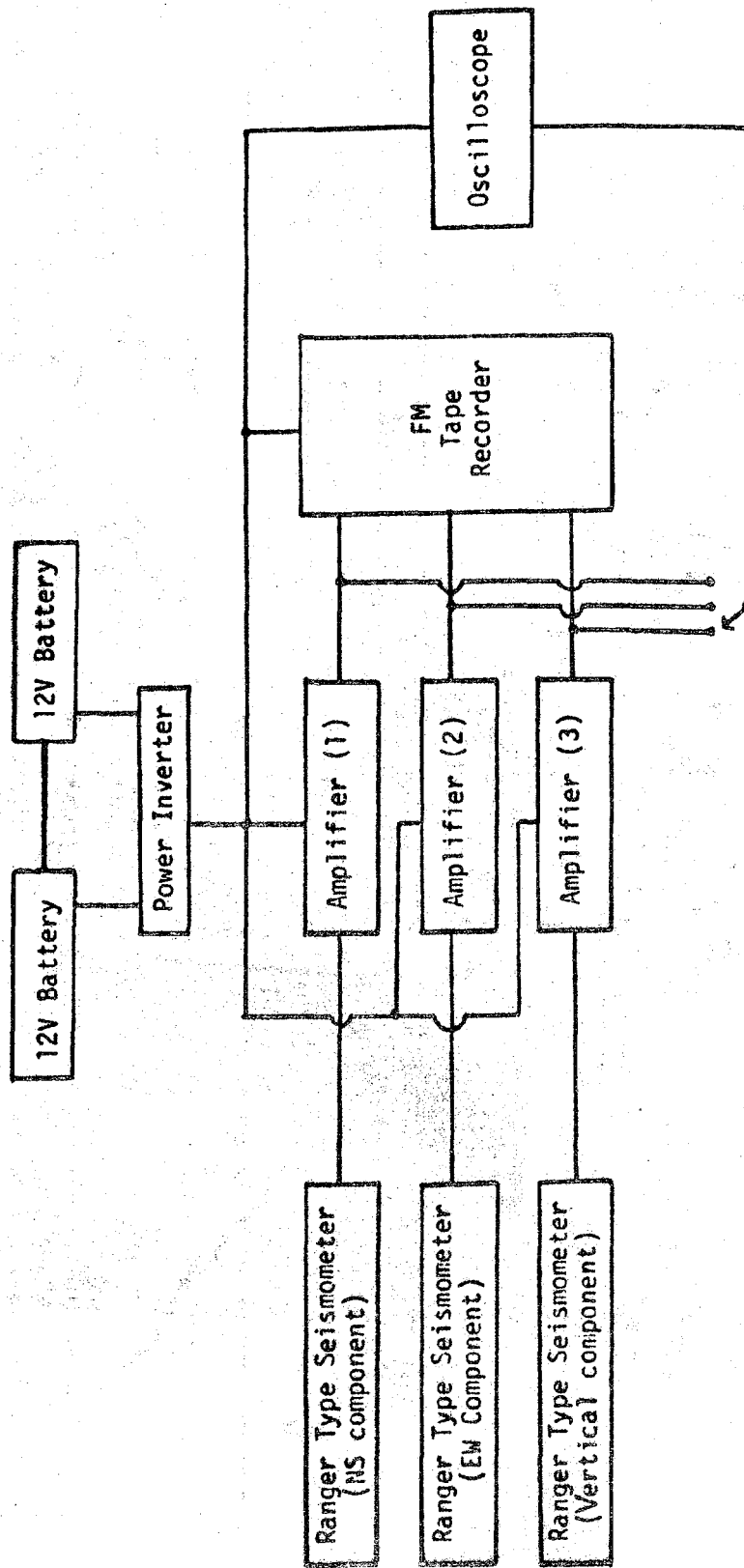


FIG. 4 A BLOCK DIAGRAM FOR EQUIPMENT USED AS PORTABLE STATION (SAME FOR BASE STATION EXCEPT OSCILLOSCOPE)

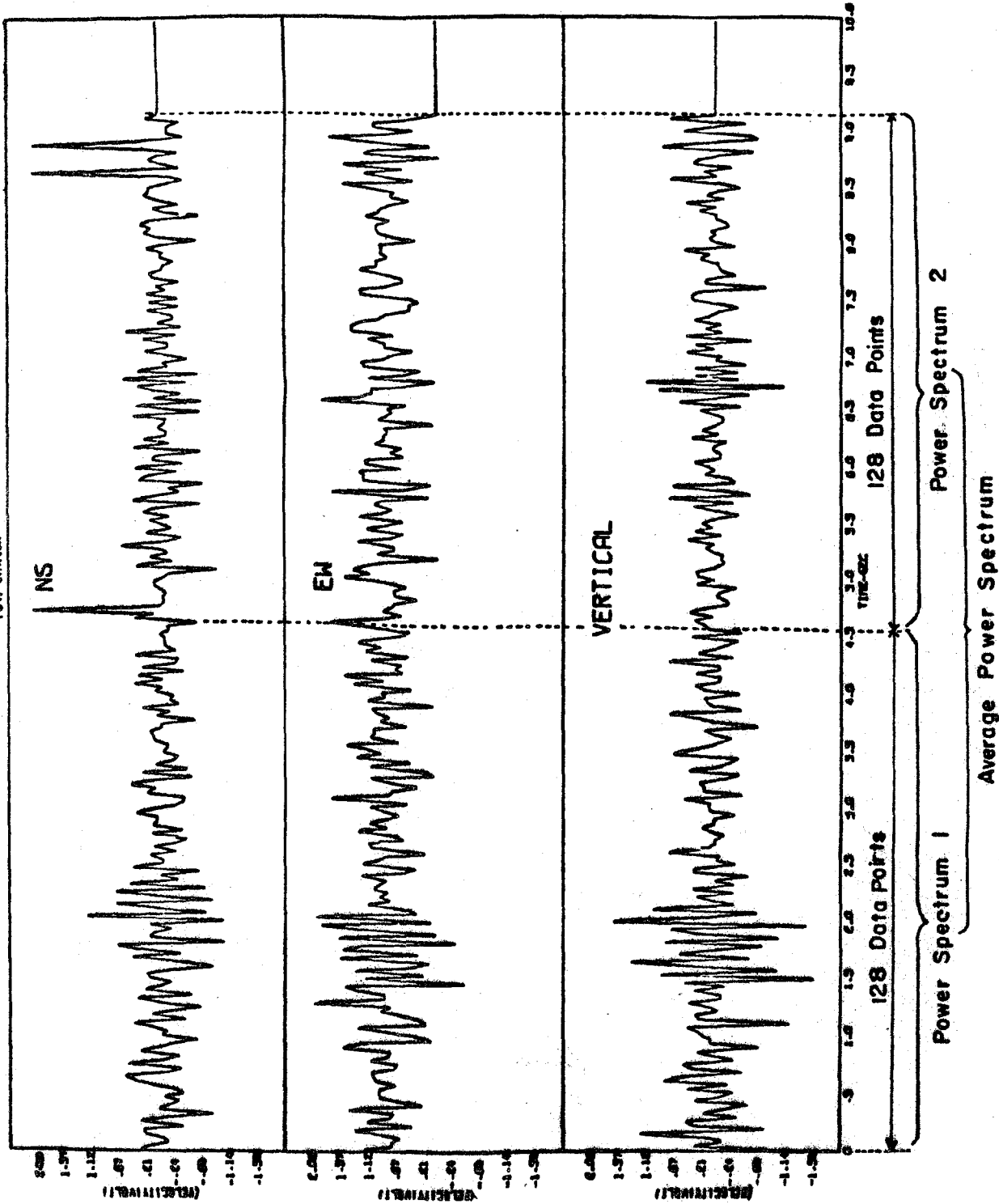


FIG 5 ILLUSTRATION OF POWER SPECTRA AVERAGING PROCESS

NO 2005 /ORTB 4/ 2/ 73 TIME 14:40 65.80. 3

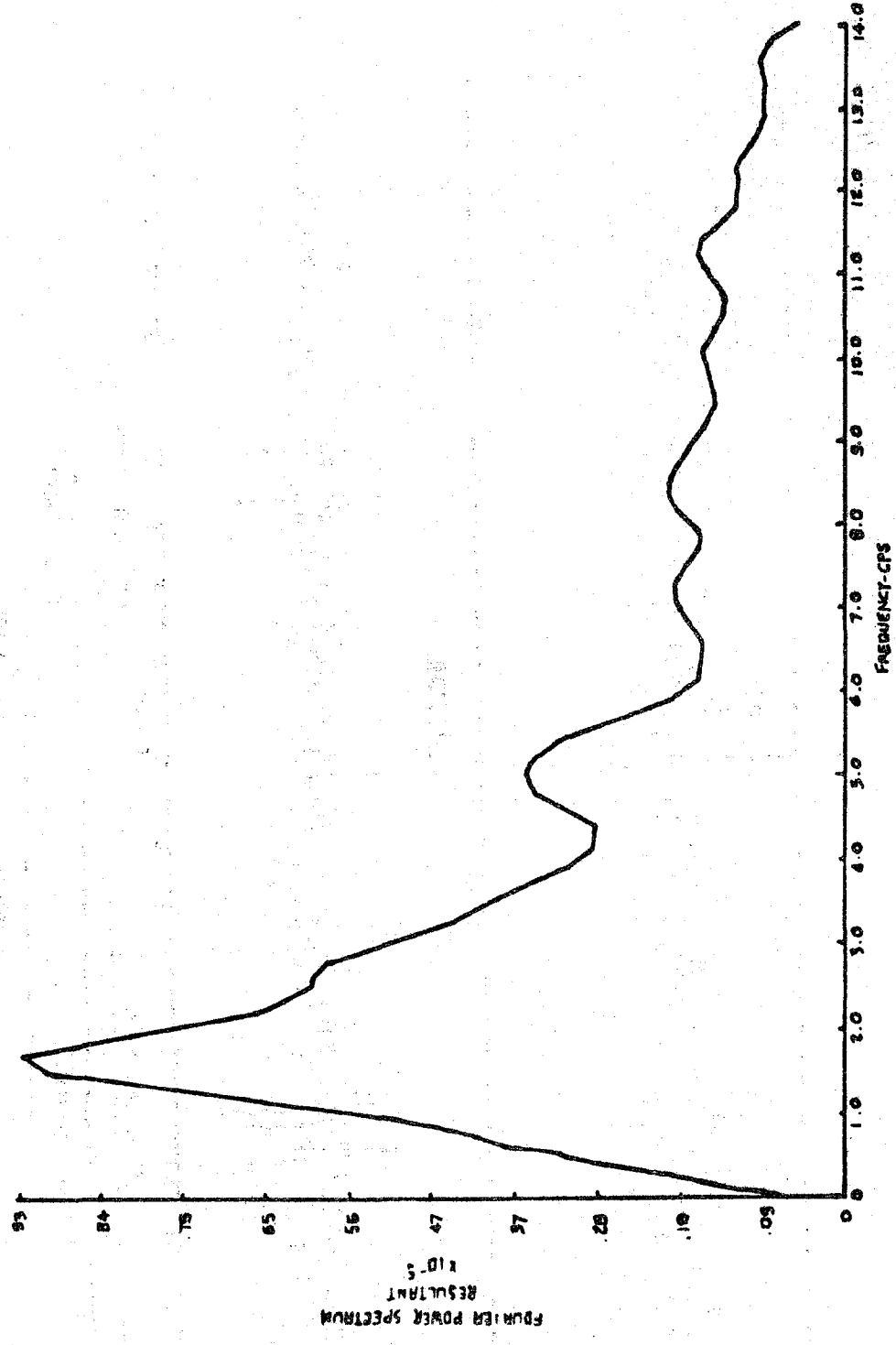


FIG 6 PORTABLE STATION AVERAGE RESULTANT POWER SPECTRUM

○ - MAJOR PREDOMINANT FREQUENCY
 ○ - MINOR PREDOMINANT FREQUENCY

DOMAIN PREDOMINANT FREQUENCY IN HZ
 D₁ 0.5 < f < 2.5
 D₂ 2.5 < f < 5.5
 D₃ 5.5 < f < 8.0

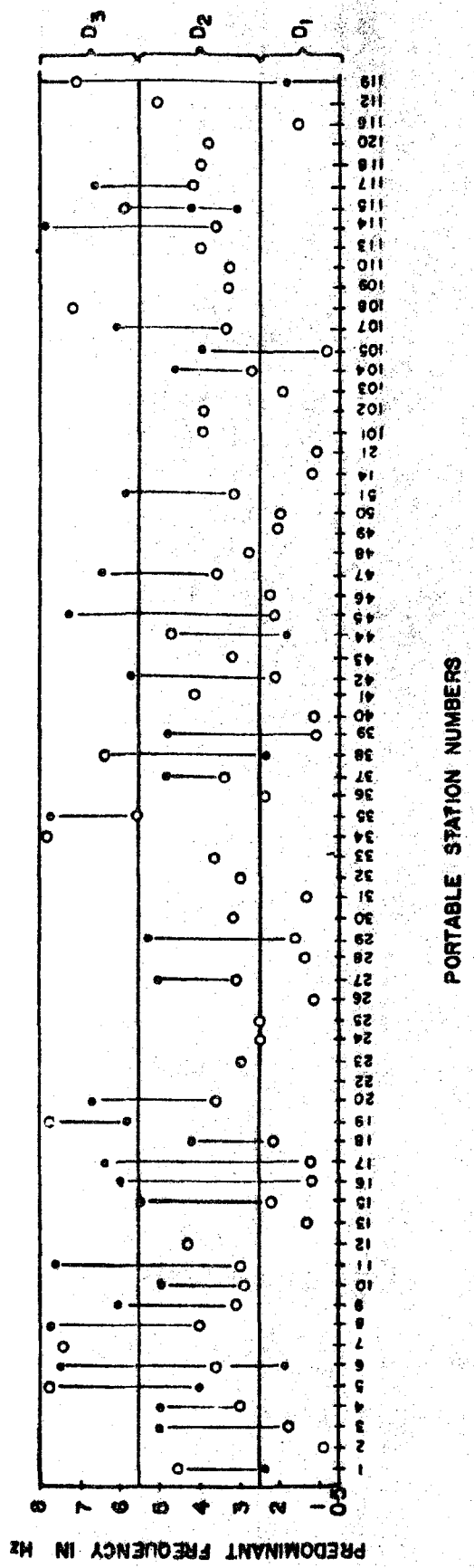


FIG 7 PREDOMINANT FREQUENCY DISTRIBUTION AS A FUNCTION OF PORTABLE STATION LOCATION

Reproduced from
best available copy.

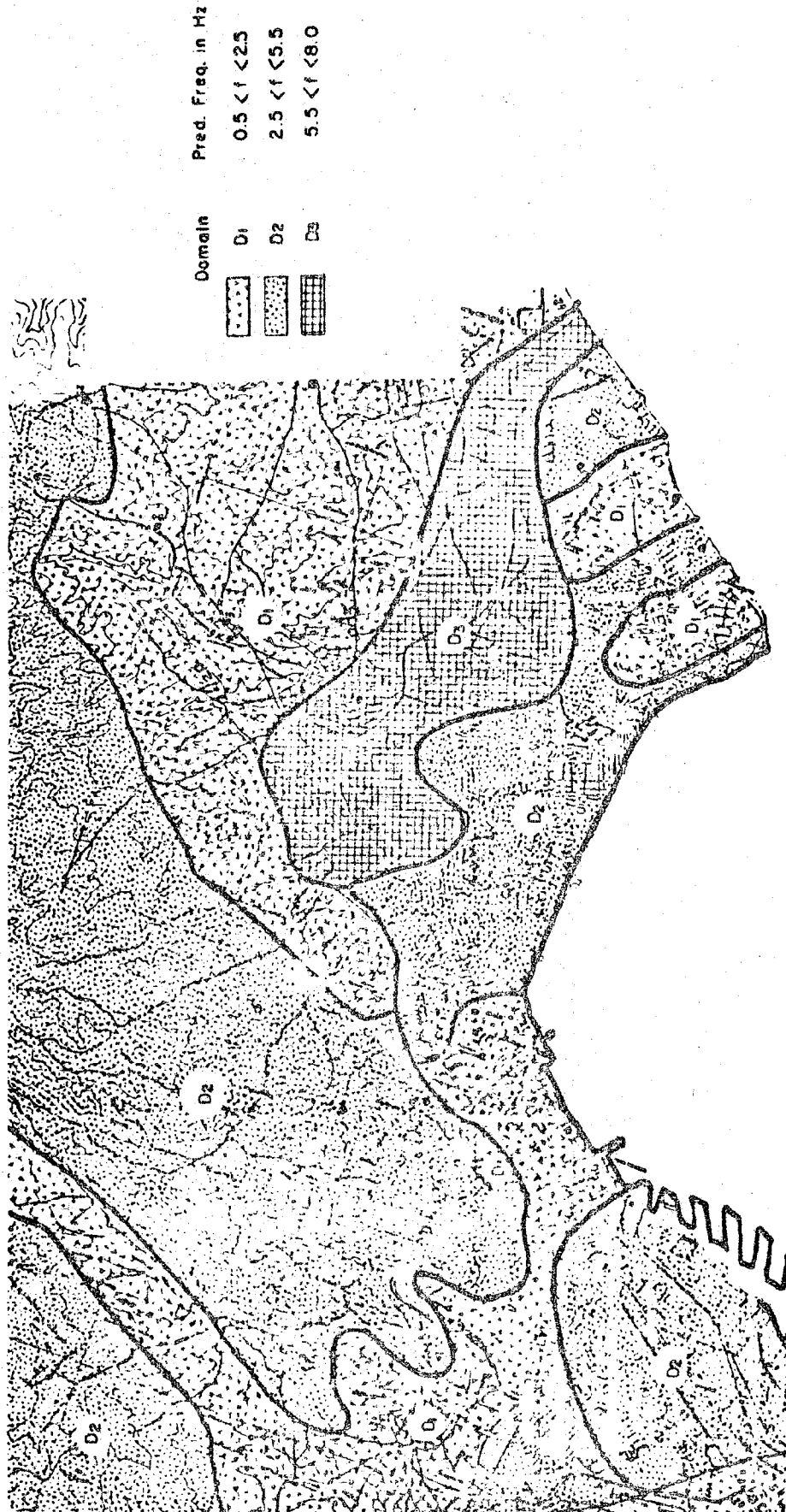
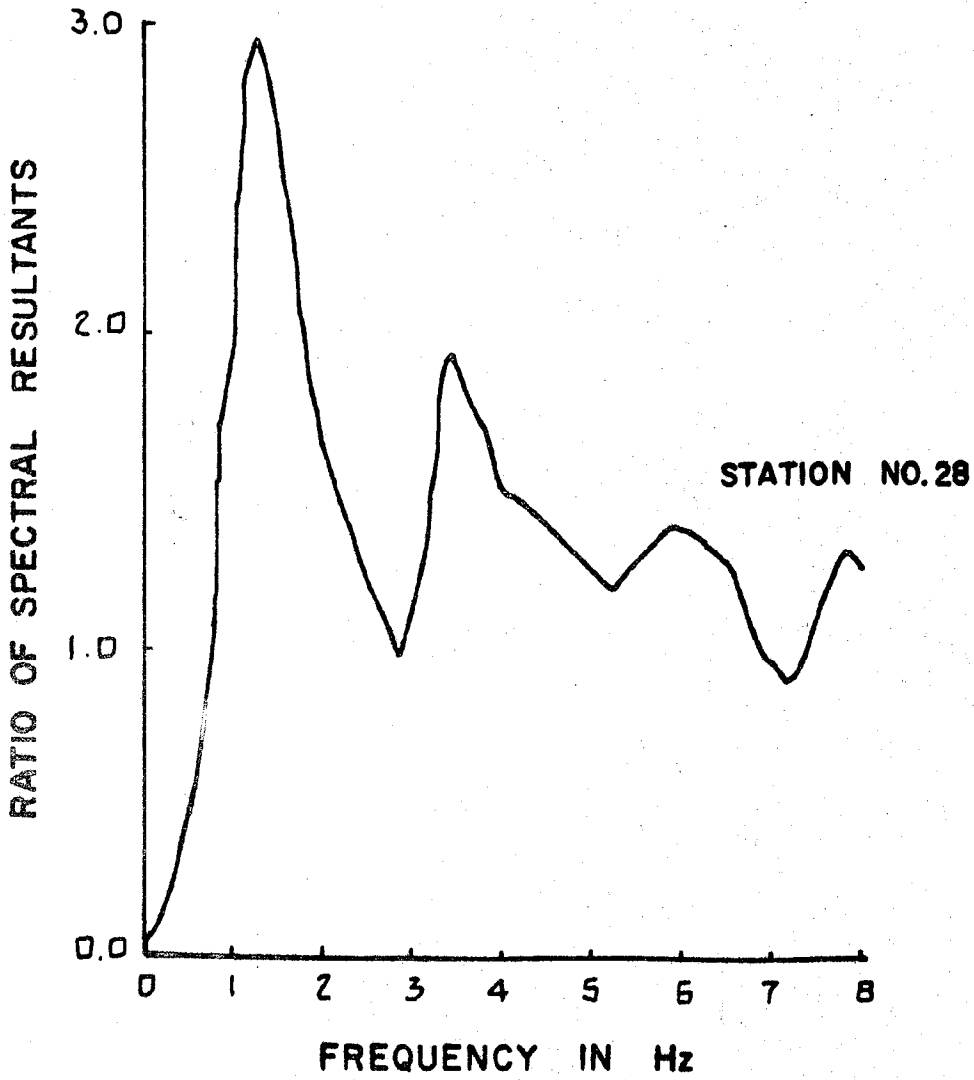


FIG 8 A MAP SHOWING THE DISTRIBUTION OF PREDOMINANT FREQUENCIES



**FIG 9 ONE OF THE TYPICAL
POWER SPECTRAL RATIO
CURVE FOR ZONE 1₂**

Reproduced from
best available copy.

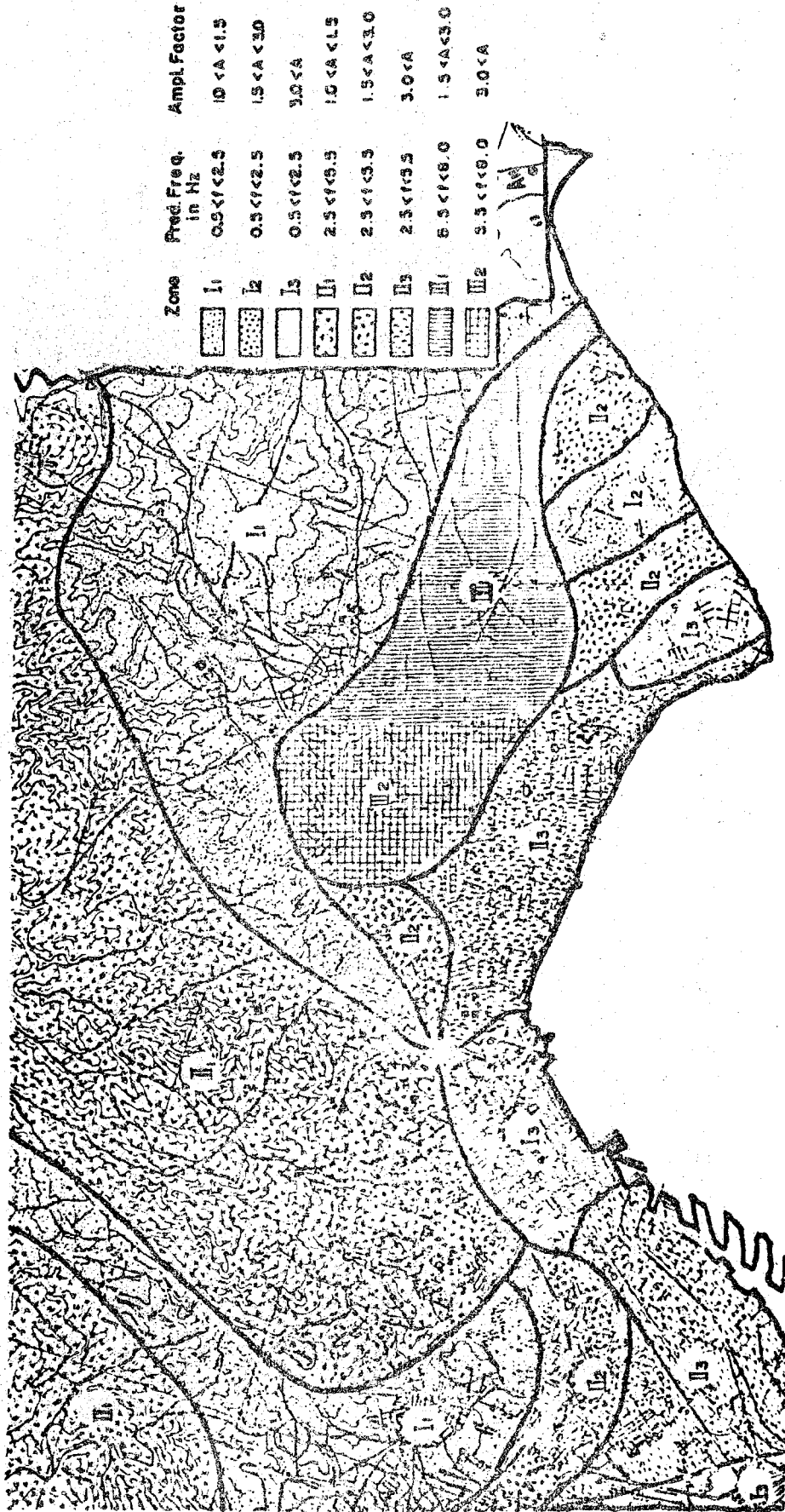


FIG 10 A MAP SHOWING SITE AMPLIFICATION FACTORS

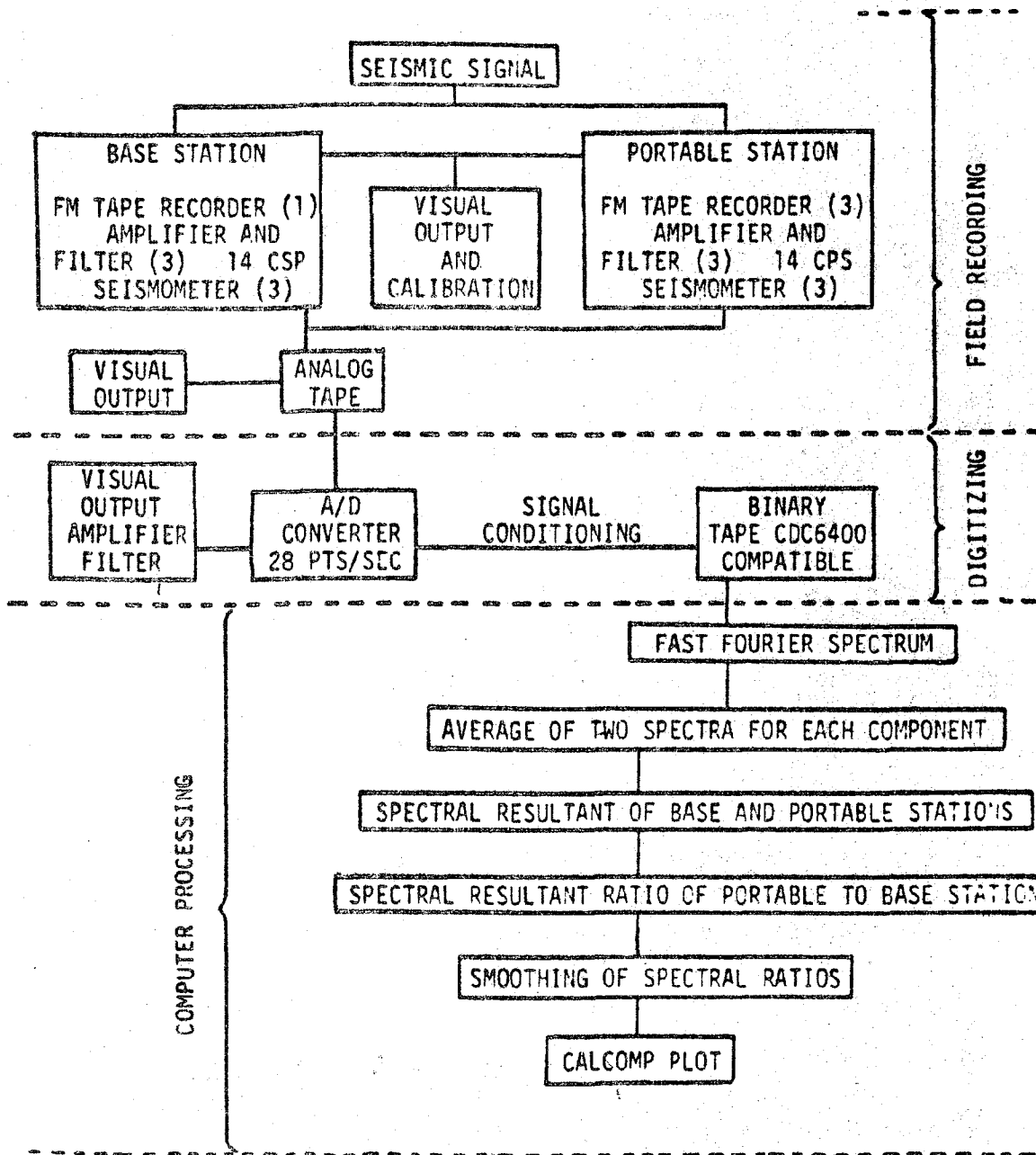


FIG. II SUMMARY OF DATA ACQUISITION & PROCESSING SEQUENCE

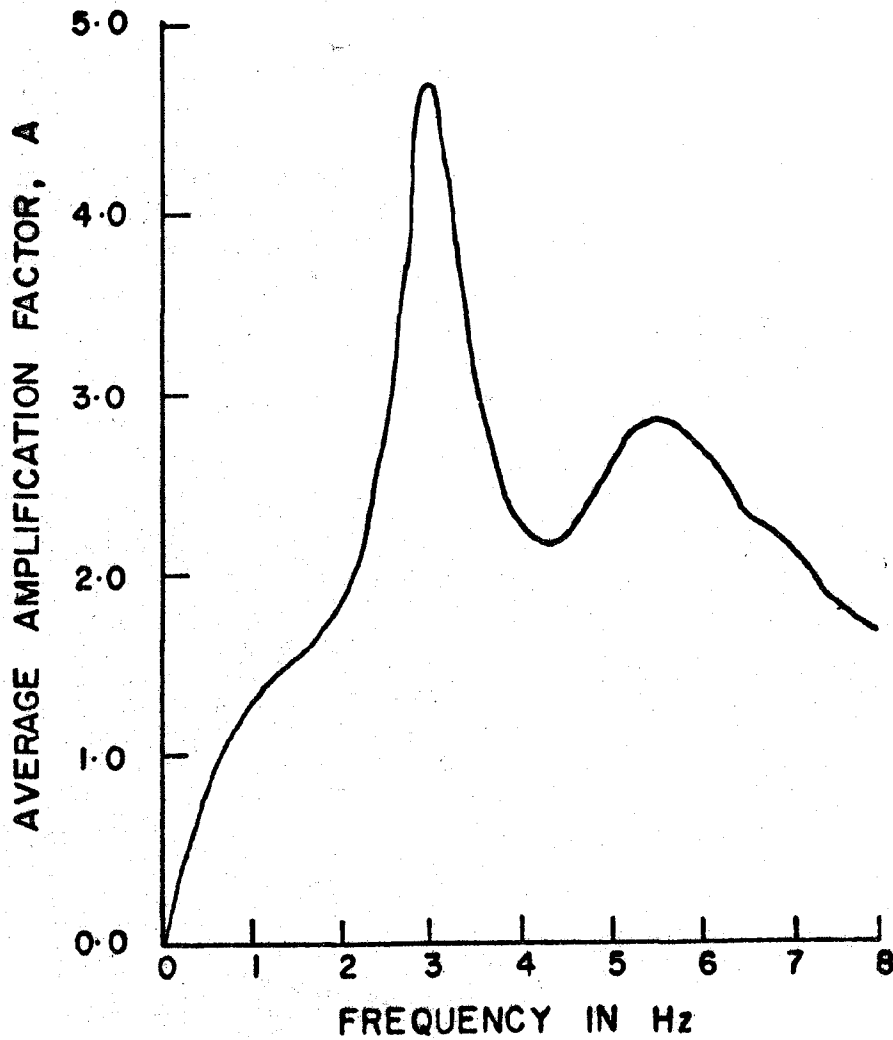
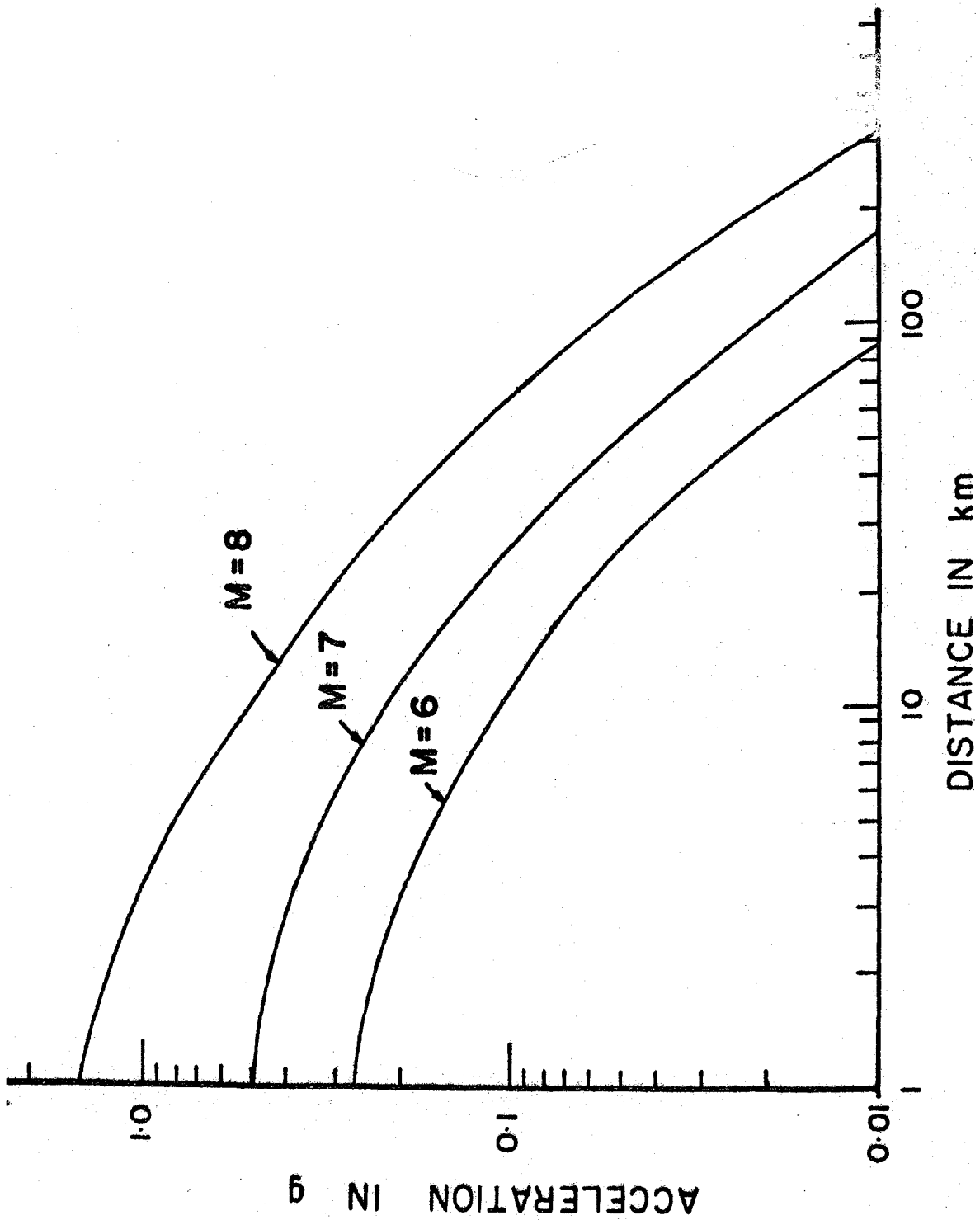


FIG.12 AVERAGE RESULTANT
AMPLIFICATION CURVE
FOR ZONE II₃



SEISMIC SIGNAL ATTENUATION CURVES
 FIG 13

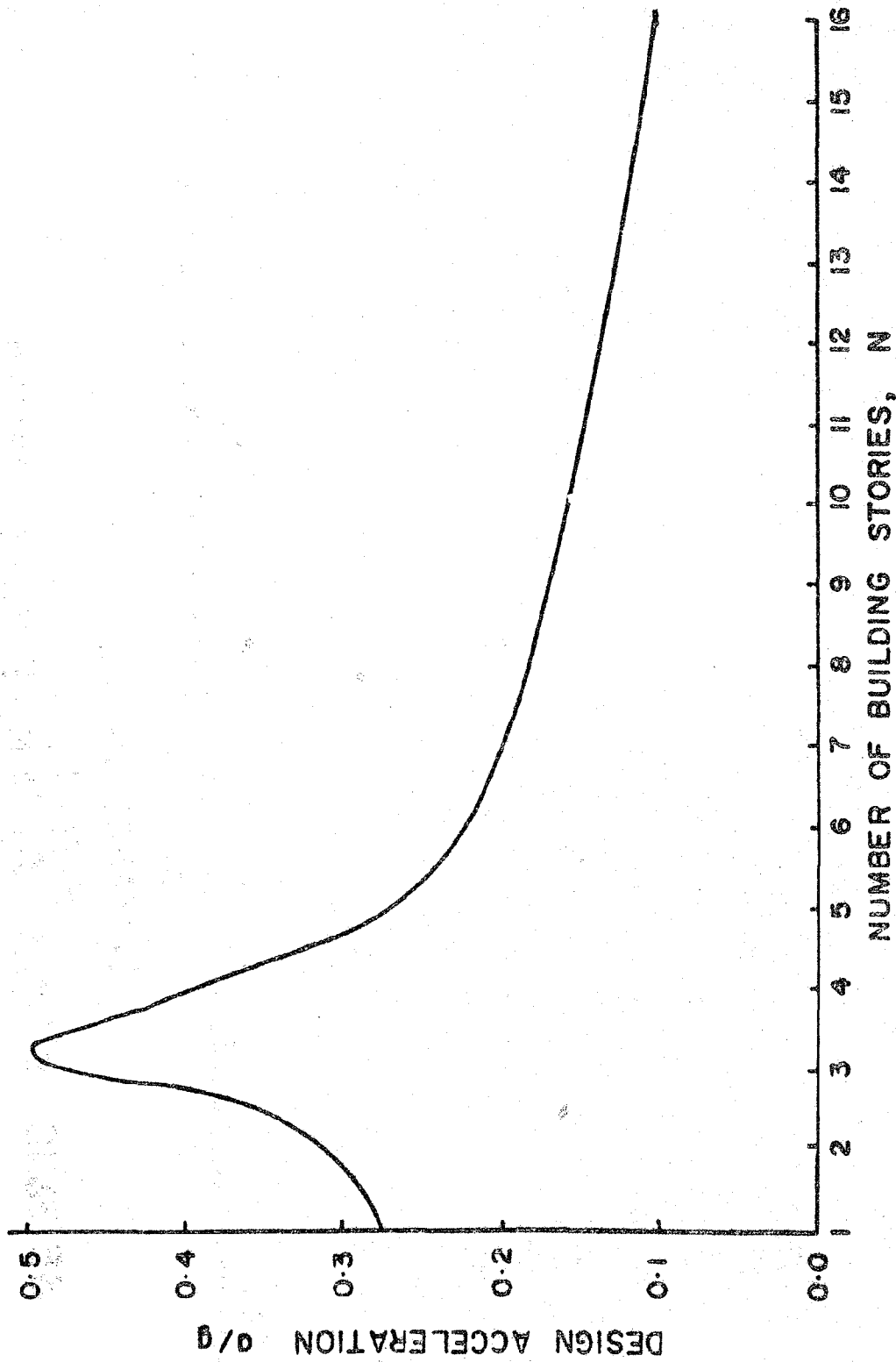


FIG 14 THE AVERAGE RELATIONSHIP BETWEEN THE NUMBER OF BUILDING STORIES N AND DESIGN ACCELERATION FOR ZONE II3

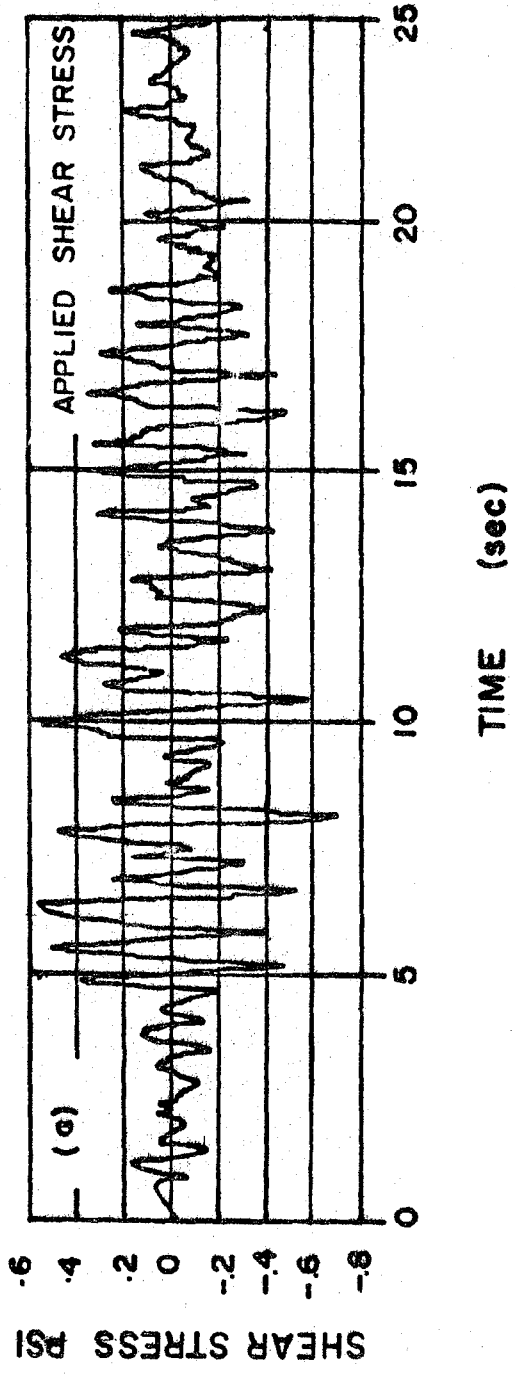


FIG 15 DESIGN EARTHQUAKE

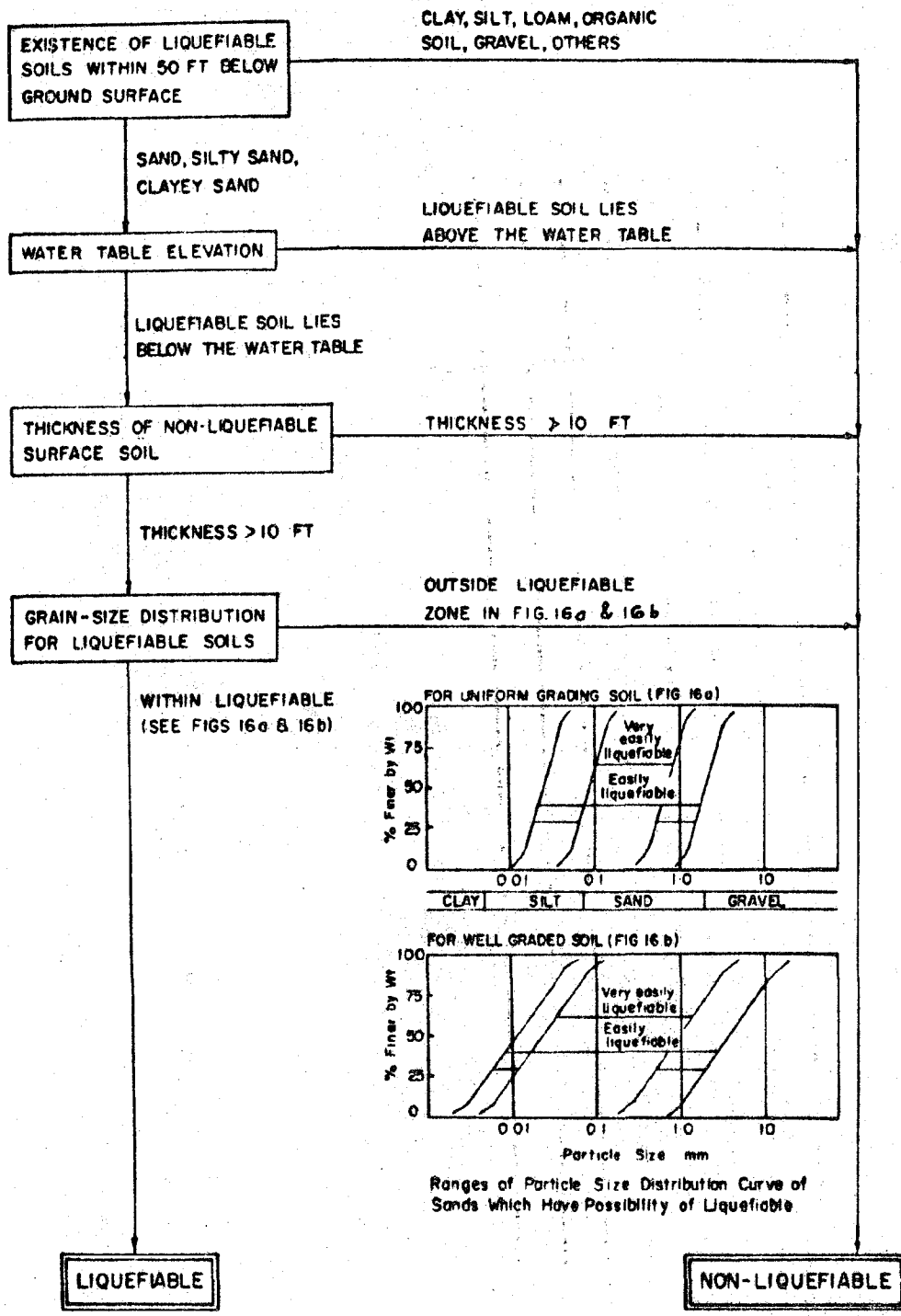


FIG 16 PRELIMINARY EVALUATION OF SOIL-LIQUEFACTION POTENTIAL

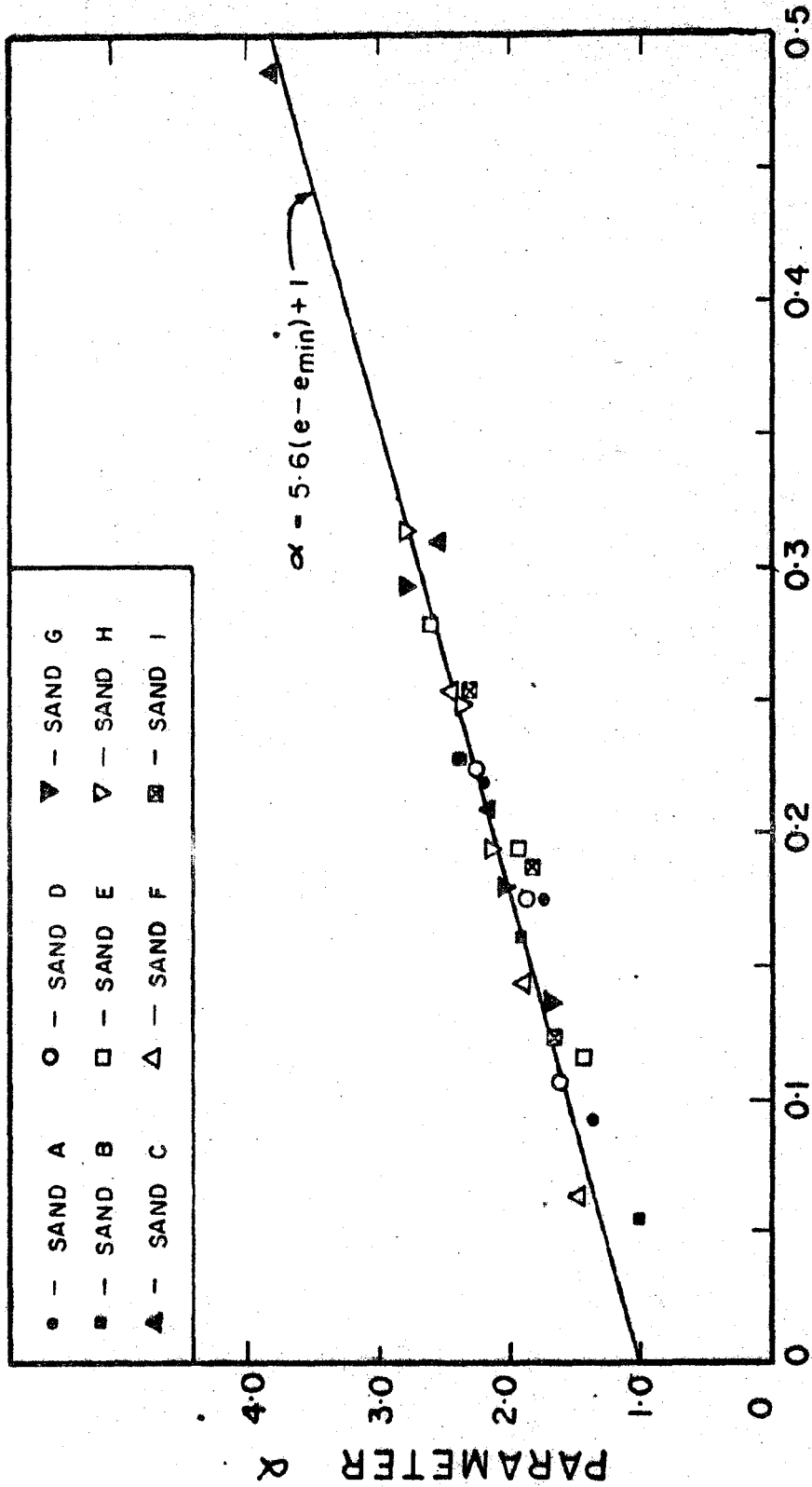


FIG.17
 VOLUME DECREASE POTENTIAL (e - e_{min})
 PARAMETER α VERSUS VOLUME
 DECREASE POTENTIAL

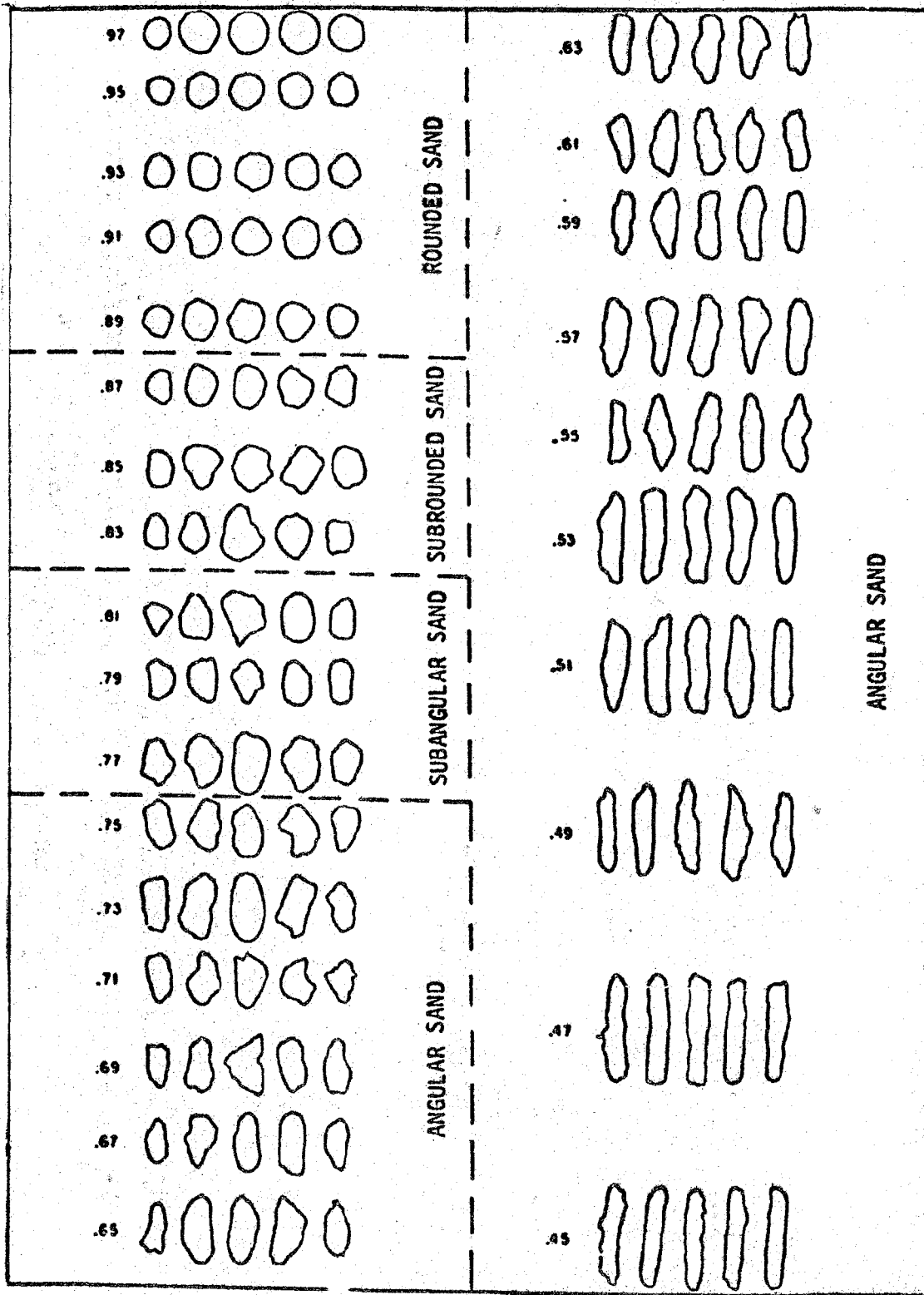


FIG.18 CHART FOR DETERMINATION OF SPHERICITY BY VISUAL METHOD

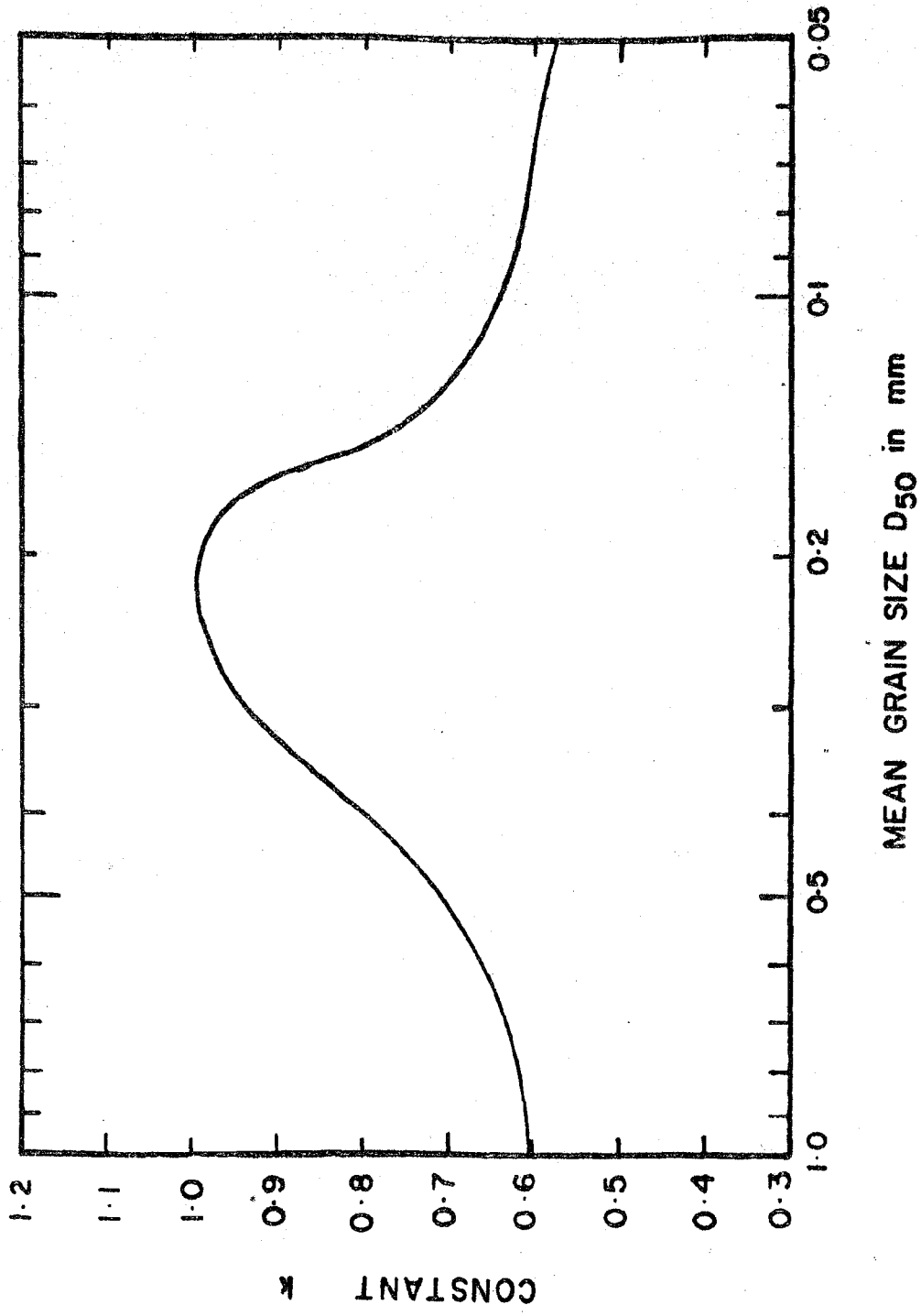
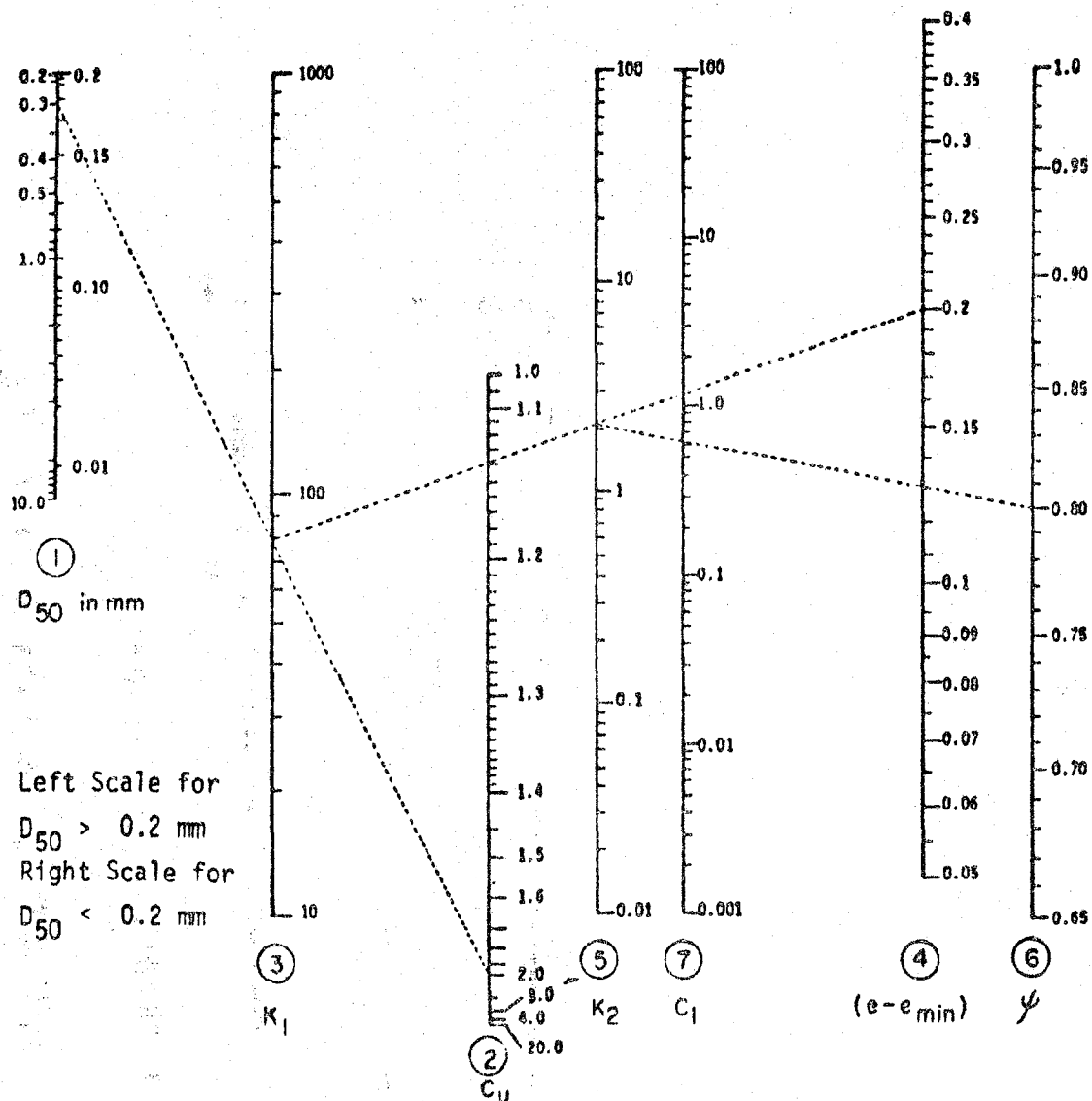


FIG.19 CONSTANT k VERSUS MEAN GRAIN SIZE D_{50}



NOMOGRAPH CHART FOR PARAMETER C_1

Nomenclature

- D_{50} - soil diameter at which 50% of soil weight is finer
- C_u - coefficient of uniformity D_{60}/D_{10}
- $(e - e_{min})$ - volume decrease potential
- ψ - degree of sphericity

Example

Given: $D_{50} = 0.3 \text{ mm}$, $(e - e_{min}) = 0.2$
 $C_u = 2.0$, $\psi = 0.8$

Find: Parameter C_1

- Step 1: Connect $D_{50} = 0.3 \text{ mm}$ on ① & $C_u = 2.0$ on ②, obtain the value $K_1 = 78$ from ③
- Step 2: Connect K_1 on ③ & $(e - e_{min}) = 0.2$ on ④, obtain the value $K_2 = 2.1$ from ⑤
- Step 3: Connect K_2 on ⑤ & $\psi = 0.8$ on ⑥, obtain parameter $C_1 = 0.63$

FIG 20 NOMOGRAPH CHART FOR DETERMINING PARAMETER, C_1

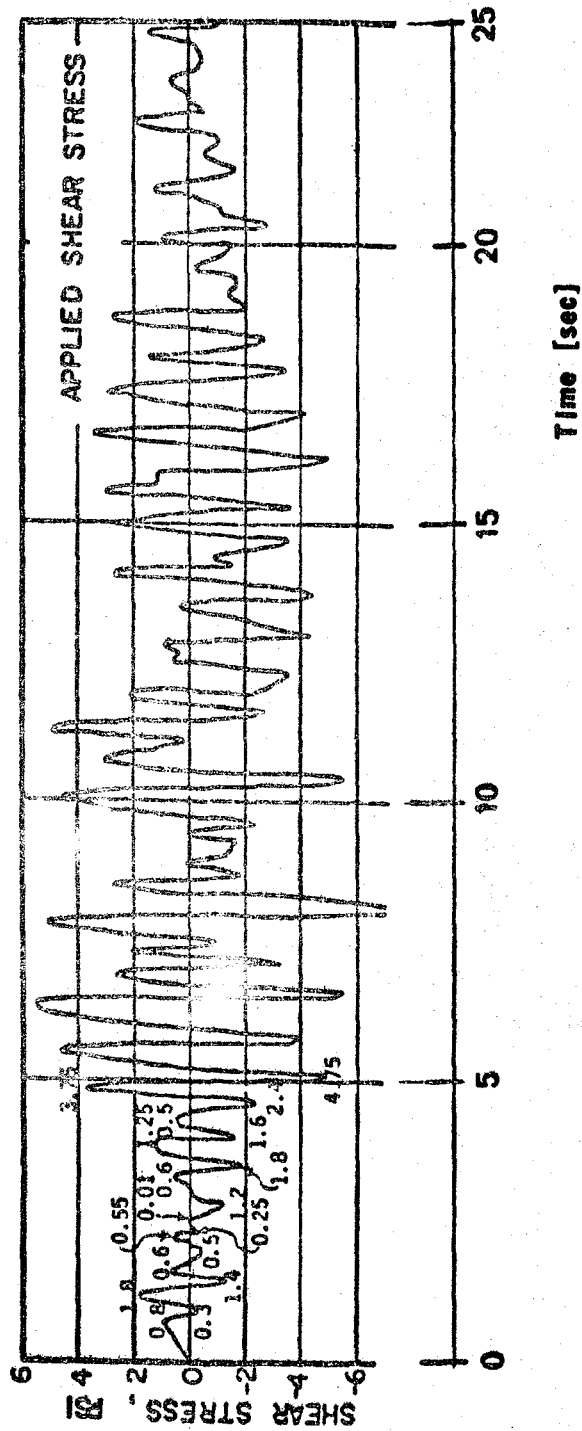


FIG. 2I STRESS CYCLES AND POSITIVE & NEGATIVE SHEAR STRESS VALUES

TABLE II



CYCLE NUMBER, N	SHEAR STRESS τ_N , PSI	$(N_{eq})^{\alpha} = \sum \left[\frac{\tau_i}{\tau_N} \right]^{\alpha}$	ΔU_{Np}^* or $\Delta U_{Nn}^* = \frac{N_{eq} C}{(1-U_{N-1}^*)} \frac{1}{N_{eq}^2 - 0.5} \left[\frac{\tau_N}{\sigma_{N-1}} \right]^{\alpha}$	$\Delta U_N^* = (\Delta U_{Np}^* + \Delta U_{Nn}^*)$	$U_N^* = U_{N-1}^* + \Delta U_N^*$	$\bar{\sigma}_N = \bar{\sigma}_0 (1-U_N^*)$ PSI
1	Positive	$\left(\frac{0.8}{0.8}\right)^{2.1} = 1.0$	$(1-0) \frac{1.2}{1.2-0.5} \left(\frac{0.8}{5.31}\right)^{2.1} = .0751$	$\frac{1}{2}(0.0751+0.0096) = 0.0423$	0 +0.0423	5.31(1-0.0423) = 5.0852
	Negative	$\left(\frac{0.3}{0.3}\right)^{2.1} = 1.0$	$(1-0) \frac{1.2}{1.2-0.5} \left(\frac{0.3}{5.31}\right)^{2.1} = .0096$	$\frac{1}{2}(0.0751+0.0096) = 0.0423$	0 +0.0423	5.31(1-0.0423) = 5.0852
2	Positive	$\left(\frac{0.8}{1.8}\right)^{2.1} + \left(\frac{1.8}{1.8}\right)^{2.1} = 1.975$	$(1-0.0423) \frac{1.1075 \times 2}{1.1975-0.5} \left(\frac{1.8}{5.0852}\right)^{2.1} = .2773$	$\frac{1}{2}(0.2773+0.2247) = 0.2510$	0.0423+0.2510 = 0.2933	5.31(1-0.2933) = 3.7525
	Negative	$\left(\frac{0.3}{1.4}\right)^{2.1} + \left(\frac{1.4}{1.4}\right)^{2.1} = 1.0457$	$(1-0.0423) \frac{1.0457 \times 2}{1.0457-0.5} \left(\frac{1.4}{5.0852}\right)^{2.1} = .2247$	$\frac{1}{2}(0.2773+0.2247) = 0.2510$	0.0423+0.2510 = 0.2933	5.31(1-0.2933) = 3.7525
3	Positive	$\left(\frac{0.6}{0.6}\right)^{2.1} + \left(\frac{1.6}{0.6}\right)^{2.1} + \left(\frac{0.6}{0.6}\right)^{2.1} = 11.778$	$(1-0.2933) \frac{11.778 \times 2}{11.778-0.5} \left(\frac{0.6}{3.7525}\right)^{2.1} = .0026$	$\frac{1}{2}(0.0026+0.0018) = 0.0022$	0.2933+0.0022 = 0.2955	5.31(1-0.2955) = 3.7409
	Negative	$\left(\frac{0.3}{0.5}\right)^{2.1} + \left(\frac{1.4}{0.5}\right)^{2.1} + \left(\frac{0.5}{0.5}\right)^{2.1} = 11.400$	$(1-0.2933) \frac{11.400 \times 2}{11.400-0.5} \left(\frac{0.5}{3.7525}\right)^{2.1} = .0018$	$\frac{1}{2}(0.0026+0.0018) = 0.0022$	0.2933+0.0022 = 0.2955	5.31(1-0.2955) = 3.7409
4	Positive	15.017	0.0017	0.0009	0.2964	3.7361
4 ^b	Negative	36.660	0.0001	0.0009	0.2964	3.7361
5	Positive	45426.000	0.0000	0.0264	0.3228	3.5958
	Negative	2.641	0.0529	0.0264	0.3228	3.5958
6	Positive	13.618	0.0023	0.0826	0.4054	3.1573
	Negative	2.174	0.1629	0.0826	0.4054	3.1573
7	Positive	4.138	0.0423	0.0606	0.4660	2.8355
	Negative	3.751	0.0789	0.0606	0.4660	2.8355
8	Positive	26.860	0.0009	0.1522	0.6128	2.0274
	Negative	2.667	0.3035	0.1522	0.6128	2.0274
9	Positive	1.4775	2.4390	2.8688	3.4870	-13.21
	Negative	1.681	3.2987	2.8688	3.4870	0

Notes: (a) All calculations are conducted for $\sigma_0 = 5.31$ psi, $\alpha = 2.1$, $C_1 = 2.0$

(b) Calculated by the same procedures as shown immediately above

APPENDIX-A

UNIVERSITY OF WASHINGTON
COLLEGE OF ENGINEERING

SOIL ENGINEERING RESEARCH REPORT NO. 19

SOIL LIQUEFACTION DURING EARTHQUAKES--
UNIVERSITY OF WASHINGTON RESEARCH

BY

MEHMET A. SHERIF
ISAO ISHIBASHI

JANUARY, 1980

DEPARTMENT OF CIVIL ENGINEERING
UNIVERSITY OF WASHINGTON
SEATTLE, WASHINGTON 98195

2-33

TABLE OF CONTENTS

	<u>Page</u>
ABSTRACT	11
Definitions and General Considerations	1
Pore-Pressure Rise under Non-Uniform Loading	4
Pore-Pressure Rise under Earthquake-Type Loading	5
Figures	10

ABSTRACT

In this report the authors advance a new theory on soil liquefaction during earthquakes. This theory utilizes the actual earthquake stress-time history and certain soil parameters, C_1 , C_2 , C_3 , and α , to predict the pore-pressure buildup as a function of time. The values of C_1 and α are shown to be functions of volume-decrease potential ($e - e_{min}$), while C_2 and C_3 appear to be constant for all soils and are almost equal to 2.0 and 0.5 respectively. The soil is said to have reached the state of liquefaction during an earthquake loading when the value of the normalized pore pressure (pore pressure divided by confining pressure) reaches unity (one). The pore-pressure values predicted by the theory agree very well with the experimental results.

SOIL LIQUEFACTION DURING EARTHQUAKES--

UNIVERSITY OF WASHINGTON RESEARCH

Definitions and General Considerations

Soil is said to have liquefied when it temporarily loses all of its supportive capacity. This happens when the value of the pore pressure in the soil during an earthquake reaches a value which is almost equal to the pre-earthquake effective confining soil pressures σ'_c around the soil sample.

To assist the reader in better understanding the process involved in the development of some of the new theories and concepts expressed in the following paragraphs it is necessary that the new loading terminologies expressed in this report be explicitly defined. Uniform loading, for example, is one in which the maximum positive and negative shear stresses (τ_p and τ_n) are equal at all times. Non-uniform loading is one where the maximum positive and negative shear stresses are not equal at all times, except within the same cycle. On the other hand, earthquake loading corresponds to random loading, where no restrictions are imposed.

Figs. 1(a, b, and c) show graphic representations of uniform, non-uniform, and earthquake loading respectively.

The basic aim of this report is the development of a quantitative analytical procedure for the prediction of the amount of pore-pressure rise in a saturated soil during an earthquake as a function of time, and hence the liquefaction potential of the soil.

For illustrative purposes, let us take a simple dynamically induced shear stress/time curve, as shown in Fig. 2(b), applied on a saturated sand, and let us assume that the pore pressure generated in the soil due to this stress is as shown in Fig. 2(a). In this figure, the incremental pore-pressure rise during, say, the N^{th} cycle equals the total pore pressure u_N

at the end of the N^{th} cycle minus the residual pore-pressure value u_{N-1} at the end of the $(N-1)^{\text{th}}$ cycle, or

$$\Delta u_N = u_N - u_{N-1} \quad (1)$$

By dividing each side of the above equation by the pre-earthquake mean effective confining pressure, we obtain

$$\Delta U_N^* = U_N^* - U_{(N-1)}^* \quad (2)$$

where $U^* = \frac{u}{\sigma'_c}$ (normalized pore-pressure value);

σ'_c = pre-earthquake in-situ effective mean confining pressure around the soil sample and equals $\frac{1}{3} (\sigma'_1 + \sigma'_2 + \sigma'_3) = \frac{1}{3} (\sigma'_1 + 2\sigma'_3) = \frac{1}{3} (\sigma'_1 + 2K_0\sigma'_1) = \frac{\sigma'_1}{3} (1 + 2K_0)$; and

$\sigma'_1, \sigma'_2, \sigma'_3$ = pre-earthquake effective vertical and horizontal pressure.

In general, it can be assumed that

$$\Delta U_N^* = H \cdot I \cdot \bar{N} \quad (3)$$

where H = stress-history function;

I = stress-intensity function; and

\bar{N} = number-of-stress-cycles function.

Based on the fact that the stress-history function H has no effect on the pore pressure generated during the first cyclic loading and that at the complete-liquefaction stage the pore-pressure value reaches a constant level, which implies that ΔU_N^* equals zero, the stress history H can be represented as

$$H = 1 - U_{N-1}^* \quad (4)$$

Also, since the pore pressure increases with increasing applied shear stresses and decreases with increasing confining pressures, the stress-intensity function I can be expressed as

$$I = \left(\frac{\tau_N}{\sigma_{N-1}} \right)^\alpha \quad (5)$$

where τ_N = applied dynamic shear stress during the N^{th} cycle;

σ_{N-1}^* = mean effective confining pressure at the end of the $N-1^{\text{th}}$ cycle; and

α = material constant.

Fig. 3* shows the experimental relationship between the modified pore-

pressure parameter $\frac{\Delta U_N^*}{1 - U_{N-1}^*}$ and the stress ratio $\frac{\tau_N}{\sigma_{N-1}}$. It is seen from

this figure that the incremental rise in the modified pore-pressure parameter increases with increasing stress ratio $\frac{\tau_N}{\sigma_{N-1}}$ and that the slopes of the lines shown in Fig. 3 are almost the same (i.e., $\alpha = 2.4$). Therefore, the following relationship can be expressed:

$$\frac{\Delta U_N^*}{1 - U_{N-1}^*} = \bar{N} \left(\frac{\tau_N}{\sigma_{N-1}} \right)^{2.4} \quad (6)$$

To obtain the value of the number-of-stress-cycles function \bar{N} , the experimental data obtained during this research is plotted as shown in Fig. 4*, from which the value of \bar{N} is expressed in Eq. 7 as the best-fit curve through the experimental data.

$$\bar{N} = \frac{6.13N}{N^{1.77} - 0.46} \quad (7)$$

*These experimental data were obtained from tests conducted on loose Ottawa sand. The values of the constants 2.4, 6.13, 1.77, and 0.46 in Eqs. 6 and 7 vary depending on soil density.

where N is the number of uniform stress cycles.

Substituting Eqs. 7, 5, and 4 in Eq. 3, the following relationship is found for ΔU_N^* :

$$\Delta U_N^* = (1 - U_{N-1}^*) \left(\frac{6.13N}{N^{1.77} - 0.46} \right) \cdot \left(\frac{\tau_N}{\sigma_{N-1}} \right)^{2.4} \quad (8)$$

From Eq. 8 the amount of the pore-pressure buildup in a loose Ottawa sand under a given uniform stress ratio $\frac{\tau}{\sigma}$ can be calculated as a function of the number of uniform stress cycles N as shown in Fig. 5. It is seen from this figure that the values of the pore pressures predicted by Eq. 8 and the ones obtained experimentally in the laboratory for loose Ottawa sand are nearly the same.

Pore-Pressure Rise under Non-Uniform Loading

Eq. 8 can also be applied to determine the pore-pressure buildup in saturated sands under non-uniform loading if we substitute an equivalent number of stress cycles N_{eq} for the regular uniform cycles N . The N_{eq} is defined as

$$N_{eq} = \sum_{i=1}^N \left(\frac{\tau_i}{\tau_N} \right)^{2.4} \quad (9)$$

where N_{eq} = equivalent number of stress cycles;

τ_i = the shear-stress amplitude corresponding to i^{th} cycle ($1 \leq i \leq N$);

and

τ_N = the shear-stress amplitude at the N^{th} cycle.

Fig. 14 illustrates the values of τ_i , τ_N , etc.

After substituting N_{eq} for N in Eq. 8, we obtain Eq. 10, which applies to the prediction of pore-pressure buildup under non-uniform loading:

$$\Delta U_N^* = (1 - U_{N-1}^*) \left[\frac{6.13N_{eq}}{N_{eq}^{1.77} - 0.46} \right] \left[\frac{\tau_N}{\sigma_{N-1}} \right]^{2.4} \quad (10)$$

It can be seen from Figs. 6, 7, 8, and 9 that there is a good correlation between the pore-pressure rise calculated on the basis of Eq. 10 and those found experimentally from tests on loose Ottawa sand in the laboratory. It is concluded therefore that Eq. 10 does indeed predict the pore-pressure buildup in loose Ottawa sand subjected to non-uniform dynamic loading.

Pore-Pressure Rise under Earthquake-Type Loading

The incremental pore-pressure-rise equation (Eq. 10) can be written in a more general form, as in Eq. 11. Eq. 11 will apply to the prediction of pore-pressure rise in any soil type once the material properties C_1 , C_2 , C_3 , and α are known.

$$\Delta U_N^* = (1 - U_{N-1}^*) \left[\frac{C_1 \cdot N_{eq}}{N_{eq}^{C_2} - C_3} \right] \cdot \left[\frac{\tau_N}{\sigma_{N-1}} \right]^\alpha \quad (11)$$

where N_{eq} = the same as before; and

C_1 , C_2 , C_3 , and α = material parameters.

Figs. 10 and 11 show the values of C_1 and α respectively as a function of volume-decrease potential ($e_{nat} - e_{min}$), and Fig. 12 shows the values of C_2 and C_3 as a function of soil void ratio. Studies undertaken to investigate the variability of ΔU^* with respect to changes in the values of C_2 and C_3 reveal that ΔU^* is not very sensitive to these parameters. Also, it is interesting to note from Fig. 12 that the values of the parameters C_2 and C_3 do not vary much with soil density or soil type; and therefore, for all

practical purposes, the parameters C_2 and C_3 can be considered constant for all soil types.

Eq. 11, which predicts pore-pressure rise in a saturated soil under non-uniform dynamic loading, can also be made to apply to the prediction of pore-pressure rise under earthquake loading, provided that the random stress variation during the earthquake stress/time history is represented by an equivalent number of uniform stress cycles. In order to do this, reference is made to Fig. 13. Let us assume that Fig. 13(a) represents any arbitrary N^{th} earthquake stress cycle in which the positive stress τ_{Np} does not equal τ_{Nn} . The random positive and negative stress variation in Fig. 13(a) can be represented by two fictitious full-cycle uniform stresses, one corresponding to the positive stress τ_{Np} and the other to the negative stress τ_{Nn} , as shown in Figs. 13(b) and (c) respectively. In view of the fact that the values of both the positive and negative shear stresses τ_{Np} and τ_{Nn} are doubled through this process, the values of the incremental pore pressures generated under the stresses shown in Figs. 13(b) and (c) should therefore equal twice the incremental pressure rise under the actual earthquake stress cycle shown in Fig. 13(a). Accordingly,

$$\Delta U_N^* = \frac{1}{2} (\Delta U_{Np}^* + \Delta U_{Nn}^*) \quad (12)$$

Considering the above relationship, the value of the total normalized pore pressure at the end of the N^{th} earthquake cycle will therefore be

$$U_N^* = U_{N-1}^* + \frac{1}{2} (\Delta U_{Np}^* + \Delta U_{Nn}^*) \quad (13)$$

When the value of the normalized total pore pressure U_N^* in Eq. 13 reaches unity (one), then the soil will reach liquefaction stage.

In view of the fact that we have separated the actual earthquake stress cycle in Fig. 13 into two uniform positive and negative stress cycles, it is necessary therefore that we consider the individual effects of the positive and negative stress components, together with their associated pore pressures and equivalent number of stress cycles separately.

Therefore, the magnitudes of ΔU_{Np}^* , ΔU_{Nn}^* , $(N_{eq})_p$, and $(N_{eq})_n$ can be calculated from the expressions outlined in Eqs. 14, 15, 16, and 17 respectively:

$$\Delta U_{Np}^* = (1 - U_{N-1}^*) \cdot \frac{C_1 (N_{eq})_p}{(N_{eq})_p^{C_2} - C_3} \cdot \left(\frac{\tau_{Np}}{\sigma_{N-1}'} \right)^\alpha \quad (14)$$

$$\Delta U_{Nn}^* = (1 - U_{N-1}^*) \cdot \frac{C_1 (N_{eq})_n}{(N_{eq})_n^{C_2} - C_3} \cdot \left(\frac{\tau_{Nn}}{\sigma_{N-1}'} \right)^\alpha \quad (15)$$

$$(N_{eq})_p = \sum_{i=1}^N \left(\frac{\tau_{ip}}{\tau_{Np}} \right)^\alpha \quad (16)$$

$$(N_{eq})_n = \sum_{i=1}^N \left(\frac{\tau_{in}}{\tau_{Nn}} \right)^\alpha \quad (17)$$

where τ_{Np} and τ_{Nn} are the maximum positive and negative stresses at the N^{th} cycle at which the normalized pore-pressure value is to be calculated, and τ_{ip} and τ_{in} are the maximum positive and negative shear stresses at the i^{th} cycle (see Fig. 14(a) for illustration).

In the following paragraphs we shall illustrate the applicability of Eqs. 13 through 17 to the prediction of liquefaction potential of saturated sands under given earthquake-induced shear stresses. Suppose that an earthquake shear stress, shown in Fig. 15(a), acts in the middle of the 2-ft. saturated medium-dense Ottawa sand layer shown in Fig. 15(b), and that we are

asked to determine whether the soil layer in question will liquefy under the shear stresses shown in Fig. 15.

Step 1

The first step in the solution of this problem involves the determination of the material properties and the pre-earthquake effective mean confining pressures on the soil. From the given information we determine the following values: $C_1 = 2.4$, $C_2 = 1.82$, $C_3 = 0.3$, $\alpha = 2.17$, and $\sigma'_m = 5.31$ psi.

Step 2

The second step in the calculation involves the identification of the magnitudes of the maximum positive and negative shear stresses within each stress cycle of the earthquake loading time history curve in Fig. 15-a. This is done by taking every consecutive two zero crossings on the earthquake shear stress curve as one cycle and only recording the magnitudes of the maximum positive and negative stresses within each cycle, as shown in Fig. 16.

Step 3

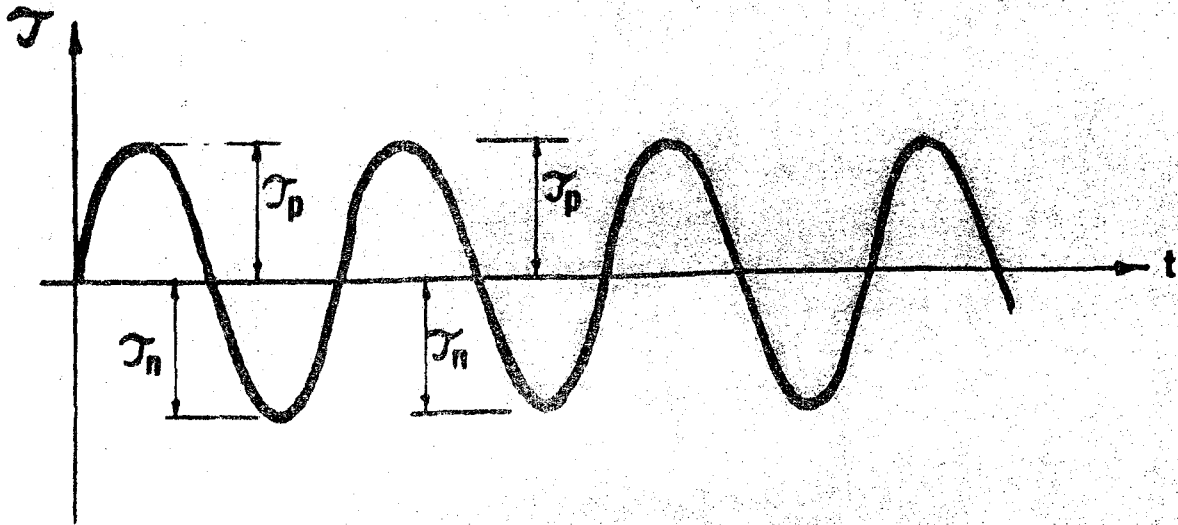
After having ascertained the above information, the calculation can be carried on as seen in Table 1, using equations 13, 14, 15, 16, and 17 to determine whether the soil under consideration will liquefy during the given earthquake loading history shown in Fig. 16. Since it is seen from the data in Table 1 and from Curve A in Fig. 17 that the value of the normalized pore pressure U_N^* exceeds unity at the end of the 8-1/2 cycles, it is concluded therefore that the 2-ft. soil layer shown in Fig. 16 will liquefy during this earthquake and that the liquefaction commences 5 seconds after the start of the earthquake.

In order to illustrate the effects of the confining pressures on soil liquefaction, it was decided to investigate the liquefaction potential of the same soil, assuming that the soil element A in Fig. 15 is at a depth of about 33 ft. from the ground surface, where the mean confining pressure

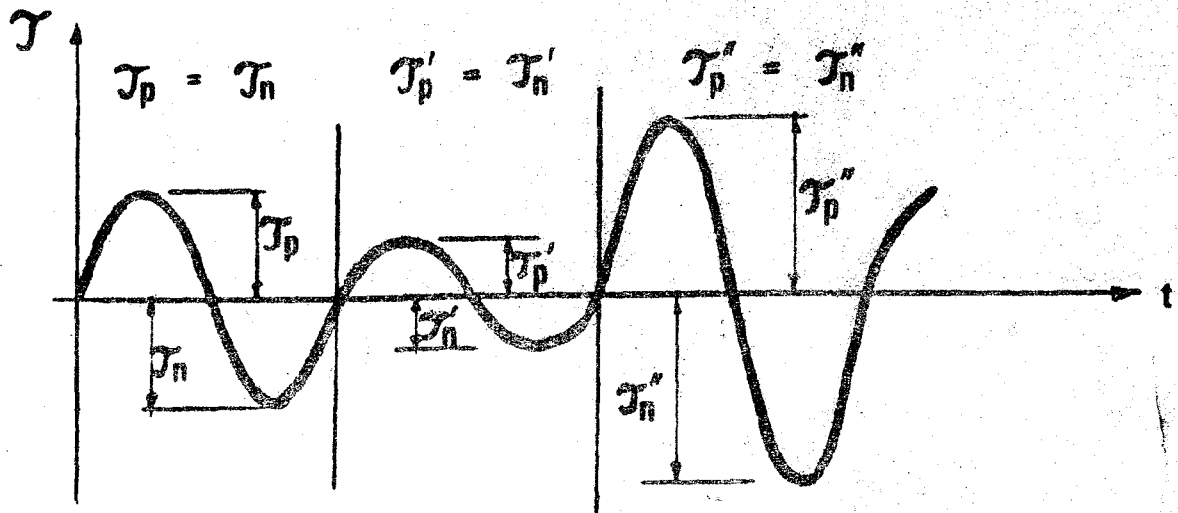
around it would have been about 20 psi instead of 5.31 psi. As shown in Curve B in Fig. 17, the maximum value of the normalized pore pressure U_N^* under those circumstances would have been equal to 0.54 at the end of the earthquake, thus suggesting that if the soil were located at a depth of 33 ft. from the ground surface, and if it were subjected to the same earthquake stresses shown in Fig. 15(a), it would not have liquefied.

In conclusion, it is believed that the liquefaction equations (Eqs. 13, 14, 15, 16, and 17) do provide an adequate basis for analyzing the liquefiability of a given soil. In fact, the results predicted by these equations and the actual pore-pressure rises observed in the laboratory appear to be in close agreement, as shown in Fig. 18. Fig. 19 shows the predicted values of the normalized pore pressures in loose, medium dense, and dense saturated sand layers excited by the earthquake-induced shear stresses shown by the top curve. It can be observed from this figure that the loose deposit liquefies after 5 seconds, while the same deposit with medium density liquefies after 10 seconds. On the other hand, if the above soil were dense it would not liquefy during this particular earthquake. It is also evident from Fig. 19 that it is mainly the large peak shear stresses that contribute significantly to pore-pressure rise.

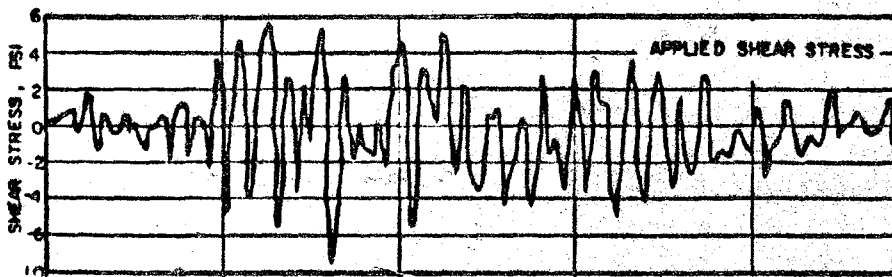
TYPES OF LOADINGS



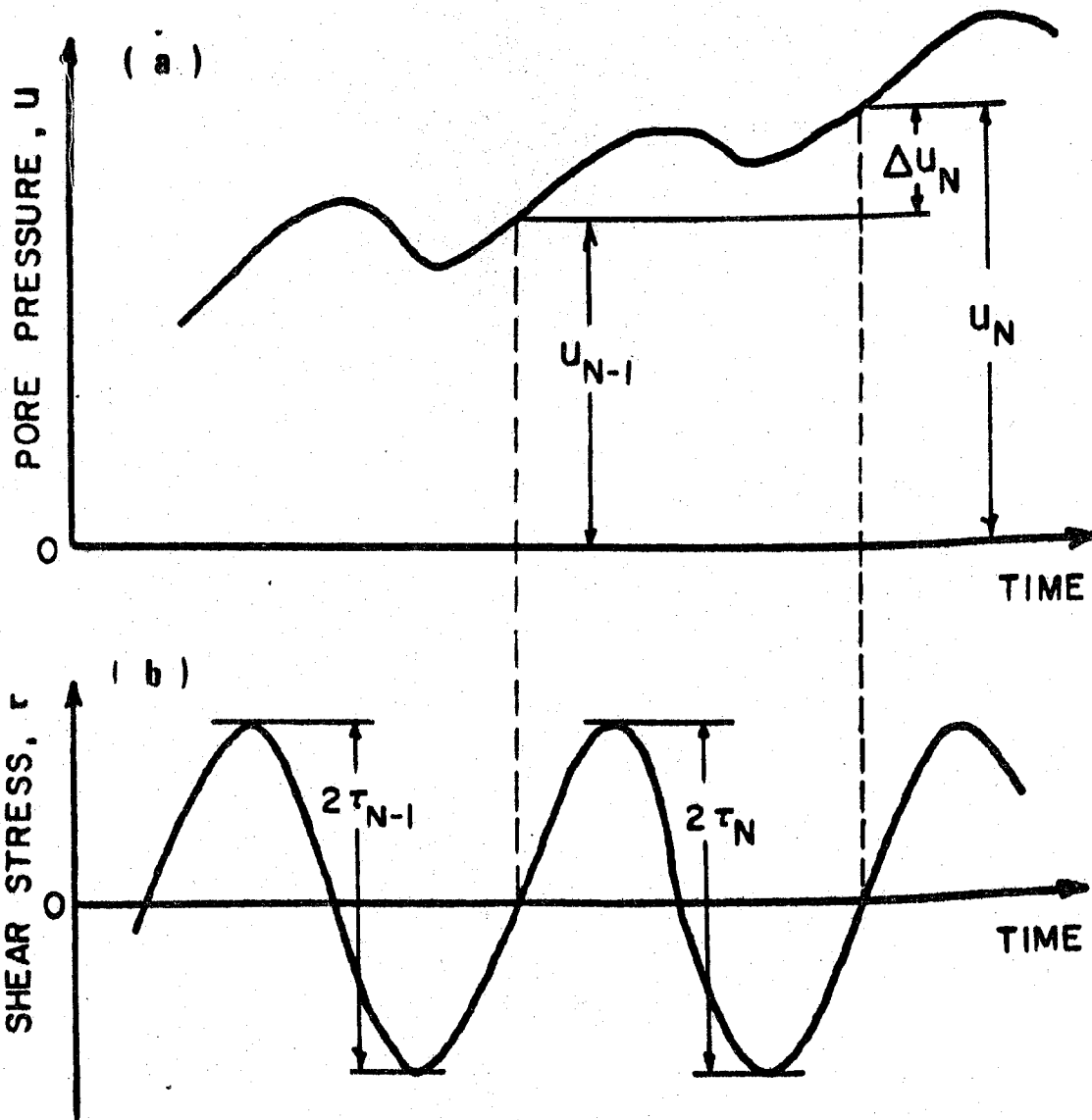
(a) UNIFORM LOADING ($\tau_p = \tau_n$ at all times)



(b) NON UNIFORM LOADING (within each cycle $\tau_p = \tau_n$)
 $f_1 \neq f_2 \neq f_3$



(c) EARTHQUAKE LOADING (no restrictions)



$$\Delta U_N = U_N - U_{N-1}$$

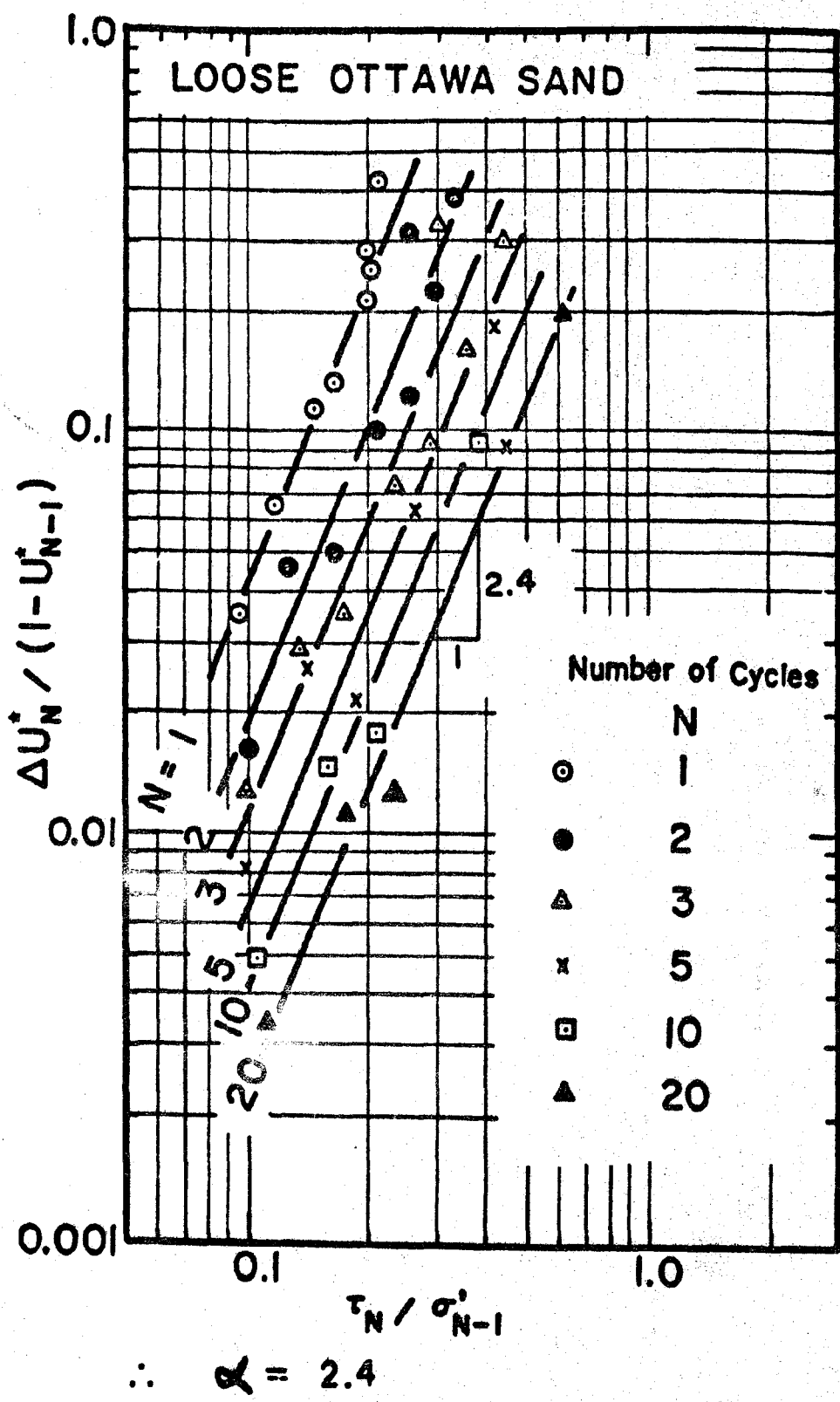
$$\Delta U'_N = U'_N - U'_{N-1}$$

where

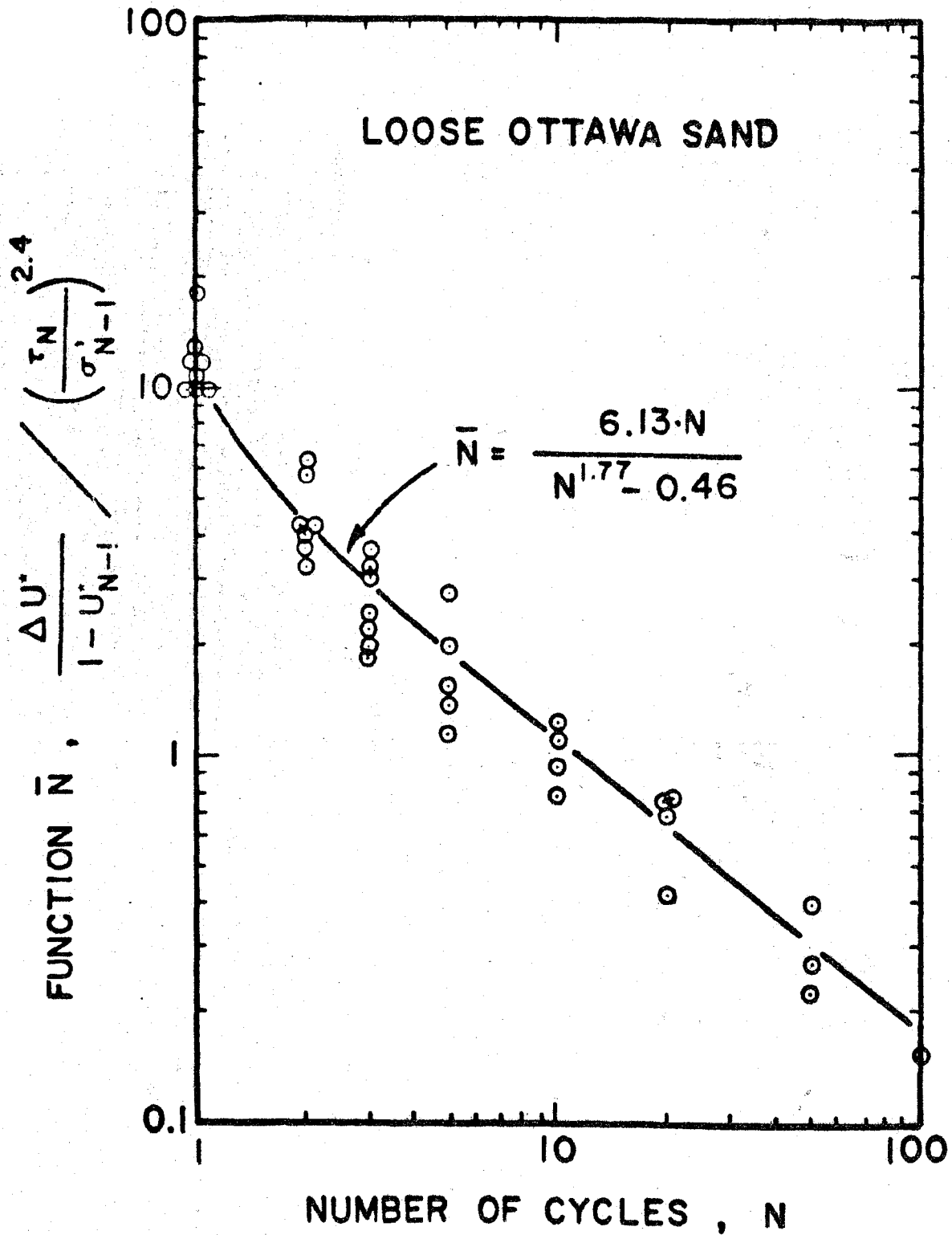
$$U' = \frac{u}{\sigma'_N}$$

σ'_N = Pre-earthquake Mean Effective Confining Pressure

FIG. 2



PORE-PRESSURE RISE PER CYCLE (EXPERIMENTAL)
FIG. 3 2-47



NUMBER OF CYCLES VERSUS CYCLIC FUNCTION \bar{N}

FIG. 4

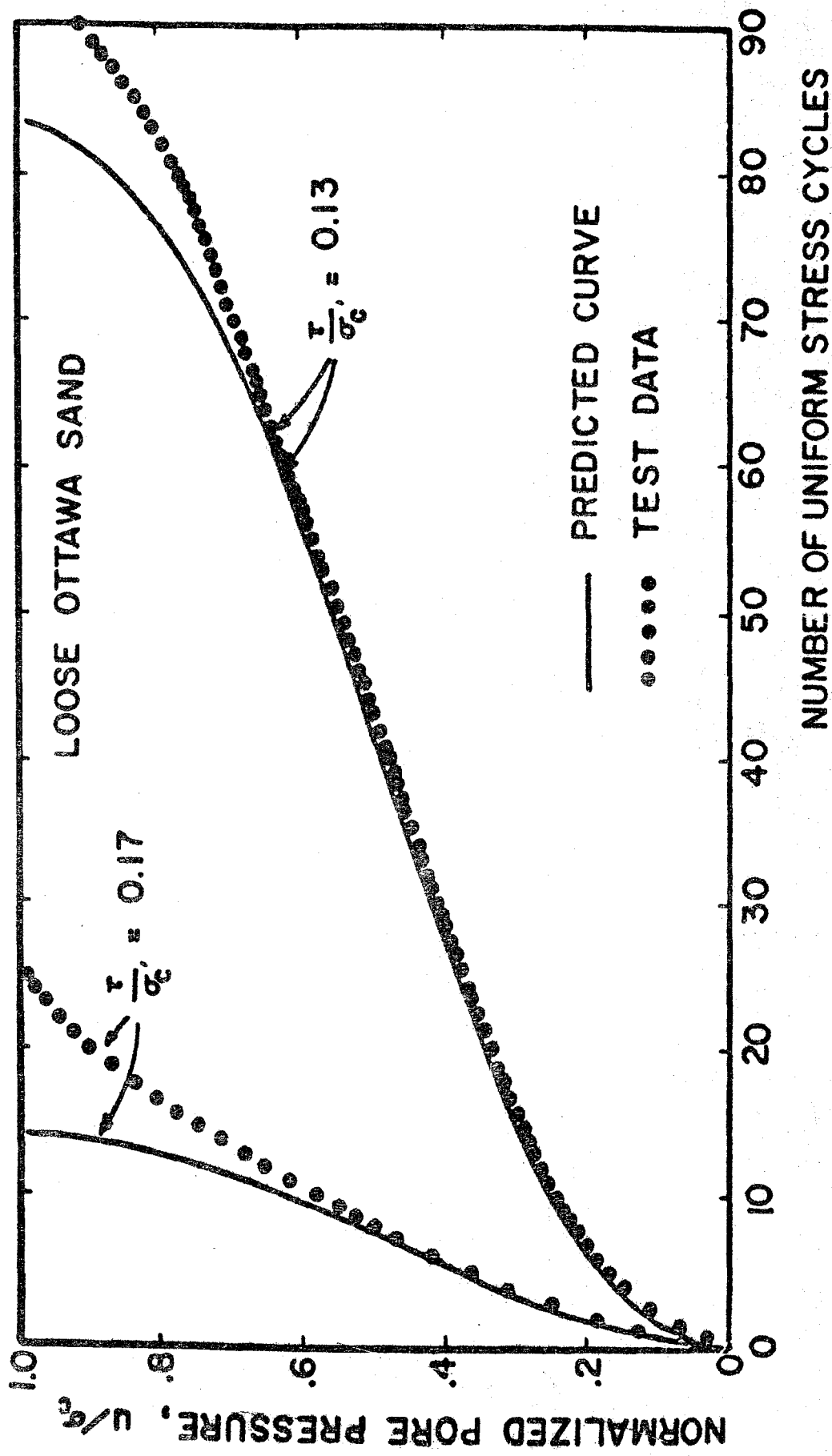
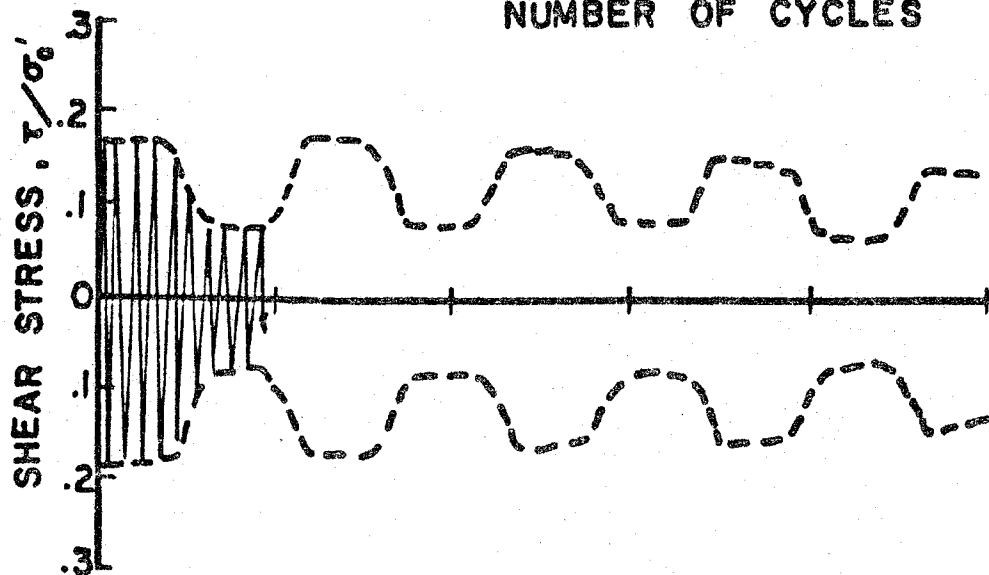
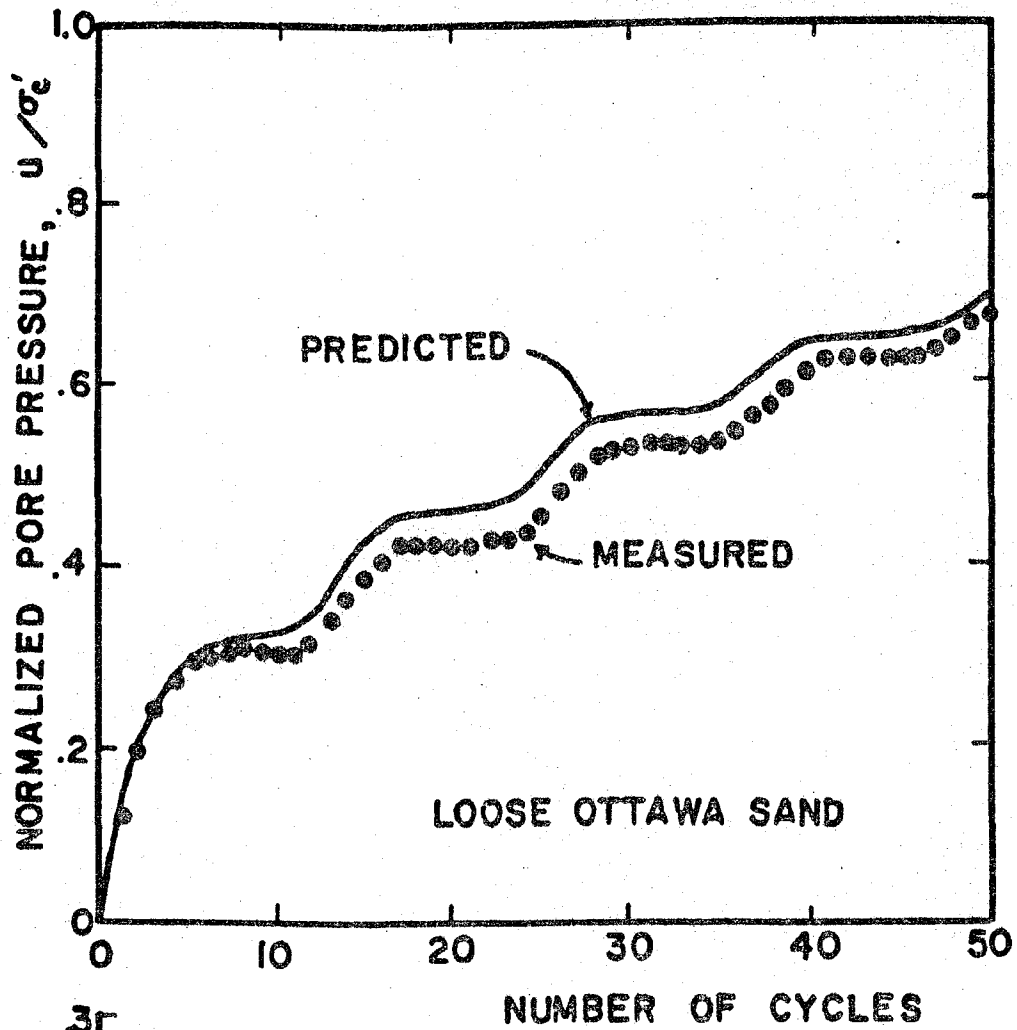
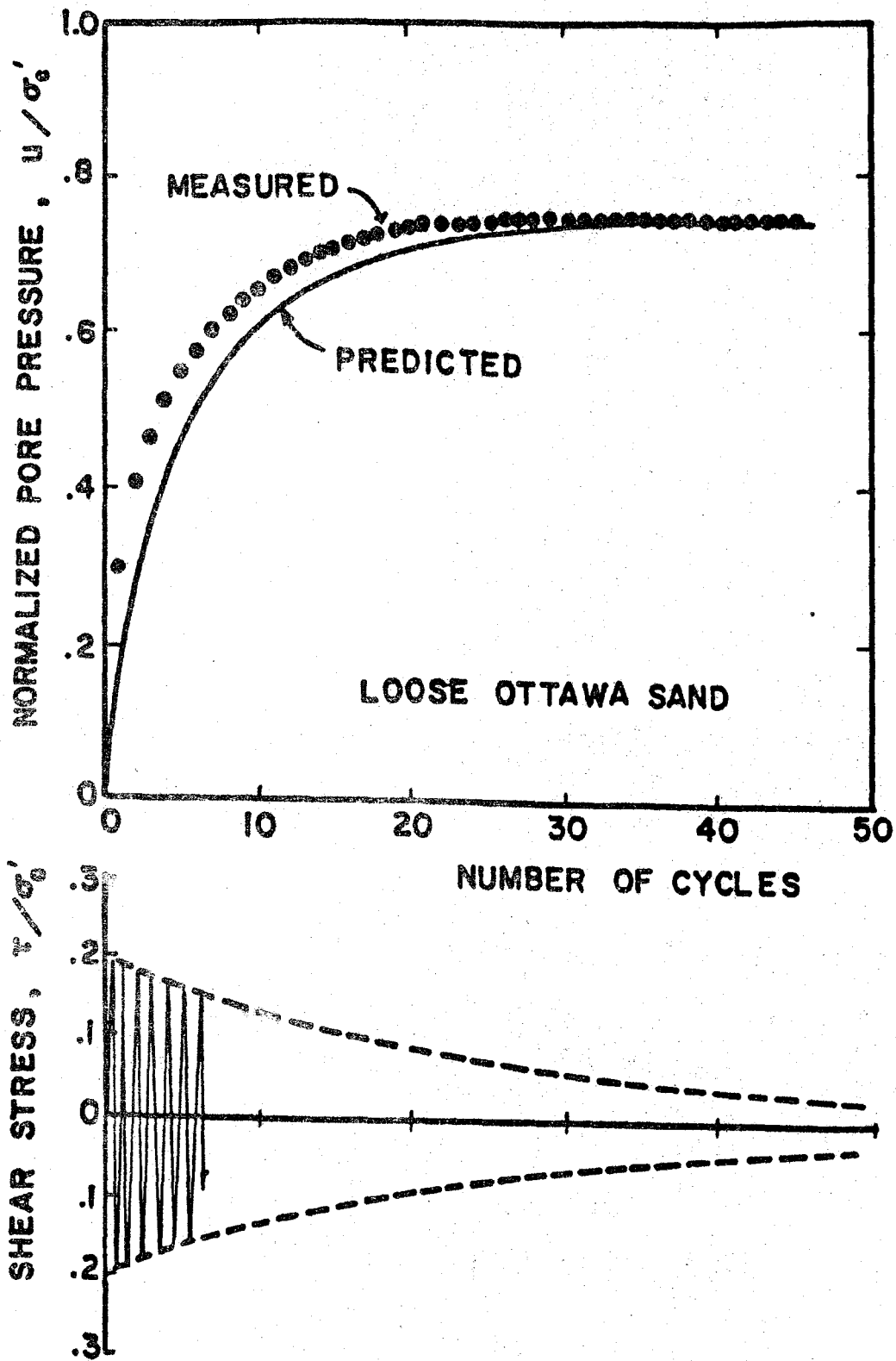


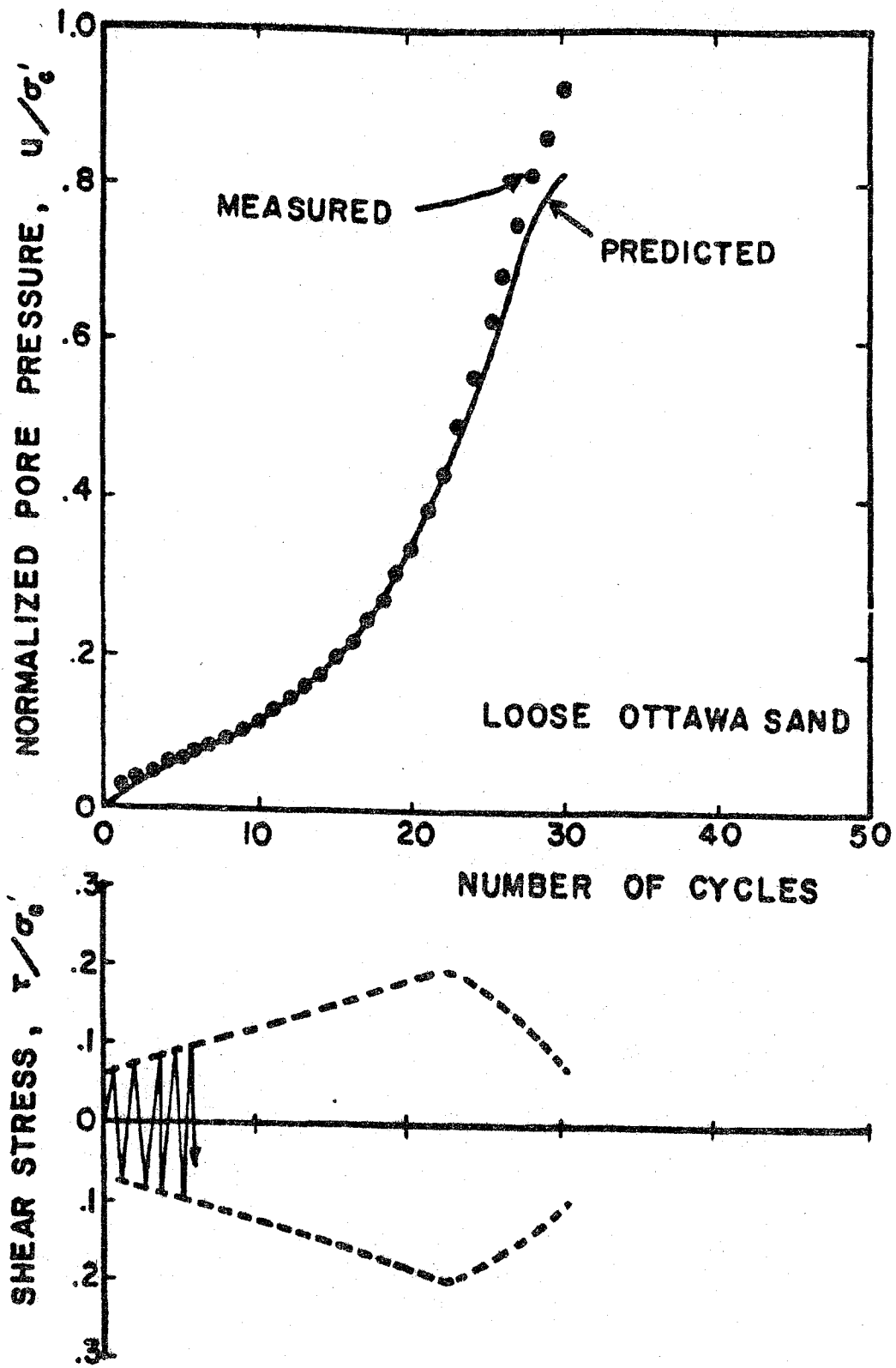
FIG. 5 PORE - PRESSURE RISE UNDER UNIFORM CYCLIC LOADING



PORE-PRESSURE RISE UNDER NON-UNIFORM CYCLIC LOADING

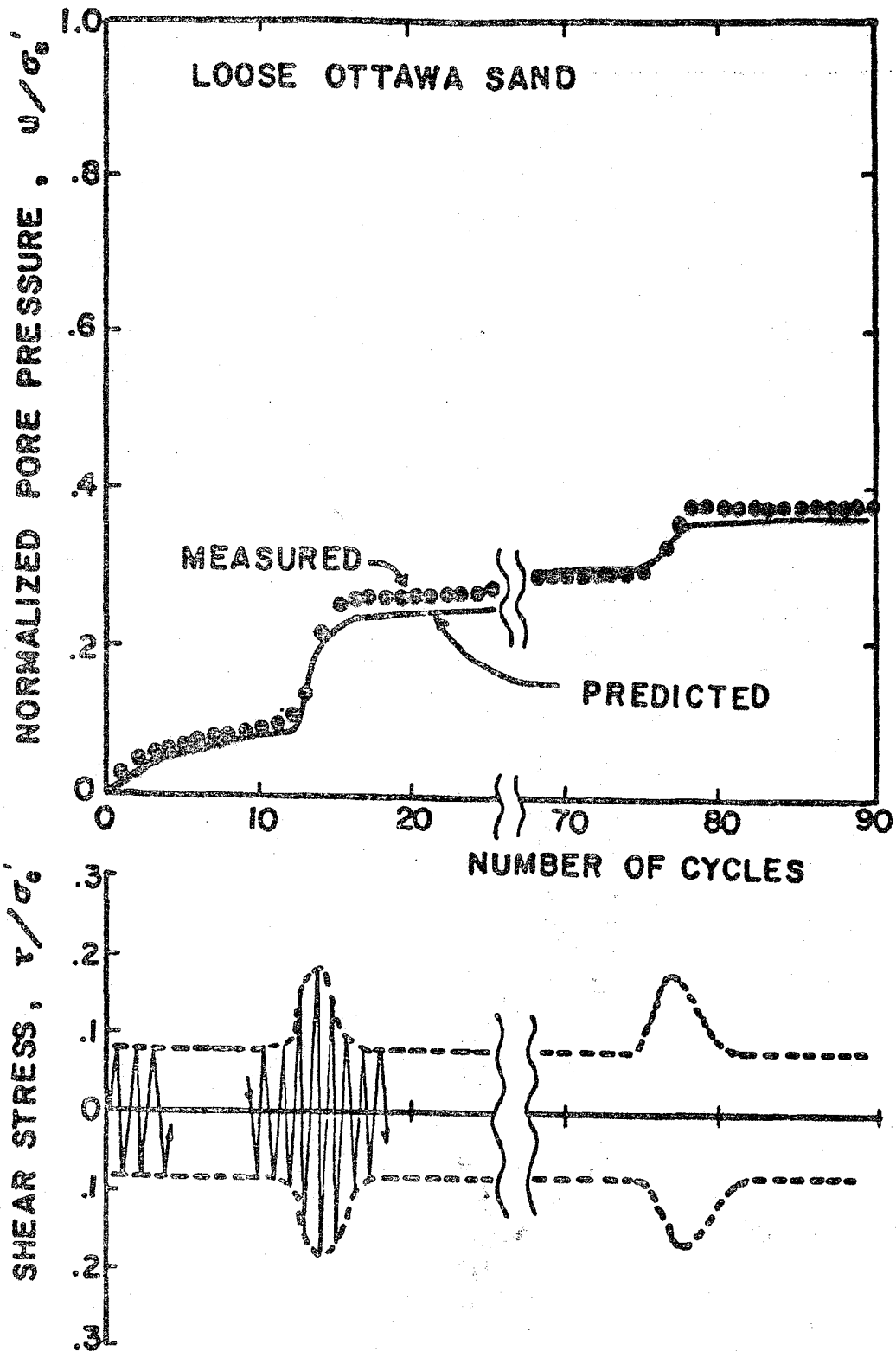


PORE-PRESSURE RISE UNDER NON-UNIFORM
CYCLIC LOADING



PORE-PRESSURE RISE UNDER NON-UNIFORM CYCLIC LOADING

FIG. 8



PORE-PRESSURE RISE UNDER NON-UNIFORM
CYCLIC LOADING

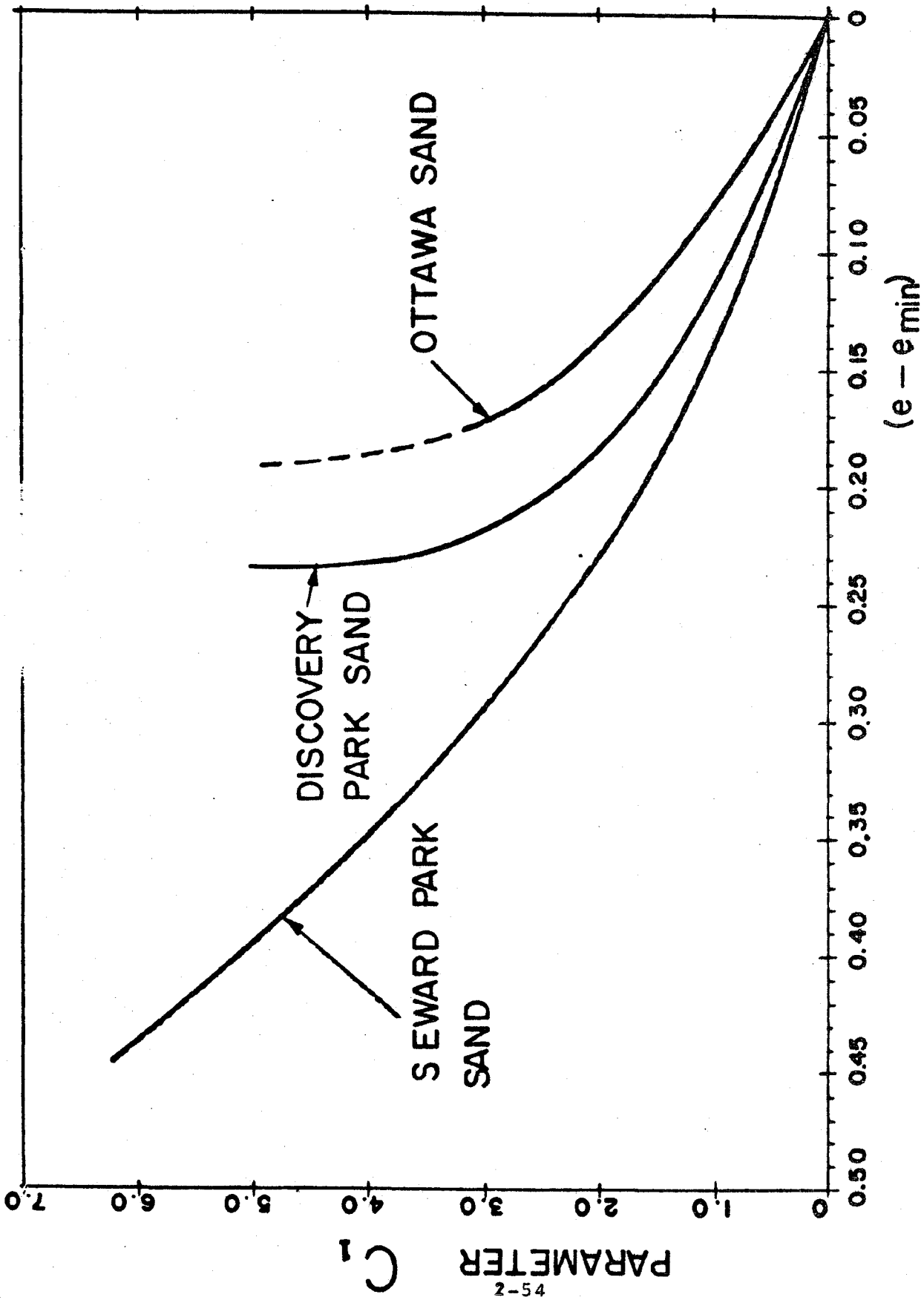


FIG.10 VOLUME DECREASE POTENTIAL

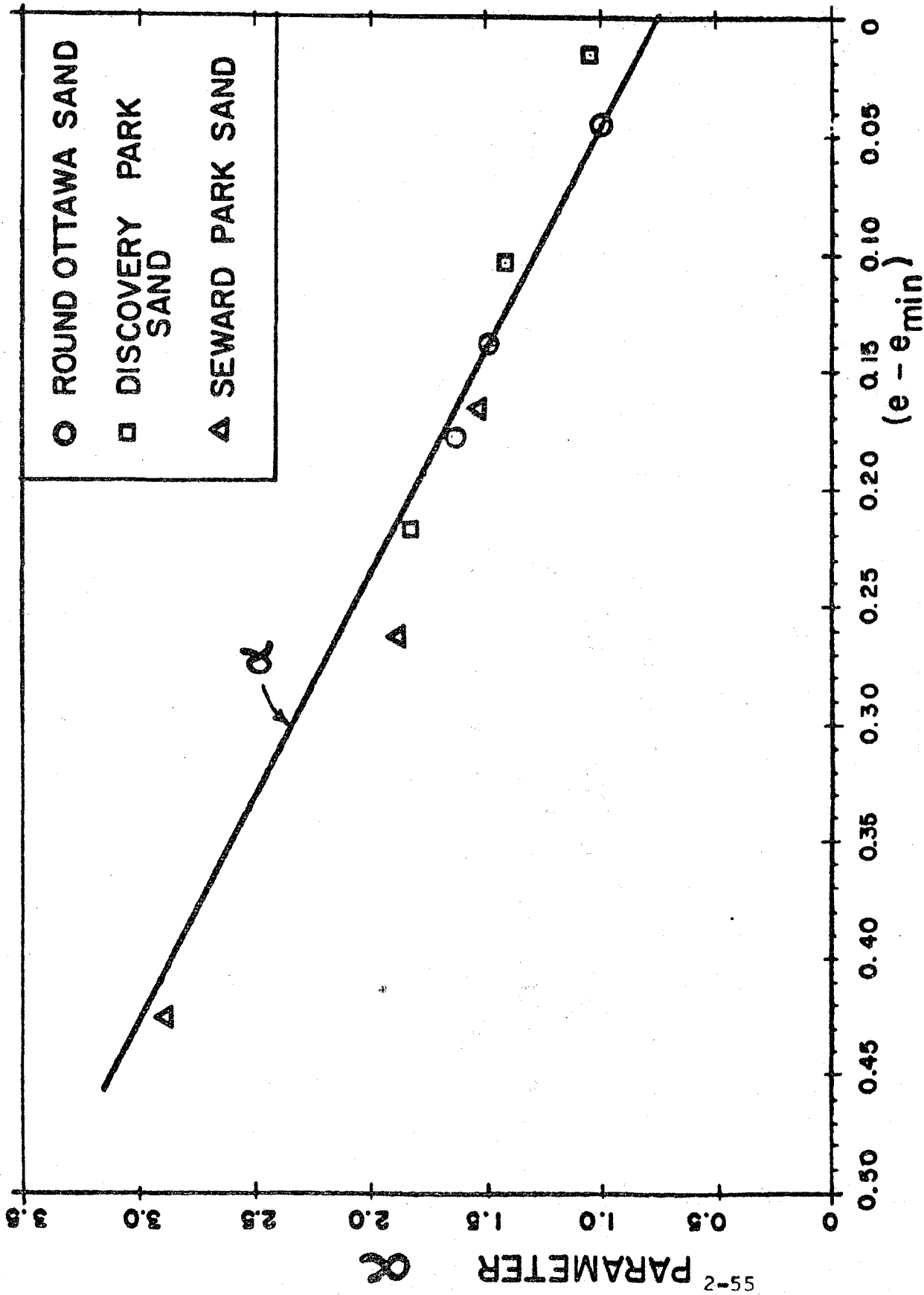


FIG. 11 VOLUME DECREASE POTENTIAL

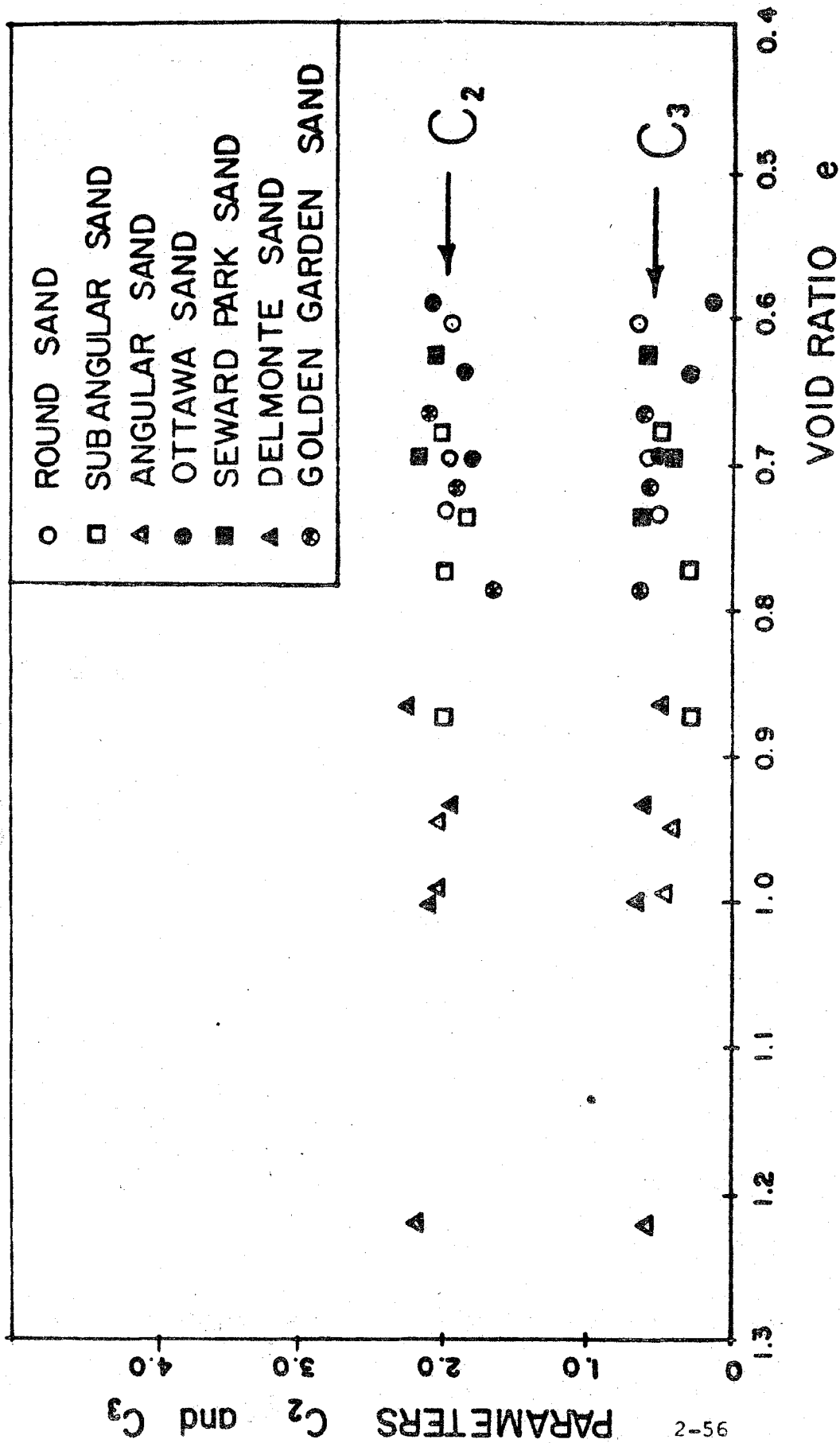


FIG. 12

ACTUAL RANDOM SIGNAL
at Nth CYCLE

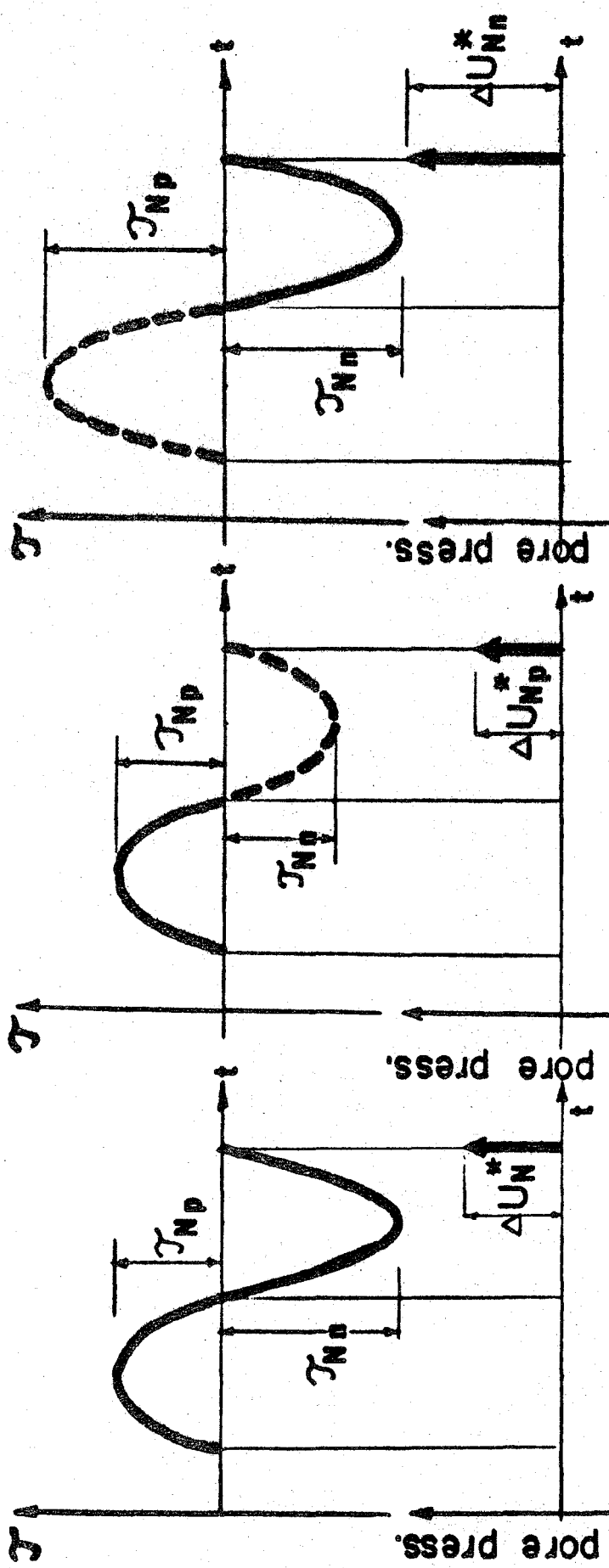
FICTITIOUS UNIFORM
SIGNAL CORRESPONDING
TO POSITIVE SHEAR
STRESS at Nth CYCLE

FICTITIOUS UNIFORM
SIGNAL CORRESPOND-
ING TO NEGATIVE SHEAR
STRESS at Nth CYCLE

$$(\tau_{Np} \neq \tau_{Nn})$$

$$(\tau_{Np} = \tau_{Nn})$$

$$(\tau_{Np} = \tau_{Nn})$$



$$\Delta U_N^* = \frac{1}{2}(\Delta U_{Np}^*) + \frac{1}{2}(\Delta U_{Nn}^*)$$

$$\text{THEREFORE, } U_N^* = U_{N-1}^* + \frac{1}{2}(\Delta U_{Np}^* + \Delta U_{Nn}^*)$$

FIG 13

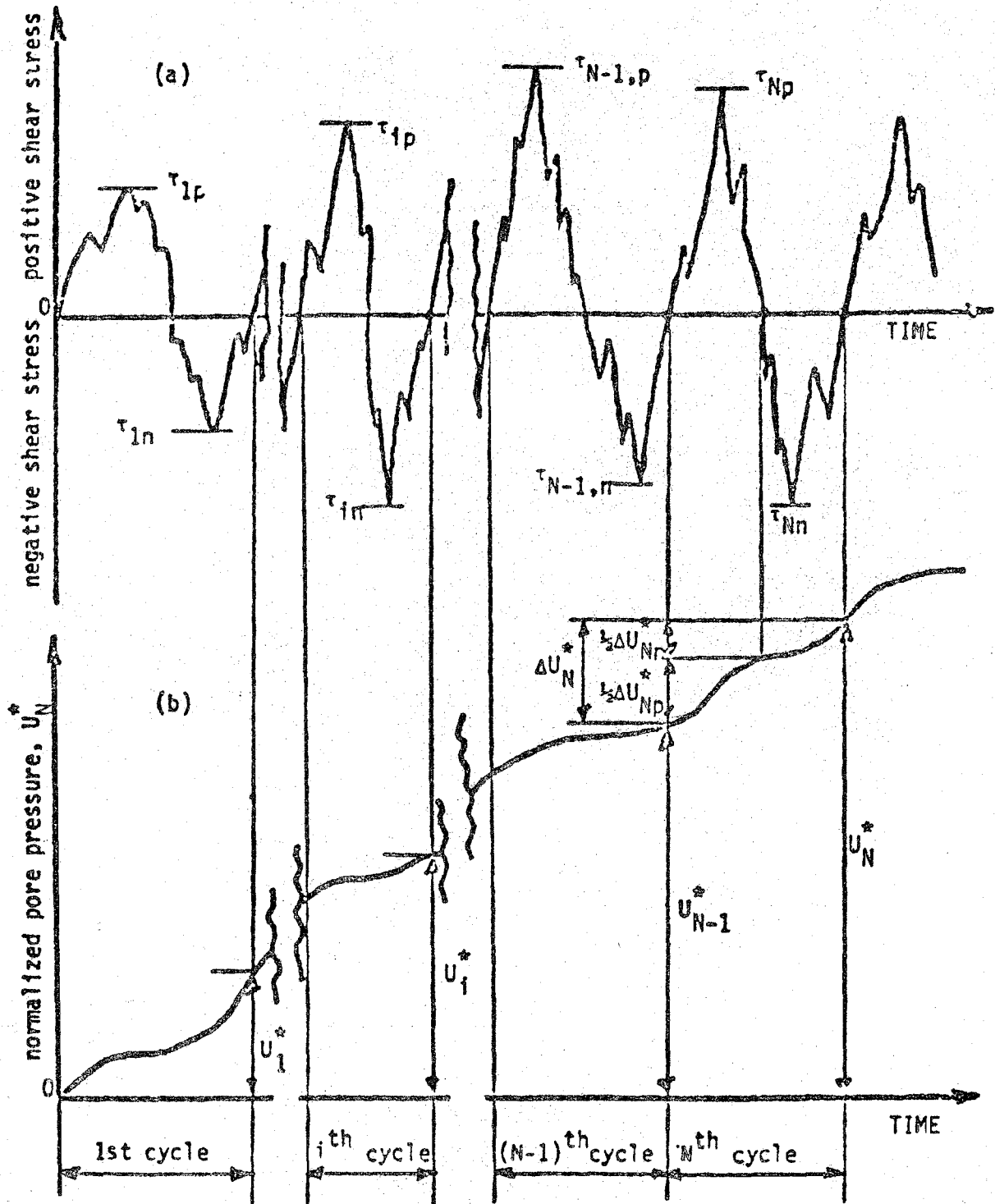


Fig. 14 Illustration of Normalized Pore Pressure Buildup as a Function of Earthquake Stress Cycles.

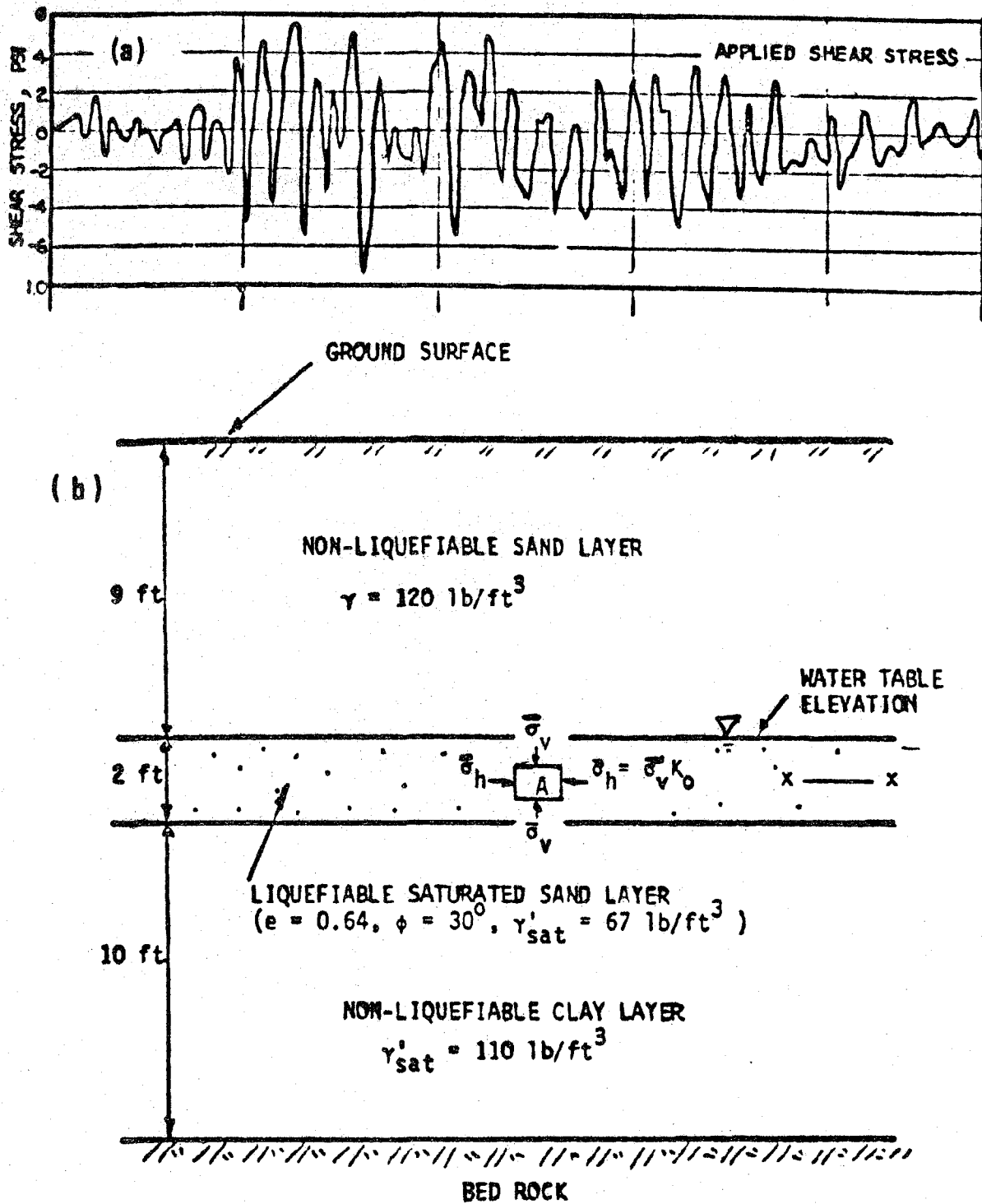


FIG. 15 ILLUSTRATIVE PROBLEM

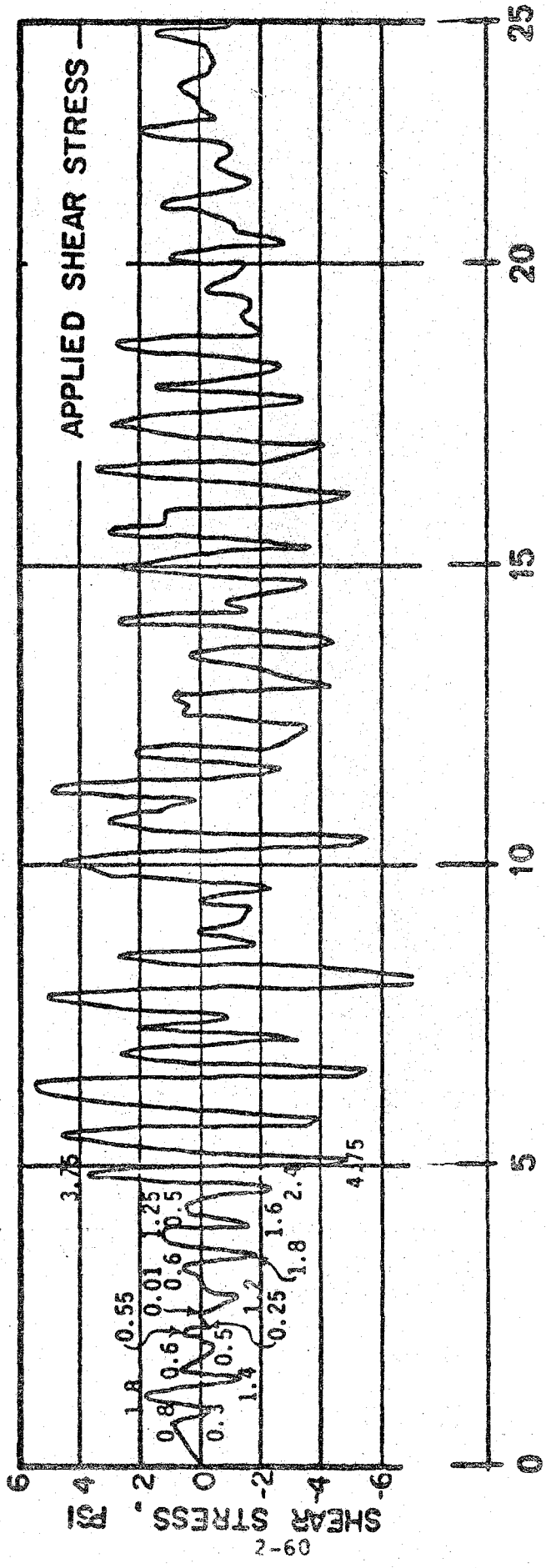


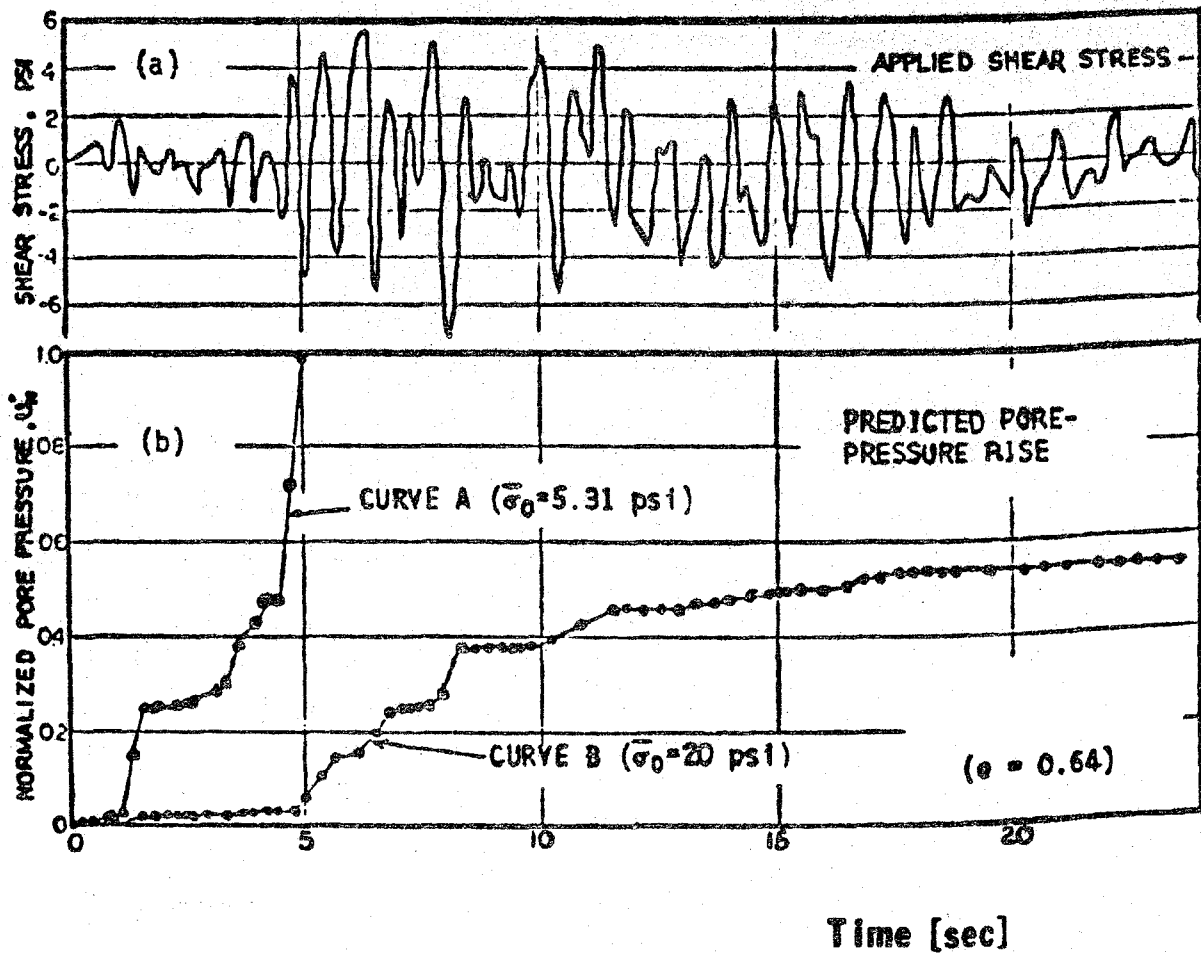
FIG. 16

TABLE 1^a

CYCLE NUMBER, N	SHEAR STRESS τ_N , PSI	$(N_{eq})^{\alpha} = \sum \left(\frac{\tau_i}{\tau_N} \right)^{\alpha}$	$\frac{\Delta U_{NP}}{(1-U_{N-1})} = \frac{N_{eq} C_1}{N_{eq} C_2 - C_3} \left(\frac{\tau_N}{\tau_{N-1}} \right)^{\alpha}$	$\Delta U_N^{\alpha} = \frac{1}{2} (\Delta U_{NP}^{\alpha} + \Delta U_{Nn}^{\alpha})$	$U_N^{\alpha} = U_{N-1}^{\alpha} + \Delta U_N^{\alpha}$	$\bar{\sigma}_N = \bar{\sigma}_0 (1 - U_N^{\alpha})$ PSI
1	POSITIVE	$\left(\frac{0.8}{0.8}\right)^{2.17} = 1.0$	$(1-0) \frac{1.1 \cdot 2.4}{1.08} \frac{(0.80)^{2.17}}{0.30(5.31)} = 0.056$	$\frac{1}{2} (0.056 + 0.007) = 0.0315$	0 + 0.0315	5.31 (1 - 0.0315)
	NEGATIVE	$\left(\frac{0.3}{0.3}\right)^{2.17} = 1.0$	$(1-0) \frac{1.1 \cdot 2.4}{1.32} \frac{(0.30)^{2.17}}{0.30(5.31)} = 0.007$	$\frac{1}{2} (0.056 + 0.007) = 0.0315$	= 0.0315	= 5.143
2	POSITIVE	$\left(\frac{0.8}{1.8}\right)^{2.17} + \left(\frac{1.8}{1.8}\right)^{2.17} = 1.172$	$(1-0.0315) \frac{1.172 \cdot 2.4}{1.172} \frac{(1.8)^{2.17}}{0.30(5.143)} = 0.270$	$\frac{1}{2} (0.270 + 0.187) = 0.2285$	0.0315 + 0.2285	5.31 (1 - 0.26)
	NEGATIVE	$\left(\frac{0.3}{1.4}\right)^{2.17} + \left(\frac{1.4}{1.4}\right)^{2.17} = 1.032$	$(1-0.0315) \frac{1.032 \cdot 2.4}{1.032} \frac{(1.4)^{2.17}}{0.30(5.143)} = 0.187$	$\frac{1}{2} (0.270 + 0.187) = 0.2285$	= 0.260	= 3.929
3	POSITIVE	$\left(\frac{0.8}{0.6}\right)^{2.17} + \left(\frac{1.8}{0.6}\right)^{2.17} + \left(\frac{0.6}{0.6}\right)^{2.17} = 13.715$	$(1-0.26) \frac{13.715 \cdot 2.4}{13.715} \frac{(0.6)^{2.17}}{0.30(3.929)} = 0.0035$	$\frac{1}{2} (0.0035 + 0.0028) = 0.0030$	0.26 + 0.003	5.31 (1 - 0.263)
	NEGATIVE	$\left(\frac{0.3}{0.5}\right)^{2.17} + \left(\frac{1.4}{0.5}\right)^{2.17} + \left(\frac{0.5}{0.5}\right)^{2.17} = 13.113$	$(1-0.26) \frac{13.113 \cdot 2.4}{13.113} \frac{(0.5)^{2.17}}{0.30(3.929)} = 0.0025$	$\frac{1}{2} (0.0035 + 0.0028) = 0.0030$	= 0.263	= 3.913
4	POSITIVE	17.565	0.0024	0.0013	0.2643	3.907
4	NEGATIVE	49.016	0.002	0.0013	0.2643	3.907
5	POSITIVE	99.000	0	0.0325	0.2968	3.734
5	NEGATIVE	2.629	0.065	0.1043	0.4012	3.180
6	POSITIVE	15.543	0.034	0.1043	0.4012	3.180
6	NEGATIVE	2.09	0.2054	0.0869	0.4881	2.718
7	POSITIVE	4.161	0.060	0.0869	0.4881	2.718
7	NEGATIVE	3.70	0.1138	0.2323	0.7204	1.4847
8	POSITIVE	31.39	0.0018	0.2323	0.7204	1.4847
8	NEGATIVE	2.535	0.4627	5.940	6.314 > 1.0	-28.2 < 0
9	POSITIVE	1.3%	4.557		Liquefaction	Liquefaction
9	NEGATIVE	1.576	6.432			

Note a. All calculations are conducted for $\bar{\sigma}_0 = 5.31$ psi, $\alpha = 2.17$, $C_1 = 2.4$, $C_2 = 1.82$, and $C_3 = 0.3$.

b. Calculated by the same procedures as shown immediately above.



PREDICTION OF SOIL LIQUEFACTION POTENTIAL AS A FUNCTION OF EARTHQUAKE STRESSES AND CONFINING PRESSURES

FIG. 17
2-62

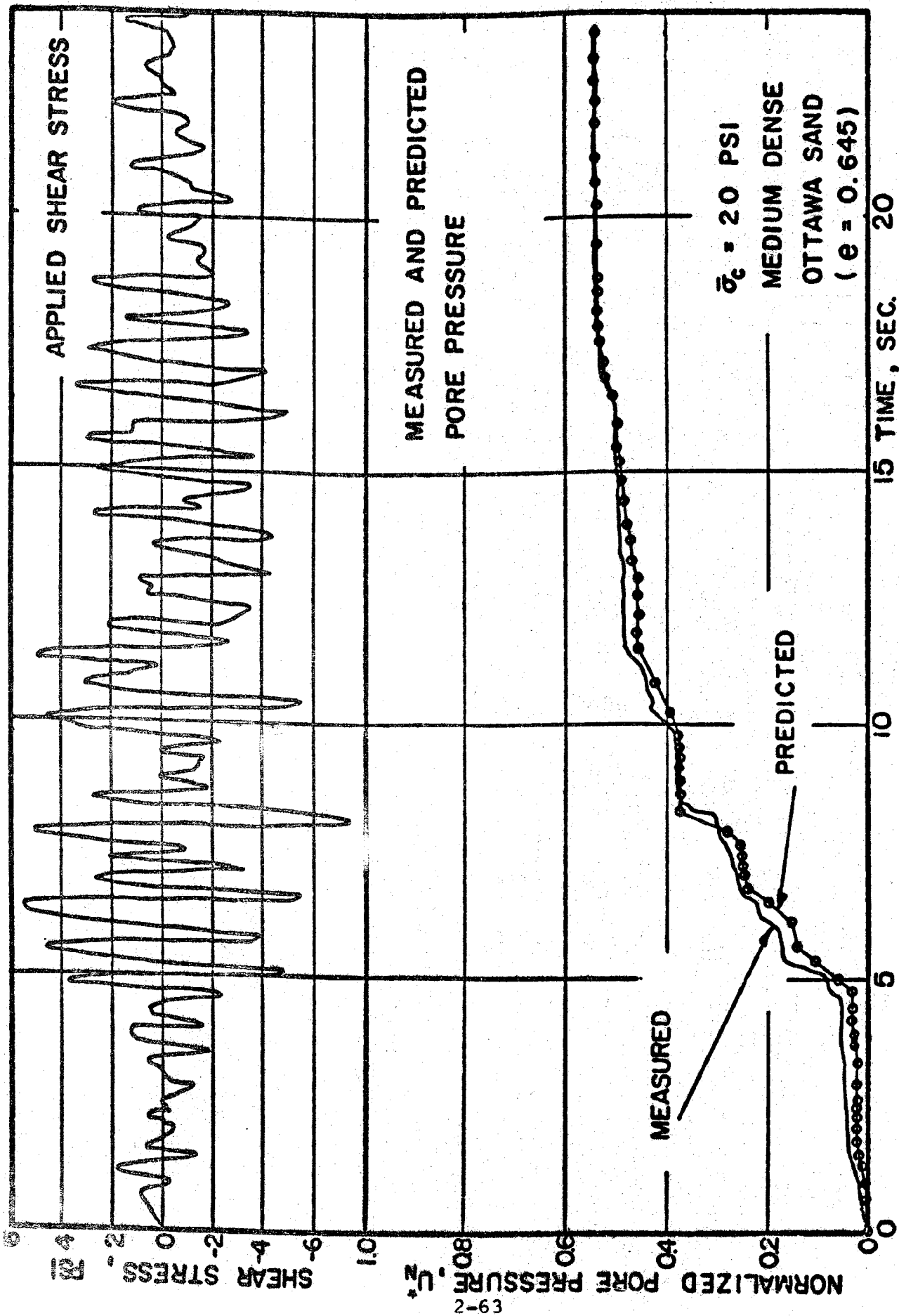
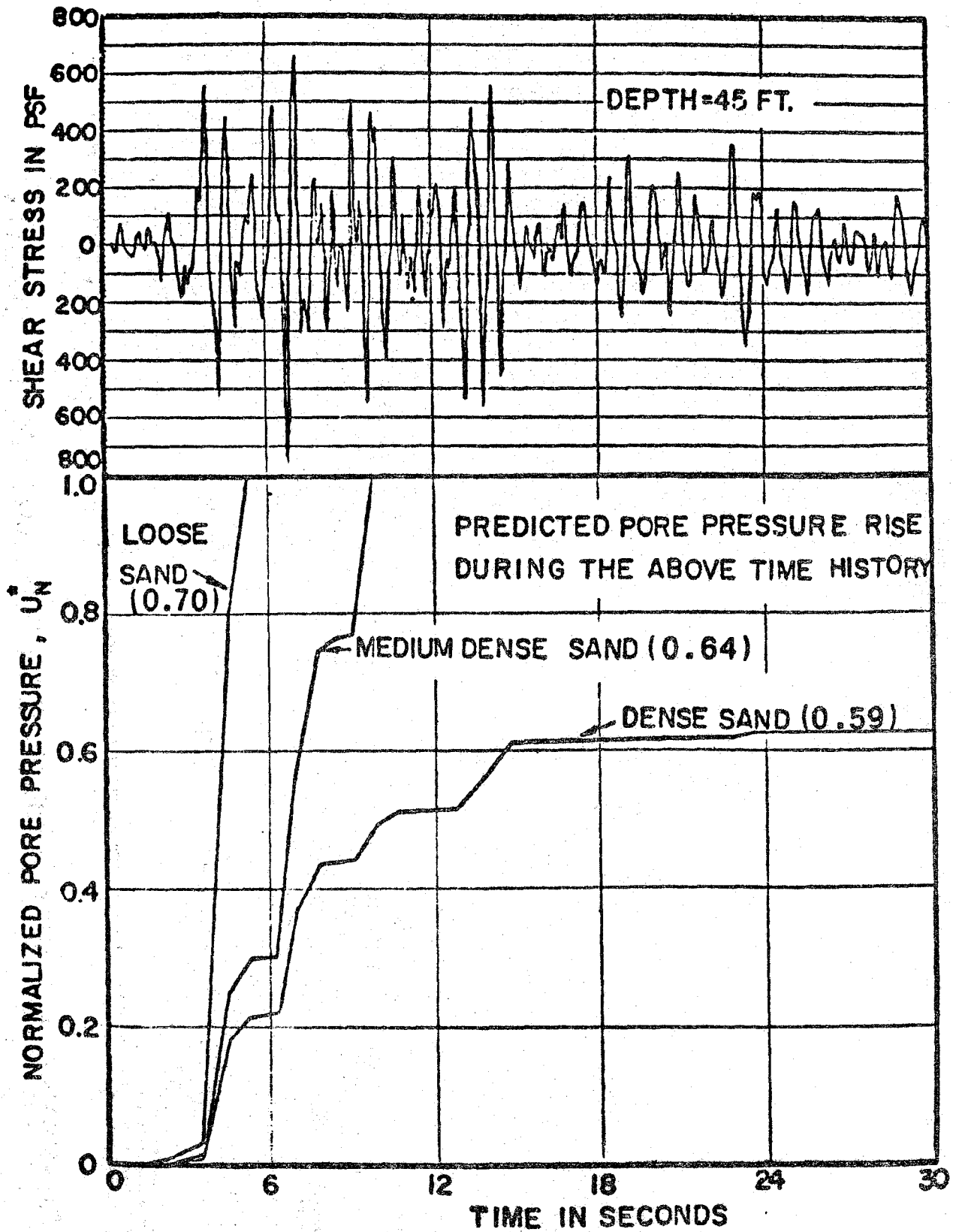


FIG.18 PORE-PRESSURE RISE UNDER EARTHQUAKE-TYPE LOADING



PREDICTED PORE PRESSURE RISE DURING
ACTUAL EARTHQUAKE.

STATUS AND PROBLEMS ARISED IN THE SEISMIC MICROZONATION
IN CHINA

ZHANG ZAIYONG*

ABSTRACT

This paper summarizes several methods of seismic microzonation which have been employed and have been employing in China. At present, the opinion that microzonation by adjusting intensity according site condition in an area should be deleted is much more approved. There is another opinion that correct differentiation should be taken between the two different kinds of earthquake effects, i.e. ground failure and ground motion. The former effect can be avoided basically by site selection and the latter effect has to be reduced by quantitative analysis of seismic response, on the basis of detailed zoning by means of geological units and soil classification, then earthquake design parameters will be determined for each microzone and earthquake damage prediction map or seismic microzoning map will be prepared.

The author discusses in the paper some basic requirements which are necessary for effective microzonation, and puts forward some problems for further investigation.

At the present stage, earthquake-resistant design in China is still based on seismic intensity. The following documents should be ready at hand: (1) seismic zoning map (1:3,000,000 scale) for the purpose of predicting the severity and location of earthquake occurrence by means of intensity; (2) macroseismic intensity scale, used for describing the damage effect resulted from earthquakes qualitatively and (3) earthquake-resistant design code for various structures, the design criterion used is a given intensity level. Determination of earthquake design parameters will be made individually only for special engineering structures of significance.

The seismic zoning map was compiled on the basis of middle-long term earthquake prediction and macroseismic effect field in terms of basic intensity, it provides the expected maximum average intensity in a given region of average site condition for a relative long period (says, 100y). Such a map can't reflect the difference in intensity in two locations resulting from the effect of local site condition. In the meantime, when the intensity rating for a given site

* Associate research professor, Institute of Engineering Mechanics, Chinese Academy of Sciences. Harbin, China.

according to 1:3,000,000 zoning map is adopted, further investigation and adjustment of the basic intensity in the investigated area and its surrounding are perfectly needed, it is, then, the task of seismic microzonation.

Up to now, there has not yet an acceptable and effective method for seismic microzonation in China. The principal existing methods are based upon experience learning from damage in the recent destructive earthquakes and measurement of some parameters characterizing dynamic behaviour of ground motion in situ. General speaking, existing methods include the following.

1. Microzonation by means of intensity adjustment.

The "Chinese building code in seismic regions (draft) of 1959" was carried out by applying Russian investigator S.V. Medvedev's microzoning method, the effect of soil condition and water table elevation on seismic intensity in a region is evaluated by seismic intensity adjustment. As a result of such procedure, seismic load applied on structures will be increased or decreased by a factor of 2 depending upon "rigidity" of soil, which is defined as the product of seismic wave velocity and density of soil layers. Then microzoning map is drafted simply by adjusting the intensity. Figure 1 is the microzoning map of Beijing (Peking) region in 1957, made by the above mentioned method. Experience of historic destructive earthquakes in the recent 20 more years on Beijing region has proved that such a microzoning map is not practical, it does not agree with the actual distribution of intensities in some recent earthquakes. Figure 2 (1) is such an example.

Medvedev's microzoning method is mainly based on the correlation between seismic intensity increment and soil rigidity. This method has not been successfully checked in recent earthquakes, which can be frequently found in references. For example, there exists difference obviously between the seismic microzoning map of Bucharest which prepared by using Medvedev's method and the damage distribution in the Vrancea earthquake, Romania, of March 4, 1977 (2),(3), but the damage distribution in the 1941 earthquake, when compared with that in the 1977 earthquake above mentioned, have similarity between them. According to the historic records, a good deal of similarity exist, such as location of epicenter, size of seismic source etc. Therefore, if source mechanism characteristics, transmission path and historic earthquake records are not comprehensively taken in consideration microzoning map based on the effect of local soil condition alone is not enough.

In spite of its uncertainties, Medvedev's method is still adopted up to the present, because it has been familiar to Chinese engineers. Microzoning method, and the like of Medvedev's, cannot distinguish the damage effects resulting from ground failure and ground motion, on the other hand,

earthquake-resistance can't be obtained by means of increasing seismic intensity. Particularly, for buildings on soft soil, increase in seismic load only will not lead design to safety and economic if structural damage resulted from ground failure is not considered.

2. Microzonation based on soil classification.

As early as 1964, the intensity adjustment method mentioned in the last paragraph has been deleted in the "Chinese building code in seismic region(draft)". Instead, building sites were classified into favorable and unfavorable sites in the code from the point of view of earthquake-resistance. At the same time seismic load and aseismic measures were adjusted appropriately on the basis of various soil and structural characteristics, and soil was also classified into four categories for the determination of design spectra. In 1974, four categories of soil were grouped into three categories in the "Aseismic building code TJ 11-74" (4). Thus, the fact that, in the adjustment of intensity, seismic coefficient was only taken in consideration has been changed, and instead, the frequency content of ground motion brought into consideration. The physical properties of various kinds of soil were specified as the following table.

Soil classification	Design strength (T/M ²)	Density(T/M)		Predominant period (sec.)	Longitudinal wave velocity (KM/Sec.)
		sandy soil	clay		
I	> 40	-	-	< 0.20	> 2
II	15--40	> 1.5	> 1.4	0.15-0.50	1-- 2
III	8--15	1.4-1.6	1.2-1.5	0.35-0.70	0.3-- 1
IV	< 8	< 1.4	< 1.2	> 0.60	< 0.3

Although the term " seismic intensity microzonation" (or site intensity) has not yet been adopted in the existing aseismic building code the contents of the code still consist of the effect of local site condition on ground motion substantially, and the meaning of microzonation has also been extended.

As for soil classification, microtremor and wave velocity measurement data are used in the soil classification besides engineering geological and hydrogeological description. The microzoning map of Tianjin region of 1967 (5) had been prepared by means of soil classification, i.e., to combine just as engineering geological data with the predominant period data in microtremor measurement in the analysis (Fig.3). Although class of seismic soil in a large number of areas based on engineering geological and hydrogeological data is well in agreement with that based on microtremor measurement, yet there is contradiction in some areas. Whether dynamic behaviour of soil layers during strong earthquake motion can be reflected in the microtremor measurements, it is still in question. For example, the relationship

between damage to buildings in Tianjin City and man-made fill in the Hejian earthquake (M=6.4) of 1967 and the relationship between damaged building zones of Tianjin City and man-made fill distribution in the Tangshan earthquake (M=7.8) of 1976 showed that zoning by the seismic soil classification based on the predominant period obtained in microtremor measurement is not agree with the damaged building zones in the strong earthquake. However simplicity of microtremor measurement and its ability of obtaining a large number of data in a short period make its use greatly increasing.

Some researchers have shown that microtremor record is an effective tool for identifying the period of surficial soil layers (i.e. predominant period). In Japan, microtremor techniques are considered as an effective tool for microzonation up to date, in the beginning of sixtieths, the microzoning maps of Toyohashi and Ichinomiya City (6) were prepared by using microtremor techniques. In some cases, those maps were agree with the practical damage distribution. In the Balkan region (7), Chile (8) and other countries, similar microzoning maps were also prepared. They have all found that the results of microtremor measurement are always not in accord with practice because the correlation between microtremor results and damage distribution are not so closely related. Therefore the microtremor techniques are merely an additional tool in microzonation. It must be pointed out that microtremors ranging from 0.1 Hz to 1 Hz are induced by mechanical vibration of industrial equipment, traffic etc. in the surficial soil layers, the total superposition of excitation is reflected through the predominant period of soil layer itself, for this reason, microtremor is only the response of characteristics of the shallow surficial soil layer. Generally speaking, the depth of earthquake focus is rather large compared with that of soil layer even in a shallow earthquake, focal depth may be score km. The seismic wave reaching to the surface depends upon the dislocation pattern of source mechanism and physico-mechanical property of rock, but the effect of property of strong earthquake mechanism and propagation path cannot be reflected comprehensively by microtremor. Moreover, the microtremor response under small strain can't particularly evaluate the response under large strain produced by strong earthquake motion owing to the nonlinear property of soil. It is meaningless to use amplitude of microtremor as an index in the soil classification of the soil, so that extrapolation from microtremor data to strong earthquake effect is unreliable. Detailed study of comparison between the strong motion records of the El Centro earthquake and the microtremor records at the same site carried out by F.E. Udwadia and M.D. Trifunac (9) has shown that the correlation between the response of strong earthquake motion and the microtremor is not obvious, or even no such correlation exists. They have come to conclusion that the microzoning technique by use of microtremor data could not be used as a chief approach. It is commonly realized.

3. Microzonation by means of average weighted shear modulus (AWSM).

Macroseismic data obtained in the past destructive earthquakes in China indicated that there is a good relation between the damage index and the dynamic properties of surficial soil layer which can be represented by the average weighted shear modulus G of soil in term of shear wave velocity. In general, the higher the damage to low-rise buildings on the site, the lower the AWSM, or vice versa. The value of AWSM of a given site may be expressed as,

$$G = \frac{\sum h_i G_i \sum h_i \rho_i v_{is}^2}{\sum h_i}$$

where h_i ---- thickness of the i th soil layer;
 G_i ---- shear modulus of the i th soil layer;
 ρ_i ---- density of the i th soil layer;
 v_{is} ---- shear wave velocity of the i th soil layer;
 $H = \sum h_i$ ---- total thickness of soil layers, 20 m is generally taken.

Average weighted shear modulus G in a region may be assumed to have a normal distribution according to the damage index i of a given site and the AWSM obtained in measurement, then the average value of AWSM G or $G + \sigma$ (where σ is standard deviation) can serve as a measure in microzonation. Further analysis on the basis of available bore-hole logging combined with the wave velocity measured at the given site is made to compute ground motion parameters of each microzone by selecting an assumed "common base" (bedrock or hard soil in a certain depth), replacing the soil layers of each microzone with lumped mass system, introducing a representative accelerometer into the system as an input to the "common base", and using one dimensional shear beam model. The nonlinear property of soil is evaluated in the process of computation. At last, the average acceleration spectra of each microzone, which is used as an earthquake resistant design spectra, are obtained. Tangshan City and Qinhuangdao City (10) microzoning maps were prepared so by the above approach. Such microzoning approach is not only different from the intensity adjustment method, but also different from that based on seismic soil classification. As this approach gives the response spectra directly from the point of view of earthquake-resistant design and for practice use, it must be pointed out that between the damage index of low-rise buildings in macroseismic statistics and AWSM of soil layers, there is certain correlation, but is this correlation available for the structures of other types? The question is far from being settled and needs for further study.

4. Analysis method.

Along with the development of numerical technique, seismic microzonation can be attributed to solving seismic response of multi-layer soil overlying on the semi-infinite bedrock corresponding to various typical site conditions.

It should be noted that applicability of such computing model is so limited that a low velocity soil layer on hard rock is required, and the more contrast the intersurface, the more effective this model. Furthermore, when the assumed "common base" is taken as a surface of bedrock, thus its depth may exert an influence on the predominant period of site, consequently on the safety of these structures, the natural period of which approaches to the predominant period of the site. Secondly, for simplifying the computing model, the horizontal shear vibration of soil layers is considered only, thus it is not feasible in the near field because where the vertical vibration component is really large. For the most simple method of solving the wave equation, the one dimension SH wave incidence is adopted vertically upward, it implies that the principal seismic wave energy arrived is independent of orientation. But, it is not always so practically.

Another similar method is to define seismic response of soil layer profile according to an input accelerogram and to determine design spectra as well as amplification factor of acceleration, their iso-value contours are taken as the basis in soil classification (11).

5. Microzonation based on the comprehensive prediction of earthquake damage.

In China, there is another method in microzoning (12) (13), called as the method of strong earthquake effects prediction which is similar to the seismic microzonation in the San Francisco Bay Region performed by the U. S. Geological Survey (14). This method differentiates two different kinds of earthquake damaging effect, i.e. effect of ground failure and ground motion, and then measures are taken in the consideration of earthquake resistance for the above effects. The regional geological, geomorphological and hydrogeological conditions are the most significant bases for differentiating earthquake effects. Therefore, in microzonation, ground failure probably occurred can be divided into the following categories: (1) collapse and landslip; (2) differential settlement; (3) sand blow and mud spout; (4) extensive settlement and landslide; (5) tectonic and miscellaneous. This method has been used in "The ground failure microzoning map of Beijing region" provided by The Institute of Geology, State Seismological Bureau of China.

The prediction map of rock motion parameters characterizing strong earthquake vibration is prepared on the basis of earthquakes expected to occur in the region, and the magnitude, epicentral distance and source depth, etc. of which are controlling parameters, determined according to data published in the references either in China or in foreign countries.

It can be seen from the previous description that methods used in seismic microzoning in China have not yet been spe-

cified at present, all methods are worth to be further investigated. The principal tendency in developing method of microzonation is to differentiate the two different kinds of earthquake effects correctly, to classify geological units and soil for determination of damage types in each microzone, moreover, quantitative analysis must also be proceeded for determination of design earthquake parameters in each microzone. The above mentioned microzoning technique takes soil effects into consideration only, as to the effect of faulting, topography and others on earthquake damage, not much are considered at present.

Even though the definition of seismic microzonation has not yet been well established so far and no unified method has been adopted, yet microzoning maps prepared by the above method provide measures of relative effect of seismic hazard in each microzone for the land-use designers and engineers. It is suggested by the author that the effective microzonation must be as follows:

1. It must reflect effect of source mechanism, transmission path and local site condition in the particular region. Of course, these effects should not be evaluated by the engineering judgement based on experience only, but also on theoretical base and experiments of earthquake engineering at present.

It is recognized from the recent knowledge of earthquake engineering that the ground motion characteristics at any site is influenced by the above mentioned three factors, certainly, it is difficult to separate these factors quantitatively individually, it is even impracticable sometimes, but for some special case, one of them may play an important role.

Strong motion records have shown that the effect of source mechanism on ground motion in certain cases is far obvious when compared with the effect of local site conditions. Analysing 15 records of earthquakes of magnitude ranging from 3 to 6.8 obtained in El Centro, Udvardi and Trifunac (1973) (15) classified them into 4 groups according to their orientation to epicenter, comparison of Fourier spectrum of each group was made. The first group consists of 4 earthquakes, three of them come from the same source region, but magnitude of each earthquake is not the same, the shapes of Fourier spectrum of each component corresponding to each earthquake are different. At the same recording site, because the transmission path and local site condition are the same, therefore difference of the shapes of Fourier spectrum may be interpreted as the difference of source mechanism and nonlinear effect of soil. Therefore, the effect of source mechanism plays more important role.

Apparently, the above mentioned conclusion is in contra-

diction with the traditional microzoning concept. Many seismologists and engineers realized for a long time that no great difference in the effect of ground motion existed in a city area or a construction site, if there did exist, such difference can be attributed to local soil condition. Such a microzoning method which is based on correlation between damage to low-rise buildings and the surficial soil layer 10-20 m in thickness in terms of macroseismic intensity is still to be adopted extensively. Thus we consider with sufficient reason that such microzoning map is only correct in cases where effect of source mechanism and transmission path can be neglected in comparison with the effect of local site condition and at the same time there are no correlations between the local site condition and the wave incident angle.

Of course, the author does not oppose the idea that local site condition has effect on ground motion characteristics, but has to emphasize the fact that the most important factors governing the damage potential of buildings are the type of incident wave to bedrock, amplification and filtration of surface soil layers and response of building itself, the effect of local site condition can be predominated only in case of the given type of incident wave.

2. For a given site, stability of repeated relative damaging effects during strong earthquake is most important which is independent of its source, and it should be testified by the strong motion records.

The typical example of repeated damaging effect was found in Yutian County, Hebei Province of China, which was a low-anomalous area both in the Sanhe-Pinggu earthquake (M=8) of 1679 and the Tangshan earthquake (M=7.8) of 1976, the epicenters in the two earthquakes were NW60 km and SE50 km respectively. It is noted that damaging effect was independent of the direction from which seismic waves travelled. Certainly, this was a macroseismic phenomenon, and it is a pity that we have not enough strong motion records up to present to testify the repeated relative damaging effect. Therefore, microzoning map based on the data of only one destructive earthquake damage is always unsuitable, because ground motion characteristics are controlled by many factors, and it is difficult to predict the damage model in a future earthquake at a given site which would be similar to that of the previous earthquake. In this sense, nothing can be done in the seismic microzonation reflecting the repeated relative earthquake effect until a large amount of strong motion records are accumulated. From the standpoint of recent knowledge, it is possible to collect strong motion records extensively for various soil condition and to obtain, by extrapolation, ground motion parameters for different soil condition directly from their statistical average values. Moreover, the nonlinear effect of soil must be estimated during extrapolation procedure from weak earthquakes

It is very effective in practice to make clear the repeated relative earthquake effect at a given site by observation of aftershocks after destructive earthquakes. Because the range of source area of aftershocks is well known in general if the source area of aftershocks has somewhat changed, aftershocks always occur so frequently that it is completely possible to obtain a large number of aftershock records in a short time for study of effect of source mechanism, frequency dependent amplitude of ground motion varying with magnitude, relationship between site response and aftershock focus, site amplification, attenuation law, differential ground motion in microzone, etc. Because aftershock records are easily accumulated in a short time, therefore it is possible to divide them into certain groups for study of individual factor. The industrial explosion data may be adopted also, if necessary.

3. On the basis of recent knowledge and technique, there will be many limitations in microzonation carried out only by individual approach (empirical, experimental, theoretical). According to different requirements, seismic microzoning map for different purpose can only be prepared by synthetical analysis using various data.

Practice has proved that destructive earthquake effect (except for secondly damage) may be divided generally into two categories: (1) ground failure effect which is closely related to geological condition, such as surface rupture, differential settlement, sand liquefaction, landslide, etc. All failures can be triggered by earthquakes of specified magnitudes; (2) damage effect resulted from ground motion. When dealing with these two effects, the former can be avoided by selecting favourable sites and deleting unfavourable sites, the latter can be avoided by checking the earthquake resistance of structures for given seismic loading coefficient. Therefore, in view of different requirements a number of microzoning maps for different purposes must be worked out, such as microzoning maps reflecting all kinds of geological effect and maps for earthquake-resistant design of various structures.

4. Measure of dividing relative earthquake effect must be related to the methods in the existing aseismic building code for the convenience of engineering practice. It must be recognized that, in the present stage, earthquake resistant design in China is based on seismic intensity, but at the same time it can't be restricted in using intensity as a criterion, and it is necessary to use quantitative parameters instead of seismic intensity as design criterion gradually, i.e. from using geological, seismological and historical data to engineering design parameters. The design earthquake parameters showing damage effect of strong ground motion can be determined in terms of rock motion expressed by magnitude, epicentral distance and focal depth of earthquakes probably occurred in the given region. For surficial soil layer, further evaluation of ground motion parameters may be calculated

by means of rock motion. The ground motion parameters given for each microzone ought to consist of a number of physical parameters (peak ground acceleration, response spectra and duration, etc.) and their probability of occurrence. For regions which are possible to carry out instrumental study, aftershocks and industrial explosion measurements may be adopted for direct comparison of peak vibration, frequency content, duration, etc. at each recording point with various soil conditions. Design parameters of the given site may be obtained from the recorded spectrum in situ and combination of various data.

5. Since the concept of seismic microzonation has been developed based on the correlation between local site conditions and damage to buildings, then it must be replaced by the soil-structure interaction analysis. No matter how the lumped parameter method or the finite element method is adopted in the interaction study, the structural model and the soil medium are analyzed as a coupling system. In the lumped parameter method, the effect of soil condition is evaluated by equivalent elastic constant and equivalent damping factor, and in the finite element method, soil nonlinear property can be analysed by using equivalent linearization procedures corresponding to given strain, that is to say, the effect of soil condition considered in microzonation will not exist naturally. The effect of source mechanism and transmission path are included in the selection of input ground motion. Such extensive computation may be feasible only, of course, for the most important structure individually. As for ordinary buildings and dwellings, seismic microzoning map is still an indispensable tool for engineers to determine design earthquake parameters and site selection.

REFERENCES

- (1) Li Tze-chiang (1957): Earthquake of Peking, Acta Geophysica Sinica. Vol. 6, No. 2.
- (2) N. Mandrescu (1978): The Vrancea Earthquake of March 4, 1977 and the Seismic Microzonation of Bucharest. 2ICM.
- (3) Lloyd. S. Sluff (1978): Geological Considerations for Seismic Microzonation. 2ICM. Vol. I, P.135.
- (4) Aseismic Building Code (TJ-11-74) (1974)
- (5) Site Intensity Research Group of Beijing and Tianjin region (1967): Report on Site Intensity of Beijing and Tianjin Region.
- (6) Yorihiro Ohsaki (1972): Japanese Microzonation Methods. 1ICM. Vol. I, P.161.
- (7) V. Karnik (1972): Microzoning Programme within the UNDP-UNESCO Survey of the Seismicity of the Balkan Region. 1ICM. Vol. I, P.213.
- (8) R. M. Lastrico (1972): Chilean Experience in Seismic Microzonation. 1ICM. Vol. I, P.231

- (9) F.E. Udawadia, M.D. Trifunac (1972): Studies of Strong Earthquake Motions and Microtremor Processes. 1ICM. Vol. I, P.319.
- (10) Institute of Engineering Mechanics and North China Institute of Prospecting (1977): Preliminary Seismic Microzonation of Fengrun Area in Tangshan City.
- (11) Fu Shengcong, Zhou Xiyuan, Yang Delin (1978): Seismic Response Analysis of Soil in Beijing Urban Area. Beijing Seismological Brigade and Beijing Geological and Geomorphological Prospecting Division.
- (12) Institute of Geology, Chinese Academy of Sciences (1976): Strong Earthquake Effect Prediction and Microzoning Problems in Beijing Region.
- (13) Institute of Geology, Chinese Academy of Sciences (1976): Geological Characteristics and Earthquake Damage Prediction of Beijing and Tianjin Region.
- (14) R.L. Wesson et al. (1972): Preliminary Analysis of Seismic Microzonation in the San Francisco Bay Region. 1ICM. Vol.I, P. 859.
- (15) Luis Esteva (1976): Microzoning Models and Reality. 6WCEE. Vol.I, P. 27.

-
- * 1ICM-- Proc. of the First International Conference on Microzonation, 1972.
 - 2ICM-- Proc. of the Second International Conference on Microzonation, 1978.
 - 6WCEE--Proc. of the Sixth World Conference on Earthquake Engineering, 1976.

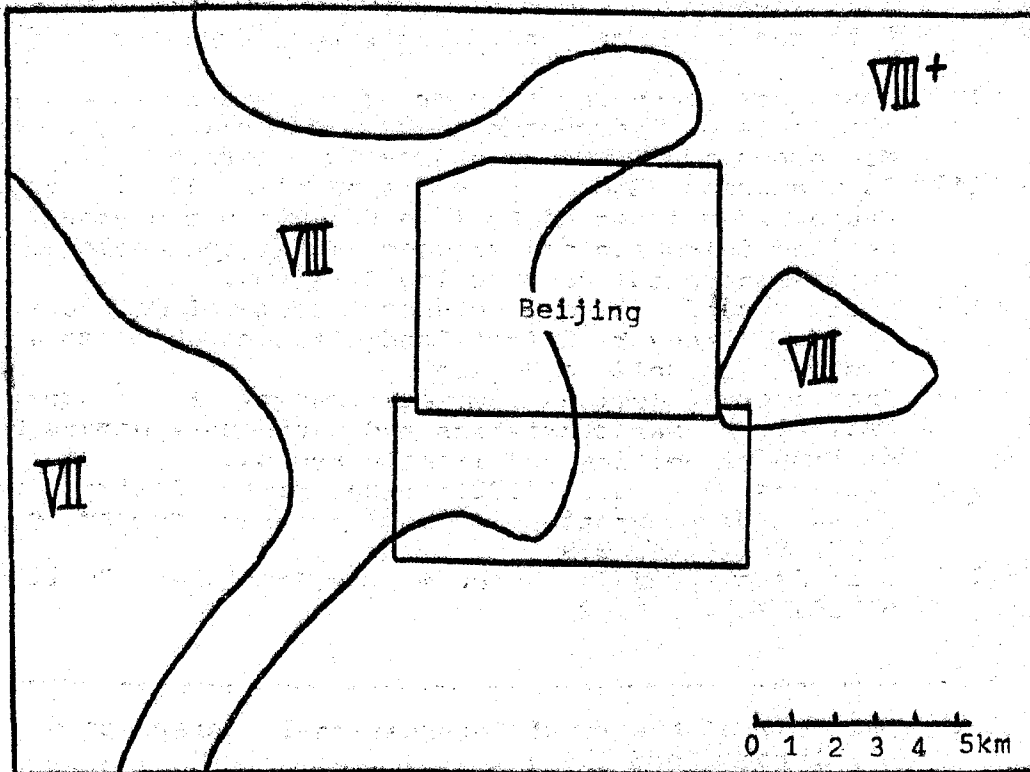


Fig.1 Seismic microzoning map of Beijing (1957)

Roman number shows the "intensity"

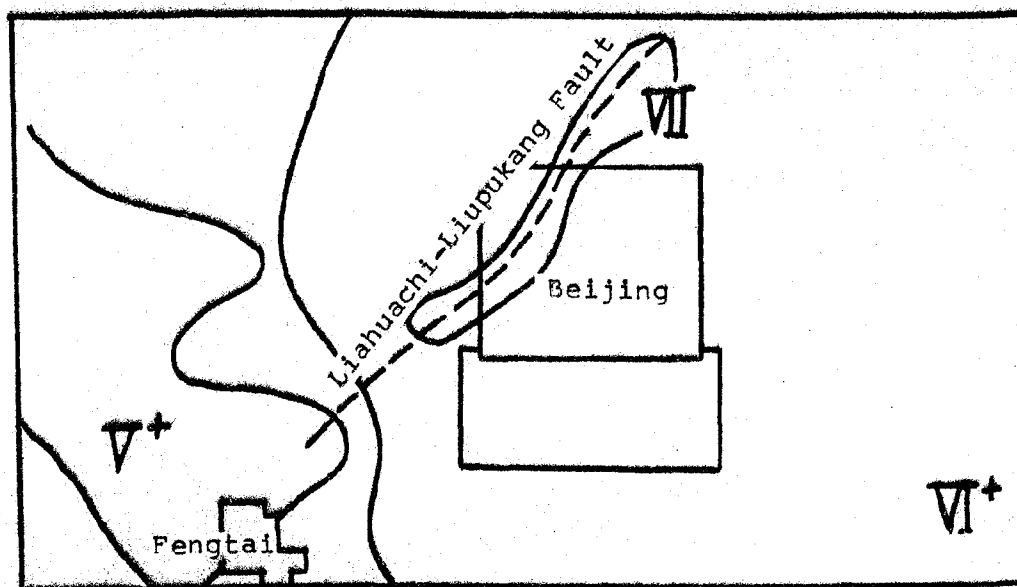


Fig.2 Generalized contour map of intensity distribution in Beijing during the 1976 Tangshan earthquake

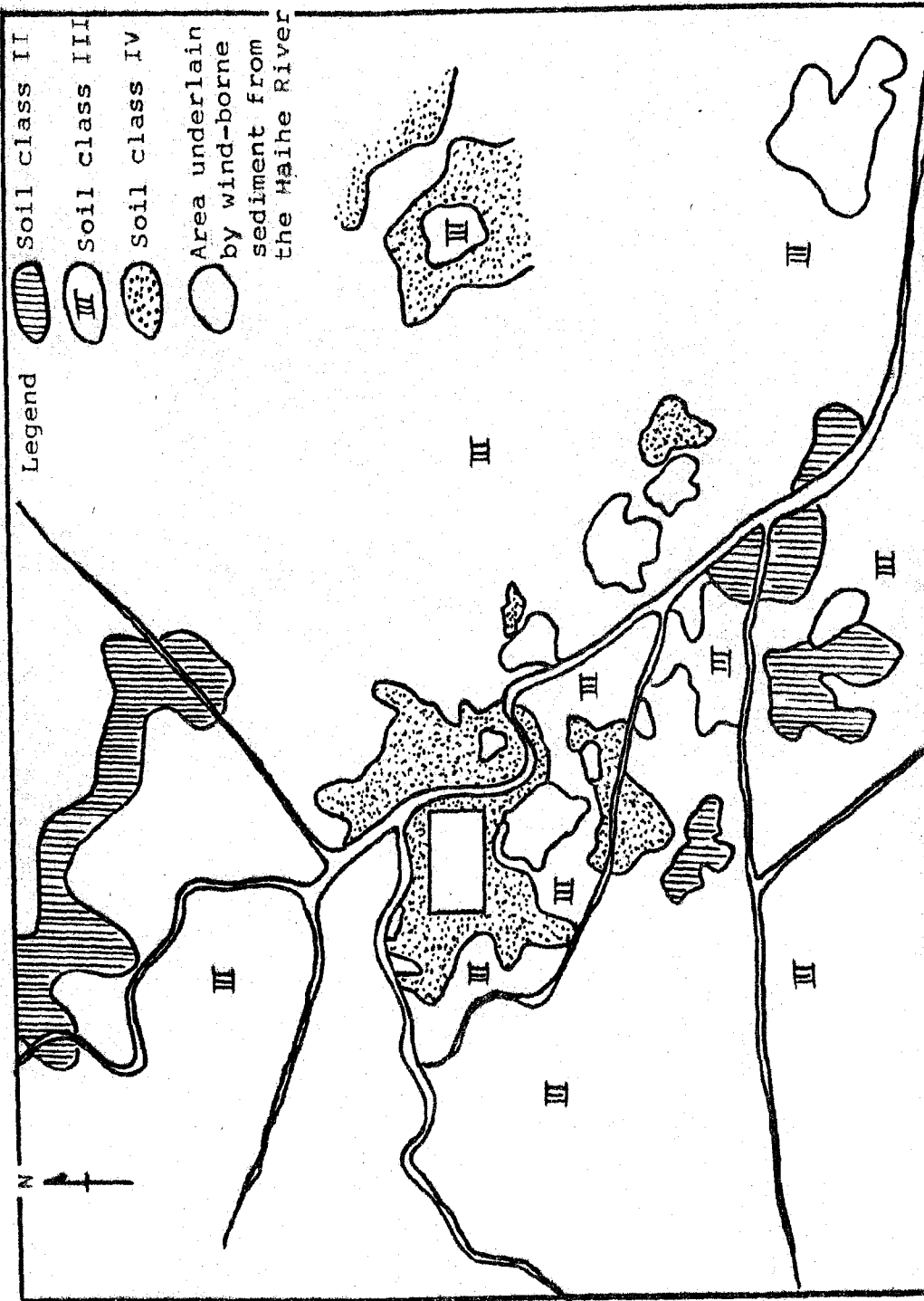
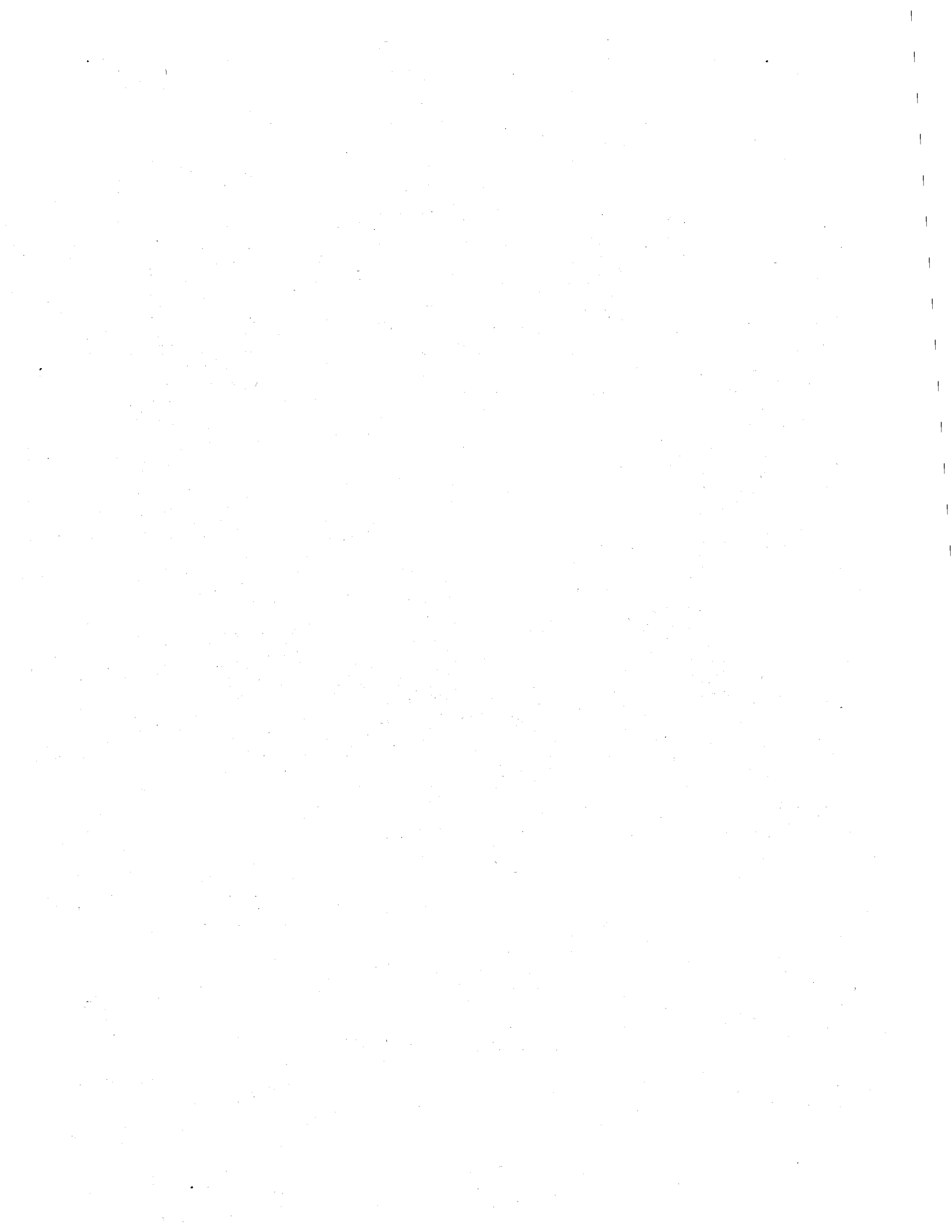


Fig.3 Map of soil classification for Tianjin City



MICROZONATION AND LAND USE PLANNING
George G. Mader

Abstract

Land use planning in the United States provides a number of opportunities for using microzonation techniques. Since most land use planning takes place at the local government level, it is at this level where microzonation applications are to be mainly found. In California, a seismically active region, there are many examples of microzonation as applied to land use planning. Specific examples, described in this paper, are embodied in seismic safety elements of general plans for Santa Clara County, Santa Barbara County and the City of San Francisco. Microzonation as applied to state level regulations are found in state designated special studies zones along active earthquake faults. At the local level, examples of zoning with respect to landslide problems and controlling the subdivision of land with respect to seismic and non-seismic problems are found in the Town of Portola Valley. Two recent programs of the Association of Bay Area Governments for the San Francisco Bay Area focus on the definition of seismic and non-seismic problems for computer systems capable of describing hazards and risks for large areas.

The advancement of microzonation techniques has allowed a steady increase in the use of seismic data in the land use planning process. Many of the increases in the utilization of microzonation techniques have taken place in the last ten years. In the long run, the success of including microzonation techniques in land use planning will depend on more and better geologic and seismic data and greater efforts to inform the public and public officials.

¹George G. Mader, AICP, is Vice-President of William Spangle and Associates, City and Regional Planners, a Senior Lecturer in the School of Earth Sciences at Stanford University, and Chairman of the California Seismic Safety Commission.

INTRODUCTION

Most city and regional planners in the United States advise governments on the desirable distribution of public and private land uses. Planners' advice is conditioned by economic, social, political and physical factors. Seismic considerations are one of the physical factors. To the extent planners have better information on how land and buildings will react in an earthquake, the better they will be able to advise client governments.

A number of advances in the application of seismic information to land use planning have been made in the last ten years in the United States. Many of these advances have occurred in the State of California, an area of high seismicity, in the aftermath of the 1971 San Fernando Earthquake in Southern California which had a Richter Magnitude of 6.4. This paper summarizes some of the most recent applications of seismic information to land use planning and describes emerging efforts to improve the state-of-the-art. Examples are drawn from the State of California.

In order to understand the role of land use planning in the United States, it is necessary to have some appreciation of governmental structure. Each of the fifty states in the United States has a large amount of control over affairs within the state other than those of national significance. Typically, each state is made up of a number of counties, and the counties are in turn made up of incorporated areas called cities, and unincorporated areas which are controlled directly by the county. Most decisions about land use are made by the city or county, the lowest levels of government. In some instances, states directly control land use when it is in the state interest to do so. The national government, while using methods to encourage certain land uses, does not directly control the use of land. In addition, there are special governments or voluntary associations of governments which are formed with the consent of the electorate for special purposes. Most applications of microzonation techniques to planning are found at the local, city or county, level while some applications are emerging at the regional level.

The major planning documents utilized at the city and county levels are portrayed in Figure 1. This figure illustrates the hierarchy of plans and regulations and their relationships to geology and development proposals. The general plan is a policy document, not a law, and forms the basis for most land use planning. It states general goals and includes a map showing land uses proposed for the next 20 to 30 years. It is the standard against which all proposals for changes in land use are judged. The zoning ordinance is based on the general plan and precisely delimits areas in which different land uses are permitted and quantifies such matters as the density of population, the size of lots, the distance buildings should be set back from property lines, and the height of buildings. The subdivision ordinance sets forth the requirements that have to be met before land can be divided for sale as individual parcels. It includes standards for such items as roads and utilities. The site development ordinance regulates the manner in which land is graded for the construction of buildings, roads and other uses. Finally, the building code regulates the manner in which buildings are constructed.

Each of the plans and regulations in Figure 1 provides an entry point for the use of geologic and seismic data. Information on microzonation, therefore, has a potential application with respect to each of these plans and regulations. The summaries that follow relate to these types of plans and regulations.

Throughout the examples presented in this paper, two recurrent themes occur:

bridging the gap between scientists, who produce data, and planners and politicians who use data; and defining risk in terms that will assist decision-makers. There has been much progress made in producing data that can be applied to land use decisions; however, often this data is not adequately translated into terms that help the planner make land use recommendations. In the examples that follow, there is a wide range of types of data used and methods of translating the data into terms useable by planners. The second recurring theme, risk, is inherent in any land use decision. The recognition of risk may be very general or may be articulated in great detail. The examples that follow provide a variety of approaches to dealing with the definition of risk.

SEISMIC SAFETY ELEMENTS

In the State of California, all cities and counties are required to have general plans. In addition, in 1971, the California State Legislature adopted a law that required general plans to include seismic safety elements. This requirement is particularly relevant to microzonation in that it requires each city and county to make an inventory of seismic hazards for the entire jurisdiction and then to take this information into account in establishing policy for the use of land and buildings. Examples of seismic safety elements from Santa Clara County, Santa Barbara County and the City of San Francisco are described below.

Santa Clara County

Santa Clara County is situated in the southern portion of the San Francisco Bay Region and encompasses 1,316 square miles (3,422 square km.), with a population of 1,235,000. Most of the county is divided into incorporated cities, but major areas are still unincorporated and therefore under the direct control of county government.

When the state requirement for seismic safety elements was imposed, detailed geologic information for the entire county was not available. The approach utilized by the county was to assemble geologic data that was available and from that data, prepare a county-wide map indicating the likelihood of seismic and geologic problems in all parts of the county. The map is shown as Figure 2 and portrays three relative stability zones:

1. Where geologic investigation is normally required.
2. Where geologic investigation may be required.
3. Where geologic investigation is not normally required.

In practice, the county geologist uses this map as an aid in determining whether the proponent of a development will be required to have soils and geologic investigations made of his property before the county will approve the project. If a report is prepared, it is reviewed by the county geologist and must meet his approval.

This is a crude approach to microzonation in that very broad areas are defined. It does, however, differentiate between areas and provides a basis for requiring detailed reports where deemed necessary. On the other hand, it does not provide guidance to the county or land owners as to the nature of geologic problems and whether proposed land uses are likely to be accepted.

In this instance, the bridge between the data producers and data users is found in the relative stability map and the county geologist who must interpret the map

and geologic reports for the planners. The question of risk is only generally dealt with in the three broad categories on the map. Further definition of risk takes place with respect to individual soils and geologic reports.

Santa Barbara County

Santa Barbara County lies about 75 miles (120 km.) north of the City of Los Angeles in California. The county contains 2,745 square miles (7,137 square km.), with a population of 294,000. Vast areas of the county are undeveloped and under the land use control of the county government.

Santa Barbara went considerably further than Santa Clara County in quantifying geologic problems. Its program included assembling data for the entire county on ground shaking, tsunami-seiche, liquifaction, slope stability, expansive soils, soil creep, compressible/collapsible soils, high groundwater and surface rupture from faulting. All of this data, with the exception of that pertaining to surface rupture, was tabulated on a 90 acre (36 ha.) grid cell system for the entire county, plus a 5 acre (2 ha.) grid cell system for four urban areas. Surface rupture, since it is a linear feature, was treated separately.

Each 90-acre grid cell was rated 1, 2 or 3 for each hazard based on the following system: 1 = none to low hazard, 2 = moderate hazard, 3 = high hazard. A second number was then used to indicate possible variability from the rating due to potential local variations, lack of basic data and subjective evaluations. Each hazard was given a weight representing its importance relative to the other hazards. The weight was a judgement based on three considerations:

1. Consequences of the problem. (Would loss be to life or property and what would be the severity?)
2. Frequency of occurrence.
3. Difficulty of prevention or mitigation.

The weights assigned to each hazard, were as follows:

Seismic severity (ground shaking)	18
Tsunami-seiche	19
Liquefaction	15
Slope stability	23
Expansive soils	7
Soil creep	4
Compressible/collapsible soils	11
High groundwater	3

100 (lowest possible score
assuming rating of 1
for all hazards)

Next, a weighted rating was obtained by multiplying the weight by the rating. The sum of weighted ratings for each land unit is called the GPI (geological problem index). The range of weighted ratings was 100 - 236 (300 maximum). No cell received a maximum rating because some problems are confined to flatland or hillside areas and no cell had a high rating for all hazards. The GPI was assigned to categories as follows:

<u>GPI Range</u>	<u>Category</u>	<u>Severity</u>
100 - 125	I	low
126 - 145	II	low-moderate
146 - 180	III	moderate
181 - 210	IV	moderate-severe
211 - up	V	severe

The GPI was calculated for each 90-acre grid cell county-wide and for each 5-acre grid cell in four urban study areas. Computer mapping of the five categories shows the relative severity of geologic hazards throughout the County and in the four urban areas. An example of the system as applied to a portion of the county is shown in Figure 3.

Based on the GPI, the following land use recommendations were included in the seismic safety element:

1. Consider areas in Category V for natural areas, recreational or agricultural use, possible low density use.
2. Consider Category IV lands for low density use or non-development. Cost of safe development may be high.

In this example, the development of weighted ratings represents a considerable step forward in bridging the gap between data producers and users. The user has specific numbers which represent the best judgement of those who provided the data. The system does not, however, indicate the severity of the hazards for different types of land uses. The matter of risk, however, has been addressed at least in comparative terms through the weighted ratings.

City of San Francisco

The City of San Francisco shares a serious problem with many other older cities in the United States, the presence of numerous old unreinforced masonry buildings. The problem in San Francisco was to identify the severity of this hazard and to undertake remedial programs.

The buildings that are most hazardous are known as pre-code Type C buildings. These buildings were constructed before 1948 when comprehensive lateral force requirements, specifically considering seismic forces, were incorporated into the San Francisco building code. Type C buildings have masonry or concrete exterior bearing walls with wood floors and roofs.

The study identified geologic conditions affecting ground motion and structural conditions. The mapping revealed over 1,400 residential buildings with nearly 35,000 living units and 2,800 non-residential buildings as pre-code Type C. Figure 4 shows the distribution of the non-residential pre-code Type C structures. Figure 5 shows estimated building damage from a "1906 Type" earthquake (The 1906 San Francisco earthquake is estimated to have had a Richter Magnitude of 8.3). A high degree of correlation between the pre-code Type C buildings and estimated building damage can be seen by comparing Figures 4 and 5. The identification of the problem, however, has not been significantly followed by a program of removal or strengthening of old buildings other than through normal building demolition for redevelopment or through conversion of older buildings to newer uses.

This study provides detailed identification of hazardous old buildings and indicates the high level of risk these buildings present. In this manner, it bridges the gap between the data producer and user, and helps define risk levels.

SEISMIC SAFETY REGULATIONS

The discussion in the preceding section addressed seismic safety elements of general plans. It should be remembered that general plans are policy documents and do not have the strong effect that laws or regulations have. In this section, several examples of regulations will be discussed. These regulations require that specific precautions be taken with respect to seismic hazards.

Regulations that govern land use based on seismic considerations are not as fully developed as are seismic safety elements. This is due to hesitancy on the part of government to enact regulations in this subject area and also the developing nature of the state-of-the-art of such regulations. Several examples will be presented, all from the State of California.

State Designated Fault Zones

Normally, states do not regulate land use, but instead leave this matter to local jurisdictions. One exception to this general rule is land use in the vicinity of active earthquake faults in California. The Alquist-Priolo Special Studies Zones Act, adopted in 1972, directs the state geologist to delineate special studies zones along potentially and recently active fault traces in the state. The zones are ordinarily less than a quarter mile wide unless special conditions warrant a wider zone. An example of a special studies zone is shown on Figure 6. Once the maps have been issued by the state geologist, local jurisdictions must require developers to prepare geologic reports for any development within the zones. When a trace is located through such a zone, state regulations prohibit construction of buildings for human occupancy across the trace or within 50 feet of the trace unless geologic investigation proves the absence of active branches of the fault.

This regulation is a significant example of microzonation applied to land use planning for a very large area. Proponents of the law thought that of all of the possible seismic problems, faulting should be the easiest one to map for regulation purposes. They also believed politicians could be convinced to recognize this hazard in land use regulations. In practice, however, the regulation has been rather difficult to develop and administer. Because the precise locations of all active faults in California were not known, the special studies zones were defined as rather wide bands. While these wide bands were justifiable, given our knowledge of fault location, they had the adverse effect, from the property owner's point of view, of casting a shadow over all properties in the zone, even though a very small percentage of properties were actually over or close to a fault. Furthermore, where faults were not recognizable from surface features, it was hard to communicate to lay persons that the faults actually existed. This later problem has led the state to concentrate the regulation on faults with surface expression. On the positive side, the regulation has greatly heightened the awareness of developers, land owners and realtors of the faulting problem. Also, the regulation has led to the mapping and avoidance of active faults.

The experience of tying state-wide regulations to geologic hazards has been enlightening. The problems encountered give cause for very careful consideration

before enacting state requirements relative to other geologic hazards. On the other hand, the significance and potential impact of state legislation in this subject area has been demonstrated.

Landslide Regulations

In California, with all of its hills and mountains, landslides are a major hazard under seismic and non-seismic conditions. Mistakes have been made in the past in allowing development in landslide terrain without recognizing the hazard. In recent years, however, increased attention has been given to the problem. Many cities and counties now require soils and geologic reports prior to approving a development. In such a process, landslides are either avoided or engineering designs are developed to handle the problems. Nevertheless, there is a need to recognize the presence of landslide terrain as early as possible in the planning and development process so that longer range plans can be prepared which take the landslide areas into account.

The Town of Portola Valley, a small community of 10 square miles (16 square km.), a population of 4,000, occupying a valley and hills in the San Francisco Bay Area, has developed a detailed microzonation approach to landslide problems. It should be pointed out that this innovative work would probably not have been undertaken had it not been for several costly landslides in the community that caused the elected officials to recognize that the town had to deal with landslides. To address the problem, the town undertook geologic mapping of the entire town at a scale of 1 inch equals 500 feet (1 cm. = 60 m.). The map of geology, however, did not provide direct information as to the likelihood of landslides and therefore a second map was prepared based on the geology map and called the "Movement Potential of Undisturbed Ground" map (see Figures 7 and 8). This derivative map rates all of the geologic formations in terms of their relative stability.

With this mapping in hand, the next step was to establish policies for land uses for each of the stability categories. To accomplish this, the town council appointed a committee composed of four geologists, two engineering geologists, a soils engineer, an attorney and a planner. Based on their professional judgements, the members of the committee prepared a table indicating land use limitations for each of the landslide categories. This table is in effect the link between scientific and engineering knowledge on one hand, and land use planning on the other. While risks were not quantified in the preparation of the table, the committee operated under instructions from the town council to prepare criteria to reduce the risk of failure of development from landslides to a very low level. The table is shown on Figure 9.

The maps and policy have been in effect since 1974 and have proven to be effective guides to development. The policy, adopted by the town council, includes provisions for modifications of the maps if subsequent investigations indicate inaccuracies in the maps. Thus, in this example, the interpretive map and policies bridge the gap between data producers and data users, and provides guidance for land use decisions in order to minimize the risk of damage from landslides.

Subdivision Regulations

If all geologic problems have not been identified in the seismic safety element or through area-wide mapping and regulation, as described above for landslides, a significant opportunity to identify and deal with geologic problems exists at the subdivision stage. A simple provision in subdivision regulations that requires

preparation of soils and geologic reports by the developer and subsequent review of such maps by a geologist, retained by the city or county, can in effect result in microzonation.

An example of the subdivision approach is again drawn from the community of Portola Valley. In this instance, a developer proposed to develop 450 acres (180 ha.) of land. The town's subdivision regulations required that before the town would approve any plan, the developer would have to prepare a geologic study of the property that would be satisfactory to the town geologist. The developer retained a geologist to prepare such a map (Figure 10). After the mapping was completed, the property owner found to his surprise that his property had several active fault traces and numerous active landslides. The developer was able, however, to design a subdivision in which these problems were avoided. In several important areas, however, he was required to undertake extensive engineering projects to solve problems of instability. The geologic information, translated into relative stability terms, and the proposed lot layout are shown on Figure 11.

This example argues strongly for government requirements for detailed geologic data at the time of development. This is a crucial stage for data producers and data users to communicate fully. Once land is subdivided, the future property owners will want to develop their land and they should be protected from major unforeseen geologic problems to the maximum extent feasible.

EMERGING APPROACHES

Problems of translating seismic risk in terms that are meaningful to planners and politicians persist. One problem is that most studies result in comparative terms such as "high", "moderate", and "low", or numbers that are abstract, such as the point system used in the Santa Barbara seismic safety element described earlier. A second problem is the need to translate seismic information into measurements of potential building damage for all geographic portions of a planning area. Each of these problems has been dealt with in two innovative studies carried out in the Association of Bay Area Governments (ABAG), one on land capability, in cooperation with the U.S. Department of Housing and Urban Development (HUD) and the United States Geological Survey (USGS), and the other on earthquake hazards mapping, in cooperation with USGS.

Land Capability Analysis

The first study, entitled, Qualitative Land-Capability Analysis, applied a land-capability analysis technique to a portion of the San Francisco Bay Area. The study relied on basic and interpretive geologic maps that had been prepared during an extensive study during 1970 to 1976 by USGS and HUD of the San Francisco Bay Area. In essence, the land capability analysis study involved the following steps:

1. Selection of basic data maps.
2. Development and use of interpretive maps on the following subjects:

- Surface-rupture potential
- Ground-shaking potential
- Stream-flooding potential
- Dike-failure inundation potential
- Dam-failure inundation potential
- Landslide potential
- Soil-creep potential
- Shrink/Swell potential

Liquefaction potential
Settlement potential
Erosion and sedimentation potential
Septic-tank limitations
Sand and gravel potential
Mercury-extraction potential
Agricultural potential

3. Selection of the following land uses for analysis:

Rural or agricultural
Semirural residential
Single-family residential
Multifamily residential
Regional shopping centers
Downtown commercial
Industrial
Freeways

4. Analysis of each land use with respect to each interpretive map for each cell in the study area. The study area included approximately 332 square miles (830 square km.), and was composed of grid cells of approximately 24.9 acres (10 ha.). The analysis consisted of an estimation of costs related to: damage potential from natural hazards (such as floods, landslides, or earthquakes); fees for special investigations, designs, or construction practices necessary to mitigate natural hazards or remedy site deficiencies; and losses of potentially valuable natural resources such as sand and gravel.
5. A computer system was used to add the costs for all factors for each cell and generate a printout for each land use. See Figures 12 and 13 for an illustration of the computer map and derived data for one land use-- multifamily residential.

This study represents a significant step forward in the utilization of earth science data in land use planning. Its advantages are that it addresses risk (except life loss and casualties) in terms of dollars, a term that people understand. It also allows the addition of costs for various hazard and resource factors. Unfortunately, this degree of sophistication has not been developed by the planning profession for dealing with all of the other factors that determine land use such as economic, social, political and other earth science and non-earth science physical factors.

Earthquake Hazard Mapping

A second ABAG study has linked earthquake information to an ABAG computer program covering the entire San Francisco Bay Area. This computer program, titled Bay Area Spatial Information System (BASIS), has recorded the entire Bay Area into cells of 2½ acres (1 ha.). The earthquake hazard component of BASIS is only partially complete at this time. Steps involved in developing the earthquake hazard component have consisted of the following:

1. Six basic earthquake hazard maps have been put in the system, as follows:

Geology
Faults

Topography
Landslides
Tsunami inundation areas
Dam-failure inundation areas

2. The basic earthquake data maps have been combined or used individually to form nine hazard maps as follows:

Maximum ground shaking intensity
Risk of ground shaking damage
Liquefaction susceptibility
Liquefaction potential
Rainfall-induced landslide susceptibility
Earthquake-induced landslide susceptibility
Fault surface rupture
Tsunami hazard areas
Dam failure hazard areas

3. The hazard maps can be manipulated to produce the following:

Computer assisted environmental assessment
Production of composite hazard maps
Assessment of property and population at risk

These manipulations are possible in part because of the vast amount of other data already in the BASIS system including the following:

Physical Environment

- . average annual precipitation
- . vegetation
- . National Flood Insurance Program maps
- . flood-prone areas
- . coastline features from U.S.G.S. 7½ minute quadrangles
- . soil associations
- . average yield from wells
- . digital terrain tape elevations
- . slope stability
- . air quality problem areas
- . water quality problem areas

Social Environment

- . 1970 census tracts
- . county boundaries
- . city sphere-of-influence boundaries
- . airports, seaports, vacant industrial lands
- . some transportation data
- . landfill sites and service areas

4. Derivative maps from the project include the following:

Maximum ground shaking intensity
Risk of ground shaking damage (to wood frame dwellings, concrete and concrete block and steel frame buildings, and tilt up concrete buildings.)
Liquefaction potential

Rainfall induced landslide susceptibility
Earthquake induced landslide susceptibility
Tsunami inundation
Dam failure inundation
Composite maximum earthquake damage (for wood frame dwellings both
with and without dam failure)

Figures 14 and 15 portray the composite maximum earthquake damage to wood frame dwellings assuming dam failure.

The ABAG study has advanced the state-of-the-art in predicting damage levels to existing and future land uses on a fairly small area basis (one hectare). The program has a major advantage of being tied in to data on a wide variety of subjects and thus allows better integration into complex planning studies. It also has the advantage of allowing the user to test a variety of input data. At this point, the BASIS system is just beginning to be used by planning agencies in the San Francisco Bay Area in developing their seismic safety elements.

CONCLUSIONS

This paper has construed the term microzonation broadly. Essentially, it has been assumed that the definition of seismic effects for specific areas can be termed microzonation. Applying this definition to the land use planning process as practiced in the United States, and in particular California, allows the identification of a number of examples where land use planning has made use of microzonation data. The eight examples cited have been intended to portray a range of applications that is rather representative of the state-of-the-art of applying microzonation techniques to land use planning. Based on this brief review, several conclusions can be reached:

1. In order for microzonation techniques to be an effective ingredient in land use planning, they must take advantage of the entry points in the established land use planning process. Thus, we find examples mainly in conjunction with general plans, zoning and subdivision processes. Most of the examples cited come under these categories.
2. In general, it is easiest to use small area seismic data at time specific developments are under consideration by government. At this time it is possible to require detailed soils and geologic information and obtain the most precise answers to questions. For decision-makers, the information and choices are specific and not abstract. An example of such an application was the subdivision in the Town of Portola Valley.
3. The larger the area being considered and the more remote the time of development, the more difficult it is to include microzonation considerations into the land use planning process. One problem is simply being able to develop sufficiently detailed basic information, such as in the case of Santa Clara County where county-wide generalized data had to be used. Another problem is the need to deal with risk in a more abstract manner than when an actual development is being planned. The two ABAG studies cited have made significant progress by describing risk in terms of dollars and specific damage estimates for large areas.

4. Requiring the use of geologic and seismic data at the local level by a superior level of government, such as the state, requires great care. The dilemma is whether to control land use relative to hazards directly or in a general or indirect way. The requirement for seismic safety elements in California is a very general requirement. It allows great variety at the local level in implementation. While this is desirable from the point of view of most local governments, one can question whether such governments are adequately addressing seismic problems. The Alquist-Priolo Special Studies Zones Act, on the other hand, requires compliance with rather specific state requirements. This later legislation has often been objected to by local governments. While the differences of point-of-view are often mainly the reflection of a provincial attitude of local government, there also is an argument to be made for the fact that the level of data available and its interpretation is important to the success of a requirement. In general, experience is showing that the better the available seismic information is, the more likely it is that the public can require that attention be paid to seismic problems. This argues, then, for increasing efforts to describe seismic hazards in terms that are meaningful to the public at large and local governments.

5. The use of microzonation techniques in land use planning is continually increasing as better microzonation techniques are perfected that provide the type of data planners need. Advances in seismic safety policy, however, are the result of a blend of factors. These include: a greater awareness by the public and public officials of earthquakes, their problems and approaches to dealing with the problems; increasing legislation requiring governments to recognize seismic hazards; and continual education of professional planners relative to seismic hazards and mitigation techniques.

BIBLIOGRAPHY

- Association of Bay Area Governments, 1980, A Guide to ABAG's Earthquake Hazard Mapping Capability: ABAG, various pagings.
- Blair, M.L. and Spangle, W.E., 1979, Seismic Safety and Land Use Planning - Selected Examples from California: U.S. Geological Survey Professional Paper 941-B, 82 pages.
- California Public Utilities Resources Code, 1972, secs. 2621-2625, Alquist/Priolo Special Studies Zones Act.
- Hart, E.W., 1977, Fault Hazard Zones in California, 1977: California Division of Mines and Geology, Special Publication 42, 24 pages.
- Laird, R.T., Perkins, J.B., Bainbridge, D.A., Baker, J.B., Boyd, R.T., Hunstrom, D., Zucker, M.B., and Staub, P., 1979, Quantitative Land Capability Analysis: U.S. Geological Survey Professional Paper 945, 115 p.
- Livingston and Blayney, 1974, Santa Barbara County Comprehensive Plan, Seismic Safety Element: Livingston and Blayney, City and Regional Planners, San Francisco, California, 93 p.
- Mader, G.C., 1974, Earthquakes, Landslides and Public Planning: Cry California, Journal of California Tomorrow, San Francisco, Vol. 9, no. 3, pages 16-22.

Mader, G.G., 1977, Land Use Planning for Seismic Safety: Summer Institute for Architectural Faculty, American Institute of Architects Research Foundation, Washington, D.C., pages 27-58.

Mader, G.G., and Crowder, D.F., 1971, An Experiment in Using Geology for City Planning--The Experience of the Small Community of Portola Valley, California: U.S. Department of Interior and U.S. Department of Housing and Urban Development, Environmental Planning and Geology, pages 176-189.

Portola Valley, Town of, 1975, Movement Potential of Undisturbed Ground: Town of Portola Valley, map.

San Francisco Department of City Planning, 1974, A Proposal for Citizen Review, Community Safety, the Comprehensive Plan of San Francisco: Department of City Planning, San Francisco, California 69 pages.

Santa Clara County, 1975, Seismic Safety Plan, An Element of the General Plan: San Jose, California, 75 pages and appendices.

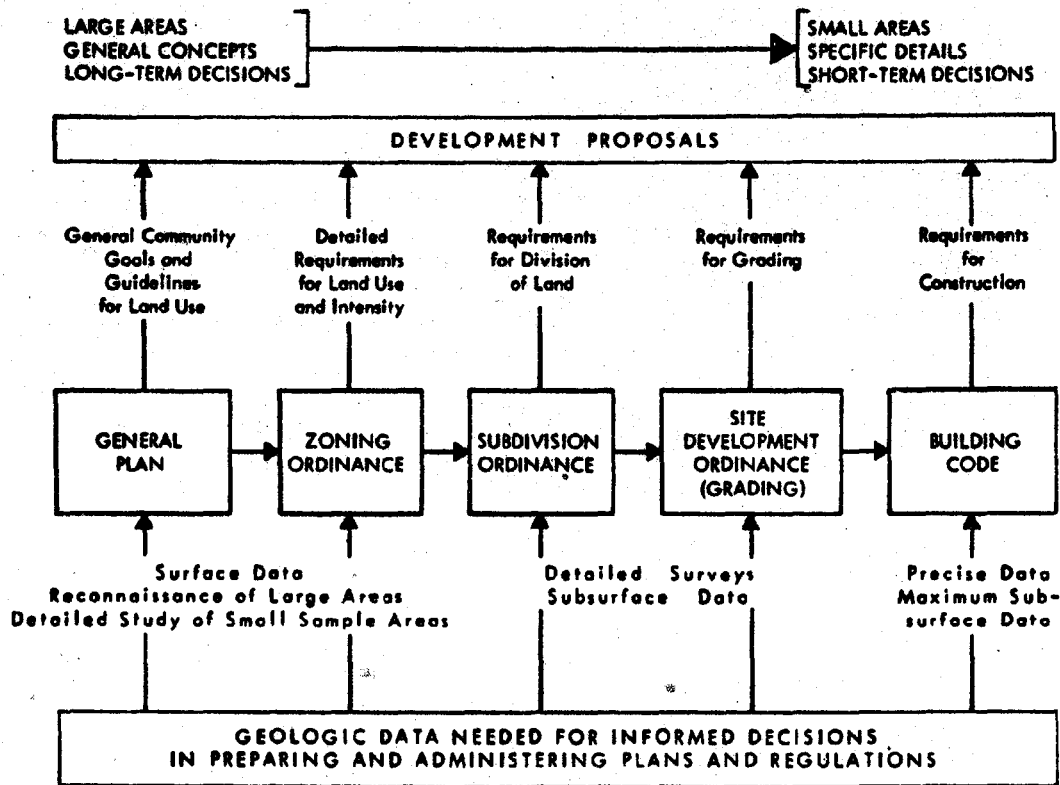


Figure 1. The sequence of plans and regulations central to the land use planning process are portrayed horizontally in this diagram, starting with the general plan. As the focus of the planning process moves from the general plan and concern for large areas, to the building code and concern for small areas, the need for geologic data gradually changes from reconnaissance type data to precise data for specific sites. (Mader, 1971)



Figure 2. An illustration from the Santa Clara County Seismic Safety Element, a portion of the County's general plan, showing zones of relative stability. (Santa Clara County, 1975)

Reproduced from
best available copy.

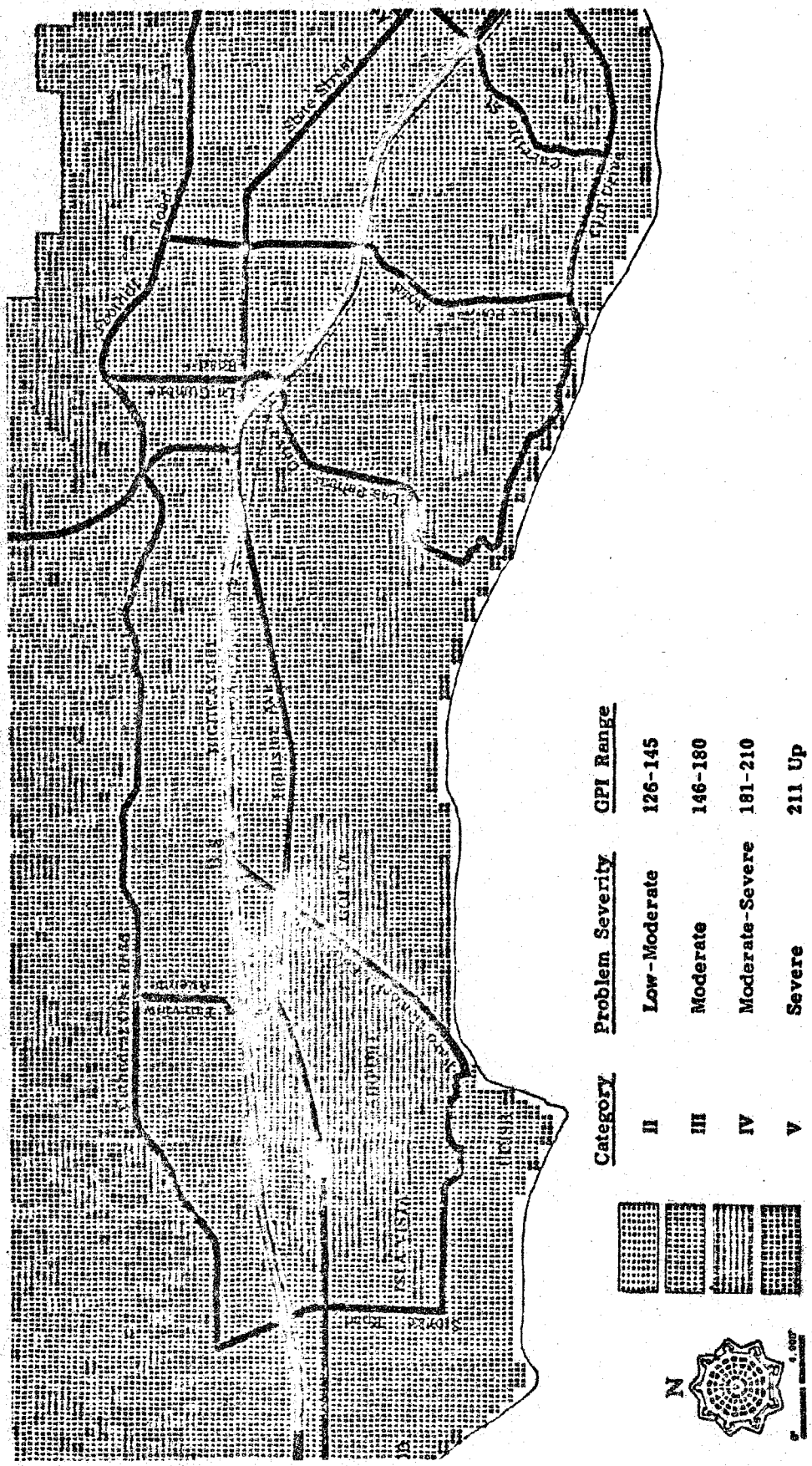


Figure 3. A portion of the computer generated map showing geologic problem index ratings for 5 acre (2 ha.) grid cells. This map is a part of the Seismic Safety Element portion of Santa Barbara County's general plan. (Livingston and Blayney, 1974)

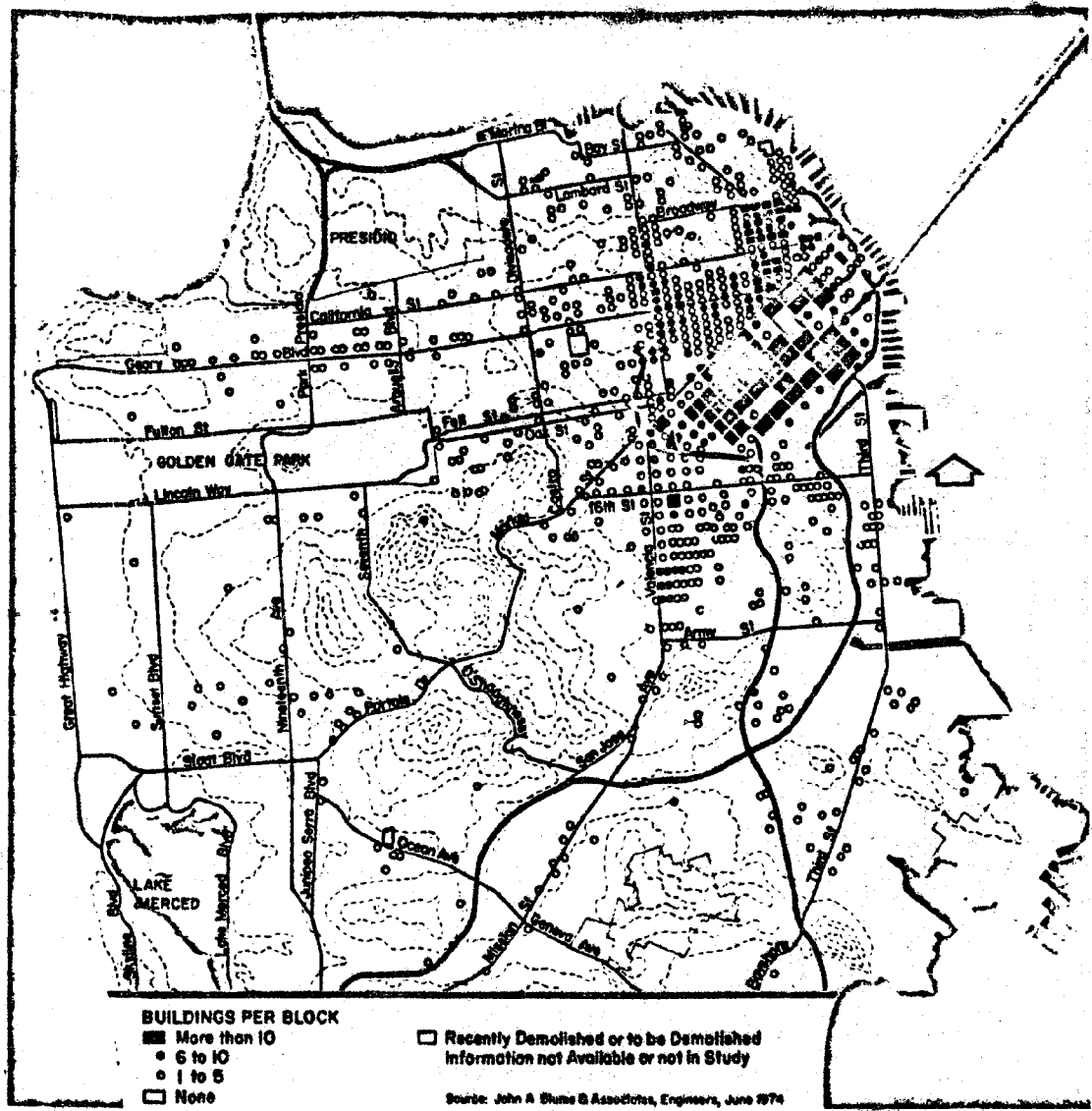


Figure 4. Distribution of pre-code Type C non-residential buildings. Scale is approximately 1 inch = 1.5 miles (1 cm. = 0.9 km). (San Francisco Department of City Planning, 1974)

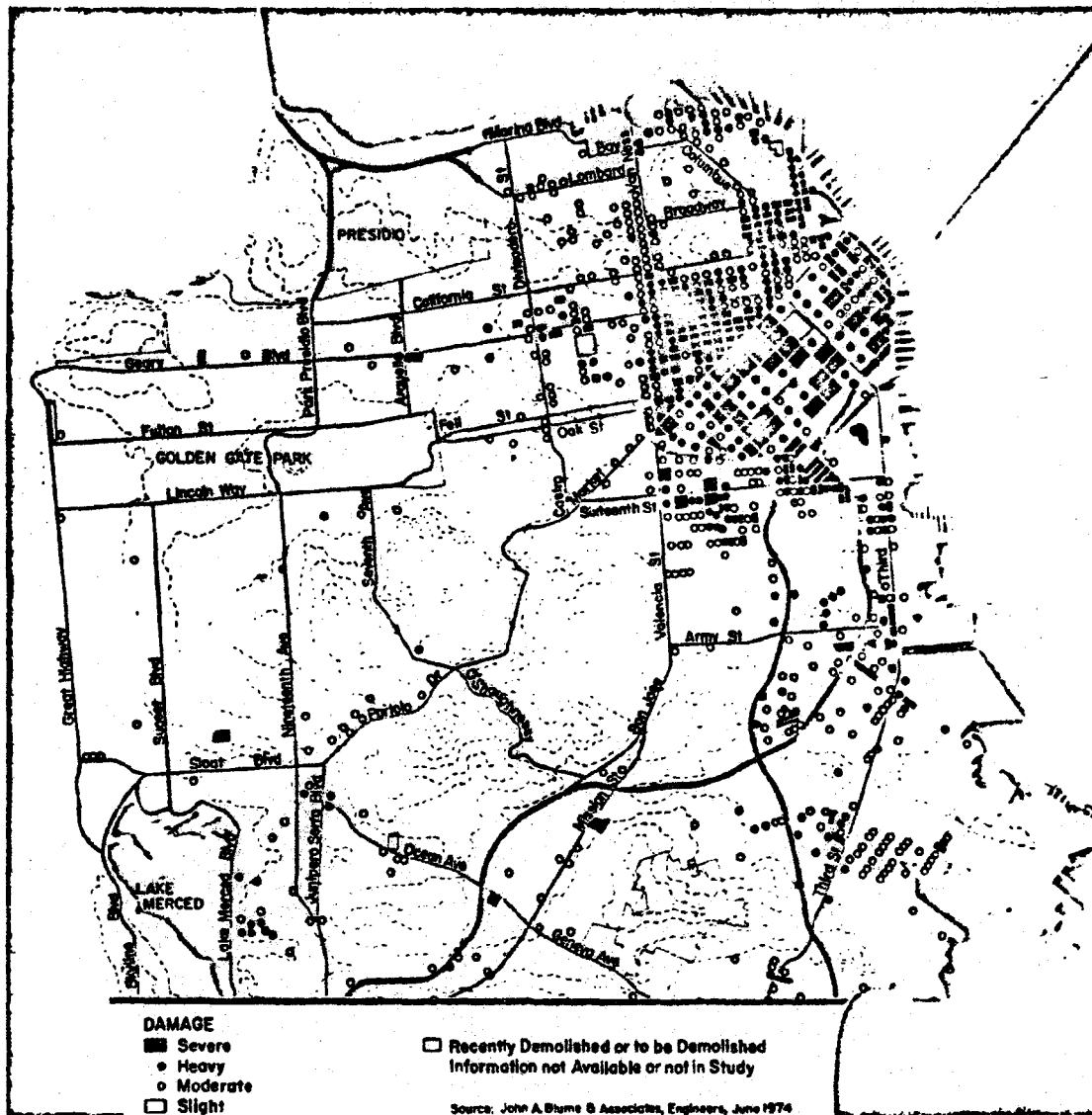
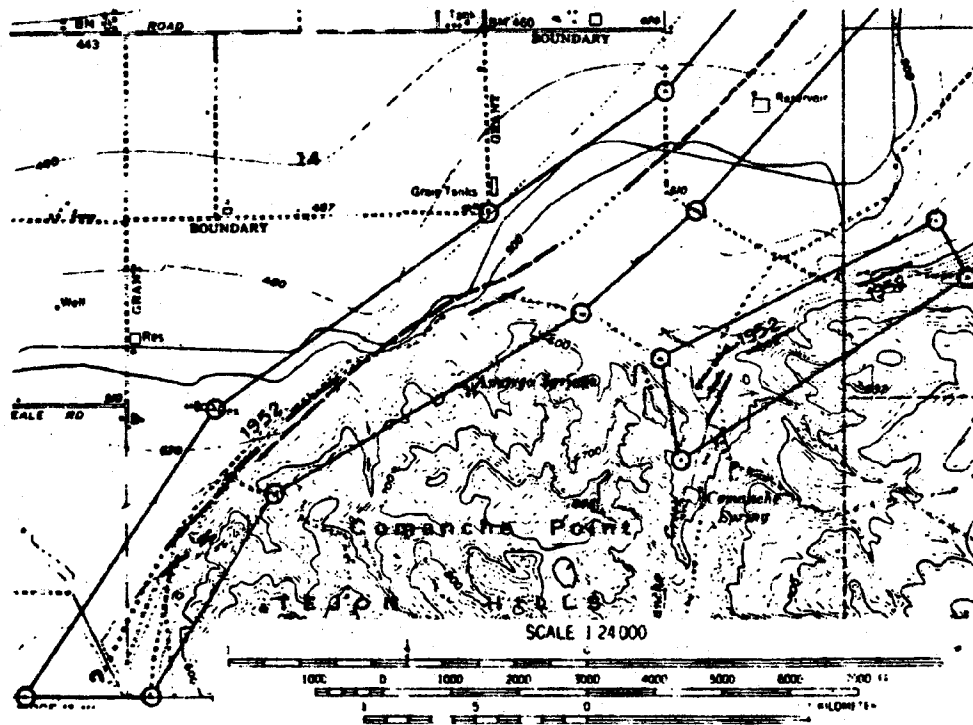



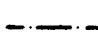
Figure 5. Estimated building damage levels for a "1906 type" earthquake. Scale is approximately 1 inch = 1.5 miles (1 cm. = 0.9 km.). (San Francisco Department of City Planning, 1974)




MAP EXPLANATION

Potentially Active Faults


 Faults considered to have been active during Quaternary time; solid line where accurately located, long dash where approximately located, short dash where inferred, dotted where concealed; query (?) indicates additional uncertainty. Evidence of historic offset indicated by year of earthquake associated event or C for displacement caused by creep or possible creep


 Aerial photo lineaments (not field checked); based on youthful geomorphic and other features believed to be the results of Quaternary faulting

Special Studies Zone Boundaries


 These are delineated as straight-line segments that connect encircled turning points so as to define special studies zone segments.


 Seaward projection of zone boundary

Figure 6. Example of special studies zones and explanation of symbols. (Hart, E.W., 1977)

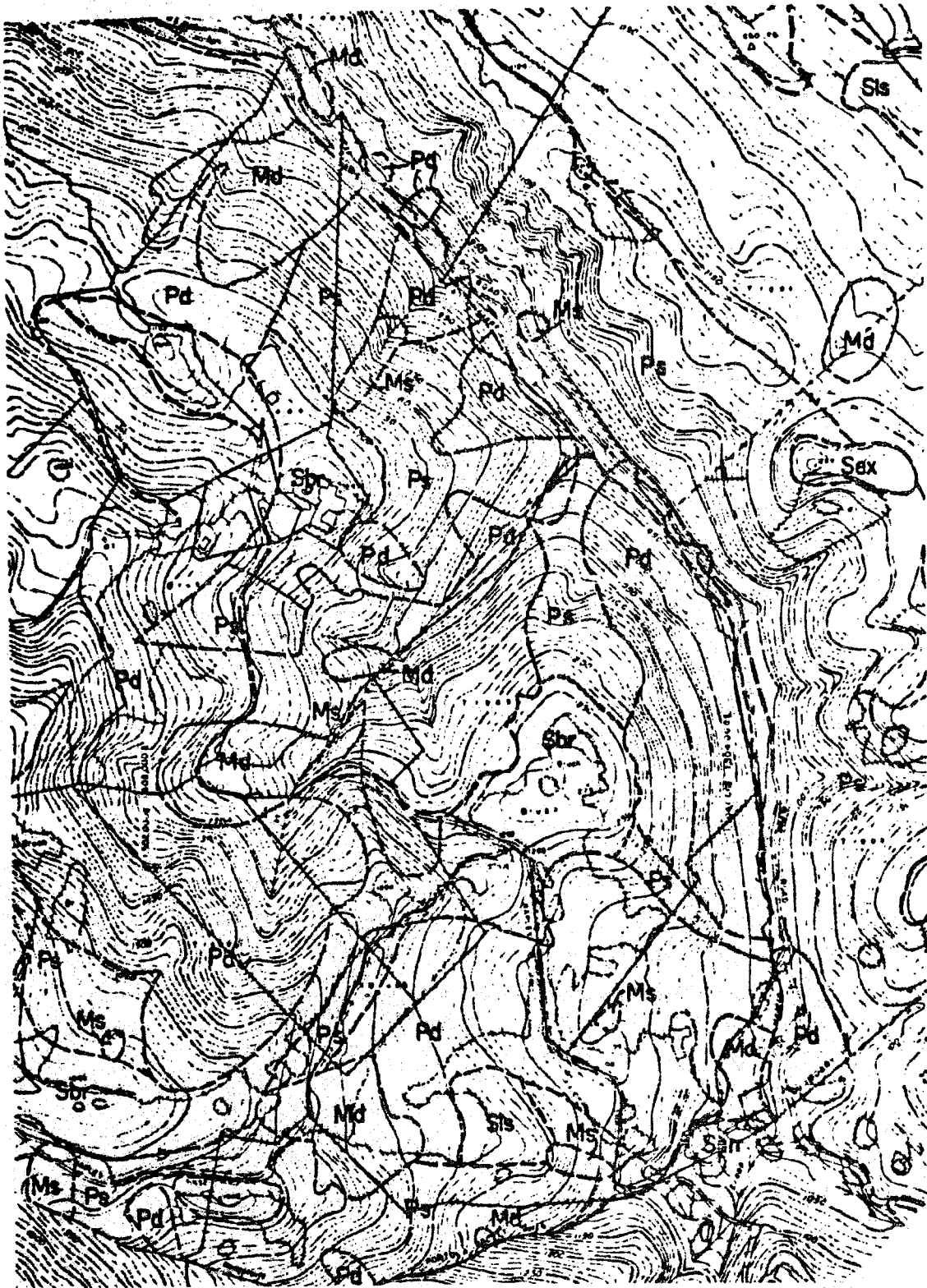


Figure 7. A portion of the Movement Potential of Undisturbed Ground Map for the Town of Portola Valley. See Figure 8 for legend. Scale is 1 inch = 500 feet (1 cm. = 59 meters). (Portola Valley, Town of, 1975)

Relatively Stable Ground

- Sbr** Level ground to moderately steep slopes underlain by bedrock within approximately three feet of ground surface or less; relatively thin soil mantle may be subject to shallow landsliding, settlement, and soil creep.
- Sun** Unconsolidated granular material (alluvium, slope wash, and thick soil) on level ground and gentle slopes; subject to settlement and soil creep; liquefaction possible at valley floor sites during strong earthquake.
- Sls** Naturally stabilized ancient landslide debris on gentle to moderate slopes; subject to settlement and soil creep.
- Sex** Generally highly expansive, clay-rich soils and bedrock. Subject to seasonal shrink-swell, rapid soil creep, and settlement. May include areas of non-expansive material. Expansive soils may also occur within other map units.

Areas with Significant Potential for Downslope Movement of Ground

- Pmw** Steep to very steep slopes generally underlain by weathered and fractured bedrock; subject to mass-wasting by rockfall, slumping, and raveling.
- Ps** Unstable, unconsolidated material, commonly less than 10 feet in thickness, on gentle to moderately steep slopes subject to shallow landsliding, slumping, settlement, and soil creep.
- Pd** Unstable, unconsolidated material, commonly more than 10 feet in thickness, on moderate to steep slopes; subject to deep landsliding.

Areas with Potential for Surface Rupturing and Related Ground Displacements Associated with Active Faulting

- pf** Zone of potential permanent ground displacement within 100 feet of active fault trace.

Unstable Ground Characterized by Seasonally Active Downslope Movement

- Ms** Moving shallow landslides, commonly less than 10 feet in thickness.
- Md** Moving deep landslides, commonly more than 10 feet in thickness.

Contacts between map units: solid where known, long dashes where approximate, short dashes where inferred, queried where probable.

Figure 8. Legend for Movement Potential of Undisturbed Ground map. See Figure 7. (Portola Valley, Town of, 1975)

CRITERIA FOR PERMISSIBLE LAND USE IN PORTOLA VALLEY

	LAND STABILITY SYMBOL	ROADS		HOUSES (parcel acreage)			UTILITIES	WATER TANKS	
		Public	Private	¼-Ac	1-Ac	3-Ac			
MOST STABLE	Sbr	Y	Y	Y	Y	Y	Y	Y	
	Sun	Y	Y	Y	Y	Y	Y	Y	
	Sex	[Y]	Y	[Y]	Y	Y	Y	[Y]	
	Sls	[Y]	[Y]	[N]	[Y]	[Y]	[Y]	[N]	
	Ps	[Y]	[Y]	[N]	[Y]	[Y]	[Y]	[N]	
	Pmw	[N]	[N]	[N]	[N]	[N]	[N]	[N]	
	Ms	[N]	[N]	N	N	N	N	N	
	Pd	N	[N]	N	N	N	N	N	
	Psc	N	N	N	N	N	N	N	
	Md	N	N	N	N	N	N	N	
	LEAST STABLE	Pf	[Y]	[Y]	(Covered by zoning ordinance)			[N]	[N]

- LEGEND:**
- Y Yes (construction permitted)
 - [Y] Normally permitted, given favorable geologic data and/or engineering solutions
 - N No (construction *not* permitted)
 - [N] Normally *not* permitted, unless geologic data and/or engineering solutions favorable
- S Stable
P Potential movement
M Moving
- LAND STABILITY SYMBOLS:**
(as used on geologic hazards map)
- br bedrock within three feet of surface
 - d deep landsliding
 - ex expansive shale interbedded with sandstone
 - f permanent ground displacement within 100 feet of active fault zone
 - ls ancient landslide debris
 - mw mass wasting on steep slopes, rockfalls and slumping
 - s shallow landsliding or slumping
 - sc movement along scarps of bedrock landslides
 - un unconsolidated material on gentle slope

Figure 9. Table indicates policy of the Town of Portola Valley regarding appropriateness of land stability categories for selected land uses. (Mader, G.G., 1974)

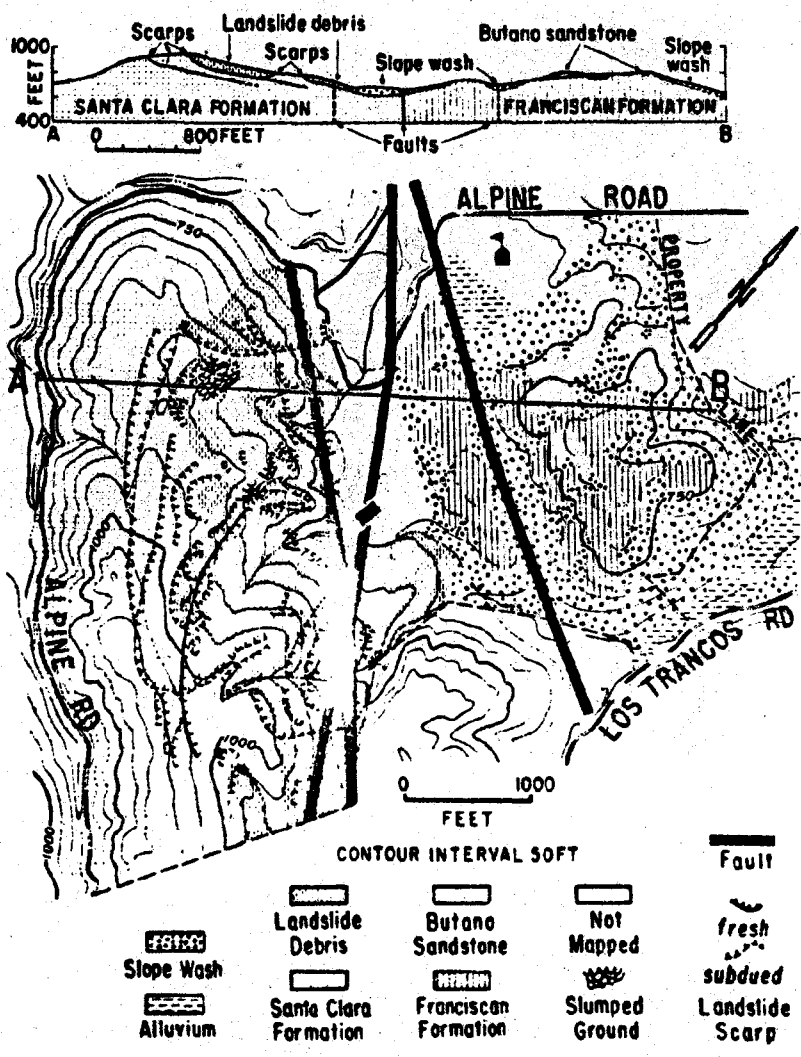


Figure 10. Geologic map of property proposed for subdivision in the Town of Portola Valley. (Mader, G.G., 1971)

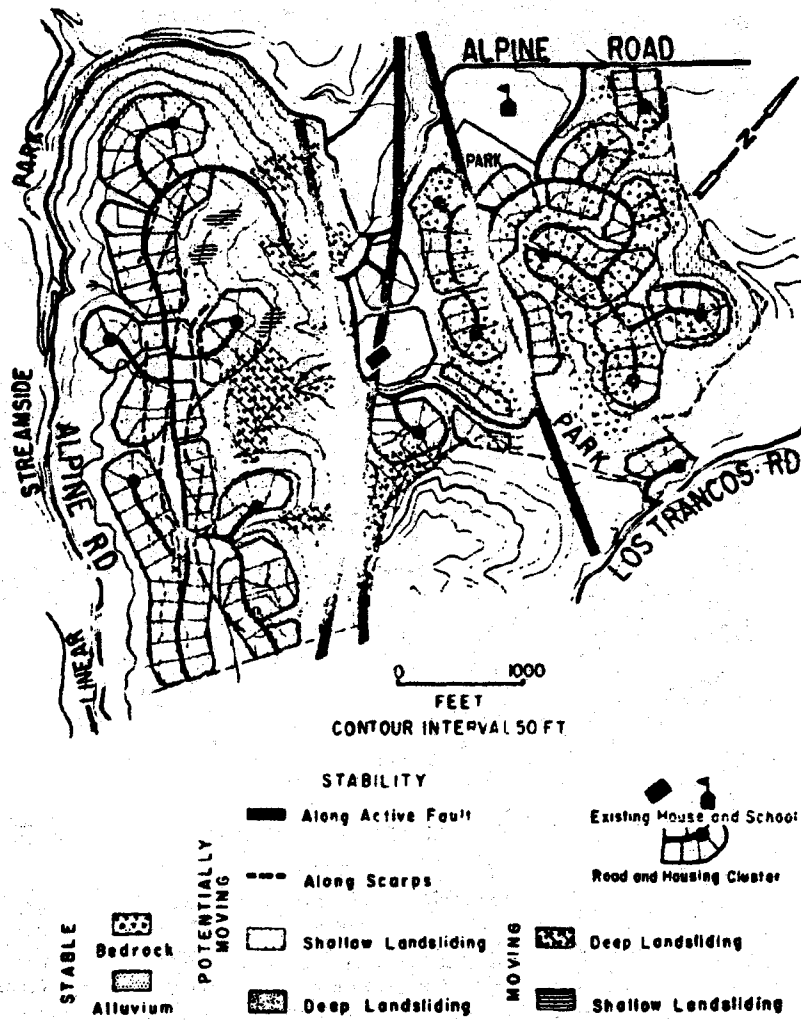


Figure 11. Relative stability map, derived from geology map (Figure 10), on which proposed subdivision in the Town of Portola Valley has been superimposed. (Mader, G.G., 1971)

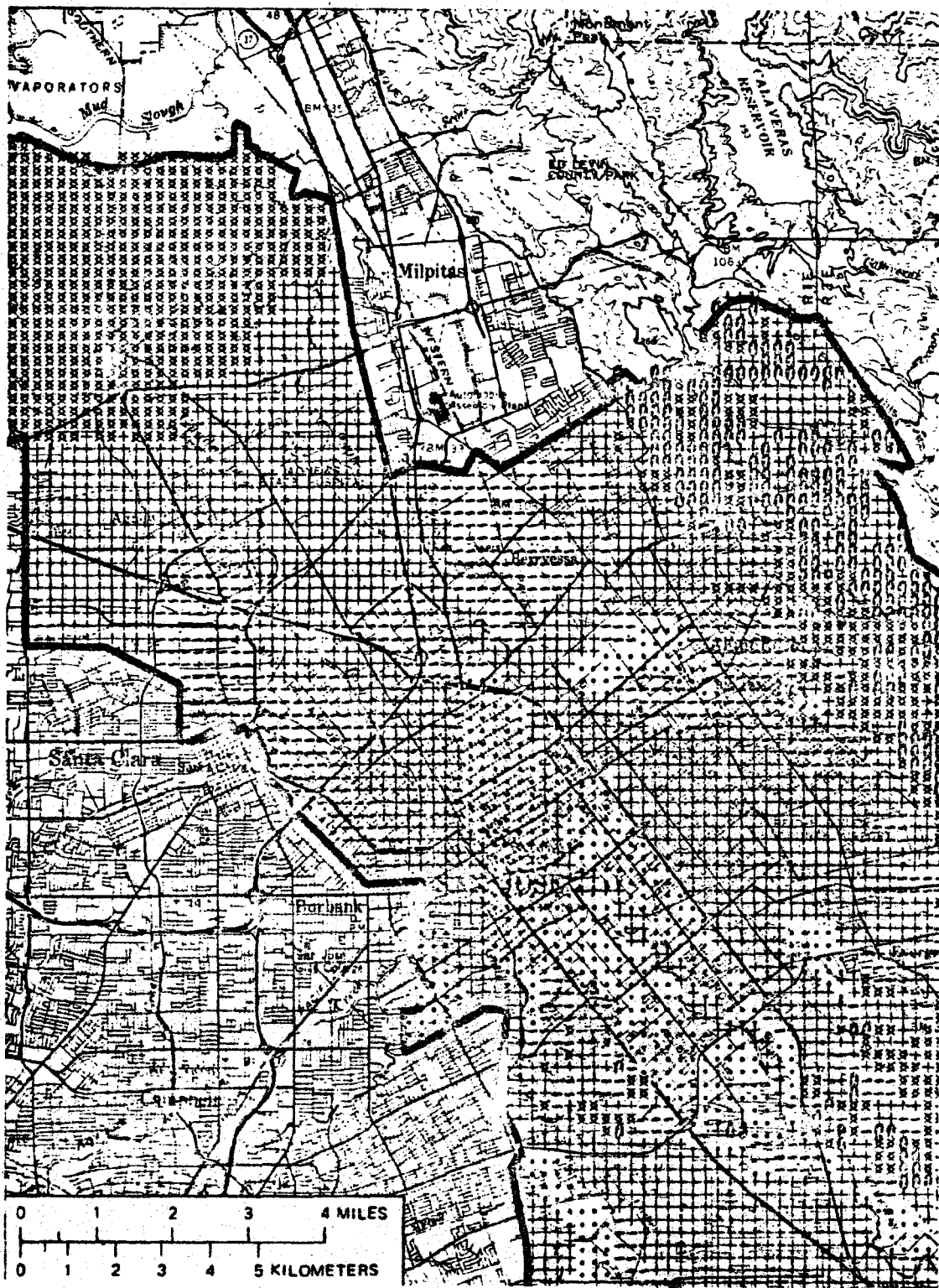


Figure 12. Land-capability map for multifamily residential use for a portion of Santa Clara County. Each grid cell includes 24.9 acres (10 ha.). See explanation, Figure 13. (Laird, R.T., 1979)

Hazard, constraint, or resource	Severe ← → Slight				
Surface rupture	\$200	\$300	\$0	---	---
Ground shaking—San Andreas, Hayward	20,000	20,000	5,000	\$2,000	\$200
Ground shaking—Southern Hayward	2,000	2,000	500	200	20
Ground shaking—Calaveras	20,000	5,000	2,000	200	---
Stream flooding	40,000	0	---	---	---
Dam failure	0	---	---	---	---
Dike failure	20,000	0	---	---	---
Shrink/swell soils	20,000	7,000	0	0	---
Settlement	20,000	30,000	20,000	2,000	---
Liquefaction	4,000	3,000	300	20	0
Subsidence	0	---	---	---	---
Landslides	200,000	100,000	50,000	9,000	0
Soil creep	40,000	40,000	0	0	---
Erosion and sedimentation	200	30	10	0	---
Septic tanks	0	---	---	---	---
Sand and gravel	20,000	0	---	---	---
Mercury	0	---	---	---	---
Agricultural land	5,000	0	---	---	---

EXPLANATION


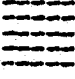




Level	Symbol	Total cost range (in dollars per acre)	
1		0.01	21,500.00
2		21,500.01	46,300.00
3		46,300.01	100,000.00
4		100,000.01	215,000.00
5		215,000.01	463,000.00
6		463,000.01	1,000,000.00

Figure 13. Summary of costs for multifamily residential use, in dollars per use, at top of page. Explanation for symbols used in Figure 12, at bottom of page. (Laird, R.T., 1979)



Figure 14. Composite maximum earthquake damage (with dam failure) to wood frame dwellings. Map shows computer printout for the northerly portion of San Mateo County. Each cell contains 2½ acres (1 ha.). See Figure 15 for explanation. (Association of Bay Area Governments, 1980)

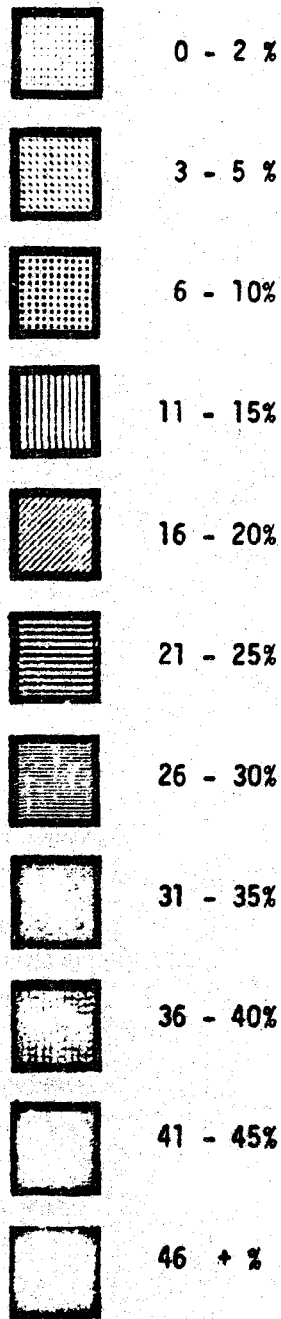


Figure 15. Explanation for Figure 14. Percentages are estimates of the average damage per event to wood frame dwellings. (Association of Bay Area Governments, 1980)

EARTHQUAKE RISK ANALYSIS IN PUBLIC POLICY

**This Article Discusses the Anatomy and Ingredients
of Earthquake Risk Analysis as it May be Used in Public Policy**

by

**JOHN H. WIGGINS
PRESIDENT**

**J.H. Wiggins Company
1650 South Pacific Coast Highway
Redondo Beach, California 90277**

SUMMARY

Earthquake risk assessment in policy analysis has blossomed in the last ten years as a method for analyzing risks and benefits and consequently the decisions pertaining to potentially dangerous technologies. Nuclear power, liquid natural gas facilities and large dams, are some areas that have been assessed by various investigators and have apparently, at least in the public eye, backfired. The recent Three Mile Island nuclear power station accident and the Teton dam failure are examples of situations that have brought technologists to a severe test of their credibility in the risk assessment arena. This paper outlines the ingredients for analyses which, if included, will mitigate criticism of future studies in the field of earthquake risk assessment.

INTRODUCTION

The Concept of Risk and State of the Decision Process

Risk analysis is now being discussed more and more in the public policy arena. Decision makers want to know the "acceptable risk" involved with a technology. The Three Mile Island accident and recent air crashes have forced earthquake engineers to start seriously facing risk assessment as a necessary part of their job. But establishing an explicit level of risk which is "acceptable" is only one small part of a many faceted problem.

Let us begin our investigation of the parts of this problem by first identifying the involved parties as well as the motivations, recognized or de facto, that thrust these parties into the earthquake risk-taking and, therefore, decision-making process. These are outlined in Table 1 below.

Table 1. Motivations of Decision Makers Involved in Earthquake Risk

INVOLVED PARTIES	MOTIVATION (RECOGNIZED OR DE FACTO)
CITIZEN	PERSONAL SAFETY
LEGISLATOR	COMPROMISE AND REFLECTION
CODE-BUILDER AND POLICY ENFORCER	PUBLIC SAFETY
DESIGNER, ENGINEER AND CONSTRUCTOR	DESIGN SAFETY
MATERIALS SUPPLIER	PROFIT SAFETY
OWNER	PROFIT OR MISSION OPTIMIZATION
LENDER	LOAN SAFETY
INSURER	DAMAGE MINIMIZATION
LOSS EVALUATOR	DAMAGE ESTIMATION

The citizen, naturally, wants the structure in which he is housed to be safe enough so that he is not injured or killed. On the other hand, the legislator, being buffeted by many interests from all sides, wants to organize the various influences in such a way that he can be reelected. The reelection motivation is a valid one, for if he has not fulfilled his constituents' ambitions and the ambitions of those who influence the constituents, he cannot be reelected. The public administrator is responsible for the "health, safety and welfare" of the community which he represents whereas the designer, engineer and constructor want failure free structures. If the structure fails, lawsuits may ensue with possible loss of reputation as well as monies and time - time which could otherwise be used in a profit-generating activity.

In trying to balance the risk between all parties two key ideas present themselves:

- risk knowledge
- equitable risk

Earthquake risk, for it to be acceptable or not, has to be known within some level of uncertainty. This risk can be computed whether by the inductive or the deductive approach. The balance between cost of risk reduction and expected loss establishes degrees of equitability, wherein ultimately the value of human life is either explicitly or implicitly treated. I believe that through the careful description of risk computation, a number of benefits can accrue:

- cost minimization
- loss reduction
- the establishment of equitable earthquake insurance policies and rates
- the determination of whether certain construction should proceed or not.

Costs should be minimized because the important time element and cost of capital should be reduced. Likewise, losses can be reduced because the construction would not come about in an unforeseen manner.

Earthquake insurance is an important consideration in any project since, with very large owners, large capital outlays in the remote instance of failure would be detrimental to any commercial or private owner as well as the consumer. Three Mile Island and the associated pass-through losses are an example.

Probably the most important benefit which could result from the application of what I call the "Balanced Risk" rationale is a determination of whether or not nuclear power plants, dams, gas transmission lines, liquid natural gas facilities, etc., should or should not be built at certain locations. All of the details should be developed, considered and resolved between all parties before costly construction activities begin.

Two key words involved in the Balanced Risk approach are "knowledge" and "decision." Within the "knowledge," area there are facts and circumstances that are known, unknown, knowable, and unknowable. Certain things will always be known. Other facts may be unknown, but they are knowable. However, the amount of money that is set aside for determining new knowledge must be decided in advance of any major design effort. The unknowable will always be present. That is why society is finally working with the concept of risk and the concept of uncertainty. It is imperative that the unknowable future, which accounts for states of nature or states of man that cannot be estimated at time of study, be accepted as a state of "humanbeingness."

"Policy makers must stop waiting for consensus where none is possible and concentrate instead on how to minimize the societal costs of uncertainty."

The word "decision" has benchmarks associated with it which are termed:

- acceptable risk
- unacceptable risk
- tolerable risk
- intolerable risk

Webster defines "acceptable" as "...capable or worthy of being accepted; welcome; pleasing; barely satisfactory or adequate." On the other hand, the idea of "tolerable" is defined by the phrases "...capable of being borne or endured [e.g., pain]; moderately good or agreeable." In other words, society may tolerate certain automobile risks which are higher than those inherent in regulation promulgated to reduce those risks to acceptable levels. Consequently, the concepts of risk acceptance or toleration must be carefully perceived regarding earthquake codes and standards for new construction on the one hand, and the rehabilitation of existing construction on the other.

One perspective of risk can be gained by comparing three sets of individuals and how they approach work, travel and pleasure. Depending on whether the person is a cautious man, a risky man or a housewife, it has been computed [1] that the risky man who works in a coal mine, rides

motorcycles and climbs mountains takes more than 10 times the risk of a cautious man who works at a desk, rides a bus and does little for pleasure. The risky man is about 6 times more apt to die from accident than the housewife. Plus, if one considers the different activities which are a specific option to the individual, one can make average decisions about his or her own individual safety.

Another perspective of risk can be learned from studying Figure 1, which distributes annual losses from earthquake and tornado as a function of damage state [2]. Since the average losses from each of the hazards shown is equal, from dollar loss considerations, the risk may not be accepted as equal because the damage states are different. On the one hand, a tornado involves considerable total collapse and severe damage. Consequently the chance for death, per dollar lost, is greater for tornado than for earthquake. Decision about safety and the cost of mitigating death from these hazards must be considered to be a function of the damage state afforded by them. This introduces the concept of utility which will be discussed later.

Figure 2 presents yet a third perspective on safety [3]. It compares risk with the degree of regulation and judged benefit associated with various modes of transportation. On the one hand, the benefit from private automobile, commercial air, intercity bus, urban bus, transit bus, and elevator are judged to have a high benefit; however, the degree of regulation associated with private auto travel seems to be too low while that for transit bus is too high for the relationships on the graph to apply. Private automobile has a death risk of approximately 700 per billion exposure hours whereas commercial aviation has a lower death risk of 573 per billion exposure hours. Yet the stringency of safety regulations is judged to be "medium" for private automobile and "very high" for commercial air travel. Similarly, intercity rail and boating are not regulated properly from the purely balanced benefit/risk point of view.

Several other observations can be made from Figure 2. If the degree of regulation can be thought of as an order-of-magnitude situation, as presented, low benefit risks are tolerated by society to be about 1000 times riskier than high benefit risks. This agrees with Starr's first observation about voluntary and involuntary risks [4]. Similarly, high benefit transportation risks seem to receive more attention from government than risk associated with work. Underground coal mining (580×10^{-9}), construction (220×10^{-9}) and desk work (1×10^{-9}) receive "high," "medium" and "low" ratings regarding safety regulation. These would then compare with the medium benefit rather than the high benefit transportation modes. Swimming (3500×10^{-9}), mountain climbing (2700×10^{-9}) and smoking (2600×10^{-9}) all have a "low" degrees of regulation and would plot below the low benefit line.

Starr [5] also attempted to develop a benefit-risk toleration curve for involuntary risks. He regarded the average disease level, even for the very high benefit activities, to be the maximum risk toleration level. On the other hand, natural hazards, which are implicitly

KEY:
 L = Low
 M = Moderate
 H = Heavy
 S = Severe
 C = Total Collapse

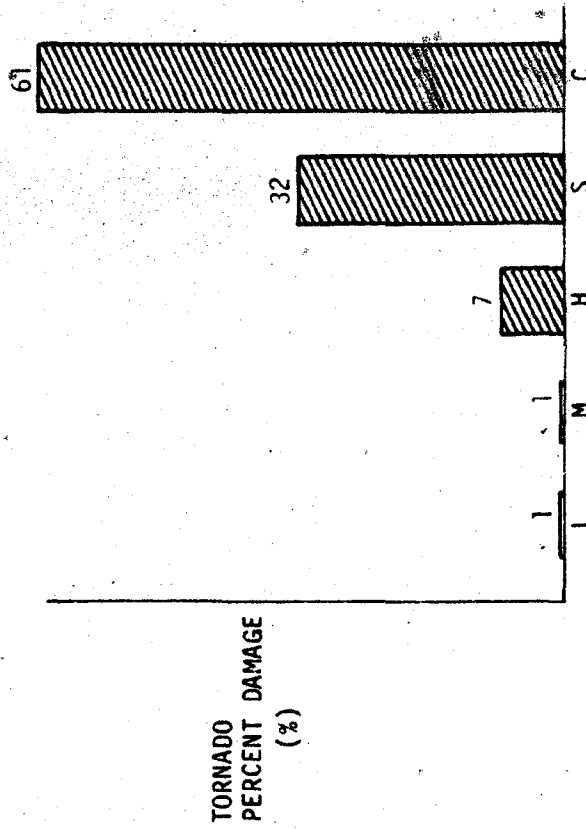
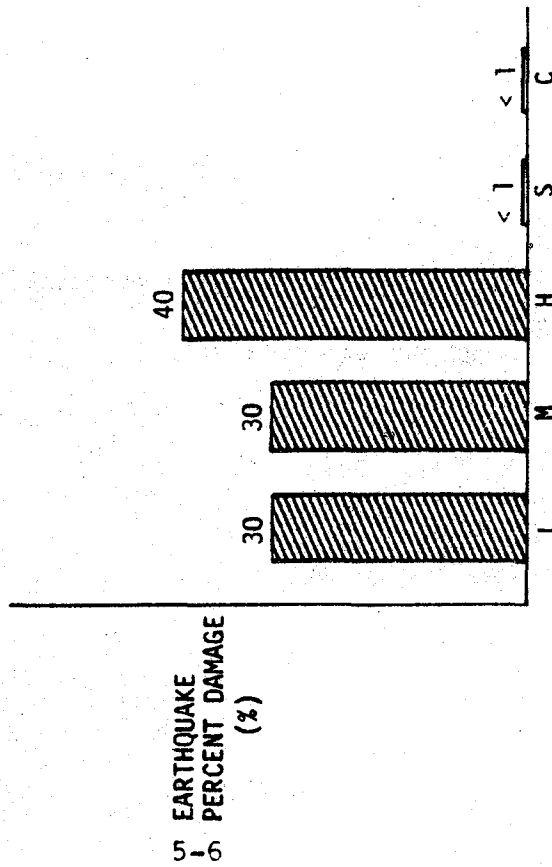


Figure 1. Distribution of Annual U.S. Building Losses for Two Natural Hazards Which Cause About the Same Monetary Losses

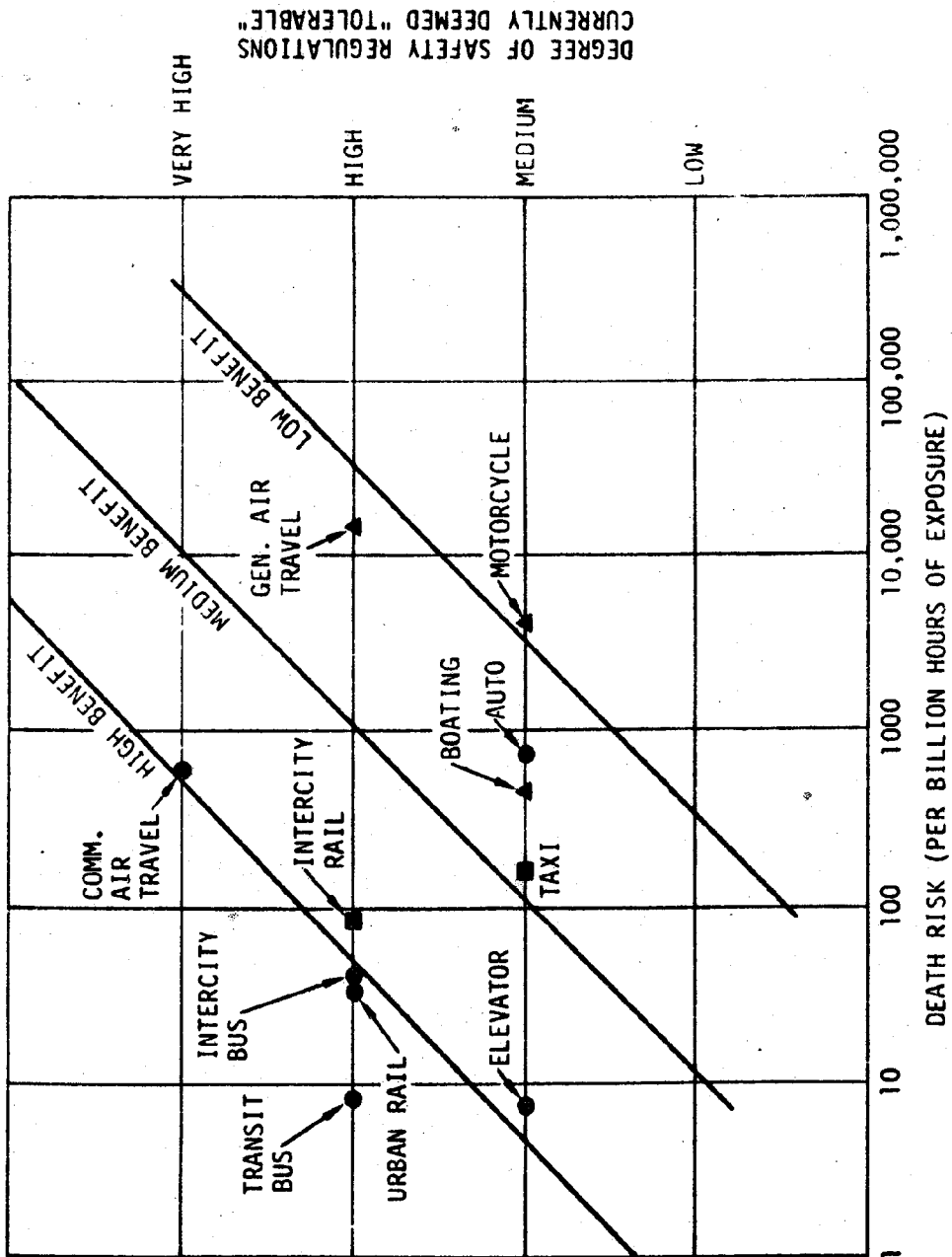


Figure 2. Mortality Rates per Billion Exposure Hours (1971-1975) for Various Transportation Modes Plotted by Stringency of Safety Regulations and Benefit Judged by the Author

considered to be Acts of God and develop little benefit, should represent the lowest risk toleration level. Anything above the S-shaped benefit/risk curve could be termed "Acts of Man"; anything below the S-shaped curve could be considered "Acts of God."

With the foregoing as a brief introduction to the concept of Balanced Risk and the various perspectives in which general risks can be addressed, let us examine three other definitions associated with earthquake:

- policy-risk-level
- life loss
- economic loss

I define the policy-risk-level as that which a governmental or a standards making body considers to be acceptable. In the case of earthquake, this degree of acceptance can equal the current de facto earthquake risk associated with structures designed to the Uniform Building Code (UBC), or some lower level. For example these lower levels can be either one-tenth the UBC risk level, or one-one hundredth the UBC risk level. However, in selecting the policy-risk-level for a community, the nation, or for a standard of design, one must balance the costs and losses in social and economic terms.

The de facto value that society puts on a human life can be computed. Adding up all of the home, work, public and motor vehicle deaths and the associated dollars lost on accidents, society is currently tolerating the average value of a life to be about 400,000 1977 dollars ([1] factored to 1977). On the other hand, the discounted earning power of the average individual was about \$150,000 in 1977 dollars ([6] factored to 1977 conditions). Looking at the de facto value of death in a slightly different way, the cost of maintaining a malformed child from birth to death is about \$400,000 ([7] factored to 1977 conditions.) Currently, economists are attempting to compute the value of a human life based on the amount of money an individual is willing to spend on safety devices. Consider the smoke-alarm as a potential preventor of life loss in home building fires. There are about 70,000,000 homes wherein about 7,000 people die per year from fire. Considering that the average smoke alarm costs in the neighborhood of \$30 each, the average perceived value of a human life, if all homes buy an alarm, is about \$300,000. Consequently, no matter how one wants to phrase the value of human life, we currently tolerate and for the future are willing to accept a value between \$150,000 and \$400,000 as the nominal, de facto value of an American's life.

What about economic loss from accidents, whether manmade or natural? It can be computed that auto, public, work or home accidents (those activities in which we are engaged 24 hours every day of the year) cost \$3.20 per \$100 of GNP in 1977 [8]. This is the tolerable loss rate

that society has been willing to accept under 1977 conditions. In 1967 the figure was \$2.70 per \$100 of GNP. For earthquake it is computed that the economic loss from structures designed to Uniform Building Code conditions would be about \$0.01 lost per \$100 exposed on an annualized basis [9]. Compare this with the insurance rate on dwellings of \$.15 to \$.20 per \$100 exposed with a 5% deductible. Further, compare natural hazards loss rates with manmade risks: auto, public, work and home accidents. They cause about \$10 billion in losses [10] compared with \$62 billion [8] from manmade risks.

An attempt to balance the loss reduction in persons killed and damage dollars lost versus the added cost of construction aimed at reducing those losses can be made by examining earthquake codes [9]. It is conservatively estimated that the average costs to reduce the risk to one-tenth current UBC level in California would be about one percent higher than current UBC values. If this cost is spread throughout the State of California which in 1970 spent about \$9.3 billion on construction, and the de facto value of human life is increased tenfold to \$3,000,000, the optimum public safety from construction should only be increased by a factor of between 2 and 3. This example shows the non-linear effect of arbitrarily increasing the value of a human life from a tolerable one to a hypothetical, acceptable one.

Figure 3 shows a schematic of the foregoing discussion. Three quantities are plotted thereon: the benefit derived from taking the earthquake risk; the loss expected from taking the risk; and the cost to mitigate the risk. The hard money losses can be identified through inductive or deductive models to represent reproducible assets and lost time. However, losses represented by human safety, mental and physical health and the welfare of a community are a function of moral and political values. The question revolves around what should be the value weighting options which increase the hard money losses.

Several observations can be made from Figure 3:

1. The higher the value one places on health, welfare and life safety, in comparison to today's tolerable values, the lower becomes the benefit until society can derive no benefit. Thus, one can determine when the activity in question becomes useless to society and the construction should not proceed.
2. Even today we may not be operating at optimum benefits using de facto tolerable losses as the starting point. There is a maximum point for benefit...a greater pay-off for taking lower or higher risks depending on which side of the benefit curve the risk activity is currently located.
3. An analysis of the type shown in Figure 3 is not static in time. It is everchanging as new means for reducing costs of risk taking are discovered. Further, benefits are not static since the reduction or increase of side effects (secondary and higher order benefits or losses) may prove to have serendipitous

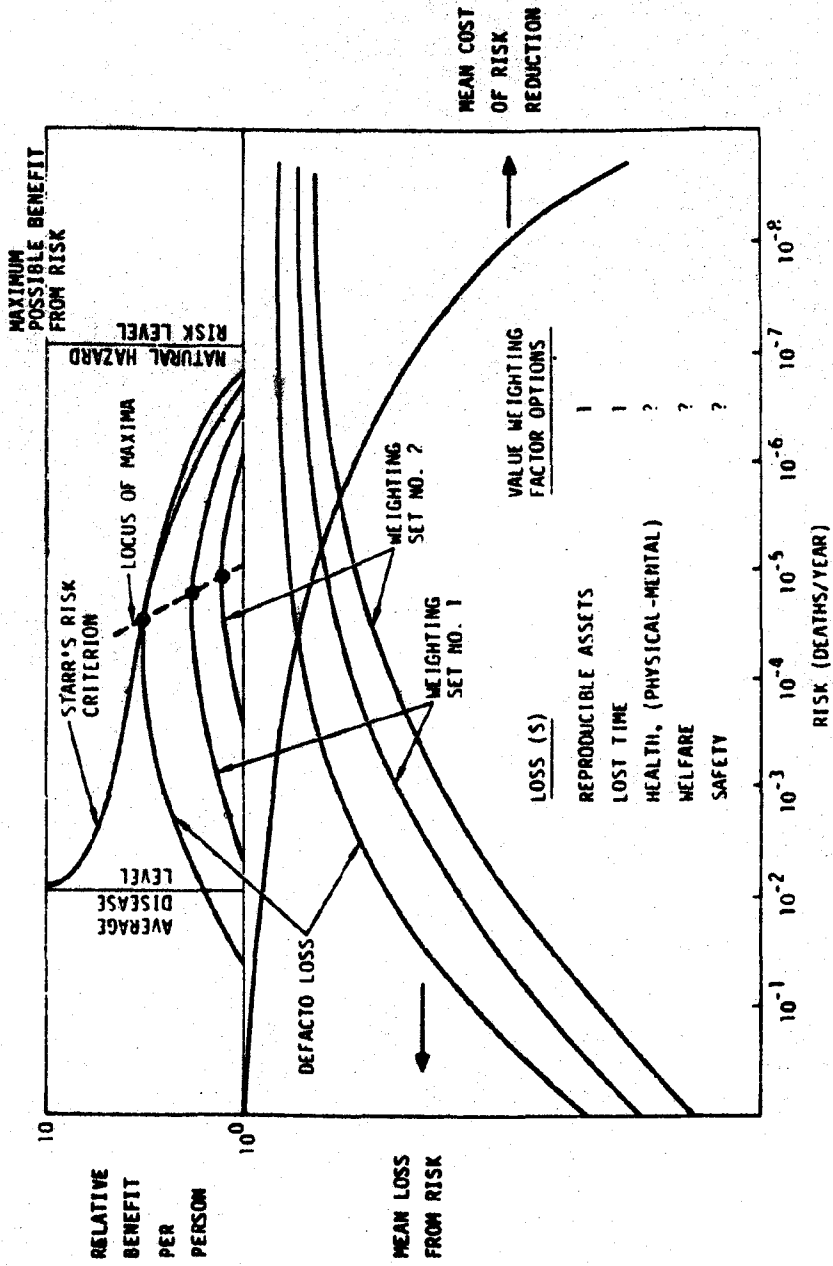


Figure 3. A Schematic Showing the Influence of Value Weighting Factors on Initial Benefit/Cost/Risk, Trade-off Decisions Made for the Lifetime of a Project. Concepts Shown Include a Maximum Risk Level Based on an Uncontrollable Risk Level

effects. This set of curves is simply a documented, best-estimate of the situation at the time of the decision.

2. RISK MANAGEMENT AS IT PERTAINS TO THE EARTHQUAKE COMMUNITY

"Risk Management" is a term that has been determined by the insurance industry to represent that function which balances principally the economic risk within a company or an industrial complex. I use it in the broader sense to include social consequences as well; however, I shall discuss it principally from the insurance point of view.

There are various techniques for reducing or otherwise allocating for earthquake risk (used herein to mean chance of loss). First, by increasing knowledge about earthquake risk, one might mitigate the risk strictly through this knowledge. For example, if expensive batteries or other types of equipment are perched on a high shelf in a building it might be wise to relocate these items on the floor so that secondary damage from a fall under earthquake action would not take place. A second technique for treating earthquake risk is through loss prevention. In other words, by reducing the vulnerability of a structure or item, the loss might be reduced or prevented. By simply bolting down generators, losses under earthquake action might be prevented. Risk transfer is a third way of treating risk. That is, by purchasing insurance one can transfer the earthquake risk to the insurer in the event of a damaging event at a nominal annual cost. A fourth technique for treating earthquake risk is through retention. One can retain a risk either through simply assuming it and betting nothing will happen; then if something happens, by assuming it will somehow be compensated for in another way (federal relief, say) or through self-insurance. In the self-insurance case, one simply sets aside a certain amount of money every year which would be drawn on by the risk-taker in the event of loss.

In risk management there are various kinds of financial losses which may be incurred by various parties: 1) personal loss, 2) commercial loss, and 3) governmental loss. These losses might be incurred in the form of life loss, property loss or liability. Another way of examining sources of financial loss would be with the "balance sheet" approach. Herein, losses might result from: 1) a reduction in income, 2) an increase in expenses, 3) a reduction in assets, or 4) an increase in liabilities. Earthquake risk management simply aims at treating sources of financial loss through balancing knowledge, loss prevention, risk transfer, and risk retention.

Up to this point, I have been using the word "risk" but I wonder if all readers have the same understanding of what the word means. For example, to some the word "risk" means measurable uncertainty - something or some phenomenon which varies in some random fashion. Yet another definition of "risk" is the uncertainty regarding the occurrence of an undesirable event. A third describes "risk" as a combination of hazards measured by probability. A fourth, which I choose to use, involves the

uncertainty of loss. In other words, it is necessary that an exposure to a hazard be present for a loss to occur.

There are several classifications of risk which, depending upon the use, would require different game rules for accepting or tolerating. The first type of risk is called speculative risk, which involves chance for gain or loss. This involves the gambler or entrepreneur. The second type of risk is called pure risk. Pure risk involves the chance of loss or no loss; most often in risk analysis exercises it is pure risk which is of interest. Two other definitions come to use from the insurance industry. One involves fundamental risk and the other particular risk. A fundamental risk is impersonal in origin and consequence. On the other hand, a particular risk originates in individual events taking place and the object in question experiencing the risk.

Since risk is defined as the chance of loss, there are four associated fundamental parameters which interlink to cause the risk. The first involves the "hazard." The hazard, of course, is the source of loss. The earthquake, flood, and the air-polluting smokestack are all hazards. The second is the "exposure." This involves the quantity of loss possible; in the case of earthquake, the nearby city. The third parameter is the "vulnerability" of the exposure. In the case of earthquake, a block of granite would behave quite differently than a very weak unreinforced masonry structure. When the exposure is people, not only the physical vulnerability but also the moral or socio-economic aspects must be traced. For example, all of the physical elements which make up a human being are valued by chemists to be worth less than \$20. Yet earlier it was computed that the average life is worth about \$400,000. Obviously socio-economic conditions enter the situation. The fourth parameter that affects risk is the "location" of the exposure in relation to the hazard. One may have a very vulnerable structure that is worth a great deal of money; however, it is simply too far from the earthquake for the risk to be severe.

Figure 4 represent the earthquake risk analyst's risk management process. The hazard can be modified by strain relief in the earth while the vulnerability is decreased by improved codes or design practices. The location can be modified by land use codes while the exposure can be reduced through warning.

3. DECISION ANALYSIS

Let us turn now to the process of decision analysis. This involves making decisions regarding mitigations or risk from a purely technical viewpoint.

Figure 5 outlines the technical process. It requires several steps:

1. Generation of mitigation alternatives which may reduce the risk.

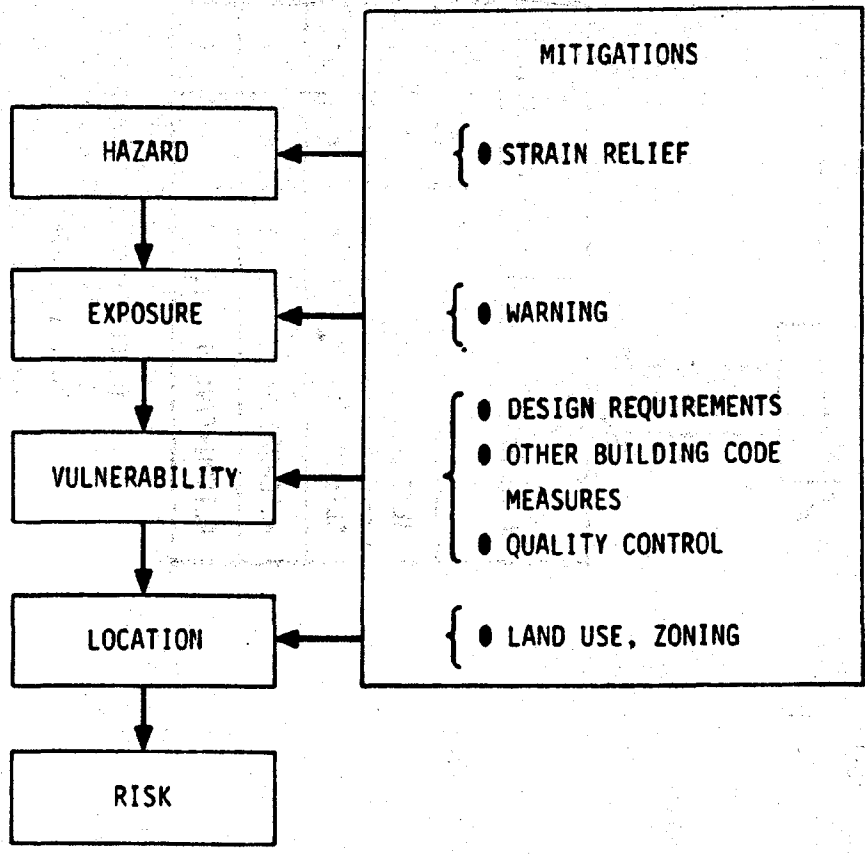


Figure 4. The Management of Risk from Earthquake by Mitigating the Hazard, the Vulnerability of the Exposure, the Amount of Exposure and the Location of the Exposure

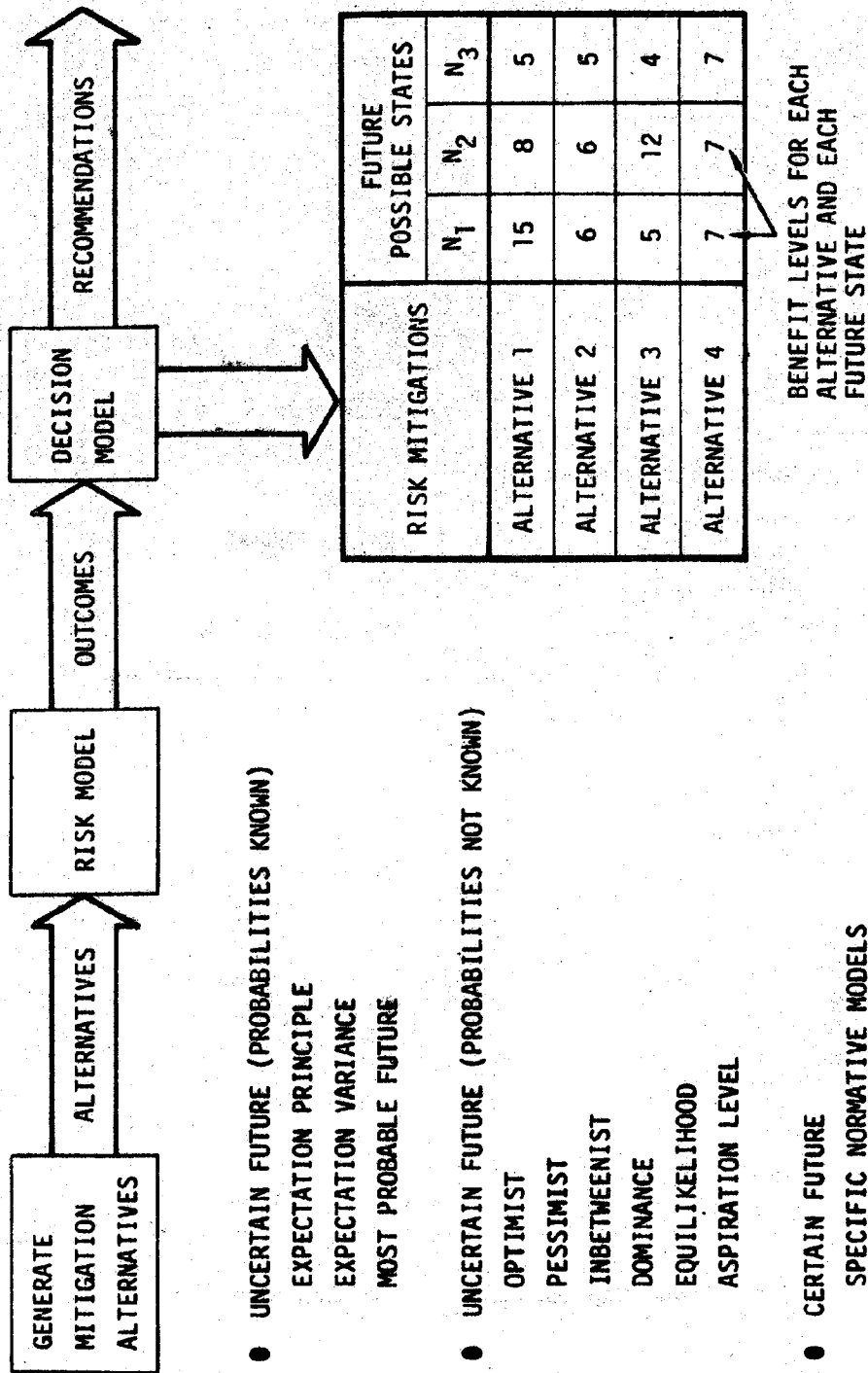


Figure 5. The Quantitative Decision Analysis Using Various Methods (from Jon Collins)

2. Development of a risk model involving hazard, exposure, vulnerability and location of the exposure.
3. Computation of outcomes using the risk model.
4. Incorporating the outcomes into a decision model.
5. Making recommendations based strictly on quantitative risk outcomes as modified by various decision processes.
6. Depending upon the decision process that appears to be "good" for the decision maker in question, recommending the alternative for selection.

In defining the decision model one should list the alternatives in a table such as that presented in Figure 5 and list the outcomes as a function of possible future states of nature or states of man.

Figure 5 also specifies three types of futures which could result from various outcomes: the uncertain future, wherein the probabilities are not known; the uncertain future in which probabilities are known; and the certain future.

Risk models assume some type of physical model described by other types of information. Using data or statistical models three possibilities of an uncertain future when the probabilities are known can be described:

1. The expectation principle simply computes the expected value from each outcome, and one selects the best alternative from the standpoint of minimum loss, minimum cost, or maximum gain.
2. The expectation variance principle includes the amount of uncertainty involved with each outcome computed. In the case where two expected values are the same, the outcome with the high variance is weighted lower. That is, uncertainty plays a role in weighting the outcome.
3. In the case of the most probable future, if one alternative dominates all states of nature with a higher or lower probability, depending on whether benefit or risk is being computed, then the dominant alternative may be selected.

Decision under uncertainty, where no probability, is known is the area where policy decisions are found. Figure 5 shows an example of three states of nature and four alternatives with different outcomes in the box. Having only these numbers for decision making there are seven techniques which can be used for a single selection.

1. The optimist ... looks at all states of nature for each alternative and selects that alternative which provides the highest, highest benefit (or least, least risk). The highest benefit that can accrue from each alternative from each state of nature is 15 identified with alternative 1.
2. The pessimist ... does not want to lose very much. He is willing to sacrifice the largest gain if he eliminates the risk of a smaller loss. So he examines the highest, lowest benefit for each alternative and for each state of nature. In the case cited in Figure 5, this would be alternative 4.
3. The in-betweenist ... examines each alternative by weighting the highest possible benefit and the lowest possible benefit from each state of nature and for each alternative in the same way. He then selects that alternative which provides the highest in-between result. Again, examining Figure 5 and weighting each benefit both high and low equally, the in-betweenist would select alternative 1 for his recommendation.
4. The question of dominance ... involves the desire to eliminate the alternative which is dominated for all future states of nature by some other alternative. Since alternative 4 dominates alternative 2 for all future states of nature, alternative 2 can be eliminated. However, since no other alternative is dominated by any remaining alternative, the dominance principle leaves three alternatives to be considered by some other principle.
5. The equi-likelihood principle ... averages all outcomes for each alternative and for each state of nature, and selects the highest average. In this case, alternative 1 would be selected.
6. The aspiration level ... requires the decision maker to select some benefit level below which no alternative is acceptable. Put another way, he wants a benefit level of x or greater. The value of x is strictly a subjective value. If the decision maker selects the aspiration of 5 as his minimum acceptable level, alternatives 1, 2 and 4 would be acceptable. However, if he selected the benefit level to equal 6 as his aspiration level, only alternative 4 meets the aspiration rule.
7. The principle of least regrets ... selects the alternative that provides the least possible, maximum regret from each state of nature. Noting that the maximum regret for alternative 1 is 4, for alternative 2 is 9, for alternative 3 is 10, and for alternative 4 is 8, one would select the least maximum regret to be alternative 1. The worst selection under this principle would be alternative 3.

Up to this point, risks and benefits have been weighted equally, depending upon the type of decision principle one wishes to employ. The question of utility has arisen, however. Is a loss which costs twice as much twice as bad? Let's examine the difference between a single national loss from an earthquake which costs \$62 billion and a loss of \$62 billion spread hourly throughout the nation, which is worse? One

single loss of this size would be catastrophic and would ripple through every economic sector of the United States. However, \$62 billion was lost from all accidents in 1977 [8]. These accidents did not appear to impair the ability of the nation to conduct business-as-usual. Another way of looking at the utility principle is to examine the gambler who goes to Las Vegas with \$1,000 and the gambler who has only \$10 to bet. A \$5 bet to the \$10-limit gambler is much more important than a \$5 bet to the gambler who has \$1,000 to spend.

Has the nation actually included the utility principle in its de facto decision making processes? Figure 6 says that it has [8, 11]. In the case of transportation safety, Congress has decided to invest more safety research and development money per fatality per year in commercial aviation than it is willing to invest in motor vehicle safety. In 1973 the number of deaths per fatal accident for commercial aviation was about 43. On the other hand only 1.14 persons died per fatal accident in motor vehicles. Yet the Federal government spends about \$100,000 per death in research and development aimed at improving safety in commercial aviation compared with about \$870 per death per year for motor vehicles. A regression curve plotted through the transportation safety data suggests that the nation views safety as worth the number of deaths per accident to the $3/2$ power. This is a non-linear utility curve. It states that the nation wants to reduce risk to the least maximum regret.

Using the same procedure for natural hazard research, [12], but plotting the curve parallel to that for transportation, one finds that the nation is willing to spend about 20 times more on risk in transportation than natural hazards. Consequently, when the visibility of a hazard is high and where there is a possibility of many deaths per fatal accident, the nation is willing to spend more for safety and to be nonlinear in its allocation of funding. This outcome is neither good nor bad. It simply reflects the public's conscience about the risks from the hazards in question. Nevertheless, these tolerable utility curves can be used in the decision-making process as starting points for determining acceptable risk for some earthquakes.

Another perspective for considering risk and utility may be derived by comparing average annual losses computed for hurricane winds at different time periods. It is estimated that the loss to property from hurricane wind will escalate almost four times in the thirty years between 1970 and the year 2000 [10, 13] due to population movement to the eastern and southeastern seaboard. A one billion dollar average annual loss in 1970 may be tolerable. However, if nothing is done between 1970 and 2000 to mitigate hurricane loss, the question arises as to whether the almost four billion dollar projected loss in 2000 would similarly be acceptable. Consequently, one must look at the trends in time concerning a particular risk.

Another example of trends in transportation safety is presented in Figure 7 [3]. Depending on the indicator of risk that the decision maker is concerned about, different safety R&D budget allocations can be made. In the case of commercial aviation, the number of deaths per

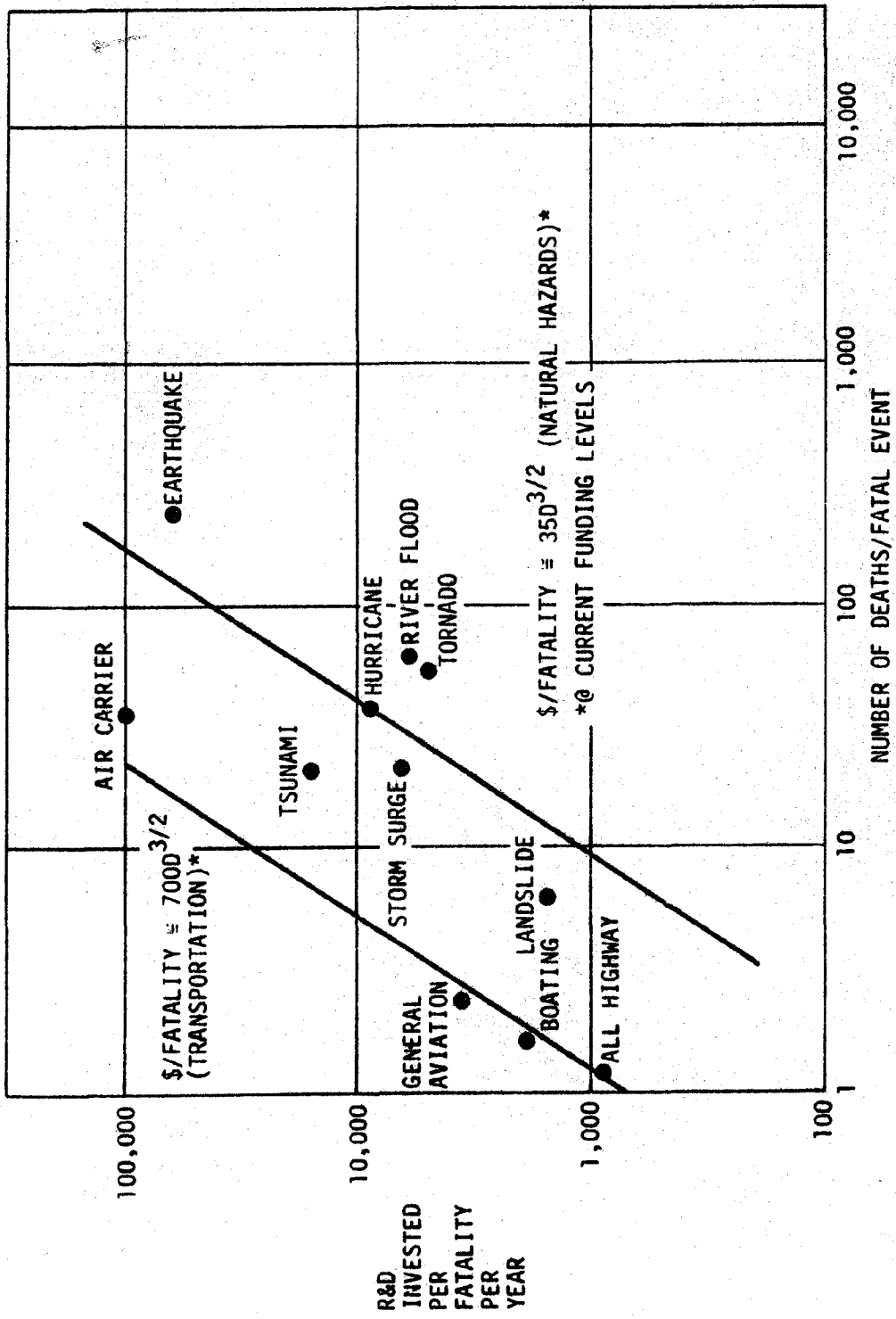


Figure 6. Safety Research and Development Funding Levels for the U.S. Government Agencies During 1973 Plotted vs. Fatalities per Fatal Accident for Various Transportation Modes and Natural Hazards

MODE	DEATHS ACCIDENT	DEATHS YEAR	DEATHS FATAL ACCIDENTS	ACCIDENTS YEAR	FATAL ACCIDENTS YEAR	ACCIDENTS TRIP	DEATHS PERSON-HR.
COMMERCIAL AVIATION	22% ↗	4% ↗	100% ↗	38% ↘	38% ↘	83% ↘	90% ↘
GENERAL AVIATION	20% ↗	--	1% ↗	11% ↘	--	--	18% ↘
PASSENGER AUTO	--	--	18% ↘	11% ↗	4% ↗	6% ↘	20% ↘
BUS	--	--	--	15% ↗	42% ↗	--	15% ↗
BOATING	5% ↘	9% ↗	5% ↗	15% ↗	--	2% ↗	--
COMMERCIAL VESSEL	6% ↘	20% ↗	--	29% ↗	--	--	--
INTERCITY RAIL	18% ↘	--	--	--	--	--	16% ↗

SCORE
17 - ↗
12 - ↘

Figure 7. Transportation Safety Trends Plotted from 1965-1975 Trend Data for Various Safety Descriptions

accident is increasing significantly; however, the deaths per person-hour are decreasing even more significantly. Combining utility curves for deaths per accident and deaths per person-hour, one could develop an optimum R&D budget for reducing losses. Yet a different budget could be developed for any one or combination of indicators the decision maker considers pertinent.

These three examples of utility demonstrate that the decision process is not a simple one. It depends on a number of normative scales which are subjectively chosen by the decision maker. It is the task of the decision analyst, however, to present the various alternatives using the concept of utility and the decision concepts in such a way that the decision maker can rationally justify the alternative or combination of alternatives selected.

In order to present an idea of the different processes which might affect the earthquake risk decision when considered from different perspectives, Table 2 ranks decision under uncertainty, with no probability given, for various people.

1. The legislator ... represents the public conscience and is influenced by it and special interest groups. His main motivation is to get reelected; however, in order to do this, he can't make too many waves. He must start as an in-betweenist.
2. The public administrator ... administers the law in the public interest. He is charged with the responsibility of building a mechanism to do what the law says. Being a bureaucrat, he wants to make sure that the least maximum regret is not experienced during his tenure in office.
3. The courts ... interpret the administration of the law within the Constitutional framework. They are not gamblers, and they are not pessimists; however, they definitely consider the principle of dominance (preponderance of the evidence) a first order in interpreting the law.
4. The big businessman ... represents the stockholders' interest for long term growth with an adequate annual dividend to keep the stock value up. Because he is big he has very little chance for a rapid growth rate which would drive stock prices up, and therefore attract capital. He must maintain at least a 5% dividend every year with a good rate of growth on assets. Therefore, he too is interested in the dominance principle first, with regard to the first-order of business in decision making.
5. The small businessman ... is first and foremost involved with the company's survival. Secondly, he wants to maintain an adequate annual growth rate that is hopefully about 20%. This growth rate is usually not achievable for big business, but is very possible for a small business. Therefore, the small businessman shares the same attitude as the public administrator, in that he applies the regret principle first.

Table 2. The Author's Opinion of the Probable De Facto Order of Usage of Seven Methods Giving Uncertain Futures Where No Probabilities are Known

METHOD	LOGIC	LEGISLATOR	ADMINISTRATION	COURT	BIG BUSINESS	SMALL BUSINESS	CITIZEN GROUP	AVERAGE
DOMINANCE	1	4	2	1	1	3	5	2.66
ASPIRATION LEVEL	2	2	4	7	2	4	1	3.33
LEAST REGRET	3	3	1	4	6	1	3	3
EQUILIKELIHOOD	4	5	3	2	3	5	6	4
INBETWEENIST	5	1	6	3	7	6	7	5
PESSIMIST	6	6	5	5	4	7	2	4.83
OPTIMIST	7	7	7	6	5	2	4	5.16

6. The citizen and citizen-groups ... attempt to maximize an immediately perceived gain for a definite aspiration level. They want "no nuclear power plant here", therefore they wipe out the nuclear power plant alternative and leave the gas, coal, or hydroelectric plants as the only alternatives. They drive the benefits from the nuclear plant alternative so low that it must be excluded.

You may opine different rank orders of decision making than that presented in Table 2; however, it shows that different people can see the same problem from different angles and therefore use different decision making processes. I have tried to compare the different perspectives with logic, but the logic presented is my logic and not necessarily correct logic. However, the rank order of the average of the six perspectives is virtually the same as the "logic" column.

In the final analysis, the quantitative risk analyst, using risk models and various earthquake decision alternatives, provides recommendations based on quantitative yet uncertain measures of dollars, lives or utilities. He cannot automatically include in the outcome the social, political, legal, administrative, and other secondary and higher order impacts or aspects of the problem. The final actions will be based on the incentive and the liability perceived by the decision maker, and on his authority for making decisions.

Therefore, I maintain that responsible action by the earthquake engineer involves a number of tasks and activities.

- Identifying the problem and the uncertainties associated with the problem. Spelling out all of the alternatives clearly.
- Developing various methods of analysis and detailing the problems and limitations with each method.
- Identifying various mitigation alternatives, strategies and their costs that can be used to lower risk.
- Performing a quantitative analysis of the alternatives under uncertainty.
- Identifying all the impacted elements, the authorities for action, the economic, political, social and legal constraints.
- Identifying the non-quantitative considerations and presenting possible alternative impacts for further evaluation.
- Developing results in a clear, concise and accurate communique to the socio-political audience. This audience includes the impacted persons, the decision makers involved.

These steps require the earthquake engineer to move beyond his models and numbers. He must know something about economics, politics, law, social systems, behavioral science, as well as secondary and higher order outcomes. He does not need to model these in a decisional framework; however, he must be aware of these elements in the problem. Since decision makers, for the most part, will not learn the technical problem at hand, it behooves the technical person to learn about the social, administrative, political, legal and economic aspects of each problem.

Some observations can be made at this point about the technical risk management processes:

1. The techniques are seldom practiced outside the university or research community./
 2. However, they allow us to get a total picture within the knowable world.
 3. They permit us to withhold final judgment until all of the knowable facts are in.
 4. They require the development of models which are developed by people who know their business.
 5. They tend to make an obscure solution translucent, if not transparent.
 6. Most importantly, they show us how to ask the right questions.
 7. They allow us to question each premise made within all parts of the analysis.
4. TECHNOLOGY ASSESSMENT
- 4.1 Methodology for Integrating Technical With Non-Technical Judgment

In the preceding discussion I alluded to social, administrative and economic aspects that influence the decision making process. Technology assessment is an attempt to integrate these "soft" parameters into the total analysis. Simply stated, technology assessment attempts to address the secondary and higher-order outcomes when a new technology is introduced or an old technology is modified.

What is a "technology"? It is defined as "...the technical method of achieving a practical purpose." A "secondary" impact is one that is immediately derived from the primary outcome. For example, if a person is killed, one direct outcome from the death is bereavement by the loved one. In a lighter vein secondary and higher order impacts could be related to the story, "for want of a nail a shoe was lost... for want of

a shoe a horse was lost... for want of a horse a general was lost... for want of a general the battle was lost... for loss of a battle, the war was lost..."

Technology assessment is not science, engineering, economics, political science or law. Rather, it is an art requiring talent, experience, and free thinking, structured by logic which is implicit within the technology being assessed. See Joseph Coates writings for a complete description of its process [14].

Schematically, I have presented an overview of an earthquake technology assessment in Figure 8. The assessment system is divided into three basic parts. The realm of quantitative calculations, which computes primary effects, has been discussed. The economic and environmental system is the second area addressed by technology assessment, and can only be looked at from a semi-quantitative standpoint. One looks at bounds, estimates, or orders of magnitude of outcomes. The third area for inclusion in the technology assessment process is qualitative in nature. The socio-political system depends principally upon psychological and emotional considerations: therefore, one must compare the goodness or badness of an alternative with other risks which have similar outcomes by using different types of decision processes (Table 2). These comparisons give the decision maker a perspective on the outcomes generated by the mitigation measure for intervention or strategy.

Table 3 was prepared from a recent report by Petak, Atkisson and Gleye [2] dealing with earthquake and other natural hazards problems. They set forth various secondary and higher-order impact areas which can be considered when implementing a mitigation. Remember that the mitigation or "cure" can be worse than the risk. Risk reduction is treated separately. Say that damage from an earthquake could be reduced by strengthening buildings through modification of the building code. One could trace five potential higher order outcomes (Figure 9). If the cost of construction is changed, this influences three more outcomes, one of these being the cost of housing. Cost, in turn, affects the quantity of housing, the demands for other goods, and so on.

In the end, one must understand that the mitigation as well as the losses influences all areas of social concern. It is the job of technology assessment to identify these variables and their impacts and to address them in as logical, free thinking, and complete a manner as possible. It will not be perfect. However, technology assessment attempts to identify the logical consequences of any decision as far into the future as possible.

5. CASE LAW AND SOCIO-ECONOMIC RISK AND DECISION ANALYSIS

In the foregoing discussion I briefly mentioned the legal ingredient in the decision/risk "stew." How do the courts treat risk and safety in

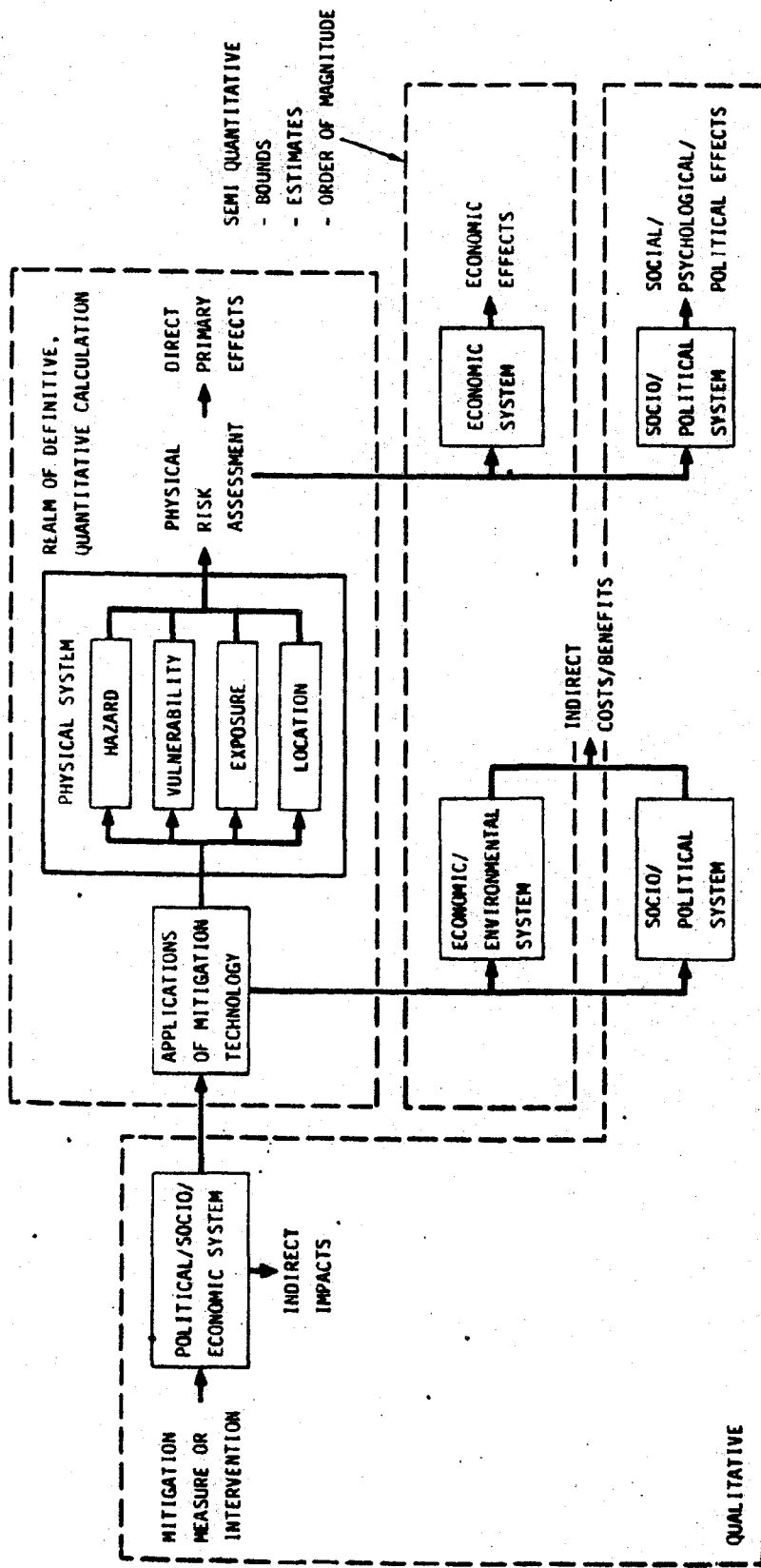


Figure 8. The Technology Assessment Process

Table 3. Areas of Impact That Could Be Considered When a Mitigation is Applied for the Purpose of Reducing a Natural Hazard

ECONOMIC
<p>PUBLIC: ADMINISTRATIVE, IMPLEMENTATION COSTS IMPACT ON TAX ROLES, ETC. PUBLIC UTILITY DESIGN, LOCATION, CAPACITY IMPACTS ON INDUSTRIAL LOCATION PREFERENCES IMPACTS ON PUBLIC HOUSING: COSTS, LOCATION, DESIGN</p> <p>AGGREGATE: EMPLOYMENT IMPACTS ON CONSTRUCTION INDUSTRY IMPACTS ON LABOR UNION (ORGANIZATION, JURISDICTION, ETC.)</p> <p>PRIVATE: IMPACTS ON MATERIAL SUPPLIERS COSTS OF HOUSING PURCHASE COSTS OF HOUSING MAINTENANCE COSTS OF BORROWING</p>
ENVIRONMENTAL
<p>SHAPE AND SIZE OF CITY POPULATION DENSITY LAND USE, OPEN SPACE ENERGY CONSERVATION MATERIALS SUPPLY ALTERNATIVE ENERGY SOURCES (SOLAR, ETC.)</p>
SOCIAL/POLITICAL
<p>LOCAL/STATE/FEDERAL AUTHORITY, JURISDICTION INSTITUTIONAL CHANGE (NEW REGULATORY BODIES?) EDUCATIONAL (TRAINING OF INSPECTORS, ETC. AND NEW ENGINEERING SPECIALTIES?) DISTRIBUTIVE JUSTICE (DISPROPORTIONATE COST FOR POOR? AGED? MINORITIES?) TOTAL HOUSING SUPPLY? LOW COST HOUSING SUPPLY? USE OF MOBILE HOMES? SECOND HOMES? POLITICAL COSTS OF IMPLEMENTATION FEELINGS OF SECURITY, SAFETY ETC.</p>

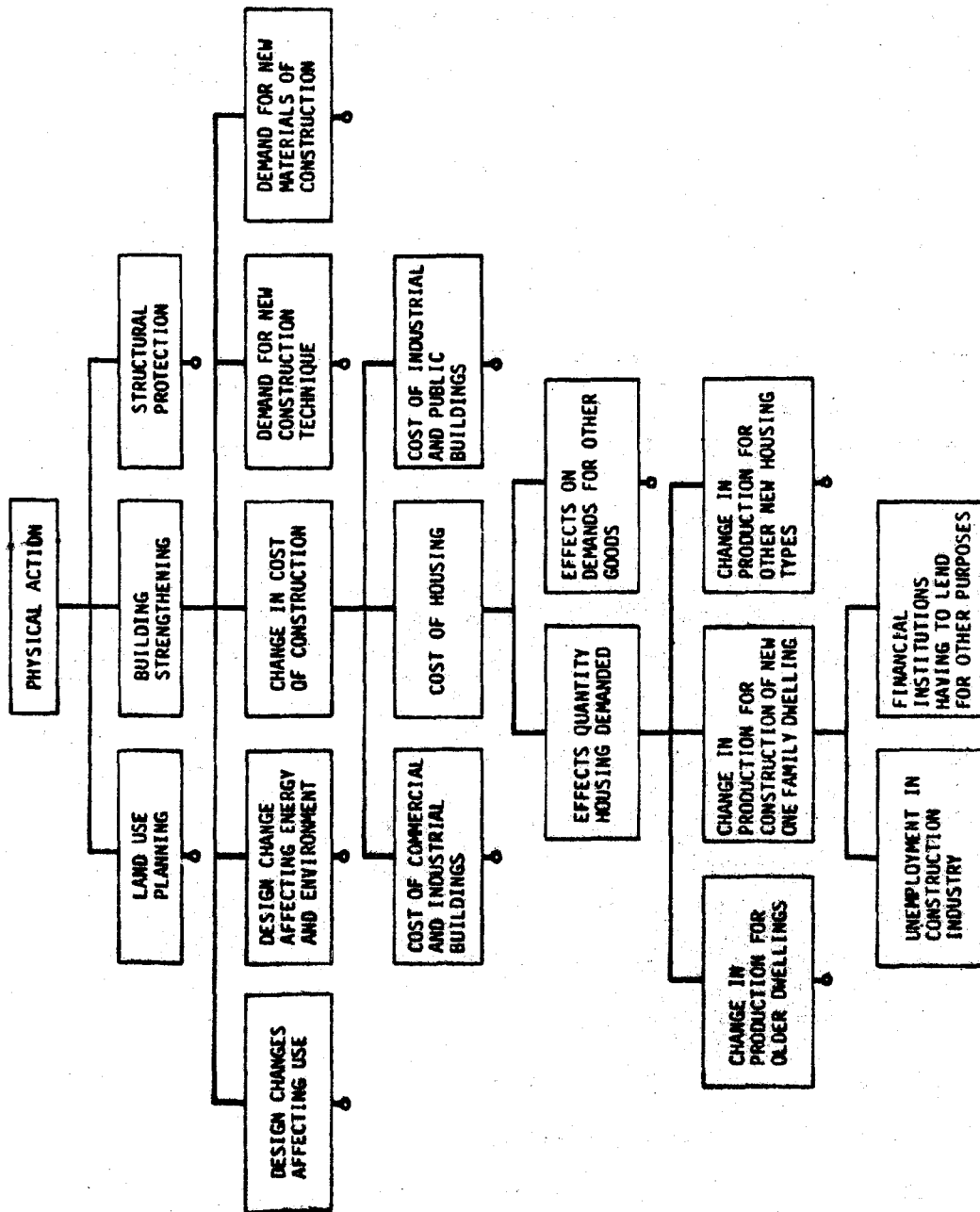


Figure 9. An Example of Tracing the Secondary and Higher Order Impacts by Applying a Building Code Change in Order to Mitigate a Natural Hazard

their decisions? Since the legal consequences are of first order importance to the outcomes of risk analysis and technology assessment, we must examine some of the tenets involved in order to put this principal piece of the puzzle into its proper place. Do safety considerations affect the outcome of litigation, or do court decisions affect safety regulations? This is the big question of today, since the courts are more and more becoming involved in social arguments. I maintain that safety considerations and court decisions should not be related:

- Safety, in design, seeks an acceptable risk which is a priori design.
- The courts seek out the loss-bearer which involves a posteriori fault.

However, we must recognize the trends in our legal system. They are such that fault no longer seems to take precedence. The old legal tenet "...did he do wrong or did he do right..." does not seem to be the question any more. Rather, the new doctrine in the courtroom is to spread the loss from those who can't pay to those who can.

Thus, it seems to me that the courts are forcing Congress back into the position of representing the "public interest" when making laws. They have done this by developing twelve major considerations that are delineated in almost every court decision in its findings of facts and conclusions at law [15]. These findings can help the earthquake risk and decision analyst to scope the problem. If the role players in every major project assumed during project conception that a court action would be brought against the project it is my guess that many problems would not arise. Let us examine the following and imagine the results if risk analysts religiously referred to these guidelines:

1. The usefulness of the mitigation.
2. The availability of a safer replacement structure.
3. The likelihood of injury.
4. The probable seriousness of injuries.
5. The obviousness of the danger involved.
6. The public's expectations concerning the structure's performance.
7. The possible elimination of risk through care or warnings.
8. The possibility of eliminating the risk without impairing the structure.
9. The "state-of-the-art" of the earthquake community.

10. The financial cost of making the structure safer.
11. Consumer willingness to pay for a higher priced but safer structure.
12. The bargaining power of the owner as contrasted with that of the consumer.

6. CONGRESS AND THE RISK MANAGEMENT PROCESS

As I have indicated, the political process is involved in assessing the consequences of risk and mitigations for risk reduction. Let me outline some of the things I have observed from past Congressional actions. First, one must recognize that Congress does not solve problems! Rather, it delegates power to administrative bodies who then solve the problems. Second, Congress originally passed laws which created the right of limited judicial review, and the courts supported this limited judicial review alternative. However, with the recent citizen movement, various citizen's groups have challenged Congress in creating the right of limited judicial review. Because of this buffeting, Congress required citizen participation in administrative action. In effect, this allows citizens to sue the government in order to test the "most reasonable" concept, not whether an administrative decision is reasonable.

Some advocates say that judicial review is the only answer for solving today's problems. However, changing the judicial system from one which resolves problems to one which develops most reasonable concepts was not the intent of the founding fathers. Yet another suggestion has been to require more detailed and more involved Congressional standards. I disagree. People are people; and to force Congress into a straight jacket will only inhibit the process, not make Congressmen better persons.

I principally disagree with the above postulates because the original intent of Congress was that it should decide vaguely, because Congress can't solve problems. Congress says: "Define the problem and solve it." And this is good, because problems are not defined for Congress. They are usually too complex for general solution by a lay community. Further, bit by bit solutions may lead to general solutions, if Congress performs its proper oversight review duty. In my estimation, there has been a shortfall here. The current technological and other problems that we face partly result from Congress transferring part of its responsibility into the judicial system, where it does not belong.

7. AN EXAMPLE OF RISK MANAGEMENT DECISION MAKING

This example involves assessment of alternatives regarding the correction of the earthquake hazards in the California State Capitol Building [17]. The building was more than 100 years old and constructed

of unreinforced masonry. The original engineering report presented alternatives in terms of costs and general risks. Yet no decisions by the Senate, the Assembly or the Governor's Office had been made. Therefore in order to provide a perspective for these bodies to make a decision, the risks and costs were translated in terms of bills each body had passed or signed into law that addressed the earthquake problem. The first bill, Assembly Bill 2300, required the adoption of the Uniform Building Code by all communities. Then in Senate Bill 519, the state mandated design levels for hospitals. By translating the design levels in terms of de facto risk and associating them with legislation which each one of these decision bodies had already made law, the decision to rehabilitate or reconstruct was immediately made. It is rather ironic to recognize that the only "risk" numbers that were persuasive in this example were "2300" and "519." Neither the cost nor the risk rate was seriously considered. Only the legislation involving risk that had already been passed by the politicians was the determinant.

8. PUBLIC INTEREST

In concluding this paper, I would like to briefly touch on the "public interest" which many believe should be used as a baseline for earthquake risk analysts. If a decision in any way involves the public at large, some discussion of this term is required. Today, we recognize six national goals that have been stated over and over again. They must be integrated through a Balanced Risk rationale to serve the public interest. These are:

- Energy
- Ecology
- Economy
- Effectiveness
- Environment
- Safety

INTEGRATED BY RISK BALANCING

These five E's and an S must be balanced in the earthquake technology that is being produced. Safety cannot be the sole ingredient.

Many scholars in the public administration field have asked the question: "Is public interest a guide or a goal?" Or "Is it a flag raised by special interest groups?" [18]. Very simply stated, the public interest is either a "moral imperative" or a "process of accommodation." If it is an imperative, then the moralistic guidelines behind that imperative should be stated. These are nebulous and individualistic indeed. If it is a process of accommodation, then it only involves "muddling through."

Who guards the public interest? The governments involved as well as private interests guard it. In other words, government in and of itself is not the sole policeman for the public; responsible action by interest groups - both citizen and corporate - is also required. In this case, the goal is to: (1) define what the public interest is in terms of the private and government interests; (2) assess the organizational effectiveness intended to serve the public interest.

In the case of seismic safety regulations, one must be responsive to the public desires and not necessarily to developing stronger codes because stronger codes seem better. It is obvious that some people are ambivalent in this case. They think nothing of letting old buildings go unstrengthened. Yet they cry "earthquake" when a nuclear power plant is planned; or they try to find a fault under a Liquid National Gas facility. In either case, I believe it is the task of the professional to:

1. Inform the groups at risk about his findings.
2. Communicate the information in such a way that a high degree of comprehension is attained.
3. Be persuasive that he is "doing his best."
4. Constructively involve management in order to be persuasive.

What we are all looking for is responsible action; but how is this action to be promoted? Figure 10 indicates three basic ingredients: a sense of responsibility and accountability, the awareness of the public, and presentation of alternative methods for risk reduction. The degree of responsible action is enlarged as these three ingredients are enlarged by the following pressures [19]:

1. Research findings in the technical community
2. Communication of research findings to the citizenry at large
3. Citizen input from special interest groups
4. The frequency and time since the last earthquake event against which responsibility action is to be taken
5. Decisions of the courts as they influence the sense of responsibility and accountability
6. Professional and political ethical standards

In the end, responsible action for serving the public interest depends on technical communication and an integration of the social, technical, political, economic, legal and administrative frameworks which

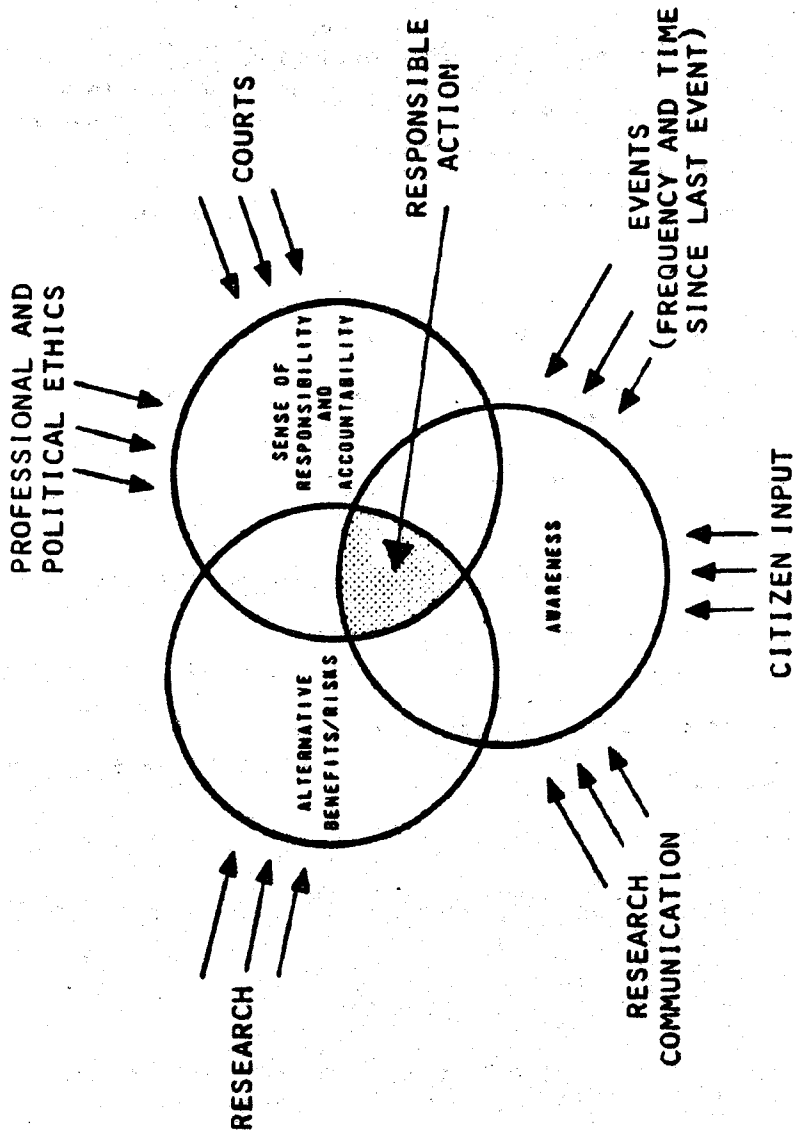


Figure 10. Ingredients and Forces Leading to Responsible Action on Technological Risks

at the same time involve and influence the public interest. The concept of balanced socio-economic risk analysis as applied to earthquake engineering is yet in its infancy; however, I believe it is the technical community's responsibility to take the lead in developing a process for achieving responsible action that not only is right but also persuasive.

References and Notes

1. J.H. Wiggins, The Risk Imbalance in Current Public Policies (Proceedings of Session IV, International System Safety Society Symposium, 1973).
2. W.J. Petak, A.A. Atkisson, P.H. Gleye, Natural Hazards: A Policy Assessment (J.H. Wiggins Co. Report #1246 supported by the National Science Foundation under Grant Numbers ERS-75-0998-A01 and AEN-74-23992, 1978).
3. J.H. Wiggins, Risk Perspective and Liability in Transportation (Proceedings, Engineering Foundation Conference on Product Liability, Franklin Pierce College, New Hampshire, 1977).
4. C. Starr, "Social Benefit vs. Technological Risk," Science 165, 1232 (1969).
5. C. Starr, Benefit-Cost Studies in Socio-Technical Systems (Perspective on Benefit-Risk Decision Making, Committee on Public Engineering Policy, National Academy of Engineering, 1972).
6. J.H. Wiggins, An Examination of Technical, Legal and Economic Factors Associated with Sonic Boom (Federal Aviation Administration Report FAA 70-1, 1969).
7. Summary Proceedings, Perspective on Benefit-Risk Decision Making, (Committee on Public Engineering Policy, National Academy of Engineering, 1972).
8. National Safety Council, Accident Facts: 1965 through 1978 Chicago, Illinois.
9. J.H. Wiggins, L.T. Lee, W.J. Petak, Seismic Safety Study, City of Los Angeles, (Dept. of City Planning, Los Angeles, 1974).
10. J.H. Wiggins Company, Building Losses from Natural Hazards: Yesterday, Today and Tomorrow. (Prepared under National Science Foundation Grant No. ENV-77-08435, 1978).
11. Chief, Memorandum: Draft of Preliminary Evaluation of DOT Safety R & D (R & D Plans and Programs Analysis Division, TST-24, Department of Transportation, Office of Secretary, Memorandum to Messrs. Paullin, Ward, Maxwell and Goodson, 1976).
12. G.F. White and E.J. Haas, Assessment of Research on Natural Hazards (Cambridge, Mass., 1975).
13. J. Hirschberg, P. Gordon, W.J. Petak, Natural Hazards: Socioeconomic Impact Assessment Model (J.H. Wiggins Company under Grant No. ERP-75-0998, 1978).
14. J.F. Coates, The Role of Formal Models in Technology Assessment (Technology Forecasting and Social Change, Vol. 9, 1976).

15. D.S. Hoffman, Unreasonable Risk of Injury Revisited. (Proceedings, Engineering Foundation Conference on Product Liability, Franklin Pierce College, New Hampshire, 1977).
16. National Transportation Safety Board, Special Study of Proposed Track Safety Standards (Report No. NTSB-RSS-71-2, 1971) and Code of Federal Regulations, 49 Transportation (U.S. Government Printing Office, Washington, 1974) Rev. 1, Parts 200-999.
17. W.J. Petak, The Engineers Professional Responsibility and the Public Interest, (Proceedings, 1976 Annual Reliability and Maintainability Symposium, 1341-76 RM 025, 1976).
18. J.H. Wiggins, Earthquake Risk Analysis of the West Wing, California State Capitol Building, Bulletin of the Association of Engineering Geologists, 11, pp. 147-159, 1974.
19. J.D. Collins, Alternatives for Risk Evaluation in Decision Making (Floodproofing and Flood Plain Management Conference, Engineering Foundation, Asilomar, Calif., 1977).

The Research of the Engineering Geological Features of the
Epicentral Area of an Earthquake of Magnitude 6 in Li Yang
in 1979.

Tong Ji University

Duan Guang Xian^I

Wang Jia Jun^{II}

Fei Han Chang^{III}

Abstract

This article is based on the three macroscopic investigations undertaken after the Li Yang earthquake in 1979. It is the result of the geological engineering work, prospecting and researching the Li Yang epicentral area from November to December in 1979. It states the west-north structure of the earthquake source from the view points of geomorphology, seismic geology and the mechanism of seismic focus. It gives a strong proof of some anomalies appearing in the epicentral area. It analyses the conditions of engineering geology with facts for the anti-seismic work in seismic focus. It provides a valuable information for the coming reconstruction and lays a foundation for the division of the water region of the earthquake.

Introduction

An earthquake of Ms=6.0 took place in the west-north part of Li Yang country, Kiangsu province, at 18.57 on July 9, 1979. The epicentral area was from Nan Dou to

I. Associate Prof. Tong Ji Univ.

II. III. Lecturer. Tong Ji Univ.

Sang Pei and the intensity was VIII. After the earthquake, the departments concerned came to this place and did a lot of research work, such as macroscopic investigations about the disaster and seismic observations. In the whole work, there were two different view points about the structure which induced the earthquake. It was short of a strong proof of the repetition of earthquake. There was no sufficient understanding about the strata texture, the distribution of clay and the characteristics of engineering geology of the overburden in the earthquake area. There were no quantitative and qualitative analysis of the clay. All these were harmful to the analysis of the earthquake, to the adoption of the anti-seismic measures, and to the precautions against earthquake. For the reasons mentioned above and on the basis of the long axis from Nan Dou to Sang Pei was selected and was arranged a prospecting line along NW 235° (figure 1) to carry out the seismic engineering geological exploration. The amount of work that was done is shown in figure 1.

Table 1

Item	Amount of Works
The total length of the prospecting line	about 11 Km
Drill holes	12, total accumulating depth 196.10 M
Screw drill holes	9, total accumulating depth 12.40 M
Static penetration test holes	18, total accumulating depth 207.80 M
Standard penetration test	5
Wave speed test in drill hole	15
Samples of the undisturbed soil	50 (for physical and mechanical tests)

(Continued)

Item	Amount of Work
Samples of the disturbed soil	75
The appraisal of the polarizing microscope	4

I. The survey of the earthquake of magnitude of 6 in Li Yang. This earthquake spread widely and was felt in Lin Yi, Zao Aon in Shantung province in the north, in Lon You, Yu Huan, in Chekiang province in the south, in the Yellow Sea in the east, and in Jiu Jiang in Kiangsi province in the west.

Over 800 aftershocks (up to the end of Dec. 10, 1979) had been recorded after this earthquake. One of the aftershocks reached the magnitude of 4.8 at 16.48 on July 11, 1979.

The parameters in connection with this earthquake are given in table 2.

Table 2

Microscopic epicenter	East longitude 119°15' 31°27'5" north latitude
Depth of seismic focus	12.6 KM
Seismic sequence	The type of main shock and aftershock
The type of seismic cause of formation	Tectonic earthquake
The mechanism of seismic focus	Joint plane I, strike 313°, dip 222.5° dip angle 54° Joint plane II, strike 18°, dip 118° dip angle 71°

The mechanism of focus was supplied by the eophysical Institute of the National Seismic Bureau.

After TANG SHAN earthquake on July 28, 1976, a short time-interval of forecast of seism-earthquake was made for Li Yang area. According to the analysis of tectonic system, some geologists confirmed that there was the seismic geological background in that area. But the prelude of the earthquake was not so obvious that they could make the forecast exactly.

Details about the macroscopic phenomena before and after the earthquake were described in our article in July 1979, and a supplement is made here about earthquake sound, sand eruption and overflow of water.

(1) Earthquake sound:

The earthquake sound appeared before and at the beginning of the shock. People there gave a vivid picture of the sound. Among the 91 examples of macroscopic investigations, 62 examples were concerned with the sound. The macroscopic sound of 47 examples came from the north-west direction. This shows that the sound obeys a certain rule and there is a relation existing between the sound and the earthquake. From the direction of sound (figure 2), we believe that it was associated with the structure in the NW direction which induced the earthquake. This is worth studying, because the structure that induces the earthquake is the place where stress is accumulated and energy is released. Especially, it is more important to regard it as a sign of prequake, because the signals are strong and a good relationship exists between sound and earthquake. During Li Yang earthquake, a great many people who had experienced the earthquake in 1974 rushed out of their houses as soon as they heard the earthquake sound. The earthquake starts from a gradual change to a sudden one, which causes the rock to break and results in a fierce shock. Therefore we should study another kind of

sound which is called "microscopic earthquake sound." Of course, it will need the specialists in geomechanics, rock-mechanics and the geophysic to make a concerted effort in carrying out the seismic forecast by earthquake sound.

(2) Sound eruption and overflow water:

The phenomena of sand eruption and overflow water occurred in Mr. Jiang's home in Nan-Dou town, in Si-Jia, Zhan-Ke and Yu Jia Lo Te - Dong Mei brigade of Qiang Fu commune. All these places are in the area of 8 degree. The phenomena is the most serious in the village called Yu Jin Lo Te. When the earthquake started, at more than ten places in an area about 0.3 mu, sand eruption and overflow water occurred 200 meters from the village in the North-East, and lasted for 4 days until the mid-day on July 13, 1979. In this area, the ground water table was rather high and the water surface in the river nearby was only 20 cm below the land surface, the materials erupted are light mild clay called microsilt (figure 3) whose grain size, ingredient and differential thermal curves are basically similar to those of the microsilt erupted in Mr. Jiang's home in Nan Dou. The distributive direction of the sand eruption and overflow water holes in Yu Jia Lo Te is NW 280° and the general direction of the holes is NW. It is obvious that the phenomena have a connection with the earthquake structure. As the liquefied sand soil made the house foundation ineffective, a two storeyed brick house belonged to Mr. Jiang was collapsed (figure 4). Both the building of the Nan Dou Supply and Marketing Cooperative and that of Nan Dou Farm Machinery Plant are brick-cement buildings. Comparing these two, the former was not much damaged by the liquefied sand soil, whereas the latter got much damage, the house being built on back-filled soil which caused differential settlement. It can be seen that the

vibrating inertial force of the house on the liquified sand soil seems to be smaller than that on the unliquified sand soil. Hence we may conclude that if the foundation loses effectiveness, the damage will usually be greatly increased by earthquake, but it is not necessarily so with the liquified sand soil.

II. The inducing seismic tectonic. The Li Yang earthquake of magnitude of 6 is an indication of the movement of the Kiangsu block. It is certain that there must exist regional geological tectonic background and the inducing seismic structure. The Li Yang earthquake is of tectonic seism.

(1) The regional geological tectonic background:

This area is in the south-west part of Kiangsu province. It is in the region of the reflected arc of the east wing of Huai Yang orographic type, which is in the second rise band of the new Hua Yia system in the eastern part of China.

The eastern part of this seismic area, Li Yang to Son Wang, belongs to the rise area. The strata of Paleozoic group and Mesozoic group are exposed to the surface. The middle part, Shang Pei to Nan Dou belongs to settle area, and is covered with Quaternary System except exposure of basalts of Tertiary Period in a few places. From the data of drill holes in Ya Xi town, Shang Pei, Jin county, it is found that down to 800 meters it is still Tertiary Period. Thus, a block basin of graben type has been formed - Nan Dou basin (figure 7). Mao mountain is rising continuously and Nan Dou basin is sinking without any interruption, therefore this is the area where the perpendicular differential movement is the strongest.

In the south of Kiangsu province, the depth (4) of the basement is 5 to 7 KM and the deepest is 9 KM.

It is 7 KM in Li Yang. The bearing of the contour line is NE - NEE and NW. It is shown from the contour that the deposit of the overburden is controlled by two fault groups in the directions of NE or NEE and NE.

(2) The inducing seismic structure:

So far there are several papers (2) (3) (4) (5) (6) on the exposition of Li Yang inducing seismic structure, and on the discussion in common. They confirm that the intersection of the two fault groups NE and NW is the place of inducing seism, but they have two different kinds of view points -

- a) NWW fault is the inducing seismic tectonic.
- b) NNE fault is the main inducing seismic tectonic.

Our view belongs to the first (3). We must understand the fault of inducing seism from the view point of seismic engineering and must take anti-seismic measures against inducing seism.

First: From the map of the distribution of seismic intensity, someone thinks that the main tectonic is in NNE because the total formation of the intensity line map shows the direction of NNE. But it is obviously affected by the conditions of landforms and lithological characters. The west of the seismic area is Mao mountain and the east is the hilly land. It is narrow in the east-west direction and wide in the north-south direction. When the seismic waves arrive at the mountains of west or east, they will attenuate quickly. The VII. degree area is long in the south-north direction and short in the east-west direction, and therefore it shows that the NNE is in development. But it is not sufficient to determine that the direction of NNE is the main tectonic.

Second: Looking at the VIII degree area (figure 8), we can see that the long axis is NWW and the VIII degree anomaly area is also NWW, about 290° - 310° , similar as

the NW fault, and it coincides with joint plane 1. Furthermore the long axis of the VIII degree anomaly area of Song Xin to Yan Xia is also NW.

Third: Zhang Zuo-Nan Dou-Bai Ma-Li Shui NW rift band is active and its bearing is 290° - 310° . The existence of the NW rift made the Mao mountain separate into several segments. The places where the rift past through became mountain passes. The rift can clearly be seen from the satt lite photos. Crossing through different units, the rift which stretches right over a hundred kilometres is a bed rock rift and active erupting hand of volcanoes.

Fourth: To the south of the valley of Song Pei river lie six rivers cutted. From geomorphology and the distribution of rivers it is determined that the N-S rivers are cut by N-W rivers at the contemporary age. This is caused by the underground tectonic movement of NW valley that becomes the powerful proof of recent actions of NW tectonic.

Fifth: After the investigation of buildings we have found that to the north of Nan Dou-Tang Zhu-Shang Pei, the buildings become dextral (figure 9, 10) and on the contrary the earth surface became sinistral. To the south of that district, the buildings became sinistral and the earth surface dextral. The 河角广 mechanism theory of seismic focus enlightens us to consider that Nan Dou-Tong Zhu-Shang Pei must be an inducing seismic rift.

Sixth: Nanking seismic brigade did the investigation before Li Yang earthquake of magnitude of 5.5 on April 22, 1974. They discovered the macroscopic anomalies in 20 surveyed water points (figure 11). In or around the seismic focus the groundwater table was universally ascended but it was decended in most round areas. The ascending area became the ellipse type of NW which was similar to

the seismic focus of macroscopic investigation. Hence these had the reference value about the NWW ellipse of groundwater ascending area in 1974. Figure 12. The compound columnar section of Quarternary strata.

Seventh: In Dong Mei brigade where had fierce erupting sand and overflow water, the distribution of the holes was 290° . It showed that the phenomenon was controlled by NWW tectonic.

Eighth: Within 62 examples of the macroscopic investigation of earthquake sound, the sound came from the NW in 47 example. The sense of vibration was that it pushed people to the south-east. It is obvious that there is an inter-connection between the vibrating sense and the direction of inducing seismic rift.

To sum up all these we consider that the NWW rift is the inducing tectonic.

III. The characters of engineering geology of Quarternary strata in Li Yang seismic focus area of magnitude of 6. In this seismic focus area the thickness of Quarternary strata is about 15-20 M. After prospection, the results of the tests are the following:

1a. Soil-It is brown yellow and brown grey clayey loam with a few ironstones, calderites, a great many plant roots and a lot of humuses. The thickness is 0.2-0.6 M.

1b. Mixed backfilled soil- It is grey black and rather dense with a lot of pieces of broken bricks and tilles. It is 0.5-1.7 M. In thickness.

2a. Clayey loam- It is brown yellow, grey yellow and wet with ironstones and calderites in soft plastic state. It is 0.7-1.5 M. In thickness.

2b. Mud- It is black grey with a lot of humuses, pieces of broken bricks and titles and plant roots. It

is 0.8-1.0 M. In thickness.

3a. Light clayey loam- It is brown yellow and wet with a few ironstones and calderites in soft plastic state. It is 2.3-4.0 M. In thickness.

3b. Muddy clayey loam- It is grey, grey white and grey with a little humus and a few plant roots and shells. In some places it is intercalated with clayey loam and thin layers of silt. It is 7-12 M. In thickness and is distributed in the bank of cofferdam. Its engineering character is bad. It is the main stratum to control the damage of shock and the stability of engineering structure.

3c. Clayey loam- It is grey and wet with ironstones and a few lime nodules in plastic state. It is 1.3-3.5 M in thickness.

4. Clay- It is dark green and rather wet with ironstones in stiff plastic states. It is 2-5 M. in thickness.

4L. Silt- It is light yellow with calderites and lots of mica in medium dense state. It is 0.9 M. in thickness.

5. Light clayey loam- It is brown yellow and wet with ironstones and a few lime nodules in soft plastic state. It is 1.3-3.1 M. in thickness.

5L. Medium sand- It is grass green, earth yellow and rather wet with the grains of rhombic quartz and a small quantity of silt in medium dense state. It is 1.42-1.8 M. in thickness and is partly in these areas,

6. Clayey loam- It is red brown and wet and is the sediment of shale weathered in stiff plastic state.

Fig. 12 is the compound columnar section of Quaternary strata.

Table 3 is the physical and mechanical characters of

each strata.

IV. The analyse of seismic damage of the ground and foundation of seismic focus. The earthquake related to Li Yang county on a large scale. According to the statistics there were over 120,000 houses collapsed, over 100,000 houses partially collapsed and about 123,000 houses tilting with gaps. The total amount is over 340,000 houses. Nine reservoirs were damaged. The capacity of each reservoir was over one million cubic metres. More than 500 culverts and sluice gates were damaged in various degrees. Twenty bridges were damaged. The seismic waves caused damages in sixteen communes. 90% of the houses in Song Pei commune were collapsed. Over 70% of the houses in Song Xin commune were collapsed too. The disasters were serious. From the investigative results of seismic damage we can see that except for the distributing rule of intensity controlled by the inducing tectonic, there is an anomaly of intensity which is concerned with landforms, topography, soil and type of foundation.

There are two completely different kinds of scenes of seismic damage that are only ten metres away from each other. Then it is necessary to analyse the relationship between the condition of foundation and the seismic damage and to analyse relative "anormalt" with the help of longitudinal section of the main axis bearing of Seismic focus.

(1) The influence of topography, landforms and inducing seismic tectonic to seismic damage:

The inducing seismic rift of Li Yang earthquake of magnitude of 6 past through the seismic focus in the direction of NW. In VIII degree area the space is rather long in the NW-SE direction and quite narrow in the NE-SW direction. In connection with the two anomalies

of Nan Dou town and Song Pei town, the total space is also NWW. It illustrates that NWW inducing seismic tectonic takes the controlling function.

The range of prospection is from the west to the east, Song Pei- Xi Tong-Zhang Jia Jiao- Qin Fong- Nan Dou. From the analysis of the geological profile we can see that the landform is gradually inclined and the elevation is from +5 - +6M to +2 - +3M. The elevation of the area from Xi Tong to Dong Tong is partly about +7 M. The piedmont of Li Yang area is widely covered with "Xia Shu Soil". Since the time of upper Pleistocene of Quarternary, a fierce erosion has occurred. Then the furrows have been cut downward and the earth surface has moved upward. It gradually forms an incomplete mound. A series of marshes has been formed because the furrows are cut downward to be depressions and the Zong river has been cut out. For example, a certain thickness of muddy clayey loam has deposited in the Nan Dou marsh because the deposition of static water and man-made coffer have reduced the scope of marsh and enlarged the coffer. The areas, lower than +4.5 M are coffer lands on which there is muddy soil of certain thickness. With the macroscopic investigation we get the rules of seismic damage. The mound is damaged lightly. The gentle slope in front of the mound, depressions of coffer and the areas along the river are damaged seriously. For example, Nan Dou town is in Nan Dou marsh and Zhang Jia Jiao, Xin Cai Yu villages are in the depressions along the river. All these seismic damages are controlled by microcosmic landforms.

In the macroscopic investigation we found an anomaly. To the east of Song Pei, 3 kilometres away, is the Dong Zhang primary school in which there are two rows of classrooms in the direction of east-south, about 10 metres away to each other. Built with bricks and stones, these

classrooms were all the same in form, structure, material and construction. But at the time of earthquake, the south row was all collapsed and only some crevices were caused in the north row which has been in use till now. We did a main prospecting on the anomaly. We arranged a drill hole, two static prospecting holes and four screw drill holes near the primary school. It showed that the northern classrooms were on the mound, the upper part of which is only about one metre brown yellow clayey loam and the lower part is clay in stiff plastic state. 8.6 M downward, it is the bedrock lightly weathered. The classrooms of the south row were on the gentle slope. The basement of the southern walls were just on the edge of coffer land under which there is muddy clayey loam which is 1.0 M in thickness. Because the two rows were on the different conditions of microscopic landforms and soil characters, it is certain that there were two different results.

(2) The influence of basement soil to seismic damage:

As the basement of buildings, the layers were subjected to the attack of seismic waves during the time of earthquake. Under the action of building, the layers bear the feedback function of the vibrating energy of the buildings, therefore buildings and the basement together prevent the movement of seismic force. The seismic effect of the characters of the basement soil should be an important factor of seismic damage. One kind is the basement failure, such as seismic sinking, crevice, sliding and liquefied sand soil etc, which break the upper construction. The other kind is that the effects of filtering and intensifying of the basement soil reduce or sharpen the damage of buildings under the seismic action. It is very important to clarify the engineering characters

of the basement soil in the analysis of seismic damage. The engineering characters of the surface soil of the prospecting area is in table 4.

According to the analysis of the profiles of engineering geology, from the east of Dong Zhang primary school to Lo Tai Yu, the earth surface belongs to depression deposited with muddy clayey soil to a depth of 7-12 M. Its water content and compressibility are large ($=0.064$). The soil belongs to the layer of high compressibility and its bearing capacity is $9T/M^2$. The buried depth is about 1.0 M.

As the travelong speed of the seismic wave is $V_s=98M/see$ this layer plays a controlling function in the whole range. It directly affects the serious degree of seismic damage. For example, there were two static sounding holes J14 J15 in the east and west of San Ca He village.

From the static sounding curves we can see that there is such a thick muddy clayey loam and that almost all the houses of San Ca He village were collapsed. Another example is that both of Zhang Jia and Xie Cei Yu demonstrated the same scenes.

The J16 hole is on the thinning out of muddy layer where the light clayey loam is only 2.5 M to earth surface. There is a village around the J16 hole, then the serious degree of seismic damage cannot be determined. But observing the martyrs grave stones and the irrigation ditch nearby we know that the seismic damage was light.

On the both sides of Nan Dou town two drill holes, CK1 CK2 were arranged. The soil samples of the holes show that there is a layer of muddy clayey loam of 12 M intercalated with thin layer of light clayey loam of 2-4 M. Based on calculating the critical liquefied

rumming number of standard penetration of the layer, N equaled 8.3 rumming number (the light clayey loam of caculation minus one degree according to the determined liquefied standard of anti-seismic rules). Although this layer was not done the standard penetration test, to compare with the lower layer, light clayey loam and silt, the void ratio liquid index were larger than the lower layer but the unit weight of soil was smaller than the lower. We estimated its standard penetration rumming number was smaller than the critical rumming number. It is the main layer to make the erupting sand and overflow water. The erupting sand of the well of Nan Dou Jiang Xi Zong home and water becoming muddy had the relationship with the layer.

Though there is no muddy clayey loam layer in Song Pei town near the Song Pei post office, there is a layer of mud of 2 M in the depth of 1.7 M. The layer is soft but it directly influences the serious degree of seismic damage.

During the time of earthquake the accumulating energy of the layer travels through the layer to the earth surface in the form of elastic wave. Because of the different media the earth surface effects are various and express different seismic damage. On view of anti-seismic the soft basement soil can enlarge the vibrating amplitude with the long vibrating period and postpones the time of vibration. This phenomenon aggravates the damage of buildings. The liquefied cutting off seism of the saturating sand and the damping function of eliminating seism of the soft soil are useful for anti-seism. However which kind of the foundation it is, it will aggravate the seismic damage, when the self vibrating period of the building is as similar as the vibrating period of the foundation soil and it will produce the harmonic vibration.

With the evaluation of the condition of the foundation soil, Li Yang seismic effect expressed the function of amplification and filter of the foundation soil. The function will be enlarged as the thickness of the soft soil is increased. The most houses were civil houses in the district of seismic focus. The type of foundation was a unitary strip of wall made of bricks. There was a few simple factories which had not formally been designed and calculated in the side of foundation. It could not clearly show the relationship between the seismic damage and the type of foundation.

V. The repeatability of the distribution of seismic damage:

To compare with the earthquake $M_s=5.5$ in 1974, the distributing region, the type of seismic damage and the damage degree were almost the same. Li Yang area had the earthquake twice in 5 years. It expresses the repeatability of earthquake and seismic damage. Our country has many earthquakes. It is calculated that in the history of our country there were over 9000 times of earthquake among which 6.7% belonged to disastrous earthquake. After liberation, there have been more than 200 times of earthquake which were over the magnitude of 6. Hence we must have strength to research the repeatability of the distribution of seismic damage.

So far in our country or abroad people are still in the perceptual stage of cognition about the phenomenon of the repeatability of seismic damage in the same area. Lanchow seismic team gave us a useful consideration about the problem. Based on the data of magnetotelluric method, they found where had been happened the huge earthquake in history the underground temperature is high. On the contrary the underground temperature of other

places is lower. Furthermore the high temperature band of the seismic focus has the obvious direction. When the huge earthquake is happened, a great deal of heat energy is produced because of the faulting, friction and fierce deformation in the place of seismic source. It makes that rock strata of the faulting plane raise the temperature. When the temperature of rock is raised, its stress will be relaxed very quickly. Therefore the efficiency of accumulating the energy of elastic deformation will be decreased as soon as possible in seismic focus. Then the place of seismic source cannot accumulate a great deal of stress and break out huge earthquake. As the time passing away, the temperature of the place of seismic source will decrease to the former state. At that time, the media can accumulate the energy of elastic deformation once again and will break out another huge earthquake. Because the conduction of rock heat is slow, the interval of time is rather long. By the experiments of solid physics it declares when there is a fast tectonic function, it can compensate the decreasing of accumulating energy of elastic deformation induced by raising temperature. The frequency of huge earthquake may be increased. We consider that the Mao mountain is continuously rising and Nan Dou basin is decending without a break. As the functional force of tectonic is at high speed, it induces the repeatability of Li Yang earthquake. This assumption is not well considered and only the reference.

The another side of the repeatability of seismic damage. There is a weak link in geologic body. By the prospecting study we can see that from Nan Dou to Shang Pei, the depth of groundwater table is rather shallow and the upper soil layer is quite soft (mud, muddy clayed loam etc.) The layer also consists of easily liquefied

light clayey loam and landforms are special. These weak links were not changed in the two earthquakes of Li Yang. This condition shows the ability of anti-seism is quite weak. While the tectonic of inducing seismic of the two earthquakes were all NWW, the tectonic lithological character are the basic factors of the repeatability of seismic damage.

The stack problem is the third side of the repeatability of seismic damage. The earthquake in 1974 had a potential influence (3) (13) to the earthquake in 1979. Sun Pin Shan and Qin Yong Chang comrades of engineering-mechanical institute gave a good exposition for the problem. We also paid attention to the problem in the time of macroscopic investigation. The seismic damage of houses was analysed in my article (3) last year. We take Nan Dou highway and Song Xin bridge as an example. In the earthquake of 74, the Nan Dou highway bridge which is a double-curvature arch bridge was lightly harmed, but this time the bridge was heavily damaged. This time, the platform lost stability and the damage was produced. Under the action of seismic force, the road surface of the bridge heads and the soil body along the river lost stability sank and slid toward the middle of the river along a faulting plane. At the same time, the platforms also sank and slid toward the middle of the river. At last there were 5-6 cm difference between the road surface of the bridge heads and the pavement of the bridge platform. It is reported that if you did not pay attention to the problem, you could not find the difference in height of pavement and the crevices in the arch ring. That was just the internal harms attacked in '74. This earthquake increased the damage of them (fig. 16). It is more obvious in Song Xin bridge. It is told that the bridge was not repaired and solidified after it was harmed by

the earthquake of 1974. The earthquake of 1979 widened the crevices of the stone arch bridge and the stone steps near the bridge and the collapsing space (fig. 17).

These facts stated that after the attack of earthquake, the problem of anti-seism and solidying is very important.

VI. Conclusion:

1. In the coming macroscopic investigation, we should gradually combine seismic geology with earth surface movement, geological prospection of seismic engineering (consisting of engineering geophysics) and the structure of buildings. Then we can do against earthquake in quality and quantity. It has the very important meaning to reconstruct the damaged area and reeuce the future seismic damage.

2. After the study of NW tectonic of Li Yang earthquake of magnitude 6, considering the earthquake in Xin Tai, He Jian, Hai Cheng and Tong Shan, we deeply feel that it is necessary to observe the faulting action from north to west. It is just the N-W fault which has the new and strong activing. When we take further step to analyse Peking, Tientsin and Shanghai, the N-W fault cannot be ignored.

3. By the investigating result of this macroscopic seismic damage, one end of the seismic focus (VIII degree) is at Dan Song village of Song Pei commune and the other end is at Da Li Shu town of Qin Feng commune. We use the result of the prospecting experiments to analyse the division of seismic intensity in small area. Except for considering the base of the tectonic of inducing seism we should pay attention to the influence of cutting off seism of basement soil, eliminating seism or filter and amplifying function. According to the rules of dividing

the site soil (II) of the designing standard of anti-seism of industry-civil-architecture, to the west of Dong Zhang primary school belongs to II site band and to the east belongs to III site band in where mud is buried in the depth of 10 M and is harmful for anti-seism of buildings. With the investigation of seismic damage, we suggest that the distributing position of seismic focus should be the Dong Zhang primary school as one end and Lo Tai Yu village of Qin Feng Commune as the other end which conform with the practice condition. It is a reference for the seismic department in duty.

4. The permissive bearing force of foundation of muddy clayey loam is $9T/M^2$. Based on the rule 8 of the standard of anti-seism design, if the soft clay layer of VIII degree R $10T/M^2$ is in the main forced region of the foundation of buildings we must adopt suitable measures of anti-seism. When the plan of building and foundation is designed, the common function of upper structure and foundation must be considered. The model of building, condition of load, type of structure and geological condition must synthetically be analysed. We should determine the reasonable architectural measures, structural measures and the treating plan of foundation. For example, we may use pile foundation or other artificial treating foundation, enlarge the bottom area of basement, deepen the foundation, reduce the weight of load, increase the whole character of structure and the balanced symmetry etc. In Li Yang earthquake area, the strip foundation wall is used in a great many houses. The wall bodies are soil wall, hollow masonry wall etc. There were various degrees of damage in this earthquake. The rigidity of the whole body is little which is the main reason. As if the contact character of the mud brick wall is bad and the intensity of mortar joint used

in hollow masonry wall is too low. We suggest that the mortar index should not be less than No. 25 and the brick index should not be less than No. 75. When pond is used as architectural site, people must scoop up sludge (mud and muddy soil) and fill the soil of medium sand, coarse sand and rubble, slag and clay soil and other materials which has no erosion and has stable character. Then it may prevent the appearance from the guest house of Nan Dou Farm Machinery Plant.

5. There were only five years from Li Yang earthquake of magnitude of 6.0 to the earthquake of magnitude of 5.5 in April 22, 1974. It is such a short time to accumulate a great deal of the releasing of energy that we must earnestly research the seismic repeatability. Now we should pay attention to the latent influence of the earthquake in '74 to the earthquake in '79 and earnestly take the measures of anti-seism and increase the quality of construction. Then we can reduce the future damage induced by the seismic repeatability.

REFERENCES

(1) The speech of comrade Zhen Xi Wen in the discussing meeting of seismic trend called by Li Yang seismic office.

Comrade Zhen is the member of the second geological team of the geology bureau of Kiangsu Province.

The speech of the author of this paper in Oct, 1979.

(2) The indicing seismic tectonic of Kiangsu Li Yang Sun Yan and Wang Zong Jing in Oct, 1978.

(3) The preliminary investigation of seismic damage of Li Yang earthquake in 1979.

Duan Guang Xian, Qu Ze Sheng,
Yu An Dong in Sept, 1979.

(4) The character of Kiangsu seismic tectonic and the discussion of seismic harmfulness

Xie Rui Zheng, Zhu Yong Zheng,
Qui Ran Zhong in Feb, 1979.

(5) The basic character of seismic geological tectonic and the discussion of nowadays stress field in the area of

Ning Zhen - Yi Li Wu Lian Ying,
Sun Shou Cheng in Nov, 1979.

(6) The preliminary discussion of geological tectonic of Li Yang earthquake of magnitude 6

Chen Xi Wen in Dec. 1979.

(7) Seismic disaster (Japan)

He Jiao

(8) Seismic geology

Nanking University Geological Dept. in Oct, 1977.

(9) The engineering geological prospecting standard of industrial and civil architecture (TJ21-77)

(10) The designing standard of ground foundation of industrial and civil architecture (TJ7-74)

(11) The designing standard of industrial and civil architecture (TJ11-78)

(12) The teaching materials of the condition of seismic source.

Lanchow seismic brigade in Oct, 1972.

(13) The distribution and the site affection of Kiangsu Li Yang earthquake.

Sun Pin Shan, Qin Yong Chang in Oct, 1979.

Figures, photographs:

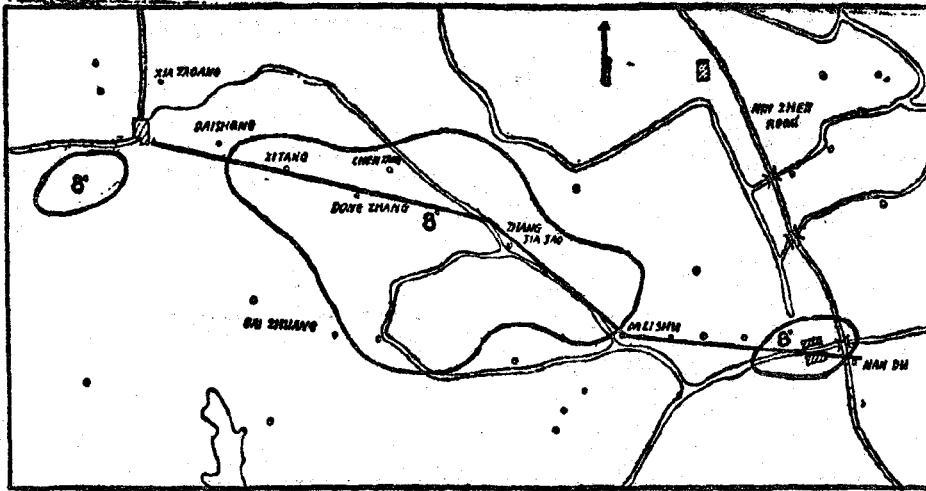
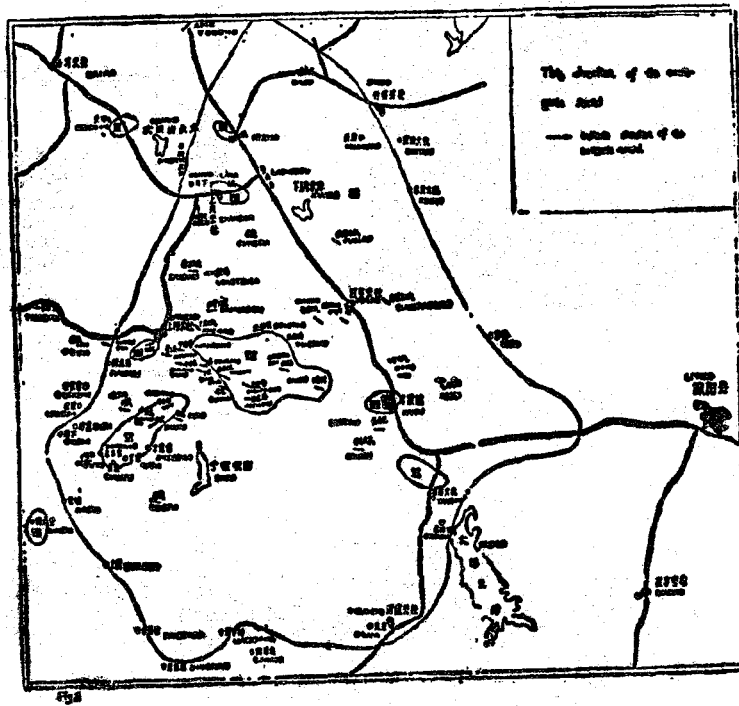
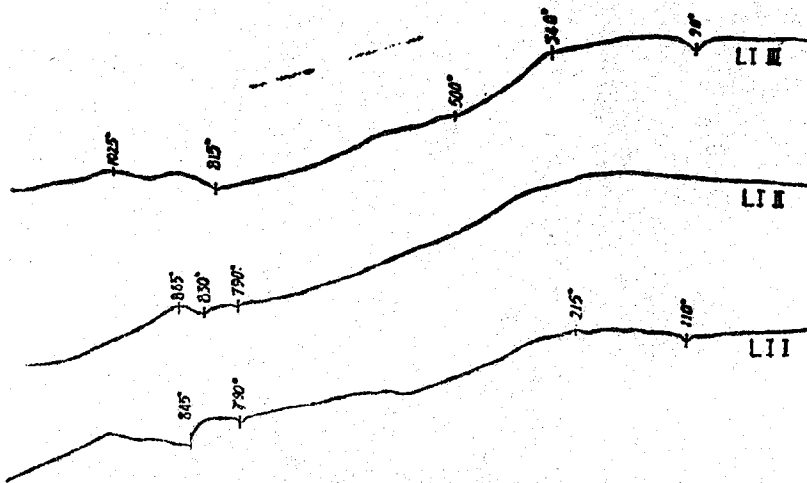


Fig 1 The sketch map of the distribution of prospecting lines in magmatogenic area.
 — the straight line is prospecting line



Reproduced from
best available copy.



Sample number	Location	Drilling and temperature in the rock	Temperature	Weight of sample	Amplifying times	Date
LI I	8m deep in the wall of the Tang Basin	11"/mm	15°C	300 mg	350	at 11:00 on 10.12.79
LI II	3m deep in the wall of the Tang Basin	"	"	"	350	at 9:30 on 10.12.79
LII	"	"	10°C	"	400	at 0:30 on 10.12.79

Fig 3 The differential thermal analysis curves of the light clayey loam.



Fig 4

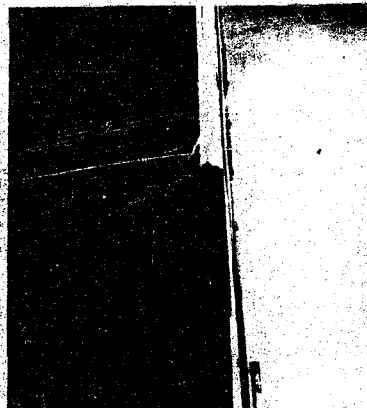


Fig 5



Fig 6

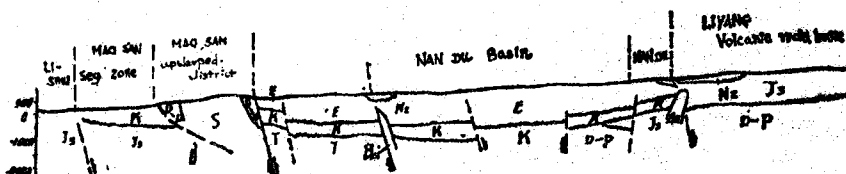


Fig 7 The profile of NAN DU Basin



Fig 9A The reversing Chimney



Fig 9B The reversing Chimney



Fig 10A Crevices in a wall



Fig 10B Crevices in a wall

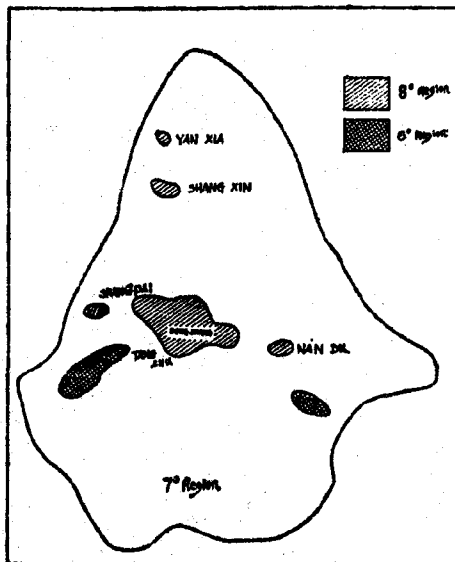


Fig 8

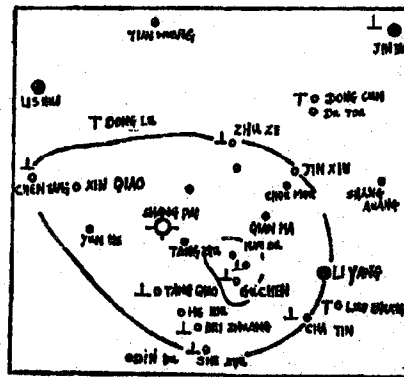
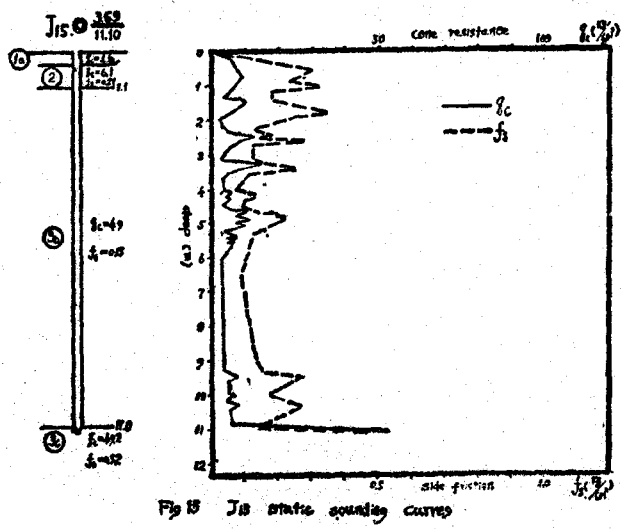
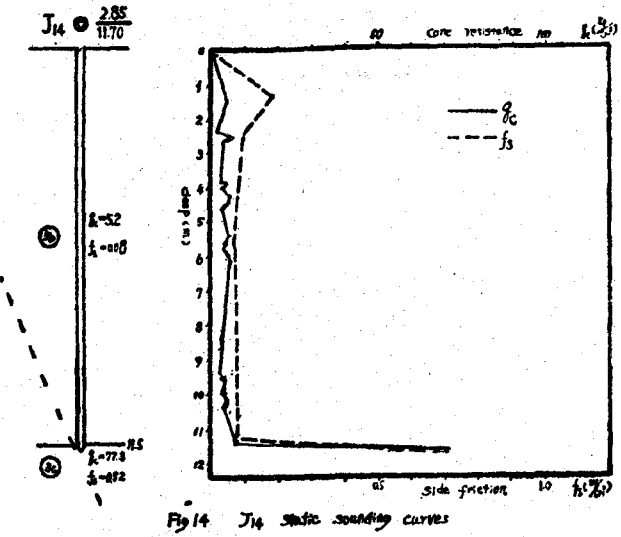
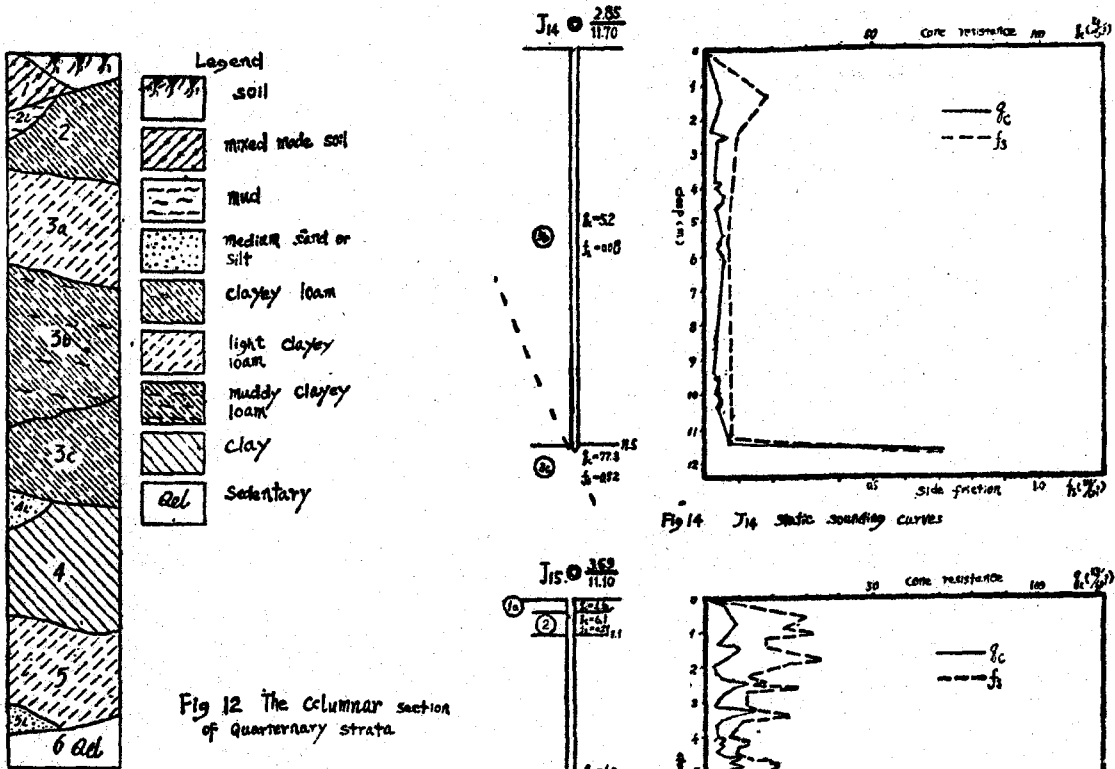


Fig 9 The variation of ground water induced by the earthquake of magnitude of 5 in LIYANG in May 1974

- Legend
- ascending of groundwater Table
 - descend of groundwater Table
 - groundwater becomes and its colour and taste changing
 - Seismic focus
 - The magnitudinetic area of macroscopic investigation
 - the ascending area of ground water



Fig 13



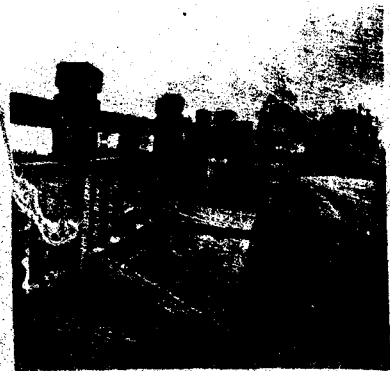


Fig 16 Sinking of the platform
of Nan Dou bridge



Fig 17 The staggen of Song Xin
bridge, the collapsing and
faulting of steps

The physical and mechanical characters of each strata

Table 3

Strata number	Soil	Thickness of strata	W	r	e	G	W _w	W _p	I _p	I _L	Solidifying		consolidated quick compres- sion test		static penetration test		N ₆₀	
											C	E _s	C	φ	q _u	q _c		f _s
2 _L	clayey loam	07-15	349	104	1.00	273	374	216	15.8	0.81	0.040	50	0.22	21°30'	0.73	14.9	0.29	
3 _a	light clayey loam	23-40	322	185	0.94	271	338	244	9.4	0.83	0.016	122	0.20	28°				
3 _b	stuffy clayey loam	10-120	388	185	1.06	272	357	207	15.0	1.21	0.064	32	0.16	17°10'	0.68	6.0	0.10	
3 _c	clayey loam	13-35	305	191	0.87	273	343	182	16.1	0.76	0.043	44	0.30	12°30'		16.5	0.38	
4	clay	2-5	249	199	0.73	274	404	206	19.8	0.22	0.020	87	0.78	21°20'		24.3	0.50	15
4 _L	silt	0.9	303	193	0.82	270					0.016	113	0.26	29°				12
5	light clayey loam	13-31	227	197	0.68	271	246	164	8.2	0.77	0.021	80	0.22	27°				
5 _L	medium sand	14-18	215	195	0.66	267												7



GEOLOGIC CONSIDERATIONS FOR EARTHQUAKE MICROZONATION

by

D. Burton Slemmons

Department of Geological Sciences

Mackay School of Mines

University of Nevada

Reno, Nevada 89557

ABSTRACT

The purpose of this report is to summarize the current state-of-the-art and state-of-practice in the United States of microzoning for geologic factors that affect earthquake hazard and risk. The basic procedure for microzonation is similar to that for macrozonation or for site specific evaluations, but has the specific purpose of detailed zoning for a variety of geologic factors over a limited area. The process of microzonation consists of establishing probable or credible (maximum probable) earthquakes, for specific faults or sources, or for a region, and the zoning of an area for local geologic factors that control the specific hazard or risk in that area. This review summarizes the geologic factors that influence microzonation decisions for the following hazards: surface faulting and deformation, ground shaking, ground failure, liquefaction, subsidence, tsunamis, seiches and splashes.

INTRODUCTION

General Statement

The general methods for assessing earthquake hazards are similar for macrozonation, the determination of global or regional zones that are defined by plate tectonic related boundaries; microzonation, the more detailed zoning for local conditions; and site specific studies, the precise determination of the hazards at a given point or site. Microzonation for seismic hazards is herein defined as the process for detailed zoning of areas for geologic, seismologic, hydrologic, geotechnical, regulatory, and planning factors to delineate areas of equal or similar exposure to hazards in order that planning, site selection, and engineering design can proceed in such a manner that the seismic risk is mitigated or minimized.

The above definition is close to that of Sherif (1980) who states:

"Microzonation is a process for identifying relevant geological, seismological, hydrological, and geotechnical site characteristics in a specific region and incorporating them into land-use planning and the design of safe structures in order to reduce damage to human life and property resulting from earthquakes."

Cluff (1978) includes similar considerations in his definition:

"Seismic microzonation is herein defined as the subdivision of a region into areas or zones that have relatively similar exposure to various earthquake-associated effects (such as surface fault rupture, ground shaking, ground failure, and water inundation). The aim of microzonation is to estimate the location, recurrence interval, and relative severity of future seismic events in an area so that the potential hazards can be assessed and the effects can be mitigated or avoided."

The most comprehensive review of geologic considerations for seismic microzonation is by Cluff (1978), who emphasizes the importance of multidisciplinary efforts, including combining data and judgements from geology, seismology, geophysics, engineering, and planning. The newness of the rapidly expanding field of seismic risk and hazard analysis, and the limited data base for predicting earthquake effects for specific zones and sites, make it necessary to include all possible types of data in microzonation. Microzonation is a continuing process and data from future earthquakes and new research will make it possible to improve upon the present state-of-the-art and practice.

The rapid advance in application of microzonation, and recognition of its importance, is indicated by the wider use of microzonation in many seismically active regions of the world and the increasing refinement in methods. The first major publication on microzonation is the proceeding's volumes of the First International Conference on Microzonation for Safer Construction-Research and Application in 1972, with 64 papers. The proceeding's volumes of the Second International Conference on

(Hays, 1980).

Microzonation is generally by hazard zoning expressed as the effect, or the probability of the effect, generally in the format of a map, as in detailed predicted earthquake intensity maps, seismic wave amplification maps, liquefaction maps, active fault or fault zone maps, etc. Microzonation for the degree of risk to man or his works is generally not considered. Generally, the completed microzonation is by a series of maps that show one or more hazards. Some maps integrate the hazards into a single microzonation map (Bell and others, 1978). However, when planning for the use of an area is completed or implemented, so the land use is known, it is possible to prepare microzonation maps for earthquake risk.

Deterministic and Probabilistic Methods in Microzonation

Until recently, most seismic hazard and risk analyses have used deterministic methods of analysis and most regulatory agencies require deterministic methods for assessment of major or vital engineered structures. Examples of deterministic regulations include those summarized in Appendix B under U. S. Nuclear Regulatory Commission; California Division of Mines and Geology; U. S. Bureau of Reclamation and U. S. Corps of Engineers. The standards, or criteria for decisions are clearly expressed, commonly in specific quantitative terms of geologic age or degree of fault activity, design ground motions (acceleration, velocity, displacement, spectral character, etc.), or specific geologic or seismologic settings. The zoning or microzoning specified for exclusion of buildings for human occupancy as specified in California by the Alquist-Priola Act (1977), is the area within fifty (50) feet of an active fault that has experienced displacement during Holocene time (about the last 11,000 yrs). This type of regulation is deterministic in character.

Deterministic methods have the character that a single number describes each independent variable and formulations of relations use a specific value for a dependent variable. Results are generally presented in a single form.

Probabilistic methods have the character that the uncertainties are organized with a probabilistic model that evaluates sources of uncertainty from either natural variation or incomplete knowledge. Basic assumptions are clearly stated and the relations commonly are expressed in terms of exceedance probability.

Probabilistic methods were introduced for seismic risk analyses by Cornell (1968), and contributions that relate to zoning include Merz and Cornell, (1974); Lomnitz ((1974)), Douglas and Ryall (1975), Algermissen and Perkins (1976), Esteva (1976), Ryall (1977), Applied Technology Council (1978), Cluff and others (1980), and Ryall and Van Wormer (1980). The factors of probabilistic methods for microzonation include:

- (1) analysis of acceptable hazard and risk,
- (2) recurrence relations and,
- (3) the probabilities of exceedance for various exposure times.

This type of approach has been proposed and used for regional acceleration, velocity and displacement relations (Algermissen and Perkins, / 1976; Applied Technology Council, 1978), but the short period of observation in relation to low recurrence rate, and the lack of allowance for a possible

Microzonation in 1978 included 119 papers. Because these two conferences summarize the current state-of-the-art, and practice, this paper will draw heavily on the data in these proceeding's volumes. The summary of Cluff (1978) on the geologic considerations for microzonation is an especially useful discussion of the topic considered in this paper. Other basic contributions include Cluff and others (1972). The methods for evaluation of faults are reviewed by Slemmons (1972 and 1977), and Glass and Slemmons (1978).

Purpose and Scope of Paper

The primary purpose of this paper is to prepare a summary that reflects current state-of-the-art and practice in assessment of the geological considerations that are essential for microzonation for earthquake hazards. The paper summarizes the basic parameters and methods that are used in United States. The scope of the paper is intended to provide a basis of comparison of the state-of-the-art in China and the U.S. for discussion at a joint U. S. - People's Republic of China Microzonation Workshop and field review of earthquake effects in China.

Geological Topics for Consideration

Although microzonation for earthquakes requires an interdisciplinary approach to zoning for earthquake hazards, several types of evaluations are primarily based on geologic studies, but some evaluations require parallel studies to be integrated. For example, the definition of active faults and active tectonic belts should consider both the long term geologic evidence and the briefer seismologic and historic records. The seismologically defined epicenters, focal points, and focal mechanisms complement geologic data on the location and nature of activity along tectonically active structures.

The main topics to be considered in microzonation studies are:

- * Detection, delineation, and definition of the character of faults which are capable or have the potential for earthquakes.
- * Compilation of earthquake recurrence and time-history data on rates of slip along active faults, or on non-activity for dead or inactive faults.
- * Compilation of data on past faulting events for estimating the size of potential future earthquakes in terms of earthquake magnitude or seismic moment.
- * Delineation of zones of surface fault rupture or localized deformation in order to evacuate surface rupture or disturbance by subsidence, uplift or warping.
- * Delineation of potential seismic sources in order to calculate location and distribution of zones of attenuated strong ground motion and earthquake intensity.
- * Collection of data on the nature and distribution of areas of secondary ground failure by earthquake generated landslides, liquefaction, and subsidence or consolidation.
- * Identification of areas of potential hazard from waves caused by

tsunamis, seiches or splashes.

Plate Tectonic Control of Earthquake Sources

Recent worldwide improvements in earthquake detection, with the installation of the World-Wide Network of Standardized Seismographs (WWNSS) by the United States in the early 1960's, and the installation of comparable networks by several other countries, universities and research organizations have made it possible to define focal mechanisms, focal depths, and epicenters with a greatly improved accuracy and precision (Kisslinger, 1978). On a worldwide basis most earthquakes of $M_s = 5$ are located, and in the western United States the detection capability varies regionally from $M_s = 1$ to $M_s = 3$ in local, well instrumented areas (Smith, 1978). This improved detection level has led to the identification of: (1) seismic belts and zones at plate and, or boundaries; (2) stable zones of aseismic or weakly seismic character; and (3) improved location of focal mechanisms and hypocenter depths (Isacks and others, 1968; Oliver, 1972; Kisslinger, 1978). It is well recognized (Lomnitz, 1974; Dewey and Bird, 1970) that the seismic zones correlate with active faults and folds in orogenic belts. The seismic character of different global tectonic settings is as follows:

Convergent Plate Boundaries : Convergent plate boundary zones have the highest rates of differential plate movement of the three types of plate boundaries, up to 16 cm/year. These zones are long, wide and thick, as defined by the boundaries of the usually associated subducting plate. They contain large volumes of strained lithosphere characterized by intermediate to deep focus earthquakes, which release a large percentage of the earth's seismic energy. Because of the rapid strain accumulation due to rapid differential movement, these zones have short recurrence intervals (some less than 100 years). Maximum earthquake for this type of megathrust zone may be up to $M_s = 8.5$ to 9. These zones generally have active surface thrust faults and may have an associated pattern of strike-slip faults (Huzita and others, 1973).

Divergent Plate Boundaries: The oceanic ridge or rift systems are divergent plate boundaries and are generally marked by extensional features including relatively short fissures, elongate depressions and ridges. Earthquakes occur up to about $M_s = 8$ to 8.3, have normal-slip focal mechanisms, shallow hypocentral depths, and short rupture lengths (up to about 100 km). Some conjugate strike-slip faults are usually present, including active transform faults that may have earthquakes with magnitudes of up to about 8.25.

Transform Plate Boundaries: Transform plate boundaries are major fault zones that connect divergent plate boundaries to each other or divergent-convergent plate boundaries. These zones are characterized by earthquakes with strike-slip mechanisms and shallow hypocentral depths. The pattern of faulting may be complex with splays or branches. The maximum historical magnitude, is $M_s = 8.25$. The earthquake volumes are smaller than for convergent boundaries because the volume of the elastically strained lithosphere is thinner and generally not as wide (only about 10km thick for the 1906 earthquake on the San Andreas fault).

Intraplate blocks: Most areas of intraplate blocks are tectonically and seismically stable regions of the earth's crust, with widely dispersed earthquake activity, which commonly cannot be associated with causative

faults, structures, or topography. There is generally little or no evidence for active or capable faults. The earthquakes are generally of shallow focus, mostly less than 20 km. Suggested causes include loading-unloading effects from changes in sea level and pluvial lake levels, sediment loading or unloading, glacier and ice cap advance-retreat, crustal density differences, isostatic adjustments and other various causes that involve gradual stress changes and local structures. The maximum historic earthquake for United States to the east of the Rocky mountain Front (except for three special intraplate seismic zones--the Charleston, South Carolina area, the New Madrid, Missouri region, and the St. Lawrence River region) is about 5.5 to 5.75. The maximum credible earthquake for such regions appears to be less than 6 with a maximum intensity of about MM VIII. Bergman and Solomon (1980) note that for oceanic intraplate regions, the earthquakes from 1963 to 1979 show correlation between preexisting zones of weakness, are not generally associated with large bathymetric relief and have shallow foci (generally less than 20 km). The highest magnitude earthquakes that are not associated with known zones of weakness or large bathymetric relief in the oceanic intraplate regions is $M_s=6.3$, for worldwide earthquakes in the oceanic intraplate regions.

The boundaries of intraplate blocks may be transitional for substantial distances. The seismic and tectonic activity in Western United States extends inland from the San Andreas transform fault to the Rio Grande rift and the Rocky Mountains of Colorado, about 1300 km. Within this zone, there is a distributed pattern of active faults (Howard and others, 1978). Some definitions include such regions as part of intraplate blocks. The maximum earthquake for the Basin and Range Province is about $M_s=7.7$ (Pleasant Valley, Nevada in 1915 or the Bakersfield, California earthquake of 1957).

The normal method for estimating maximum earthquakes for the intraplate regions is to assign a "tectonic province" approach (Cluff, 1978; Hays, 1980; and U. S. Code of Regulations, 1973). This method assumes that for regions with no capable or causative faults, the maximum earthquake of a given tectonic, geomorphic, or geographic region is the maximum historic earthquake, or this value plus a safety factor for conservatism because of the very short period of historic observation and the low rate and long recurrence interval of seismic activity. For such regions, probabilistic methods of analysis are commonly applied (Algermissen and Perkins, 1976; Applied Technology Council, 1976; Cornell, 1968, 1971; Merz and Cornell, 1974).

TERMINOLOGY

Active, Capable and Dead or Inactive Faults

The concept of active and dead faults dates back to at least 1916, when Wood referred to "living" faults, and 1923 when Willis distinguished "active" and "dead" faults. Microzonation for earthquakes is critically dependent upon recognition of active faults for establishing the magnitude, seismic moment, and ground motion parameters for earthquakes that control the size and location of the zoned areas. The historical background and main definitions used for describing active and capable faults is reviewed in Slemmons and McKinney (1977), and up-dated in Appendix B of this report. Within this report the following terms are used:

Active fault: An active fault is a fault that has slipped during the present seismotectonic regime and is likely to have renewed displacement in the future (see Appendix A and p. 1 of Appendix B).

Dead Fault: A dead fault is a fault that was active during an earlier orogenic period, but is not active within the present tectonic regime and, accordingly does not offset late Cenozoic deposits or surfaces, and is not seismically active.

Capable Fault: A capable fault is an active fault that is specified by regulatory agencies, as for the U. S. Nuclear Regulatory Commission, U.S. Code of Federal Regulations (1975) or the U. S. Corps of Engineers in Regulation No. 1110-2-1806 (1977).

Controlling or Design Earthquake Terminology

Microzonation for earthquakes is generally based on assumed or estimated earthquake sources that control the nature of the earthquake hazard for the zone specified. The concept is similar to that used for design of a structure at a given site, as indicated in the following definitions:

Design Earthquake (after Newmark) : The design earthquake is that earthquake for which a structure is proportioned and constructed so that, in the event of an earthquake with motion at the site, there will be no loss of life resulting from damage or deformation of the structure.

Design Earthquake (from U. S. Corps of Engineers Regulation No. 1110-2-1806) : A design earthquake defines the ground motion at the site of the structure and forms the basis for dynamic response analyses. Usually, several design earthquakes for both the maximum earthquake and the operating basis earthquake as applicable, are investigated.

Controlling Earthquake Value: The Controlling earthquake value, or threshold value for microzonation is the source earthquake that affects a region, zone or site in such a manner that a given hazard exists. The controlling earthquake size (magnitude, intensity, seismic moment, etc.) may either be an event that may occur at any point within the zone ("floating earthquakes"), or it may be from an active fault or fault zone outside the area, with ground motion attenuated to the site. The controlling value earthquake is that earthquake, or those earthquakes that provides zone or site effects that equal or exceed a threshold value. Commonly the maximum, maximum expectable or maximum credible earthquake is

used for zoning, but zoning may be specified for a maximum probable earthquake, one that is likely to occur within a specified period, such as the life of a structure or the land use that is planned. The following definitions have been used for design basis purposes and with modification can apply to use as controlling values or events for establishing zones or areas for microzonation.

Maximum Credible Earthquake: The maximum credible earthquake is the largest earthquake that can be reasonably expected to occur (same as maximum expectable earthquake).

Maximum Earthquake: The maximum earthquake is defined as the severest earthquake that is believed to be possible at the site on the basis of geological and seismological evidence. It is determined by regional and local studies which include a complete review of all historic earthquake data of events sufficiently nearby to influence the project, all faults in the area, and attenuations between causative faults and the site (same as maximum credible earthquakes).

Maximum Earthquake (values) : The maximum earthquake is that which occurs within the region which provides the strongest ground motion or hazard effects at a specific microzone.

Hazard and Risk

The microzonation for earthquake hazard and earthquake risk is influenced by the philosophy and purpose of the "Earthquake Hazards Reduction Act of 1977" (P.L. 95-124), which states:

...to reduce the risks of life and property from future earthquakes in the United States through establishment and maintenance of an effective earthquake hazards reduction program.

Hazard is defined as a source of danger, or a chance of danger.

Earthquake Hazards are the probability that natural events accompanying an earthquake such as ground shaking, ground failure, surface faulting, tectonic deformation, and inundation, which may cause damage and loss of life, will occur at a site during a specified exposure time (Hays 1980).

The National Academy of Sciences (1975) publication on "Earthquake Prediction and Public Policy" summarizes earthquake hazards as having the following effects: violent shaking resulting in vibrations, avalanches, soil liquefaction, lurching, seiches (oscillations and fluctuations in levels of bodies of water), and tectonic movement, expressed as regional uplift and subsidence, fault breaks reaching the earth's surface, and tsunamis (seismic sea waves).

Risk is the exposure to a hazard or danger. Risk considers the effect of the hazard in terms of a loss and is commonly expressed in terms of probability of occurrence or exceedance.

Earthquake risk is the probability that social or economic consequences of earthquakes, expressed in dollars or casualties, will equal or exceed specified values at a site during a specified exposure time

seismic cycle may limit the validity of this method for some regions (Ryall and Van Wormer, 1980).

The use of deterministic methods for earthquake recurrence is explained by Cluff (1978) and Cluff, Patwardhan and Coppersmith (1980). These methods include the concept of earthquake cycles (Fedotov, 1968 and 1969; Ryall, 1977; and Ryall and Van Wormer, 1980). This method commonly uses (1) the earthquake recurrence relations of Wallace (1970) for accumulated strain energy across the fault rupture surface in order to accumulate strain on the total available fault surface, (2) then the size of the earthquake (magnitude or seismic moment) as determined by the relative dimensions of the rupture surface, (3) slip rate, and (4) stress conditions and the shearing resistance of the materials at the fault. The earthquake generation process is shown in Figure 1.

Regulatory definitions for Microzonation

Although mapping for microzonation has been conducted in the United States for all of the main types of earthquake hazards, the threshold parameters selected for mapping zones are generally determined by the researcher, or the agency conducting the microzonation studies, commonly on a case by case basis. Regulation has been established for only one type of microzonation, mapping, and development of active fault zones in California regulated by the Alquist-Priola Special Studies Zones Act of 1972 and subsequent revisions (Hart, 1977, and summarized in Appendix A of this report). Hart (1978) has described this type of zoning in relation to microzonation.

GEOLOGIC-SEISMOLOGIC FACTORS FOR MICROZONATION

Source Mechanisms and Parameters

Study of more than 100 examples of historic surface faulting reveals that most shallow focus earthquakes of over 6 magnitude have related earthquake size (magnitude and seismic moment), fault rupture length, and maximum or average displacement (Richter, 1957; Tocher, 1958; Iida, 1959 and 1965; Bonilla, 1967 and 1970; Bonilla and Buchanan, 1970; Slemmons, 1977; Mark, 1977; Mark and Bonilla 1977, and Bonilla, 1980). Geodetic by Savage and others (1966, 1969), focal mechanism studies by Smith and Lindh (1978), evaluations of earthquake stress drop (Wyss and Brune, 1968) and the stress orientations of the United States (Zoback and Zoback, 1980a, 1980b) provide strong correlations between the geologic evidence for faulting and orogeny, geodetic changes, seismic effects, and the general state of the stress. Regional geologic studies of faults and tectonism provide many examples of associated systematic relationships between the type of faults and their orientation in conjugate patterns (Huzita, others 1973; Wright, 1976).

The present data indicates that from earthquakes which have extensive surface faulting, including well documented prehistoric examples, it is possible to estimate the magnitude and seismic moment of the earthquakes (Wallace, 1977; 1978a, 1978b), determine seismic gaps, provide estimates of source earthquakes and their mechanisms. This data delineates fault regions, and zones of high activity (Slemmons; 1967; Wallace, 1978b) and provides a critical input into microzoning.

Seismic Gap Relations

The detection of seismic gaps to predict future or imminent earthquakes is important to adequate microzonation. Seismic gaps are the active tectonic zones between recently active fault segments that have a high potential for reactivation in the near future. The use of geologic methods has not been widely used, for detailed evaluations of active faults is a new field. Several gaps in the historic belt of historic faulting noted by Slemmons (1967) and Ryall and others (1966) are apparent. A detailed and systematic study of active faults in central Nevada by Wallace (1978) led to detection of an important gap between the Pleasant Valley (1915) and Dixie Valley (1954) earthquake areas. The patterns and sequences of activity along the Northern Anatolian fault zone and along major subduction zones has led to delineation of gaps of special seismic potential.

Attenuation of Seismic Waves

The greatest loss of life and earthquake is from the effects of shaking on the surface and engineered structures. Shaking is generally strongest at the source and is attenuated with distance (Neumann, 1954), as shown in Figure 2 from Krinitzsky and Chang (1975). The effect is drastically affected by local conditions, however, including type of bedrock and or soil, topography, and local and regional geologic structure.

Earthquake Magnitude

The estimation of potential earthquake magnitudes from geologic data has been reviewed by Slemmons (1977) and Glass and Slemmons (1978). The main methods relate to the study of active faults for evidence of historic or pre-historic earthquakes that provide evidence of maximum or average displacement and total rupture length from single earthquakes to plot on the graphs or linear regression formulations of Slemmons (1977), Mark (1977) and Bonilla and Mark (1978). The relation having the highest correlation coefficient, and most readily applied method is from the magnitude vs. displacement relation (fig. 3 and table 1). The magnitude vs. total rupture length is also widely applied (fig. 4 and table 2).

The most recent quantitative method proposed for strike-slip faults is by Woodward-Clyde Consultants (1980). Their compilation suggests the fault slip rate may be directly related to maximum earthquake magnitude that occurs along faults of this type (fig. 5).

The use of fault half-length was proposed by Wentworth and others in 1968 for estimating the maximum earthquake magnitude to be expected (maximum probable earthquake) for strike-slip faults. Subsequent usage of this method has commonly used a one-half or one-third fault length for estimation magnitude from the Bonilla or Slemmons formulations. In order to provide a statistical basis for this method, Table 3 is prepared. The data on this chart are preliminary, but suggest that use should be made of the one-fourth length, method, or the one-third method for about one standard deviation of conservatism.

Seismic Moment

The field data on rupture length and average displacement, either with or without geodetic data, provides essential information for estimating the

seismic moment (Wyss and Brune, 1968; Brune, 1970). This measurement of earthquake size can be related to earthquake magnitude by the formulations of Thatcher and Hanks (1973), Kanamori (1977), and Anderson (1975). To date, this earthquake parameter has not been applied to microzonation methods, but its better correlation with earthquake volume and size, as well as improved correlation with earthquake intensity patterns and seismic energy release, will make wide use of this parameter in the future.

Stress Drop

This parameter has not been widely used in microzonation, but is related to the intensity of energy release, it tends to be low near major plate boundary faults, moderate near interplate boundaries, and high within plates (Liu and Kanamori, 1980).

Seismicity and Earthquake Distribution

The use of geological data for detecting, delineating, and determining the character of active faults provides a more extensive distribution than is shown by the short historic and seismologic record. The primary cause for the variability in degree of correlation between active faults and seismicity is the generally long recurrence interval between major seismic events on most faults. Within the Great Basin the seismicity is widely dispersed and commonly cannot be related to known active faults during the period preceding large earthquakes. The aftershocks generally define the faults that are activated during the main shock, or branches or extensions developed during the following readjustments. Much of the segment of the San Andreas fault zone that was ruptured in 1906 is aseismic, but actively creeping segments, the Sargent fault and adjacent segments of the Hayward and Calaveras faults, are well defined by epicenters (Borchert 1975). Allen (1975), Ambraseys (1970) and others emphasize the need to conduct thorough geologic searches and evaluations to determine future hazard and risk. This will be discussed in "Assessment of Fault Activity and Earthquake Size".

Determination of Earthquake Frequency or Recurrence

One of the main approaches to earthquake risk analysis is to determine the relative seismicity of various seismic regions, or of faults, using seismologic and/or geologic-tectonic criteria. The method establishes the frequency, recurrence interval, or return period for earthquakes of a given range of intensity or magnitude. The selection of the limits of the seismic area, structural-tectonic region, or fault zone is generally taken with an adequate size to provide an adequate historic record of activity, or to include a region with similar seismic potential and tectonic affinity, or a single fault rupture system or fault. The method can be used for deterministic evaluations or is amenable to probabilistic analysis. Generally, results of the seismologic-historic method are correlated or compared with geologic results. The two approaches are both subject to important limitations and should be considered to provide complementary information. The methods are:

Geologic Method: The long period of time between repetition of large earthquakes on major faults is commonly measured in hundreds of years to tens of thousands or, perhaps, even hundreds of thousands of years. The geologic methods of estimating this time interval between repetitions is described in Slemmons (1977).

The recurrence interval or return period is defined as the time interval between repetitions of large earthquakes along faults or fault zones. Wallace (1977, 1970) based his method of estimating the recurrence interval by evaluation of the strain rate (also fault slip rate) and maximum earthquakes determined by historic records, fault rupture lengths, or by maximum displacements (Bonilla, 1977, 1967). Wallace proposed the following formula for defining the relation:

$$R_x = D/S - C$$

Where:

R_x = recurrence interval at a point on the fault.

D = displacement accompanying an earthquake of given magnitude (related empirically to Richter magnitude).

S = long-term strain rate (from offset of geologic units, and

C = tectonic creep rate

The results of Wallace's analysis for the San Andreas fault system are shown in Figure 6. Basic components of this analysis are: (1) estimated 2 cm/yr average fault slip rate from the geologic offsets reported by Dickinson and Grantz, 1977, 1968; (2) magnitude-fault rupture length relations; (3) magnitude-displacement; (4) recurrence i

nterval for a fault with an average slip rate of 2 cm/yr, derived from (3) above; and (5) relationships with adjustment for entire fault length and creep effects. This relationship shows that for a characteristic or assumed earthquake of 8.25 and a 2 cm/yr slip rate (strain rate with no drag), the recurrence interval is about 350 years. Slemmons (1977) used more extensive worldwide earthquake data to classify faults by degree of fault activity to develop the earthquake recurrence interval-magnitude-slip rate relations of figure B1 in Appendix B. This chart suggests, and field data from many parts of the world indicate (Allen, 1977, 1975; Wallace, 1977, 1978; Ambraseys, 1977, 1971; Sieh, 1977, 1978a, 1978b,) that return periods for major faults are from 100 years or less for major plate tectonic boundaries with boundary slip rate of 10 cm/yr or greater, to perhaps 100,000 years or greater for faults with slip rates of about 0.001 cm/yr. Sieh (1977, 1978a, 1978b) has shown that prehistoric earthquakes for the Palette Creek

area of the San Andreas fault zone (with an average slip rate of about 3-4 cm/yr) is about 160 years.

Cluff (1977, 1978) classifies and compares faults by degree of activity with recurrence intervals shown schematically (Figure 7). Cluff, and others (1980) show a schematic diagram to define time within a cycle or interval, with the size of the energy steps in earthquake magnitude related to the dimensions of the rupture surface, slip rate, stress conditions (stress drop), and shearing resistance of the materials at the fault. They apply these relations to the Wasatch fault zone in Utah.

Seismologic-Historic Method: This method is affected by limitations in the statistical validity of the brief historic or instrumental seismologic period of data acquisition, limited ability to detect seismic events of lower magnitudes, and the difficulty or arbitrary nature of selecting the maximum magnitude or intensity values for determination of design parameters or for microzonation.

The plotting is usually based on the following relation of Gutenberg and Richter (1965)

"N is the number per year of shallow earthquake having magnitude equal to or greater than M, in area A. The area may be selected to limit a fault zone to correlate with geologic methods for evaluating a fault."

The formula is commonly placed in the following format:

$$\log N = a - bM,$$

Where N is the number of earthquakes per unit time per unit area in a given magnitude range, with a and b the two constants to be determined for the area.

Examples of studies using the above type of analysis are given by Algermissen and Perkins (1973), Applied Technology Council (1978), Ryall and others (1966) for western United States.

The primary geological consideration for this type of analysis is to properly define the full and accurate dimensions of a fault zone, so that only earthquake activity is used in the formulation, or to subdivide the region or zones into units of similar or identical levels of seismicity, tectonic setting, stress field (Zoback and Zoback, 1980; Hays 1980) summarizes some of the regional stress relationships.

Assessment of Fault Activity and Earthquake Size

Introduction: The importance of detection, delineation, determination of character, evaluation of fault time history, and the assessment of the potential of faults as a hazard or risk is a problem that has received attention from geologists in the United States for more than a century. The range in action or approach by geologists in relation to the hazard and risk has varied from academic studies of faults with no attention paid to potential activity, to ignoring or withholding evidence for faults, to complete and integrated studies with thorough assessment of hazard and risk. The ideal microzonation for faults and determination of controlling or design earthquakes from fault data should be undertaken with a "multi"

approach (Slemmons, 1972; Cluff and others, 1972; Slemmons, 1977; Glass and Slemmons, 1978; and Cluff, 1978). This completes the assessment using as many sources of information as possible. The methods for applying the data to microzonation for faults are discussed in Cluff and others (1972; Slemmons (1972), Cluff (1978) and particularly in Hart (1978). The general methods of evaluating active faults for the determination as source earthquakes for design or zoning purposes is reviewed in Slemmons (1977) and Cluff (1978).

Detection of Active Faults: The detection of active faults is possible from the youthful geomorphic expression of scarps, the offset of geologically young deposits, historic observations of rupturing and offset, and seismologic evidence that defines a segment of the fault that has experienced activity. The most important single source of information is from the geomorphic expression (Appendix A of Slemmons, 1978 and Slemmons, 1979) by characteristic types of geologic expression. Many dozens of kinds of landforms are developed by surface faulting, and some features are characteristic or suggestive of the type of fault or slip direction on the fault surface. The "shopping list" of features that should be sought for are included in Tables 3, 4, and 5, from Glass and Slemmons (1978).

The single most important method for searching for young fault scarps is by use of low-sun-angle aerial reconnaissance and photography. The method was first described by Slemmons, (1969), Cluff and Slemmons, (1972), and Clark (1971). The basic method uses either the highlighting effects on subtle geomorphic features of low-sun illumination or shading effects by back illumination (Glass and Slemmons, 1978; Walker and Trexler, 1975). The methods may use either seasonal or daily variations in sun azimuth according to the specific orientation of the fault zone being evaluated, or the general orientation of faults of the region (Figure 8). The daily and seasonal sun angles are accurately tabulated by Clark (1971), with the variations for 40 degrees latitude shown in Figure 9.

Delineation of Active Faults: Delineation of active faults is generally conducted by photogeologic studies, particularly with the aid of low-sun-angle aerial photography or radar imagery that provides a similar effect (Grant and Cluff, 1976). The use of "multi" imagery analysis is recommended, using a variety of scales, and types of imagery, including multistation (stereoscopic), multiband (multispectral), multirate (multiseasonal), multistage or multilevel (multiscale), multipolarization (for side-looking airborne radar, SCLAR), and multi-enhancement (computer or optical modification of images), using multiobservers (to reduce personal biases in interpretation). This "multi" approach is described by Glass and Slemmons (1978). The best results are obtained if synoptic or small scale imagery is used to supplement more detailed scales, and if aerial reconnaissance is used to supplement laboratory and field studies (from Slemmons, 1972).

Characterization of Faults: The characterization of faults is the determination of the slip direction or separation of faults. This is important for determining the type of fault i.e., normal-slip, strike-slip, or reverse-slip as general types, or for a more detailed classification, the use of the diagram of Bonilla and Buchanan (1970). Any classification is best accomplished from field observation or trenching of faults, but may be preliminarily assigned by the geomorphic expression (Slemmons, 1972; Cluff and Slemmons, 1972, and Glass and Slemmons, 1978) or regional conjugate field relations (Huzita, and others 1973; and Wright, 1976).

Classification of Activity: The classification by activity may be general or descriptive, as by assignment of activity or capability as listed in Appendix B, or by determination of slip or strain rate using the classifications of Slemmons, (1977) or Cluff (1978). Thus the classification may be a simple "active", or "dead" type (Appendix B) or one of degree of activity, as with "extremely high", "high", "moderate", etc. Quantitative measures of the degree of activity may also be used for application of probabilistic approaches to microzonation, including recurrence rates.

The determination of the rate of activity of a fault may be defined by recurrence. This can be expressed by either geomorphic expression or stratigraphic or soil-stratigraphic methods. For scarp morphology of young faults, the preservation of faulting events may be preserved by levels that can be detected by field measurements or by low-sun-angle effects. Wallace (1977) proposes a sequence of degradation (Figures 10 and 11) that is exhibited by a fault from its initial steep fault controlled scarp, through a series of lower slopes or gradients that are initially debris-controlled, to an eventual gentle slope that is controlled by slope wash. The age relations of scarp slopes for the Great Basin of Nevada are shown in Figures 12 to 14. Bucknam and Anderson (1979) note that in addition to the factors described by Wallace, the scarp height affects the rate of degrading of the slope angle (Figures 15 and 16). The type of surficial material by the fault also affects the rate of degradation (Dodge and Grose, 1980) as shown in Figure 17. Nash (1980) evaluates rates of scarp degradation by computer modeling (fig. 18, 19, and 20). The age of soils cut by faults can be used to date the fault time-history as noted by Pease (1979) and Bell and Pease (1980). Their studies indicate various conditions that may complicate the use of the methods described by Wallace (1977) and Bucknam and Anderson (1979). The general use of soil stratigraphy has been summarized in relation to geomorphic applications to engineering geology by Slemmons (1979).

Design Earthquake Values: The analysis of faults, including the determination of total length, maximum or average displacements during past earthquakes, total rupture length during past earthquakes, percentage of total length ruptured during single event, and determination of slip rates for strike-slip faults all have been used to estimate the magnitude of past earthquakes. Examples include the mapping of "fossil" earthquakes in the central Nevada region by Wallace (1978b), to determine seismic gaps and to determine the maximum probable earthquakes for many of the regional major faults (from rupture lengths and maximum displacement), and approximate recurrence interval (for Holocene scarps).

Woodward-Clyde Consultants (1980) have evaluated the slip rates for many strike slip faults in the world (fig. 5) in order to estimate the maximum probable earthquake for the Newport-Inglewood fault zone with a slip rate of 0.5 mm/yr. This chart suggests that there is a relationship between slip-rate and the maximum probable earthquake magnitude.

In order to estimate maximum probable earthquake magnitudes for strike-slip faults, Table 6 relates maximum historic surface rupture length to total fault length of the fault zone. The mean historic rupture length for 11 faults of 200 to 1300 km length is 22 % with one standard deviation of 7 percent. Thus a fault of 1000 km length would be expected to have a maximum probable earthquake, by rupturing as 220 km length, segment with a magnitude of about 7.8.

MICROZONATION FOR SURFACE FAULTING AND DEFORMATION HAZARDS

The identification, classification, characterization, and delineation of active faults with respect to permanent ground displacement (surface rupture or deformation) can greatly reduce earthquake hazards in urban areas (Slemmons, 1972). Microzonation for these hazards should consider the above parameters, using photogeological, geological, geophysical, hydrological, and sub-surface exploration data.

Microzonation of this type was first discussed by Slemmons (1972) and Cluff and others (1972), although the discussion of the problem has many earlier reviews, including Lawson (1908), Willis and Woods (1923), Louderback (1950), and many others. The first (and only) regulatory adoption of microzonation for active fault hazard, including surface displacement, is the Alquist-Priola Special Studies Zones Act of the State of California in 1972 (Appendix A) with subsequent revisions. Hart (1977, 1978) reviews fault hazard zones in California including the policies and criteria (although not regulated by legislation) of the State Mining and Geology Board, the Guidelines for Evaluating the Hazard of Surface Fault Rupture, and the Suggested Outline for Geologic Reports on Faults.

The normal process of study of active faults for microzonation uses the general methods suggested by Slemmons (1972) and Cluff and others (1972). Slemmons (1977) suggests guidelines for assessment of faults and earthquake magnitude, and Glass and Slemmons (1978) summarize the use of imagery and imagery analysis in active fault studies. The process of evaluation for microzonation generally involves a sequence of steps as in Table described by Slemmons (1972, p. 352) and determination of activity as in Table 7.

MICROZONATION FOR GROUND SHAKING HAZARD

Ground shaking during an earthquake is a major cause of loss of life, injury, and damage. Secondary effects include liquefaction, landslides, tsunamis and subsidence, initiated by ground shaking, and discussed in other sections of this paper. This section deals with the primary effects of ground shaking, mainly the failure of engineered structures in response to earthquake induced cyclic vibrations. Failure (or competence) of these structures is dependent on several factors including (1) basic design of the structure, (2) acceleration and direction of acceleration exerted on the structure by the ground shaking, (3) frequency of the shaking, (4) duration of the shaking, and (5) regional and local attenuation and/or focusing of the shaking (i.e., location of the source earthquake). The first of these factors does not fall within the scope of this paper.

The conspicuous effect of various geologic formations on the strength of ground motion (intensity, acceleration, velocity, and displacement), the frequency, and the duration has long been recognized for historic earthquakes (Lawson, 1908; Kanai, 1952, 1953, 1956; Medvedev, 1965; and Hays, 1980). Neumann (1954) has examined the 1949 Puget Sound earthquake for effect intensity of local geologic conditions (fig. 2). Seed and Idriss (1968) and Donovan and Mathiesen (1978) have used equivalent lumped mass systems and wave propagation theory of ascending shear waves in explaining local effects on San Francisco. Some of the factors influencing the response of the surface to seismic waves are summarized by Housner (1970, 1975); and Schnabel and Seed (1973); and Seed and others (1976).

Widely used ground motion parameters for microzonation include effective peak acceleration (EPA), peak acceleration, velocity, displacement, and response spectra (Applied Technology Council, 1977; Donovan and others, 1978; and Hays, 1980.)

MICROZONATION FOR GROUND FAILURE HAZARD

General Statement: The widespread distribution of secondary ground failures of rock, debris, and earth, at distances of up to several hundred miles from causative earthquake epicenters provides extensive examples of the effect of earthquake motion on or in stable materials. The types of ground failures that may occur are dependent upon site-specific conditions and include all of the types listed in Varnes (1979) as shown in Figure 21, 22, 23. These ground failures occur in rock, debris, soil, and combinations of these in the following manner:

1. Falls
2. Topples
3. Rotational slides
4. Translational slides
5. Lateral spreading
6. Flows
7. Complex movements of combinations of two or more of the above.

Those ground failures (some translational slides, lateral spreading and flows), which are liquefaction induced, are discussed in the microzonation for liquefaction susceptibility section of this paper.

Macrozonation for landslide potential has been accomplished by Radbruch-Hall and others (1976) for the United States, primarily using slope and geologic parameters, and topographic and geologic maps. These maps on geologic settings, when taken in combination with seismic source are useful for initial evaluations of the importance of this hazard or risk.

Ground Failure Associated with Historic Earthquakes: Reports of the occurrence of ground failure triggered by earthquakes and the ensuing damage and loss of life is numerous in the literature, including Lawson (1908), Youd (1978), Morton (1971), Nason and others (1975), Nilsen and Brabb (1975), Youd and Perkins (1978), Youd and Hoose (1978), Keefer and others (1978), Hays and others (1978), Youd and Hoose (1978), Cluff (1971), Shepherd and others (1970), Tocher (1962), and numerous others.

The hazard of ground failure is well discussed by Keefer and others (1978) in a review of the May 31, 1970, Peru Earthquake. The earthquake triggered ground failure in a large mass of ice and rock. The ensuing debris flow traveled over 60 km at velocities for 280-400 km per hour. Within four minutes the flow had killed over 18,000 people, mostly in two buried towns. Geologic and historic evidences (Keefer and others, 1978) indicate the ground failure potential was extreme in the area, and 8 years before, a debris slide which was not seismically induced, had killed 4000 people in one of the towns buried in 1970. Also, one of the towns was built on a debris flow.

Harp and others (1978) report "The Ms=7.5 Guatamala earthquake of February 4, 1976, generated at least 10,000 landslides, which caused hundreds of fatalities as well as extensive property damage." Landslide data from 15 historic earthquakes by Keeton and others (1978) indicate the relative abundances of different types of landslides as shown in Table 8.

Physical Conditions Conducive to Earthquake Triggered Ground Failure: Ground failure from earthquake effects is dependent on many parameters

including magnitude, distance, attenuation (both local and regional, focusing, rock or soil type, degree of weathering, jointing, consolidation, slope angle, and previous tectonic history.

Table 9 shows a preliminary assessment of Keefer and others (1978) of seismically induced landslide susceptibility.

Methods for Detecting Ground Failure Potential for Microzonation: Data for assessing ground failure potential for the purpose of microzonation can be obtained by various methods including: (1) field investigations, (2) photogeology, (3) geologic and topographic maps, (4) computer-generated slope maps, and (5) sub-surface investigation e.g. boreholes and trenching.

An excellent example of microzonation for landslide potential for the La Honda, California, area has been prepared by Keefer and others (1978). Their interpretation is based on data from a detailed engineering-geologic field investigation, a published map of unconsolidated Quaternary materials, and a computer generated slope map.

Bell and others (1978) have developed a computer-simulated earthquake hazard model for the Reno, Nevada, 7.5' minute quadrangle. Included with their hazard model is the potential for slope instability, based on a composite computer generated seismic response classification and digitized slope map of the area.

Glass and Slemmons (1978) indicate that the geomorphic features of landslides are diagnostic and very long lived. Photogeologic methods can detect landslides of up to tens of thousands years in age. Morton (1971), Glass and Slemmons (1978), and Keefer and others (1978) indicate seismically induced landslide potential may be evaluated by observing existing landslides in the study area primarily by photogeologic interpretation. It should be noted that various authors including Keefer and others (1978) suggest that reactivation of existing ground failure occurs at a low rate (Table 10) but areas which have many existing landslides are especially susceptible to reactivation of new landslides during an earthquake.

MICROZONATION FOR LIQUEFACTION HAZARD

General Comments

The identification and determination of the potential damage from seismically induced liquefaction is an important geological-seismological element of earthquake microzonation. Assessment and zoning for this phenomena may be accomplished by either: (1) simple, deterministic methods using earthquake sources in combination with geological hydrologic data on soils and sedimentary units, or (2) deterministic methods using susceptibility concepts as outlined by Youd and Perkins (1978) and Youd and others (1978).

Youd (1973) and Youd and others (1975) define liquefaction as the transformation of a granular material from a solid state into a liquefied state as a consequence of increased pore-water pressure.

Sherif and Ishibashi (1978) define liquefaction as a:

"Phenomena whereby certain sands and sandy soil totally lose their supportive capacity and behave almost like liquids under dynamic or earthquake-type loading."

Sherif and Ishibashi (1978) report:

"liquefaction is brought about to a great extent as a consequence of pore-pressure buildup and to a lesser extent due to favorable reorientation of soil particles in such a way that the soil-water system enters a stage at which it exhibits least resistance to applied forces. In engineering practice the soil is considered to have liquefied when the pore-pressure rise reaches the value of the total overburden stresses on the soil. When this happens, the strength of the soil reduces to zero.."

The liquefaction process is a transformation process primarily resulting from earthquake motion in susceptible materials rather than a liquefied flow or type of ground failure, although ground failure is a common consequence of liquefaction. Ground failure does not occur at random but is limited to certain types of susceptible materials which are in certain geologic-hydrologic settings, and occurs when a threshold shaking intensity (acceleration and duration) is exceeded.

Youd and others (1975) define three categories of liquefaction related ground failure:

- (1) Flow landslides, generally on moderate to steep slopes that are underlain by water saturated, loose, granular, low density soils (or dry loess - Varnes, 1979) : Susceptibility may be partly controlled by variations in annual climate or groundwater level.
- (2) Lateral spreading, commonly on gentle or nearly horizontal slope: This type of failure is common along free faces at stream banks that expose deposits of susceptible material.
- (3) Quick-condition failures in flat areas with high water tables and loose to moderately dense granular materials: This type of failure results in loss of bearing capacity, resulting in sinking

and tilting of structures, embankments and other types of surficial loads into underlying liquified sediments (e.g., Nigata, Japan and San Francisco, California). This type of failure commonly is accompanied by "sand volcanos" and water spouts from the exhalation of the liquified material or pore-water by overburden pressure.

Nature of Liquefiable Materials

The types of materials which are susceptible to liquifaction are described in geologic terms for specific areas in several studies: Youd and others (1975) for the San Francisco, California area, Bell and others (1978) in the Reno, Nevada area, Youd and others (1978) for the San Fernando Valley, California, area, and Ishihara and Ogawa (1978) for the Tokyo, Japan, area.

In general, materials susceptible to liquifaction are described by numerous other authors, including the Japan Society of Civil Engineers (1973), Youd and Perkins (1978), Ferritto and Forrest (1978), Sherif and Ishibashi (1978), Anderson and others (1980).

The Japan Society of Civil Engineers (1975) published graphs of liquifaction of sands using percentage of fines vs. particle size. These graphs give limiting bounds of very easily and easily liquified sands as shown in Figure 24. Youd and Perkins (1978) tabulate the estimate susceptibility of sediments to liquifaction during strong seismic shaking, considering depositional environment and age of sediments. Their results are shown in Table 10. Ferritto and Forrest (1978) define susceptibility to liquifaction of materials in geological engineering parameters, including dynamic shear stress level, characteristics of the shear stress record, relation density, initial effective confining stress, drainage conditions, grain characteristics, previous stress history, and other parameters which indirectly affect liquifaction.

Sherif and Ishibashi (1978) report sands, silty sands and clayey sands are soils which are potentially liquifiable while clay, silt, loam organic soil gravel and others are less susceptible. The use of techniques and parameters similar to Ferritto and Forrest (1978) is indicated.

Anderson and others (1980) consider susceptibility to depend essentially on the nature and age of deposition of subsurface soils and their grain size distribution, relative density, and topographic aspects, as well as the depth to the water table. They use the factors and conditions compiled by Helley and Lajoie (1979) as shown in Table 11.

Liquifaction Associated with Historic Earthquakes

An excellent report on three cases of liquifaction of the same area near Tokyo, Japan is well documented by Ishihara and Ogawa (1978) and Kuribayashi and Tatsuoka (1975). The very short recurrence interval for earthquakes in the Tokyo area, and the high population density make this a special example for liquifaction recurrence. The data for this area shows a similar susceptibility for the three earthquakes. This suggests the importance of past events in a given area for determining liquifaction potential for future earthquakes.

Examples within the United States include the 1954 Fallon-Stillwater

earthquakes in Nevada (Tocher, 1956; Youd and Perkins, 1978), the 1906 San Francisco, California earthquake (Lawson, 1908; Youd and Perkins, 1978), the 1964 Alaska earthquake (Youd and Perkins, 1978), and the 1917 San Fernando Valley, California earthquake (Youd and others, 1978).

Approaches to Microzonation for Liquefaction Susceptibility :

Development of liquefaction potential maps for microzonation is described by Youd and Perkins (1978) using two factors:

- (1) Whether soils or subsoils are present which are susceptible to liquefaction and,
- (2) The probability of the occurrence of sufficient ground shaking which will liquefy susceptible material. The following is a brief summary of their method:

Ground failure susceptibility is a function of the geotechnical properties of a unit and its topographic position. Using the data in Table 10 of this report, a geologic map of the area is prepared and susceptible units are shaded to indicate their relative susceptibility to liquefy on a separate ground-failure susceptibility map (figs. 25a and 25b). This step may also account for water table level as a deep water table, below 33 ft (10m), lowers susceptibility by removing the pore-water.

Faults and other source areas for a study area are mapped and data of the activity of the seismic sources is gathered (fig. 25c). From this map a contoured map of seismic sources is drawn (fig. 25d) showing average return periods for earthquakes of the seismic sources. Contours are drawn using fault lines or areas rather than epicenters. Epicenters define only the first point of seismic release and not the zone of seismic energy release. The contours are based on the empirical data of Youd and Perkins (1978) as shown in Figure 25e. The map of return periods is shaded for various return periods and overlain on the ground failure susceptibility map. This yields a map of liquefaction-induced ground failure potential (fig. 25f). More study information is required to quantify liquefaction and ground failure susceptibility and to differentiate between susceptibility levels of different geologic units for use in probabilistic analyses and site specific studies.

Liquefaction susceptibility determination methods : Various methods of defining the susceptibility of materials to liquefaction is outlined in the literature. Historic data on liquefaction phenomena may be used where the records are adequate, e.g., compiled by Ishihara and Ogawa (1978) and Iwasaki and others (1978) for areas in Japan.

In-situ methods include penetration tests conducted in the field as outlined by Ferritto and Forrest (1978) and Dexfulian and Prager (1978). Geologic mapping for layered sediments is useful (Ishihara and Ogawa, 1978). Arya and others (1978) outlined methods for the verification of liquefaction by field blast tests.

Various liquefaction theory and laboratory tests from borings and samples are described by Ferritto and Forrest (1978), Sherif and Ishibashi (1978), Youd and others (1975), Youd (1973), and Nemet-Nosser and Shokoch (1978).

MICROZONATION FOR SUBSIDENCE HAZARD

Settlement of Cohesionless Soils

The cyclic vibrations of earthquake shaking may cause surface subsidence by any of three basic mechanisms or combinations thereof: (1) reduction in volume from realignment of soil grains, (2) reduction in volume from removal of pore water during liquefaction, and (3) lateral motion of soil profile on unrestricted slopes.

Reduction of soil volume by about 2.5 feet of settlement by compaction in an alluvial deposit of 468 feet thick is reported by Grantz and others (1964) from the realignment of soil grains during the 1964 Alaskan earthquakes. Measurement was made possible by a rigid well casing imbedded in bedrock below the alluvium. Seed (1970) reports differential settlement in several examples between abutments and backfills on bridges, highways, and railroads. This type of failure occurs in unsaturated, non-compacted deposits.

Seed (1970) also reports various case histories of surface subsidence from a combination of loss of pore water (liquefaction) and grain realignment. Examples include coastlines, islands, river and stream banks, highways and building foundations. Numerous examples of loss of pore water are discussed earlier in the liquefaction section of this report. A secondary hazard from subsidence of unsaturated and saturated fills may exist as flooding of the subsided areas, either from nearby bodies of water, or the water forcefully ejected during liquefaction.

Lateral motion of soil profiles may occur during earthquake vibration where soil profile is unrestricted horizontally. This situation may occur on coastlines, river and stream banks, and artificial fills for buildings, dams, canals, highways, railroads, and reclaimed lands.

MICROZONATION FOR TSUNAMI, SEICHE AND SPLASH HAZARD

Tsunamis are long period water waves (5 to greater than 60 minutes, Wiegel, 1970) which historically have caused great loss of life and property at great distances from the causative event. It is likely that the major cause of catastrophic tsunamis is rapidly occurring tectonic displacement of the ocean floor (Wiegel, 1970). Additional causes may be underwater volcanic explosions, landslides and nuclear tests. Leet (1948) reports that tsunamis in Japan in 1896 caused over 27,000 casualties and destroyed over 10,000 homes.

Seiches, or oscillation of a body of water within its reservoir, and splashes, waves caused by rapid landslides, may cause damage in two manners. The first is flooding of low lying areas adjacent to the body of water, and the second is cresting of the retaining structure, if the water is impounded by a dam. A rockfall during the 1964 Alaskan earthquake (Bolt and others, 1977) caused a splash on a bay which scoured trees from the shore at the mouth of the bay to an elevation of 1550 feet (500 m). In "before and after" photographs of the bay entrance (Bolt and others, 1977) the "before" photo shows scour marks on the terrain bounding the mouth of the bay, but not as high as in the "after" photographs, indicating the problem is recurring in some cases.

Excellent histories of other tsunami, seiche, and splash disasters are given in Weigel (1970) and Bolt and others (1977). In addition, theory of long wave motion is received by Weigel (1970).

Microzonation for tsunami, seiche and splash hazard is difficult because of economic feasibility. Run-up (maximum water elevation) in Japan has been in excess of 105 feet about sea level. Configuration or topography of the ocean bottom and the shoreline are determining factors in run-up height, as well as source parameters and wave properties. The danger from these hazards is inherent in most low lying topography near oceans, lakes and reservoirs.

ACKNOWLEDGEMENTS

I am very grateful for the competent assistance of all the following workers: Bob Whitney of the Mackay School of Mines, who assisted in writing and editing this manuscript. His assistance greatly improved the content and organization of the report. Cheryl Valcarce and Loretta Sabini inducted the word processing, formatting, and final editing of the manuscript. Mark Molinari, George Bergantz and Lonnie Harriet prepared figures, references, and searched the literature.

REFERENCES

- Algermissen, S.T., and Perkins, D.M., 1976, A probabilistic estimate of maximum acceleration in rock in the contiguous United States: U.S. Geol. Survey Open File Report, 76-414.
- Allen, C.R., 1975, Geological criteria for evaluating seismicity: Geol. Soc. Amer. Bull., v. 86, p. 1041-1057.
- Alquist-Priola, 1977, Special studies act: California Div. of Mines and Geol.
- Ambraseys, N.N., 1969, Maximum intensity of ground movements caused by faulting: World Conference Earthquake Eng., 4th Santiago, Chile, Jan. 13-18, 1969, Proc., v. 1, A2 p. 154-171.
- Ambraseys, N.N., 1971, Value of historical records of earthquakes: Nature, v. 232, p. 375-379.
- Anderson, L.R., Keaton, J.R., and Gordon, W.J., 1980, Liquefaction potential maps for land use planning in Utah: in Proc. Conference 10 -- Earthquake Hazards along the Wasatch and Sierra Nevada Frontal Fault Zones, U.S. Geol. Survey Open File Report 80-801, p. 153-171.
- Applied Technology Council Associated with Structural Engineers Association of California, 1978, Tentative provisions for development of seismic regulations for buildings: National Bureau of Standards Publication 510.
- Arya, A.S., Nandakumaran, P. Puri, V.K., and Mukerjee, S., 1978, Verification of liquefaction potential by field blast tests: in Proc. Second International Conference on Microzonation, v. II, p. 865-872.
- Bell, J.W., and Pease, R.C., 1980, Soil stratigraphy as a technique for fault activity assessment in the Carson City area, Nevada: in Proc. Conference 10--Earthquake Hazards along the Wasatch and Sierra Nevada Frontal Zones, U.S. Geol. Survey Open-File Report 80-801, p. 577-600.
- Bell, E.J., Trexler, D.T., and Bell, J.W., 1978, Computer-simulated composite earthquake hazard model for Reno, Nevada: in Proc. Second International Conference on Microzonation, v. I, p. 471-483.
- Bergman, E.A., and Soloman, S.C., 1980, Oceanic intraplate earthquakes: Implications for local and regional intraplate stress: Jour. Geophys. Res., v. 85, n. B10, p. 5389-5410.

Bolt, B.A., Horn, W.L., MacDonald, G.A., and Scott, R.F., 1977, Geological Hazards: Springer-Verlag, 330 p.

Bonilla, M.G., and Buchanan, J.M., 1970, Interim report on worldwide historic surface faulting: U.S. Geol. Survey Open-File Report.

Borcherdt, R.D., 1975, Studies of seismic zonation of the San Francisco Bay region: U.S. Geol. Surv. Prof. Paper 941-A, 102 p.

Brune, J.N., 1970, Tectonic stress and the spectra of seismic shear waves from earthquakes: in Jour. Geophys. Research, v. 75, p. 4997-5009.

Bucknam, R.C., and Anderson, R.E., 1979, Estimation of fault ages from a scarp-height-slope-angle relationship: Geology, v. 7, p. 11-14.

Clark, M.M., 1971, Solar position diagrams - solar altitude, azimuth, and time at different latitudes. Geol. Survey Research 1971, U.S. Geol. Surv. Prof. Paper 750-D, D145-148.

Cluff, L.S., 1971, Peru Earthquake of May 31, 1970: Engineering geology observations: Seismol. Soc. of Amer. Bull., v. 61, n. 3, p. 0511-0534.

Cluff, L.S., Hansen, W.R., Taylor, C.L., Weaver, K.D., Brogan, G.E., McClure, F.E., Idriss, I.M., and Blayner, J.A., 1972, Site evaluation in seismically active regions - an interdisciplinary team approach: in Proc. Conference on Microzonation for Safer Construction Research and Application, v. 2, p. 957-987.

Cluff, L.S., 1978, Geologic considerations for Seismic Microzonation: in Proc. Second Internat. Conf. Microzonation, v. 3, p. 135-152.

Cluff, L.S., Patwardhan, A.S., Coppersmith, K.J., 1980, Estimating the probability of occurrences of surface faulting earthquake on the Wasatch fault zone, Utah: Seis. Soc. of Amer. Bull., v. 70, p. 1463-1478.

Cornell, C.A., 1968, Engineering seismic risk analysis: Bull. Seism. Soc. America, 58, p. 1583-1606.

Cornell, C.A., 1971, Probabilistic analysis of damage to structures under seismic loads: in Dynamics in Civil Engineering, John Wiley, New York, p. 473-493.

Dewey, J.F., and Bird, J.M., 1970, Mountain belts and the new global

tectonics: Jour. Geophys. Res., v. 75, p. 2625-2647.

Mezfulian, H., and Prager, S.R., 1978, Use of penetration data for evaluation of liquefaction potential: in Proc. Second International Conference on Microzonation, v. II, , p. 873-884.

Dickinson, W.R., and Grantz, A., 1968, Indicated cumulative offsets along the San Andreas fault in the California Coast Ranges: in Proc. Conference on Geologic Problems of San Andreas Fault System, Stanford Univ. Pubs. in Geol. Sci., v. 11, p. 117-119.

Dodge, R.L., and Grose, L.T., 1980, Tectonic and geomorphic evolution of the Black Rock fault, northwestern Nevada: in Proc. of Conf 10—Earthquake Hazards along the Wasatch and Sierra Nevada Frontal Fault Zones, U.S. Geol. Survey Open-File Report 80-801, p. 494-499.

Douglas, B.M., and Ryall, A., 1975, Return periods for rock acceleration in western Nevada: Seismol. Soc. America Bull., v. 65, n. 6, p. 1599-1612.

Esteva, L., 1966, Seismicity, Chapter 6: in Seismic Risk and Engineering Decisions; Developments in Geotechnical Engineering 15: Elsevier Scientific Publishing Co., New York.

Esteva, L., and Bazan, E., 1978, Seismicity and seismic risk related to subduction zones: in Proc. Second International Conference on Microzonation, v. II, p. 657-668.

Fedetov, S.A., 1968, On the seismic cycle, possibility of collective seismic regionalization, long term seismic prediction: Seismicheskoe raionirovanie SSR, Moscow, p. 121-150.

Fedetov, S.A., 1969, Seismicity in the south of the Kurile Island Arc. The disastrous Etorofu earthquake of 6 November 1958 and the seismic regime of the southern Kurile zone before and after it: in Earthquakes and the Deep Structure of the South Kurile Island Arc. "Nauka", Moscow, p. 58-121.

Ferritto, J.M., and Forrest, J.B., 1978, Seismic liquefaction potential: Civil Engineering Lab. Tech. Note TN-N-1530, U.S. Dept. of the Naval Constr. Bat. Center, Post Huenerne, CA., 187 p.

Glass, C.E., and Slemmons, D.B., 1978, Imagery in earthquake analysis: State-of-the-Art for assessing earthquake hazards in the United State Series; Report 11: Misc. Paper 5-78: U.S. Army Engineer Waterway Exp. Station, Vicksburg Miss.

- Grant, T.A., and Cluff, L.S., 1976, Radar imagery in defining regional tectonic structure: Annual Review of Earthquake and Planetary Sciences, v. 4, p. 123-145.
- Gutenberg, B., and Richter, C.F., 1965, Seismicity of the Earth: Stechert-Hafner (reprint), New York.
- Harp, E.L., Wilson, R.C., Wieczorek, G.F., and Keefer, D.K., 1978, Landslides from the February 4, 1976 Guatemala earthquake: Implications for seismic hazard reduction in the Guatemala City area: in Proc. Second International Conference on Microzonation, v. 1, p. 353-366.
- Hart, E.W., 1977 (Revised), Fault hazard zones in California: California Div. of Mines and Geol. Spec. Pub. 42, 24 p., plus Supplemental nos. 2 and 3.
- Hart, E.W., 1978, Zoning for the Hazard of surface fault rupture in California: in Proc. Second Internat. Conf. Microzonation, v. II, p. 635-646.
- Hays, W.W., King, K.W., and Park, R.B., 1978, Duration of nuclear explosion ground motion: Seis. Soc. Amer. Bull., v. 68, p. 1133-1146.
- Hays, W.W., 1980, Procedures for estimating earthquake ground motion: U.S. Geol. Survey Prof. Paper 1114, 77 p.
- Helley, E.J., and Lajoie, K.R., 1979, Flatland deposits of the San Francisco Bay region - their geology and engineering properties and their importance to comprehensive planning: U.S. Geol. Survey Prof. Paper 943, 88 p.
- Howard, K.A., and others, 1978, Preliminary map of young faults in the U.S. as a guide to possible fault activity: U.S. Geol. Survey Misc. Field Studies Map, MF-916, scale 1:5,000,000.
- Huzita, K., Kishimoto, Y., and Shiono, K., 1973, Neotectonics and seismicity in the Kinki area, southwest Japan: Osaka City Univ., Jour. Geosciences, v. 16, p. 93-124.
- Iida, K., 1959, Earthquake energy and earthquake fault: Nagoya Univ. Jour. Earth Sci., v. 7, n. 2, p. 98-107.
- Iida, K., 1965, Earthquake magnitude, earthquake fault, and source dimensions: Nagoya Univ., Jour. Earth Sci., v. 13, n. 2, p. 115-132.

Isacks, B., Oliver, J., and Sykes, L.R., 1968, Seismology and the New Global Tectonics: Jour. of Geophys. Res., v. 73, p. 5855-5899.

Ishihara, K., and Ogawa, 1978, Liquefaction susceptibility map of downtown Tokyo: in Proc. Second International Conference on Microzonation, v. II, p. 873-884.

Iwasaki, T., Tatsuoka, F., Tokida, K., and Yasuda, S., 1978, A practical method for assessing soil liquefaction potential based on case studies at various sites in Japan: in Proc. Second International Conf. on Microzonation, v. II, p. 885-896.

Japan Society of Civil Engineers, 1973, Earthquake resistant design for civil engineering structures: Earth structures and Foundations in Japan, p. 58.

Kanamori, H., 1977, The energy release in great earthquakes: Jour. of Geophys. Res., v. 82, p. 2981-2987.

Kefer, O.K., Wieczorek, C.F., Harp, E.L., and Tuel, D.H., 1978, Preliminary assessment of seismically induced landslide susceptibility: in Proc. Second International Conf. Microzonation, v. 1, p. 279-290.

Kisslinger, C., 1978, Seismicity and global tectonics as a framework for microzonation: in Proc. Second International Conference on Microzonation, v. I, p. 3-26.

Krinitzsky, E.L., and Chang, F.K., 1975, Earthquake intensity and the selection of ground motions for seismic design: U.S. Waterways Experiment Station, Misc. Paper S-73-1, Report 4, 59 p.

Kuribayashi, E., and Tadayuki, T., 1975, An evaluation study on the distribution of property losses caused by earthquakes: in Proc. Second International Conference on Microzonation, p. 1499-1503.

Lawson, A.C., and others, 1908, The California earthquake of April 18, 1906--Report of the State Earthquake Investigation Commission: v. 1, Part 1, p. 1-254; Part 2, p. 255-451, Carnegie Institution of Washington, Publication 87.

Liu, H.L., and Kanamori, H., 1980, Determination of source parameters of mid-plate earthquakes from the wave forms of body waves: Seismol. Soc. of Amer. Bull., v. 70, n. 6, p. 1989-2004.

- Lomnitz, C., 1974, Global tectonics and earthquake risk: Developments in Geotectonics, 5, Elsevier Scientific Publ. Co., Amsterdam, 320 p.
- Louderbach, G.O., 1950, Faults and engineering geology: in Paige, S., Chmn. Application of Geology to Engineering Practice: Geol. Soc. Amer. Berkeley, v. p. 125-150.
- Mark, R.K., 1977, Application of linear statistical models of earthquake magnitude versus fault length in estimating maximum expectable earthquakes: Geology, v. 5, p. 464-466.
- Mark, R.K., and Bonilla, M.G., 1977, Regression analysis of earthquake magnitude and surface fault length in estimating maximum expectable earthquakes: U.S. Geol. Surv., Open-File Report 77-614.
- Matsuda, T., 1975, Magnitude and recurrence interval of earthquakes from a fault (in Japanese) : Earthquake, Series 2, v. 28, p. 269-283.
- Medvedev, S.V., 1965, Engineering seismology: U.S. Dept. of Commerce, Nat. Tech. Info. Service, Rept. TT65-50011. 260 p.
- Merz, H.A., and Cornell, C.A., 1973, Seismic risk analysis based on a quadratic frequency law: Seismol. Soc. of Amer. Bull., v. 63, n. 6, p. 1999-2006.
- Morton, D.M., 1971, Seismically triggered landslides in the area above the San Fernando Valley: in The San Fernando, California Earthquake of February 9, 1971, U.S. Geol. Survey, Prof. Paper 733, p. 99-104.
- Nash, D.B., 1980, Morphologic dating of degraded normal fault scarps: Jour. Geol., v. 88, p. 353-360.
- Nason, R., Harp, E.L., LaGresse, H., and Malley, R.P., 1975, Investigations of the 7 June 1975 earthquake at Humboldt County, California: U.S. Geol. Survey Open-File Report 75-404, 37 p.
- National Oceanic and Atmospheric Administration, 1972, A study of earthquake losses in the San Francisco Bay area, U.S. Dept. of Commerce. Washington, D.C.: U.S. Government Printing Office.
- Nemet-Nasser, S., and Shokoch, A., 1978, A new approach for the analysis of liquefaction of sand in cyclic shearing: in Proc. Second International Conference on Microzonation, v. II, p. 957-970.
- Neumann, F., 1954, Earthquake intensity and related ground motion, Univ.

Press, Seattle, Washington, 77 p.

Nilsen, T.H. and Brabb, E.E., 1975, Landslides: in Studies for Seismic Zonation of the San Francisco Bay Region, U.S. Geol. Survey Prof Paper 941-A, p. A75-A87.

Oliver, J., 1972, Contributions of seismology to plate tectonics: Amer. Assoc. Petrol. Geol. Bull., v. 56, n. 2, p. 214-225.

Pease, R.C., 1979, Scarp degradation and fault history south of Carson City, Nevada: Unpublished M.S. thesis, Univ. of Nev. Reno, 90 p.

Redbruch-Hall, D.H., Colton, R.B., Davies, W.E., Skipp, B.A., Lucchitta, I., and Varnes, D.J., 1976, Preliminary landslide overview map of the conterminous United States: U.S. Geol. Survey Misc. Field Studies Map, MF-771.

Richter, C.F., 1958, Elementary Seismology: W.H. Freeman and Co., San Francisco, 768 p.

Ryall, A.S., Slemmons, D.B., and Gedney, L.D., 1966, Active seismic zones in the western United States (abs.): Geol. Soc. Amer. Spec. Paper 101, p. 331-332.

Ryall, A., 1977, Earthquake hazard in the Nevada region: Seismol. Soc. Amer. Bull., v. 67, n. 2, p. 517-532.

Ryall, A.S., and VanWormer, J.D., 1980, Estimation of maximum magnitude and recommended seismic zone changes in the western Great Basin: Seis. Soc. of Amer. Bull., v. 70, p. 1573-1582.

Savage, J.C., and Hastie, L.M., 1966, Surface deformation associated with dip-slip faulting: Jour. Geophys. Res., v. 71, p. 4897-4904.

Savage, J.C., and Hastie, L.M., 1969, A dislocation model for the Fairview Peak, Nevada earthquake: Seismol. Soc. Amer. Bull., v. 59, n. 5, p. 1937-1948.

Schultz, J.R., and Cleaves, A.B., 1955, Geology in engineering: John Wiley and Sons, Inc., New York, 592 p.

Seed, B.H., 1970, The response of earth dams during earthquakes: in Proc. of Seismic Instrumentation Conference on Earth and Concrete Dams, U.S. Army Engineer Waterways Experiment Station, Vicksburg, Miss.

Shepard, R., Dodd, T.A., Sutherland, A.J., Moss, P.J., Carr, A.J., Gordon, D.R., and Bryant, A.H.. 1970, The 1958 Inangahua earthquake: Report of the University of Canterbury team: Seismol. Soc. of Amer. Bull., v. 60, n. 5, p. 1561-1606.

Sherif, M.A., 1980, Definition of Microzonation: Newsletter, Earthquake Engineering Research Institute, v. 14, no. 4, p. 68.

Sherif, M.A., and Ishibashi, 1978, Soil dynamic considerations for microzonation: in Proc. Second International Conf. on Microzonation, v. I, p. 81-110.

Sieh, K.E., 1977, A study of Holocene displacement history along the south-central reach of the San Andreas fault: Ph.D. thesis, Stanford Univ., 219 p.

Sieh, K.E., 1978a, Prehistoric large earthquakes produced by slip on the San Andreas fault at Pallet Creek, California: Jour. of Geophys. Res., v. 83, n. B8, p. 3907-3939.

Sieh, K.E., 1978b, Slip along the San Andreas fault associated with the great 1857 earthquake: Seismol. Soc. of Amer. Bull., v. 68, n. 5, p. 1421-1448.

Slemmons, D.B., 1967, Tectonic movements and seismicity (abs.): in Proc. of the Second United States-Japan Conf. on Research Related to Earthquake Prediction Problems, p. 82.

Slemmons, D.B., 1969, New methods for studying regional seismicity and surface faulting: EOS, American Geophys. Union Transaction, v. 50, p. 397-398.

Slemmons, D.B., 1972, Microzonation for surface faulting: Proc. Int. Conf. on Microzonation, v. 1, p. 347-361.

Slemmons, D.B., 1977, Faults and earthquake magnitude, Report 6 of State-of-the-Art for assessing earthquake hazards in the United States: U.S. Corps of Engineers Mis. Paper 5-73-1, 129 p.

Slemmons, D.B., 1979, Evaluation of geomorphic features of active faults for engineering design and siting studies: syllabus for course on Geomorphological Applications to Engineering Geology, California State Univ., Los Angeles, November 10-11, 1979.

Smith, R.B., 1978, Seismicity, crustal structure, and intraplate tectonics of the interior of the western Cordillera: in Cenozoic Tectonics and

- Regional Geophysics of the Western Cordillera, Geol. Soc. Amer. Mem. 152, p. 111-114.
- Smith, R.B., and Lindh, A.G., 1978, Fault plane solutions of the western United States: A compilation: in Cenozoic Tectonics and Regional Geophys. of Western Cordillera., Geol. Soc. of Amer. Memoir 152, p. 107-110.
- Thatcher, W., and Hanks, T.C., 1973, Source parameters of southern California earthquakes: in Jour. of Geophys. Research, v. 78, p. 8547-8576.
- Tocher, D., 1956, the Fallon-Stillwater earthquakes of July 6, 1954; Seismol. Soc. America Bull., v. 46, n. 1, p. 10-14.
- Tocher, D., 1958, Earthquake energy and ground breakage: Seismol. Soc. America Bull., v. 48, no. 2, p. 147-153.
- U.S. Army Corps of Engineers, 30 April 1977, Earthquake design and analysis for Corps of Engineers dams: Dept. Army, Office of the Chief of Engineers, Regulation No. 1110-2-1806, 8 p.
- U.S. Atomic Energy Commission, 1973, Nuclear power plant, seismic and geological siting criteria; Federal Register, v. 38, n. 218, pp. 31, p. 281-31, 282.
- U.S. Code of Federal Regulations, 1975, Title 10 (Energy), Part 100 (Reactor Site Criteria), Appendix A (Seismic and Geologic Siting Criteria for Nuclear Power Plants).
- U.S. Nuclear Regulatory Commission, 1975, Rules and Regulations: N.R.C., title 10, Chapter 1, p. 100-1-100-5.
- Van Wormer, J.D., and Ryall, A., 1980, Seismicity related to structure and active tectonic processes in the western Great Basin, Nevada and eastern California: in Proc. of Conf. 10, Earthquake Hazards along the Wasatch and Sierra Nevada Frontal Fault Zones; U.S. Geol. Surv., Open-File Report, p. 37-61.
- Varnes, D.J., 1978, Slope movement types and processes: in Landslides, Analysis and Control, Special Report 176, p. 11-33.
- Walker, P.M., and Trexler, D.T., 1977, Low sun-angle photography: Photogrammetric Engineering and Remote Sensing, v. 43, p. 493-505.

Wallace, R.E., 1970, Earthquake recurrence intervals on the San Andreas fault, California: Geol. Soc. America Bull., v. 81, p. 2875-2890.

Wallace, R.E., 1977a, Profiles and ages of young fault scarps, north-central Nevada: Geol. Soc. America Bull., v. 88, p. 1267-1281.

Wallace R.E., 1977b, Time-history analysis of fault scarps and fault traces--A longer view of seismicity: in Proc. 6th World Conference on Earthquake Engineering, New Delhi, India, v. 2, p. 409-412.

Wallace, R.E., 1978a, Geometry and rates of change of fault-generated range fronts, north central Nevada, Jour. Research, U.S. Geol. Survey, v. 6, no. 5, p. 637-650.

Wallace, R.E., 1978b, Patterns of faulting and seismic gaps in the Great Basin province: Proc. Conference VI, Methodology for Identifying Seismic Gaps and Soon-to-Break Gaps, U.S. Geol. Survey Open File Report 78-983, p. 857-868.

Wentworth, C.M., Bonilla, M.G., and Buchanan, J.M., 1969, Seismic environment of the sodium pump test facility at Burro Flats, Ventura County California: U.S. Geol. Survey Open-File Report, 42 p.

Wiege, R.L., editor, 1970, Earthquake Engineering: Prentice Hall, Inc., Englewood Cliffs, N.J., 518 p.

Woodward-Clyde Consultants, 1980, Report of the Evaluation of Maximum Earthquake and Site Ground Motion Parameters Associated with the Offshore Zone of Deformation San Onofre Nuclear Generating Station.

Wright, L.W., 1976, Late Cenozoic fault patterns and stress fields in the Great Basin and westward displacement of the Sierra Nevada block: Geol. v. 4, p. 489-494.

Wyss, M., and Brune, J.N., 1968, Seismic moment, stress, and source dimensions for earthquakes in the California-Nevada region: Jour. Geophys. Res., v. 73, n. 14, p. 4681-4694.

Youd, T.L., 1973a, Liquefaction, flow and associated ground failure, U.S. Geol. Surv., Circular 688. Reston, VA., 1973, p. 12.

Youd, T.L., Nichols, D.R., Helley, E.J., and Lajoie, K.R., 1975, Liquefaction potential in Studies for Seismic Zonation of the San Francisco Bay Region: U.S. Geol. Surv., Prof. Paper 941-A, p. A68-A74.

Youd, T.L., and Hoose, S.N., 1978, Historic ground failures in northern California triggered by earthquakes: U.S. Geol. Surv., Prof. Paper 993, 177 p.

Youd, T.L., and Perkins, D.M., 1978, Mapping liquefaction-induced ground failure potential: Journal of the Geotechnical Engineering Division, Proc., The American Society of Civil Engineers, v. 104, no., GT3, p. 433-446.

Youd, T.L., Tinsley J.C., Perkins, D.M., King, E.J., Preston, R.F., 1978, Liquefaction potential map of San Fernando Valley, California: in Proc. Second International Conference on Microzonation, v. I, p. 267-278.

Zoback, M., and Zoback, M., 1980, State of stress in the western United States: in Proc. Conference 10--Earthquake Hazards along the Wasatch and Sierra Nevada Frontal Fault Zones; U.S. Geol. Surv., Open-File Report 80-801, pp. 359-432.

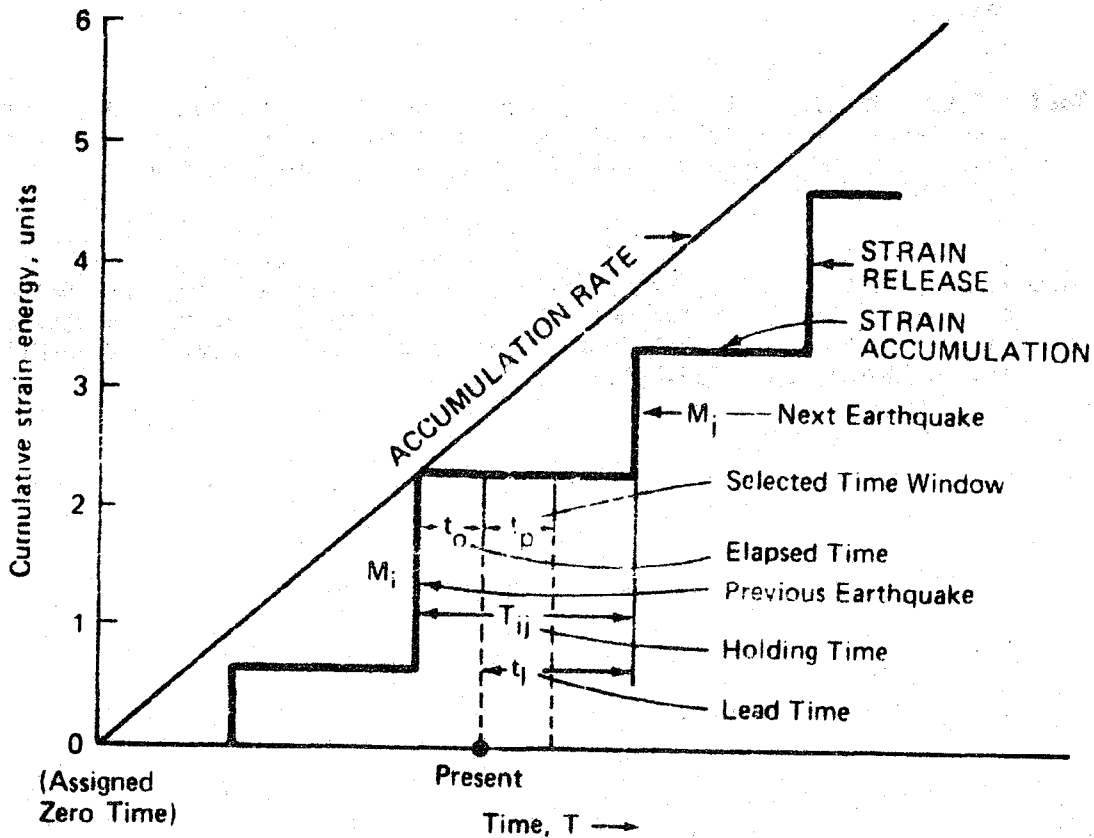


Figure 1: Schematic diagram of the earthquake generation process (Cluff and others, 1980). The following terms are used:

- M_i , the magnitude of the most recent major earthquake
- t_o , the elapsed time since the most recent major earthquake
- M_j , the magnitude of the next major earthquake
- T_{ij} , the holding time between the occurrence of two successive major earthquakes M_i and M_j
- t_p , the period of interest (e.g., design life of a structure or the selected time window for the future)
- t_l , the lead time between the present and the next major earthquake

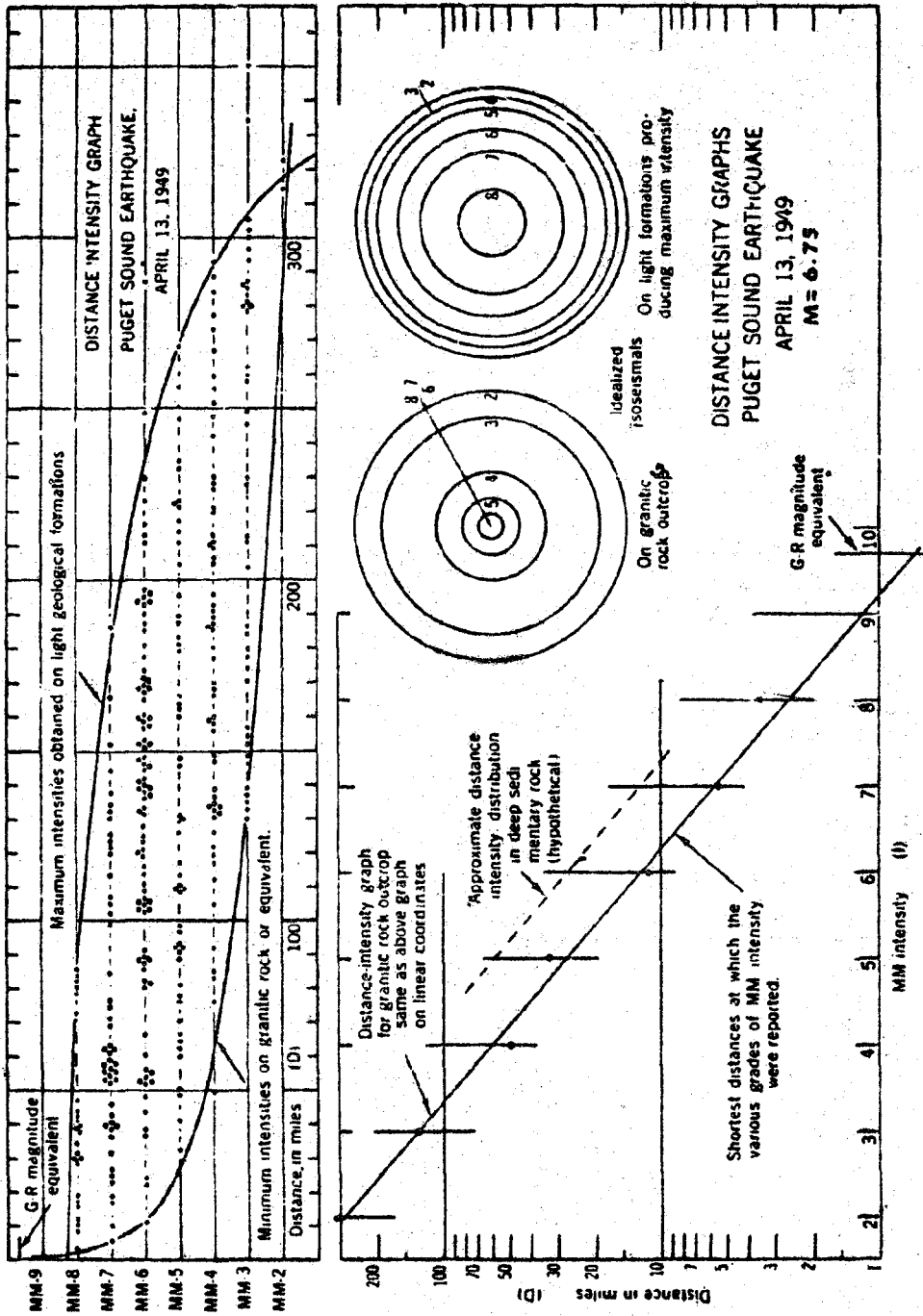


Figure 2: Effects of soil type and distance on intensity (Neumann, 1954).

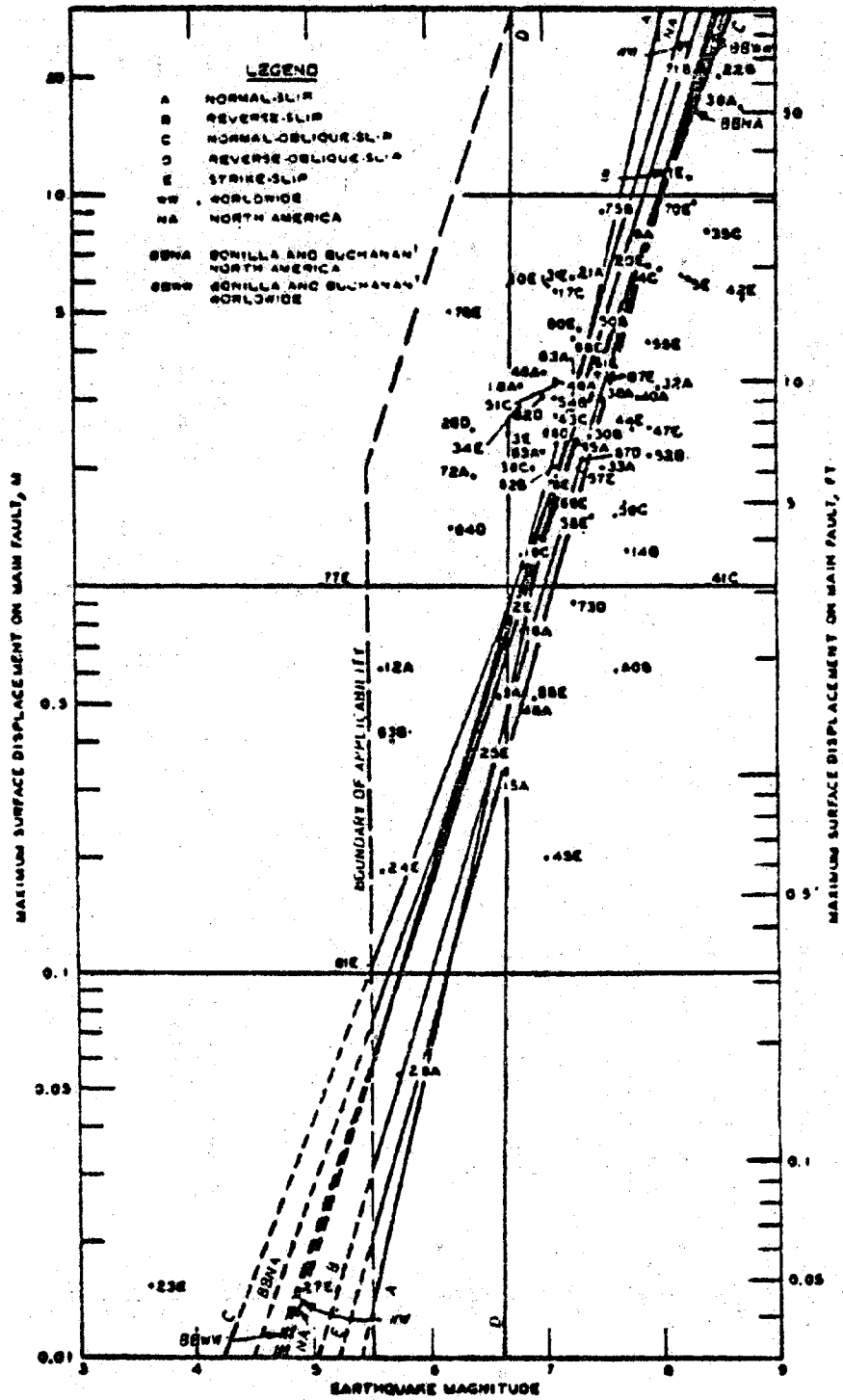


Figure 3: Maximum surface fault displacement on main fault as related to earthquake magnitude (Slemmons, 1977).

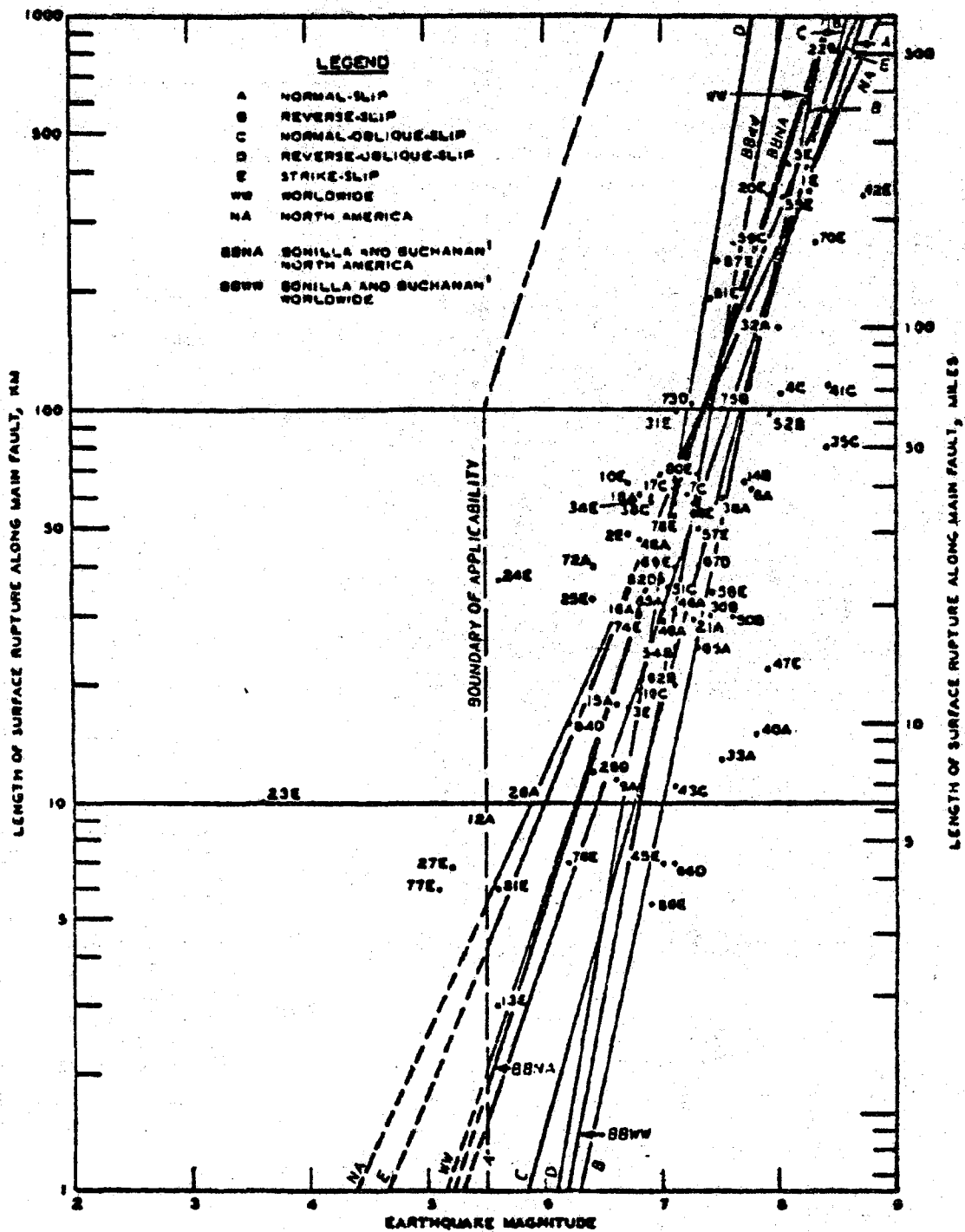


Figure 4: Relation of earthquake magnitude to length of zone of surface rupture along the main fault zone (Slemmons, 1977).

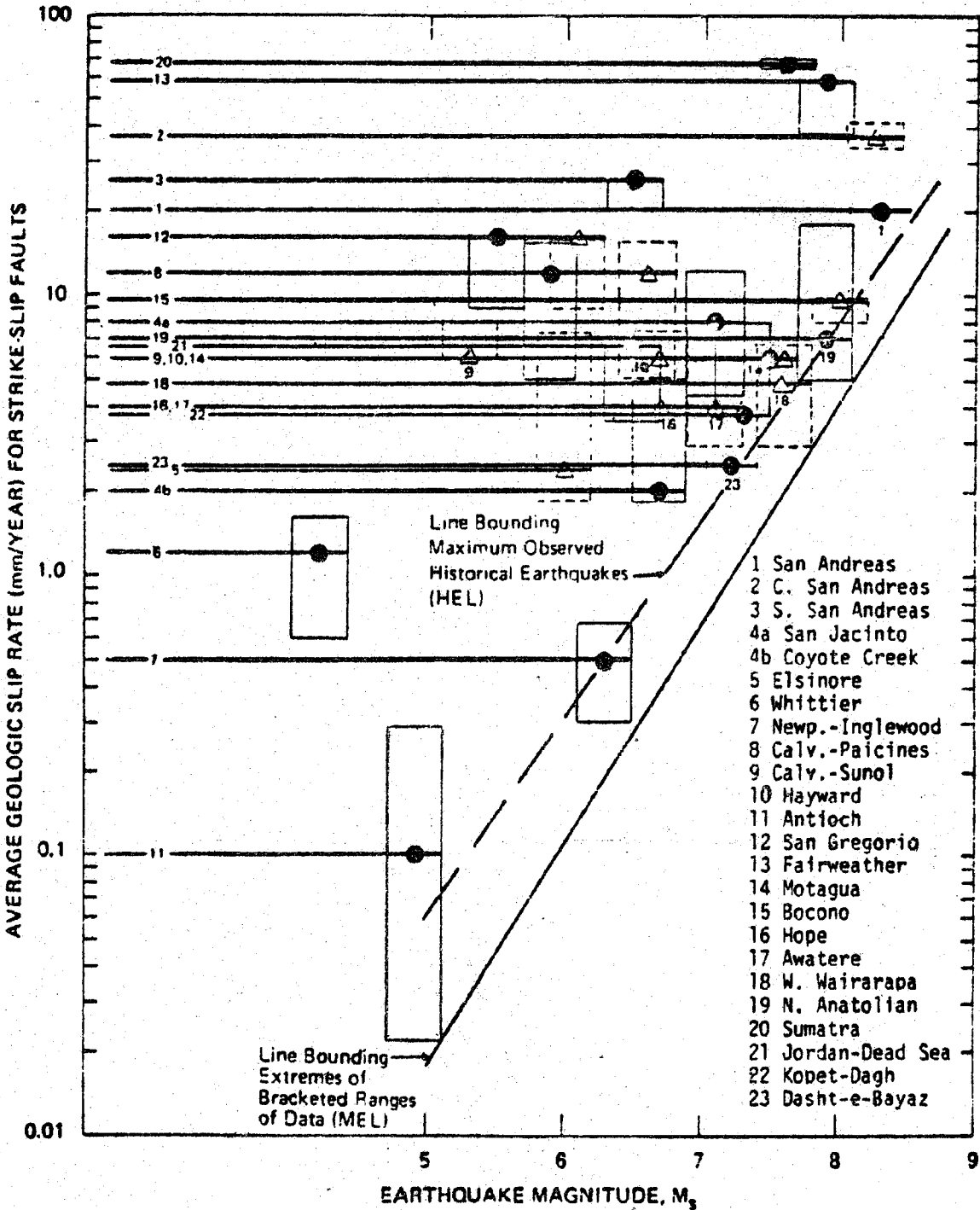


Figure 5:

Data Range Analysis
Geologic Slip Rate VS Historical
Magnitude for Strike-Slip Faults

(After Woodward-Clyde
Consultants, 1980)

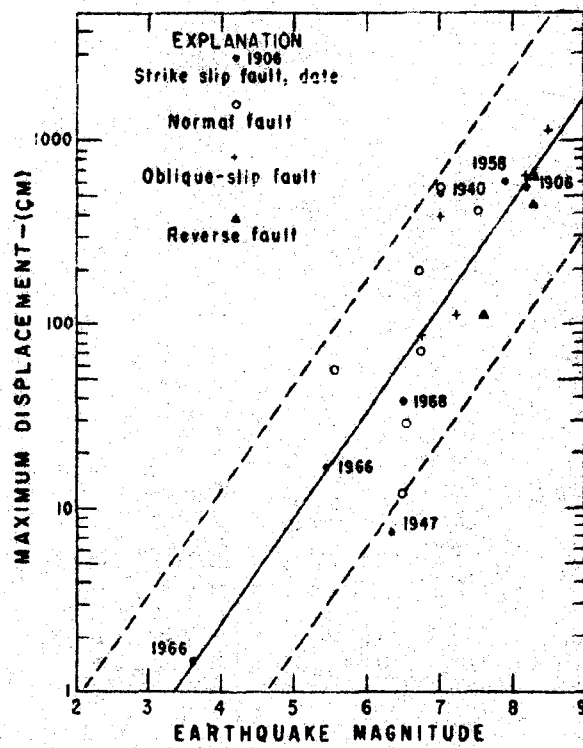


Figure 3. Magnitude-displacement relation in historic faulting in western North America (after Bonilla, 1967).

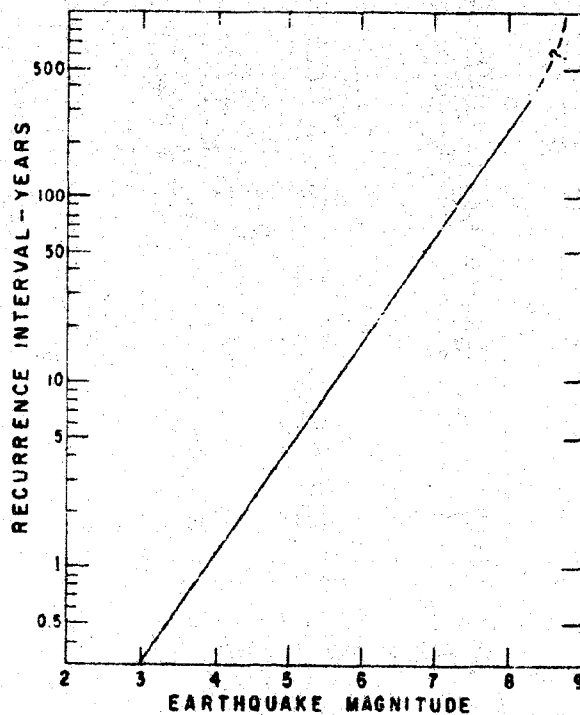


Figure 4. Recurrence interval at a given point on a fault, assuming average displacement rate of 2 cm/yr.

Fig. 6c, d: Wallace recurrence method of analysis of fault activity for the San Andreas fault zone (Wallace, 1970).

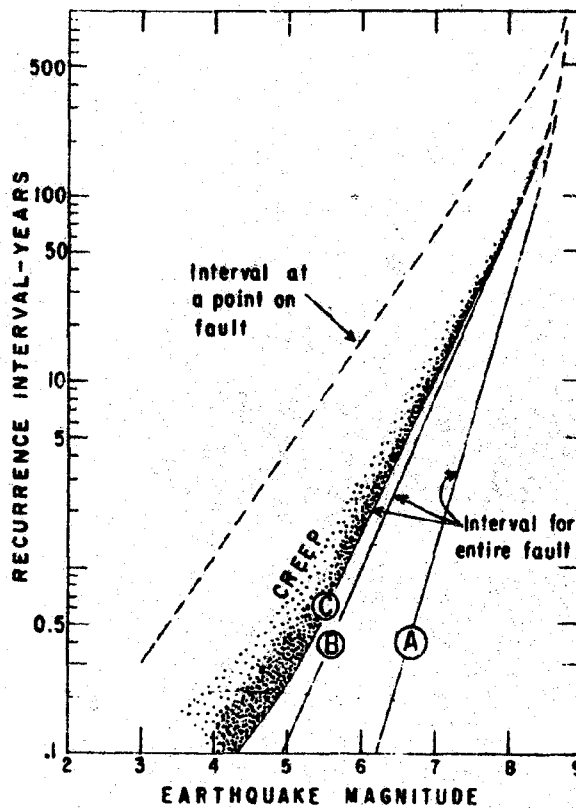


Figure 5. Recurrence interval showing adjustment of "basic" curve from Figure 4 adjusted for entire length of fault. Curve "A" uses data points in curve "A," Figure 2. Curve "B" uses data points in curve "B," Figure 2. See text heading "Effect of creep on recurrence" for explanation of curve "C" and "creep" field.

Fig. 6e: Wallace recurrence method of analysis of fault activity for the San Andreas fault zone (Wallace, 1970).

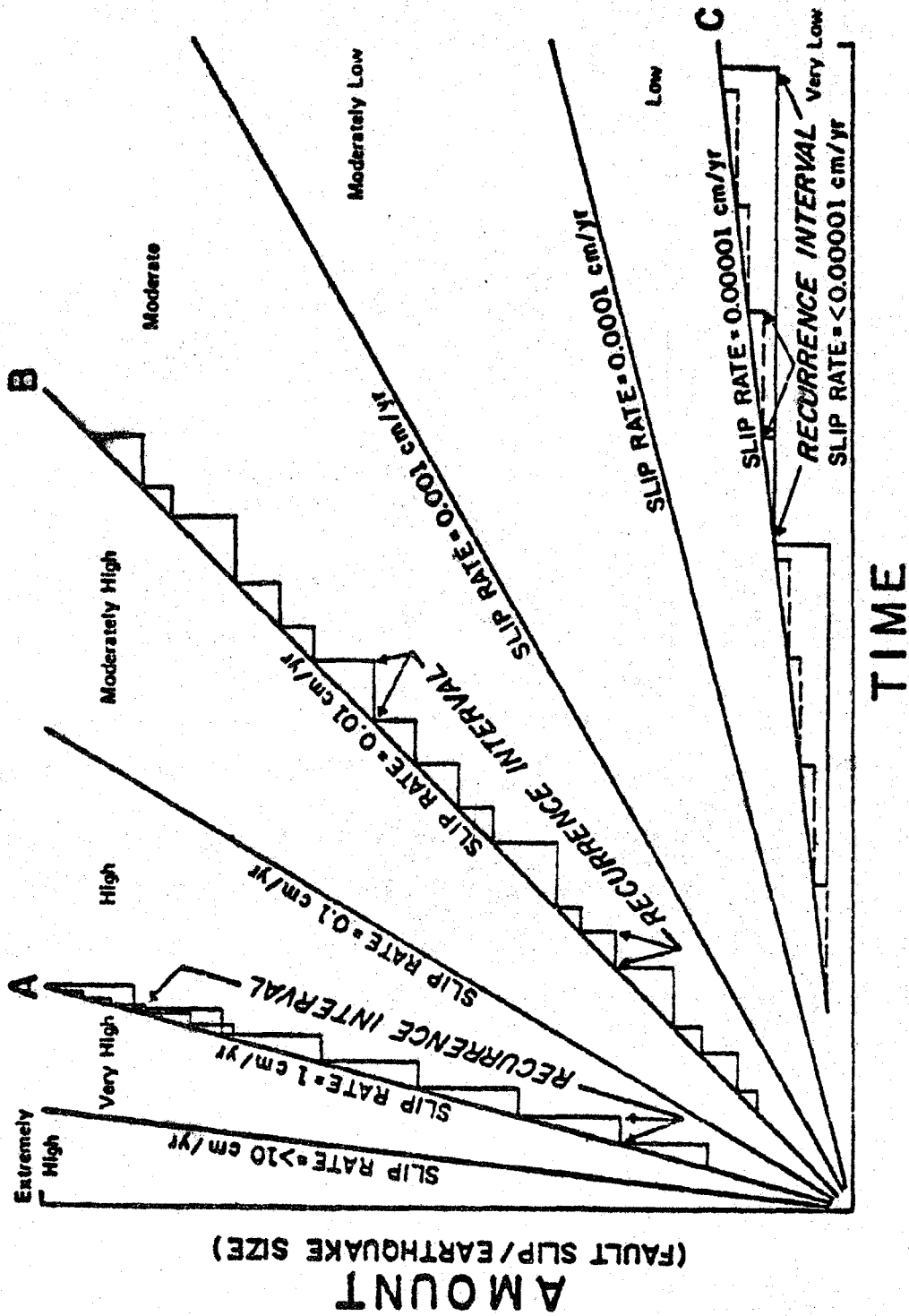
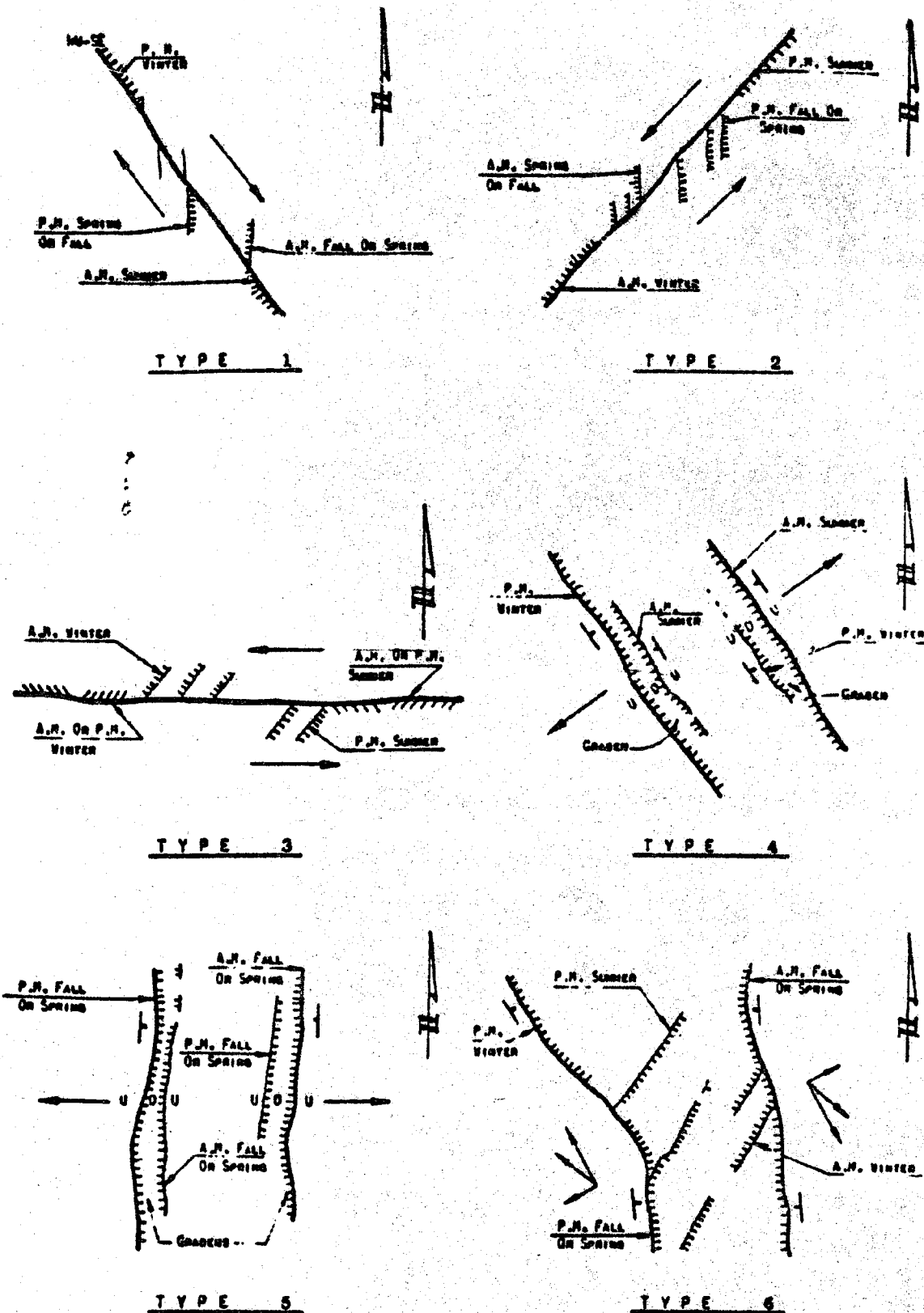


Figure 7 - RELATIVE DEGREE OF FAULT ACTIVITY



HAUGHURED INDICATE AREA OF SHADOW.

Figure 8. APPLICATION OF LOW SUN ANGLE PHOTOGRAPHY TO STUDY ACTIVE FAULTING
TYPICAL TYPES OF FAULTING

DEPARTMENT OF THE INTERIOR
UNITED STATES GEOLOGICAL SURVEY

LATITUDE - 38 DEGREES

SOLAR POSITION DIAGRAM

Heavy lines show paths of the sun across the sky on the indicated dates.

To use in the Southern Hemisphere add 6 months to dates, 12 hours to times, and 180° to azimuths.

Dates from U.S. Naval Oceanographic Office Pub. No. 260. Azimuths of the sun (1964). "Local solar time" of this diagram is based on the average position of the sun and may be in error by as much as 16 minutes during certain parts of the year.

To convert time from this diagram to zone time (for example Pacific Standard time), add 4 minutes for each degree of longitude west of the zone's standard meridian (one that is a multiple of 15), or subtract 4 minutes for each degree east of the standard meridian.

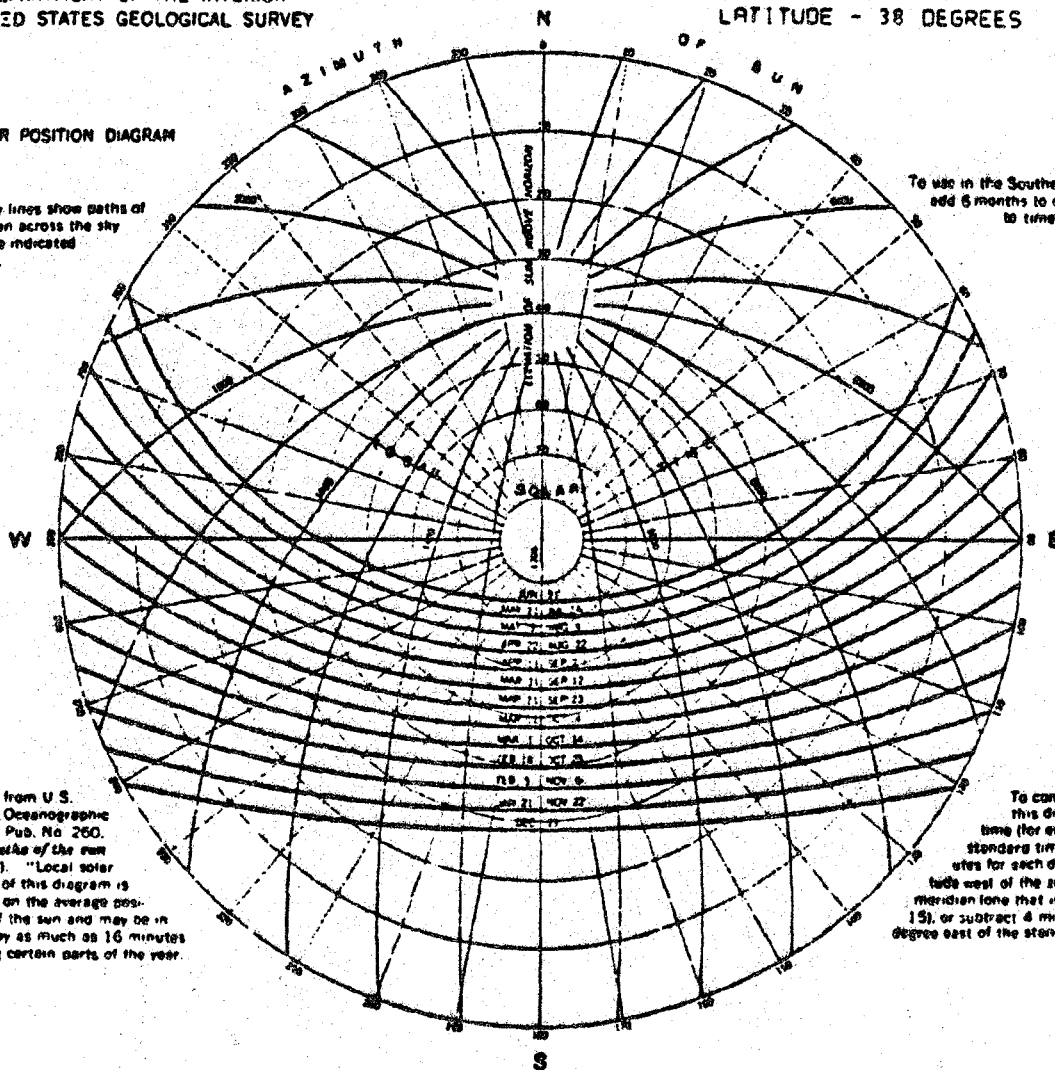


Figure 9: Diagram for use in determining optimum time of day and day of year for low-sun angle imaging(Clark,1971).

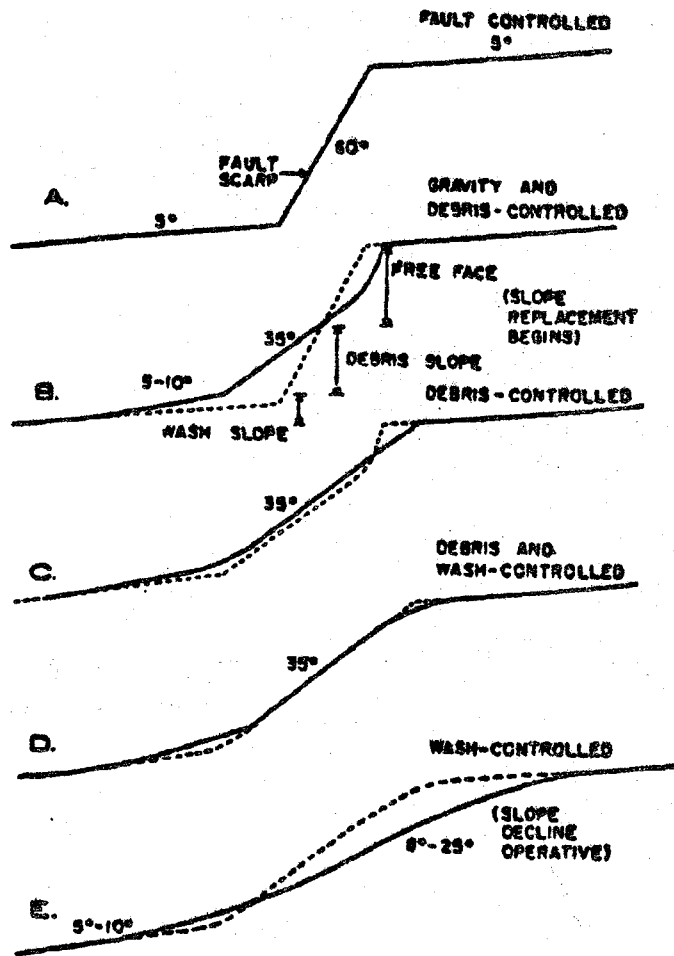


Fig. 10: Sequences of fault-scarp degradation. To show incremental change, dotted line represents solid line of previous profile (Wallace, 1977).

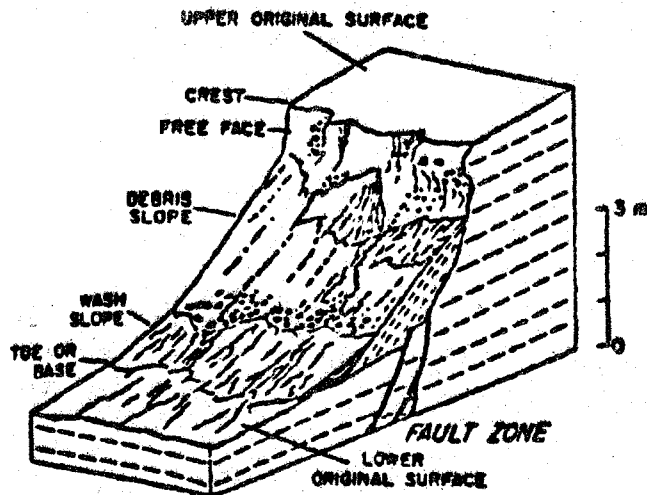


Fig. 11: Block diagram of a fault scarp showing terminology used for scarp description (Wallace, 1977)

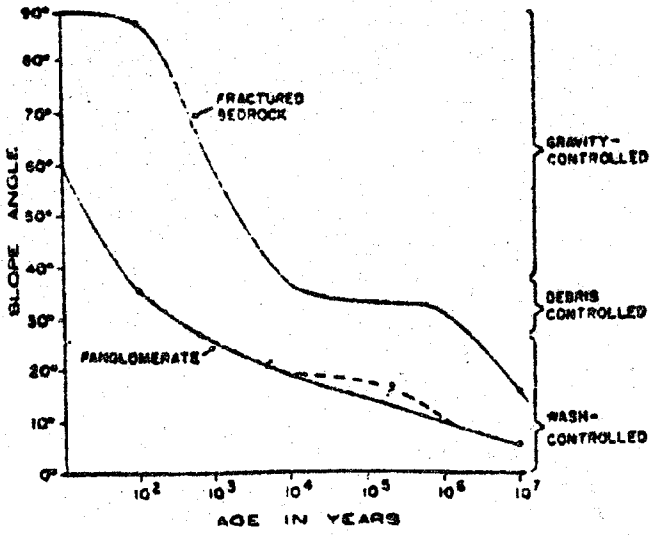


Figure 12: Limits of the principal slope angle versus age of fault scarp (Wallace, 1977).

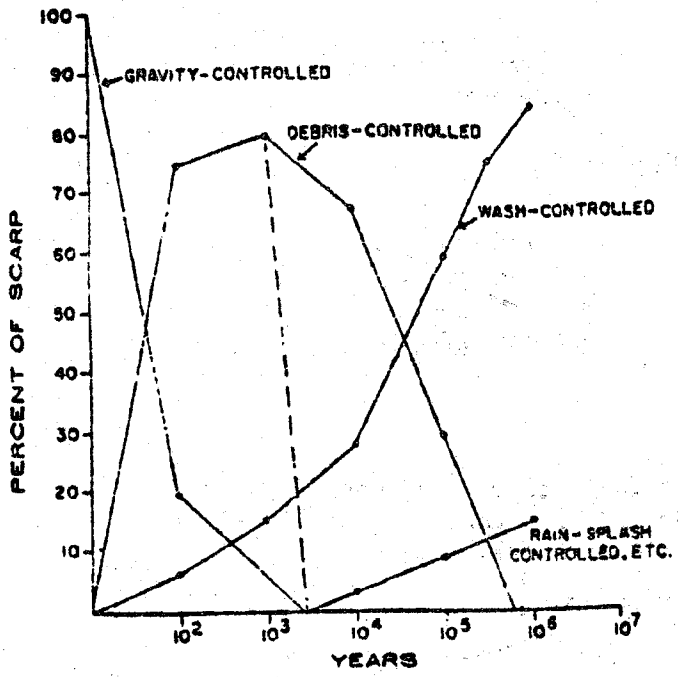


Figure 13: Process control versus age of scarp (Wallace, 1977).

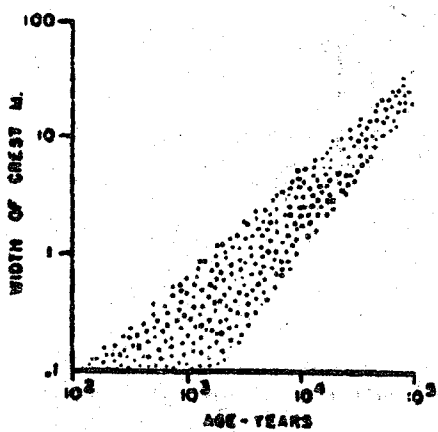


Figure 14: Width of crestal break in slope versus age of scarp (Wallace, 1977).

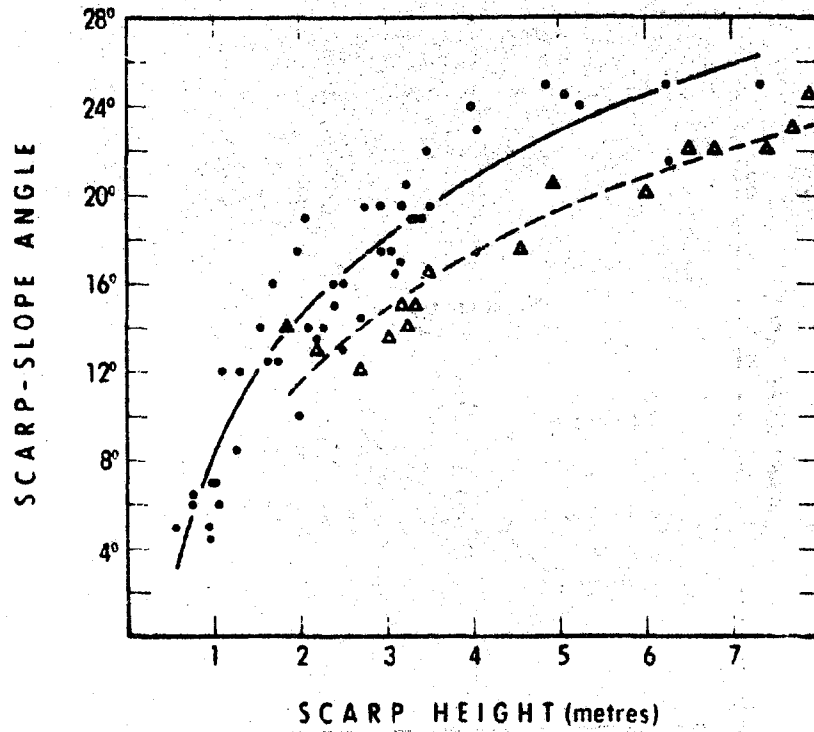


Fig. 15: Scarp-slope versus scarp height data for Drum Mountain scarp (dots) and Lake Bonneville shoreline (triangles) (Bucknam and Anderson, 1979).

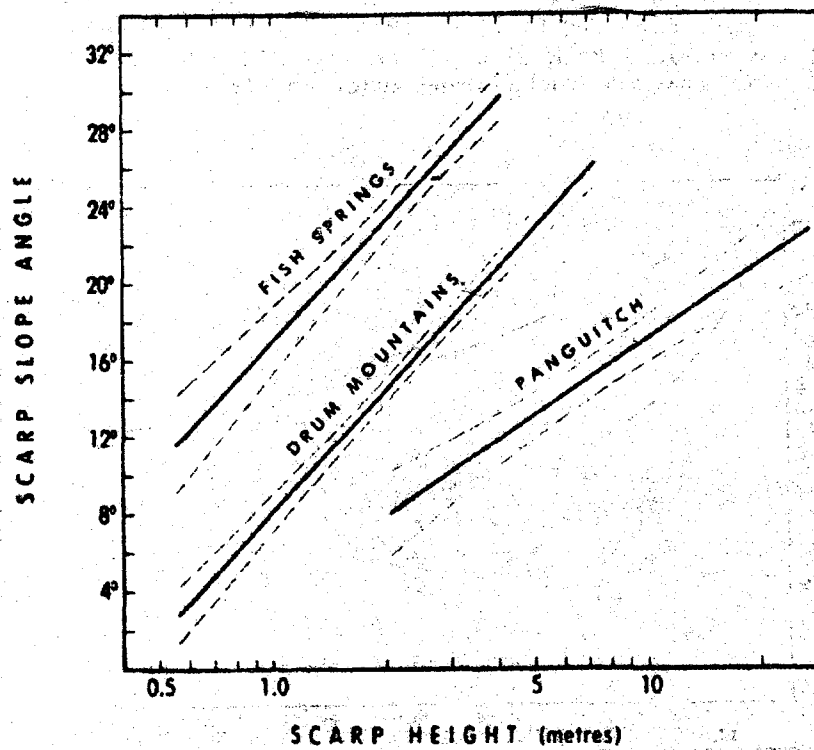


Fig. 16: Regression lines of scarp-slope angles on the log of scarps of varying age. Dashed lines define the 95% confidence interval (Bucknam and Anderson, 1979).

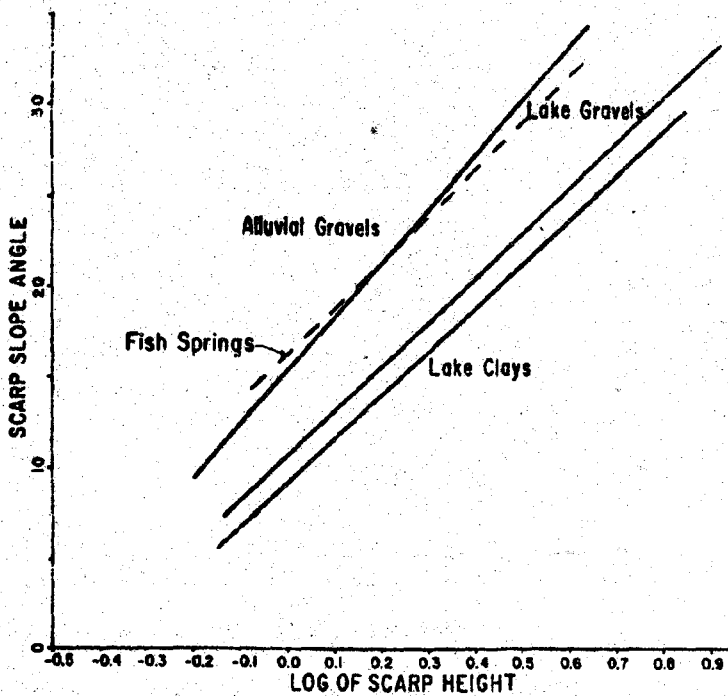


Fig. 17: Linear regression best-fit lines for maximum scarp angle versus log scarp height for three materials cut by the Black Rock fault (from Dodge and Grose, 1979). Also shows closeness of fit between Black Rock alluvial gravel data and Fish Springs data (alluvial) of Bucknam and Anderson (1979).

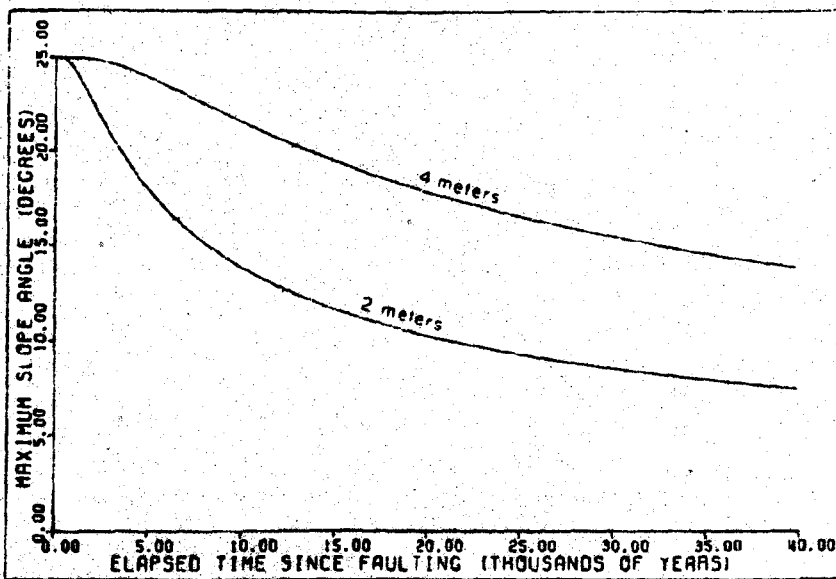


Fig. 18 Decrease in maximum slope angle with time of scarps with initial heights, H , of two and four m and slope angles of 25° . A value of $4.4 \times 10^{-4} \text{ m}^2 \text{ year}$ is assumed for c .

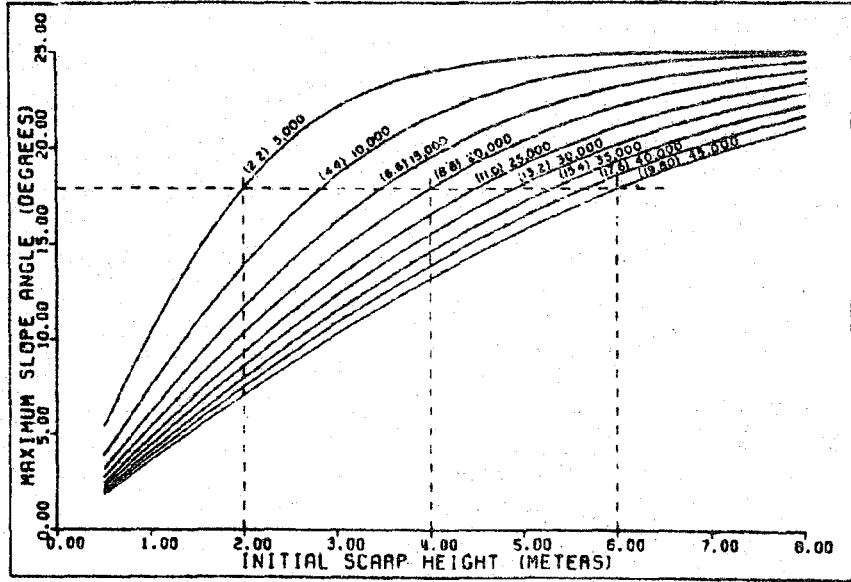


Fig. 19: Relation of slope angle and scarp height predicted by the slope degradation model for scarps with initial slope angles of 25°. Each curve represents a different value of t/c (value in parentheses). Values of t , assuming a value of 4.4×10^{-4} m²/year for c , are printed outside parentheses. The times needed for scarps with initial heights of two, four, and six m to degrade to an angle of 17.9° are indicated (5,000; 20,000; and 45,000 years respectively).

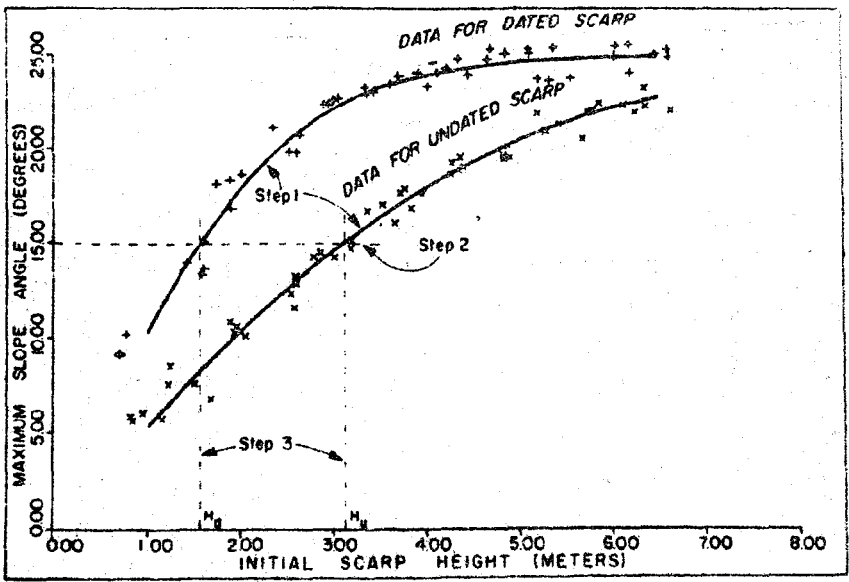
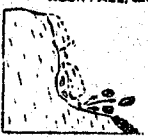
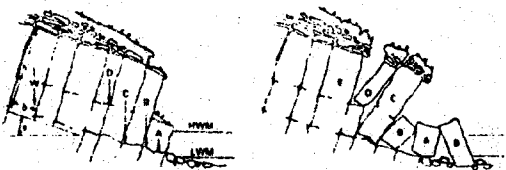
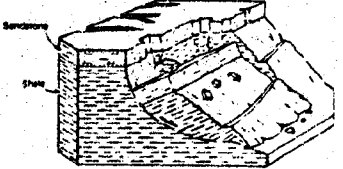

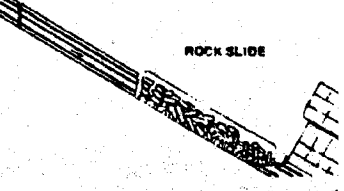
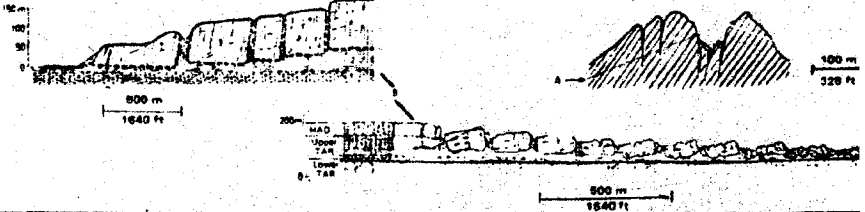
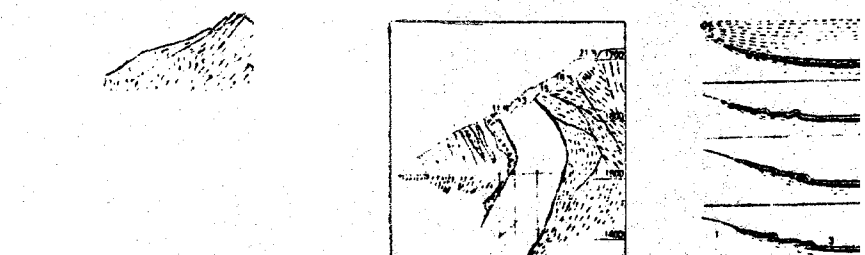
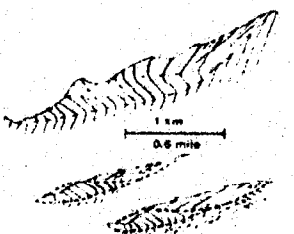

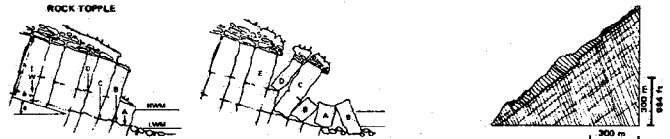
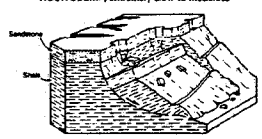
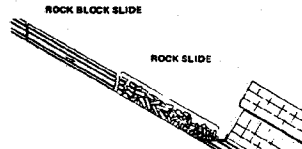
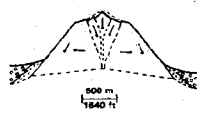
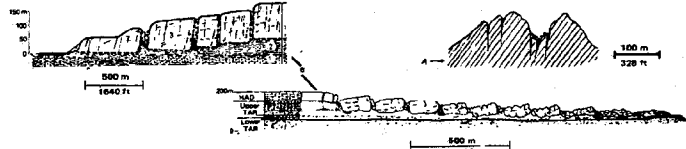
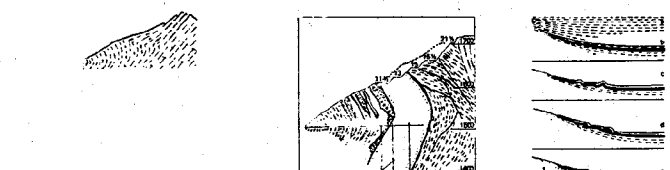
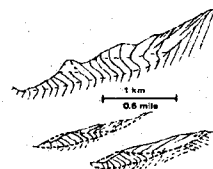
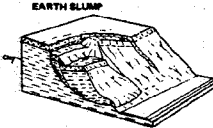
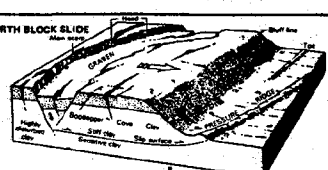
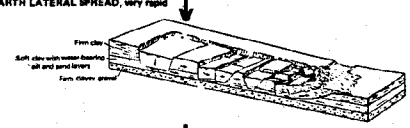
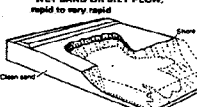
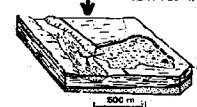

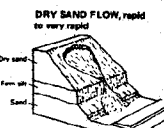

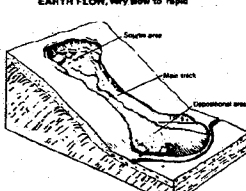



Fig. 20: Procedure for determining the age of an undated normal fault scarp in cohesionless material: (1) Free hand curves are fitted to the data from the dated and undated scarps (simulated data used in this example); (2) A horizontal line is drawn that will intersect both curves (drawn at 15° in this example); (3) Verticals are drawn through the intersections of the horizontal line with the curves for the dated and undated scarps to derive H_d and H_u respectively ($H_d = 1.57$ m and $H_u = 3.14$ m in this example); (4) Assuming the value of c to be the same for both scarps, if t_d is the age of the dated scarp and t_u is the age of the undated scarp: $t_u = t_d(H_u/H_d)^2$. For this example, if the age of the dated scarp is $t_d = 5,000$ years the undated scarp is $t_u = 20,000$ years.

Figure 21: Landslide Types in Bedrock (Varnes, 1978).

DOMINANT TYPE OF MOVEMENT	TYPE OF MATERIAL (BEFORE MOVEMENT)																
<p>FALLS</p> <p>Movement due to forces that cause an overturning moment about a pivot point below the center of gravity of the unit. If unchecked, will result in a fall or slide.</p>	<p>BEDROCK</p> <p>ROCK FALL, extremely rapid</p> 																
<p>TOPPLES</p> <p>Movement due to forces that cause an overturning moment about a pivot point below the center of gravity of the unit. If unchecked, will result in a fall or slide.</p>	<p>ROCK TOPPLE</p> 																
<p>SLIDES</p> <p>Movement involves shear displacement along one or several surfaces or within a zone, which may be visible or may reasonably be inferred.</p>	<p>ROCK SLUMP, extremely slow to moderate</p> <p>Movement due to forces that cause a turning moment about a point above the center of gravity of the unit. Surface of rupture concaves upward.</p> 																
<p>SLIDES</p> <p>Movement predominantly along more or less planar or gently undulatory surfaces. Movement frequently is structurally controlled by surfaces of weakness, such as faults, joints, bedding planes, and variations in shear strength between layers of bedded deposits, or by the contact between firm bedrock and overlying detritus.</p>	<p>ROCK BLOCK SLIDE</p>  <p>ROCK SLIDE</p> 																
<p>LATERAL SPREADS</p> <p>Distributed lateral extension movements in a fractured mass.</p> <ol style="list-style-type: none"> Without a well-defined controlling basal shear surface or zone of plastic flow (predominantly in bedrock). In which extension of rock or soil results from liquefaction or plastic flow or subjacent material. 																	
<p>LOW VELOCITIES</p> <p>IN BEDROCK</p> <p>Includes essentially continuous deformation and surficial as well as deep creeps. Involves extremely slow and generally nonaccelerating differential movements among relatively intact units. Movements may:</p> <ol style="list-style-type: none"> Be along many shear surfaces that are nonparallel and not connected; Result in folding, bending, or bulging; or Roughly simulate those of viscous fluids in distribution of velocities. <p>IN SOIL</p> <p>Movement within displaced mass such that the form taken by moving material or the apparent distribution of velocities and displacements resemble those of viscous fluids. Slip surfaces within moving material are usually not visible or are short-lived. Boundary between moving mass and material in place may be a sharp surface of differential movement or a zone of distributed shear. Movement ranges from extremely rapid to extremely slow.</p>	 <p>Gravity downslope movements of clay rocks and coal on the margin of a sedimentary basin.</p>																
<p>RATE OF MOVEMENT SCALE</p> <p>Approximate ranges of rates of movement are according to the scale below.</p> <table border="1"> <tr> <td>10¹</td> <td>extremely rapid</td> </tr> <tr> <td>10⁰</td> <td>rapid</td> </tr> <tr> <td>10⁻¹</td> <td>very rapid</td> </tr> <tr> <td>10⁻²</td> <td>rapid</td> </tr> <tr> <td>10⁻³</td> <td>moderate</td> </tr> <tr> <td>10⁻⁴</td> <td>moderate</td> </tr> <tr> <td>10⁻⁵</td> <td>very slow</td> </tr> <tr> <td>10⁻⁶</td> <td>extremely slow</td> </tr> </table>	10 ¹	extremely rapid	10 ⁰	rapid	10 ⁻¹	very rapid	10 ⁻²	rapid	10 ⁻³	moderate	10 ⁻⁴	moderate	10 ⁻⁵	very slow	10 ⁻⁶	extremely slow	 <p>7-52</p>
10 ¹	extremely rapid																
10 ⁰	rapid																
10 ⁻¹	very rapid																
10 ⁻²	rapid																
10 ⁻³	moderate																
10 ⁻⁴	moderate																
10 ⁻⁵	very slow																
10 ⁻⁶	extremely slow																

<p>(DOMINANT) TYPE OF MOVEMENT</p>	<p>TYPE OF MATERIAL (BEFORE MOVEMENT) BEDROCK</p>																										
<p>I. FALLS Mass in motion travels most of the distance through the air. Includes free fall, movement by leaps and bounds, and rolling of fragments of bedrock or soil.</p>	<p>ROCK FALL, extremely rapid</p> 																										
<p>II. TOPPLES Movement due to forces that cause an overturning moment about a pivot point below the center of gravity of the unit. If unbraced, will result in a fall or slide.</p>	<p>ROCK TOPPLE</p> 																										
<p>III. SLIDES Movement involves shear displacement along one or several surfaces, or within a relatively narrow zone, which are visible or may reasonably be inferred.</p> <p>A. ROTATIONAL Movement due to forces that cause a turning moment about a point above the center of gravity of the unit. Surfaces of rupture concave upward.</p> <p>B. TRANSLATIONAL Movement predominantly along more or less planar or gently undulatory surfaces. Movement frequently is structurally controlled by surfaces of weakness, such as faults, joints, bedding planes, and variations in shear strength between layers of bedded deposits, or by the contact between firm bedrock and overlying detritus.</p>	<p>ROCK SLLMP, extremely slow to moderate</p>  <p>ROCK BLOCK SLIDE</p>  <p>ROCK SLIDE</p> 																										
<p>IV. LATERAL SPREADS Distributed lateral extension movements in a fractured mass.</p> <p>A. Without a well-defined controlling basal shear surface or zone of plastic flow (predominantly in bedrock).</p> <p>B. In which extension of rock or soil results from liquefaction or plastic flow or subjacent material.</p>																											
<p>V. FLOWS</p> <p>A. IN BEDROCK Includes spacially continuous deformation and surficial as well as deep creep. Involves extremely slow and generally nonaccelerating differential movements among relatively intact units. Movements may:</p> <ol style="list-style-type: none"> 1. Be along many shear surfaces that are apparently not connected; 2. Result in folding, bending, or bulging; or 3. Roughly simulate those of viscous fluids in distribution of velocities. <p>B. IN SOIL Movement within displaced mass such that the form taken by moving material or the apparent distribution of velocities and displacements resemble those of viscous fluids. Slip surfaces within moving material are usually not visible or are short-lived. Boundary between moving mass and material in place may be a sharp surface of differential movement or a zone of distributed shear. Movement ranges from extremely rapid to extremely slow.</p>	 <p>Gravity downslope movement of chevron rocks and soil on the margin of a secondary basin.</p>																										
<p>RATE OF MOVEMENT SCALE Approximate ranges of rates of movement are according to the scale below</p> <table border="1"> <tr> <td>10¹</td> <td>extremely rapid</td> </tr> <tr> <td>10⁰</td> <td>10 ft yr - 3 m/s</td> </tr> <tr> <td>10⁻¹</td> <td>very rapid</td> </tr> <tr> <td>10⁻²</td> <td>1 ft mo - 0.3 m mo</td> </tr> <tr> <td>10⁻³</td> <td>rapid</td> </tr> <tr> <td>10⁻⁴</td> <td>1 ft yr - 1.5 m yr</td> </tr> <tr> <td>10⁻⁵</td> <td>moderate</td> </tr> <tr> <td>10⁻⁶</td> <td>5 ft mo - 1.5 m mo</td> </tr> <tr> <td>10⁻⁷</td> <td>slow</td> </tr> <tr> <td>10⁻⁸</td> <td>5 ft yr - 1.5 m yr</td> </tr> <tr> <td>10⁻⁹</td> <td>very slow</td> </tr> <tr> <td>10⁻¹⁰</td> <td>1 ft 5 yr - 0.05 m yr</td> </tr> <tr> <td>10⁻¹¹</td> <td>extremely slow</td> </tr> </table> 	10 ¹	extremely rapid	10 ⁰	10 ft yr - 3 m/s	10 ⁻¹	very rapid	10 ⁻²	1 ft mo - 0.3 m mo	10 ⁻³	rapid	10 ⁻⁴	1 ft yr - 1.5 m yr	10 ⁻⁵	moderate	10 ⁻⁶	5 ft mo - 1.5 m mo	10 ⁻⁷	slow	10 ⁻⁸	5 ft yr - 1.5 m yr	10 ⁻⁹	very slow	10 ⁻¹⁰	1 ft 5 yr - 0.05 m yr	10 ⁻¹¹	extremely slow	
10 ¹	extremely rapid																										
10 ⁰	10 ft yr - 3 m/s																										
10 ⁻¹	very rapid																										
10 ⁻²	1 ft mo - 0.3 m mo																										
10 ⁻³	rapid																										
10 ⁻⁴	1 ft yr - 1.5 m yr																										
10 ⁻⁵	moderate																										
10 ⁻⁶	5 ft mo - 1.5 m mo																										
10 ⁻⁷	slow																										
10 ⁻⁸	5 ft yr - 1.5 m yr																										
10 ⁻⁹	very slow																										
10 ⁻¹⁰	1 ft 5 yr - 0.05 m yr																										
10 ⁻¹¹	extremely slow																										

(DOMINANT) TYPE OF MOVEMENT		TYPE OF MATERIAL (BEFORE MOVEMENT)																											
		ENGINEERING SOILS	PREDOMINANTLY FINE																										
I. FALLS Mass in motion travels most of the distance through the air. Includes free fall, movement by leaps and bounds, and rolling of fragments of bedrock or soil.		EARTH FALL																											
II. TOPPLES Movement due to forces that cause an overturning moment about a pivot point below the center of gravity of the unit. If unchecked, will result in a fall or slide.		EARTH TOPPLE																											
III. SLIDES Movement involves shear displacement along one or several surfaces, or within a relatively narrow zone, which are visible or may reasonably be inferred.	A. ROTATIONAL Movement due to forces that cause a turning moment about a point above the center of gravity of the unit. Surface of rupture concaves upward.	EARTH SLUMP 																											
	B. TRANSLATIONAL Movement predominantly along more or less planar or gently undulatory surfaces. Movement frequently is structurally controlled by surfaces of weakness, such as faults, joints, bedding planes, and variations in shear strength between layers of bedded deposits, or by the contact between firm bedrock and overlying detritus.	EARTH BLOCK SLIDE 																											
IV. LATERAL SPREADS Distributed lateral extension movements in a fractured mass. <p>A. Without a well-defined controlling basal shear surface or zone of plastic flow (predominantly in bedrock).</p> <p>B. In which extension of rock or soil results from liquefaction or plastic flow or subseismic material.</p>		EARTH LATERAL SPREAD, very rapid 																											
V. FLOWS <p>A. IN BEDROCK Includes spatially continuous deformation and surficial as well as deep creep. Involves extremely slow and generally nonaccelerating differential movements among relatively intact units. Movements may: <ol style="list-style-type: none"> Be along many shear surfaces that are apparently not connected; Result in folding, bending, or bulging; or Roughly simulate those of viscous fluids in distribution of velocities. </p> <p>B. IN SOIL Movement within displaced mass such that the form taken by moving material or the apparent distribution of velocities and displacements resemble those of viscous fluids. Slip surfaces within moving material are usually not visible or are short-lived. Boundary between moving mass and material in place may be a sharp surface of differential movement or a zone of distributed shear. Movement ranges from extremely rapid to extremely slow.</p>		WET SAND OR SILT FLOW, rapid to very rapid  <p>WET FLOWS RAPID EARTH FLOW (CLAY FLOW), very rapid  <p>MUDFLOW  </p></p>																											
SCALE OF MOVEMENT Approximate ranges of rates of movement are according to the scale below <table border="1" style="margin-left: auto; margin-right: auto;"> <tr><td>10²</td><td>extremely rapid</td></tr> <tr><td>10</td><td>10 h = 3 m =</td></tr> <tr><td>1</td><td>very rapid</td></tr> <tr><td>10⁻¹</td><td>1 h = 0.3 m =</td></tr> <tr><td>10⁻²</td><td>rapid</td></tr> <tr><td>10⁻³</td><td>1 h = 1.5 m =</td></tr> <tr><td>10⁻⁴</td><td>moderate</td></tr> <tr><td>10⁻⁵</td><td>3 h = 1.5 m =</td></tr> <tr><td>10⁻⁶</td><td>slow</td></tr> <tr><td>10⁻⁷</td><td>3 h = 1.5 m =</td></tr> <tr><td>10⁻⁸</td><td>very slow</td></tr> <tr><td>10⁻⁹</td><td>1 h = 0.3 m =</td></tr> <tr><td>10⁻¹⁰</td><td>extremely slow</td></tr> </table>		10 ²	extremely rapid	10	10 h = 3 m =	1	very rapid	10 ⁻¹	1 h = 0.3 m =	10 ⁻²	rapid	10 ⁻³	1 h = 1.5 m =	10 ⁻⁴	moderate	10 ⁻⁵	3 h = 1.5 m =	10 ⁻⁶	slow	10 ⁻⁷	3 h = 1.5 m =	10 ⁻⁸	very slow	10 ⁻⁹	1 h = 0.3 m =	10 ⁻¹⁰	extremely slow	DRY SAND FLOW, rapid to very rapid  <p>LOESS FLOW (dry, caused by earthquakes), extremely rapid. Also moist or wet  <p>EARTH FLOW, very slow to rapid  <p>DRY FLOWS  </p></p></p>	
10 ²	extremely rapid																												
10	10 h = 3 m =																												
1	very rapid																												
10 ⁻¹	1 h = 0.3 m =																												
10 ⁻²	rapid																												
10 ⁻³	1 h = 1.5 m =																												
10 ⁻⁴	moderate																												
10 ⁻⁵	3 h = 1.5 m =																												
10 ⁻⁶	slow																												
10 ⁻⁷	3 h = 1.5 m =																												
10 ⁻⁸	very slow																												
10 ⁻⁹	1 h = 0.3 m =																												
10 ⁻¹⁰	extremely slow																												

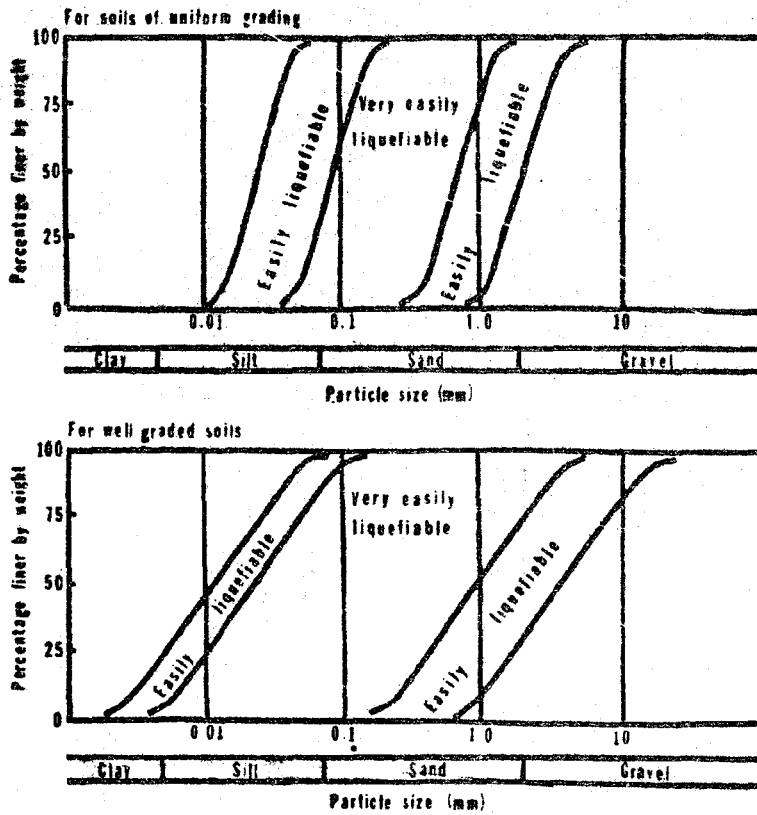


Fig. 24: Ranges of particle size distribution curves of sands which have possibility of liquefaction(Japan Society of Civil Engineers,1973).

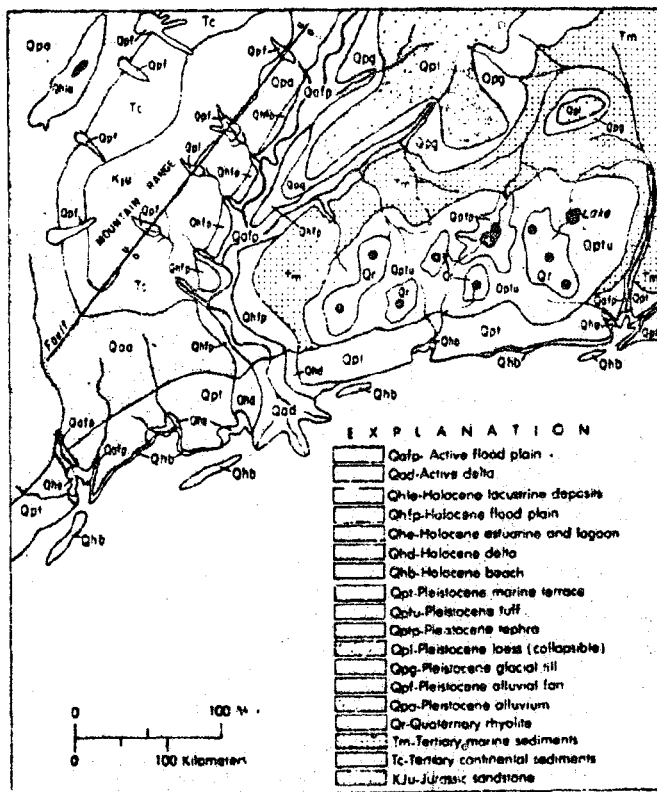


Fig. 25a: Geologic map of hypothetical area (Youd and Perkins, 1978).

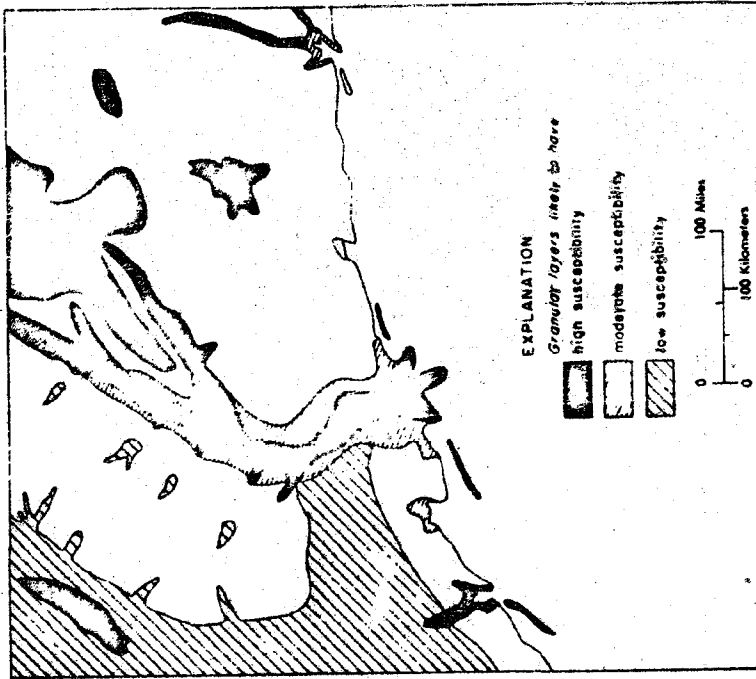


Fig. 25b: Map of liquefaction-induced ground failure susceptibility for the area (Youd and Perkins, 1978).

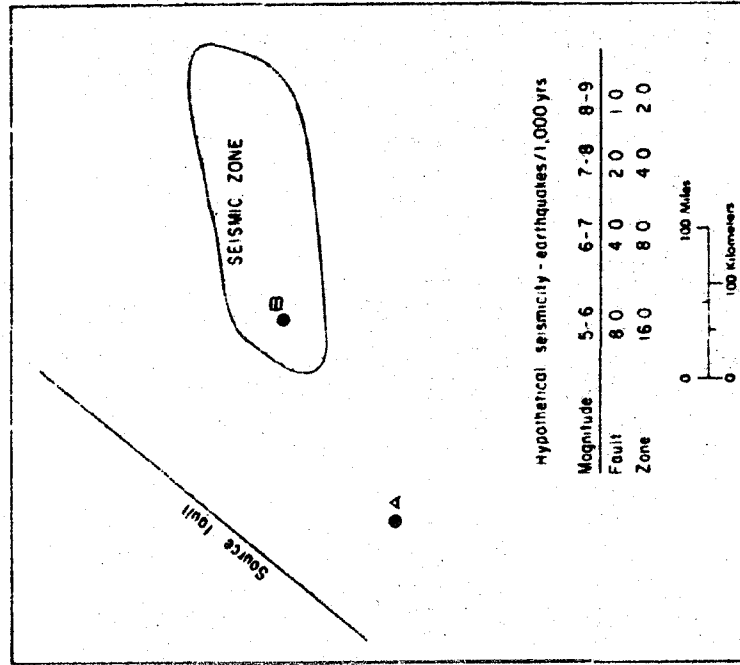


Fig. 25c: Map of the area containing source fault and seismic zone (Youd and Perkins, 1978).

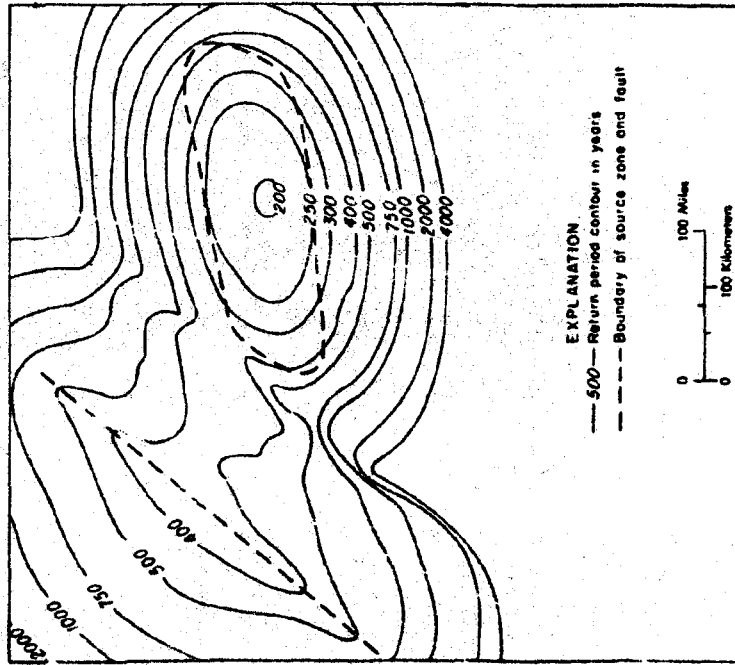


Fig. 25d: Map of ground failure opportunity return period for the area (Youd and Perkins, 1978).

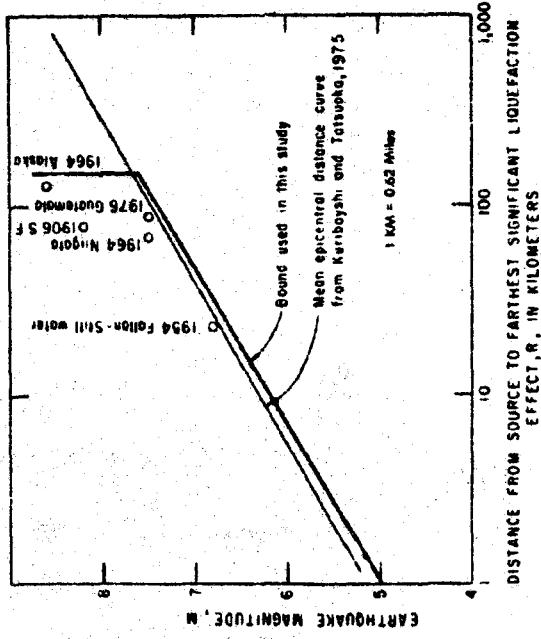


Fig. 25e: Earthquake magnitude versus maximum distance to significant liquefaction-induced ground failures (Youd and Perkins, 1978).

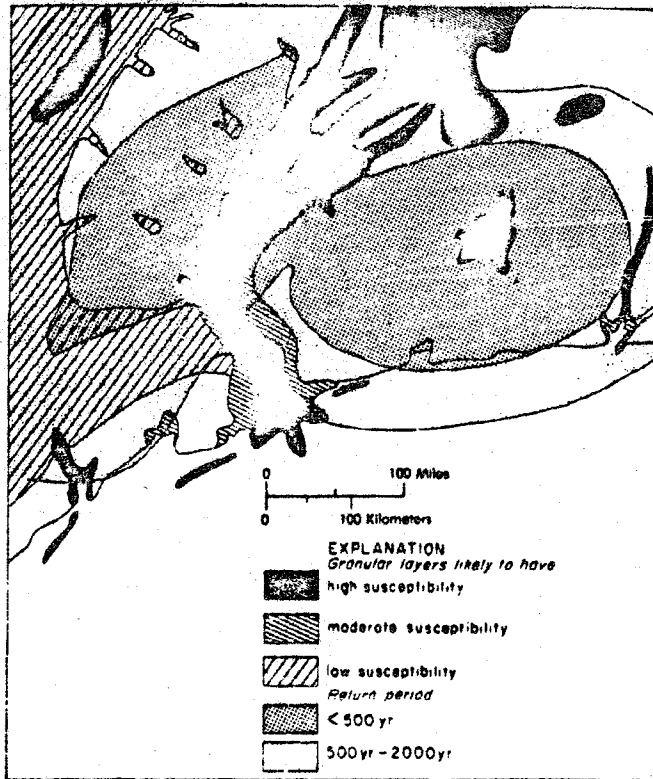


Fig. 25f: Map of liquefaction-induced ground failure potential for the area (Youd and Perkins, 1978).

You have all of the original Tables except Table 7 and 8.

Table 1: Equations of Best Straight-Line for Magnitude

Versus Log Displacement: $M = a + b \text{ Log } D$ (from Slemmons, 1977).

Fault	No.	a	b	Standard Deviation	Correlation Coefficient
North America	24	6.745	0.995	0.595	0.840
Rest of world	51	6.821	1.120	0.549	0.643
Worldwide	75	6.750	1.197	0.541	0.791
A normal-slip	20	6.827	1.050	0.449	0.777
B reverse-slip	11	7.002	0.986	0.469	0.744
C normal-oblique-slip	8	6.750	1.260	0.395	0.672
D reverse-oblique-slip	6	6.917	-0.150	0.421	-0.063
E strike-slip	30	6.717	1.214	0.639	0.814
A + C	28	6.757	1.226	0.431	0.774
B + D	17	6.846	1.023	0.506	0.674
C + D + E	44	6.705	1.206	0.586	0.794
C + D	14	6.692	1.165	0.451	0.568
B + E	41	6.767	1.200	0.606	0.811
A + C + E	58	6.737	1.221	0.549	0.806
B + D + E	47	6.742	1.188	0.597	0.795

Table 2: Equations of Best Straight-Line Fit for Magnitude

Versus Log Fault Length: $M = a + b \text{ Log } L$ (from Slemmons, 1977).

Fault	No.	a	b	Standard Deviation	Correlation Coefficient
North America	26	-0.146	1.504	0.628	0.815
Rest of world	49	2.971	0.920	0.500	0.680
Worldwide	75	1.606	1.182	0.603	0.724
A normal-slip	18	1.845	1.151	0.521	0.575
B reverse-slip	9	4.145	0.717	0.167	0.932
C normal-oblique-slip	10	3.117	0.913	0.457	0.604
D reverse-oblique-slip	7	4.398	0.568	0.340	0.522
E strike-slip	31	0.597	1.351	0.694	0.775
A + C	28	2.042	1.121	0.490	0.666
B + D	16	3.355	0.847	0.320	0.833
C + D + E	48	1.149	1.262	0.650	0.737
C + D	17	2.992	0.918	0.437	0.652
B + E	40	1.042	1.277	0.664	0.773
A + C + E	59	1.204	1.260	0.639	0.724
B + D + E	47	1.357	1.217	0.638	0.758

Table 3: Common Geomorphic Features of Normal-slip Faults

Geomorphic Feature	Ability of Imagery to Resolve Feature ^a		
	Synoptic Scale (Landsat) ^{bb}	Intermediate Scale ^{cc}	Detailed Large Scale ^{dd}
1. Scarps			
a. Simple scarps	• (for larger scarps)	•	•
b. Fissure scarps or fissure traces	0	0	•
c. Trench-trace scarps or graben-trace scarps	Only if scarp is high, vegetation is sparse, and sun angle is low	• if large feature (>1 m)	•
d. Longitudinal-trace scarps or step-trace scarps	Only if scarp is high, vegetation is sparse, and sun angle is low.	• if large feature (>1 m)	•
e. Subsidence-trace scarp	0	0	•
f. En echelon scarps	•	•	•
g. Beveled scarps	•	•	•
2. Triangular facets, faceted spurs, or battered facets	•	•	•
3. Zigzag faults on orthogonal fracture systems	•	•	•
4. Arcuate scarps, especially at terminations or in deep, poorly consolidated sediments	•	•	•
5. Rejuvenated valley or ravine floors with terraces upstream from scarps	0	•	•
6. Wine glass canyons	•	•	•
7. Alluvial aprons, fans, breached fans	•	• if large (>1 m)	•
8. Ramps (oblique slip)	•	•	•
9. Groundwater effect: Linear spring alignments, differential water tables, not or warm springs	•	•	•
10. Volcanic centers	•	•	•

Table 4: Common Geomorphic Features of Reverse-slip Faults

Geomorphic Feature	Ability of Imagery to Resolve Feature ^a		
	Synoptic Scale (Landsat) ^{bb}	Intermediate Scale ^{cc}	Detailed Large Scale ^{dd}
1. Fault scarps	• if large 10's of m	•	•
2. Blunted or oversteepened base of hills at fault	•	•	•
3. Talus and landslide alignments	0	•	•
4. Mile-track or bulldozed traces	0	•	•
5. Graben or fissure swarms on up-thrown block	0	• if large (>1 m)	•
6. Upstream terraces	0	•	•
7. Drag warping of downfaulted block fans, terraces, or sediments	0	0	•
8. Sinuous traces on planar surfaces	• if on scale of km	•	•
9. Single traces or multiple, widely separated (short cut) traces	•	• if large (>1 m)	•

Table 5: Common Geomorphic Features of Strike-slip Faults

Geomorphic Feature	Ability of imagery to Resolve Feature ^a		
	Synoptic Scale (Landsat) ^{oo}	Intermediate Scale ^{oo}	Detailed Large Scale ^{oo}
1. Scarp, eroded or battered scarp	+	+	+
2. Bench	+ if >10 m	+	+
3. Linear canyon, gully, swale, trench, trough, stream, or valley	+	+	+
4. Pond, depression, swampy depression, playa, sag pond, swampy trench	+ if >100 m and filled with water or vegetation	+	+
5. Lateral stream or drainage channel offset	+ if >100 ³ m	+	+
6. Fault gap, notch, or saddle	+ if >100 m	+	+
7. Trench, wedge		+	+
8. Offset ridgeline or hill		+	+
9. Linear or elongated ridge		+	+
10. Trough		+	+
11. Pondered alluvium		+	+
12. Shutter ridge		+	+
13. Scarplet	0	+ if >1 m	+
14. Swale	0	0	+
15. Aligned vegetation or linear boundary	+	+	+
16. Side hill trench or trough	0	+	+
17. Fault valley	+	+	+
18. Fault trace	0	+	+

Table 6

Table of major strike-slip faults, with estimated total length, and percent of fault ruptured during earthquakes of about $M_s = 6$ or greater.

FAULT, DATE	M_s	TOTAL LENGTH (KM)	RUPTURE LENGTH (KM)	PERCENT OF LENGTH
San Andreas		1380		
1857	8.25		370-400+	29.0
1906	8.25		435	<u>31.5</u>
North Anatolian		1330		
1939	7.9		350	26.9
1942	7.3		50	<u>3.8</u>
1943	7.6		265	19.9
1944	7.4		190	14.3
1957	7.1		40	3.0
1967	7.1		54	4.1
Fairweather-Queen Charlotte		1150		
1899	8.5?			
1949	8.1		380	33.0
1958	7.9		350	<u>32.6</u>
1972	7.1		170	15.8
Montagua		1100+		
1976	7.5		230-270	<u>21.4</u>
Awatere-Wellington		547		
1948	7.1		100?	<u>18.3?</u>
Clarence-West Wairarapa		600		
1855	7.5		160	<u>26.7</u>
Hope-East Wairarapa		410		
1888	6.7		55	<u>13.4</u>
San Jacinto-Cerro Prieto (incl. Coyote, Superstition Mtns., Superstition Hills and Imperial faults		290		
1934	7.1		?	
1940	6.7		64	22.1
1968	6.4		33	<u>11.4</u>
1979				
Calaveras-Green Valley		272		
1861	6		29	10.7
1979	5.9		16	<u>8.4</u>
Hayward-Rodgers Creek-Healdsburg- Maacama		285		
1868	6.7		48	<u>16.8</u>

The mean for highest percentage on each fault (underlined) = 22.1

Standard deviation

= 7.45

Reproduced from
best available copy.



Table 7: Criteria for Recognizing an Active Fault (Cluff and others, 1972).

Data source	Specific criteria
Geologic	Active fault indicated by young geomorphic features such as: fault scarps, triangular facets, fault rifts, fault slice ridges, shutter ridges, offset streams, enclosed depressions, fault valleys, fault troughs, sidehill ridges, fault saddles; ground features such as: open fissures, mole tracks and furrows, rejuvenated streams, folding or warping of young deposits, ramps, ground-water barriers in recent alluvium, echelon faults in alluvium, and fault paths on young surfaces. Usually a combination of these features is generated by fault movements at the surface. Erosional features are not indicative of active faults, but they may be associated with some active faults. Stratigraphic offset of Quaternary deposits by faulting is indicative of an active fault
Seismological	Earthquakes and microearthquakes, when well located instrumentally, may indicate an active fault. Absence of known earthquakes, however, does not ensure that a fault is inactive.
Historical	Historical manuscripts, news accounts, personal diaries, and books may describe past earthquakes, surface faulting, landsliding, fissuring or other related phenomena. Usually for a large earthquake, there will be several accounts in the historical record. Evidence of fault creep or geodetic movements may be indicated

TABLE 8: RELATIVE ABUNDANCE OF DIFFERENT TYPES OF LANDSLIDES

Most Abundant	Falls and shallow, disintegrating slides in rock Avalanches, falls, and shallow disintegrating slides in soil Lateral spreads Cut-slope failures Slumps and block slides in soil Slumps and block slides in rock Wet flows Rock fall-avalanches Liquefaction-induced landslides in artificial fills Re-activation of dormant landslides Landslides in artificial fills not due to liquefaction
Least Abundant	Sub-aqueous landslides

Table 9: Preliminary Assessment of Seismically Induced Landslide Susceptibility (Keefer and others, 1978).

LANDSLIDE TYPES	SOME ENVIRONMENTS IN WHICH LANDSLIDES ARE LIKELY TO OCCUR
Rock fall-avalanches	Very steep, very high slopes that are composed chiefly of deeply weathered, closely jointed, or highly sheared rock and that are being over-steepened by active erosion
Slumps and block slides in rock	Moderate to steep slopes in many different types of rock
Rock falls and shallow, disintegrating rock slides	<ol style="list-style-type: none"> 1. Rock slopes steeper than 35° 2. Rock slopes with talus accumulations at their bases 3. Slopes containing weathered, sheared, or closely jointed rock
Falls, avalanches, and shallow, disintegrating slides in soil	<ol style="list-style-type: none"> 1. Steep, high slopes containing certain kinds of weakly cemented materials such as some kinds of loess and some volcanic pumice soils. 2. Steep ridge flanks and stream banks containing unsaturated sandy or silty soils with little or no cohesion
Slumps and block slides in soil	Moderate to steep slopes in soils derived from many different types of rocks, particularly in areas with abundant, preexisting landslide deposits
Re-activation of dormant landslides in soil	Only relatively small numbers of dormant landslides are re-activated by earthquakes
Lateral spreads	<ol style="list-style-type: none"> 1. Areas of generally low relief underlain by many different kinds of unconsolidated saturated Holocene sandy or silty materials 2. Steep, high bluffs containing layers of sensitive clay or liquefiable sand or silt as defined in 1. 3. Uncompacted saturated sandy artificial fills
Wet flows	Steep to very gentle slopes underlain by some kinds of saturated sandy or silty soils
Sub-aqueous landslides	Fronts of deltas or fan deltas, particularly in areas underlain by saturated, liquefiable sand or silt
Cut-slope failures	Artificial cuts
Liquefaction-induced landslides in artificial fills	Uncompacted, saturated, sandy fills
Landslides in artificial fill not caused by liquefaction	Many different types of fill

Table 10. Estimated Susceptibility of Sedimentary Deposits to Liquefaction during Strong Seismic Shaking (Youd and Perkins, 1978).

Type of deposit (1)	General distribution of cohesionless sediments in deposits (2)	Likelihood that Cohesionless Sediments, When Saturated, Would Be Susceptible to Liquefaction (by Age of Deposit)			
		≤500 yr (3)	Holocene (4)	Pleistocene (5)	Pre-Pleistocene (6)
(a) Continental Deposits					
River channel	Locally variable	Very high	High	Low	Very low
Flood plain	Locally variable	High	Moderate	Low	Very low
Alluvial fan and plain	Widespread	Moderate	Low	Low	Very low
Marine terraces and plains	Widespread	-	Low	Very low	Very low
Delta and fan-delta	Widespread	High	Moderate	Low	Very low
Lacustrine and plays	Variable	High	Moderate	Low	Very low
Colluvium	Variable	High	Moderate	Low	Very low
Talus	Widespread	Low	Low	Very low	Very low
Dunes	Widespread	High	Moderate	Low	Very low
Loess	Variable	High	High	High	Unknown
Glacial till	Variable	Low	Low	Very low	Very low
Tuff	Rare	Low	Low	Very low	Very low
Tephra	Widespread	High	High	?	?
Residual Soils	Rare	Low	Low	Very low	Very low
Solka	Locally variable	High	Moderate	Low	Very low
(b) Coastal Zone					
Delta	Widespread	Very high	High	Low	Very low
Estuarine	Locally variable	High	Moderate	Low	Very low
Beach	Widespread	Moderate	Low	Very low	Very low
High wave energy					
Low wave energy	Widespread	High	Moderate	Low	Very low
Lagoonal	Locally variable	High	Moderate	Low	Very low
Fore shore	Locally variable	High	Moderate	Low	Very low
(c) Artificial					
Uncompacted fill	Variable	Very high	-	-	-
Compacted fill	Variable	Low	-	-	-

Reproduced from
best available copy. 

DEFINITION OF "ACTIVE FAULT", "CAPABLE FAULT", AND "DEAD FAULT"

Currently there are no universally accepted definitions for "active fault" and "inactive fault", or "capable fault." The wide range in definitions varies from those based on very low rate of activity or recurrence (as used for siting of nuclear reactors and other vital structures) to definitions restricting the term "active" to faults with historic offset. The original definition by Willis and Wood (Willis, 1923) included the following four essential elements, which are still widely used:

- (1) Active faults have been offset during the present seismotectonic regime.
- (2) Active faults have the probability or potential for future renewal or recurrence of offset.
- (3) Active faults have evidence of recent activity, as may be shown by physiographic evidence.
- (4) Active faults may have associated earthquake activity.

Some earlier definitions of active faults (Wood, 1916; Willis, 1923) classified faults as "alive" or "active" with potential for future recurrence of offsets, or "dead" and no longer likely to be reactivated. A few definitions restrict the term "active" to faults with historic evidence of activity. In view of the inadequacy of the historic period of observation to sample the long-term activity of many faults, most workers prefer to include geological evidence of activity. Examination of the definitions listed in Table 1 suggests the following general characteristics for active fault, capable fault, and dead fault :

Active fault : An active fault is a fault that has slipped during the present seismotectonic regime and is therefore likely to have renewed displacement in the future. The fault activity may be indicated by historic, geologic, seismologic, geodetic, or other geophysical evidence of activity. The activity or fault slip rates may vary from very low, with long recurrence intervals, measured in tens or hundreds of thousands of years, to very high, with short recurrence intervals, measured in tens to hundreds of years. Recent offset along faults with long recurrence intervals may either be recent or ancient. Some workers compare active faults with active volcanoes, which show either historic or geologically recent activity, or are dormant, but with the potential for future activity. Definitions generally include a time indication of either the most recent offset or a recurrence interval. The most widely used definition of active faults in current engineering practice is those faults with evidence of Holocene displacement (approximately the last 10,000 years). Some definitions include the connotation that active faults may move or have offsets during the life of man-made structures, but most workers prefer to define the term independently of applications or man-made structures.

Capable fault : The term, capable fault, is defined by the U. S. Nuclear Regulatory Commission (1975) for siting nuclear reactors (see also U. S. Atomic Energy Commission, 1973). A similar definition by the International Atomic Energy Agency (1972) is summarized in Krinitzsky (1974). These definitions restrict this term to faults that have been

displaced once during the last 35,000 years, or more than once during the last 500,000 years, as shown in Figure A1. The U.S. Corps of Engineers (1977) also use the term capable fault, with a definition that is similar to that of the U.S.N.R.C.

Dead fault: A dead fault is a fault that was active during an earlier orogenic period, but is not active within the present tectonic regime and accordingly does not offset late Cenozoic deposits or surfaces, and is not seismically active.

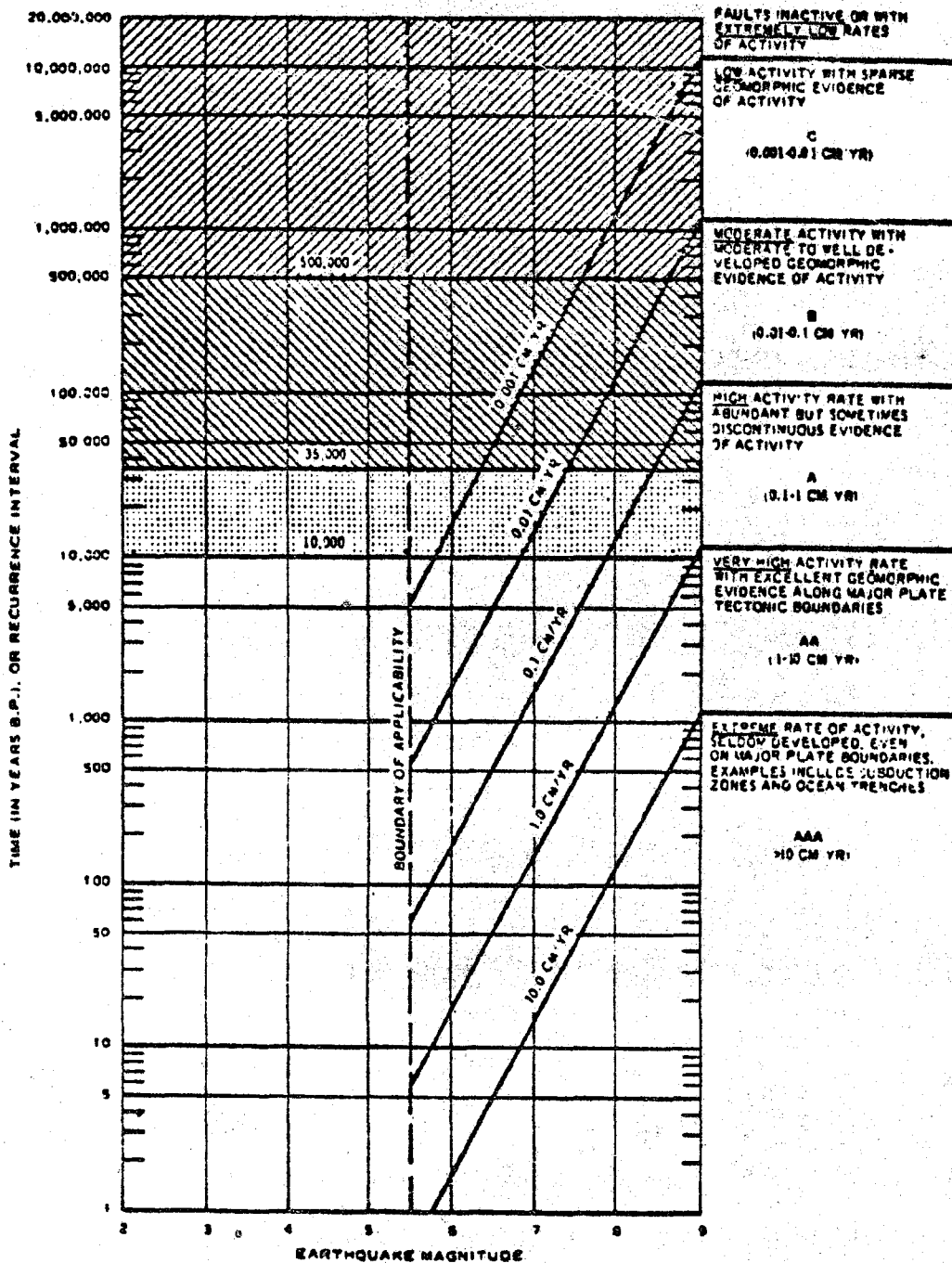


Fig. B1: Relationship between time or recurrence interval (in years), fault-slip or strain rates across fault zones (in cm/yr), and earthquake surface magnitude (Slemmons, 1977). Letter classification of rates is from Matsuda (1975).

TABLE B1: REPRESENTATIVE GEOLOGIC USAGE OF THE TERMS "ACTIVE FAULT" AND CAPABLE FAULT," 1923-1976.

Reference	Definition
<u>Wood (1916)</u>	Wood recognized geologic evidence for recurrent great earthquakes along "recognizable belts-- 'living' zones of geological faulting." He called for "a thorough <u>search for living faults: a specialized survey of surface geology.</u> "
<u>Willis (1923)</u>	"...two classes of faults are distinguished: <u>active and dead.</u> These terms are used very much in the sense in which we speak of active volcanoes or dead volcanoes. An active fault is one on which a slip is likely to occur. A dead fault is one on which no movement may be expected...Wood designated as active all faults on which there has been a movement within historic time, and also all faults upon which physiographic evidence of recent surface dislocation--'trace' phenomena--could be obtained.... Hence any fault that is related to growing mountain is reasonably subject to the suspicion of being an active fault in the sense that a slip may occur."
<u>Louderback (1937)</u>	"The criteria for arriving at a judgement that a fault is active are geological, historical, and seismological.... The best geological criterion is based on evidence of recent displacement along the fault, and especially on evidence of a series of displacements, running through a long period of time and coming down close to the present....If a fault shows evidence of repeated movements during Quaternary time, up to and including very recent offsets, as, for example, in very young alluvium...future movements are practically certain... Observational evidence includes fresh or youthful nonerosional scarps, offset streams and alluvial fans, longitudinal depressions and sag ponds, deformed and displaced recent deposits, and similar phenomena along the fault or shear zone....Historical evidence lies in the records of earthquakes the descriptive accounts of which permit reasonable reference to a particular fault. A seismographic method of learning what faults in a region are active is that of determining the locations of centers of origin of recurring small earthquakes. These earthquakes... indicate that the faults along which they are generated are unstable and subject to repeated adjustments."
<u>Louderback (1950)</u>	"...active faults are those which are undergoing movement now or have moved in recent geologic or in historic time, and are liable to recurrent movements in the future...In the study of a fault as to its active-dead status, it is desirable to determine if possible, the diastrophic period and phase to which it owes its existence. Although there is evidence that under certain conditions some faults which originated in an earlier period have been reactivated, sometimes with a different type or direction of movement in a later period of disturbance, most faults have an active life history that is dependent on a local or regional phase of acute diastrophic activity which is limited in time.

"The active group cuts all formations, including the Recent, with which they come in contact, have direct expression in the topography, and a number have undergone movements accompanied by earthquakes in recent historic time...

"Criteria...that a fault is active are geological, historical, and

seismological...

"The actual observable evidence includes such of the following as may be available in the particular case: fresh or youthful scarps offset streams or alluvial fans, a line of horizontal depressions (not the effect of erosion) or sag ponds, and deformed or displaced Recent deposits.

"Historical evidence lies in the records of earthquakes whose descriptive accounts permit reasonable reference to a particular fault, and especially records of actual displacements of the ground along a fault line.

"A seismographic method of learning what faults of a region are active is to determine the locations of centers of origin of recurring small earthquake...

"The most convincing occurrences are naturally those in which geological, historical, and seismological types of evidence are all available and concordant for the fault under consideration."

Schultz and Cleaves (1955) : "Fractures that are known to have experienced dislocation within historic time are known as active faults....If the seismograph records show that earthquakes occur along a fault, it should ... be regarded as active. Similarly, if accurately located bench marks exhibit horizontal or vertical displacements, any faults known to exist in the area should be regarded as active....

"If a fault is...overlain by younger strata that are not displaced, it is...inactive....The physiographic evidences of active faulting are (1) bold escarpments, (2) sag ponds, (3) offset streams, and (4) shutter ridges."

Trefethen (1959) : "A fault is considered live if displacements have occurred along it within historic time whereas a fault on which no recent slipping has taken place is considered dead.

Sherard and others (1963) : " By definition, active faults are those which either are clearly undergoing movement in historical or geological time. Dead faults are those which show no sign of having been active in recent geological time."

Cluff (1964) : "An active fault is a fault that shows conclusive evidence of movement in Recent geologic time. To be classed as active, the fault must cut the Recent deposits such as alluvial fans or alluvium, have had ground rupture during historic times, or show seismologic evidence (epicentral plots along the fault of activity). Many of the known active faults mapped today show all three types of evidence, i.e., geologic, historic, seismologic."

Allen and others (1965) : "In the absence of strain-accumulation data or historic records of major earthquakes along a given fault, the only satisfactory criterion for activity lies in geological evidence that displacements have taken place along the fault in the recent geologic past...

"Faults that have had sufficiently recent movement to displace the ground surface is a very young and ephemeral feature. Such physiographic

evidences of faulting (e.g. scarps, sag ponds, offset drainage lines) are powerful tools in identifying and studying active faults, but in practice it is difficult to use these features to compare the degree of activity between different faults or to establish the time interval since the last major displacement

"...if stream offsets and scarps in alluvium are to be used as criteria for activity of faults, then the term 'active' must apply to events dating well back into the Pleistocene epoch, perhaps as much as 100,000 years.."

Albee and Smith (1966) : "...the use of the term 'active fault' ...reveals that most geologists use the term 'active fault' in the sense expressed in Webster's (dictionary) definition that active means 'in action, moving.' Although various workers have used various types of criteria for recognizing action, the length of time since last displacement has been considered to be an essential criterion. Whatever the criteria, the use of the term implies a judgement on the part of the geologist that the fault is in action and that it will eventually break again.

"Activity is not just a single state, but varies over a broad spectrum of degrees of activity. For example, some faults are exceedingly 'active,' others are moderately 'active,' and some are only slightly 'active.' Use of the term 'active fault' without qualification rings of greater authority than is usually possible in most cases regarding faults and engineering works.

"The more obvious evidences of fault activity are historic surface faulting, the occurrence of large earthquakes related to a fault, and measurements of accumulated strain."

"In addition to the seismic record, geodetic measurements may provide a criterion for recognizing activity and estimating the degree of activity...."

"Geologic evidence on 'the degree of activity' is a more powerful tool than seismic or geodetic evidence because the geologic evidence monitors a fault over a time period 1000 or more times as long as the accurate seismic and geodetic records."

Bonilla (1967 and 1970) : "An active fault can be defined as one that has moved in the recent past and may move in the near future. The 'recent past' as used here includes the current hour and extends back an indefinite time that many geologists would take to include at least the Holocene Epoch (about 10,000 years). The 'near future' as used above includes a length of time on the order of the useful life of engineering structures or the time span considered in long-range plans for the future. The determination of whether a fault is 'active' as defined above involves geology, geophysics, geodesy, and engineering. Some criteria currently in use are (1) the occurrence of earthquakes that can be related to the fault with reasonable assurance; (2) one or more episodes of surface ruptures (including tectonic creep) or acute bending in the recent past as defined above; (3) instrumental evidence of elastic and inelastic strain; and (4) structural coupling to another fault (or other tectonic feature such as a monocline) that is active. At present, some active faults may not be identifiable, but the ability to identify them should improve with time."

International Atomic Energy Agency (1968) : "The most serious problems appear to exist in those regions characterized by long, continuous faults and fault zones that have had a history of recurring surface displacements within the past few million years. Such zones can generally be recognized by geologists on the basis of physiographic evidence of geologically recent ground displacements, although this virtually demands the availability of high-quality regional aerial photographic coverage.... A much difficult problem is the determination of the probable degree of 'activity' or the likelihood of a surface break within the lifetime of the projected structures, and this must be judged on the basis of (i) how recently the fault has broken, (ii) how frequently it has broken in the past, and (iii) regional seismological, geological and geodetic considerations. In such regions, the largest displacements as well as the largest earthquakes can usually be associated with the longest and most throughgoing fault systems. Auxiliary and branch faulting adjacent to the main fault represent an additional hazard during a major earthquake, and the geologist should be able to make an estimate of such a possibility on the basis of the previous history of faulting in the local area.

"Another hazard is the possibility of slippage (or creep) along a fault even in the absence of earthquakes. Recent studies suggest that this is most likely to occur along the same kinds of major fault zones that are the probable sources of large earthquakes, and this is therefore one more reason to be careful in avoiding such faults in the construction of critical facilities such as nuclear power plants."

Cluff and Bolt (1969) : "Active faults usually are associated with one or more of the following: an historic record of faulting, the occurrence of earthquakes along their courses, evidence of geologically recent movement (the last few thousand years), and slow fault slippage. A fault should be considered active if it has displaced recent alluvium or other recently formed deposits, whose surface effects have not been modified to an appreciable extent by erosions, which has earthquakes located in the near vicinity and whose recurrence of movement is expected."

Wentworth and others (1969) : "A fault is active if because of its present tectonic setting, it can undergo movement from time to time in the immediate geologic future. This active state exists independently of the geologists ability to recognize it...."

"...selection of the criteria used to identify active faults for a particular purpose must be influenced by the consequences of fault movement on the engineering structures involved..."

"Positive identification of specific faults as active, or as sufficiently active to be of concern for a particular engineering problem, is not possible except for those few faults that have exhibited repeated activity in historic or very recent geologic time.... In the following discussion, all faults exhibiting evidence of late Quaternary movement with appropriate length to site-distance ratios are included as worthy of consideration...."

Flawn (1970) : "Active faults are faults along which there has been movement in historic or recent geologic time, or along which recurrence of movement is predicted or is likely to occur; dead faults are those along which there is no indication of movement in historic or Recent geologic time and no reason to predict a recurrence of movement... Studies that

demonstrate accumulation of strain in rocks in an area would justify reclassification of a dead fault to the active category. Faults in seismic areas, even without a history of movement, are more likely to slip than faults in regions without a history of seismic activity."

Wentworth, Ziony, and Buchanan (1970) : "A fault is active if, because of its present tectonic setting, it can undergo movement from time to time in the immediate geologic future. This active state exists independently of the geologists' ability to recognize it. Geologists have used a number of characteristics to identify active faults, such as historic seismicity or surface faulting, geologically recent displacements inferred from topography or stratigraphy, or physical connection with an active fault. However, not enough is known of the behavior of faults to assure identification of all active faults by such characteristics...."

"Selection of the criteria used to identify active faults for a particular purpose must be influenced by the consequences of fault movement on the engineering structures involved."

U. S. Atomic Energy Commission--Proposed Amendment to 10 CFR Part 100 Appendix A (1971) : "An active fault" is a fault which has exhibited one or more of the following characteristics:

"(1) Movement at or near the ground surface at least once in the past 35,000 years or more than once in the past 500,000 years. In the absence of data permitting absolute dating, faults with sufficiently recent movement to leave perceptible evidence of surface rupture, surface warping, or offset of geomorphic features are considered active faults.

"(2) Instrumentally well-determined macro-seismicity for a fault located in the continental United States west of the Rocky Mountain Front, or in Alaska, Hawaii, or Puerto Rico.

"(3) A relationship to an active fault according to characteristics (1) or (2) such that movement on one could be reasonably expected to be accompanied by movement on the other."

Gary and others (1972) : "A fault along which there is recurrent movement, that is usually indicated by small, periodic displacements or seismic activity."

International Atomic Energy Agency (1972) : The following summary is from Krinitzsky (1974) - "The International Atomic Energy Agency criteria are similar to the U. S. criteria, but add:

"(a) Evidence of creep movement along a fault. Creep is slow displacement not necessarily accompanied by macroearthquakes.

"(b) Topographic evidence of surface rupture, surface warping, or offset of geomorphic features.

"They would further classify active faults on a geomorphic basis as follows:

"Class A - High rate of movement, greater than 1 m per 1000 yr.

"Class B - Topography shows clear evidence of dislocation.

"Class C - Topography shows indistinct evidence of dislocation.

"Class D - No evidence of amount or rate of dislocation on which quantitative assessment can be based, but fault is considered capable of causing surface faulting.

"In general engineering practice a fault is considered to be active if there is displacement within Holocene deposits regardless of datable evidence. (Examples: fault displacements within surface gravels, alluvium, or glacial outwash.)"

Wesson and others (1972) : "Faults with a potential for generating damaging earthquakes have been identified by the following criteria --ordered by decreasing certainty of current activity; (1) historic and/or current seismicity or ground breakage; (2) physiographic faulting features and disturbances in Holocene sedimentary deposits which indicate displacement in the last ten thousand years; (3) structural geologic evidence for displacement in Quaternary time (last three million years); and (4) geophysical anomalies suggesting displacements in buried bedrock coincident with anomalous distribution of surficial deposits."

Grading Codes Board (1973) : "With regard to seismic activity, faults can be divided into three major groups (A) active faults; (B) potentially active faults; and (C) inactive faults. This grouping is based on the following criteria, listed in order of decreasing hazard.

"A. Active faults: These faults are those which have shown historical activity. This category includes such faults as the San Andreas, San Jacinto, and Newport-Inglewood.

"B. Potentially active faults: These faults are those, based on available data, along which no known historical ground surface ruptures or earthquakes have occurred. These faults, however, show strong indications of geologically recent activity.

"Potentially active faults can be placed in two subgroups that are based on the boldness or sharpness of their topographic features and the estimates related to recency of activity. These subgroups are:

"1. Subgroup One - High Potential

- a. Offsets affecting the Holocene deposits (age less than 10-11,000 years)
- b. A groundwater barrier or anomaly occurring along the fault within the Holocene deposits.
- c. Earthquake epicenters (generally from small earthquakes occurring close to the fault).
- d. Strong geomorphic expression of fault origin features (e.g. faceted spurs, offset ridges or stream valleys or similar features, especially where Holocene topography appears to have been modified).

"2. Subgroup Two Low Potential

This subgroup is the same as 1a, b, or d above, with the exception that the indications of fault movement can be only determined in Pleistocene deposits (less than 1,000,000 years ago) .

"C. Inactive faults: these faults are without recognized Holocene or Pleistocene offset or activity."

U. S. Atomic Energy Commission (1973) : "A 'capable fault' is a fault which has exhibited one or more of the following characteristics:

"(1) Movement at or near the ground surface at least once within the past 35,000 years or movement of a recurring nature within the past 500,000 years.

"(2) Macro-seismicity instrumentally determined with records of sufficient precision to demonstrate a direct relationship with the fault.

"(3) A structural relationship to a capable fault according to characteristics (1) or (2) of this paragraph such that movement on one could be reasonable expected to be accompanied by movement on the other."

Ziony, Wentworth, and Buchanan (1973) : "Faults of a region can be ranked according to likelihood of future movement on the assumption that those with the most recent displacements probably have relatively short recurrence intervals. Selection of those faults considered to be active, and thus requiring more detailed site investigations, must be influenced by the consequences of possible displacement on the engineering works involved. For example, all faults in the region with proved or likely movement during late Quaternary time (past 500,00 years) may be considered active for purposes of siting nuclear power reactors and other structures that require large safety factors, whereas many such faults might not be considered active for less critical land uses."

Grant-Taylor et al. (1974) : "A Class I Active Fault is one that has shown repeated movement over the last 5,000 years, but may also include those with a single movement in the last 5,000 years and repeated movement in the last 50,000 years (Officers Geological Survey, 1966). A class I fault moves sufficiently often and the displacement that occurs is so large that it has definite planning relevance. Officers Geological Survey (1966) states: 'Class I Active Faults are liable to movement of up to 4.5 m in a period of time that could be the same as the life of a structure. As no structure can hope to withstand such a dislocation it is recommended that no structures be built across the trace of a class I Active Fault, or across the presumed continuation.'"

Nichols and Buchanan-Banks (1974) : "The definition of what constitutes an 'active fault' may vary greatly according to the type of land use contemplated or to the importance of the structure. For example, the Atomic Energy Commission regards a fault as active or 'capable' with respect to nuclear reactor sites it has moved 'at or near ground surface' at least once in the past 35,000 years, or 'more than once in the past 500,000 years' (Atomic Energy Commission, 1971). A definition for purposes of town planning in New Zealand defines as active, any fault on which movement has taken place at least once in the last 20,000 years (Town and Country Planning Branch, Ministry of Works, 1965; originally published as 1,000 years by typographical error). Commonly, faults are regarded as active and of concern to land-use planning when there is evidence that they have moved during historic time or, through geologic evidence, there is a significant likelihood that they will move during the projected use of a particular

structure or piece of land. Because geologic evidence may be lacking, obscure, or ambiguous as to specific times of past movement, geologists may be able to estimate relative degree of activity only after a regional analysis that may extend far beyond the locality under consideration. Such analysis may be based on historic evidence of fault movement, seismic activity (occurrence of small to moderate earthquakes along the fault trace even though not accompanied by obvious fault movement), displacement of recent earth layers (those deposited during the past 10,000 years), and presence of geomorphically young, fault-produced features (scarps, sag ponds, offset stream courses, and disruption of man-made features such as fences and curbs)."

Sherard, Cluff, and Allen (1974) : "...an active fault (or potentially active fault) is defined as one on which there is sufficient evidence of displacement within the recent geological past to make it reasonable to anticipate that future surface displacements could occur within the lifetime of a dam (about 100 years) . It must be emphasized, however that this definition implies the exercise of judgement by geologists, and that there will be honest differences of opinion among competent geologists specializing in this field as to the likelihood of displacements on a given fault."

U. S. Nuclear Regulatory Commission (1975) : "A 'capable fault' is a fault which has exhibited one or more of the following characteristics:

"(1) Movement at or near the ground surface at least once within the past 35,000 years or movement of a recurring nature within the past 500,000 years.

"(2) Macro seismicity instrumentally determined with records of sufficient precision to demonstrate a direct relationship with the fault.

"(3) A structural relationship to a capable fault according to characteristics (1) or (2) of this paragraph such that movement on one could be reasonably expected to be accompanied by movement on the other."

Wesson and others (1975) : "It is not now possible to determine with certainty if a fault will sustain movement in the future. We must assume that if a fault has been active over a considerable length of time (millions of years) and has been historically active or shows evidence of movement in the geologically recent past, it will most likely sustain movement in the future. Evidence from historically active faults both here and abroad indicates that this assumption is generally valid. Extensive studies of the geologic and tectonic settings of historic earthquakes... reveal that the faults responsible for these earthquakes were characterized by at least one or more of the following features: (1) historic earthquakes with or without surface fault displacement, (2) ephemeral physiographic features such as sag ponds, offset streams, and linear ridges that suggest recent fault displacement, and (3) offset Holocene and Pleistocene deposits and geomorphic features...Faults along which these characteristics are developed are commonly termed 'active fault.'"

Lensen (1976) : "An active fault can be defined as a fault that has moved in late geological time and will move again. The N. Z. Geological Survey (Report N.Z.G.S. 7, 1966) defines an active fault more precisely as a fault 'along which there is either evidence of movement since the beginning of the last glaciation (50,000 years ago) or evidence of repeated movement

in the last 500,00 years.'

"The main advantage of classifying active faults lies in assessing their liability to future movement, based on the assumption that a fault that has moved frequently in the immediate geological past is likely to move with a similar frequency in the future.

"Classification of active faults must thus be designed to reflect the history of past fault movements and classes with high, medium, and low frequency of demonstrable past activity can be assigned.

"The classification of active faults adopted by the N. Z. Geological Survey is shown below:

"A Class I Active Fault is thus either a fault that has shown repeated movement over the last 5,000 years or with a single movement over that period and repeated movement in the last 50,000 years.

"A Class II Active Fault is less active with either repeated movement over the last 50,000 years, or one single movement in the last 5,000 years and repeated movement in the period of 50,000 to 500,000 years.

"A Class III Active Fault is the least active with either a single movement over the last 50,000 years or repeated movement during the 50,000-500,000 year period."

U. S. Bureau of Reclamation (1976) : The U. S. Bureau of Reclamation is considering for some regions the use of new criteria for the basis of a definition in which "active faults" are defined as those that have exhibited relative displacement within the past 100,000 years."

Calif. Div. of Mines and Geology (Hart, 1977) : Alquist-Priola Act. "Active faults are those faults which have had surface displacement within Holocene time (about the last 11,000 years). Such faults are considered as active and hence as constituting a potential hazard"

U.S. Corps of Engineers (1977) : A capable fault is one that is considered to have the potential for generating an earthquake. It is defined as a fault that can be shown to exhibit one or more of the following characteristics: (a) movement at or near the ground surface at least once within the past 35,000 years; (b) macro-seismicity (3.5 magnitude or greater) instrumentally determined with records of sufficient precision to demonstrate a direct relationship with the fault; (c) a structural relationship to a capable fault such that movement on one fault could be reasonably expected to cause movement on the other."

Hays (1980) : An active fault is "active if, because of its present tectonic setting, it can undergo movement from time to time in the immediate geologic future. A capable fault is "a fault that has the potential to undergo future surface displacement. A fault is capable if: (1) it has had late Quaternary or more recent movement, or (2) macroseismic activity has been associated with it, or (3) it has demonstrated structural relations to a known capable fault such that movement of the one may cause movement of the other, especially during the lifetime of the project under consideration."

U.S. Code of Federal Regulations (1980) : For a site specific definition

of fault activity "... the recency of movement is based on the determination of movement within Quaternary time..."

REFERENCES

- Albee, A.L., and Smith, J.L., 1966, Earthquake characteristics and fault activity in southern California, *in* Lung, R., and Proctor, R., eds., Engineering geology in southern California: Glendale, Calif., Assoc. Eng. Geologists, pp. 9-33.
- Allen, C.R., St.-Amand, P., Richter, C.F., and Nordquist, J.M., 1965, Relationship between seismicity and geologic structure in the Southern California region: Seis. Soc. of America Bull., v. 55, p. 753-797.
- Association of Engineering Geologists, 1973, Geology and earthquake hazards--Planners guide to the seismic safety element: AEG, Southern California Section, 44 p.,
- Bonilla, M.G., 1967, Historic surface faulting in Continental United States and adjacent parts of Mexico: Open-file Report, U.S. Geol. Survey, Washington, D.C., also Atomic Energy commission Report TID-24124.
- Bonilla, M.G., 1970, Surface faulting and related effects, *in* Wiegel R. L., ed., Earthquake engineering: Prentice Hall, Inc., Englewood Cliffs, N. J., p. 47-74.
- California Division of Mines and Geology, 1973, Guidelines to geologic and seismic reports: CDMG Notes 37.
- California Division of Mines and Geology, 1975, Recommended guidelines for preparing engineering geologic reports: CDMG Note 44.
- Bonilla, M.G., 1970, Surface faulting and related effects: *in* Weigel, R.L., ed., Earthquake Engineering, : Englewood Cliffs, N.J., Prentice-Hall, p. 47-74.
- Cluff, L.S., 1964, Active fault problems: *in* Earthquakes and the practice of soil and geological engineering: Symposium by Woodward-Clyde-Sherard and Assoc., 227 p.
- Cluff, L.S., and Bolt, B.A., 1969, Risk from earthquakes in the modern urban environment, with special emphasis on the San Francisco Bay area, *in* Urban Environmental Geology in the Bay area: Assoc. Engin. Geol., Spec. Publ., p. 25-63.
- Code of Federal Regulations, 1980, 49 CFR Part 194: Department of Transportation, Liquefied Natural Gas Facilities; New Federal Safety Standards, Federal Register, v. 45, n. 29, February 11,

1980, Rules and Regulations, 9184-9209.

Hart, E.W., 1977, Fault hazard zones in California: California Division of Mines and Geology Special Publication 42, 37 p.

Hays, W.W., 1980, Proceedings for estimating earthquake ground motion: U.S. Geol. Survey Prof. Paper 1114, 77 p.

International Atomic Energy Agency, 1972, Earthquake guidelines for reactor siting: Technical Report Series No. 139, Vienna Austria. p. 9-10.

Joint committee on Seismic Safety, California legislature, 1974, Meeting the earthquake challenge: California Division of Mines and Geology Special Publication 45, 223 p.

Flawn, P.T., 1970, Environmental geology: Harper and Row, Pub. Inc., New York, N.Y., 313 p.

Gary, M., McAfee Jr., R., and Wolf, C., 1972, Glossary of Geology Amer. Geol. Inst., Washington, D.C., 857 p.

Grading Codes Advisory Board and Building Code Committee, 1963, Geology and earthquake hazards: Planners guide to the seismic safety element: Southern California Section, Assoc. of Engineering Geologists, 44 p.

Grant-Taylor, T.L., Adams, R.D., Hatherton, T., Milne, J.D.G., Northey, R.D., Stephenson, W.R., 1974, Microzoning for earthquake effects in Wellington, New Zealand: New Zealand Department of Scientific and Industrial Research, Bull. 213, 62 p.

Louderback, G.O., 1937, Characteristics of active faults in the Central Coast Ranges of California, with application to the safety of dams: Seismol. Soc. America Bull., v. 27, n. 1, pp. 1-27.

Louderback, G.O., 1950, Faults and engineering geology, in Paige, S., chmn., Application of Geology to Engineering Practice: Geol. Soc. America, Berkeley Volume, pp. 125-150.

Nichols, D.R., Buchanan-Banks, J.M., 1974, Seismic hazards and land use planning: U.S. Geol. Survey Circ. 690, 33 p.

Schulz, J.R., and Cleaves, A.B., 1955, Geology in Engineering New York, John Wiley and Sons, Inc., 592 p.

- Sherard, J.L., Cluff, L.S., and Allen, C.R., 1974, Potentially active faults in dam foundations: *Geotechnique*, v. 24, n. 3, p. 367-428.
- Slemmons, D.B., and McKinney, R., 1977, Definition of "active fault:" U.S. Army Engineer Waterways Exper. Sta., Vicksburg, Miss. Mis. Paper S-77-8.
- Slemmons, D.B., 1972, Microzonation for surface faulting: *in* Proc. of the International Conference on Microzonation, Seattle, Washington, October-30-November 3, 1972, p. 348-361.
- Taylor, C.L., and Cluff, L.S., 1973, Fault activity and its significance assessed by exploratory excavation: *in* Proc. Conference on Tectonic Problems of the San Andreas fault system: Stanford University Publication, Geological Sciences, v. XIII, p. 239-247.
- U.S. Army Corps of Engineers, 30 April 1977, Earthquake design and analysis for Corps of Engineers dams: Dept. Army, Office of the Chief of Engineers, Regulation No. 1110-2-1806, 8 p.
- U.S. Atomic Energy Commission, 1973, Nuclear power plants; seismic and geologic siting criteria: *Federal Register*, v. 38, no. 218, 13 Nov 1973, p. 31, 281-31, 282.
- U.S. Nuclear Regulatory Commission, 1975, Rules and Regulations: N.R.C., Title 10, Chap. 1, p. 100-1-100-5.
- Wallace, R.E., 1975, Fault scarp geomorphology and seismic history north-central Nevada (abstract) : Geological Society of America, Cordilleran section, 71st Annual Meeting--Abstract with Programs, v. 7, no. 3, p. 385.
- Wentworth, C.M., Ziony, J.I., and Buchanan, J.M., 1970, Preliminary geological environmental map of the greater Los Angeles area, California: U.S. Geol. Survey, TID 25363, 41 p.
- Wentworth, C.M., Bonilla, M.G., and Buchanan, J., 1969, Seismic environment of the sodium pump test facility at Burro Flats, Ventura County, California,: Open-File report, U.S. Geol. Survey Washington, D.C.
- Wesson, R.L., Helley, E.J., Lajoie, K.R., and Wentworth, C.M., 1975, Faults and future earthquakes: *in* Studies for seismic zonation of the

San Francisco by region: U.S. Geol. Survey Prof., Paper 941-A,
p. A5-A30.

Willis, B., and Wood, H.O., 1923, A fault map of California: Seismol. Soc.
America Bull., v. 13, p. 1-12, with map.

Wood, H.O., 1916, The earthquake problem in the western United States:
Seismol. Soc. America Bull., v. 6, p. 181-217.

Ziony, J.I., Wentworth, C. M., and Buchanan, J.M., 1973, Recency of
faulting: A widely applicable criterion for assessing the
activity of faults: Fifth World Conference on Earthquake
Engineering, Rome, Italy, p. 1680-1883.

1. The first part of the document is a list of names and addresses.

168

2. The second part of the document is a list of names and addresses.

169

3. The third part of the document is a list of names and addresses.

170

4. The fourth part of the document is a list of names and addresses.

171

5. The fifth part of the document is a list of names and addresses.

172

6. The sixth part of the document is a list of names and addresses.

173

7. The seventh part of the document is a list of names and addresses.

174

8. The eighth part of the document is a list of names and addresses.

175

9. The ninth part of the document is a list of names and addresses.

176

10. The tenth part of the document is a list of names and addresses.

177

11. The eleventh part of the document is a list of names and addresses.

178

12. The twelfth part of the document is a list of names and addresses.

179

13. The thirteenth part of the document is a list of names and addresses.

180

14. The fourteenth part of the document is a list of names and addresses.

181

15. The fifteenth part of the document is a list of names and addresses.

182

A SURVEY OF INTENSITY ANOMALY DURING DESTRUCTIVE EARTHQUAKES

CHEN DASHENG^I

ABSTRACT

In accordance with local site conditions, such as faults, local topography and ground soil, various instances of intensity anomaly during destructive earthquakes occurred in China since the sixties are illustrated in the paper. On account of the fact that these influence factors are ever changing and often mix together, when studying the possible intensity anomaly due to a specified factor, the other factors in the case will be selected to be nearly the same in other cases as far as possible, or from the statistical point of view discarding the possible influence of other factors.

The results are as follows: effect of non-causative faults on intensity is not obvious. Those villages located on the top or ridge of isolated and projecting hills are much seriously damaged. Damage of structures on rock site is generally not so heavy as those on other ground soil. In distant area far from the epicenter of strong earthquake, tall and flexible structures on soft and deep soil are more heavily damaged than low and rigid structures because of long period vibration. Ground failure is one of the main causes making the structures damage seriously on soft soil, but soil liquefaction occurred under several meters of overburden has the advantage as an isolation layer against vibration, and lowers the degree of damage of structures. All these are the main causes of various anomaly of intensity.

INTRODUCTION

Since liberation, we have paid great attention to field investigation of destructive earthquakes and study of great historic earthquakes. A lot of isoseismal maps have been collected (Ref.1), and areas of high or low intensity anomaly are often shown in these maps. For some historic earthquakes occurred early in the past, the records are generally very simple, from which only meizoseismal area, heavily damaged area, slightly damaged area and felt area can be obtained or evaluated, but the existence of intensity anomaly can still be seen in some isoseismal maps. For example, in the isoseismal map of the Sanhe-Pinggu earthquake (M=8) of September 2, 1679 (see Fig.1), Yutian (no record of damage to buildings), Anci and Yongqing (both had minor damage) were low intensity anomalous areas, while about 500 km far from the epicenter, in

^I Associate Research Professor, Institute of Engineering Mechanics, Academia Sinica.

the neighbourhood of Xugou and Taigu of Shanxi province, there was an area of high intensity anomaly (minor damage). In many isoseismal maps, areas of intensity anomaly will not be found because of the limitation of the scale or other reasons. As for intensity anomaly locations, they are often to be neglected and hardly seen in isoseismal maps.

Study of distribution and causes of intensity anomaly has an important and practical significance. It is one of the major bases for selecting engineering construction sites and land use planning, and is also the main basis for checking up result of theoretical analyses. We consider that local site conditions, such as faults, local topography and ground soil are the main factors for intensity anomaly. Since local site conditions are ever changing, and several factors often mix together, so in the study of the possible intensity anomaly due to a specified factor, the other factors in the case will be selected to be nearly the same in other cases as far as possible, or from the statistical point of view, discarding the possible influence of other factors. It should be noted that the causes of many intensity anomalous areas are often not clear due to the lack of engineering geology and geological tectonic informations. Some causes are just conjective, and may be unreliable. For instances, during the Haiyuan, Ningxia earthquake ($M=8.5$) of December 16, 1920, there was a high intensity anomalous area (intensity X) with approximately 100 square kilometers around Tongwei County in the region of intensity VIII (see Fig. 2). The soil condition and building structures were both essentially similar inside and around the anomalous area. Researchers of the Lanzhou Seismological Brigade, State seismological Bureau deduced that the intensity anomalous area was due to existence of the underlying active fault which moved during the earthquake. Further investigations are needed to explain the causes of some high intensity anomalous areas, such as Liaoyang, Xiaoshangwuqi and Wolongquan etc. during the Haicheng earthquake ($M=7.3$) of February 4, 1975 (see Fig. 3) (Ref.2), and Wanggezhuang low intensity anomalous area in the east of Tangshan City during the Tangshan earthquake of July 28, 1976 (Ref.3). Somebody also assumed that the special condition of inner structure of the earth and propagating paths of seismic waves may lead to intensity anomaly (Ref. 4). In interpreting the cause why Jingxing- Huolu high intensity anomalous area (80-100 km from epicenter) occurred during the Xingtai earthquake ($M=7.2$) of March 22, 1966 (see Fig. 4), the researchers of Institute of Geophysic, Academia Sinica considered that the main cause was due to the total reflection of seismic waves at the bottom of the earth crust. Field observation was carried out in that anomalous area by us, and we considered that the main causes are due to the existence of a certain depth (more than 20 m) of spongy loess and isolated and projecting topography (loess ridge and terrace with gullies on both sides). And there were no high intensity anomalous areas within a radius of epicentral distance of 80-100 km.

A survey of intensity anomaly during destructive earthquakes which occurred since the sixties is presented in this paper. Various instances of intensity anomaly are illustrated in accordance with faults, local topography and ground soil respectively. These available data are mainly adopted from the field observation reports of the Institute of Engineering Mechanics, Academia Sinica. It should be noted that intensity evaluations are mainly based on the damage of single or several storey buildings in villages or cities.

EFFECT OF FAULTS ON INTENSITY ANOMALY

From earthquake engineering point of view faults can be divided into causative faults and non-causative faults. The former one is the fault which generates earthquake while rupturing. In a strong earthquake, the causative fault can be judged according to the distribution of damage, ground breakages and source mechanism. Those faults not in the areas expected to occur are belong to non-causative faults.

Generally speaking, the shape of meizoseismal area is controlled by causative fault. Everybody agrees to this opinion. Even so, sometimes the damage distribution along the entire rupture varies considerably. For example, during the 1975 Haicheng earthquake the new fault traces at Xiaogushan stretched from Toudaogou in the west, passed through Erdaogou, Xiadian, Yangjiapu to the northern part of Yaopu. At Toudaogou, only fine cracks could be seen on the wall of several buildings on rock site located ten more meters from ground breakages. The damage index of the village was 0.17-0.33. Xiadian is situated on terrace of Muxi River along the fault trace near Toudaogou. The surface layer consists of gravel with a small amount of sand. The level of underground water table was roughly 3 meters under the surface, and the damage index was 0.66. If we plot the damage indexes of 19 villages located near the causative faults versus fault distance in accordance with various kinds of ground soil, the damage index does not decrease with the fault distance, but varies obviously with the categories of ground soil, as shown in Fig.5. In the figure, ground soil I is corresponding to the overburden on bedrock, the depth of which is less than 2 meters; ground soil II is the general stable overburden other than ground soil I and III; ground soil III is saturated fine sand, silt, silty soil and various kinds of filled land up to four meters under the ground surface, and the level of underground water table is rather shallow. It implies that the trend of intensity rating along and near the new ground breakages is not higher than the epicentral intensity.

Geologists and seismologists often explain that intensity anomaly results in the existence of fault underneath. According to what we observed in earthquake sites, those non-causative faults far from meizoseismal area or located near epicenter but not intersected with the causative faults do not have

obvious effects on damage. Only those non-causative faults located near meizoseismal area and intersected with causative faults or wide and seriously ruptured non-causative faults near the edge of causative faults may cause damage more serious than usual.

During the Tonghai, Yunnan earthquake ($M=7.7$) of January 5, 1970 we inspected 35 villages located just on the right of non-causative faults, and compared their damage indexes with those on similar soil, as shown in Fig. 6(Ref.5). From the difference of such damage indexes, we got a similar result consistent with the result mentioned above. The ground soil is classified according to the overburden of ground breakages.

During the Yongshan-Daguan, Yunnan earthquake ($M=7.1$) of May 11, 1974 an area of high intensity anomaly existed around Xiaping-Huilongwan within the region of intensity VII in the northwest of Jishajiang River. Near the east boundary of the anomalous area the Damaotan Fault passes through. Somebody suspected that the anomalous area was related to the fault (Ref. 6). According to our field investigation, in the anomalous area intensities of villages such as Huilongwan, Lujiawan and Xiaping were all VIII. They scattered 1 to 2 kilometers far from the west of Damaotan Fault. Villages of Xiwولو, Yaziwán, Zhujialiangzi and Wayaoping distribute in an area between the villages mentioned above and Damaotan Fault. Their intensity ratings were all rather low, nearly VII. In addition, there were no phenomena of high intensity anomaly in the villages located on the southern part of the fault or in an area 1 to 2 kilometers from the east of the fault (see Fig. 7). This means that the existence of Damaotan Fault was not the cause of high intensity anomaly.

According to the figure in the report of the Haicheng earthquake published by the Liaoning Seismological Bureau, we determine the villages through which the non-causative faults pass. Then, we plot the damage indexes of these villages in the figure showing mean damage attenuation curves, as shown in Fig. 8. The distribution of damage indexes is random, so there is hardly that non-causative fault causes damage to be more seriously. In Xiaoshangwuqi high intensity anomalous area mentioned above, there is really a fault passing through, but the distribution of villages heavily damaged doesn't fall into a strip and the effect of faults is not obviously seen (see Fig. 9). According to the result of our field investigation the actual area of high intensity anomalous area in Liaoyang is much smaller than that given by the report of Haicheng earthquake published by Liaoning Seismological Bureau (see Fig.3 and 10). And damage to buildings in villages located between the anomalous area and the Daizihé River main faults was not so heavy as that in the anomalous area. So we can negate that the occurrence of Liaoyang anomalous area was due to the effect of faults.

During the 1976 Tangshan earthquake, an area of high intensity anomaly occurred in a basin surrounded with mountains around Zhenzizhen, Luanxian County, as shown in Fig.11. The Taoyuan Fault passes from Yougezhuang through Yujiatuo in the south of Zhenzizhen toward Ganhecao and Xindianzi. According to aerial photographs, the shape of high intensity anomalous area, in which the percentage of totally collapsed buildings was greater than or equal to 80%, was roughly consistent with the strike of Taoyuan Fault. But damage in villages through which Taoyuan Fault passed and outside the anomalous area was not so heavy. For example, in Xiying and Xindianzi, percentage of totally collapsed buildings is only 20%. The intensity anomalous area was completely located in basin. A typical log in Longtuo indicates that the overburden is a kind of purple soil with shells and the bedrock is never seen up to 130 meters depth. Xiying and Xindianzi both are located at the foots of mountains. Consequently, the high intensity anomaly was mainly due to the effect of ground soil but not the effect of Taoyuan Fault.

Fig.12 is the isoseismal map of the Songpan, Sichuan earthquakes (both $M=7.2$) of August 16 and 23, 1976. Location of faults is also plotted in the map. The researchers of Sichuan Seismological Bureau (Ref.7) suggested that there were three areas of high intensity anomaly caused by faults during the earthquakes: a high intensity anomalous area (intensity rating VII) around Tanzishan of Taiping Commune, Beichuan County was just consistent with the strike of Beichuan-Zhongtanpu Fault; other two high intensity anomalous areas (both intensity ratings equal to VII) were around Majia-Hujiao and Nanping-Hanan. There were faults just passing through the middle of anomalous regions. Besides, they assumed the shape of intensity VII area around Nanping County and Wenxian County to be an arc and this should be related to the movement of Wenxian active faults. This is too farfetched. It can be seen in the map that either Taiping high intensity anomalous area or other high intensity anomalous areas, such as Majia-Hujiao, Nanping-Shuanghe-Hanan, Sierzhai and Songpan-Zhenjianguan etc. were all scattering along the river banks. So the high intensity anomaly may be mainly due to the softness of soil.(see Fig.13 and 14)

In addition, from the shapes of isoseismals of some earthquakes, such as isoseismal maps of the Yangjiang, Guangtong earthquake ($M=6.4$) of July 26, 1969 and the Liyang, Jiangsu earthquake ($M=6$) of July 9, 1979, it can be seen that even though the non-causative faults which may control the region are deep and big they have no obvious effect on intensity.

EFFECT OF LOCAL TOPOGRAPHY ON INTENSITY ANOMALY

In mountainous region and hilly land, effect of elevation and local topography on intensity are obvious. This has been

identified many times by field observations that buildings located on the top or ridge of isolated and projecting hills are damaged more seriously than the similar buildings on the plain with similar ground soil. But, as for rock site the effect is not obvious if the elevation is less than 30 meters.

During the Tongchuan, Yunnan earthquake (M=6.5) of February 5, 1966, Silicosis Hospital in Xincun, located on the top of Suoshan mountain and some villages on spurs or ridges of Xiniushan mountain and Houzibo mountain suffered more seriously damage than those on the plain (Ref.8).

The Luhuo, Sichuan earthquake (M=6.8) of August 30, 1967 occurred in mountainous region along the Xianshuihe River (Ref.9). Buildings in Xinda scattered on the diluvial fan at the exit of the Rilonggou gully. Those totally collapsed buildings were located on the spur of the diluvial fan which was formed in the early era and was disrupted in the recent era, and only a small number of buildings located on the middle part of the diluvial fan which was formed in the recent era collapsed. Rilongcun village, at the right hand side of the Rilonggou gully, was situated on the plain near the foot of a mountain and was only one kilometer to the north of Xinda. Except a case that walls of three buildings were partially collapsed, only fissures could be seen on the walls of the remainder. Dangka, Shawan and Kaga of Shawan Brigade scattered along a straight line of 1.5 kilometers long. Building construction and ground soil condition of these three villages were similar. At Dangka, buildings scattered on a rather steep slope and one of them on a spur. At Kaga, buildings also scattered on a slope and a spur, only Sawan was located on a plain between the two villages. During the earthquake, buildings on the spur were totally collapsed, those on the slope were partially collapsed, and for those on the plain, only fissures could be seen on earth walls of buildings, except that one building collapsed.

During the 1970 Tonghai earthquake, there were many cases which showed the significant effects of isolated and projecting hills on damage: (1) Tangzicun village (more than 30 dwellings) and Mahuangchong village (roughly 70 dwellings) of Jianshui County were six kilometers far from the epicenter, and were located on the ridge slope of a projecting hill and the corrosive low land, two sides of which were facing the hills and the other side of which were cut by a gully, respectively. Both ground soil consists of a certain depth of weathered residual slate clay. The damage indexes were 0.73 and 0.55 respectively, the difference of which was roughly equal to one intensity rating. (2) Yutangcun village (more than 70 dwellings) and Xiaoyutangcun village (15 dwellings) of Eshan County both were 15 kilometers from the epicenter. The buildings scattered respectively on a ridge of a red soil hill and a gradual inclined slope at the foot of a mountain of sandy clay with crushed stones. The damage index of

the former was 0.86, and 0.23 for the latter. (3) Pulongzhai village of Jianshui County located in the region of intensity VII was 19 km far from the epicenter. Buildings scattered on the ridge of a rock hill (48 dwellings) and an earth slope (20 dwellings). The damage indexes of these two parts were 0.42 and 0.20 respectively. Paishagou village (79 dwellings) was situated at the foot of a weathered rock hill not far from Pulongzhai, and its damage index was equal to 0.28. (4) Lihaozhai of Jianshui County was located on a hilly land of weathered rock, 13.5 km far from the epicenter and had a damage index equal to 0.44 (more than 170 dwellings). But the damage index of Abuguancun village (100 dwellings) which was 1.2 km to Lihaozhai village and more nearer to the epicenter was equal to 0.29. (5) Jizicun village of Jianshui County (more than 70 dwellings) was located on a ridge of a mountain, 60 m higher than the surrounding in the region of intensity VII and 12.5 km far from the epicenter. The damage index was as high as 0.7 (corresponding to intensity IX) and the intensity rating was nearly two higher than the surrounding. According to the statistic analysis of damaged dwellings of 67 villages located on isolated and projecting topography, the damage indexes were greater than those on plain (0.07 to 0.25) (Ref.5). Effect of isolated and projecting topography on damage on various ground soil are shown in Fig. 15. In the figure, the abscissa $D_1(I)$ denotes the damage index at the location of village considered in the damage contour map of ground soil I; and the ordinate denotes the practical damage index i of the village considered. It can be seen from the average tendency that, in statistical sense, the effect of topography is enlarging the damage to structures.

During the 1974 Yongshan-Daguan earthquake (Ref.6) there were also many cases which showed the effect of isolated and projecting topography on intensity. For example, in Huilongwan, Lujiawan-liudui, Xiaping, Zhujialiangzi, Juejiping (see Fig.7), on the ridge in the west of Wayaoping, upper portion of Heiboluo and on the massif in Shawan etc., the damage increased. Fig.16 shows the relief of Lujiawan-liudui. In the figure, the arrow indicates the direction of inclination, from high elevation to low elevation. Lujiawan-liudui was located in the high intensity(VIII) anomalous area. The dwellings scattered along a narrow band on an isolated and projecting massif at the edge of a ridge, the saddle-like portion in the middle part and the upper portion of the ridge near the piedmont. Their intensity ratings were IX, VII and VIII respectively, and it means that the high intensity anomaly in Lujiawan-liudui was due to the effect of local topography. Xiaping was situated on an isolated massif in front of a mountain, and a sketch of its local topography is shown in Fig. 17. The ground soil was of talus material, consisting of weathered product of igneous rock. The upper layer was loose and cohesionless soil, and the bedrock at the bottom is seriously weathered. This village was also located in an area of high intensity anomaly (intensity rating is equal to

VIII) in the region of intensity VII. Under such circumstances, the high intensity anomaly was due to the effect of isolated and projecting ridge and thick loose overburden.

During the 1975 Haicheng earthquake the topography of the earthquake site was rather smooth in the west part and hardly no isolated and projecting topography existed; the east part was of low hilly land. Most isolated and projecting topography where villages located were formed by bedrock, and villages located on the nearby plain were on the Quaternary overburden. Thus, both factors, local topography and ground soil, were mix together, so the effect of topography was not prominent. But there were still some cases, by which the effect mentioned can be explained. For example, in Houyingcheng, Bali Commune, Haicheng County there were three buildings located at the edge of a steep slope on the top of a hill, totally collapsed, and the damage index of the other buildings was only 0.40. At Tashanpu village, the damage index of single storey brick buildings located on bedrock of the foot of a ridge slope was equal to 0.20, but similar buildings on the upper portion (bedrock) of the ridge, about 40 meters higher than the former one, suffered more seriously damage and its damage index was equal to 0.27. Although the effect of bedrock on damage was not noticeable, but it was enough to explain the fact that as elevation increased damage to buildings was heavier.

During the Helingeer, Neimeng earthquake (M=6.3) of April 6, 1976 (Ref. 10), in Dongfushishan village, Xindianzi Commune, there were nine buildings located on a radial projecting platform surrounded by gullies on three sides, and the remainders located on a slope of the neighbouring hill. The damage indexes of these two groups of buildings were equal to 0.89 and 0.46 respectively. In Chafangcun village the residential area in the east was located on a spur with gullies at both sides, and the residential area in the west distributed on a slope. The damage indexes of these two areas were equal to 0.77 and 0.55 respectively. But for the buildings on the spur, the damage indexes in front of and behind the spur were equal to 0.96 and 0.64 respectively. The damage indexes of buildings in Lamadongyao village, located on isolated massif with thin overburden and on the plain of ravine base, were equal to 0.73 and 0.47 respectively. But those buildings located on bedrock massif with a gentle slope between the two residential areas mentioned above had a damage index only equal to 0.40. Besides, the shape of massif was different, the fact reflects that bedrock is beneficial to earthquake resistance.

During the Longling, Yunnan earthquakes (M=7.3 and 7.4) of May 29, 1976 (Ref. 11), a grain storage in Maocaozhai village and primary school of Zhaoyang Commune, Longling County scattered on an isolated and projecting massif which was 40 meters higher than the plain, at one side of the

intersection of the Pazhang River and the Supa River and on a spur of isolated ridge, respectively. Their damage indexes were equal to 0.83, 0.64 and 0.79 respectively. In addition, five masonry workshops of Luxi Machinery Factory were located on a plain formed by a gully, and 72 single storey adobe buildings with timber frame scattered on isolated slopes aside of the workshops. The damage index of the former was equal to 0.30, and the latter was 0.75.

During the 1976 Tangshan earthquake, a block of Chinese temple buildings with timber framed structure (built in the Ming Dynasty and rebuilt in 1957 for the last time) scattered on the top of Jingzhongshan mountain (bedrock) with an elevation of 507 meters near Sanyingtun of Qianxi County. The frame of the structures was seriously damaged or collapsed, and the intensity rating reached IX. But there were no buildings collapsed in the nearby villages (Zhishanzhuang, Mengzhuang, Liaozihuang and Nanyangzhuang etc.) which were all located on bedrock or thin overburden at the foot of the mountain. There were roughly 130-170 buildings in each village, and only the upper portion of a small number of stone-built gable walls and the outer part of wall toppled down. The intensity ratings were all roughly equal to VI. Those villages are roughly on a level of 220 to 250 meters above sea level. It should be noted that there was a fault with N50E strike direction passing through the east part of Jingzhongshan mountain to the east of Zhishanzhuang village at the foot of the mountain, but there was no evidence that damage of the surrounding villages became heavier due to the existence of the fault. It was thus clear that the block of temple buildings was seriously damaged merely due to the effect of topography.

Moreover, the researchers of Lanzhou Seismological Brigade, State Seismological Bureau discovered that during the 1920 Haiyuan earthquake, in loess plateau at Tianshui district the intensity ratings of some villages on elevation approximately 100 meters above riverbed were generally one degree higher than those on the banks of rivers.

EFFECT OF GROUND SOIL ON INTENSITY ANOMALY

Intensity anomaly due to ground soil have absorbed people's attention for a long time. Bedrock and thin overburden on rock are generally to be considered as the cause of low intensity anomaly, and thick and loose overburden may cause high intensity anomaly. Difference in intensities on bedrock and soil site, although a small distance apart, occurred in many cases and this identifies the fact above mentioned. It can also be testified by the intensity attenuation on various soil during the same earthquake.

In Guangzhou, along the river banks of the Zhujiang River, ground soil are of diluvium (sludge from river bed) and filled land, and in the northeast part of the city is the Tertiary

mountainous region. During the Heyuan earthquake ($M=6.1$) of March 19, 1962 the residential area on diluvium soil and filled land was heavily damaged, but that on the mountainous region was slightly damaged.

During the 1970 Tonghai earthquake (Ref.5), high intensity anomalous areas distributed along the shore of Jiluhu Lake in Tonghai County and Talong of Qujiang, and the low intensity anomalous areas scattered in the west of Tonghai County at Laojianshan and Muchengshan. In the high intensity anomalous area, the soil is usually not good, and contrarily, the soil in the low intensity anomalous areas mentioned above is of ground soil I. Some villages on bedrock in high intensity anomalous area at the shore of Jiluhu Lake, such as Shilongcun, Wangjiaba and Hujiashanchong etc., were also damaged considerably slightly. According to the correlation between damage versus ground soil obtained by means of statistic analysis, using large amount of field data of field observation. It can be seen that in comparison with the other types of ground soil, damage to structures on rock site were always more slight, as shown in Fig. 18.

During the 1975 Haicheng earthquake, there were approximately 50 villages, of which the damage was significant different in different locations. Among these, there were 23 villages in which difference in damage indexes was greater than 0.2 (corresponding to one intensity rating), and most of them were due to ground soil (Ref.2). It was usually that buildings located on bedrock or thin talus accumulation near mountain slightly damaged, and buildings located on loose overburden of alluvial soil near riverbanks damaged heavily. There were also many cases showing significant difference in damage in the neighbouring villages. For example, Xiadian ($i=0.66$) of Manggou Brigade of Gushan Commune was located on terrace of Muxi River. No bedrock was found in a well of ten meters in depth, and the level of underground water table was about 3 meters. Yangjiapu ($i=0.64$) was not far from Xiadian and also situated on the terrace. Yaopu was close to a mountain. Majority of buildings in Yaopu-qidui ($i=0.29$) scattered on both slopes of a small gully. Lijiapu ($i=0.25$) and Linjiajie ($i=0.19$) were located at the upstream of the gully on both slopes. The trend of damage attenuation from terrace to the upstream of the gully was rather obvious. In addition, low intensity anomalous areas occurred in a wide area of ground soil I or stiff ground soil II, such as Qingshiling area of Zhoujia Commune of Yinggou County, Caijiagou area of Guantun Commune, an area from Tangchi Commune to Xujiagou and Xiaodaogou, and Fanjiayu area of Haicheng County etc.. Niuzhuang area of Haicheng County was a high intensity anomalous area of ground soil III.

Residential areas in the 1976 Helingeer earthquake site scattered mainly on terraces and valley flats of loess overburden (Ref.10). Some buildings in low intensity area of Qingshuihe and Youyu were seriously damaged mainly due to

differential settlement of the ground. In lamadongyaocun village, those buildings on soil suffered damage more serious than those on bedrock.

During the 1976 Longling earthquake (Ref.11), intensity rating in a basin was found higher than the surrounding, and it was mainly due to ground soil. Zhenan basin extended in northwest direction with an area of 6 km long and 1 to 1.6 km wide. Inside the basin there were three-step terraces which were 2-3 m, 8-10m, and 25-30m above the bottom of basin respectively. Ground soil inside the basin consists of Cainozoic strata more than 200 meters deep with six layers of coal bed (the thickest layer was about 60-70 meters). And ground soil outside consists of granite of Yenshan period, residuum with a certain thickness on the margin of the mountain top. Sand, gravel and residual deposit covered the slope of the mountain. The highest percentage of totally collapsed buildings on granite in the surrounding of the basin was not higher than 30%, but the percentage of those on loose deposit in the basin was equal to 50% generally, some even reached 70%. In the Mengmao basin the damage indexes of villages or buildings in the basin, such as Mengmaojie, Mengmao primary school and Zhongbianzhai, ranged from 0.56 to 0.67, but villages located on granite near the boundary of the basin, such as Xibianzhai, Wujiacun and Yangjiazhai etc., were not so heavily damaged, the damage indexes ranged from 0.27 to 0.32. The overburden of the Mengmao basin consists of, from surface downward, one meter of clay in grey-black colour, 2-3 meters of sandy clay in grey-brown colour, 3 meters of white clay, and an interlayer of grey-white clay and alluvial gravel, but no bedrock was found. The underground water table is approximately one meter in depth.

During the 1976 Tangshan earthquake, overburden in the north part of the meizoseismal area was rather thin, limestone outcrop existed on Dachengshan and Fenghuangshan mountains and a low intensity anomalous area was formed. No.422 Cement Factory, Tangshan Steel Plant and Building Porcelain Factory near Dachengshan mountain were not so heavily damaged as buildings in the south part of the meizoseismal area. Percentages of totally collapsed buildings estimated from the aerial photographs were only 50%, but those in the other parts of the meizoseismal area were more than 90%. In Tangjiazhuang Coal Mine, majority of buildings in residential area on thick overburden collapsed, but in the northwest residential area at the foot of a hill (about 2 meters of deposit above limestone), not far from the former area, similar single storey stone buildings were only slightly or moderately damaged, and only a small number of buildings collapsed. Zhaozhuangzi (intensity rating VI) in the northwest of Sandunying of Jianxi County is located near the exit of a gully on thick overburden. Along the gully to the upstream direction the damage decreased gradually. At Jizhuangzi, as the overburden became thinner, the intensity rating decreased to V, and the

effect of earthquake on Xietuoai village in the upstream portion of the gully was hardly seen if not carefully observed. These villages were all located in an area of intensity VII. Such phenomenon, that damage decreases gradually along a gully from the exit to upstream, was not individual. The cases of seven brigades including Liaozhuangzi of Baimiaozi Commune not far from Zhaozhuangzi were also similar. The high intensity anomalous area in Zhenzizhen of Luanxian County mentioned above was due to the deep deposit in basin. The researchers of the Tianjin Seismological Bureau assumed the urban area of Tianjin and Tanggu region as an area of high intensity anomaly of rating VIII. When analyzing the cause of high intensity anomaly, they considered that besides the effect of ground soil, seven old river courses and a great number of filled pits also played an important role. According to the geologic mass properties of petrographic facies and the characteristics of earthquake response of geologic mass, the researchers of Institute of Geology, State Seismological Bureau, explained the cause of high intensity anomaly in the suburb of Beijing, such as the following villages: Wangjiachang of Shunyi, Changgou of Fangshan, Lutuan of Changping, Langfu of Tongxian and Caiyi of Daxing etc., and they considered that the main cause was ground soil.

It should be noted that intensity anomaly may also due to the particular case of soil layers. For example, Yutian was a low intensity anomalous area, twice in the past earthquakes, once during the 1679 Sanhe-Pinggu earthquake, and the other during the 1976 Tangshan earthquake. In comparison with the surrounding of anomalous area, it can be seen from the geological settings that the tectonic structure within the anomalous area is not developed and the bedrock under the overburden remains intact. Ground soil in the anomalous area consists of deep and medium dense sand with multi-inter layers of cohesive soil, filtering or isolating the high and low frequencies of seismic waves propagating upward, thus causing low anomalous intensity. As for another example, when there is a layer of moderate dense cohesive soil, several meters thick, over a saturated fine sand layer, the liquefied layer will act as an isolated layer and reduce the vibration of the superstructure, if after liquefaction, the layer still has the capacity to support the load transmitted from superstructure. During the 1975 Haicheng earthquake, field investigation of damage to buildings in 15 villages was made. It was found that damage to buildings in villages where serious sand blows were found was not so serious as those in the surrounding where no sand blows or minor sand blows occurred (Ref.2). People called such liquefaction phenomenon as "wet shock", and said that damage in wet shock is not serious, but that in "dry shock" is serious. Similar phenomena were also occurred in the 1970 Tonghai earthquake and the 1976 Tangshan earthquake. Certainly, if the overburden above the liquefied sand is too thin or too soft, then ground failure to a certain extent will occur and increase the damage to

superstructure. Such phenomenon had been seen during the 1975 Haicheng earthquake in Suxi of Qigou Commune, Hongguang of Haicheng City Commune, and Dangjiatun of Ganwang Commune etc.

Moreover, during the 1975 Haicheng earthquake we discovered that damage to flexible high-rise brick chimneys in Panshan, Dawa (both intensity VII), Yinggou City (intensity VIII), Haicheng and Dashiqliao (both intensity IX) was nearly the same. In Hongyang Coal Mine, more than hundred kilometers from the epicenter, high-rise structures, such as winch house of 15 meters high in the mine shaft, auxiliary shaft of 41.7 meters high, brick chimney of 40 meters high, charging hopper of 29.3 meters high, boiler building of 16.7 meters high with inner-frame structure, transformer substation and machinery workshop of masonry structure etc. damaged in various degree, but scores of small buildings in the neighbourhood were almost intact (in the area of intensity VI). This phenomenon implies that at distance far from the epicenter, especially on loose and deep ground soil, long period component of earthquake vibration is predominant. During the 1976 Tangshan earthquake, in Tianjin region we also found the similar phenomenon. Flexible structures, such as chimneys and high-rise plants damaged more seriously than the rigid buildings.

SUMMARY

Summarizing what mentioned above, it can be seen that the main cause of intensity anomaly is practically due to local site conditions. The effect of various parameters of local site conditions on intensity anomaly are as follows:

(1) Effect of non-causative faults on intensity anomaly is not obvious, and ground soil in the fault rupture zone as well as the ordinary soil will influence the severity of damage. Those non-causative faults intersected with causative fault and located near the meizoseismal area, or those seriously broken or large-scale non-causative faults near the edge of a causative fault may increase the severity of damage. But some geologists still suggest that the existence of fault will cause intensity anomaly.

(2) Buildings on isolated and projecting massif or ridge will be more seriously damaged than those on the plain with the same ground soil. But on the rock site, if elevation is not higher than 30 meters, such effect is not obvious.

(3) Effect of ground soil on intensity anomaly are rather complex. Existence of bedrock or thin overburden is generally the reason why intensity anomaly occurs, and loose and deep soil deposit may cause high intensity anomaly. Although ground failure may increase the extent of damage to structures on loose soil, but the liquefied saturated fine sand underlain by several meters of cohesive soil may play an important role in isolation and thus reduce the vibration and may decrease the superstructure damage. In addition, at places far from epicenter, long period vibration on loose and

deepground soil may cause damage to tall and flexible structures more heavier than those of short and rigid structures. Local topography often relates to ground soil condition. For example, in mountain area, as the thickness of overburden decreases from the exit of a gully to its upstream direction, damage also decreases gradually; ground soil at the low land site, such as old river courses and ancient pits, is rather soft.

REFERENCES

- (1) Working Group on Seismic Intensity Regionalization Map, State Seismological Bureau (1979): Collection of Iso-seismal Maps in China. Seismology Press. (in Chinese)
- (2) Institute of Engineering Mechanics, Academia Sinica (1979): Damage in the Haicheng Earthquake. Seismology Press. (in Chinese)
- (3) Chen Dasheng (1979): Field Phenomena in Meizoseismal Area of the 1976 Tangshan Earthquake. Proc. of the Second U.S. National Conference on Earthquake Engineering 22-24 August, 1979. Stanford University.
- (4) Wei Qun (1978): The Secret of Intensity Anomaly. EARTHQUAKE FRONT, 1980 No.1 (in Chinese)
- (5) Investigation Group of the Tonghai Earthquake (1977): Intensity Distribution and Effect Of Sites during the Tonghai Earthquake. Collection Papers on Earthquake Engineering, Institute of Engineering Mechanics, Academia Sinica. Kexue Press (in Chinese)
- (6) Seismological Bureau of Yunnan Revolutionary Committee and Kunming Seismological Brigade, State Seismological Bureau (1974): Primary Summary of Field Observation during the Yongshan-Daguan, Yunnan Earthquake (M=7.1) of May 11, 1974 (in Chinese)
- (7) Sichuan Seismological Bureau (1979): The 1976 Songpan Earthquake. Seismology Press (in Chinese)
- (8) Institute of Engineering Mechanics, Academia Sinica (1966): Earthquake Damage in the Tongchuan, Yunnan Earthquake of February 5, 1966. (in Chinese)
- (9) Earthquake Field Investigation Group of Ganzi Region (1967): Field Survey of the Luhuo Earthquake of August 30, 1967. (in Chinese)
- (10) Research Group of the Hellingeer Earthquake (1976): Primary Summary of the Hellingeer, Neimeng District Earthquake (M=6.3). (in Chinese)
- (11) Chen Lide, Zhao Weicheng et al. (1979): The 1976 Longling Earthquake. Seismology Press. (in Chinese)
- (12) Jiang Pu et al. (1979): Research on the Cause of Several Damage Areas during the Tangshan Earthquake. SEISOGEOLOGY. Vol.1, No.1. (in Chinese)

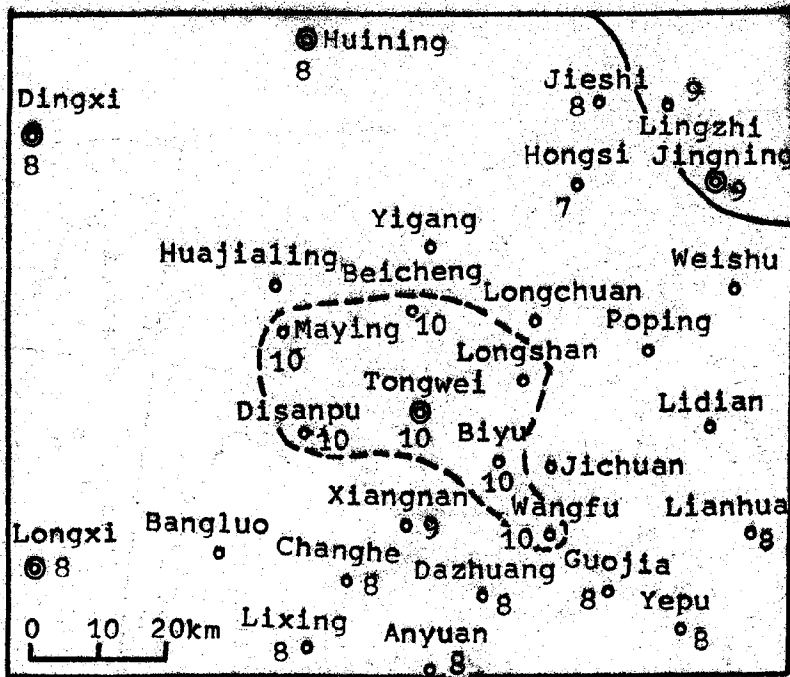


Fig.2 Tongwei high intensity anomalous area during the 1920 Haiyuan earthquake

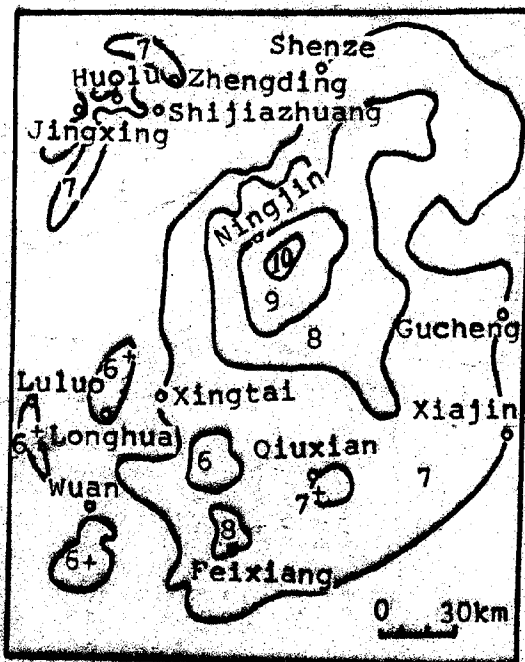


Fig.4 Isoseismal map of Xingtai earthquake of March 22, 1966

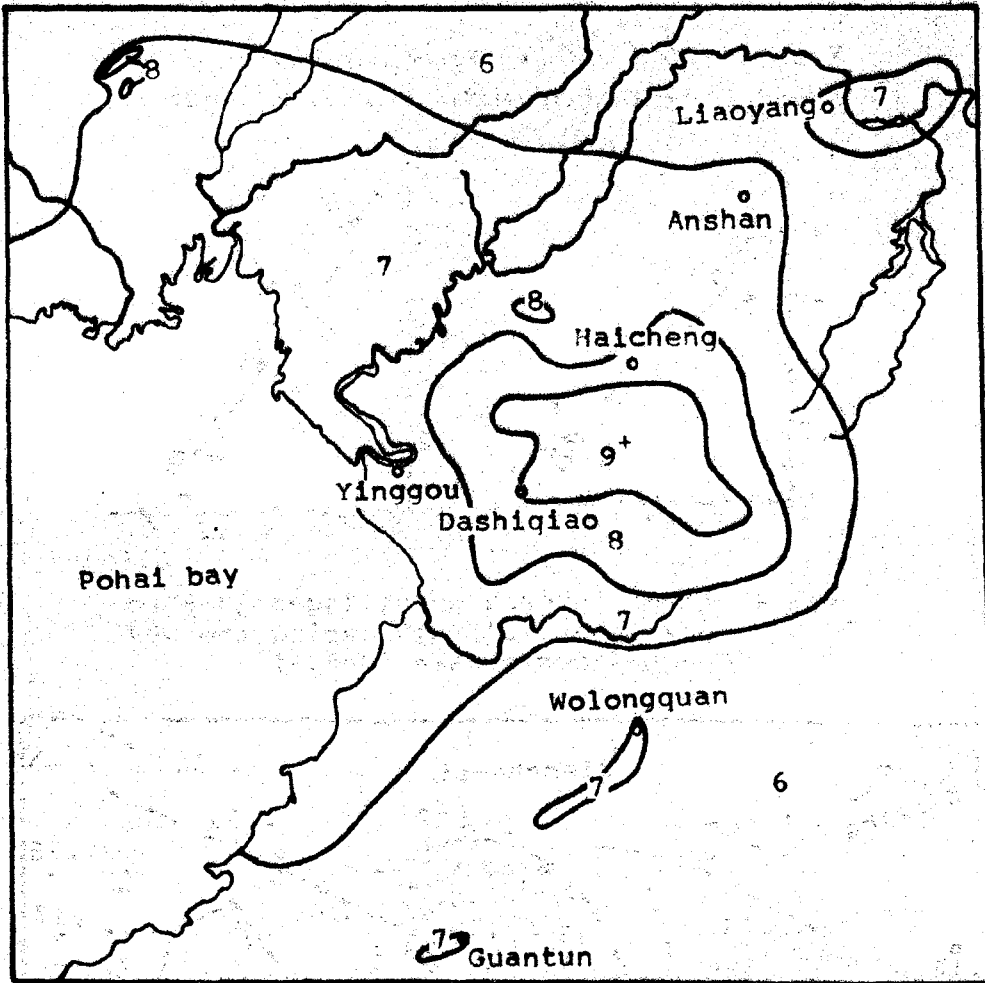


Fig.3 Isoseismal map of the 1975 Haicheng earthquake (Ref.1)

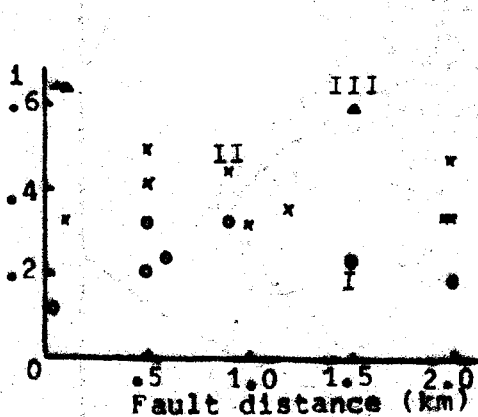


Fig.5 Relation between earthquake damage and fault distance near Xiaogushan Fault (Ref.2)

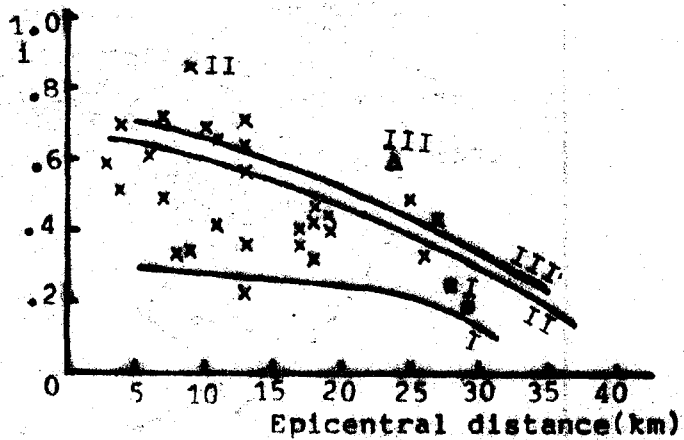


Fig.8 Relation between damage index of villages just on non-causative fault and attenuation curve of mean damage index

X intersected with causative fault
 ● not intersected with causative fault

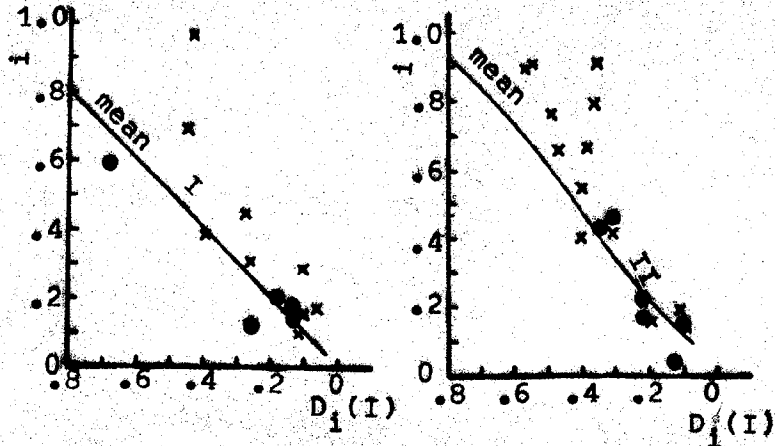


Fig.6 Damage indexes of villages just on non-causative fault during the 1970 Tonghai earthquake (Ref.5)

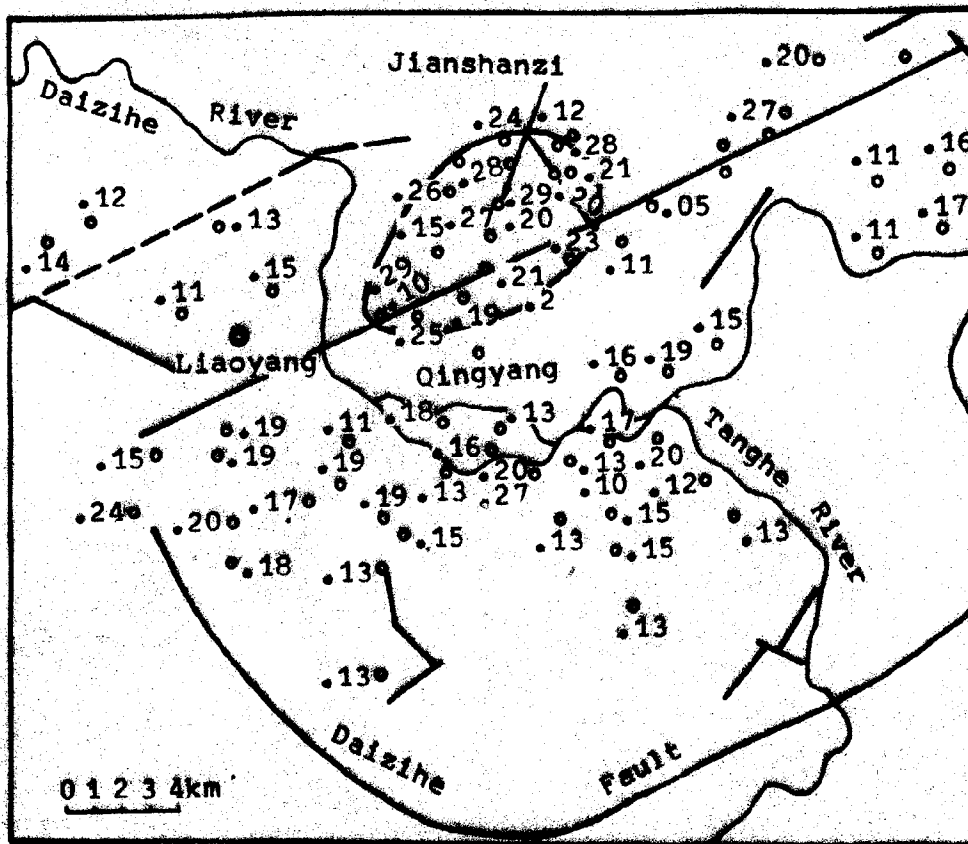


Fig.10 Distribution of earthquake damage index near Liaoyang high intensity anomalous area

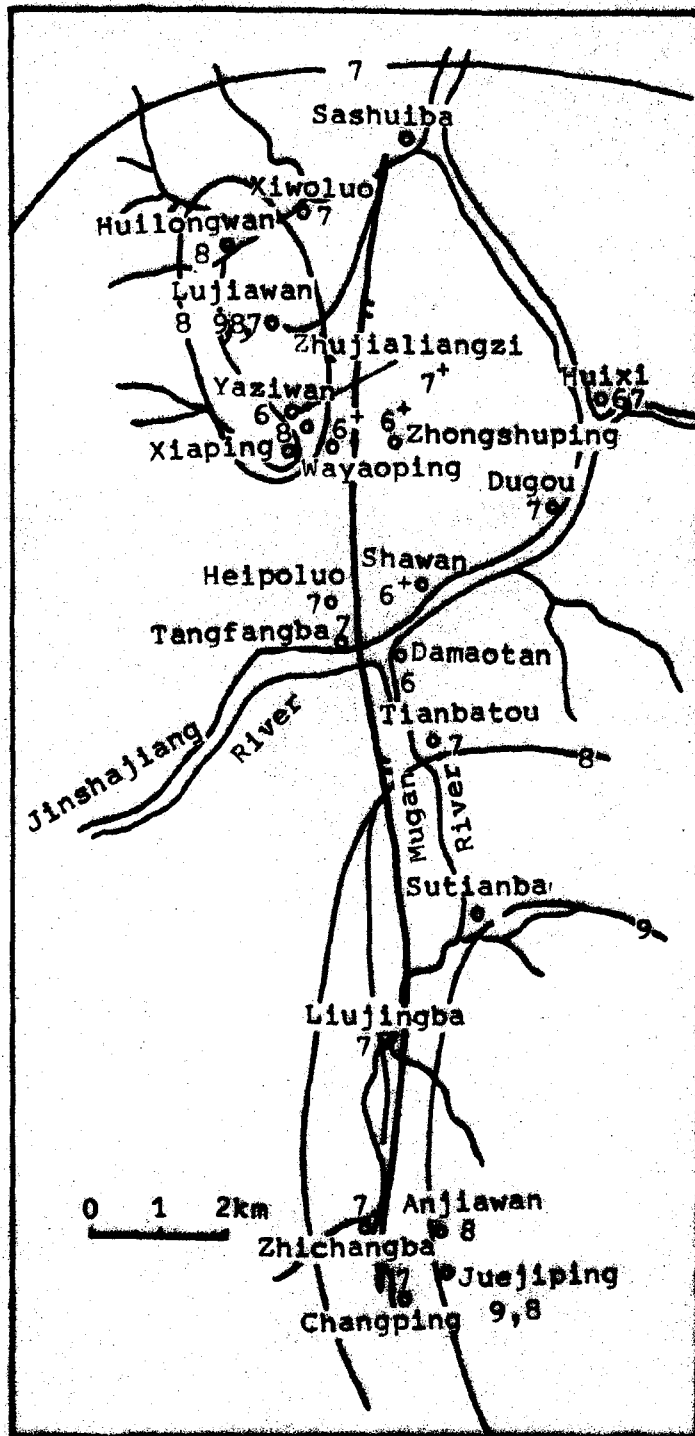


Fig.7 Distribution of damage indexes near Damaotan Fault during the 1974 Yongshan-Baguan earthquake

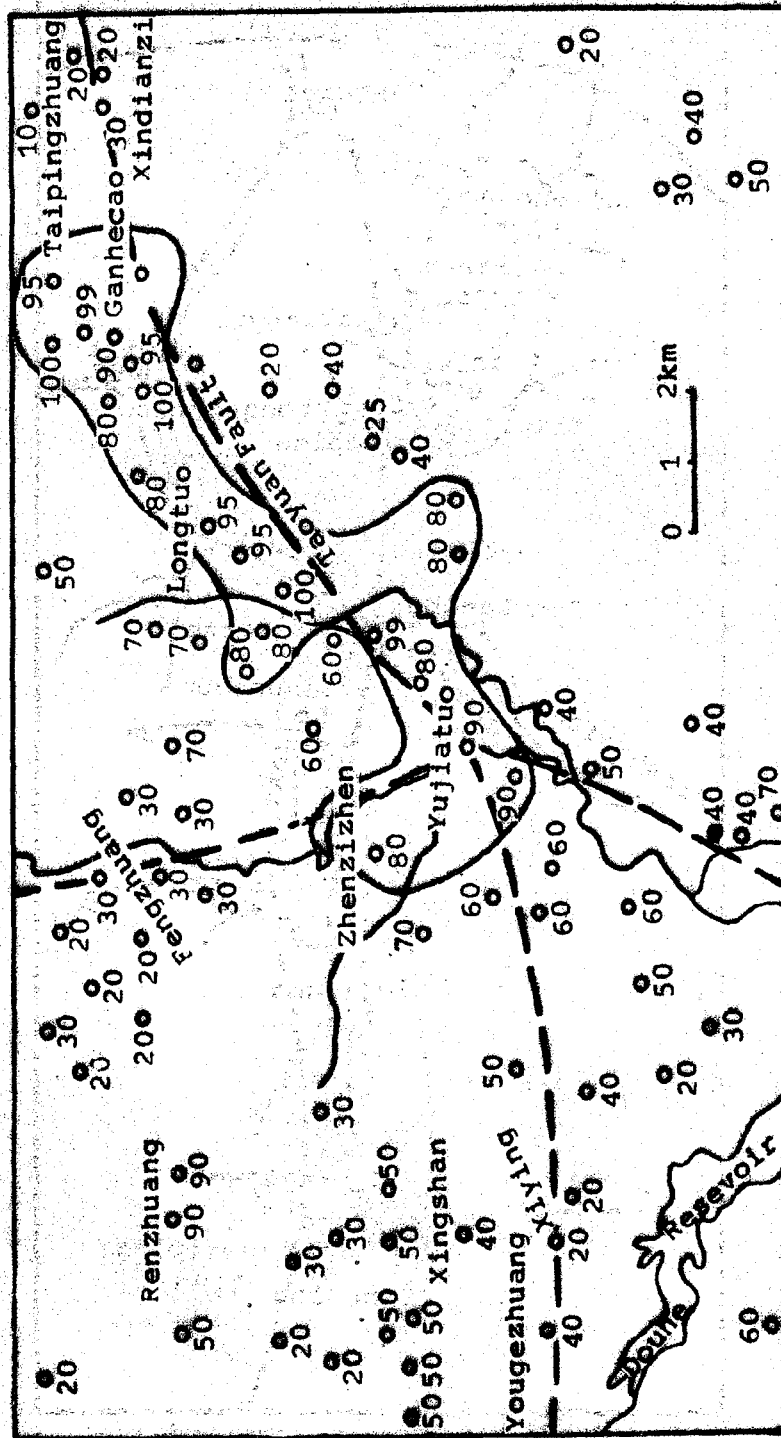


Fig.11 Zhenzizhen high intensity anomalous area

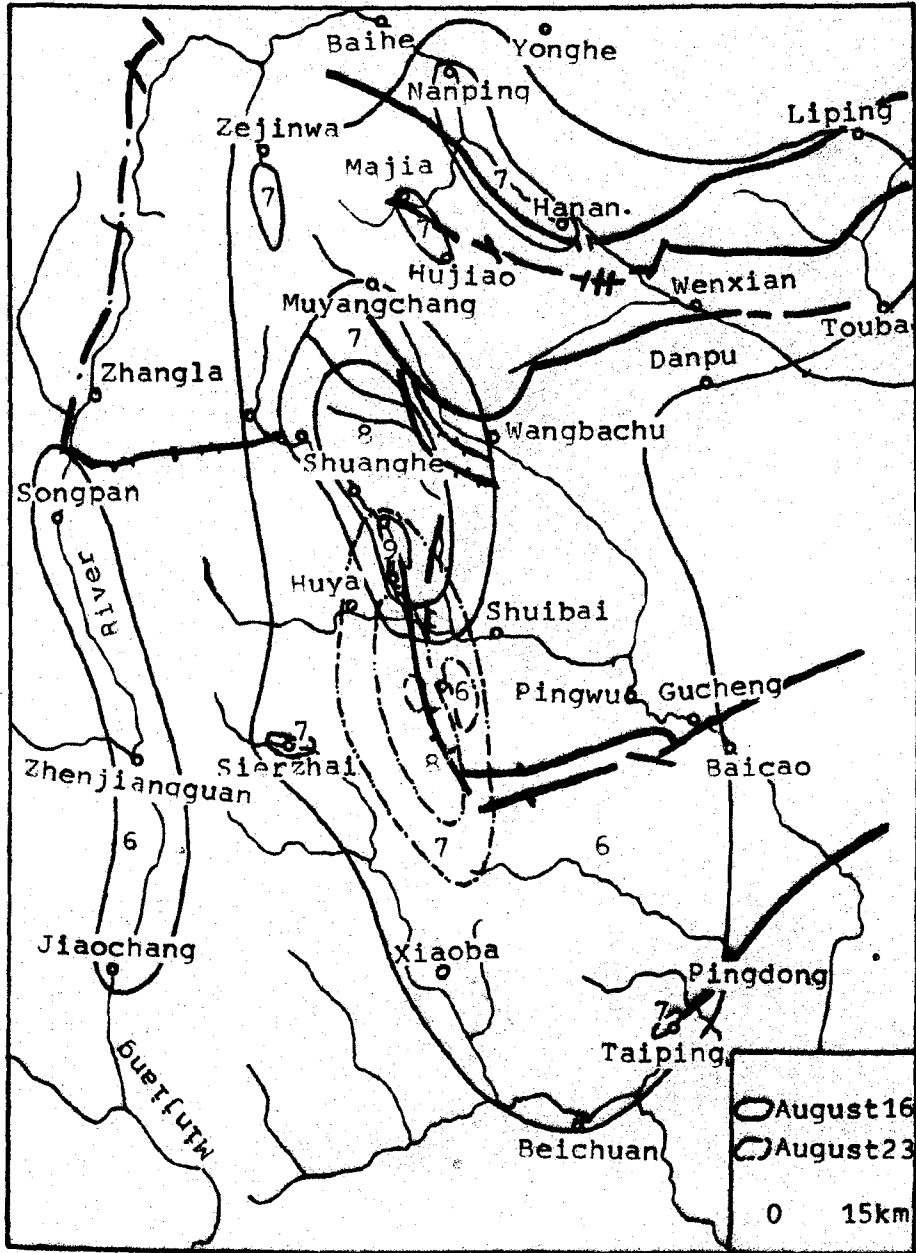


Fig.12 Isoseismal map of Songpan earthquake of August 16 and 23, 1976 (Ref.1)

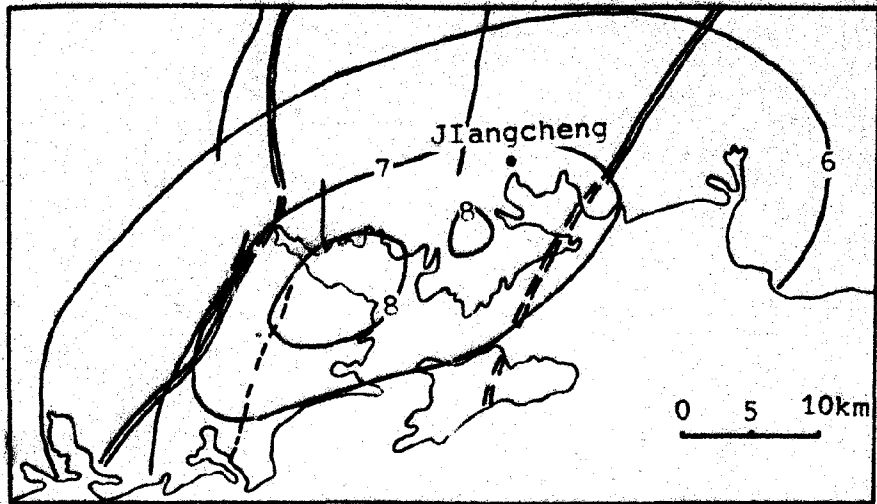


Fig.13 Isoseismal map of the 1969 Yangjiang earthquake

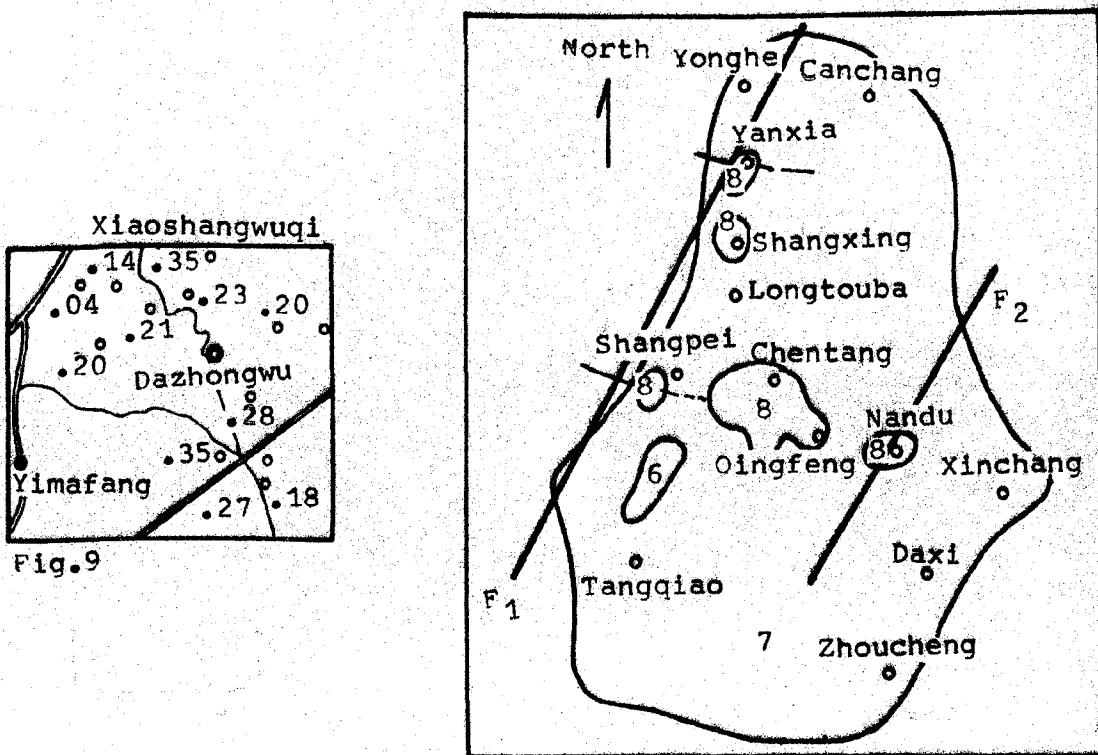


Fig.14 Isoseismal map of the 1979 Liyang earthquake

F₁-Maoshan East Fault

F₂-Jintan-Nandu Fault

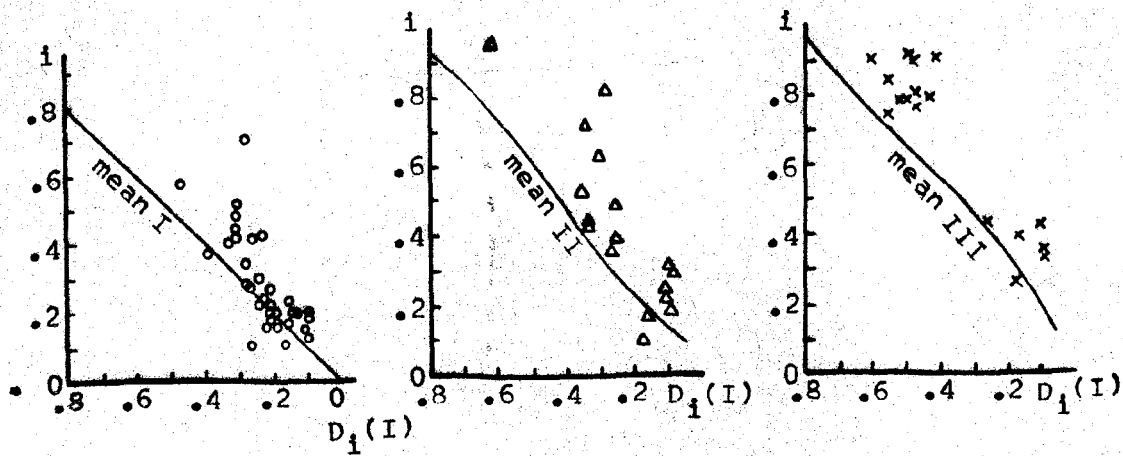


Fig.15 Effect of local topography during the 1970 Tonghai earthquake (Ref.5)

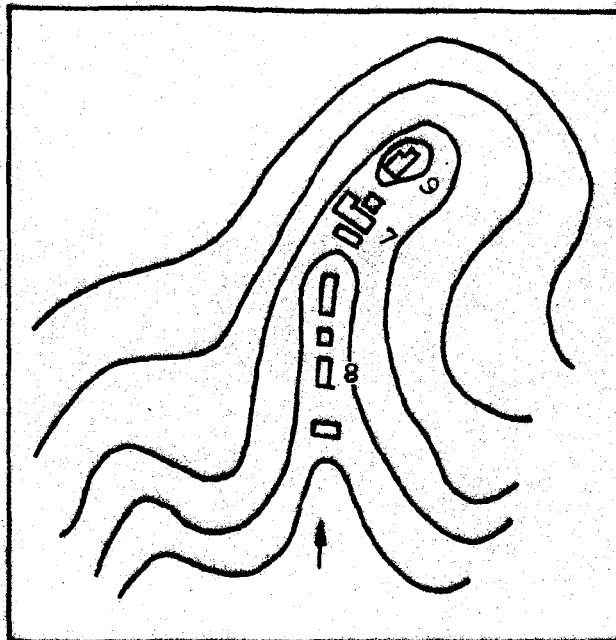


Fig.16 Inclination topography of Lujiawan-liudui

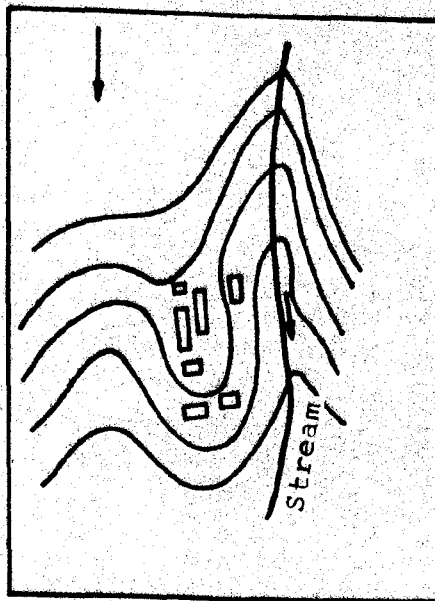


Fig.17 Inclination topography of Xiaping

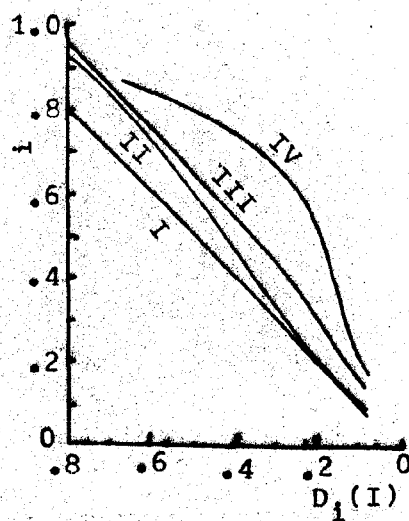


Fig.18 Relation between earthquake damage and ground soil classification in the 1970 Tonghai eqk.

CONSTRUCTION OF A ZONING MAP OF THE EARTHQUAKE GROUND-SHAKING HAZARD WHICH SHOWS THE EFFECTS OF GEOLOGY ON SEISMIC WAVES

By

Walter W. Hays (I)

ABSTRACT

Zoning of the earthquake ground-shaking hazard - the division of a region into geographic areas having similar response to ground shaking - is a complex research task. Current zoning maps use the best available geologic and seismological data to depict the ground-shaking hazard in terms of contoured values of the peak ground motion (acceleration or velocity) expected at sites underlain by rock in a 50-year period of time at the 90-percent probability level. The usefulness of such maps can be improved substantially by incorporating the frequency-dependent effects which the earthquake fault mechanism and the geology have on propagating seismic waves. Although more empirical data and research are needed, incorporation of information about the ground response in a region appears to be a feasible and physically meaningful way at this time to extend zoning maps of the ground-shaking hazard.

INTRODUCTION

Seismic zoning is defined as the division of a region into geographic areas or zones, each having a similar response throughout its extent to a particular earthquake hazard. The goal of zoning is to define as precisely as possible the location, frequency of occurrence, and relative severity of hazards (e.g., surface fault ruptures, ground shaking, ground failures, tectonic deformation, and inundation) expected within a zone. Once these parameters have been defined for all zones and hazards in a region, the potential physical effects of each hazard can be mitigated through appropriate actions such as: avoidance, land-use planning, engineering design, and distribution of losses through insurance.

This paper discusses zoning of the ground-shaking hazard, which is a complex research task (Figure 1) requiring the best available information on: (1) frequency of earthquake occurrence, (2) mechanics of faulting for past and present earthquakes, (3) the attenuating characteristics of the regional paths along which the seismic waves travel, and (4) the physical properties of the local rock and soil column underlying the site of interest and controlling the ground response. Progress in constructing zoning maps of the ground-shaking hazard has been slow, because data are very limited in each of these four general areas of research. For example, the historical record of seismicity in the United States is short, encompassing about 100 to 300 years; and variable spatially, making recurrence relations difficult to define. Only a few strong-motion accelerograms such as recorded at Pacoima Dam during the 1971 San Fernando, California, earthquake and at El Centro

(I) Deputy for Research Applications, U.S. Geological Survey, Reston, Virginia 22092

during the 1940 and 1979 Imperial Valley, California, earthquakes, have been obtained sufficiently near the causative fault to contain the signature of the dynamic fault rupture. Very few accelerograms have been recorded on arrays extending a few hundred kilometers from the earthquake source and underlain by the same type and thickness of rock or unconsolidated material; therefore, regional attenuation relations are either imprecise or nonexistent for most regions of the United States. Also, data showing the variation of ground response as a function of the spatially varying physical properties of the underlying soil and rock are very limited.

Current zoning of the ground-shaking hazard - The map shown in Figure 2 is an example of the current state-of-the-art in zoning of the ground-shaking hazard in the United States. This map, which might be classified as a macrozoning map, was prepared by Algermissen and Perkins (1976) and was used to define the seismic risk zones in the Applied Technology Council's 1978 model code. Unlike prior zoning maps, it depicts the variation of a ground-shaking parameter (peak ground acceleration) in terms of the probability that a certain level of ground motion will occur at a specific location underlain by the same material, rock (i.e., a solid material exposed at the surface or underlying soil and having a shear-wave velocity greater than 765 m/s at small (10^{-4} percent) strains) in a given interval of time (50 years). This map represents the ground-shaking hazard in terms of the peak amplitude of acceleration, one characteristic of the strength of the seismic signal. The map incorporates known differences in the Eastern and Western United States of: (1) seismicity, (2) geologic characteristics of seismic source zones, and (3) seismic attenuation rates.

Construction of the zoning map shown in Figure 2 involves the steps shown schematically in Figure 3. The first step is to assemble the historical seismicity data and to decide upon the spatial and temporal distribution of the historic earthquakes in discrete seismic source zones (inset A of Figure 3). In defining the seismic source zones, all available information about the correlations between earthquake occurrences and other geologic processes and structures are used, including:

- (1) location of the boundaries of crustal blocks which are undergoing contrasting displacements (Howard and others, 1977)
- (2) history of vertical and horizontal regional tectonic movements (Castle and others, 1975)
- (3) location and history of active faults (Sieh, 1978), and
- (4) tectonic stress (Zoback and Zoback, 1980).

Each seismic source zone is chosen so that it encloses an area of seismic activity and, to the extent possible, an area of related tectonic elements. Earthquakes are assumed to be equally likely anywhere in a source zone, to have an average rate of occurrence that is constant in time, and to follow a Poisson distribution of recurrences. At present, 71 seismic source zones have been defined for the United States (Figure 4). The fact that the seismic source zones are shown as being larger in the Eastern United States than in the Western United States reflects the relative lack of knowledge in the east.

Seismic attenuation curves (inset B of Figure 3) that specify how peak ground motion decreases with increasing distance from the causative fault in a region are essential when constructing a zoning map of the ground-shaking hazard. In spite of the limited ground-motion data the curves shown in Figure 5 are considered to be physically reasonable, albeit simplified, estimates of the regional attenuation rates for peak acceleration at rock sites in the Western and Eastern United States. The curves for the Western United States were proposed by Schnabel and Seed (1973); those for the Eastern United States by Algermissen and Perkins (1976).

The cumulative probability distribution function (inset C of Figure 3) is calculated for each site in a region in the construction of a zoning map of the ground-shaking hazard. This function allows one to determine (1) the number of times that a particular level of ground shaking (e.g., peak acceleration) is likely to occur in a given period of years at a given site, and (2) the maximum level of acceleration for any level of probability. Contour maps, such as shown in Figure 2, are then prepared to show the variation of peak ground motion in terms of specific exposure times and probability levels (inset D of Figure 3).

Characterization of the ground motion close to an active fault is one of the most difficult parts of the problem of constructing a zoning map of the ground-shaking hazard. The current data set is too limited to resolve all of the technical issues concerning this problem. However, unique ground-motion data (Figure 6) acquired in the 1979 Imperial Valley, California, earthquake reinforced current thinking in some areas and revised it in other areas. These data showed that the peak ground accelerations and velocities can be quite large (i.e. greater than 1 g and 100 cm/sec. respectively) and can vary considerably from site to site within 10 km of the fault (Porcella and Matthiesen 1979). The peak acceleration was about 0.5 g greater than that recorded in any prior earthquake and the value of peak acceleration on the vertical component was larger close to the causative fault than that on the horizontal component.

IMPROVED ZONING MAPS

One way to improve current zoning maps of the ground-shaking hazard, which are based on mapping peak ground motions, is to incorporate the frequency-dependent characteristics of ground shaking caused by the filtering effects of the geology. Body (P, SH and SV) waves generally cause the high-frequency (2-10 Hz) components of ground shaking and surface (Rayleigh and Love) waves generally cause the low-frequency (< 1 Hz) components of ground shaking. The mechanics of fault rupture at the earthquake source and the geology along the transmission path and at the local site modify the amplitude, temporal, and spectral characteristics of the seismic waves as they propagate from the causative fault to the site, enhancing the wave amplitude and duration in some narrow range of frequencies and reducing them in others. At the site, structures also act as filters having fairly well-defined frequencies of vibration and respond to the ground shaking approximately as damped mass-spring mechanical systems (Figure 7). Hence, zoning maps that depict the frequency-dependent characteristics of ground shaking are physically more correct and have a wider variety of potential applications in earthquake-resistant design than do zoning maps that are based on mapping peak ground motion.

Current knowledge of the frequency-dependent effects of the source, transmission path, and site has been gained from observational and instrumental data from past earthquakes aftershock sequences nuclear explosions, analytical models and laboratory measurements. These data, although limited, have collectively provided evidence of the most important frequency-dependent effects, including

- (1) The dominant spectral composition of ground motion and the corner frequency (i.e., the frequency where the high- and low-frequency trends intersect) shifts to the long period end of the spectrum (Figure 8) as magnitude and seismic moment increase. (Magnitude and moment are related to the mechanics of fault rupture).
- (2) The Earth's crust, which acts like a low-pass filter on the propagating body and surface waves, causes the high-frequency spectral energy to attenuate more rapidly than the low-frequency energy as distance from the causative fault increases (Figure 9).
- (3) The regional seismic attenuation rates, which depend on the physical properties of the Earth's crust and upper mantle in a region, can vary considerably from one region to another (Figure 10).
- (4) Duration of shaking, which depends on fault rupture characteristics, can differ markedly for high- and low-frequency spectral components (Figure 11).
- (5) The amplitude and frequency characteristics of ground motion recorded at two adjacent sites, dependent on the physical properties (thickness, shear modulus, density) and geometry of the soil and rock column underlying the sites, can differ greatly as a consequence of the amplification of body and surface waves (Figures 12 and 13).

Local ground response - Incorporation of the filtering effects of the local soil and rock column underlying adjacent sites in a region is probably the most physically meaningful and practical way, in terms of current knowledge, to improve zoning maps of the ground-shaking hazard. Technical literature of earthquake engineering and engineering seismology since the early 1900's has recognized and documented that structures founded upon unconsolidated material are frequently damaged in earthquakes. More important, the damage distribution on many occasions has been recognized as being site related. In this case (Figure 14), man-made structures having natural periods of vibration coinciding with those of the underlying soil column have a greater susceptibility to damage than structures having natural periods of vibration that differ from those of the soil column.

Past studies (Seed and Idriss, 1969; Murphy, Weaver, and Davis, 1971; Borchardt, 1975; Murphy and Hewlett, 1975; Hays, 1977, a,b: 1978; 1979; Rogers and Hays, 1978; and Hays and others, 1979-1980) have used ground-motion data to define the ground response of local areas. These and other studies have shown that the transfer function, defined as the average ratio of the 5 percent damped, horizontal velocity response spectra for a pair of sites, is a function of the shear-wave velocity, thickness, water content, and geometry of the unconsolidated material and rock underlying the sites. The study by

Rogers and Hays (1978) suggested an important research result: namely, that the horizontal transfer function for a pair of sites is repeatable and can be determined fairly accurately from ground-motion data encompassing a wide range in levels of peak ground acceleration and in dynamic shear strain (defined as the ratio of peak ground velocity recorded at the site and the shear-wave velocity of the near-surface material underlying the site). Experience has shown that the most useful estimate of the transfer function is obtained by averaging the spectral ratios derived from several recordings at a pair of stations, rather than from a single recording. The ideal case is to record ground-motion data at two sites whose separation is small relative to their epicentral distances. In this case, the azimuthal dependence of the earthquake source function is not a biasing factor and the transfer function will mainly depict the frequency-dependent effects caused by the differences in the physical properties of the soil and rock underlying the two sites. The transfer function is not source dependent that is, it is not dependent on azimuth or angle of wave incidence unless complex 3-dimensional structure is present at the source region.

An example of horizontal transfer functions derived from the ground-motion data sample recorded in the 1971 San Fernando earthquake is shown in Figure 15. These transfer functions correspond to Holiday Inn (HOI), 3838 Lankershime, and Glendale Municipal Building (GMB) and are calculated relative to Griffith Park Observatory (GOC) (Rogers and Hays, 1978). The levels of dynamic shear-strain estimated from the values of peak ground velocity and shear-wave velocity at these four sites were on the order of 10^{-4} percent. The levels of peak ground acceleration were 18 to 28 percent g. Essentially identical transfer functions for these sites were also obtained for ground-motion data recorded from explosions.

Although the San Fernando earthquake produced more strong-motion accelerograms than any prior earthquake, the ground-motion data sample was insufficient to define the ground response within the Glendale, California, area accurately enough for use in zoning. The aftershock data recorded on the seismic array of broad-band instruments (Figure 16) deployed in Glendale after the earthquake, however, complimented the strong-motion data sample and provided a basis for calculating site transfer functions in Glendale. Figure 17 illustrates horizontal transfer functions for: (1) Verdugo Park (station 38) relative to Griffith Park Observatory (station 46), (2) Verdugo Park relative to Glendale Municipal Building (station 41), and (3) Glendale Municipal Building relative to Griffith Park Observatory. Station 41 is located on thick (>30 m) alluvium; station 38 is located on thin (< 30 m) alluvium at the base of the Verdugo Mountains; and station 46 is located on granitic rock. The first two transfer functions show a significant increase in the amplitude of ground response at the 0.2-second period. The transfer function for thin to thick alluvium shows substantial amplification for periods less than 0.3 second and essentially identical response for periods greater than 0.4 second. Thus, the short-period components are attenuated more in the thick section of alluvium than in the thin section of alluvium. The transfer function for thick alluvium to rock does not show the amplification at short periods that the transfer function for thin alluvium to rock shows.

Two maps of ground response for the Glendale area are shown in Figures 18 and 19. The first map (Figure 18) shows the ground response, relative to

rock, for the period band 0.055 - 0.16 second. Because of the lack of adequate control in some parts of the area the contours are arbitrarily drawn to conform with the interpreted distribution of soil and rock in the area (Figure 16). The largest values of relative ground response for this short-period band occur in the vicinity of station 38 and coincide with the distribution of thin alluvium along the mountain front, especially in the northeast part of the area. This zone is where amplification of the high-frequency ground motions would be expected. The second map shows the ground response, relative to rock, for the period band 1.82 - 2.46 seconds. The largest values of ground response occur in the center of the area and correspond with the thick alluvium deposits.

Ground-response maps, such as those shown in Figures 18 and 19, can be used in conjunction with a map of the probabilistic ground shaking (see Figure 2) or a map of the actual ground shaking (Figure 20) experienced during the San Fernando earthquake to divide the Glendale area into ground-shaking hazard zones. Such zones could be used to guide construction and land-use planning and to modify earthquake-resistant designs. On the basis of ground response maps, planners and decisionmakers might choose to locate, for example, low-rise, acceleration-sensitive buildings at sites other than sites along the Verdugo mountain front where thin alluvium overlying rock causes the high frequencies and peak ground acceleration to be amplified. Also, high-rise buildings having fundamental modes of response of 1.8 - 2.5 seconds range might be located at sites other than in the center of the area where thick alluvium deposits cause amplification of the long-period seismic waves. The ultimate application would be to utilize frequency-dependent ground-response maps, such as these, to zone for the ground-shaking hazard as well as for other earthquake hazards (e.g., landslide susceptibility and liquefaction potential) and to guide structural design considerations.

TECHNICAL PROBLEMS

Construction of zoning maps which incorporate frequency-dependent effects caused by the local geology is controversial, primarily because of the limitations of the available empirical data. The data are simply too limited to establish accurate frequency-dependent relations and to resolve completely technical issues such as:

- (1) Over what range of ground-motion data and levels of dynamic shear strain is the site transfer function repeatable and essentially unchanged?
- (2) How does ground response vary with depth below the surface?
- (3) What uncertainty is associated with a mean site transfer function?
- (4) What physical properties control the spatial variation of ground response in various geographical regions of the United States?

High-strain ground shaking - The question of the dependence of a transfer function on the level of dynamic shear strain is one of the most important questions needing resolution. Local ground response is complicated by the fact that soils can behave nonlinearly their shear modulus and damping characteristics are strain dependent. Resolution of this technical question

will not be possible until ground-motion data are acquired near the causative fault for earthquakes of magnitude (M_s) 7 and greater. Such data will permit more precise zoning of the ground-shaking hazard in the vicinity of the fault zone--the area where high-strain effects are greatest.

Velocity seismograms (see Figures 21 and 22) can be used in conjunction with the shear wave velocity of the surficial materials to estimate the strain level induced in the soil and rock at a site during past earthquakes. The procedure is to divide the peak particle velocity recorded on the seismogram by the shear-wave velocity of the material underlying the site to obtain an estimate of the level of dynamic shear strain. Tables 1-3 contain peak values of velocity recorded in past earthquakes. Representative values of shear-wave velocity, determined for unconsolidated materials in the San Francisco Bay region (Gibbs and others, 1976), are:

- (1) 55 to 115 m/sec - very soft to soft clay and silty clay
- (2) 160 to 190 m/sec - medium stiff clay and silty clay
- (3) 170 to 305 m/sec - very stiff to hard clay and silty clay
- (4) 210 to 310 m/sec - sandy clay and silty loam
- (5) 240 to 270 m/sec - interbedded sandy gravels and silty clay
- (6) 150 to 250 m/sec - loose to dense sand
- (7) 250 to 400 m/sec - dense to very dense near-surface sand 0-12 m thick
- (8) 250 to 570 m/sec - dense to very dense sand 12-30 m thick
- (9) 400 to 500 m/sec - near-surface gravel
- (10) 420 to 750 m/sec - deep gravel

On the basis of these data, the greatest level of dynamic shear strain induced in soil and rock during past earthquakes (for which accelerograms were recorded) was about 2×10^{-3} percent.

The regional attenuation relation for peak velocity proposed by Seed and others (1976) can be used in conjunction with values of shear-wave velocity to estimate the epicentral distance to specific levels of shear strain (e.g., 10^{-3} , 10^{-4} , etc.) in an earthquake. Such an estimate is shown in Figure 23 for a geographic area assumed to have surficial materials characterized by a shear-wave velocity of 200 m/sec. The epicentral distance to the 10^{-3} level of shear strain is about 19 km; the distance to the 5×10^{-3} level is about 2 km. If the 5×10^{-3} level of shear strain marks the first onset of significant nonlinear behavior (as suggested by data reported by Hays and others 1979) at sites underlain by unconsolidated material, relative to that for rock sites, the size of the zone to account for the effect of high shear-strain effects is not very large, even when the ground is poor. For better ground (e.g. $V=500\text{m/sec}$), the size of the high-strain zone is smaller. Thus, the task of incorporating high-strain effects and local ground response in zoning maps of the ground-shaking hazard appears to be feasible.

The overall complexity of the earthquake faulting mechanism makes it difficult to predict the seismic wave type that will cause the peak ground velocity and induce the shear strain in the soil column at a given location. However, some general guidelines can be given on the basis of current knowledge about wave propagation and the available empirical data. Close to the fault, the location of the site relative to the fault rupture surface is the controlling factor. Because of the complex nature of a propagating fault rupture, marked differences in the levels of peak ground motion will occur at points located in different directions from the fault surface (Archuleta and Brune, 1975). Very near the center of a fault surface, the predominant low-frequency motions are in the direction of fault slip. Large transverse motions are observed at the ends of the fault and near the front of a propagating rupture (e.g., 1966 Parkfield and 1971 San Fernando, California, earthquakes). In a strike-slip earthquake (e.g., 1940 Imperial Valley, California), vertical ground motions are generally smaller than horizontal ground motions and richer in high frequencies. (However, the opposite was true in the 1979 Imperial Valley earthquake). It appears that a location directly in line with a propagating fault rupture will likely experience high amplitude shear waves having particle motions transverse to the plane of the fault. Relatively higher frequencies and amplitudes will be experienced at points ahead of the rupture than behind it. In contrast, a location at 45° relative to the fault plane will likely be rich in P-waves having particle motion radial to the earthquake source. Thus, the location and geometry of the fault rupture surface is very important when describing the velocity ground motion field close to the earthquake source.

At distances of several rupture lengths or more from the causative fault, the characteristics of ground shaking are relatively easier to define. Because the earth acts like a low-pass filter, the high-frequency body-wave energy causing the peak ground acceleration is sharply attenuated within a few tens of kilometers. Beyond this range, the Rayleigh wave, which propagates at about 0.9 the shear-wave velocity and attenuates more slowly with distance than the P and S waves, frequently produces the peak velocity on the seismogram (Figure 21). There are exceptions, however: it appears that sites underlain by several tens to several hundred meters of unconsolidated materials will frequently record a well developed Rayleigh wave (Hanks, 1976) that causes the peak ground velocity at the site. Such a wave typically shows dispersion, has wavelengths ranging from a few hundred meters to several kilometers, and samples a fairly large portion of the Earth's crust as it propagates.

The focal depth of the earthquake should also be considered in zoning. Increasing the focal depth tends to reduce the surface wave energy relative to the body wave energy. Therefore, one would expect earthquakes having shallow focal depths (e.g., 0-30 km in the New Madrid, Missouri, and Charleston, South Carolina areas) to be more efficient generators of surface waves than earthquakes having deep focal depths (e.g., 50-60 km in the Puget Sound, Washington area). For the deep-focus earthquakes, other considerations are important in evaluating the likelihood of strong surface waves at the site. The most important consideration is whether the geologic structure and the distribution of the near-surface unconsolidated materials can cause trapped or channel waves to form.

Variation of ground response with depth - Data showing the variation of ground response with depth are meager in the United States. Recently, data have been acquired at sites in Nevada using surface and subsurface instrument arrays. At one site, identical instruments were emplaced in rock (tuff) in the bottom of a 41 m drill hole at Beatty, Nevada, and at the surface on alluvium. Explosions were recorded on the array and used to establish the mean transfer function (Figure 24). The spectral amplitudes of the subsurface ground motions are less than those on the surface, with the subsurface values being about one-tenth of the corresponding surface values in the vicinity of 0.3 second, the characteristic site period (i.e., the period that corresponds approximately to four times the thickness of the alluvium divided by its shear-wave velocity). This result is valid only for low-strain ground motions.

Uncertainty associated with a mean transfer function - The best data available for defining the mean transfer function was obtained in the 1971 San Fernando earthquake. Although the available data correspond to low-strain conditions, the mean transfer function appears to be remarkably repeatable. Figure 25 shows the mean transfer function for station 38 relative to station 41; it was derived from 10 aftershocks recorded in Glendale, California and has a standard deviation of 1.50.

Horizontal spatial variation of ground response - The ground response in an area is uniquely related to the laterally varying physical properties of the subsurface geology. Each geographic area has its own characteristics of ground response which are controlled by one or more physical properties of the soil and rock: thickness, lithology, geometry, water content, shear-wave velocity, and density. For example, Las Vegas, Nevada, is a classic example of an area where the principal characteristics of ground response appear to correlate with the effect of lateral changes in thickness and lithology of the alluvium in Las Vegas valley (Figure 13) on propagating Rayleigh waves (Murphy and Hewlett, 1975). In Salt Lake City, Utah, thickness and degree of water content by weight appear to have the greatest effect (Hays and others, 1980) on the spatial variation of ground response.

If one could define the subsurface geology at sites within an area more accurately, it would be easier to predict the principal characteristics of local ground response. A site model, such as shown in Figure 26 for the El Centro, California, site, is needed for all sites in an area. Models like this require borehole data and geophysical measurements (e.g., seismic reflection lines, velocity spectra) and are generally unattainable without great expense.

SUMMARY

Although current zoning maps of the ground-shaking hazard will remain in use for some time, improved maps that incorporate the frequency-dependent effects of the fault rupture and of the regional and local geology on seismic waves will evolve only as advances in data gathering, physical understanding, and capability to model numerically occur. Such zoning maps will require additional data, including: (1) strong ground-motion records at surface and subsurface locations in many areas for a wide range of levels of dynamic shear-strain, (2) seismic-wave transmission characteristics of a wide range of unconsolidated materials overlying rock for a wide range of shear-strain levels, (3) information from in situ and laboratory measurements on the static and dynamic properties of a wide range of subsurface materials, and (4) better understanding of the faulting mechanism and the important differences it has on near-and far-field seismic radiation patterns.

REFERENCES

- Algermissen S. T. and Perkins. D. M., 1976 A probabilistic estimate of maximum acceleration in rock in the contiguous United States U.S. Geological Survey Open-File Report 76-416, 45 p.
- Applied Technology Council, 1978, Tentative provisions for the development of seismic regulations for buildings. ATC-3-06, 514 p. (Available from National Bureau of Standards, Special Publication 510, Washington. D.C.).
- Archuleta, R. J. and Brune, J. N., 1975, Surface strong motion associated with a stick-slip event in a foam rubber model of earthquakes. Seismological Society of America Bulletin, v. 65, p. 1059-1071.
- Borcherdt, R. D., (editor), 1975, Studies for seismic zonation of the San Francisco Bay region: U.S. Geological Survey Professional Paper 941-A, 102 p.
- Castle, R. O., Church, J. P., Elliott, M. R., and Morrison, N. L., 1975, Vertical crustal movements preceding and accompanying the San Francisco earthquake of February 9, 1971: A summary in Pavoni, N. and Green, R., eds., Recent Crustal Movements: Tectonophysics, v. 29, p. 127-140.
- Gibbs, J. F., Fumal, T. E., and Borcherdt, R. E., 1976, In-situ measurements of seismic velocities in the San Francisco Bay region, part 3. U.S. Geological Survey Open-file Report 76-731, 145 p.
- Hanks, T. C., 1976, Observations and estimation of long-period strong ground motion in the Los Angeles Basin: International Journal of Earthquake Engineering and Structural Dynamics, v. 4, p. 473-488.
- Hays, W. W., 1977a, The ground-shaking hazard an important consideration in land-use planning: California Division of Mines and Geology Special Report 129. p. 1-7.
- Hays, W. W., 1977b, Evaluation of the seismic response in the Sylmar - San Fernando area, California, from the 1971 San Fernando earthquake: American Society of Civil Engineers, Engineering Mechanics Division, Specialty Conference on Dynamic Response of Structures, Los Angeles, Proceedings, p. 502-511.
- Hays, W. W., 1978, Ground Response Maps for Tonopah, Nevada Seismological Society of America Bulletin, v. 68, p. 451-470.
- Hays W. W., Rogers, A. M., and King, K. W., 1979, Empirical data about local ground response: Earthquake Engineering Research Institute, 2nd National Conference on Earthquake Engineering, Stanford, California, Proceedings, p. 223-232.
- Hays, W. W., Miller, R. D., and King, K. W., 1980, Ground response in the Salt Lake City-Ogden-Provo, Utah, Urban Corridor. World Conference on Earthquake Engineering, 7th, Ankara, Turkey, Proceedings, v. 2, p. 89-96.
- Howard, K. A., Aaron, J. M., Brabb, E. E., Brock, M. R., Gower H. D., Hunt,

- S. J., Milton, D. J., Muehlberger, W. R., Nakata, J. K., Plafker, G., Prowell, D. C., Wallace, R. E. and Witkind, I. J., 1977. Preliminary map of young faults in the United States as a guide to possible fault activity. U.S. Geological Survey Miscellaneous Field Studies Map MF-916, 1:5,000,000 and 1:7,500,000.
- Murphy, J. R., Weaver, N. L., and Davis, A. H., 1971. Amplification of seismic body waves by low-velocity surface layers. *Seismological Society of America Bulletin*, v. 61, p. 109-146.
- Murphy J. R., and Hewlett, R. A., 1975. Analysis of seismic response in the city of Las Vegas, Nevada; a preliminary microzonation. *Seismological Society of America Bulletin*, v. 65, p. 1575-1598.
- Porcella, R. L. and Matthiesen, R. B., 1979. Preliminary summary of the U.S. Geological Survey Strong-Motion Records from the October 15, 1979 Imperial Valley earthquake. U.S. Geological Survey Open-File Report 79-1654, 41 p.
- Rogers, A. M. and Hays, W. W., 1978, Preliminary evaluation of site transfer function derived from earthquakes and nuclear explosions. 2nd International Conference on Microzonation, San Francisco, Proceedings, v. 2, p. 753-764.
- Schnabel, R. P. and Seed, H. B., 1973, Accelerations in rock for earthquakes in the Western United States. *Seismological Society of America Bulletin*, v. 62, p. 501-516.
- Seed, H. B., 1975, Design Provisions for assessing the effects of local geology and soil conditions on ground and building response during earthquakes, in *New Earthquake design provisions: Proceedings of Seminar sponsored by Professional Development Committee of Structural Engineers Association of Northern California and San Francisco Section American Society of Civil Engineers*, p. 38-63.
- Seed, H. B. and Idriss, I. M., 1969. Influence of soil conditions on ground motions during earthquakes. *Journal of Soil Mechanics and Foundations Division, American Society of Civil Engineers*, v. 95, p. 1199-1218.
- Seed, H. B., Murarka, R., Lysmer, John. and Idriss, I. M., 1976. Relationships of Maximum acceleration, maximum velocity, distance from source, and local site conditions for moderately strong earthquakes. *Seismological Society of America Bulletin*, v. 66, p. 221-244.
- Sieh, K. E., 1978, Prehistoric large earthquakes produced by slip on the San Andreas fault at Pallett Creek, California. *Journal of Geophysical Research*, v. 83, p. 3907-3939.
- Trifunac, M. D., 1971, Response envelope spectrum and interpretation of strong earthquake ground motion. *Seismological Society of America, Bulletin*, v. 61, p. 343-356.
- Zoback, M. L., and Zoback, M., 1980, State of stress in the conterminous United States. *Journal of Geophysical Research* v. 85, no. B11, p. 6113-6156.

Table 1.—Peak horizontal ground velocity and displacement derived for rock sites from past earthquakes

Earthquake	Date	Magnitude	Approx. source distance (km)	Component of motion	Maximum velocity (cm/sec)	Maximum displacement (cm)	Recording site
Helena, Mont.	10/31/35	6.0	8	NS ES	7.3 13.3	1.4 3.7	Carroll College, Helena, Mont.
Kern County Calif.	7/21/52	7.7	43	N. 21 E. S. 69 E.	15.7 17.7	6.7 9.2	Taft, Calif.
San Francisco Calif.	3/22/57	5.25	11	N. 10 E. S. 80 E.	4.9 4.6	2.3 0.8	Golden Gate Park, San Francisco, Calif.
Lytle Creek, Calif.	9/12/70	5.4	13	S. 25 W. S. 69 E.	9.6 8.9	1.03 2.21	Wrightwood, Calif.
Parkfield, Calif.	6/27/66	5.6	7	N. 65 W. S. 25 W.	14.5 22.5	4.7 5.5	Temblor Calif.
Rorrogo Mountain, Calif.	4/8/68	6.5	134	N. 33 E. N. 57 W.	3.7 4.2	1.6 2.9	SCE Power Plant, San Onofre Calif.
Lytle Creek Calif.	9/12/70	5.4	19	NS EW	--- ---	--- ---	Devils Canyon, San Bernadino, Calif.
San Fernando, Calif.	2/9/71	6.6	3-5	S. 16 E. N. 76 W.	115.5 57.7	37.7 10.8	Pacoima Dam

Table 1.--Peak horizontal ground velocity and displacement derived for
rock sites from past earthquakes
continued

Earthquake	Date	Magnitude	Approx. source distance (km)	Component of motion	Maximum velocity (cm/sec)	Maximum displacement (cm)	Recording site
San Fernando, Calif.-----	2/9/71	6.6	21	N. 21 E. N. 69 W.	14.7 12.4	1.8 8.9	Lake Hughes, Sta. 12
San Fernando Calif.-----	2/9/71	6.6	24	NS EW	12.3 15.0	4.9 5.4	3838 Lankershim Blv., Los Angeles Calif.
San Fernando, Calif.-----	2/9/71	6.6	26	S. 69 E. S. 21 W.	9.9 6.2	7.0 4.6	Lake Hughes, Sta. 4
San Fernando, Calif.-----	2/9/71	6.6	30	S. 08 E. S. 82 W.	9.9 6.2	7.0 4.6	Santa Pelicia Dam. (outlet)
San Fernando, Calif.-----	2/9/71	6.6	31	NS EW	20.5 14.5	7.3 5.5	Griffith Park Observatory
San Fernando, Calif.-----	2/9/71	6.6	30	NS EW	5.8 11.6	1.6 5.0	Cal. Tech. Seismol. Lab. Pasadena, Calif.
San Fernando, Calif.-----	2/9/71	6.6	40	N. 03 W. N. 87 E.	5.3 6.7	3.2 5.9	Santa Anita Dam

Table 2.--Peak horizontal ground velocity and displacement derived for stiff soil sites from past earthquakes

Earthquake	Date	Magnitude	Approx. source distance (km)	Component of motion	Maximum velocity (cm/sec)	Maximum displacement (cm)	Recording site
San Fernando, Calif.	2/9/71	6.6	21	N. 21 E. N. 69 W.	16.5 27.2	4.2 9.3	Castaic, Old Ridge Route
San Fernando, Calif.	2/9/71	6.6	28	N. 11 E. N. 79 W.	28.2 23.5	13.4 10.3	15250 Ventura Blvd., Los Angeles, Calif.
San Fernando, Calif.	2/9/71	6.6	28	S. 12 W. N. 78 W.	31.5 17.8	18.3 9.5	14724 Ventura Blvd., Los Angeles, Calif.
San Fernando, Calif.	2/9/71	6.6	35	NS EW	16.5 21.1	8.0 14.7	Hollywood Storage P.E. Lot, Los Angeles, Calif.
San Fernando, Calif.	2/9/71	6.6	39	NS EW	22.3 18.5	11.4 11.6	1470 Wilshire Blvd., Los Angeles, Calif.
San Fernando, Calif.	2/9/71	6.6	39	NS EW	18.0 22.1	10.3 12.9	3710 Wilshire Blvd., Los Angeles, Calif.
San Fernando, Calif.	2/9/71	6.6	39	NS EW	18.3 16.5	9.0 10.3	3407 W. Sixth St., Los Angeles, Calif.
San Fernando, Calif.	2/9/71	6/6	39	NS EW	14.7 16.1	9.9 9.1	3345 Wilshire Blvd., Los Angeles, Calif.
San Fernando, Calif.	2/9/71	6.6	67	N. 65 E. S. 25 E.	4.1 5.0	2.6 3.4	2516 Via Tejon

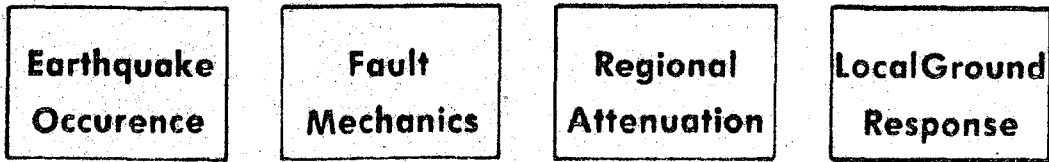


Figure 1. Elements involved in zoning of the ground-shaking hazard.

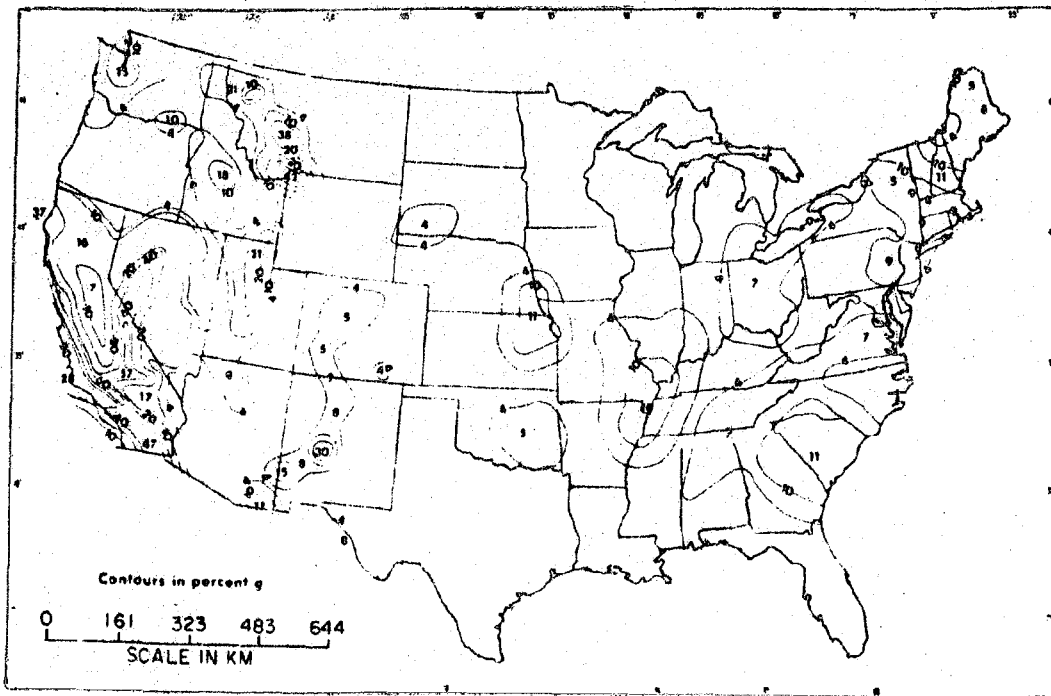


Figure 2. Probabilistic zoning map showing the peak acceleration at sites underlain by rock in the conterminous United States (Algermissen and Perkins, 1976). A 10-percent probability exists that the specified level of ground-shaking will be exceeded in 50 years.

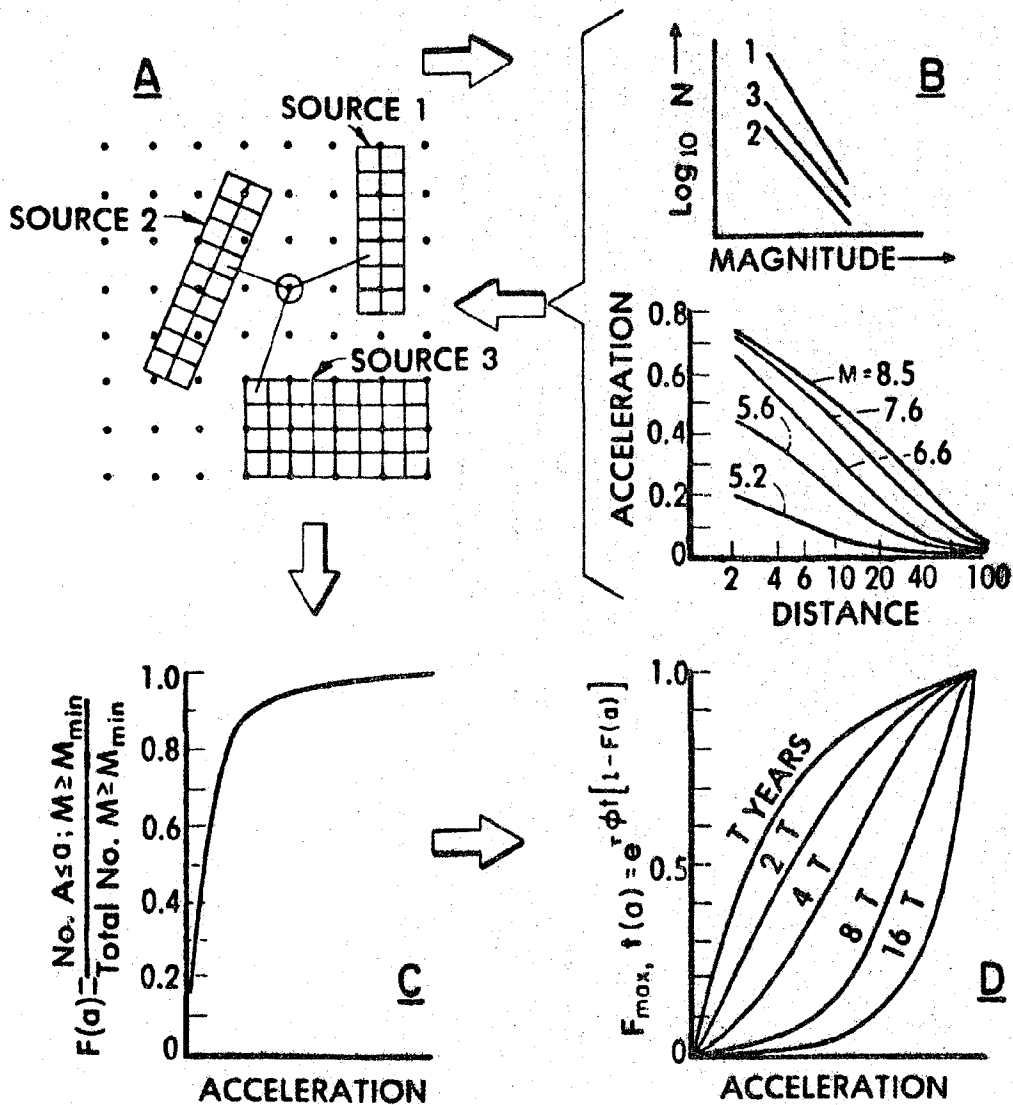


Figure 3. Schematic illustration of the elements involved in constructing a probabilistic zoning map of the ground-shaking hazard. **A** shows three typical seismic source zone configurations and the grid of points at which the ground-acceleration hazard is calculated. **B** shows typical statistical representations of seismicity for the three seismic source zones and peak acceleration attenuation curves for the region encompassing the three seismic source zones. **C** depicts a typical cumulative probability distribution $F(a)$ of ground acceleration at a given site. **D** shows the extreme probability $F_{\max, t(a)}$ for various levels of peak ground acceleration and exposure times t at a given site. Acceleration values obtained in **D** for every site form the basis for constructing a countour map such as shown in figure 2. (Algermissen and Perkins, 1976).

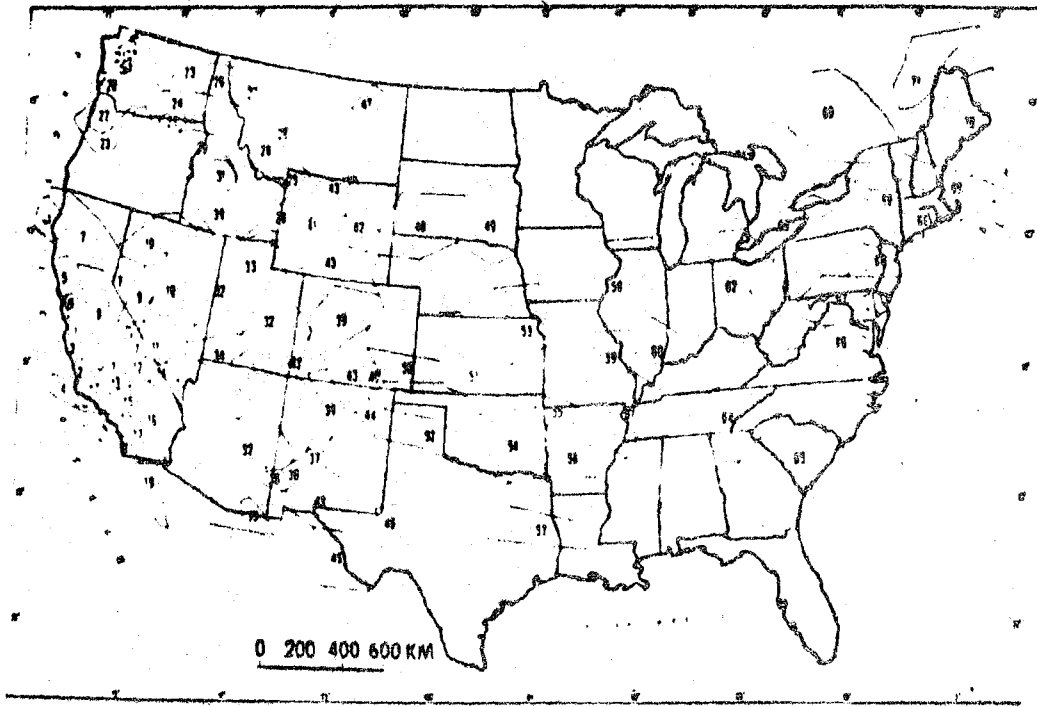


Figure 4. Map showing seismic source zones in the conterminous United States (Algermissen and Perkins, 1976).

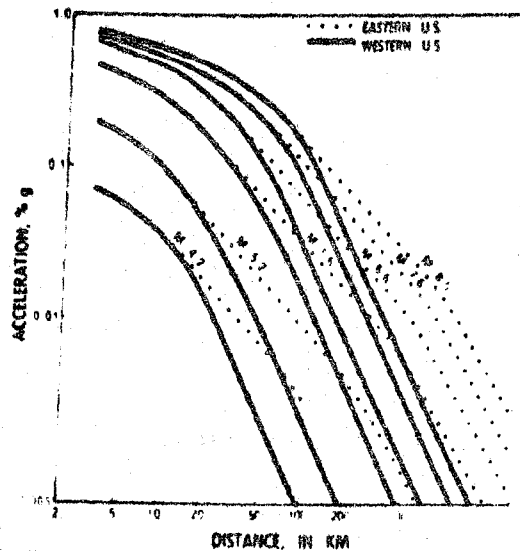


Figure 5. Average value of peak acceleration at sites underlain by rock in relation to distance from the causative fault. The solid curves for the Western United States were proposed by Schnabel and Seed (1973); the dashed curves for the Eastern United States by Algermissen and Perkins (1976).

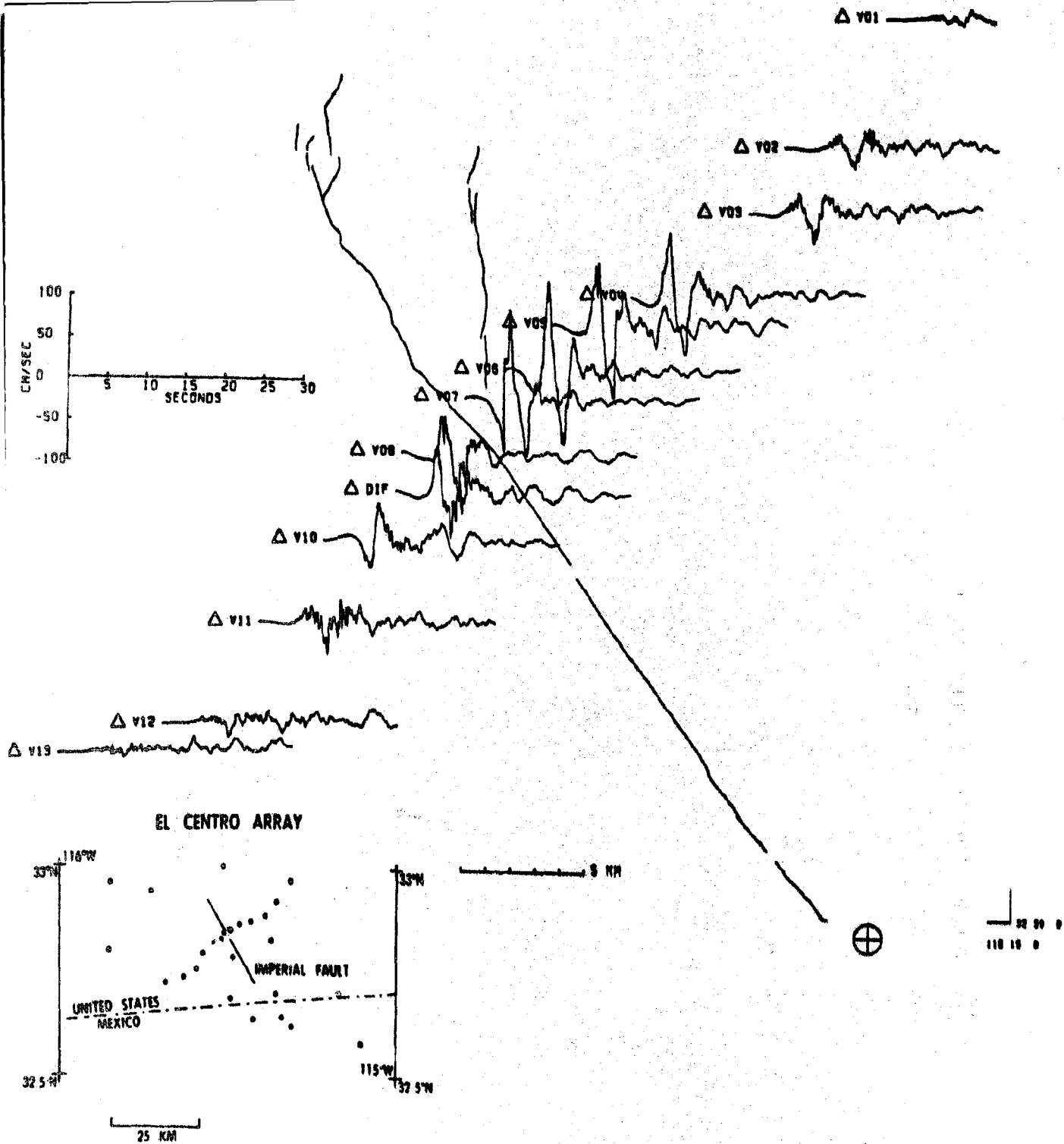
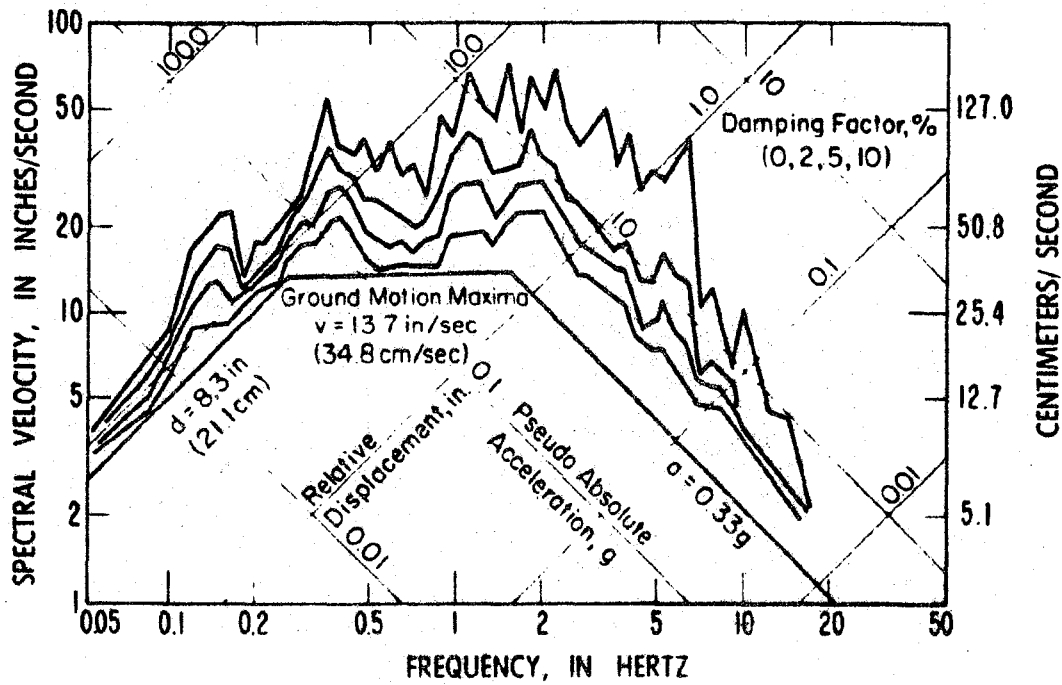
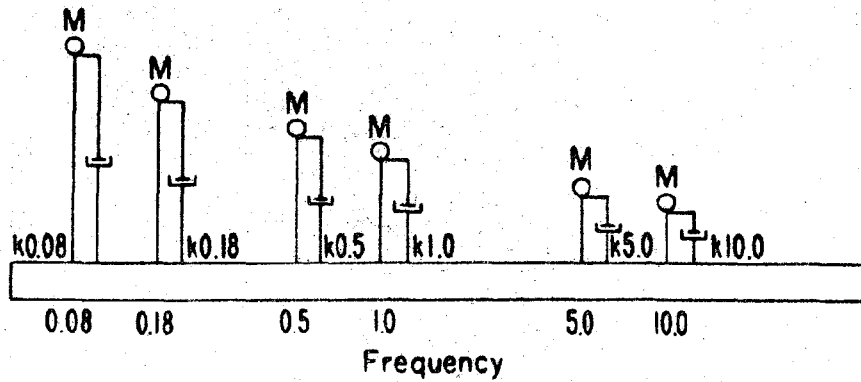


Figure 6. Diagram showing the location of stations recording the 1979 Imperial Valley, California earthquake. The epicenter is shown at the bottom right; the trace of the fault cuts across the seismic array near station V07. The scale of the horizontal component of particle velocity perpendicular to the fault is shown at the top of the illustration (Data Courtesy of Ralph Archuleta, USGS).

Schematic Ensemble of Single Degree-of-Freedom Systems



>7 Story	3-7 Story	1-2 Story
----------	-----------	-----------

Building Natural Frequency Range

Figure 7. Schematic illustration of the ensemble of damped mass-spring systems which are used to estimate the frequency-dependent response of structures to ground shaking from the 1940 Imperial Valley, California, earthquake recorded at El Centro.

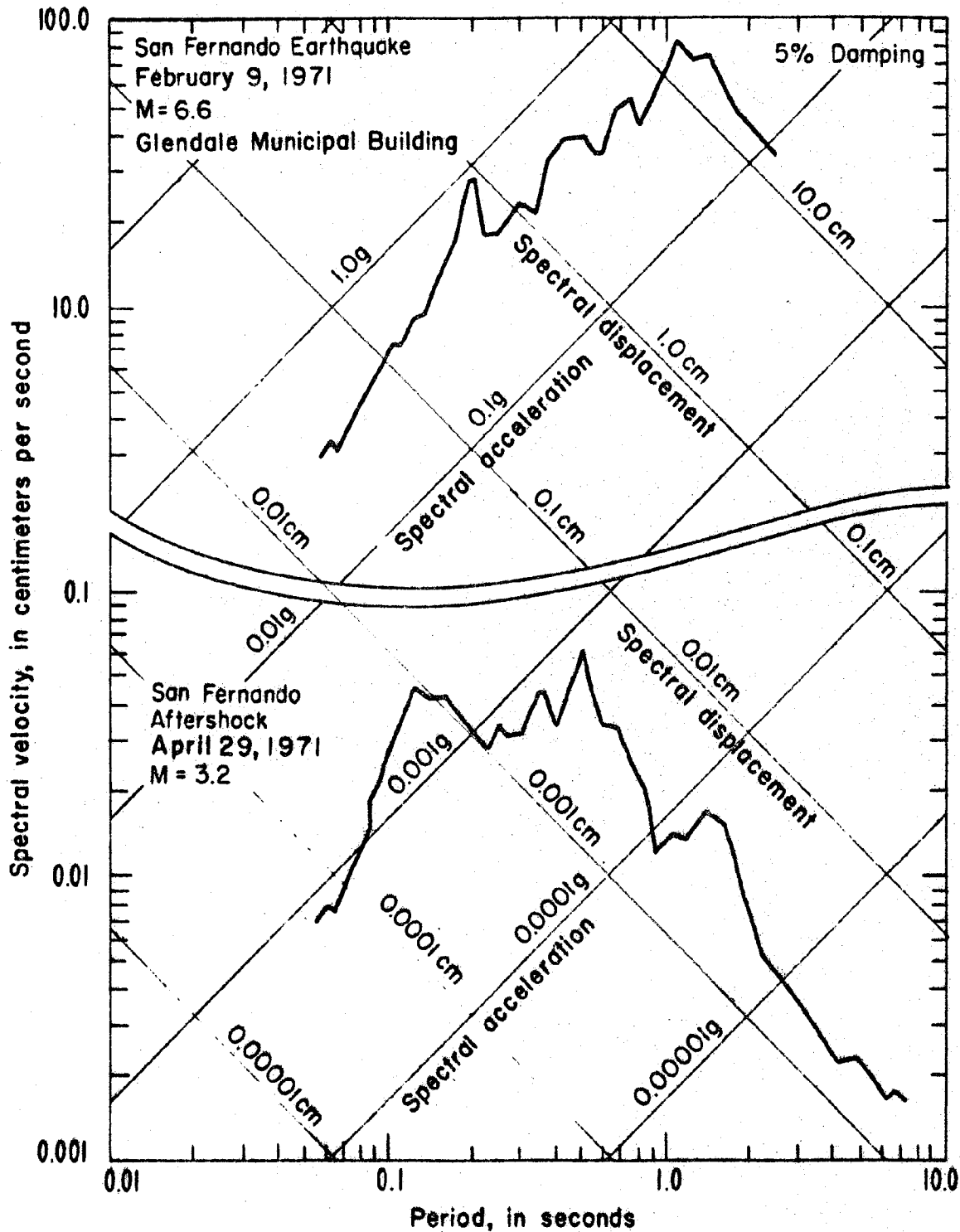


Figure 8. Example of earthquake source effects on the spectral composition of horizontal ground motion. The response spectra were derived from time histories recorded at the same site in Glendale, California from the San Fernando earthquake and an aftershock. The geology of the transmission path and local site is essentially identical for the two recordings; the variation in source parameters causes the shift in dominant energy to the long period end of the spectrum.

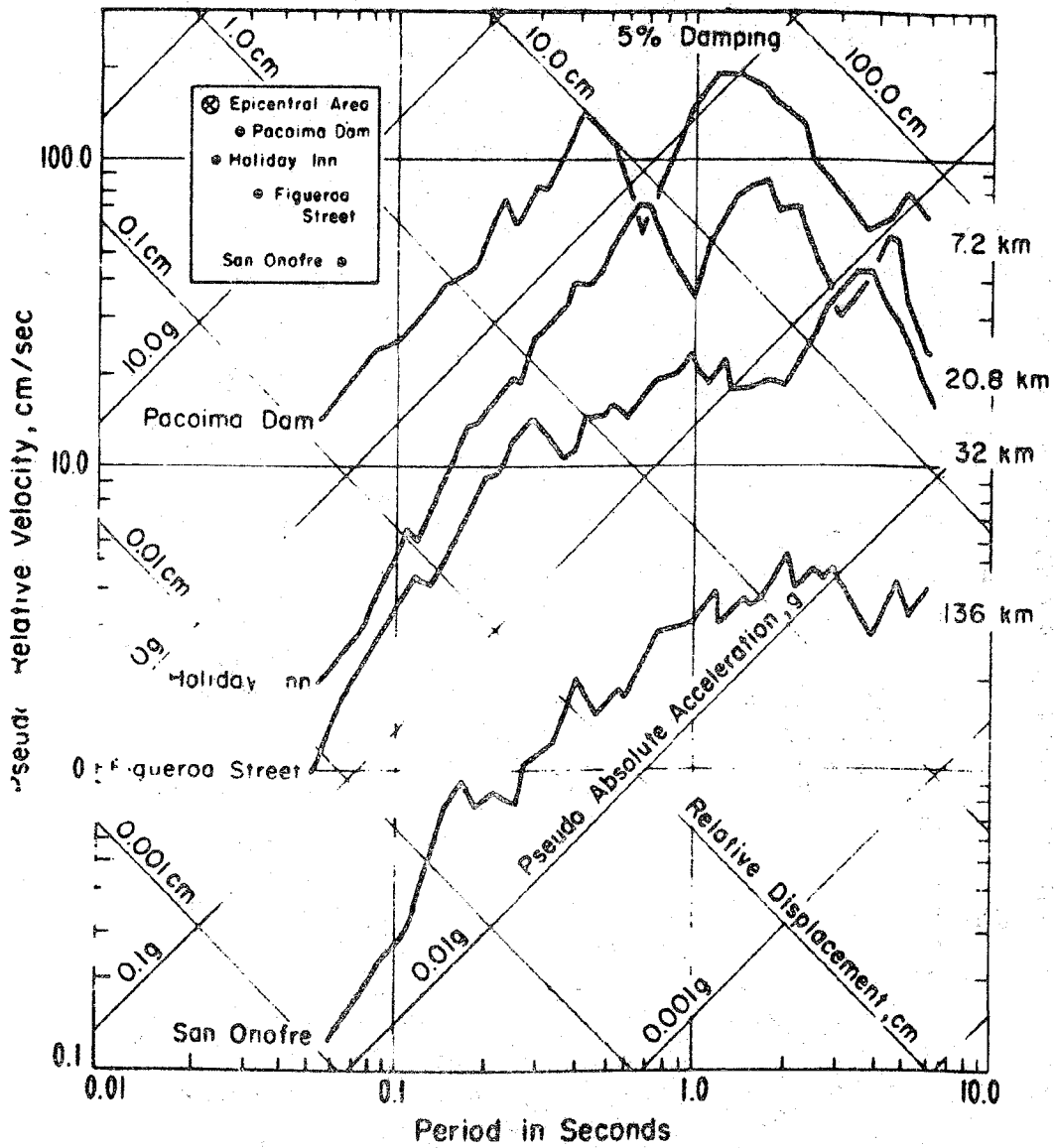


Figure 9. Example of transmission path effects on the spectral composition of horizontal ground motion, 1971, San Fernando, California, earthquake. The low-pass filtering effects of the Earth's crust cause the high frequencies to attenuate more rapidly than the low frequencies.

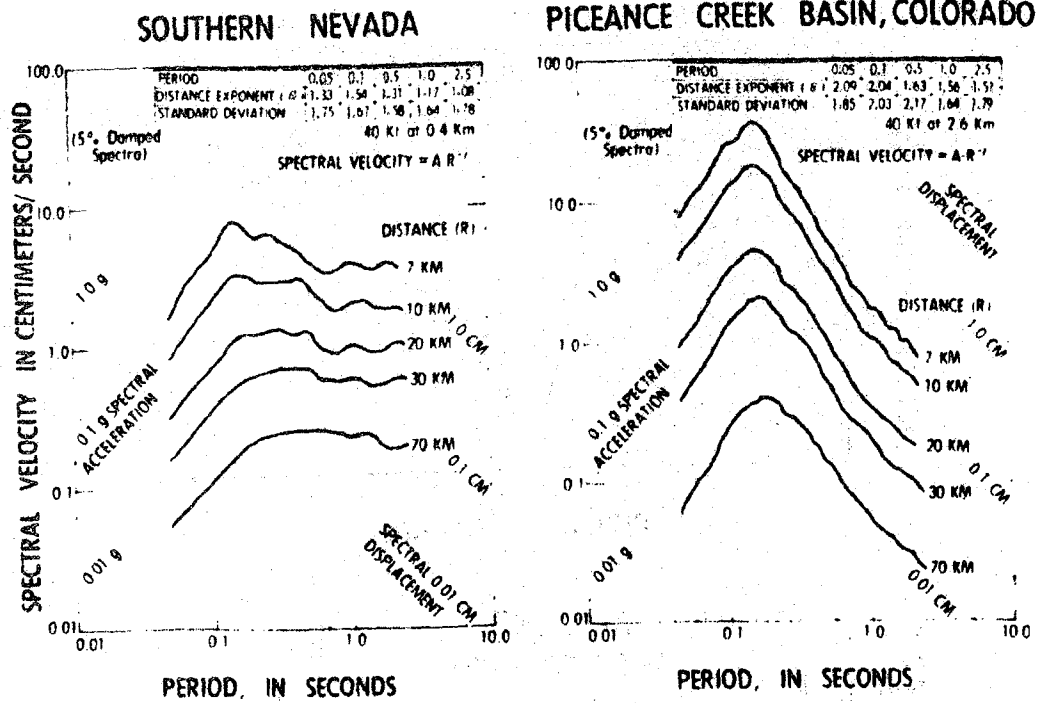


Figure 10. Examples of frequency-dependent attenuation of horizontal ground motions, southern Nevada and Colorado. These curves were derived from explosion data.

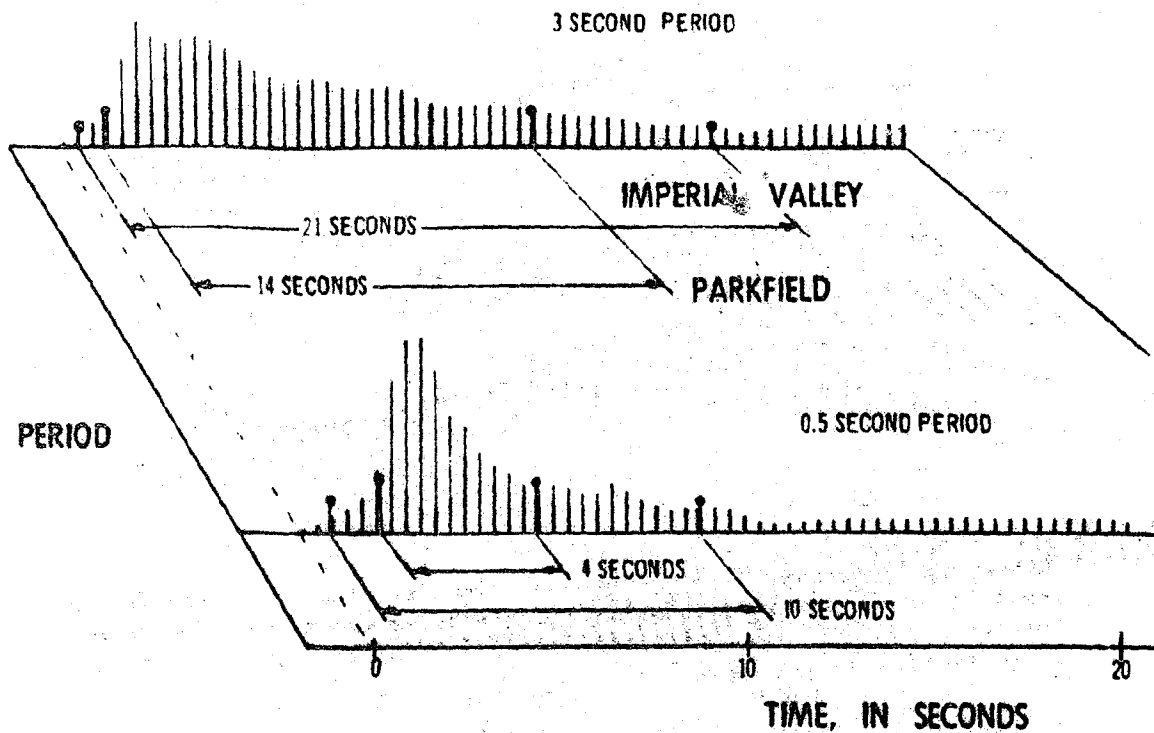


Figure 11. Example of frequency-dependent duration of shaking, 1940 Imperial Valley and 1966 Parkfield, California earthquakes.

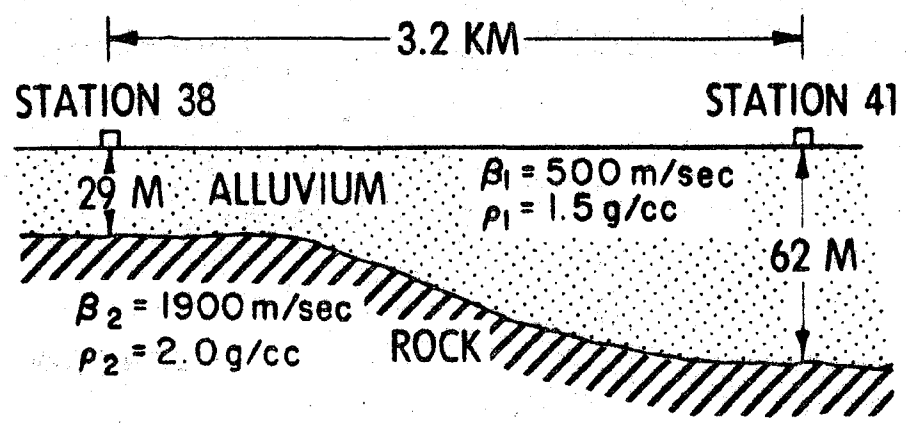
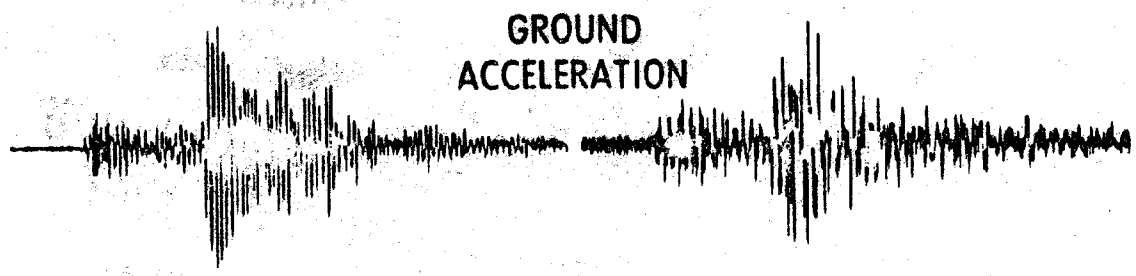
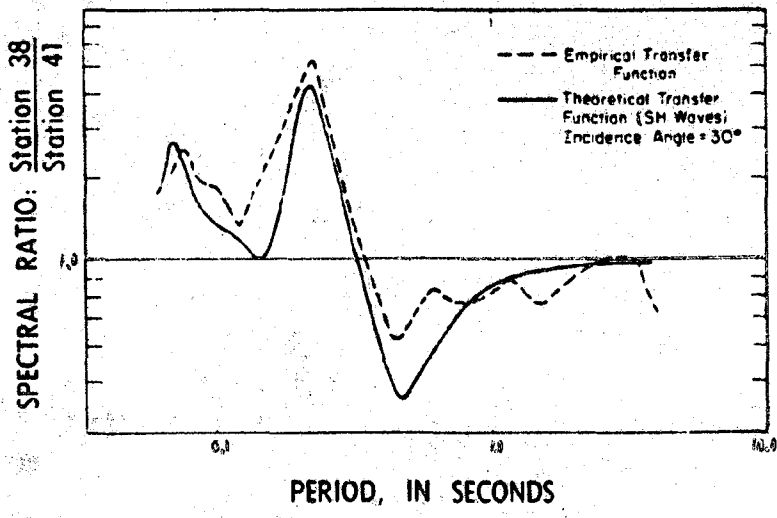
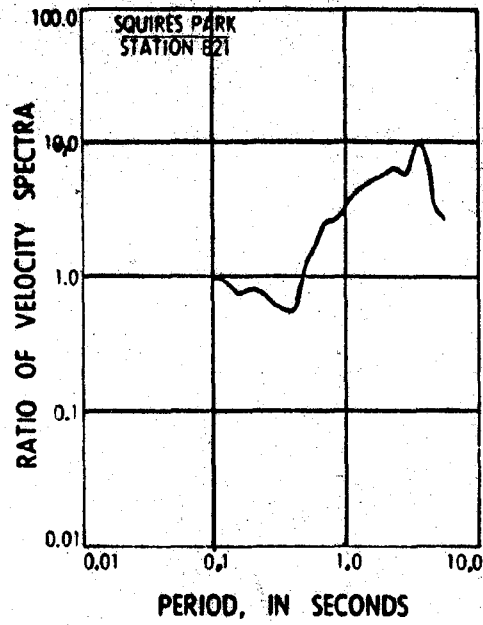
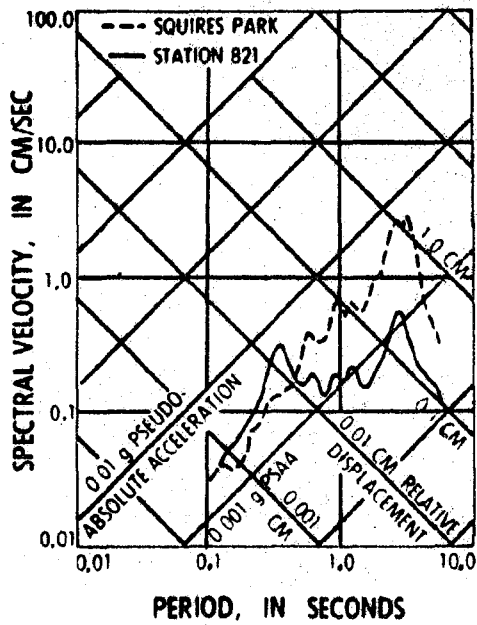
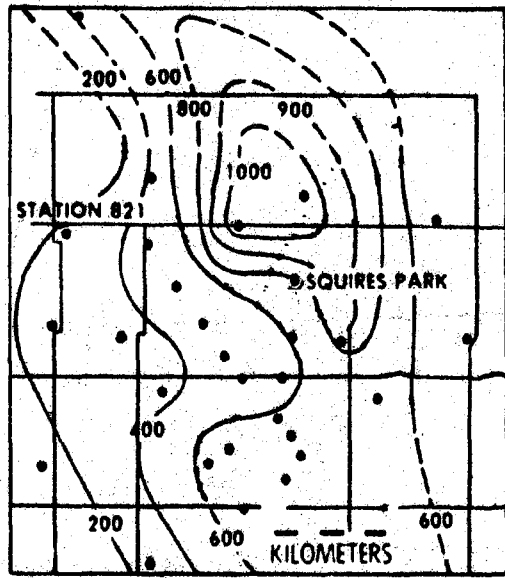


Figure 12. Example of body wave amplification, Glendale, California. The 1971 San Fernando earthquake aftershock sequence provided data for the empirical transfer function. The local geology was defined by refraction surveys and field mapping.



LAS VEGAS AREA



• Seismograph Station 400 Alluvium Depth in meters

Figure 13. Example of surface wave amplification, Las Vegas, Nevada. Ground motions are from explosions. The transfer function is for station Squires Park relative to station 821. Raleigh waves are amplified (Murphy and Hewlett, 1975).

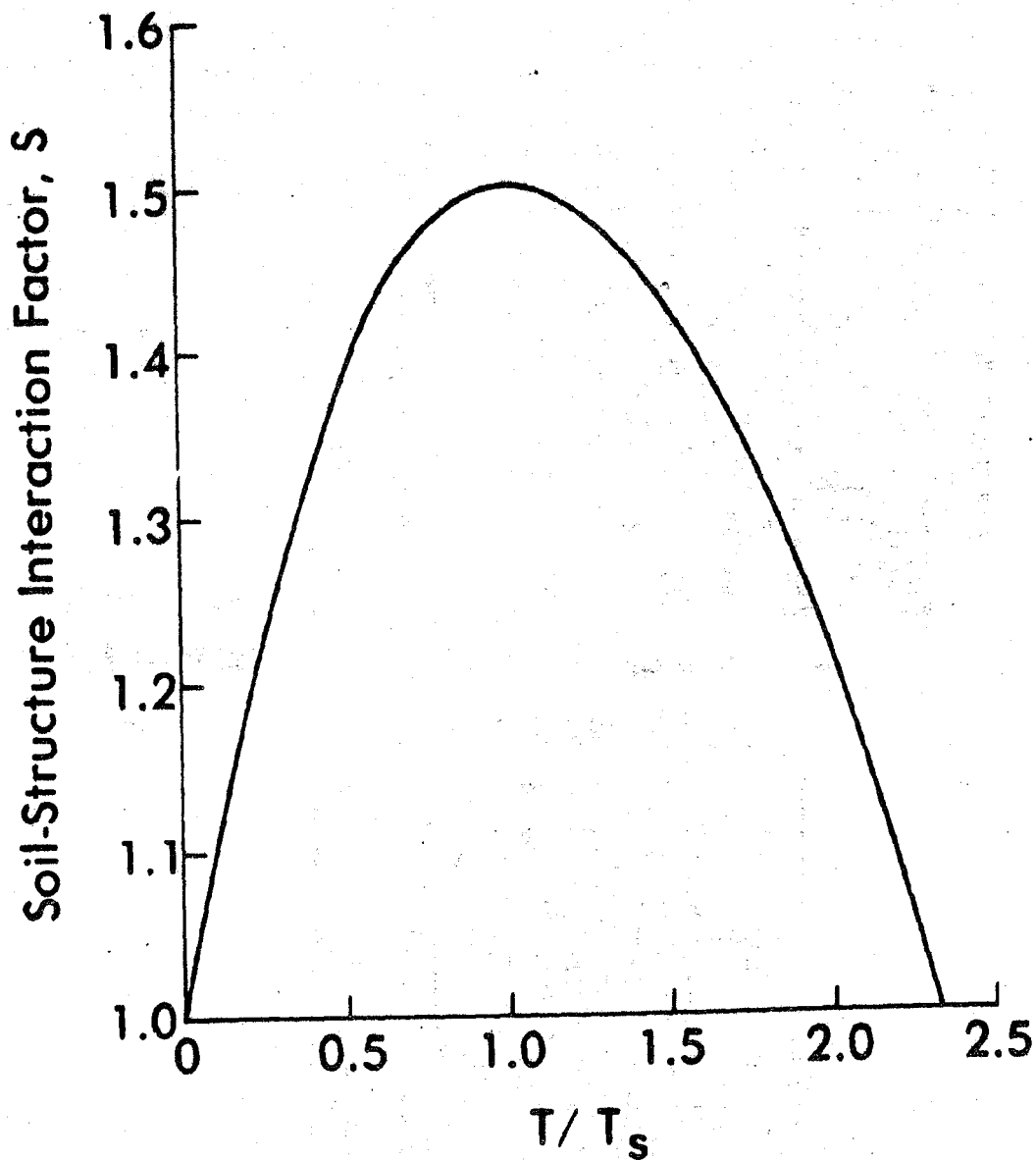
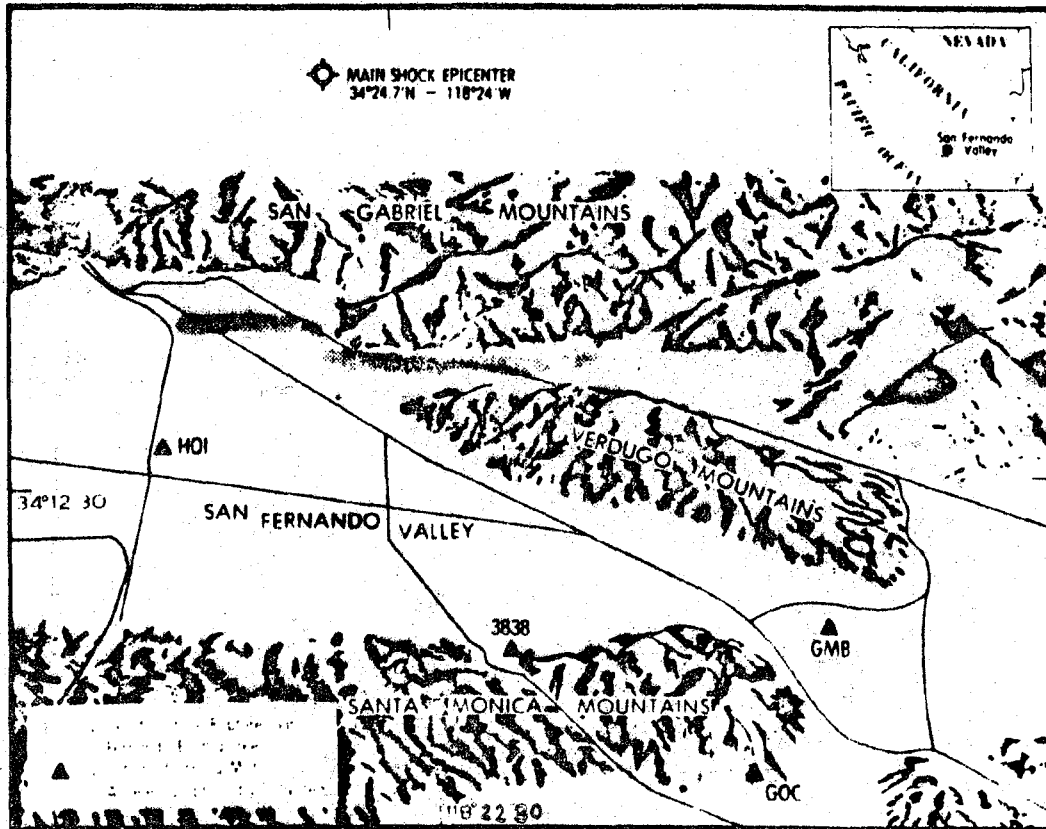


Figure 14. Soil-structure interaction factor proposed for the 1976 Uniform Building Code (from Seed, 1975). The site period is approximated by the relation $T_s = \frac{4H}{\beta R}$ where H is the depth of soil over bed-rock, β is the average shear-wave velocity of the soil layer as measured under low-strain conditions in the field, and R is a correction factor to allow for the reduction in shear-wave velocity when the soil is excited by high-strain ground motion during an earthquake.



STATION NAME	ABBREV.	DISTANCE (KM.)	AZIMUTH FROM EPICENTER TO STATION	PEAK ACCEL (g)	PEAK VEL. (cm/s)
HOLIDAY INN	HOI	20	197	0.27	30
GLENDALE MUNI BLDG	GMB	32	154	0.28	28
3838 LANKERSHIME	3838	30	172	0.18	15
GRIFFITH PARK	GOC	33	164	0.18	20

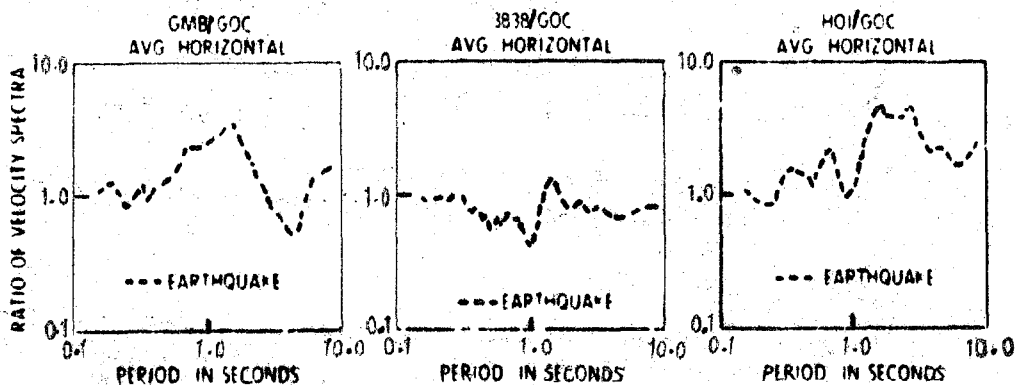


Figure 15. Horizontal site transfer functions derived for sites in the San Fernando Valley from accelerograms of the 1971 San Fernando, California earthquake. All transfer functions are calculated relative to Griffith Park Observatory (GOC). HOI is Holiday Inn, 3838 is 3838 Lankershim, and GMB is Glendale Municipal Building.

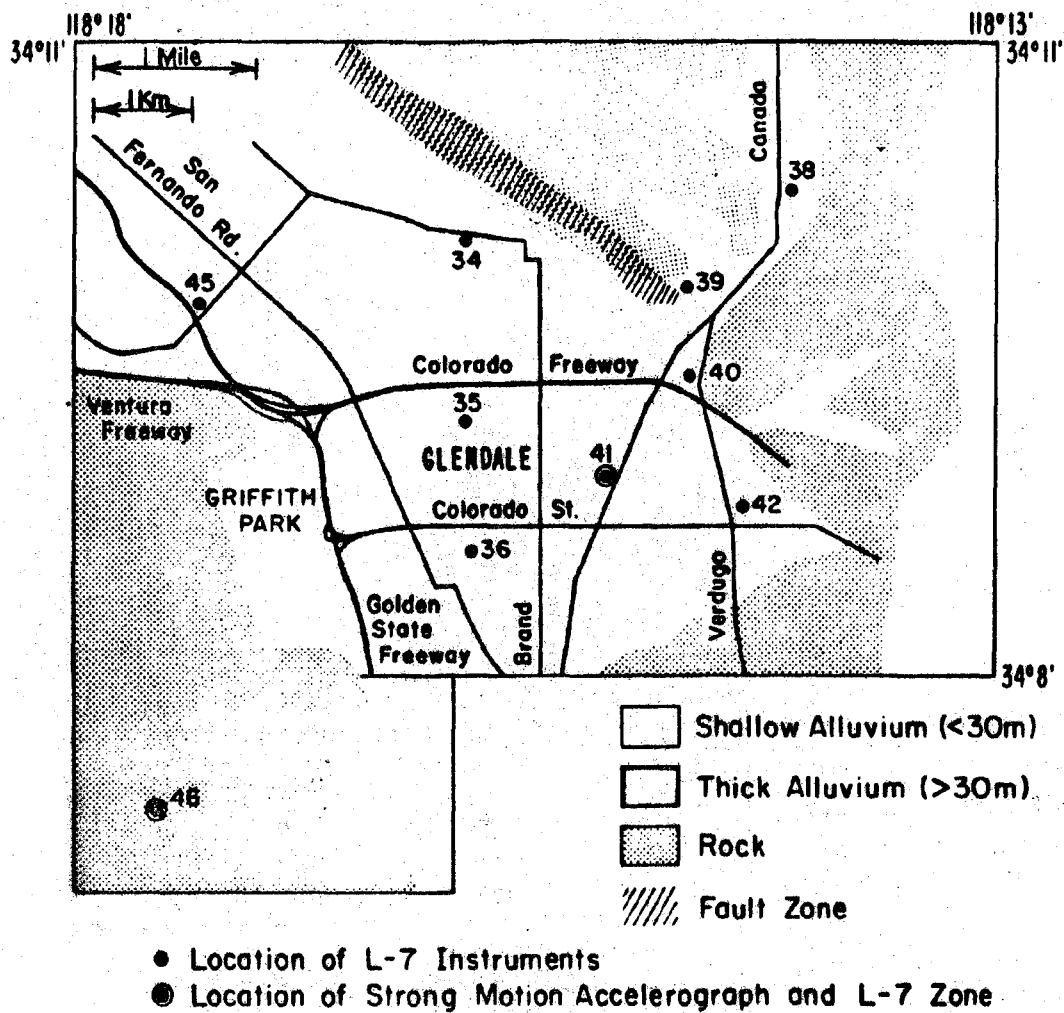


Figure 16. Generalized surficial geology and location of seismic array, Glendale, California area. Stations 46 (Griffith Park Observatory) and 41 (Glendale Municipal Building) recorded the main shock and aftershocks, all other stations recorded aftershocks only.

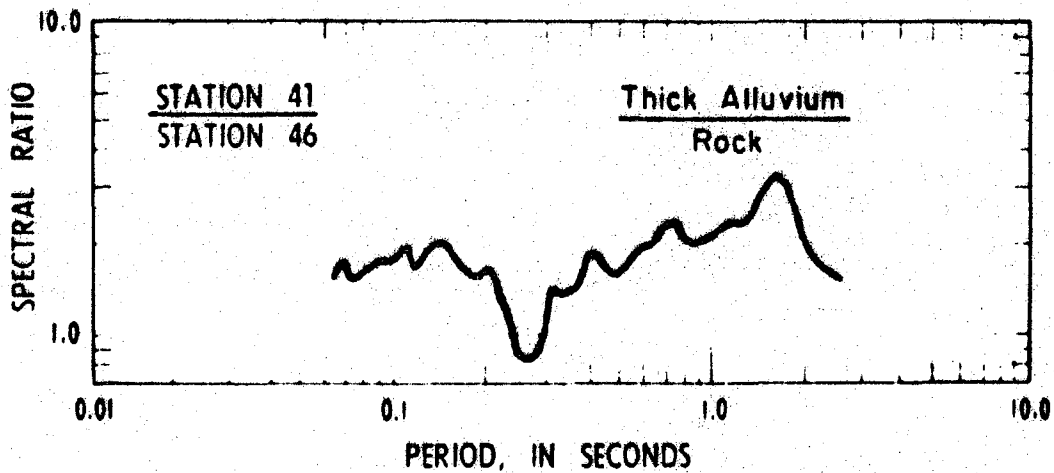
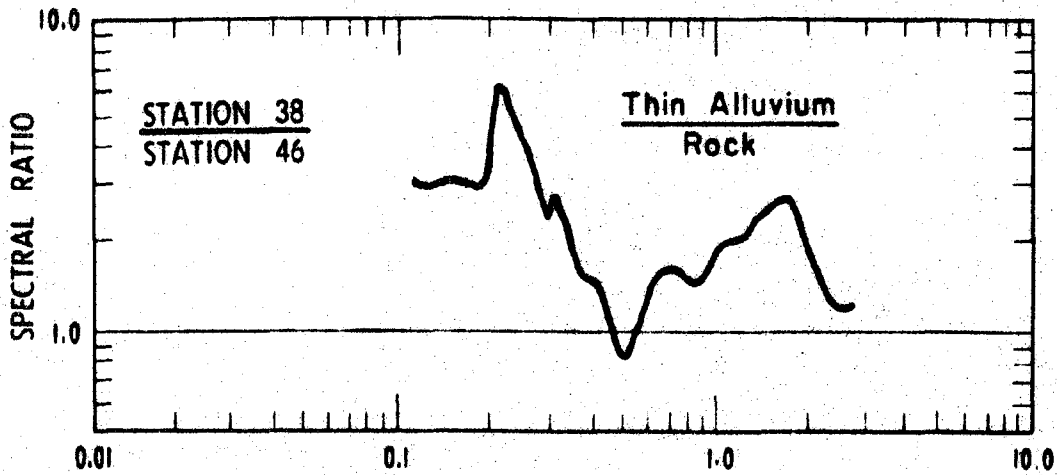
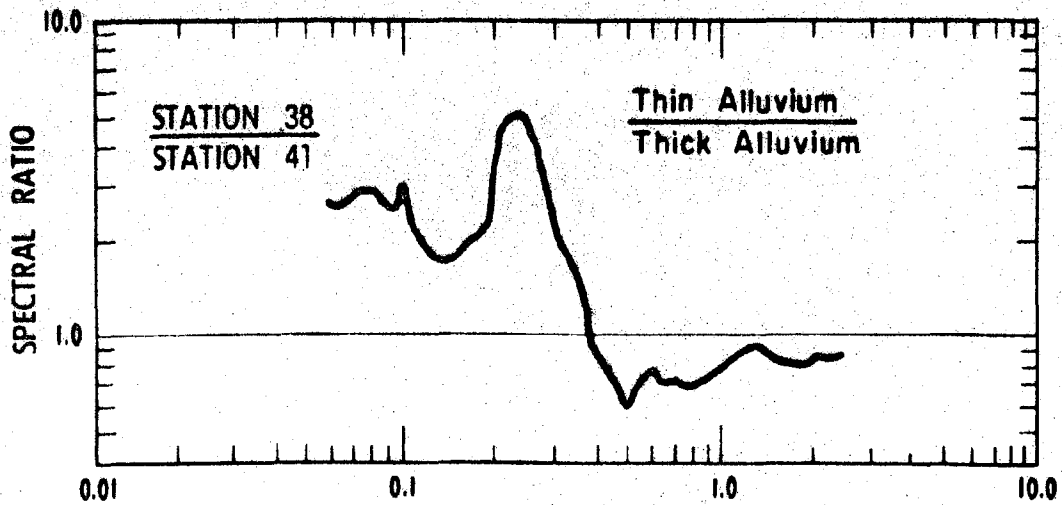


Figure 17. Average horizontal component transfer functions for sites underlain by thin alluvium relative to thick alluvium (top), rock (center) and sites underlain by thick alluvium relative to rock (bottom), Glendale, California area.

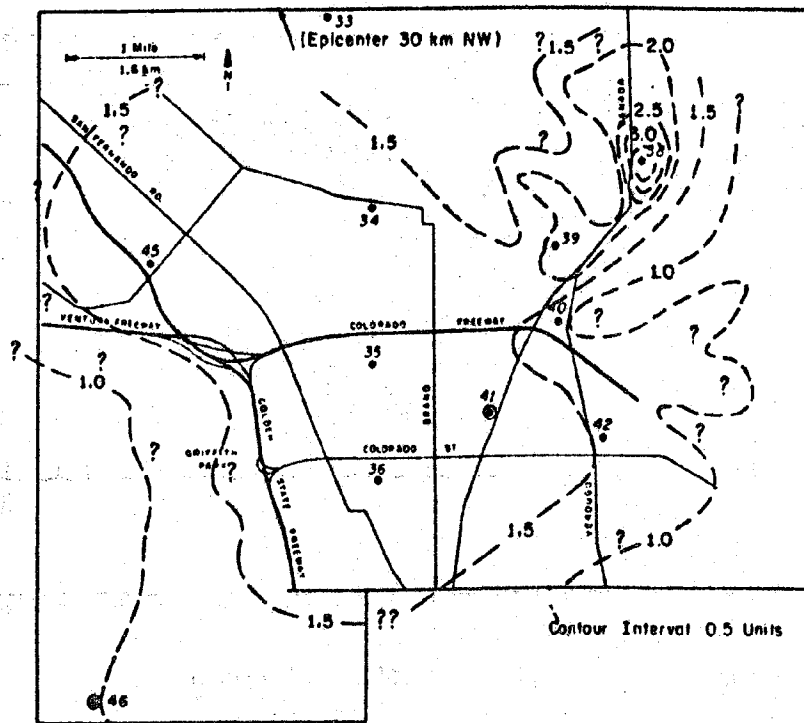


Figure 18. Generalized contour map of horizontal ground response relative to rock, 0.055-0.16 second period band; Glendale, California area. Ground response is in terms of spectral velocity and was derived from the horizontal transfer functions.

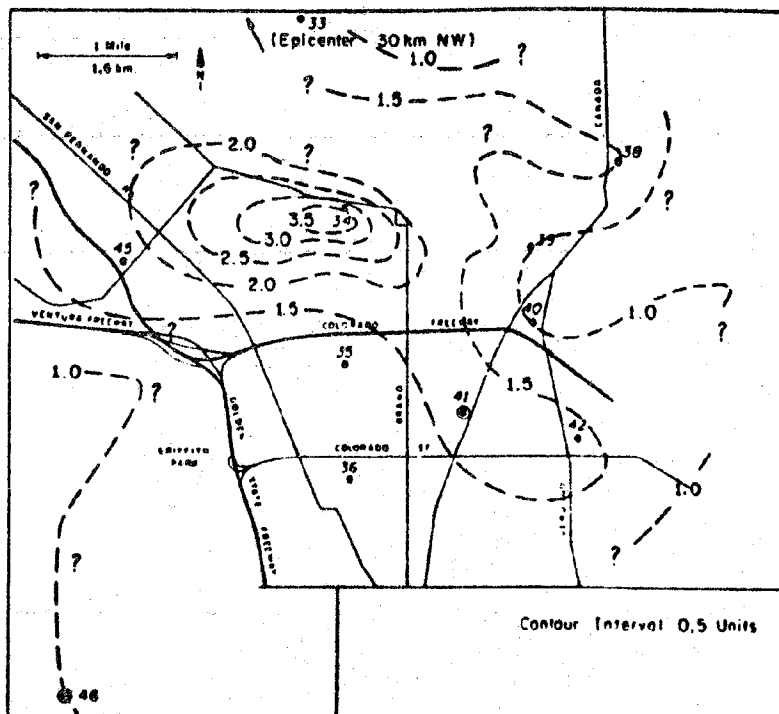


Figure 19. Generalized contour map of horizontal ground response relative to rock, 1.8-2.5 second period band; Glendale, California area. Ground response is in terms of spectral velocity and was derived from the horizontal transfer functions.

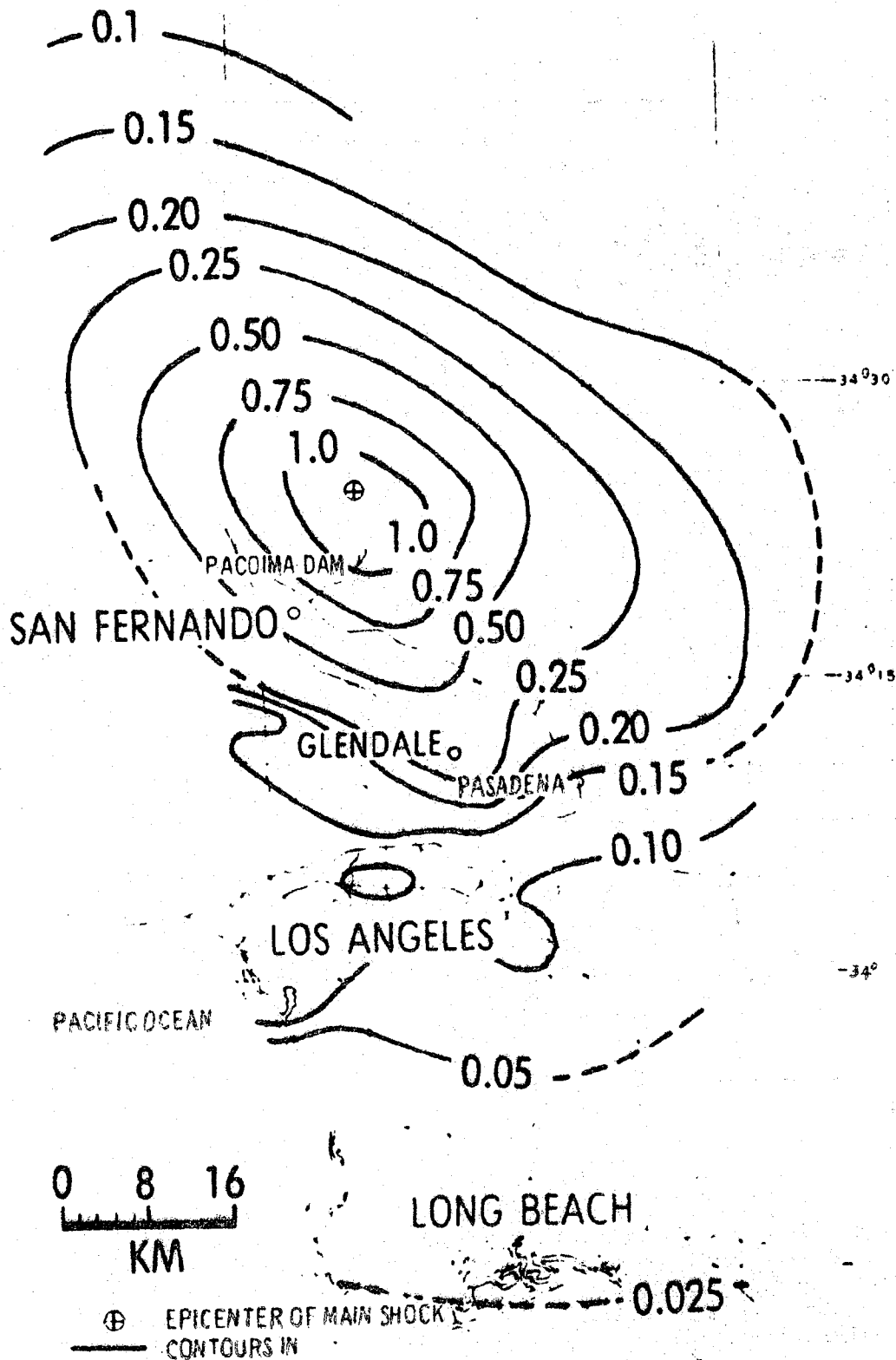


Figure 20. Map of peak ground acceleration derived from celerograms recorded in the 1971 San Fernando, California, earthquake.

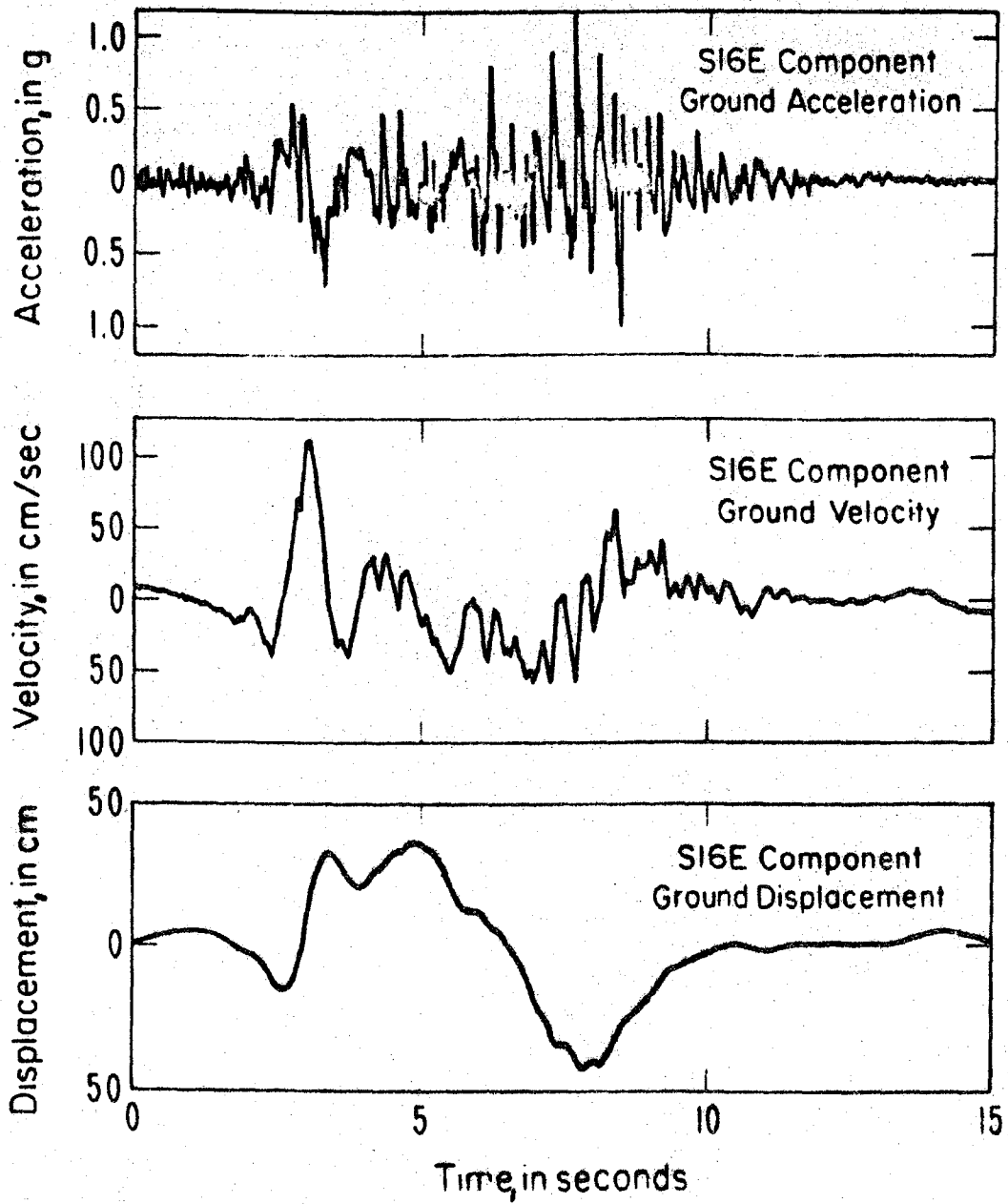


Figure 21. Accelerogram recorded at Pacoima Dam and the velocity and displacement records derived from it. 1971 San Fernando, California, earthquake. The peak acceleration is generally attributed to the surface faulting which occurred during the earthquake.

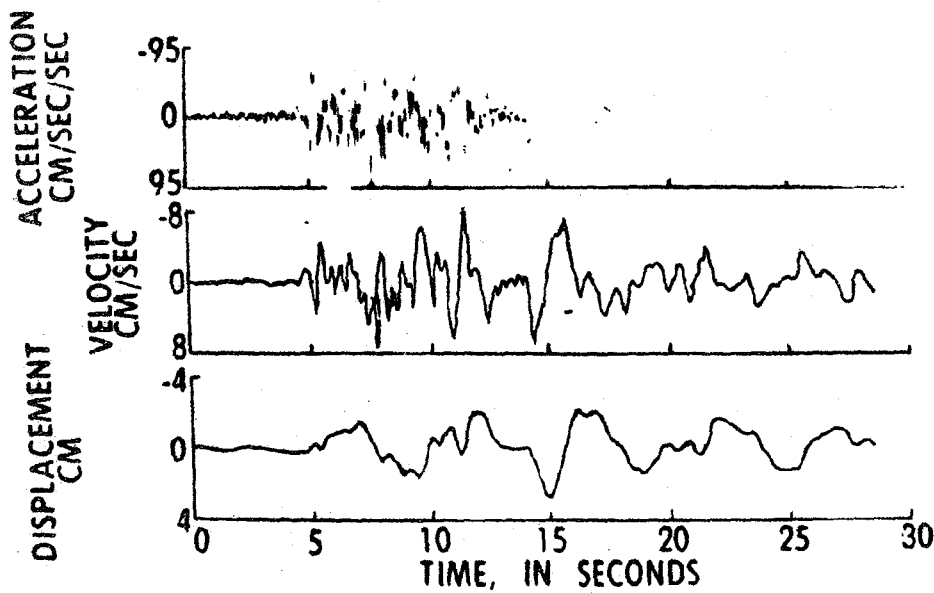
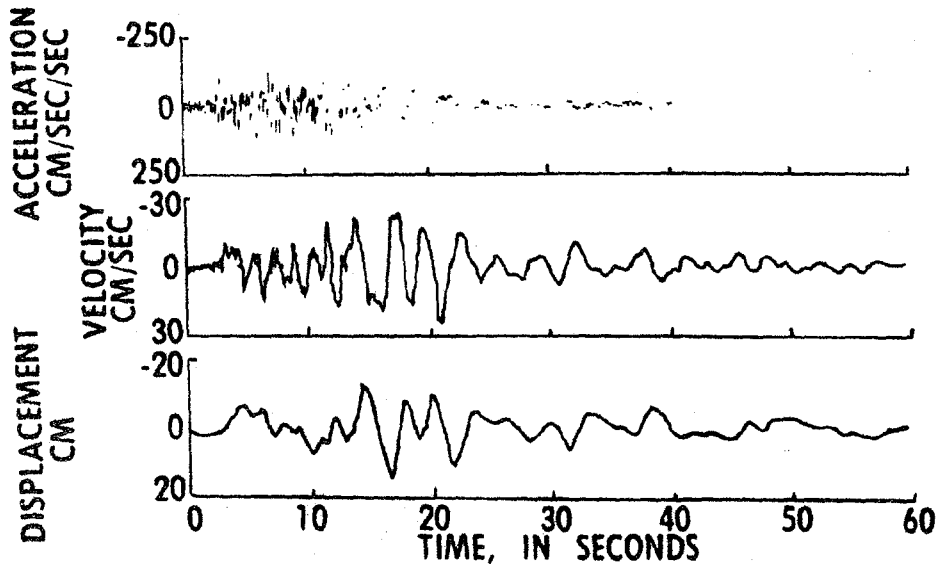


Figure 22. Accelerograms recorded at Holiday Inn (top) and California Institute of Technology Athenaeum (bottom) and the velocity and displacement seismograms derived from them, 1971 San Fernando, California, earthquake. The peak velocity occurs in the surface wave time window.

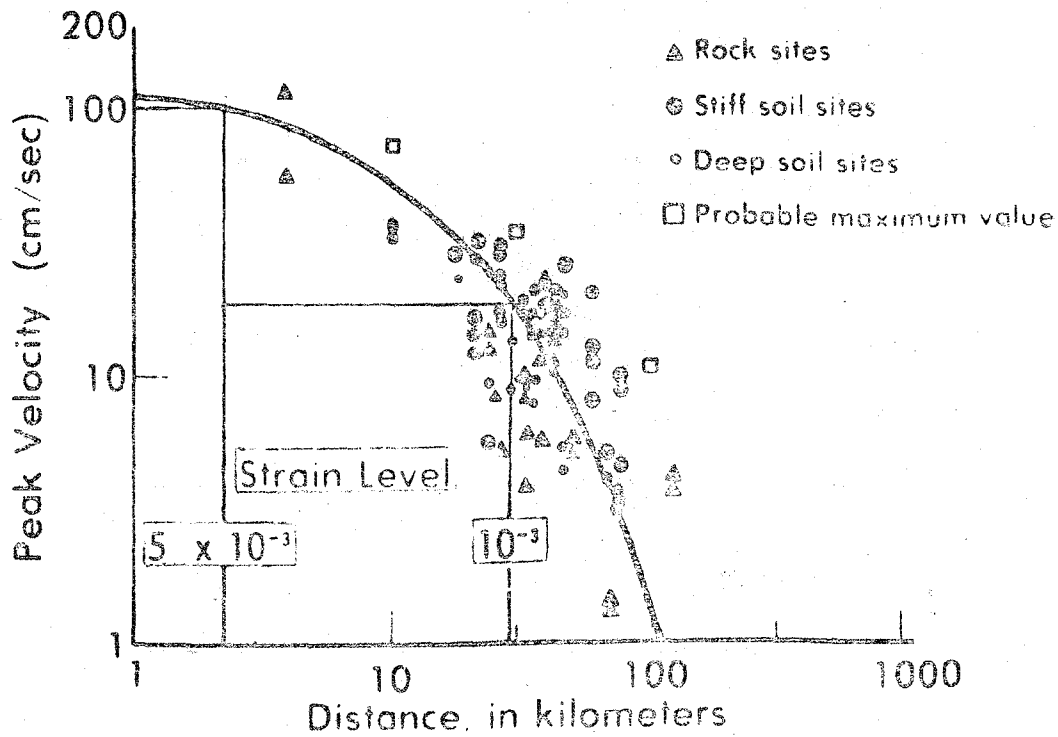


Figure 23. Estimate of the epicentral distance to various levels of dynamic shear strain. The attenuation curve for peak velocity is from Seed and others (1976). The estimated level of dynamic shear strain is obtained by dividing the value of peak velocity by 200 m/sec, a value of shear-wave velocity representative of stiff to hard clay and silty clay in the San Francisco Bay region.

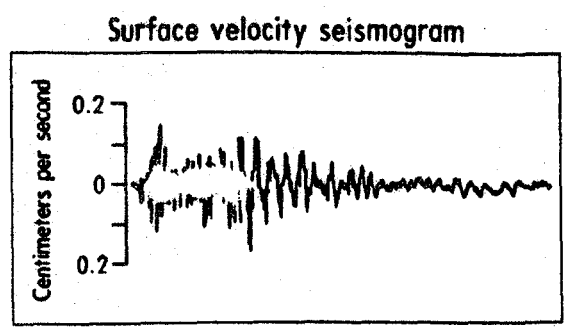
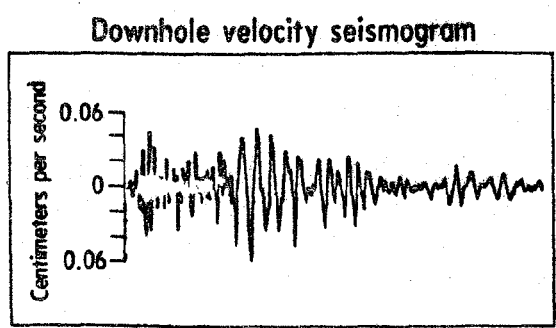
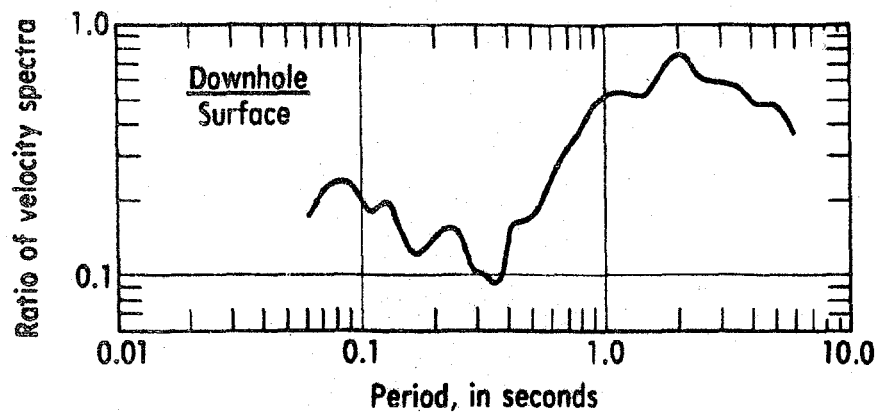
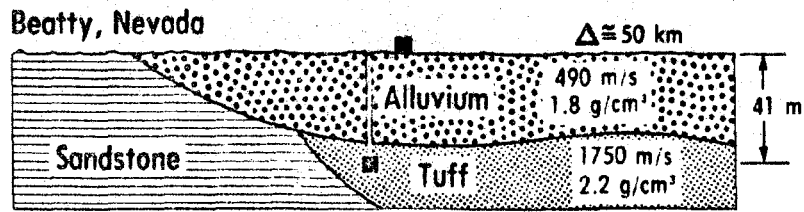


Figure 24. Variation of ground motion with depth, Beatty, Nevada. The mean transfer function was derived from explosions.

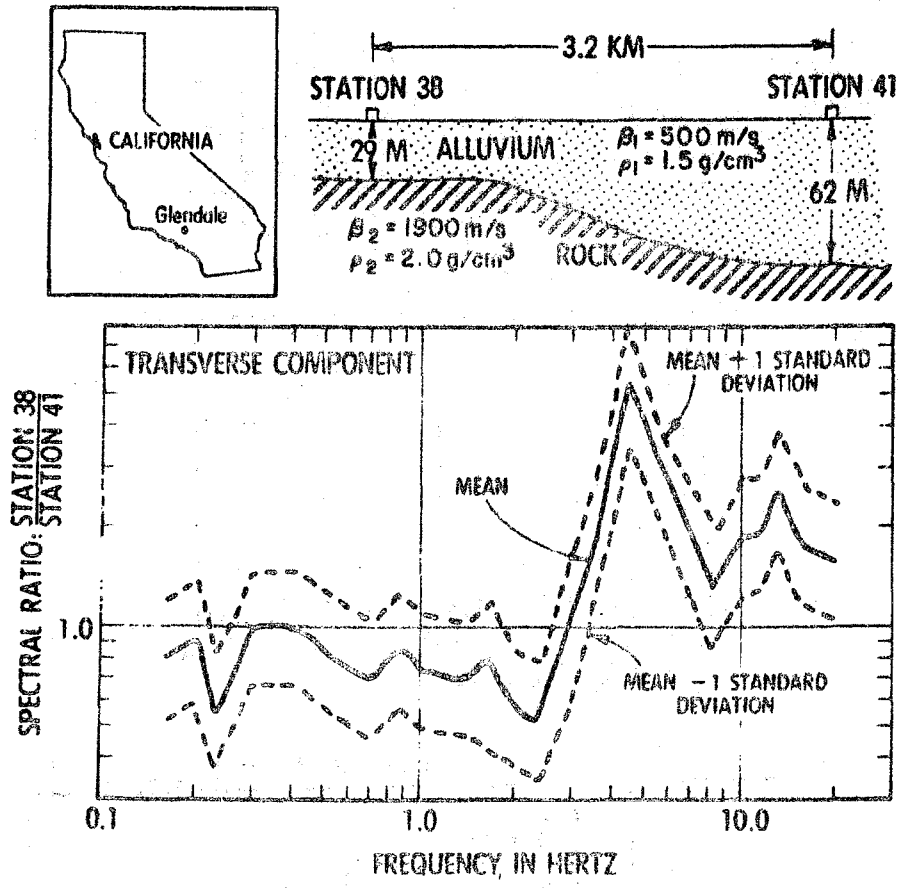


Figure 25. Uncertainty of mean transfer function, Glendale, California. The standard deviation is 1.50.

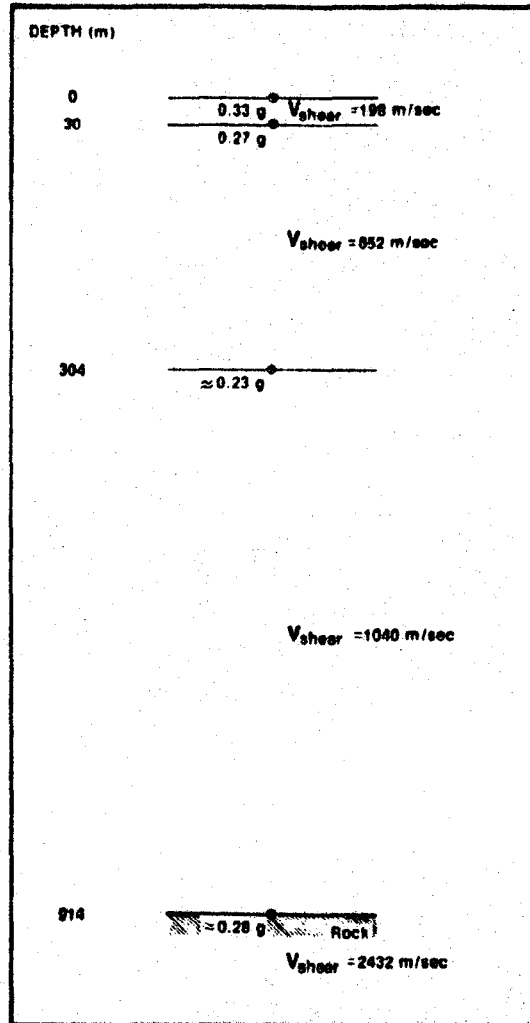


Figure 26. Model of the El Centro, California, site.



A METHOD OF SIMULATING EARTHQUAKE
GROUND MOTION BY EQUIVALENT BLAST EXCITATION

ZHANG XUE-LIANG¹, HUANG SHU-TANG¹

SYNOPSIS

By comparison of the dynamic response characteristics of building structures under earthquake and blast excitations, a method is suggested to generate an equivalent blast shock with various frequency, amplitude and duration of action, which will produce same effect on structural response, as an earthquake with expected intensity. This method can be used not only for the study of structural response characteristics, but for the study of various factors, such as ground soil and topography etc., affecting earthquake ground motion in the testing field as well.

INTRODUCTION

Various experimental method are useful for the study of dynamic response of building, ground soil and local topography etc. under earthquake excitation. First, it would be better to establish some strong-motion observation stations on various site condition and buildings located in the seismic active zone to acquire strong-motion seismogram. (1) (2) The negative feature of it is that we could not precisely predict magnitude, time and place of occurrence of future earthquake. Therefore, up to the present time, only a limited number of strong motion seismograms have been acquired in the world. On other words, it is independent of man's will. Second, we can make a survey of consequences of earthquake damage, and then with appropriate judgement we get an idea about the characteristics of earthquake damage.

¹ Seismological Bureau of Jiangsu Province.

Needless to say, the meaning is only in the qualitative sense, with the change of conditions, the conclusion is doubtful. and third, dynamic model test may be proceed using earthquake simulating shaking table. Though it has been widely used in earthquake engineering, the size and weight of tested model is always restricted by the capacity of shaking table, so it is very difficult to carry on a large scale model test, satisfying dynamic similitude. ⁽³⁾ What is more, to simulate local site condition and geographical topography. Blast induced ground motion has been employed to study the dynamic response of prototype and model at site, but the estimate is also qualitative, for it takes into consideration only the magnitude of blast induced ground motion. ⁽⁴⁾ Our method takes the advantage of desirable features of blast induced ground motion, and at the same time, we make account for frequencies, amplitudes and durations of action of blast shock, as all these factors affect the structural damages. Based on the fact, that the dynamical structure response is the same under earthquake excitation and blast induced ground motion, it is possible to generate an equivalent blast shock to simulate the earthquake ground motion. Using this method provides us possibility to carry out research work at site, not only we can study the behaviour of earthquake resistant structures, besides, we can get an idea how the local site condition affects the earthquake ground motion. The main concept of this method is described as follows.

PREDICTION OF INTENSITY OF BLAST INDUCED GROUND MOTION

There are a number of factors, which give influence on magnitude of blast induced ground motion, for example, charge size, burial depth of explosive, physical parameters of source, propagation path, local site conditions and epicentral distance etc. According to the observed results, with increasing charge size the induced maximum ground acceleration increases while with increasing dis-

tance apart from the epicenter, it decreases. Thus, an empirical formula can be expressed as follows. (5)(6)

$$a = K \left[\frac{\sqrt[3]{Q}}{R} \right]^\alpha \quad (1)$$

where

a --- maximum particle acceleration of ground motion (m./sec.);

Q --- explosive weight (kg);

R --- epicentral distance (m);

K, α --- constant, varies with local site condition.

Approximated values of coefficient K and α can be derived statistically from the data of observation, they are given below

hard bedrock	k=150,	=1.7;
medium bedrock	k=220,	=1.67;
shallow surface soil	k=300,	=1.6.

According to the formula (1), the corresponding earthquake coefficient of blast shock in the horizontal direction is

$$K_H = a/g$$

and accordingly, in the vertical direction is

$$K_V = K_H = a/g, \text{ for small epicentral distance;}$$

$$K_V = (2/3)K_H = (2/3)a/g \text{ for large epicentral distance,}$$

where

g --- acceleration of gravity.

CHARACTERISTICS OF BLAST INDUCED

GROUND MOTION

Design spectrum for blast earthquake resistant construction can be written as follows.

$$\begin{aligned} \beta &= 0.03/T^{1.5}, & T > T_m; \\ \beta &= 2.0, & T < T_m; \end{aligned} \quad (2)$$

damping ratio $\varepsilon = 0.05,$

where

T_m --- periods of the response spectrum at its peak value (sec);

β --- dynamic magnification coefficient;

T --- period (sec).

It is shown in the figure 1.

Compare the response spectra and Fourier spectra of blast induced ground motion with those of earthquakes, you can see they have the same characteristics. ⁽⁵⁾ Peak of blast response spectrum is very sharp and occur within the range of very short periods, more than 0.1 sec. spectral curve decrease rapidly with increasing period, and with periods more than 1 seconds, it tends to zero.

DISCUSSION OF THE METHOD

The damage of buildings is mainly related to frequencies, amplitudes and duration of action of the ground motion. But those factors of blast induced ground motion are different from that of earthquakes. Vibration frequency of the former is very high, the main frequencies of acceleration range from 15 to 30 Hertz; duration of motion from 0.3 to 2 second; the amplitudes of acceleration may approach even to 25.3g. A large blast of nearly one thousand tons causes damages only in the vicinity of it, and apart from the epicenter more than one kilometre are rarely damaged. What about earthquake, vibration frequencies of it range from 2 to 5 Hertz; ⁽⁷⁾ duration of motion is longer, sometimes it may approaches 40-50 second; ⁽⁸⁾⁽⁹⁾⁽¹⁰⁾ peak values observed acceleration is about 1.3g. A severe earthquake may cause damages up to several hundred kilometres. Experience indicated, when the maximum acceleration of earthquake ground motion exceed 0.1g (equivalent to grade of intensity), the buildings would be damaged to some extent. But only when the maximum acceleration of blast motion more than 1g, the buildings begin to accompany with light damage. This fact can be explained by their response spectra.

At the period of 0.2 sec., the dynamic magnification coefficient of blast motion is only 1/2.25 of that of earthquakes, and at period of 0.3 sec., only 1/7.5. The vibration of general engineering structures varies from 0.2 to 0.4 sec., therefore, this may be one of the reason why building structures can resist much higher value of blast induced ground acceleration. And besides, the dynamic strength of material of buildings may be increased under short period of dynamic loadings induced by blast shock. So the main differences of blast and earthquake ground motion consist in their different response spectra and their different period of action. According to this, we may design equivalent blast shock with corresponding frequency, amplitude and duration of action which will produce same effect on structural response as an earthquake with expected intensity.

The main idea of the method is described as below. Assume the building can be represented by a straight cantilever beam, dynamic response of the building can be obtained from response spectra. Apply the condition of equivalent damage, the artificial earthquake can be generated with equivalent earthquake intensity. The equation for determining it's parameters are given below.

1. Analysis of building damage under earthquake action.

Using response spectra, the inertia force corresponding to the j-th mode of vibration at point i is

$$P'_{ij} = K_H C_z \beta_j \eta_j X_j^{(i)} W_i \quad (3)$$

where

- K_H --- horizontal earthquake coefficient;
- C_z --- synthetical influence coefficient of structures;
- β_j --- dynamic magnification coefficient of j-th mode;
- η_j --- participation factor of j-th mode;
- $X_j^{(i)}$ --- amplitude of j-th mode at point i;
- W_i --- lumped weight of building at point i.

Total shear of building at point i

$$Q_i' = \sqrt{\sum_j \left[\sum_c K_H C_z' \beta_j' \eta_j X_j^{(c)} W_c \right]^2} \quad (4)$$

base shear

$$Q_o' = \sqrt{\sum_j \left[\sum_{c=1}^N K_H C_z' \beta_j' \eta_j X_j^{(c)} W_c \right]^2} \quad (5)$$

resisting shear strength of building

$$Q^o = [\tau] F \quad (6)$$

where

$[\tau]$ --- allowed shear stress (kg/cm²);

F --- cross-section area of beam (cm²).

If the building is damaged due to shear, then at any point i, if

$$Q_i' \geq Q^o$$

failure will occur.

if

$$Q_i' < Q^o$$

but base shear

$$Q_o' \geq Q^o$$

or

$$\sqrt{\sum_j \left[\sum_{c=1}^N K_H C_z' \beta_j' \eta_j X_j^{(c)} W_c \right]^2} \geq Q^o \quad (7)$$

then failure just occurs at the building foundation.

At the critical state of failure, we have the equation

$$K_H' = \frac{Q^o}{C_z' \sqrt{\sum_j \left[\sum_{c=1}^N \beta_j' \eta_j X_j^{(c)} W_c \right]^2}} \quad (8)$$

or

$$K_H' = \frac{[\tau] F}{C_z' \sqrt{\sum_j \left[\sum_{c=1}^N \beta_j' \eta_j X_j^{(c)} W_c \right]^2}}$$

If the material and type of structures is given, then the right hand side terms of equation(8) are known. If we take the ultimate dynamical strength of material, then

$C_z' = 1$, and we obtain the critical earthquake coefficient K_H' of building failure from the equation (8).

2. Analysis of building damage due to blast shock.

We just proceed in the same way, blast induced inertia force of the j -th mode at point i is

$$P_{ij} = K_H C_z \beta_j \eta_j X_j^{(i)} W_i \quad (9)$$

shear of building at point i

$$Q_i = \sqrt{\sum_j [\sum_i K_H C_z \beta_j \eta_j X_j^{(i)} W_i]^2} \quad (10)$$

base shear

$$Q_0 = \sqrt{\sum_j [\sum_{i=1}^N K_H C_z \beta_j \eta_j X_j^{(i)} W_i]^2} \quad (11)$$

If shear failure occurs, and the base shear

$$Q_0 \geq K Q^0$$

or

$$\sqrt{\sum_j [\sum_{i=1}^N K_H C_z \beta_j \eta_j X_j^{(i)} W_i]^2} \geq K Q^0 \quad (12)$$

then the failure occurs at the building foundation,

where

K is the coefficient introduced, considering the increased dynamic strength of material.

3. Determination of equivalent blast shock.

Coefficient K can be obtained from equation (12)

$$K = \frac{K_H C_z N \sqrt{\sum_j [\sum_{i=1}^N \beta_j \eta_j X_j^{(i)} W_i]^2}}{Q^0} \quad (13)$$

or

$$K = \frac{K_H C_z N \sqrt{\sum_j [\sum_{i=1}^N \beta_j \eta_j X_j^{(i)} W_i]^2}}{[Z] F}$$

On the right hand side of equation (13) all terms are known, except the horizontal earthquake coefficient of blast

β is dynamic magnification coefficient of blast motion, obtain from design spectra for blast earthquake. If the ultimate dynamic strength of material has been taken, then $C_z = C_z' = 1$. If the blast and earthquake causes identical damage to the buildings, then we have

$$Q_0 = KQ'_0$$

or

$$\sqrt{\sum_j [\sum_{i=1}^N K_H C_Z \beta_j \eta_j x_j(\omega) W_i]^2} = K \sqrt{\sum_j [\sum_{i=1}^N K_H' C_Z' \beta_j' \eta_j' x_j(\omega) W_i]^2}$$

After rearrange the terms, we get

$$K_H = \frac{K K_H' C_Z' \sqrt{\sum_j [\sum_{i=1}^N \beta_j' \eta_j' x_j(\omega) W_i]^2}}{C_Z \sqrt{\sum_j [\sum_{i=1}^N \beta_j \eta_j x_j(\omega) W_i]^2}} \quad (14)$$

Using the formula(14), we can design equivalent blast ground motion with various frequencies, amplitudes and duration of action for any given earthquake intensity.

EXPERIMENTAL STUDY

The proposed method has been used for stability analysis of an earth dam Xingwangzhuang of Anti reservoir in Shandong province. The main instrument used is RDZ-1-12-66 type accelerometer which is of self-triggered electro-magnetic type with 12 channels. Wide frequency range of linearity (0.5-80 Hz[±]10%), adjustable sensitivity (0.5-10gal/mm), 3 speeds of recording paper (2.1, 4.8, 11.3 cm/sec). Such instrument is especially suitable for measurement of ground motion with rather high frequency content and measurement of structure vibration where simultaneous recording at a number of points is required.⁽¹¹⁾ Two columns A and B of loam ramed in layers were used as standard models located 18 and 22 meters from the epicenter respectively. The dimension of columns is: cross-sectional area 51cm×71cm, height 4m. The attenuant curves of blast ground motion, the information of source and observed test data are shown respectively in Fig.2 and given in table 1,2.

After the action of blast, the columns obviously damaged due to shear. The cracks of columns cuts through the cross section at the base, the crack wide of column A is

about 3cm, while of the column B is very fine. A relative displacement existed at 2 metre height from the base of columns, which attains to a maxima values of 2.5cm and 1.5cm for columns A and B respectively. Nearby the base of columns there are vertical and horizontal cracks and falls of pieces of soil, at the lateral surfaces of columns observed fine cracks below the section 2m height from the base.

INFORMATION OF SOURCE

Table 1

Serial number of epicenter	No.2	No.3
Position of source	Horizontal distance from the axis of dam (m)	
	70	-80
	Altitude	
	153.503	157.027
Depth of source (m)	12	12
Ground water level (m)	164	166
Explosive weight (kg)	5	200
Volume of explosive room (m ³)	0.0072	0.30
Plugged length of well (m)	10.7	12
Explosive coefficient of concentration	14	24

Experience indicated that the damage of columns are due to shear. The column B is just at the critical state of damage, then the critical earthquake coefficient of column B can be obtained from the equation(8), where right hand side terms can be obtained from the later formula. Since the columns damaged mainly due to shear, only the shear deformations of column would be taken into consideration. The j-th periods of column is

$$T_j = \varphi_j H \sqrt{\frac{P}{gG}} \quad (15)$$

where

- φ_j --- coefficient reflected the period of j-th mode;
- H --- column height (m);

g --- acceleration of gravity (cm/sec^2);

ρ --- weight of material of per unit volume (kg/m^3);

G --- shear modulus.

From the reference (12), we get

$$\varphi_1 = 4.48; \varphi_2 = 1.49; \varphi_3 = 0.895.$$

According to the test data at site, we take

$$V_s = \sqrt{\frac{G}{\rho}} = 200 \text{ m/sec}$$

substituting in the equation (15), first three periods can be calculated as follows

$$T_1 = 0.0286 \text{ sec}; T_2 = 0.0095 \text{ sec}; T_3 = 0.0057 \text{ sec},$$

corresponding mode shapes can be obtained from the reference (12).

Based on the test data, the dynamic strength of material can be raised 50% than the static value, and finally we get

$$\begin{aligned} Q^0 &= 1.5(CF + Wtg\phi) \\ &= 1.5(1.0 \times 0.51 \times 0.71 + 2.46 \times 0.23) \\ &= 1.4 \text{ t.}, \end{aligned}$$

where

C and ϕ is coefficient of friction and viscosity respectively, the magnitude of which gets from test. If we take the ultimate dynamical strength of material, then $C'_2 = 1$, substituting in the equation(8), we obtain

$$K'_H = 1.4 / 3.798 = 0.37$$

that is which the column B approaches damage of 9 grade of intensity. Substituting the observational maximum value 4.42g of acceleration at the base of column B into the equation(13), we get

$$K = \frac{K_H C_2 \sqrt{\sum_{j=1}^n [\beta_j \eta_j X_j(\omega) W_i]^2}}{Q^0} = \frac{4.42 \times 1 \times 2.407}{1.400} = 7.6$$

After getting the values K , we can calculate the earthquake coefficient of blast shock from the equation(14) for designed equivalent blast ground motion with expected seismic intensity.

For example, if we simulate an earthquake of 8 grade of intensity, that is $K'_H = 0.2$. From the equation(14), we obtain

$$K_H = \frac{K K_H' C_N \sqrt{\sum_{j=1}^N [\sum_{i=1}^M \beta_i' \eta_j X_j(i) W_i]^2}}{C_N \sqrt{\sum_{j=1}^N [\sum_{i=1}^M \beta_i \eta_j X_j(i) W_i]^2}}$$

$$= \frac{0.2 \times 7.6 \times 3.798}{2.407} = 2.4$$

Table 2

MAXIMA VALUES OF OBSERVATIONAL ACCELERATION

Serial number of test points	Serial number of seismometers	Position located	Peak values of acceleration		Epicen- tral dis tance
			Harial (g)	Verti- cal (g)	
1	04	A base	6.5		18
1	06	A top	1.45		18
1	277	A base		5.31	18
1	254	A top		3.45	18
2	05	B base	4.42		22
2	07	B top	1.67		22
3	08	Ground	4.3		30
4	09	"	3.2		42
5	10	"	1.48		58
6	11	"	1.42		73
7	12	"	0.727		100
8	13	"	0.548		146
	04	Top of dam	0.141		72
	05	Toe of dam	0.276		55.2
	06	Ground	0.358		34.7
	07	"	0.300		42
	08	"	0.171		56.8
	09	"	0.184		63.6
	10	"	0.104		72.4
	15	"	0.025		212.5

This is an example for simulating earthquake ground motion by equivalent blast excitation of instantaneousness,

but the duration of motion is short. We can adopt the blast delayed time interval in the vicinity of sections for increased duration of blast ground motion. The duration delayed time interval can be determined as follows

$$t_m = 0.23C - (R_{i+1} - R_i) / V_s, \quad (5) \quad (16)$$

where

0.23 --- mean duration of main vibration of blast ground motion;

C --- constant ($C=0.5-2.0$), varies with charge size;

R_{i+1}, R_i --- distances, source O_{i+1}, O_i to detector.

APPLICATION IN REGIONAL SEISMIC ZONING

The proposed method can be used to study individually those factors which affect the ground motion characteristics, such as mechanism of source, propagation path and local site condition etc. It can also be used to study the repeat of effects of earthquake at the same site, coming from different equivalent blast shock; to study the rule of variational characteristics of site response with respect to propagation path and local site condition; to study the dynamic characteristics of ground soil under different deformation state of it, and so on. The test results can provide useful quantitative information for structural design and for regional seismic zoning.

The method needs verification in practice and further improvement, so as to better reflect the ground motion characteristics at the site.

ACKNOWLEDGEMENT

The authors wish to thank Engineers Li Jun-chun and Li Minggo for their great support to complete the experiment at site. Useful suggestions by Professors Wang Guangyuan and Lin Gao are gratefully acknowledged.

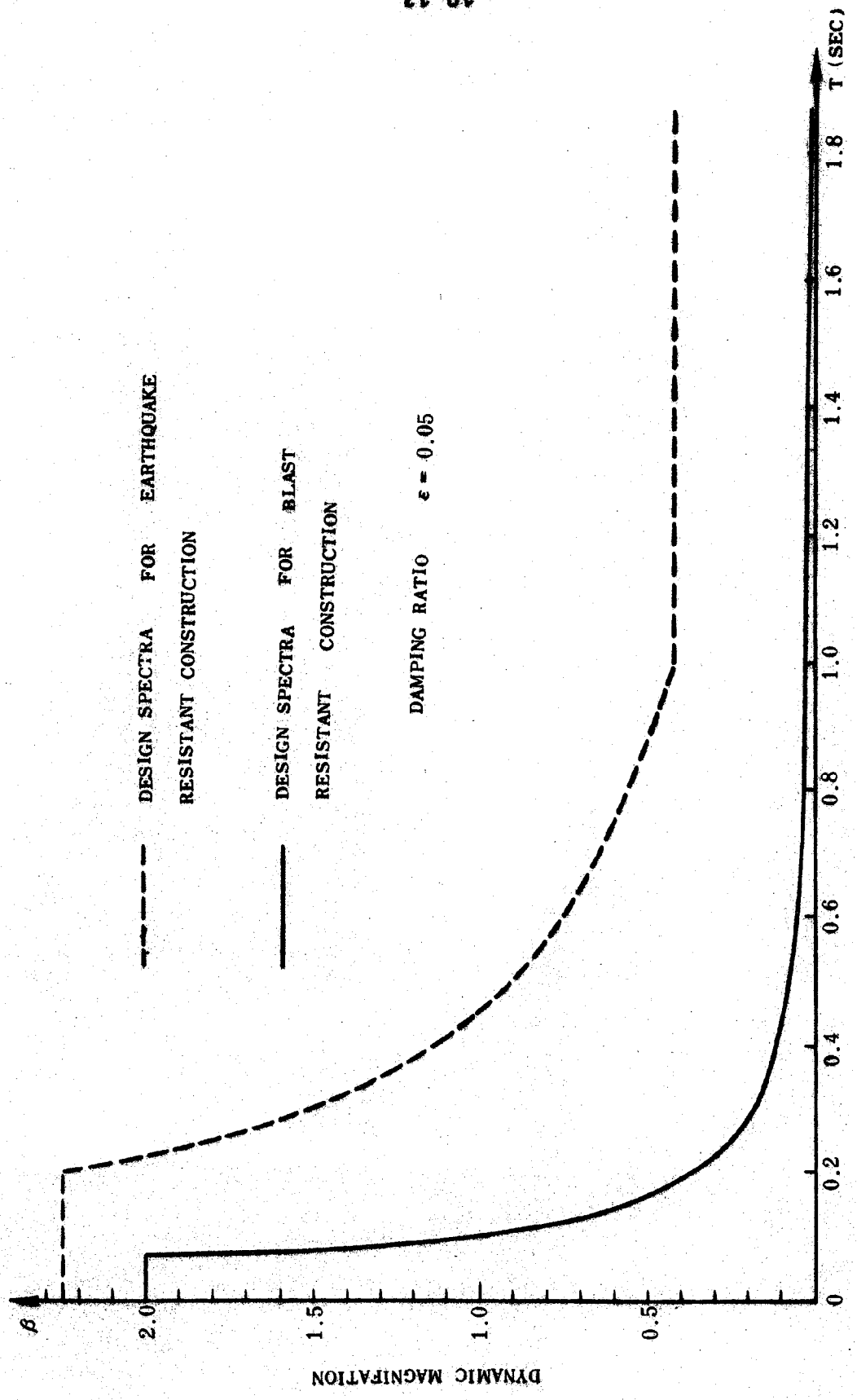


FIG. 1 RESPONSE SPECTRA

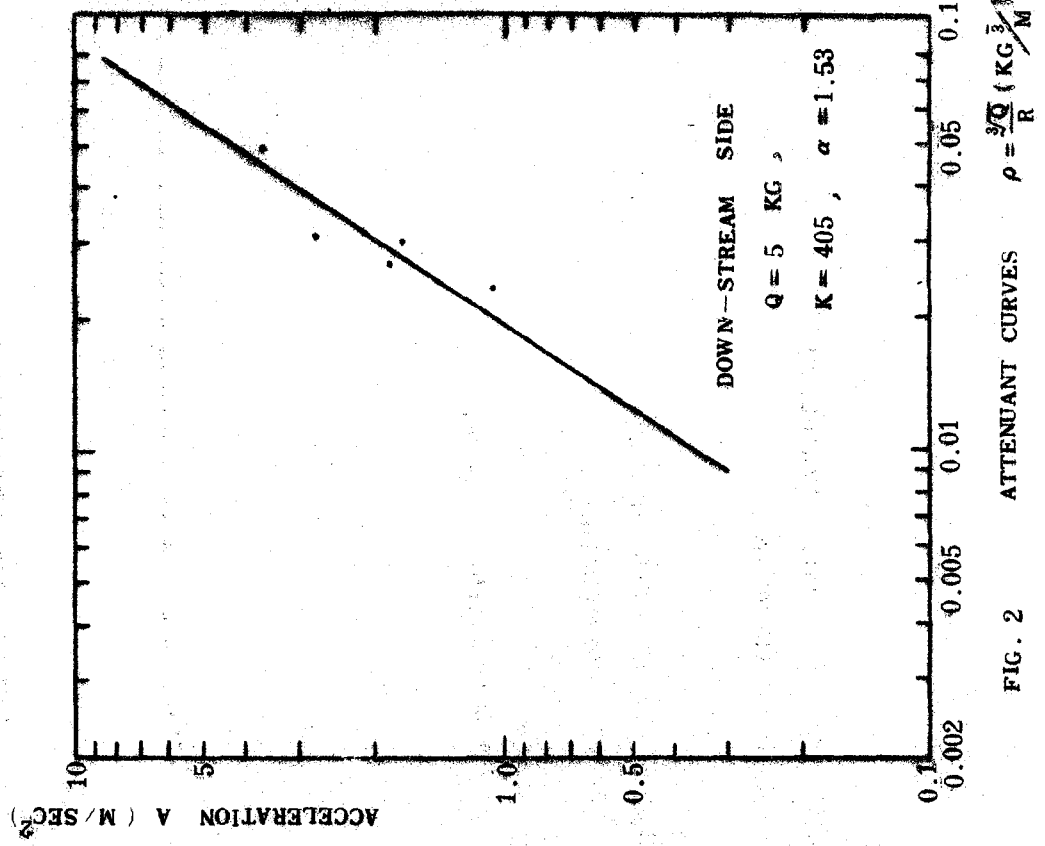
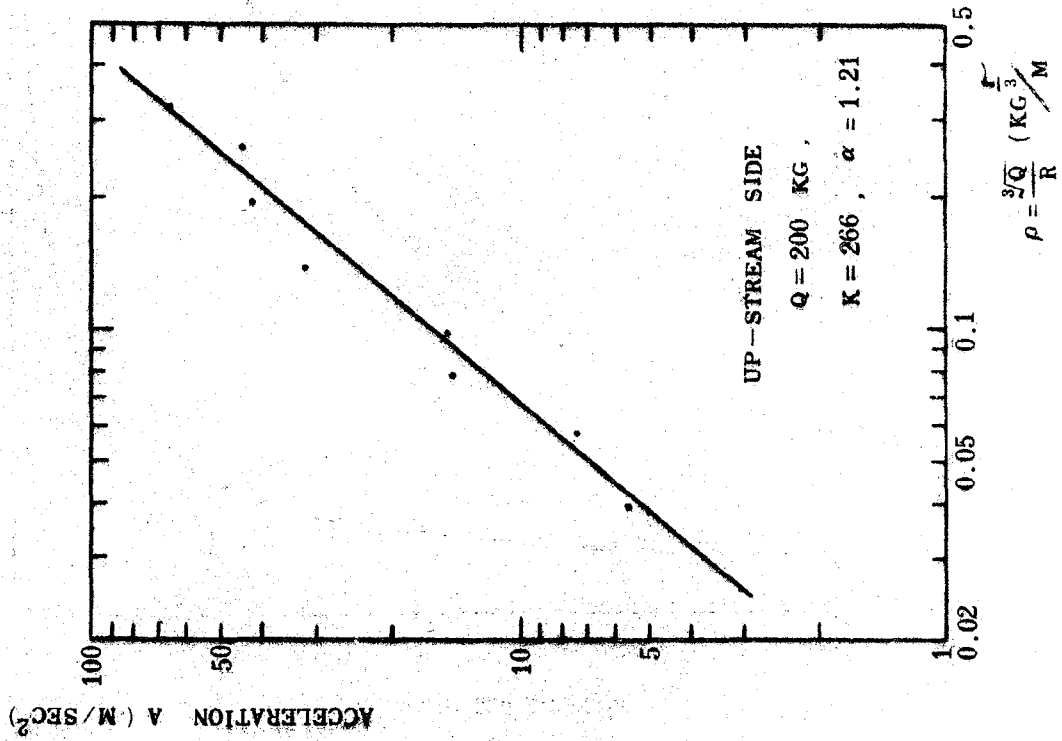


FIG. 2 ATTENDANT CURVES

REFERENCES

- (1) Zhang Xue-Liang, Yan Xin-Yu, etc: "Analysis of seismic response and earthquake resistant behavior of Nanjing Yangtse River Bridge", unpublished report, Seismological Bureau of Jiangsu province, 1978.
- (2) Robert, L. Weiegel: "Earthquake engineering", Prentice-Hall, INC., 1970.
- (3) J. Penzien, J. G. Bouwkamp, R. W. Clough, Dixon Rea: "Feasibility study large-scale earthquake simulation facility", Sep. 1967, College of Engineering University of California, Berkeley, California.
- (4) Tonghai group, section of earthquake resistant structure: "Field investigation of damage to adobe dwellings in Tonghai area and their experimental study", Collected papers of earthquake engineering, Institute of Engineering Mechanics, Academia Sinica, Vol.3, 1977.
- (5) Zhang Xue-Liang, Huang Shu-Tang: "Effects of blast earthquake", Seismology Press, 1981.
- (6) Liu Hui-Xian: "On the concept and application of earthquake intensity", ACTA Geophysica sinica, Vol.21, No.4, 1978.
- (7) Chen Da-Sheng, Lu Rong-Jian, Xie Li-Li: "Design spectra for earthquake resistant construction", Collected papers of earthquake engineering, Institute of Engineering Mechanics, Academia Sinica, Vol.3 1977.
- (8) Sarjit S. Saina, Jai Krishna, Anjur R, Chandrasekaram: "Behavior of Koyna dam, Dec. 11, 1967 earthquake", Proc. of ASCE, Jour. of the str. div. July, 1972.
- (9) D. A. Bolt: "Duration of strong ground motion", World conference on earthquake engineering, 5-th, Rome.
- (10) M. D. Trifunac and A. G. Brady: "A study on the duration of strong earthquake ground motion", BSSA. N.3 1975.
- (11) Huang Zheng-Peng, Huang Shu-Tang: "RDZI-12-66 strong motion accelerograph and its field calibration", Col-

lected papers of earthquake engineering, Institute of
Engineering Mechanics, Academia Sinica, Vol.3, 1977.

- (12) Zhang Xue-Liang, Yan Xin-Yu, etc: "Earthquake resistant
calculation of hydraulic structures", Seismology Press,
1978.

USING AIR REMOTE-SENSING TECHNIQUE IN STUDY OF
TANGSHAN EARTHQUAKE HAZARDS AND HAZARDS MICROZONING

ZOU XUEGONG *

I..Introduction

Seismology is to a great extent a science of experiment. Great earthquake in constant occurring has advanced the science of seismology. Man's knowledge of earthquake begins with the field inspection of the damages caused by earthquakes. The study of in-situ and abnormal catastrophe has promoted our understanding of the seismic science. Ours is a country with frequent shocks, having plenty of historical records on earthquakes, which supplied us, as early as 3000 years ago, with precious materials in researching on China's earthquake.

However, these materials are too simple compared with those got from a great earthquake area nowadays. In the meantime, we are unable to see back the on-site conditions of the time. Up till now we can not even catch the all-round conditions of the site for the limitation of our eye-sight in the inspection of the damages caused by an earthquake. Mallet wrote in "the Great Neopolitan Earthquake of 1857: The First Principles of Observational Seismology" : "When an observer first enters upon one of these earthquake-shaken towns, he finds himself in the midst of utter confusion. He wanders over masses of dislocated stone and is appalled by spectacles of desolation. It is only by gaining some commanding point, whence a general view over the whole field of ruin can be had, and then by patient inspection of many details of overthrow, that we at length perceive once for all that the apparent confusion is

* Earthquake Research Institute , State Seismological Bureau.
WuChang China

but surficial."

In order to find a "commanding point" which suits the inspection of any field hit by shock and directly takes down the actual spectacle of an earthquake, aerial photo is introduced into use in the investigations of earthquake damages.

The first world aerial photo for the purpose of examining earthquake damages might have been taken by G.R. Lawrence^[1], when the April 18, 1906 earthquake took place at San Francisco. His camera was as heavy as 1000 pounds and was carried up as high as 600 m by a balloon-kite with some auxiliary instruments, a photo taken in size of 1.35x2.4^M as a result.^[2] Afterwards with the development of aerial navigation and photography, a few pictures were taken after some earthquakes in the service of partial catastrophe caused.

It was not until 1940s that the aerial photo used for the purpose of inspection of earthquake damages on a large scale in a certain area developed gradually. Directly after the 1949 Fukui earthquake, a photo was taken by the U.S. Army with the scale from 1:5000 to 1:10000. And an investigation on damages on the ground surface was made at the same time by the Geographic Survey. On June 16, 1964 a Magnitude 7.7 shock hit Niigata aerial photo was carried out above the Niigata Akita regions. Over 150 pictures were got, different scales from 1:22000 to 1:25,000 included. At the same time infrared photo was also taken.^{[3][4]} In 1964 the United States photographed the Anchorage area after the great Alaska shock, scale 1:6000.^[5] We began our aerial photo in Xingtai area when it was struck in 1966. Later on we accumulated a lot of materials on the basis of taken pictures from the air in Haicheng, Lungling and Tangshan, and so developed our skill to some extent.

On speaking of the value gained through aerial photo on earthquake damages Takahashi said: "We have left precious records for our descendants." As a matter of fact, owing to its accuracy and dexterity, aerial is an important means to offer

us with necessary information on shock damages on site. This has solved concerned problems met by Mallet in his investigation of Neopolitan shock and some other recent earthquakes. And what is more, aerial photo has very high geometrical accuracy and can be scrutinized clearly. The spectacle taken in goes close to that in an earthquake that occurred in a flash and information can reach us very soon in a wide range. Even if the field has been recovered, we can still carry out research on the shaking conditions that are rich and instantaneous. For this reason aerial pictures would become the basic materials for us to see the damages and abnormal and make further study of earthquakes.

The interpretation of aerial pictures on shock damages shows the advantages of aerial photo in the investigation of earthquake hazards. Takamasa of Tokyo University spoke at the Japan-American Earthquake Predication Conference, saying "The aerial photo interpretation is very useful to the analysis of damages caused to the ground objects. Earthquake damages can be divided into a) ground deformation, b) ruins of buildings, factories, bridges, roads, embankments etc. c) flood in low-lying areas (including those below the sea level) d) combination of the three or less mentioned above. All these can be gained through the interpretation of aerial photos ." He thought this method not only useful but also defined the contents of earthquake damages. Such classification certainly is not perfectly good. For example, conflagration is not an original disaster caused by an earthquake but a secondary one. Therefore this method of classification might not be suitable for other places than Japan to which it is good. However this does not negate the wide use of the interpretation of aerial photos.

Nowadays investigations are mostly carried out qualitatively about earthquake hazards, while quantitative investigations are seldom made. The significance of analytical investigations was clearly proved after the April 1906 San Francisco

earthquake by N. R. Reid's analysis of the survey lines of both sides across San Andres faults and by his "elastic rebound hypotheses" of earthquake genesis. But it's a pity that little has been done in this respect in the heavily shocked areas. Regular aerial photo and the method of analytical survey make it possible to do quantitative analysis of the ground deformation in these areas. As mentioned above the analytical photo trigonometric survey taken after the great Alaska earthquake is one of the instances of quantitative deformation measurement. However their conclusion did not run out of the scope of photographic geodesy, not in good combination with geography, geophysics and geology so as to be able to work out any seismic analysis.

In accordance with the experience gained after the great Xingtai earthquake, we carried out some aerial photo survey drawings and interpretations on Tangshan event. In fact we have really done much more with this than with any other shock occurrences home or abroad, either in scope, content, quantity or in the results we have got so far. What we have done has much to do not only with aerial photo survey and drawing science but also with aerial remote-sensing technique. Therefore our work in Tangshan is actually an experimental investigation of aerial remote-sensing on the earthquake hazards which occurred there. We have finished the analysis of earthquake abnormality on the basis of this resulting materials.

II. BASIC MATERIALS

1. Aerial photography

The great Tangshan earthquake took place on July 28 1976. In order to get for a wide investigation various information and materials on the event and have the ruined regions soon recovered, we began our aerial photo directly the following day. The area; about 15700 square kilometers, for photo was divided into two parts: Tangshan survey region (east longitude $117^{\circ}30'--119^{\circ}00'$, north latitude $39^{\circ}05' - 40^{\circ}05'$) and Tianjin

survey region (east longitude $117^{\circ}03'45''$ - $117^{\circ}30'00''$, north latitude $39^{\circ}05'$ - $39^{\circ}15'$), covering almost all the area within the intensity VIII isoseismal.

The cameras were Swiss Rc-8 and Soviet AFA-T9 type, photo scales 1:20000, 1:15000, 1:10000 and 1:5000 respectively. The films were black-and-white, infrared black-and-white and infrared falsecolour. The repetition of flight course 60%, The repetition of transversal course 40%, the oblique angle not over 2° - 3° . More than 140 lines were passed and over 11200 aerial pictures were got. Thermo-infrared sweep photo was also taken.

2) Unrectified mosaic and controlled photomosaic

The aerial photo over we made up the following mosaic rough drawings at free distribution: four for Tangshan and one for Guye with scale of 1:5000, 344 for the whole survey area with scales of 1:10000, 1:15000 and 1:20000. For comparison we also compiled a rough drawing of Tangshan before the accident, scale 1:14000.

During the make-up we applied three methods in revising the control point, of which the best is our using electronic computers to tighten the netlevel difference in the aerial delta area. We use four methods to correct the mosaic, among which the optic came best in result. For the whole area 494 photo plane view drawings were made with identical 1:10000 scale.

3) The interpretation of earthquake damages

We carried out two interpretations, one being for compiling maps of damages, the other executed on the basis of studying large quantity of fundamental materials. The former was done mainly to show the original data of earthquake damages taken in and interpreted on the aerial pictures, while the latter done for the research on the earthquake hazards. Here mainly the former is discussed.

The phenomena shown by earthquake damages appear in many ways, containing very intricate contents. In order to meet the need for study of earthquake engineering and geognosy, damages

to the ground objects and the ground surface are considered to be the main contents in general. The damages to ground objects refer to the state and intensity (percent) of deformation, ruin, and collapse of buildings, communications and hydraulic projects, etc, including fissure, mountain avalanche, landslip, water spurting with sands, collapse and the block of the rivers, and the displacement of natural ground objects. All these can be taken down by means of aerial photo if with comparatively large scale.

The interpreting of photo was carried out line by line and picture by picture, by using the cubireflective mirror or some other interpreting instruments to magnify the pictures, with the interpreted contents marked on the pictures so as to be offered for drawing.

4) The maps of seismic damages

With the old map for reference, making use of the aerial photo plane view drawing and the result of interpretation, we made up the "1976 Tangshan Earthquake Map", 641 in all, scale 1:10000, printed in four colours. The ground objects were repaired and measured through the interpretation of the earthquake damage pictures, and the ground appearance was drawn from the old map. The contents of the map came mainly from the 1:10000 type of drawing published in 1974 by the State Survey Bureau, some symbols being added according to the damage contents. This helped us analyse the seismic abnormal.

III. SEISMIC HAZARDS AND ABNORMALS

There are different media conditions, earthquake force function and geological structures in the earthquake area. So the phenomena of damages are different and various. The correct understanding and division of the damages and abnormalities are the pre-conditions in studying an earthquake. Therefore it is vital to have an all-round investigation of the macro-seismic damage phenomenon. As a general rule this can be achieved at present by field inspection. This time we appli-

ed the remote-sensing method, which proved to be much better, making richer the contents of macroseismic study. We are to deal with such problems in the following pages as water moving out with sands, ground fissure, house falling etc, caused by earthquakes. All these can be clearly seen in the aerial photos with a wide range, being typical enough in the macroseismic earthquake hazards.

1) Water moving up with sands

This is one of the main phenomena of the damages to the ground surface. Tangshan had a wide spreading of water-saturated sands during its shaking, ranging from the south foot of Yan Mount to the beach of Bo Hai sea. Owing to the difference in ground surface and the extent to which the shaking reached, various distributions were found. We will discuss as follows:

A) the characteristics of distribution

We had four divisions classified according to the damage extent and its density. The first division showed that quantity of water-saturated sands covered the ground widely, in striped form, close, making a serious disaster. It presented white or greyish color in the aerial photo, differing greatly from the color of ground objects around. It appeared much clearer with its fresh color in the infrared false colored photo, there being intensive color difference. This was distributed across alluvium-deluvium delta of Luan River. The second division showed a better condition with water-saturated sands covering some parts of the area. It was grey-white or white-scattered on the photo's view. Its distribution lay in the central part of the area shocked. What is worth mentioning is that in the south-east of this division there were, along the ancient or the present river courses, a number of sandy-closely covered belts, going in the direction of north-north-east. Five of them looked clearer, forming the five first-division abnormal belts in this part. The third being much better with small sandy plots or belts scattered here and there, spreading mainly on the south-east part of the area. The fourth division

was the region shocked slightly. It was of separate, striped small areas, spreading mainly over the regions along the present rivers and the basins between the hills.

B) the form of water moving up with sands and the combine form

In study of the forms we divided them into two classes: the basic form and the combine form. The basic referred to the basic unit forms in this division such as circular, striped. The circular form appeared in the pictures as white circle, or near-circle with different dimensions; while the striped were clearly seen in the forms of broad stripes, which consisted of one single or more than one stripe. This might possibly be the passages formed during the sand liquifaction into cracks where water had spurted out with sands, with relation to the ancient river courses. The combine was the combination of basic ones formed under different topography. For example, there appeared at times something like grids on the ridges and slopes. In history there happened to have some zones of fan-sharp with sediment, caused by the burst of river banks, taking the shape of striped brooms. In the pictures they were clear enough with the upper part narrow and the lower spreading out. The narrow part was a single line, while the wide part put on the shape of an arc spreading outward along one side, not getting across a single length of line, sometimes along both sides, but still never getting across a single length of line, each keeping on one side respectively. They took round forms along the ancient river courses and in the zones near the modern river's turning. The picture showed grey color to the ancient river beds and a bright white color to the water-saturated sands. In addition, we found some areas taking the forms of rings, which might be the remainders of the ancient lakes, still unknown to us.

To sum up from the above, we have this moving up of water with sands divided into two large parts, that is, basic and combine, including six forms: circular, striped, gridded,

broomed, curved and ringed. It is the distributions of rivers and ancient river courses and the geographic characteristics that have effects on the formation of each state.

C) the type of moving up

As can be seen from the aerial photos, there are different colors to the moving up of water with sands, its change ranging from the bright white color to the dark grey. It looks much clearer with the infrared false colored photo, on which we can see the color changing from bright white to light blue or light green, the former having an obvious contrast in colors, while the latter appearing muddling. They cover the ground objects to different extents. With the former, all the low ground objects are covered completely. But the latter only goes along the objects, such things as fields, ditches etc. still in clear vision. Therefore according to the color intensity, we have got three types:

a) spurting type: the most intensive

b) overflowing type: rather intensive

c) saturating type: the least intensive, in which water can be seen, but no damages to the sandy ground.

The cause for forming these three types perhaps come from liquifaction extent of the sandy ground. This shows varieties of damages affected by the shaking force under different places and geograph.

2) ground fissure

In order to study the process of seismic mechanics, ground fissures are generally divided, in the investigation of ground surface, into tectonic fissure and non-tectonic fissure or original and secondary. The fissures caused for the loss of gravity in the secondary fissures are called the gravity fissure by some people in engineering investigation, such as fissures on the highway slopes, river banks and mountain bodies, owing to the loss of gravity caused by earthquake force. Some are called wet fissures for there are water-saturated sands rising out of. Contrary to them are dry fissures. Wet fissures

can be interpreted through the moving up of water-saturated sands. The aerial photo gave a clear sight with this. Dry fissures can also be scrutinized by interpreting within a certain limit. For example, the fissures along the rivers and highways on both sides of the Victory Bridge are clear enough. But sometimes because they are too small to be scrutinized, they can only be known through the displacement of the ground objects along both sides of the fissures. However if there is too little of displacement, and no obvious distinction on the colors, it would be a little difficult to interpret. Here we will discuss some of those fissures comparatively big enough in sizes, and clear enough to be seen in the photos.

The area in which fissures gathered is approximately similar to that with water-saturated sands scattered, ranging from the east part --- including Huili, Macheng Luannan, Leitong to the west --- including Tangshan, Gaozhuangtze, Jiubaihu, Guma, Shiaoji. Moreover, a few of scattered fissures could be found in the survey area.

The shapes and formations of the fissure came in various forms. They may be taken as follows: A) the shape of a single line, B) of a curve, C) of oblique arrangements, D) of parallel arrangements, E) of brooms, F) of semi-circle, G) of radiations. Among these, the dry fissures of oblique arrangements are of greater significance to the analysis of ground motion and the development of earthquake mechanism. For example, fissures in Luann district, Tangshan, were found arranged from north to east, with long extension. On the whole construction of the formation, there was an obvious distinction between the east part and the west part, the east part taking the shape of a petal, which surely has something to do with the successive changes of the Luan River. In the east part, no obvious distinction could be seen except for in the north section of this part. But there was regular destination along both sides of the present and ancient river courses.

3) the collapse and ruin of house buildings

This is one of the disasters brought by an earthquake. The investigation and research on the buildings shocked down can, in an earthquake, in turn, to promote the knowledge of some of the seismic specialities. The building damage is one of the main contents to define the criterions of intensity in making up macroseismic isoseismal map. Owing to the wide spreading of buildings in the earthquake area, it becomes the typical speciality in reflection of the earthquake, and the basis in study of the ground motion and the earthquake engineering. Because of the enormous effects caused by a great shock and lots of the inhabited points, it is rather difficult for us to get to know the conditions in time of some of the shocked areas, and we have even greater difficulties in knowing of those with their ground badly damaged. Similarly, it requires great efforts to get all-round information about the building damages, especially in mountain and water areas. If a careful inspection should be done even to those regions where some recovery has been done, the method in present use is not good enough to adapt the research on instantaneous earthquake damages. For example, there is a limitation to the inspection of the earthquake occurred in the mountainous regions so as to reduce the effect of an earthquake research. Through this experimental research on seismic damage happened in Tangshan by means of aerial remote-sensing, we hold that the two mentioned problems have found the solution. This has proved to be nice and provided us not only with a true look of the whole region, but also with some data about the damages, on the basis of which we can carry out our research work at any time about the conditions close to the instantaneous earthquake.

a) House Isoseismal Map

According to the interpreting results of the aerial photo, we have got each percent of the house damage in all the inhabited points and marked it on the "1976 Tangshan Seismic Damage Map". But there are only separate and scattered materials which can be used for further research. We have studied and

regulated all the materials for the purpose of studying the characteristics and the laws of the earthquake damage distribution. And, in combination with visual results, we have compiled the "House Building Isoseismal Distribution Map" according to the data of the percentage of the house collapse, that is, the isorithm map of the house building collapse. In accordance with the different rates of percentage, we divided the damage, when analysing the basic materials, into nine grades, namely: over 95% , 85% , 70-75% , 60-65% , 50-55% , 30-40% , 10-25% , and all compiling the map, into four sorts, namely: the first, all collapsed, over 95%; the second, basically collapsed, 80-90; the third, mostly collapsed, 50-70%; the fourth, partly collapsed 30-45% and the fifth, few collapsed, 10-25% . The criterion of "collapsing" here or in the map is approximately equal to the extent of "turning over" and "being completely fallen down" in the New Chinese Intensity Scale. The house types are one-story or multi-story buildings as seen in towns and countries, such as adobe house, wooden, brick-and-stone etc. The large types of buildings are not included in this division.

The House Isoseismal Map shows the specialities of distribution of the damages to house buildings in the earthquake area and gives the same effect as got from the earthquake iso-intensity map.

b) the comparison between the House Isoseismal Map and the Intensity scale

The "Tangshan Earthquake Isoseismal map" compiled by the Tangshan Seismic Crew after its macroseismic study is a result of large quantity of field inspection. It has the same advantages as the previous map, the diagram being brief, the intensity lines smooth and regular, the superior direction of the long axis in the epicentral region prominent and there being some zones with high and low intensity. If we compare the two maps with each other, and give the correspondance between each grade of various sorts of damages and intensity, then we can see: the first sort correspondent to eleven degrees:

the second to ten ; the third to nine; the fourth to eight; the fifth to seven. It can be found from the comparison that in the regions where they have corresponding damages their geographic locations and the range they cover are almost the same. But the outlines of the range differ greatly. Some numbers of regions with abnormal difference in height, their locations and outer range do not go in complete accordance. These distinctions require further study. However, the reason might be that the number of the resident points and the collapse percent got from the interpretation of the aerial photo are much bigger than those from macroseismic study. That is to say, the house isoseismal map might possibly offer more damages and details of some abnormal phenomenon so as to make the diagram of the isorithm more complicated. But on the other hand, to be closer to the true conditions is also possible. Therefore, putting the method of the interpretation of the aerial photo into the use of examining earthquake damages has its own advantages, being able to satisfy the needs of seismic survey in an ideal way.

Here we have an additional matter to make clear. The seismic destructiveness in Luan Count Region, because of the repetition of two shocks, has reached the first sort of seismic damage according to the interpretation of photo aerial. The intensity map has this classified into nine degrees on the basis of Mag. 7.8. If making a comparison between the first classification and degree nine, then we will find that the locations of south and north parts are corresponding on the whole, while there is a great difference in the west part.

In conclusion, using the interpretation method of aerial photo to divide the house damage and to compile the map of damages is an effective technique in the investigation of earthquake damages and in study of the seismic characteristics. This has created a new technical way for the research work on seismic damages, although there are some limitation existing. For example, there are quite a lot of factors influencing the

damages of house buildings. But at present we think it to be no other factors than the result of the earthquake force that effects. Thus the destructive characteristics got are only general macroseismic ones. Through the study of the effecting factors and the treatment of the results an ideal achievement would be obtained in applying this kind of new technique.

4) microzonation of seismic damages

We haven't so far got a method of the microzonation of earthquakes in unison in our country. It was usually measured according to the experience of earthquake damages in a destructive earthquake and some physical quantity. At present, the macroseismic characteristics are shown mainly by the intensity map. This passable in the way to the ordinary earthquakes. But in description of the damages that occur in large industrial cities like Tangshan with dense population. It is impossible to completely describe the correct characteristics of the damages, while neglecting a certain of rich phenomenon of earthquake damages is on the other hand possible. Furthermore, accurate experience couldn't be afforded, which is needed to the small zoning of the big and middle cities. So it is necessary to make research work on microzonation.

In doing this, we must classify the damages which form the small units of the area for research. For instance, we had better try to get a knowledge of each factory, street, district or even each of the house ruined in the shock. Only in this way, can we get a better foundation for our research. Here we will meet two difficulties. One is too much work to do, many hands needed. The other is the limitation of time, for we have to finish the survey in a very short time, otherwise we fail to catch the real conditions of the instantaneous shock after its recovery. The longer the time the less actual conditions we would get. Then the materials got in hand would be of little significance, with even the result of giving some conclusions so as to mislead our research work. And if we do this by relying on our hands in carrying out the field inspection,

that would be much more difficult or even impossible. In order to solve this problem we have taken the experimental division on a few of Tangshan's typical seismic instances by means of the materials of aerial photo. The microzonation of the whole city will be discussed in another paper.

We chose the following damage phenomenon for the interpretation and research in our work: the buildings of all sorts in a factory; the collapsed or semi-collapsed civil houses and buildings of other sorts; the river bank sliding motion; ground fissures; highways, railways and bridges etc. The results were good enough to be able to scrutinize easily all sorts of damages. Through the pictures of typical instances we could directly see the states of all sorts of earthquake damages. Because they are not uniform in the extent of being damaged and their spreading range different, using only one intensity level to show the damages in a heavily-shocked area could not meet the need for the further research of earthquake as well as earthquake engineering. It is therefore necessary to carry out the research on microzonation to satisfy the advanced research work.

Conclusion

Seventy-five years have passed since Lawrence took the first photo of earthquake damages in San. Francisco and it has been fifteen years since we began the interpretation of the aerial photo on Xingtai earthquake. With the development of seismology and the aerial photo technique, this new method has found its use in the research of earthquake. But owing to the limitation of some reason, it is still in the initial stage of experiment. Compared with the previous work, it is but a new try either in its scale, range, method, or the use and research of the materials. According to the good points mentioned above, it has proved to have more advantages than other means to use aerial remote-sensing technique in analysing and studying great earthquake destructiveness and some other abnormal phe-

nomenon in combination with some necessary field investigations.

The cause analysis mentioned in this article will be discussed at some other time. With the successive advance of seismology and aerial remote-sensing technique this new means will be used more and more widely and deeply in the study of earthquake. Nowadays, there is such a trace shown by the use of space satellite in investigation of earthquakes.

During the course of my writing this article I used for reference the following three reports that are not published: "Aerial Photo And Drawing Of Tangshan Earthquake" by Zou Xue-Gong, May 1978. "The Aerial Survey Drawing of Tangshan Earthquake And The Initial Study Of Seismic Damages" by Zou Xue-Gong, Chang Bu-Chun. "The Aerial Survey Drawing Of Tangshan Earthquake And the Interpretation of The Seismic Damages" by Zou Xue-Gong, Jiang Lin-Zhen and Jiang Chun-Ming. Jiang Lin-Zhen and Jiang Chun-Ming did a lot of work about the zonations of house damages and rise of water-saturated sands. Chang Bu-Chun and Chang Shi-Liang had been our cooperators with the job. To them I express my thanks here.

Mistakes are inevitable and any criticism or suggestion will be welcome.

REFERENCES

- (1) Robert G. Reeves: Manual of Remote-Sensing
1975. P.29
- (2) 马笥弘志: 新潟地震と photo Survey 写真測量
Vo/.3. pp115-118 1964
- (3) 高桥 博: 新潟地震災害調査レポート
空中写真の利用 写真測量 VO/.4
NO.3 pp.3-14 1964
- (4) 西尾元充 渊本正隆 新潟地震災害
航空写真撮影と調査計画 写真
測量 VO/.3 pp.110-114 1964
- (5) H.R.Crarat, V.Ralph, Aerial photogrammetric Crustal-Move-
ment Study at Anchorage. The Great Alaska Earthquake of
1964--Seismology and Geodesy, P.480, National Academy of
Sciences Washigton, 1972.

1945年10月

中華民國三十四年九月三十日
行政院令 公布 修正 國庫券發行辦法

修正 國庫券發行辦法

第一條 國庫券之發行，依本法之規定。

第二條 國庫券之種類，由財政部擬定，呈請行政院核定之。

第三條 國庫券之發行，應以中央公債為抵押。

第四條 國庫券之發行，應以中央公債為抵押。

第五條 國庫券之發行，應以中央公債為抵押。

第六條 國庫券之發行，應以中央公債為抵押。

第七條 國庫券之發行，應以中央公債為抵押。
第八條 國庫券之發行，應以中央公債為抵押。
第九條 國庫券之發行，應以中央公債為抵押。
第十條 國庫券之發行，應以中央公債為抵押。

USE OF AVERAGE WEIGHTED SHEAR MODULUS IN THE STUDY
OF SITE EFFECT--DISCUSSION ON THE CAUSE OF LOW INTENSITY
ANOMALY IN YUTIAN DURING THE TANGSHAN EARTHQUAKE

LIU ZENGWU, DONG ENCHANG, LU GENSHENG,
WANG DONGQIANG AND WEI PEIHENG

INTRODUCTION

During the 1976 Tangshan earthquake, an area of low intensity anomaly occurred in Yutian County, about 50 km in the north-west of the epicenter. It was an area of intensity VI enclosed in an area of intensity VII, it is not strange that there existed low intensity anomaly during at least two earthquakes in the past. In the 1679 Sanhe-Pinggu earthquake, the recorded damage in Yutian was obviously slight in comparison with the surrounding area. As for the two earthquakes mentioned, the Tangshan earthquake of $M=7.8$ located in the south-east of this area, while the Sanhe-Pinggu earthquake of $M=8$ located in the north-west, about 60 km away from this area. Magnitude and the epicenter distance to Yutian of these two earthquakes are similar, but the locations of epicenters are just opposite in direction, that means the existence of the intensity anomalous area in Yutian does not depend on the location of the epicenter and its direction. The cause of anomaly has resulted from the site characteristics. On the basis of boring and velocity measurement in the field, correlation of soil characteristics inside the anomalous area and outside to the earthquake damage is presented in this paper, using the average weighted shear modulus, G , as a criterion. Also, the cause of anomaly and the effect of the depth of soil layer on earthquake damage are discussed. In addition, reliability of microzoning, using the average weighted shear modulus, is testified by the field measurement data.

GENERAL FEATURES OF THE ANOMALOUS AREA
AND SELECTION OF MEASURING POINTS

The north part of Yutian County is near the mountain region, the overlying layer of which is thin and outcrop of bedrock occurs in some places. The overlying layer becomes thicker from north to south, the depth of the layer in the south exceeds 200 m. The topography becomes plain too. Soil layers consist of interbedding of clay, sand and sandy gravel. The soil in the north part and central part is more dense, gravel layer can be found up to 20-30 m near the ground surface, while the soil in the south is not so dense and the location of the gravel layer is deeper. The anomalous area consists of most parts in the north and the central part of Yutian County, forming a north-east zone with a length of about 30 km and a width of 10 km approximately (Fig.1).

In order to examine the soil layers in the area and find

out the cause of anomaly, 26 villages were selected for exploration. Boring was carried out in 13 villages inside the anomalous area and in the same number of villages outside that area, longitudinal and shear wave velocity in soil was also measured. Depth of the bore holes is generally 20-30m, some of which up to 40 m. Wave velocity measurement in a few boring holes was carried out only in a shallower depth owing to the collapse of the holes. Sample taken holes and standard penetration test were also performed to obtain the physical-mechanical properties of the soil in the area. Location of the measuring points is shown in Fig.1. Damage of the villages in Fig.1 is denoted by the damage index.

Downhole approach was used in the wave velocity measurement. Vibration was generated by either hammering wood plate (shear wave velocity measurement) or iron weight (longitudinal wave velocity measurement) on ground surface. Distribution of velocity of the longitudinal wave and shear wave with the depth of the bore hole was obtained. The instrument used was PS-5 seismoscope.

CHARACTERISTICS OF THE SITE SOIL

Relief in YUTIAN County is plain except in the north, which is near the mountain and the topography is complex, so the effect of relief on damage is small. Besides, Yutian is far away from the epicenter of the Tangshan earthquake, so the effect of epicentral distance can be neglected.

In the study of site effect during the Tonghai, the Haicheng and the Tangshan earthquakes, it is known that there is a good relationship between the average weighted shear modulus of the soil and the earthquake damage (Fig. 2-4). Therefore the average weighted shear modulus can be used as a criterion to measure the effect of soil.

The average weighted shear modulus is defined as:

$$G = \frac{1}{H} \sum h_i G_i$$

where $G_i = \rho_i v_{si}^2$ is the dynamic shear modulus of the i th layer, layer (ton/m²);

v_{si} = velocity of shear wave in the i th layer (m/sec);

H = effective depth of the surface soil (m);

h_i = thickness of the i th layer (m).

Based on the log diagram of the selected bore hole and the wave velocity data, average weighted shear modulus of soil layers of different depths (H) can be obtained from the above formula. The results and the corresponding damage indexes, are listed in table 1 and plotted in Fig. 5-7. Owing to the variation of the volume weight of the soil in the investigated

area is not so great (from 1.9 to 2.1 g/cm³), an average value of 2.0 g/cm³ is taken in the calculation for simplicity.

Table 1

	Name of villages	Wave velocity (3-5m)		Damage index	Average weighted shear modulus, 2×10^3 ton/m ²		
		V _s	V _p		G ₁₀	G ₂₀	G ₃₀
Inside the anomalous area	1 Mashanshi	181	410	0.16	17.4	21.8	22.4
	2 Xiaozhuangzhi	125	320	0.13	17.2	22.9	24.0
	3 Ershilipu	150	460	0.01	19.6	25.1	-
	4 Zhushuwu	117	278	0.03	23.6	27.4	-
	5 Shilituo	158	567	0.05	9.8	19.3	-
	6 North Liujia	114	267	0.20	11.8	18.0	21.3
	7 Neifuanzhuang	147	491	0.05	15.6	21.1	-
	8 Taizhangzhuang	129	550	0.01	-	-	-
	9 Jiajiapu	104	696	0.18	9.6	13.9	-
	10 Caitingqiao	188	300	0.15	11.8	14.9	16.8
	11 Xiaoshantou	210	714	0.11	24.6	26.5	28.2
	12 Houhudingfu	168	380	0.02	17.2	17.9	18.5
	13 Xiakan	161	356	0.04	33.8	25.3	24.6
Outside the anomalous area	14 Xiejiazhuang	168	456	0.40	20.0	23.2	27.4
	15 Maipo	160	638	0.46	8.4	15.9	18.9
	16 Huxiuzhuang	97	356	0.52	8.2	11.8	15.9
	17 Xiaoquan	145	400	0.29	16.2	-	-
	18 Nanchang	179	410	0.39	4.4	9.2	11.2
	19 Woluogu	111	356	0.49	4.6	8.2	10.5
	20 Zhuliao zhuang	100	400	0.62	2.6	8.7	12.2
	21 East Matou*	168	318	0.63	22.6	23.1	23.5
	22 East Xinzhuang	115	622	0.46	9.6	15.8	18.8
	23 Tangyunpu	118	350	0.38	3.8	8.0	12.2
	24 West Luzhuang	155	667	0.58	13.2	12.9	-
	25 East Luzhuang	172	320	0.12	14.0	14.4	-
	26 Shijiapu	103	376	0.49	-	-	-

* Not adopted in the calculation owing to the complexity of the topography and the base rock.

1. The depth of the site soil which should be taken in the study

From Fig. 5-7, it is shown that there exists relations between average weighted shear moduli of soil, the depth of which are 10, 20, and 30 m respectively (counting from the ground surface), and the damage index, but scattering of which is different. There is general trend that the higher the modulus, G, the smaller the damage index, i, or vice versa. It proves that the average weighted shear modulus is a good criterion in measuring the effect of site soil on damage.

Examining the relation between G and i, it is found that G is related closely with i for the soil depth of 20 m,

but not so for the depth of 10 m, showing that 10 m in depth is not sufficient showing the effect of soil on damage. As for the depth of 30 m, the relation between G and i is not better than that for the depth of 20 m. Therefore, 20 m is the required depth of soil which should be taken in the study. Of course, it is true just in the case where the bedrock is relatively deep and smooth.

At present, some, either at home or abroad, assume that the depth of the surface soil (0-5 m) plays the major role in the effect on damage. In the study of soil effect, some even use the "softness" of the surface soil to predict the earthquake damage. In order to discuss the problem, relation of longitudinal and shear wave velocities of shallow surface soil layer (0-5 m in depth) with damage is given in Fig. 8 and 9 respectively. Obviously, they are not closely related. The same result has been obtained in the Tonghai earthquake and the Haicheng earthquake (Fig. 10-12). It is known that the "softness" of soil, i.e. rigidity, can be reflected by wave velocity. The above result shows that only the "softness" of the surface soil cannot predict the effect of the site soil on the damage. It is not a critical parameter. Of course, damage also would be induced by differential settlement owing to extremely soft soil.

In summary, it is assumed that, in the evaluation of the effect of site soil on damage, surface soil of only several meters in depth is not sufficient in the consideration, and the appropriate depth to be taken in consideration should be 20 m, for the common low-rise dwellings.

2. Characteristics of soil inside the anomalous area

From the above discussion, it is known that soil layer, 20 m thick near the ground surface, plays a major role in the effect on damage. Therefore, 20 m of soil is taken for the comparison between the soil inside and outside the anomalous area. In Fig. 6, villages marked "x" are all inside the anomalous area, G values of which are almost higher, while those of the villages outside the area, which suffered serious damage, are lower. Owing to the fact that average weighted shear modulus practically reflects the average rigidity of soil layers, weighted according to their thickness, it shows that the reason why the damage of the anomalous area is slight is that surface soil of 20 m in depth has a higher "average weighted shear modulus".

CHECK OF MICROZONING BY MEANS OF AVERAGE WEIGHTED SHEAR MODULUS APPROACH

It has been attempted to microzone part of Qinhuangdao and Tangshan City using average weighted shear modulus. The reliability of this approach is of main concern to us. We have compared the microzoning using this approach with the damage

distribution in the investigated area. The procedure of the approach based on the Tangshan data is as follows:

1. Based on the data in table 1, calculate the average G of the above area

$$\bar{G} = \frac{1}{n} \sum G_i = 166.3 \times 10^2 \text{ ton/m}^2, \quad H=20 \text{ m}$$

2. Calculate the standard deviation of G_i of individual village

$$\Delta = \sqrt{\frac{\sum (G_i - \bar{G})^2}{n}} = 57.2 \times 10^2 \text{ ton/m}^2$$

3. Take $\delta = 0.675 \times \Delta = 38.6 \times 10^2 \text{ ton/m}^2$ as an index to divide the area into small regions.

4. Villages having $G \geq \bar{G} + \delta = 205 \times 10^2 \text{ ton/m}^2$ are classified into region I, where the soil condition is better and the expected earthquake damage to be occurred will be slightest; villages having $\bar{G} + \delta > G > \bar{G} - \delta$ are classified into region II, where the soil condition is moderate and the expected earthquake damage to be occurred will be also moderate; villages having $G < \bar{G} - \delta$ are classified into region III, where the soil condition is poor and the expected earthquake damage to be occurred will be serious.

In Fig.6, villages with different damage index i are plotted according to their G values and the region defined above. Obviously, damage of the villages located in region I is relatively slight ($i < 0.2$) and that of the villages located in region III is serious, while that of the villages located in region II is either slight or serious (only a few number of villages), reflecting that damage is generally moderate.

The above results testify that the microzoning in Tangshan agrees with the damage distribution at the site basically, showing that this approach is practically reliable.

RELATION BETWEEN THE PROPAGATION VELOCITY OF SHEAR WAVE IN SOIL LAYER AND ITS DEPTH

Based on boring and wave velocity measurement data, a summary of variation of velocity of shear wave in soil (inside and outside the anomalous area) is made for cohesive soil (including clay and clayey soil) and sand soil (including sand and sand gravel) (Fig. 13 and 14).

From Fig. 13 and 14, variation of shear wave velocity with depth in sandy soil is not great wherever inside or outside the anomalous area, but variation becomes obvious for the layer consisting gravel sand and gravel inside the area (marked with "x"). As for cohesive soil, there is a tendency that velocity of shear wave increases with depth, but it happens only outside of the area. The above case reflects the fact that damage anomaly is induced by the difference of soil.

Inside the anomalous area, the site soil involves many coarse particles, while outside the area, especially in the south of Yutian County, the soil particles are smaller and uniform.

A best-fit regression equation for the correlation between shear wave velocity and depth of soil by the least square method is given in Table 2. It is shown in the table that the correlation is not good for sandy soil.

Table 2

	Type of soil	Best-fit equation	Coefficient of correlation
Inside the anomalous area	cohesive soil	$V_s = 186 + 5.7H$	0.63
	sandy soil	$V_s = 317 + 1.6H$	0.21
Outside the anomalous area	cohesive soil	$V_s = 122 + 7.9H$	0.83
	sandy soil	$V_s = 223 + 4.4H$	0.48

CONCLUSION

Based on the above statement, the following conclusion can be summarized:

1. Formation of the low intensity anomalous area in Yutian is caused by the soil characteristics in that area. The common features of the site soil in the area are that the average weighted shear modulus of the soil, up to 20 m from the ground surface, is relatively high and it consists of more coarse particles.
2. In the case where the bedrock is deeply located, the depth of soil influencing the damage is about 20 m from the ground surface for common low-rise dwelling (except for the case of foundation failure). Soil, less than 5 m from the ground surface, has no obvious effect on damage.
3. In comparison with the damage at the site, it is assumed that the microzoning approach using the average weighted shear modulus is a simple, practical and basically reliable approach.
4. It is proved again that the average weighted shear modulus is a good criterion in measuring the effect of soil on damage. It is also a useful criterion in the study of soil effect.

Some of the above conclusions have been testified in the other earthquakes and seismic regions. Research work in this respect should be carried further on in order to prove the general significance of the approach in the practice. It is also of important significance in damage predicting and site selecting.

REFERENCES

- 1 Liu Zengwu et al(1978): Velocity of elastic wave and microzoning. Report of Institute of Engineering Mechanics, Academia Sinica.
- 2 Tian Qiwen et al(1980): Field investigation of Yutian low intensity anomalous area during the 1976 Tangshan earthquake. Report of Institute of Engineering Mechanics, Academia Sinica.

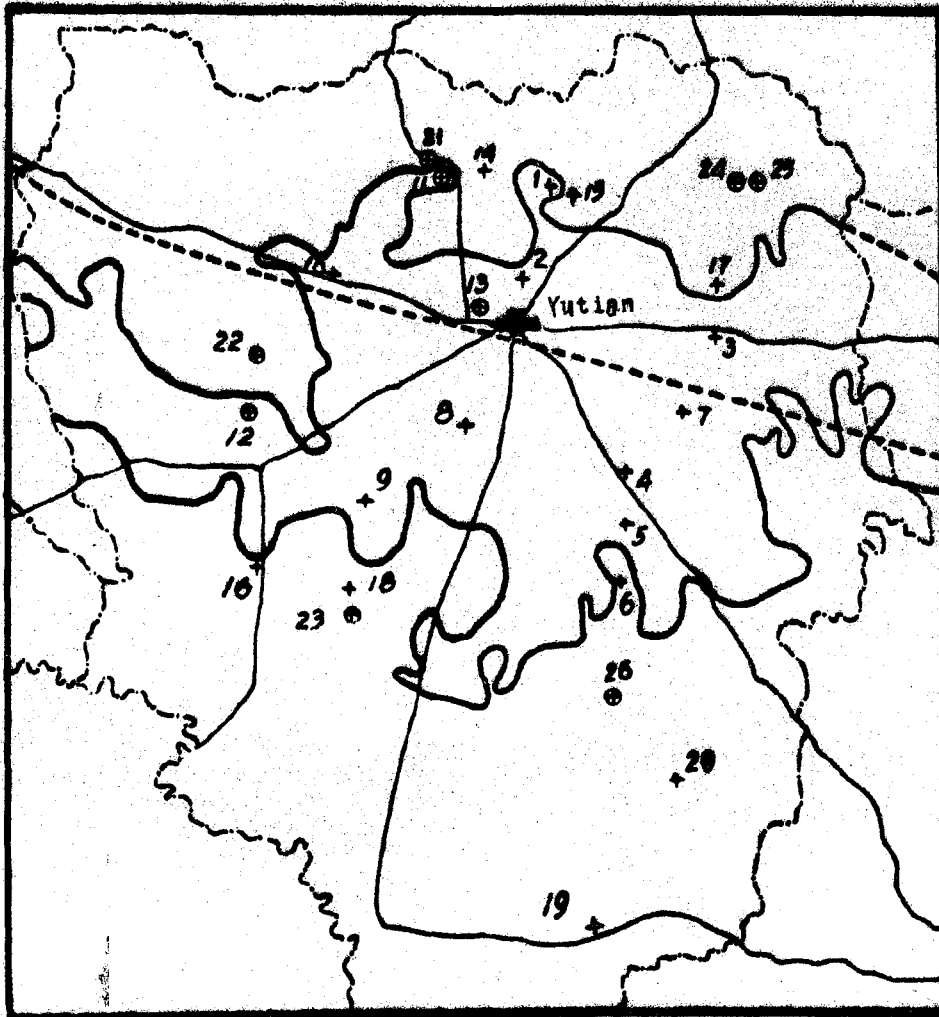


Fig.1 Location of the Yutian low intensity anomalous region and distribution of the measuring points

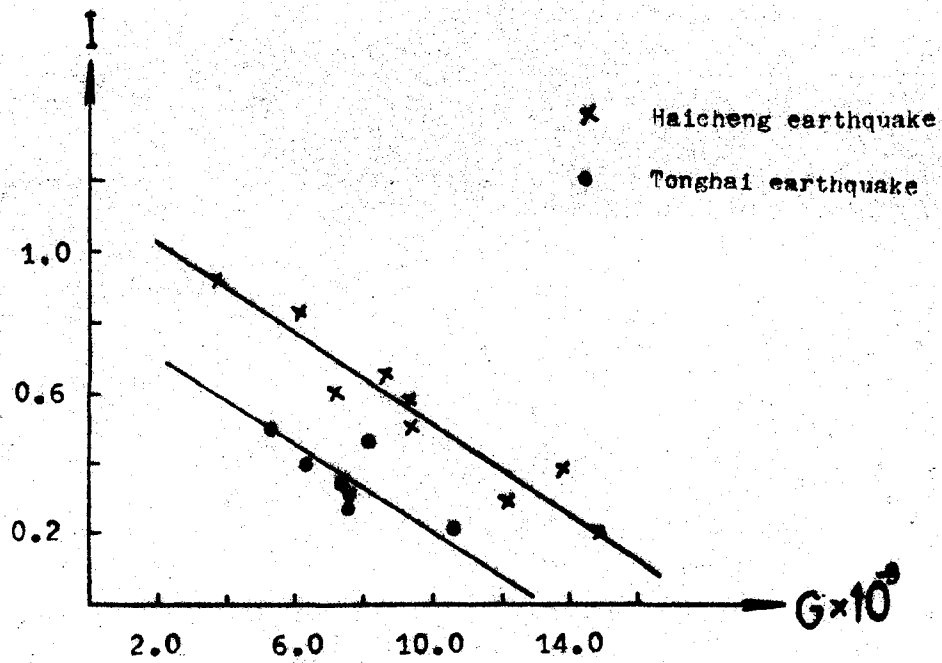


Fig.2 Relation between average weighted shear modulus and damage

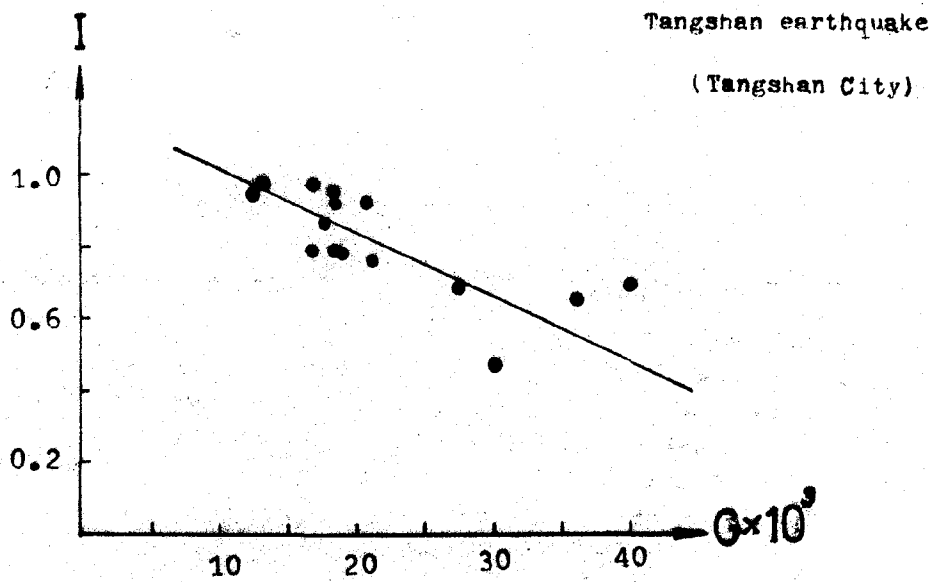


Fig.3 Relation between average weighted shear modulus and damage

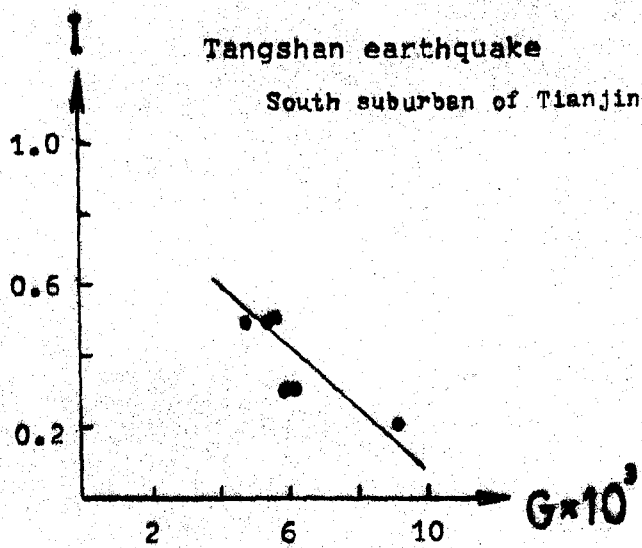


Fig. 4 Relation between average weighted shear modulus and damage

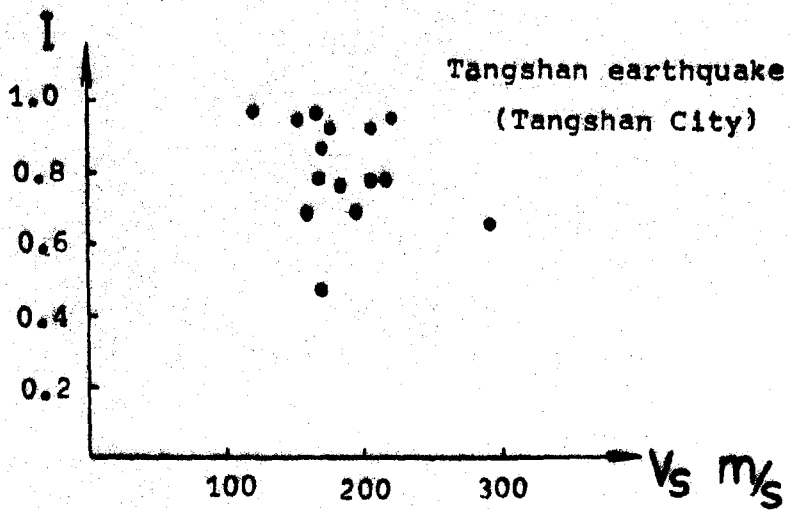


Fig. 12 Relation between shear velocity in surface soil and damage

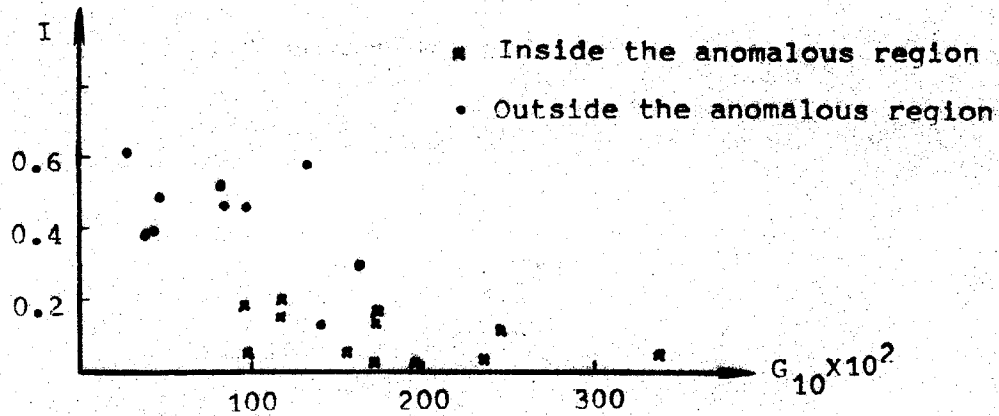


Fig.5 Relation between average weighted shear modulus and damage

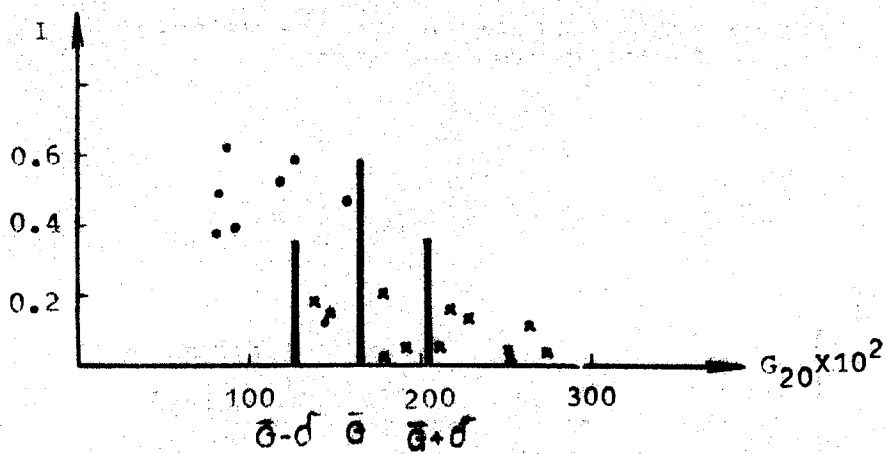


Fig.6 Relation between average weighted shear modulus and damage

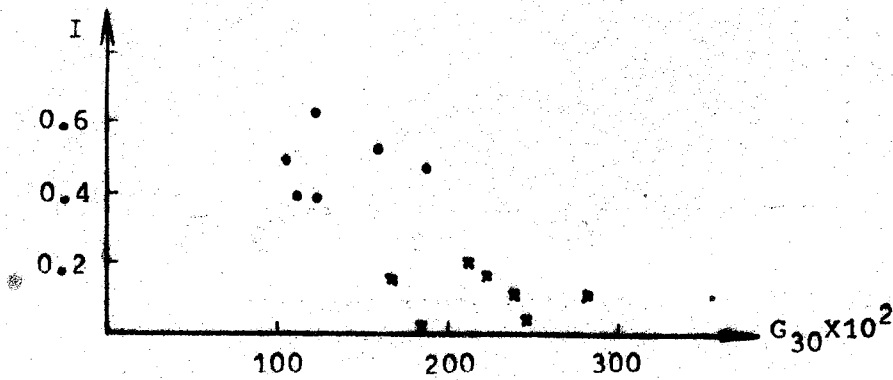


Fig.7 Relation between average weighted shear modulus and damage

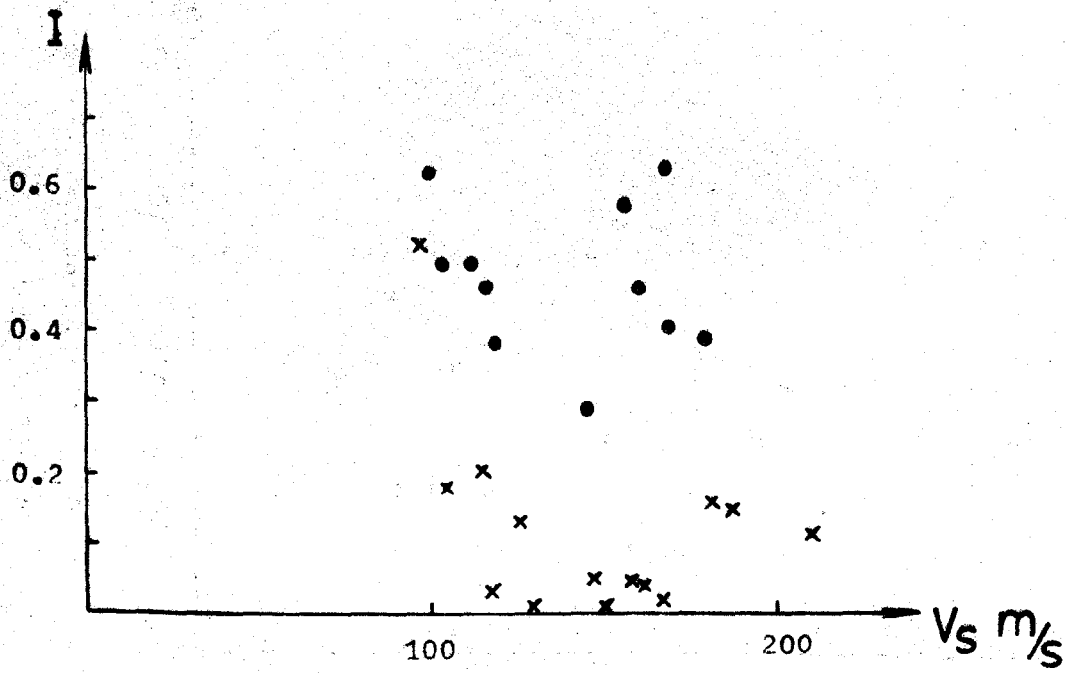


Fig.8 Relation between shear wave velocity
in surface soil and damage

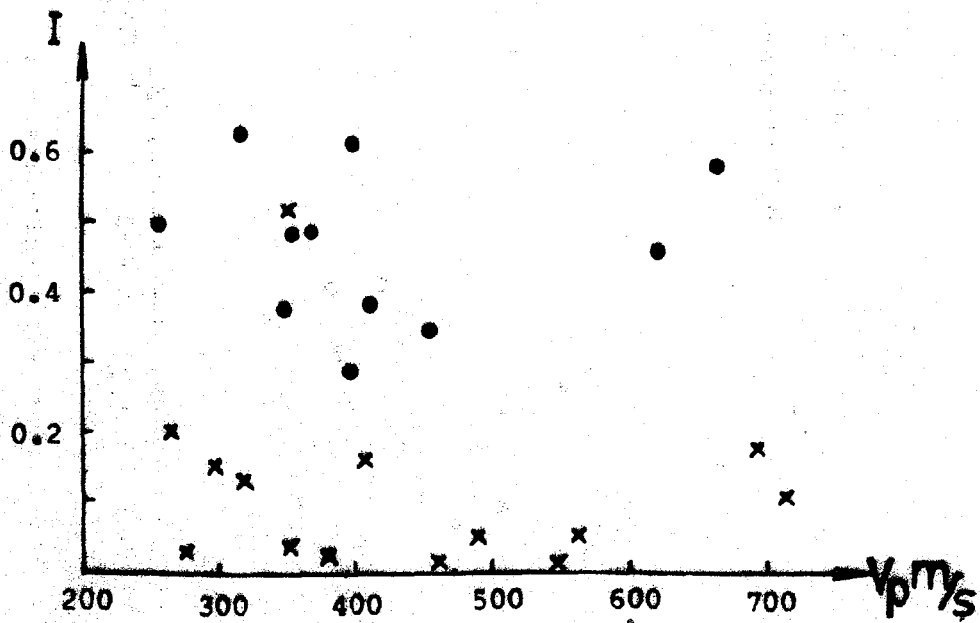


Fig.9 Relation between longitudinal wave velocity
in surface soil and damage

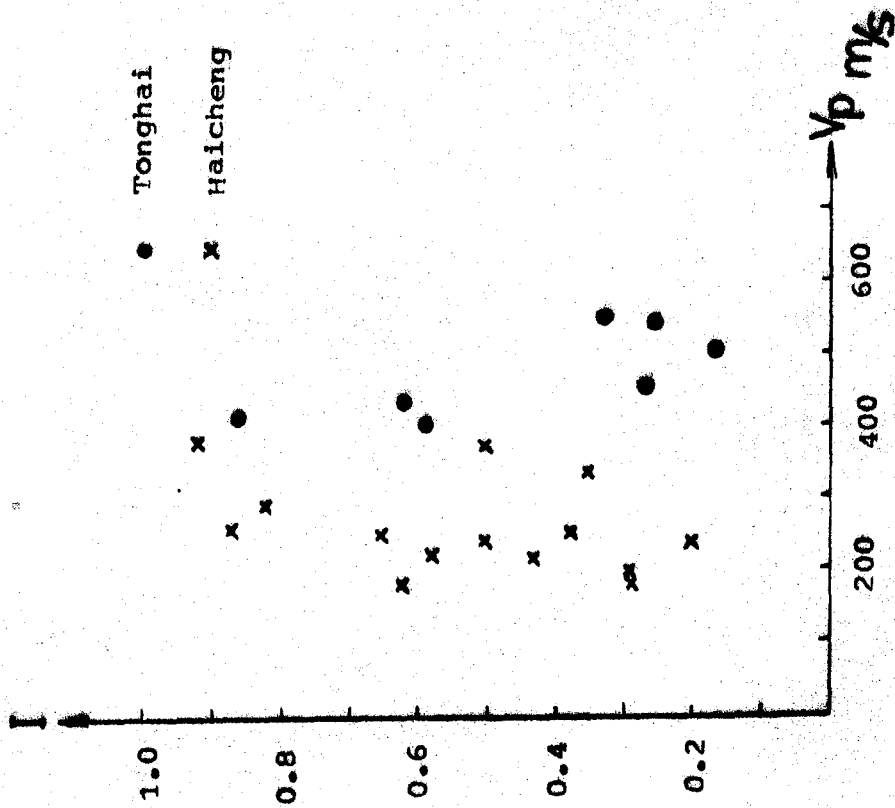


Fig.10 Relation between longitudinal wave velocity in surface soil and damage

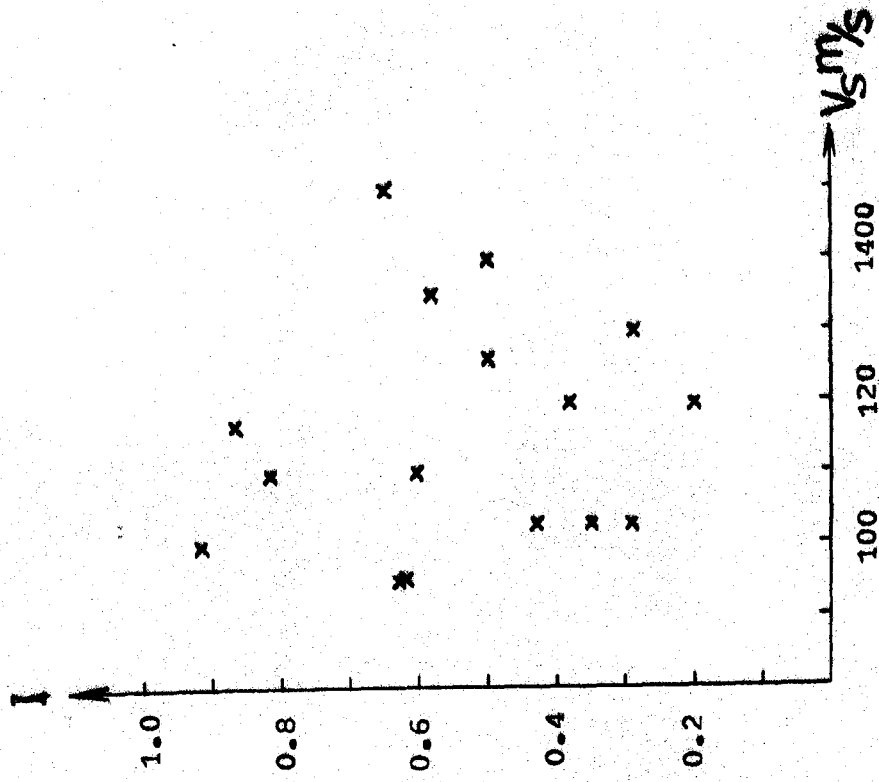


Fig.11 Relation between shear wave velocity in surface soil and damage

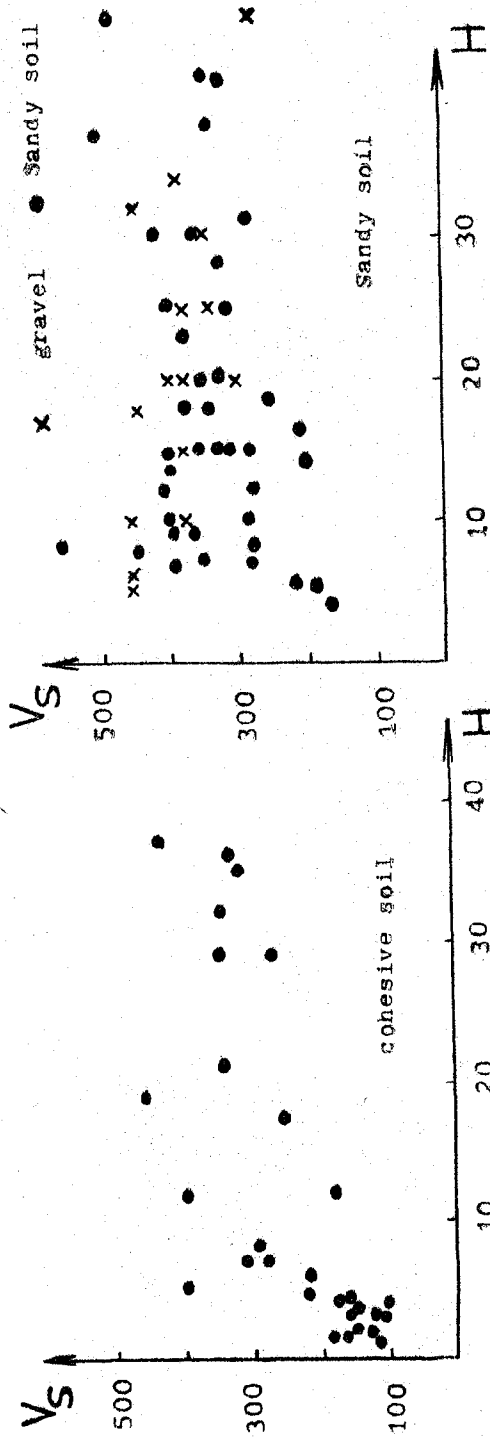


Fig.13 Variation of shear wave velocity with depth of soil inside the anomalous area

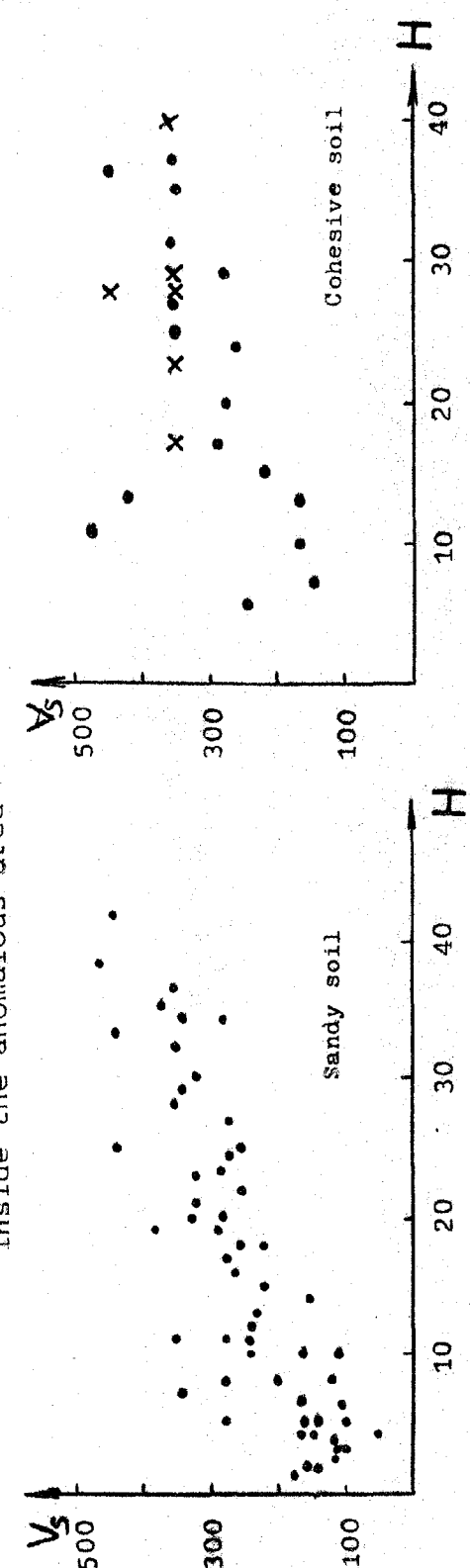


Fig.14 Variation of shear wave velocity with depth of soil outside the anomalous area



CHARACTERISTICS OF LIQUEFACTION OF CLAYEY SILT AND IT'S FIELD DISCRIMINATION

BY

Shi Zhaoji^I, Yu Shousong^{II}

ABSTRACT

The first part of this paper discusses characteristics of liquefaction of clayey silt in the cyclic triaxial test. Difference of liquefaction characteristics between sandy soil and clayey silt is pointed out. The second part of the paper reviews the current discrimination methods. It is testified by tests that different clay particle contents would be obtained from different grading analysis methods. This effect should be taken in consideration for the determination of coefficients in the discrimination formula. At last, a liquefaction discrimination formula is given both applicable to clayey silt and sandy soil, based on Chinese and foreign data.

INTRODUCTION

Since the 1975 Haicheng earthquake and the 1976 Tangshah earthquake, problem on the liquefaction of sandy soil and silty soil, containing a small amount of clay particles ($d < 0.005\text{mm}$) is more appreciated by the Chinese engineers increasingly, study of formulation of empirical formula and approach for discriminating the liquefaction of clayey silt has been carried out [1-6]. Attention has been drawn to this problem also in foreign countries with certain experimental investigation performed [7-8]. In the modified Chinese aseismic code (1979), it is pointed out that the discrimination formula for the liquefaction of sandy soil cannot be used for clayey silt, but no appropriate formula is given in the code. Therefore, it is an urgent need to solve the problem. Two respects have to be stressed on the study of the liquefaction of clayey silt: first, its liquefaction characteristics (difference of liquefaction characteristics for clayey silt and sandy soil, affecting factors etc); and secondly, developing of reliable discriminating field approach. This paper gives a summary of study performed in IEM on the above respects.

CHARACTERISTICS OF LIQUEFACTION

One of the characteristics of clayey silt is that it contains not only large amount of sand and silt particles but a small amount of clay particles which influence its charac-

^I Research Associate, ^{II} Engineer, Institute of Engineering Mechanics (IEM), Chinese Academy of Sciences.

teristics. The former makes it liable to liquefy, while the latter prevents. Obviously, when the clay particle content is sufficiently large, no liquefaction would occur. But, at the same time, such soil with large amount of clay particles is classified as another type of soil, e.g. clayey soil or clay, but not clayey silt. As for the soil with small amount of clay particles, it is necessary to examine through tests whether it is liable to liquefy or not. If it is liable to liquefy, its liquefaction characteristics, resistance or field discrimination should be taken in consideration.

Liquefaction characteristics of clayey silt in this study were obtained by means of electro-magnetic cyclic triaxial apparatus. Frequency of the sinusoidal input loading is 1 Hz. Samples used in the test are 8cm high and 3.91cm in diameter. Time of consolidation is 2 hr. for different consolidation loading. Undisturbed clayey silt samples are used, taken from Tianjin and Shansi respectively, physical properties of the samples are listed in Table 1.

1) Characteristics in the developing process of strain

It is shown in the test that "unsymmetry" occurs in the triaxial liquefaction test of sandy soil under isotropic consolidation loads, that means when cyclic dynamic stress is exerted, strain in tension and compression produced are not equal. Strain in tension is always greater than that in compression. But this difference in strain is very small (except in the case of random wave load) and can be neglected (as in Fig. 1). Typical records of liquefaction test for sands of three different densities are shown in the figure.

But, for clayey silt, such "unsymmetry" is especially obvious. For low density samples, strain in tension is 4-5 times greater than that in compression, as shown in Fig. 2. As for high density samples, even no strain in compression occurs during certain initial cycles in the test, strain in compression only occurs when number of cycles is sufficient large and is always less than that in tension (Fig.3). It is also shown in the test that the higher the density, the lower the dynamic stress, and consequently the later the strain in compression appears. Test results seem to show that undisturbed clayey silt sample differs with sandy soil sample in that, in the process of liquefaction, clayey silt sample fails chiefly in tension, the higher the density, the more obvious the phenomena, but the cause of "unsymmetry" should be further studied.

In case of consolidation under anisotropic loading, characteristics of strain in triaxial liquefaction test do not differ much with those of sandy soil, they all fail in compression.

2) Development of pore-water pressure

In case of consolidation under isotropic loading, no matter how high density is, the developing process of pore-water pressure of undisturbed clayey silt is that, in the beginning, the pore-water pressure increases rapidly and then decreases gradually to a constant value shown in Fig.2 and 3. The developing process of pore-water pressure of clayey silt

is quite similar to that of dense sand, but differs from that of loose sand and medium dense sand; in the latter, sudden rise in pore pressure often occurs in a certain number of cycles (Fig.1). In addition, increase rate of pore pressure is affected obviously by dynamic stress amplitude, i.e. the higher the dynamic stress, the quicker the rise of pore pressure (Fig.4-5). Relation between pore-water pressure ratio U/U_{max} and cycle ratio N/N_1 is given in Fig.4-5, where N_1 is the number of cycles, in which the pore pressure approaches or equals the confined pressure σ_3 in consolidation, U_{max} is the corresponding pore pressure. Such characteristics also exists in consolidation under anisotropic loading, Fig. 6 shows the test result for consolidation pressure ratio $K_c=2.5$, From the Fig. the effect of dynamic stress amplitude is very obvious.

When a sample consolidated under isotropic loading σ_0 is exerted by dynamic cyclic stress $\pm \sigma_a$, its max. and min. principal stress and direction of principal stress plane will varies periodically at an angle of 90. When pore pressure occurs in the sample, variation and calculation of the effective max. principal stress σ'_1 and min. principal stress σ'_3 are shown in Table 2.

Another characteristic of the development of pore pressure in undisturbed clayey silt is that, under loading of $-\sigma_a$, σ'_3 approaches to zero rapidly, and effective principal stress ratio σ'_1/σ'_3 reaches a very large value, while under loading of $+\sigma_a$, σ'_3 drops slowly, as shown in Fig.7. This characteristic corresponds to the "unsymmetry" of stress mentioned above, or associated with each other, because, when $-\sigma_a$ acts, rapid decrease of σ'_3 will cause the developing of strain in tension.

Developing of pore pressure in undisturbed clayey silt is quite different from that in sandy soil. Test results are shown in Fig.8-9 for sandy soils with $D_r=43\%$ and 90% respectively. It can be found that variation of σ'_3 and σ'_1/σ'_3 in both positive and negative direction is similar under loading of cyclic dynamic stress $\pm \sigma_a$, values of there two quantities are also similar. Obviously, this corresponds to the fact that unsymmetry of strain in sandy soil is not obvious.

3) Effect of density

Similar to sandy soil, density has a great effect on the liquefaction resistance of clayey silt as in the case of sandy soil. Fig.10 shows the relation between liquefaction stress ratio $\sigma_d/2\sigma_0$ and dry unit weight γ_d . Liquefaction resistance of the three undisturbed clayey silt samples all increases with their dry unit weight, but the rate of increase differs for different soil, S-1 soil has the greatest rate. Besides, density has a similar effect on the liquefaction of disturbed clayey silt.

4) Effect of initial stress state in consolidation

Initial consolidation loading is an important factor influencing sand liquefaction, in a given condition, there is a linear relation between liquefaction stress ratio and σ_3 or K_c . The similar effect has been also reflected by the

initial stress state in consolidation for undisturbed clayey silt. Fig.11 shows the relation between σ_3 and σ_1 required to produce 5% of strain in 20 cycles (i.e. $n=20$) in the range of $K_c=1.0-2.5$. σ_1 increases with σ_3 linearly but the straight line representing such relation does not pass through the origin, showing that liquefaction stress ratio which increases with σ_3 does not keep at a constant, but decreases gradually as shown in Fig.12. In addition, in the range of $\sigma_3=0.5-2.0$ kg/cm², liquefaction stress ratio increases with K_c linearly, as shown in Fig.13. Test results also show that in a certain range of σ_3 and K_c , a good linear relation exists between σ_a and max. principal stress in consolidation $\sigma_1 = K_c \sigma_3$ as follows (Fig.14):

$$\sigma_a = A + B \sigma_3 \quad (1)$$

where A and B are constants to be determined by test; for soil of S-1 type, $A=0.22$ kg/cm², $B=0.41$, when $\sigma_3=0.5-2.0$ kg/cm², $K_c=1.0-2.5$, $n=30$ and $\epsilon=5\%$. The advantage of equation (1) is that, the combined effect of σ_3 and K_c is considered, so the equation becomes more practical.

5) Effect of structure

Comparing the test results of undisturbed sample with those of disturbed sample, it is found that structure of soil has a great effect on liquefaction of clayey silt. Typical results of triaxial liquefaction test for disturbed clayey silt are shown in Fig. 15 and 16 respectively, where two different characteristics from those of undisturbed sample are found. Firstly, even though the "unsymmetry" of strain exists, but this phenomenon is not obvious; secondly, σ_3 in the tension direction does not approach zero rapidly, also σ_1/σ_3 does not approach to a higher value. If compared Fig.15-16 with Fig.1 and 9 for high density sandy soil, it is found that developing strain and pore pressure in the liquefaction process of disturbed clayey silt are quite similar to dense sand.

Such difference of undisturbed and disturbed clayey silt in liquefaction may be related to the effect of clay particle content. For S-1 soil, where $\gamma_d=1.54$ g/cm³ it is shown by the static triaxial test that internal friction angle ϕ of undisturbed sample is 33.6° and cohesive force C is 0.17kg/cm², while ϕ of disturbed sample does not change basically ($\approx 32.3^\circ$) but cohesive force C decreases to 0.07kg/cm², showing that the difference of undisturbed and disturbed sample in mechanical properties is caused by the variation of cohesive force. It is assumed that the main effect of clay particles in clayey silt is the cementation formed in the particles or soil aggregates, thus increasing the cohesion. When the structure fails, this cementation is then destroyed and consequently cohesion decreases. Therefore, certain mechanical properties, including liquefaction characteristics of disturbed clayey silt tends to those of sandy soil.

The effect of clay particles on structure is also shown in Fig.17, in which relation between the liquefaction resistance ratio R (equals the ratio between liquefaction stress

ratio of undisturbed and disturbed clayey silt) and the clay particles content M_4 is shown. The higher the M_4 , the higher the R value, i.e. the greater the clay particle content, the obvious the structure effect. It is clear that the structure of clayey silt is not only caused by cementation which is produced by the long duration action of clay particles but also by salt cementation and water film absorption etc. However it is reasonable to assume that structure is chiefly built up by cementation produced by clay particles.

FIELD DISCRIMINATION APPROACH

There are a number of approaches for the discrimination of liquefaction of clayey silt in the field, but all are of empirical approaches. Most of the approaches utilize the macro-data to obtain a discriminating formula or critical discriminating value by means of statistic analysis. These approaches have the following disadvantages: Firstly, characteristics of grading of clayey silt is not taken in consideration, discriminating formula does not include factors also related to particle grading; secondly, although some discriminating formulas consider the effect of grading, such as taking silt particle or clay particle content in consideration, but the particle analyzing method used is not illustrated and no stress has been put on the effect of methods on liquefaction discrimination. Some investigator even use combined grading data, (such as M_4), obtained from different analysis in the statistic analysis to established a discriminating formula; thirdly, test data used in most of the empirical formulas are taken from Tianjin region only, those taken from other regions are scarcely used. Discriminating formulas are scarcely related to test data of sandy soil.

It is expected to establish a convenient and reasonable discriminating approach, considering characteristics of both clayey silt and sandy soil and pointing out clearly how to obtain the data and test methods.

1) Effect of particle analysis methods on clay particle content

Experience shows that clay particle content M_4 is a good index to characterize the liquefaction potential of clayey silt, it is often utilized as a statistic data in establish a discriminating formula. In order to study the effect of particle analysis method on clay particle content of clayey silt, grading test has been carried out for 4 kinds of soil (Table 1) according to the following methods:

(a) No dispersion is performed basically, the soil sample is boiled only for 2 hr.

(b) Weak dispersion is performed, using liquid ammonia as a dispersant.

(c) Strong dispersion is performed, using $(NaPO_3)_6$ as dispersant.

Test result of the above methods is listed in Table 3. From the table, it is obvious that the composition of particles obtained depends on, to a great extent, the method of

dispersion used, clay particle content obtained in the strong dispersion is greater than that obtained in the weak dispersion, even twice greater than the latter. Therefore, clay particle contents obtained by different particle analysis methods cannot be mixed together in establishing the discriminating formula, unless check test or modification has been made previously. For the established discriminating formula above, it is necessary to point out the particle analysis method used, otherwise error will be easily made in discrimination, especially in the discrimination of critical condition.

2) Liquefaction discriminating approach applicable to sandy soil also

We have two groups of data obtained in the field for discriminating liquefaction of clayey silt, the first group was taken from Tianjin city area, the clay particle content of which was obtained by the first analysis method mentioned in the last paragraph, i.e. no dispersant was added and the sample was boiled for 1 hr. only. There are 86 data in this group, of which 49 data were taken from the liquefaction sites. The second group taken from Tianjin, Tangshan etc., consists of 126 data, of which 48 data were taken from the liquefaction sites, (NaPO_3)₆ was used as a dispersant in the particle analysis for this group.

(a) Liquefaction discriminating formula consistent with the Chinese aseismic code (for sandy soil)

Fig.18 gives the summary of certain results of the first data group, showing the relation between blow number of standard penetration test $N_{63.5}$ (for liquefied and unliquefied soil) and M_4 at three different depths ($d_5=5, 6$ and 7M. ; depth of water table $d_w=2.0\text{M.}$). Obviously, the critical blow number N'' decreases with increases of M_4 , and there seems to exist a linear relation. In the case of $M_4=0$, i.e. in the case of sandy soil, the critical blow Number N' should be taken according to the specification in aseismic code, therefore, the following discriminating formula exists

$$N'' = N' - DM_4 \quad (2)$$

when the measured N value is greater than N'' value, no liquefaction will occur, or vice versa. In the case of $M_4=0$, that means the soil is sandy soil, $N''=N'$, which is the same as the the discrimination formula in the aseismic code, therefore formula (2) is applicable both to clayey silt and sandy soil.

D in formula (2) denotes the slope of the straight line shown in Fig.18, which can be obtained by graphic solution, from the available result, it is not so closely related to the depth of the layer and the water table level. For the 1st group of data, $D=0.664$, percent of success in discriminating liquefaction is 93%, as for the 2nd group of data taken from Tianjin City (92 in number), $D=1.0$, percent of success in discriminating liquefaction is 84%, the difference in success results in the variation of particle analysis method.

Formula (2) is only suitable for region of intensity VIII, further study should be carried out to prove whether it is suitable for region of intensity VII or IX,

(b) Liquefaction discriminating formula applicable to sandy soil also

Statistical analysis using both clayey silt and sandy soil data is made in order to obtain a discriminating formula suitable for both soil. Sandy soil data are taken from ref. (4). M_4 of sandy soil is taken as zero in the analysis.

In order to increase the accuracy in discrimination, modification coefficient and nonlinear discriminating method (4,9,10) are used. Five factors which have a large effect on liquefaction are taken in the statistic analysis, namely, depth of the soil layer, X_1 in meter; blow numbers of standard penetration test, X_2 ; water table level, X_3 in meter; clay particle content X_4 (in %, but $M_4=5$ is taken when substituting in (2) and statistical formula); ground acceleration X_5 in g. (0.075 g for intensity VII, 0.15g for intensity VIII and 0.3g for intensity IX).

Statistical results of the first group of data are listed on the left column in Table 4, which gives the coefficient in the discriminating formula, mean value and standard deviation required for the modification coefficient, critical index of liquefaction potential $Z_0 = -1.217$ and percent of success $P_r = 89.1\%$. The corresponding results of the second group of data are listed on the right column, with $Z_0 = -0.4167$, $P_r = 86.4\%$.

CONCLUSION

1. Compared with the results of sandy soil, unsymmetry of strain of undisturbed clayey silt is more obvious. During liquefaction, strain in tension of clayey silt is much greater than that in compression, showing that the sample fails "in tension" principally. Consequently, when the sample is subjected to tension, its effective min. normal stress approaches to zero rapidly, but decreases slowly when the sample is subjected to compression. In addition, the pore pressure of undisturbed clayey silt would not increase suddenly on the contrary, it increases very rapidly in the beginning, then decreases its rate gradually. The increase rate of pore pressure is also affected by the amplitude of dynamic stress and increases with the latter. In the liquefaction process of undisturbed clayey silt, such developing characteristic of pore pressure and strain have been only reflected in cyclic tri-axial test, the reason should be further investigated.
2. Density and initial stress state in consolidation are also important factors affecting the liquefaction of clayey silt. It is shown by the test results that there exists a good linear relation between the dynamic stress required to produce 5% of strain and the max. principal stress σ_1 in consolidation.
3. An important effect of clay particles in clayey silt is formation of cementation, thus strengthening the structure of undisturbed clayey silt and increasing its liquefaction resistance. When its structure and cementation are destroyed, properties of clayey silt approach to those of sandy soil in advance, therefore strain and the developing process of pore

pressure in liquefaction of disturbed clayey silt are very similar to those of dense sand.

4. Liquefaction discriminating formula for clayey silt must include parameters showing the effect of grading, such as M_4 . The effect of particle analysis method on the clay particle content should be emphasized, each discriminating formula correspond to a specified method. Otherwise error would be made in discrimination. For the critical condition of discrimination (for example the calculated index Z approach the critical index Z_0), which is of main concern, effect of the error would be greater.

5. Formula (2) and Table 4 are both suitable for sandy soil and clayey silt, but formula (2) is only applicable to region of intensity VIII. If no dispersant is used in the particle analysis, D in formula (2) is equal to 0.664, while ($NaPO_3$)₆ is used as a dispersant, then $D=1.0$. It is suggested to use M_4 from the 1st particle analysis method (i.e. no dispersant is added) to establish and improve the discriminating formula for convenience and reliability.

REFERENCES

- (1) Preliminary analysis of distribution of liquefied clayey silt in Tianjin urban area and its blow Number of SPT (in Chinese). Survey and Drafting Dept. Tianjin city planning design bureau, April, 1978.
- (2) L.J.Guo, Discussion on liquefaction of clayey silt in Ninghe-Haugu region (in Chinese), 3rd National Symposium of Soil Mechanics and Foundation Engg., 1979.
- (3) Y.Q.Wang, Statistical Analysis of Liquefaction of Clayey Silt and Sandy Soil and Their Discriminating Formula (in Chinese), Report of Building Research Institute, Dept. of Metallurgy, 1979.
- (4) Yu Shousong, Shi Zhaoji, Analysis of Liquefaction Potential of Horizontal Soil Strata (in Chinese), Earthquake Engg. and Engg. Vibration, No.1, Trial issue.
- (5) G.S.Li, Discrimination Formula for the Liquefaction of Clayey Silt (in Chinese), "Metallurgy Structure", No.6, 1980.
- (6) Y.Q.Wang etc., Statistic Formula for Predicting Liquefaction Potential of Clayey Silt (in Chinese), Chinese Journal of Geotechnical Engineering, No.3, 1980.
- (7) C.K.Shen etc., The Effect of Fines on Liquefaction of Sands, Proceedings of The Ninth Inter. Confe. on Soil Mecha. and Foun. Engg., Vol.2, Okyo, 1977.
- (8) Watannaba, etc. Effect of Grain and Fine Particle Content on the Soil Liquefaction, Soil and Foundation (in Japanese), Vol.23, No.6, 1975.
- (9) K. Tanimoto and Tsutomu Noda, Prediction of Liquefaction Occurrence of Sandy Deposits During Earthquake by A Statistical Method, Proceedings of the Japan Society of Civil Engineers, No.256, 1976.
- (10) Shi Zhaoji, Yu Shousong, Program for Discriminating Liquefaction Potential of Horizontal Soil Layer (in Chinese), Report of IEM, Sept., 1979.

Table 1. Physical properties of Soil Samples

Soil No.	Natural water Content %	Natural Dry Unit weight g/cm^3	Plasticity Index %	Specific Gravity g/cm^3
T-1	26.9	$\frac{1.42}{1.31-1.56}$	6.9	2.70
T-2	23.6	$\frac{1.62}{1.59-1.64}$	8.1	2.70
T-3	28.2	$\frac{1.54}{1.50-1.59}$	9.3	2.70
S-1	25.0	$\frac{1.57}{1.53-1.62}$	7.7	2.71

Table 2. Variation of effective stress

Condition in a sample under cyclic Loading

Under Loading of $+\sigma_d$	Under Loading of $-\sigma_d$

Table 3. Results of different particle analysis methods

Location of Sampling	Method of Particle Analysis	Composition of Particle				d_{50}	C_u	$\frac{(M_{4.75})_1}{(M_{4.75})_2}$	Remarks
		M_1 0.25-0.1 mm	M_2 0.1-0.05 mm	M_3 0.05-0.005 mm	M_4 0.005 mm				
T-1	1	0.8	59.1	37.6	2.5	0.06	5.18	1.00	Particle analysis method: 1. Salt not washed, no dispersant added, boiling for 2 hr.
	2	0.8	61.4	36.7	1.1	0.062	3.5	0.44	
	3	0.8	53.1	42.8	3.3	0.053	4.5	1.32	
T-2	1	27.2	51.5	13.5	7.8	0.08	14.5	1.00	2. Salt washed, 5cc. of ammonia is added, boiling for 30 min.
	2	20.4	60.5	14.3	4.8	0.07	6.3	0.62	
	3	26.8	51.2	15.0	7.0	0.079	12.98	0.90	
T-3	1	2.4	53.8	34.6	9.2	0.043	12.3	1.00	3. Salt not washed, (NaPO ₃) ₆ 10cc. is added, boiling for 40 min.
	2	1.6	49.3	41.3	7.8	0.05	8.71	0.85	
	3	1.6	45.6	41.3	11.5	0.048	14.5	1.25	
S-1	1	0.8	59.0	36.1	4.1	0.063	6.16	1.00	
	2	0.4	57.7	34.5	7.4	0.061	8.69	1.80	
	3	0.4	55.4	35.4	8.8	0.056	10.10	2.15	

Table 4. Results of statistical analysis

No.	Variation	Data of clayey silt and sandy soil					
		1st group			2nd group		
		Mean value	Standard Deviation	Discrimination coefficient	Mean value	Standard deviation	Discrimination coefficient
1	x_1	0.5585	2.7574	1.0000	7.1547	3.1397	1.0000
2	x_2	11.3890	7.2820	-36.760	10.201	6.9477	5.2887
3	x_3	2.1541	1.8239	14.780	1.7630	1.9802	-0.29954
4	x_4	3.4557	3.4412	-10.896	5.1587	4.8746	3.8845
5	x_5	0.16472	0.059037	4.5925	0.16825	0.071981	-0.18128
6	x_1x_1	50.569	53.372	26.761	60.995	63.378	-0.30757
7	x_1x_2	83.501	88.971	-18.033	80.729	90.764	-0.14907
8	x_1x_3	16.239	30.714	-110.01	14.545	29.855	7.8888
9	x_1x_4	22.606	24.103	17.283	38.909	45.876	-1.3356
10	x_1x_5	1.0996	0.79130	6.5156	1.2242	0.88851	-3.3723
11	x_2x_2	182.41	250.44	26.610	152.08	235.36	-2.9724
12	x_2x_3	25.280	35.754	10.181	20.405	37.233	-1.1568
13	x_2x_4	40.308	49.307	-3.5444	49.479	56.941	-0.20828
14	x_2x_5	1.8834	1.5338	3.6816	1.8118	1.8172	1.1579
15	x_3x_3	7.9456	30.885	82.967	7.0080	28.883	-6.4896
16	x_3x_4	6.9114	6.8824	11.575	8.0199	12.068	-0.19992
17	x_3x_5	0.40003	0.65766	-8.4079	0.37314	0.88640	1.0149
18	x_4x_4	23.709	33.179	-13.696	50.249	78.942	0.83450
19	x_4x_5	0.51835	0.51618	-1.6004	0.84325	0.91639	-2.0056
20	x_5x_5	0.030594	0.026382	-5.3179	0.033463	0.030479	0.48514
		$Z_0 = -1.217$, $P_r = 89.1\%$			$Z_0 = -0.4167$, $P_r = 86.4\%$		
		$Z < Z_0$ Not Liquefaction, $Z > Z_0$ Liquefaction			$Z > Z_0$ Not Liquefaction, $Z < Z_0$ Liquefaction		

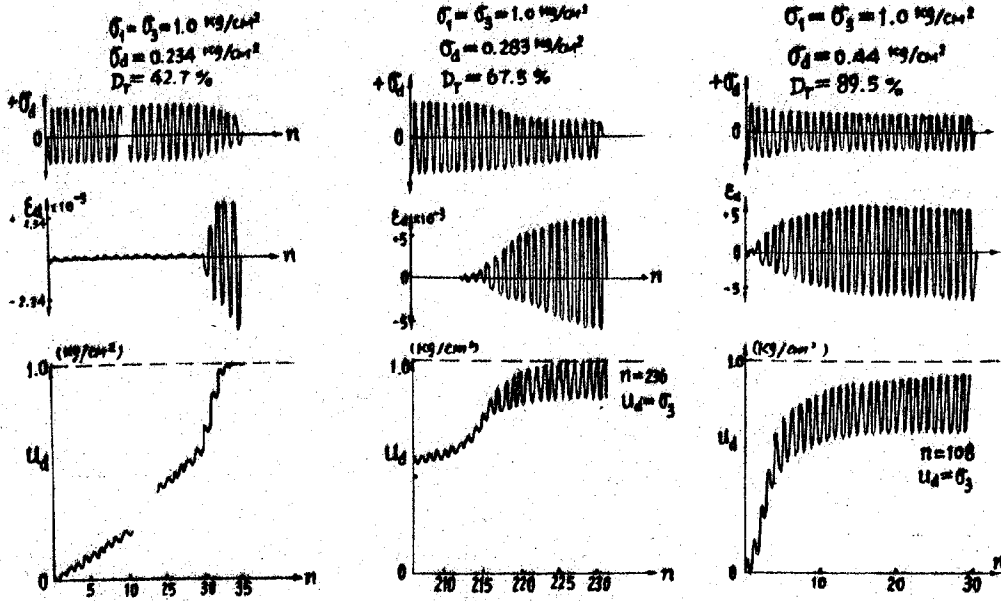


Fig. 1 TYPICAL LIQUEFIED TEST RECORD FOR SAND

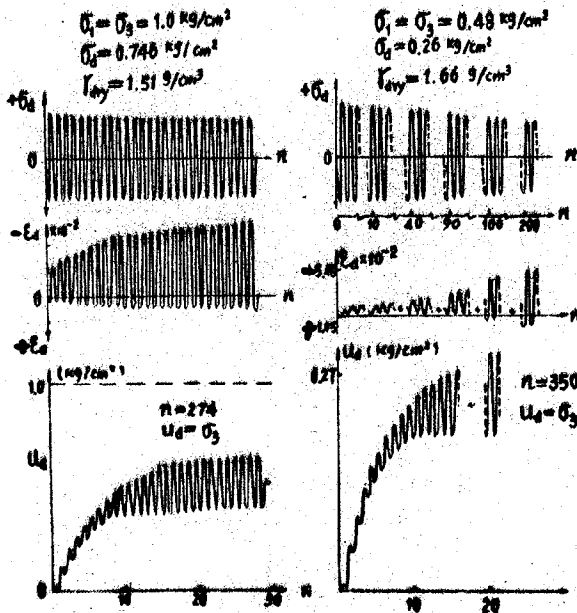


Fig. 2. TYPICAL LIQUEFIED TEST RECORD FOR UNDISTURBED CLAYEY SILT ($\gamma_{dy} = 1.51 \text{ g/cm}^2$).

Fig. 3. TYPICAL LIQUEFIED TEST RECORD FOR UNDISTURBED CLAYEY SILT ($\gamma_{dy} = 1.66 \text{ g/cm}^2$).

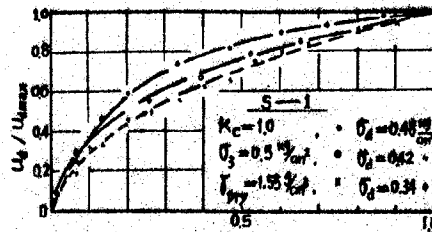


Fig. 4 N / N_L

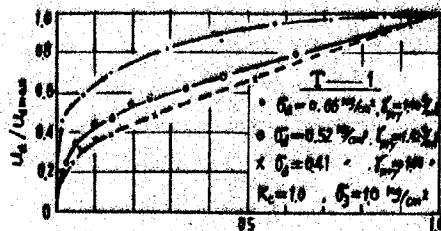


Fig. 5 N / N_L

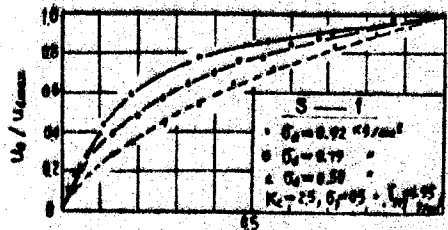


Fig. 6 N / N_L
Fig. 4, 5, 6. PORE WATER PRESSURE RATIO VERSUS CYCLIC RATIO

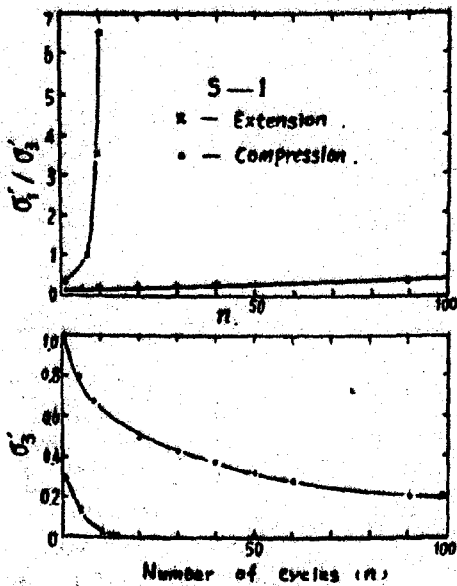


Fig. 7. DEVELOPING OF EFFECTIVE MIN. PRINCIPAL STRESS AND PRINCIPAL STRESS RATIO FOR UNDISTURBED CLAYEY SILT ($\gamma_d = 1.59 \text{ g/cm}^3$).

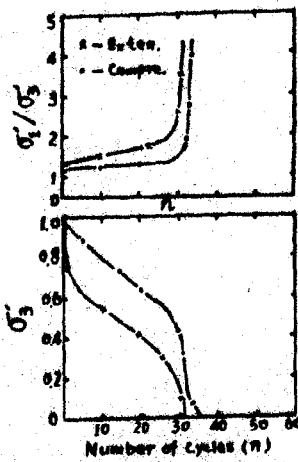


Fig. 8. DEVELOPING OF EFFECTIVE MIN. PRINCIPAL STRESS AND PRINCIPAL STRESS RATIO FOR SAND ($D_r = 42.7\%$).

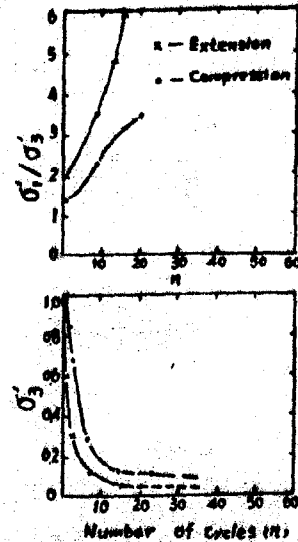


Fig. 9. DEVELOPING OF EFFECTIVE MIN. PRINCIPAL STRESS AND PRINCIPAL STRESS RATIO FOR SAND ($D_r = 89.5\%$).

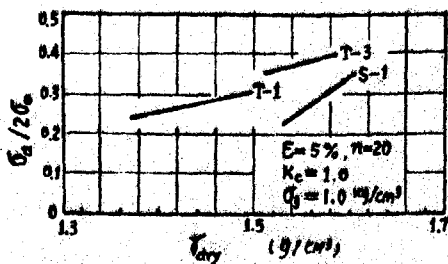


Fig. 10. LIQUEFACTION STRESS RATIO VERSUS DRY UNITE WEIGHT

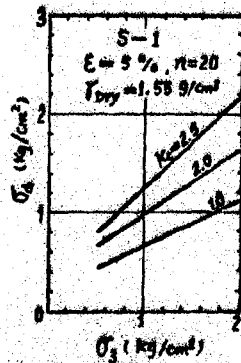


Fig. 11. DYNAMIC CYCLIC STRESS VERSUS CONFINED PRESSURE IN CONSOLIDATION.

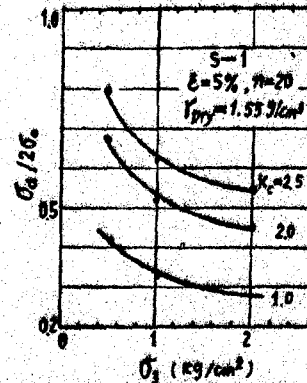


Fig. 12. LIQUEFACTION STRESS RATIO VERSUS CONFINED PRESSURE IN CONSOLIDATION.

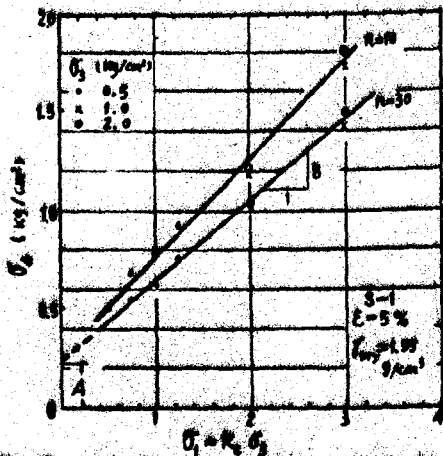


Fig. 14. DYNAMIC CYCLIC STRESS VERSUS MAX. PRINCIPAL STRESS IN CONSOLIDATION.

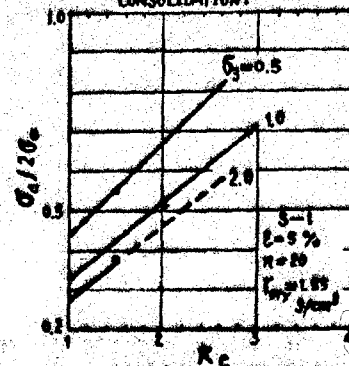


Fig. 13. LIQUEFACTION STRESS RATIO VERSUS MAX. PRINCIPAL STRESS IN CONSOLIDATION.

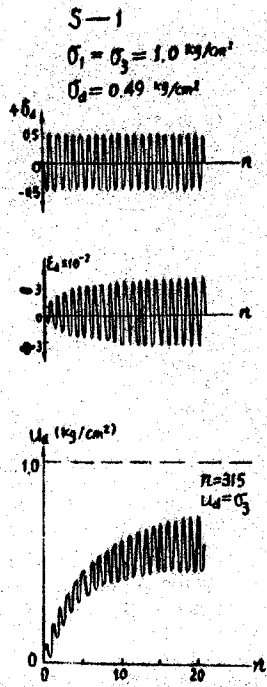


Fig. 15. TYPICAL LIQUEFIED TEST RECORD FOR DISTURBED CLAYEY SILT.

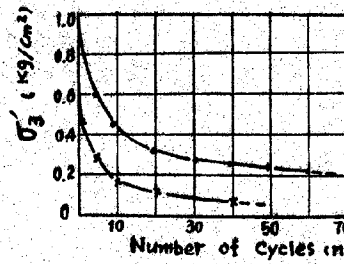
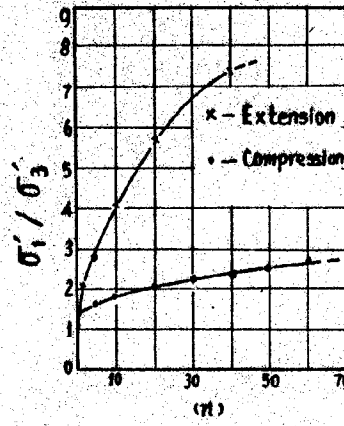


Fig. 16. DEVELOPING OF EFFECTIVE MIN. PRINCIPAL STRESS RATIO FOR DISTURBED CLAYEY SILT.

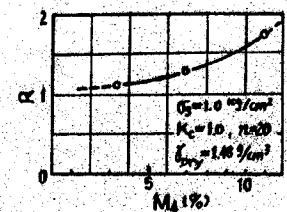


Fig. 17. LIQUEFACTION RESISTANCE RATIO VERSUS CLAY PARTICLE CONTENT.

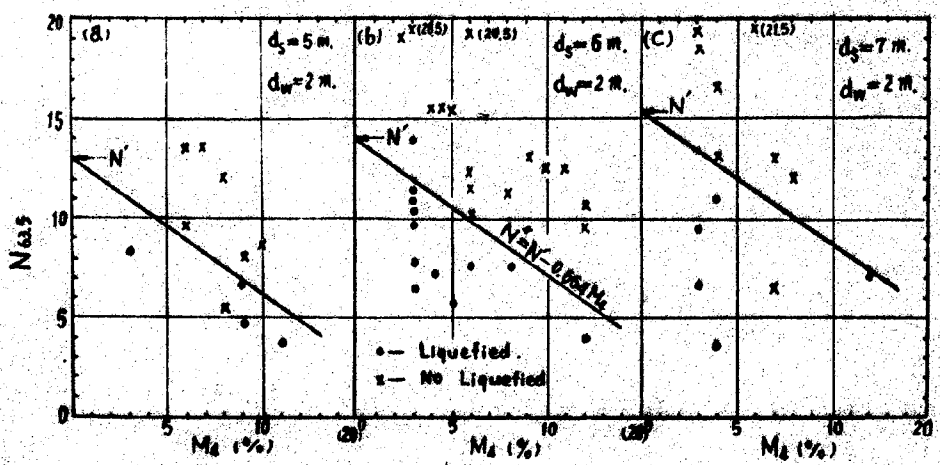


Fig. 18. BLOW NUMBER OF STANDARD PENETRATION TEST VERSUS CLAY PARTICLE CONTENT.

FOUNDATION PROBLEMS IN ASEISMATIC DESIGN OF HYDRAULIC STRUCTURES

WANG, WEN-SHAO*

SUMMARY

In aseismatic design of hydraulic structures the safety of their foundations should be studied comprehensively to meet all requirements for stability, seepage control and allowable deformation. Six main problems are discussed. They are problems of active faults, weak seams in rock foundation, soil liquefaction, soft clays, safety of seepage control system and erratic ground. Special attention has been paid to soil liquefaction and soft clays. Engineering remedies of these problems are also mentioned.

INTRODUCTION

In aseismatic design of hydraulic structures a comprehensive study should be made to meet all the requirements of foundation safety against instability, seepage failure and unacceptable deformation according to the type and form of superstructure, the engineering and hydrological geology of foundation, the hydraulic and operational condition of project and the seismic aspect and ground motion at the site. Six main foundation problems are considered based on field records of earthquake damaged areas in China during past two decades, questions raised by many our design engineers for new hydraulic establishments and experiences obtained in other part of the world.

PROBLEM OF ACTIVE FAULT

There are a few cases appearing in records that some hydraulic structures have been damaged by fault breaks during strong earthquakes (Sherard, etc., 1974). San Andreas Dam, Upper Cristal Springs Dam and Old San Andreas Dam were all sheared by the San Andreas Fault during 1906 San Francisco earthquake. All American Canal was sheared at one place by the Emperial Fault during 1940 El Centro earthquake. The bed rock of Hebgen Reservoir and its dam site subsided about 3 m in average with maximum of about 6.7 m due to vertical displacement of the main Hebgen Fault during 1959 West Yellowstone earthquake.

* Head, Department of Earthquake Engineering, Water Conservancy and Hydro-electric Power Research Institute

Table 1 gives some statistical data of historical fault breaks and their maximum displacements. A rough correlation between length of break and maximum relative displacement of ground on opposite sides is shown in Fig. 1.

Since there is no way to prevent fault break to occur, it is required to avoid erecting hydraulic structures across potentially active faults. It is certainly prohibitive to build concrete or stone masonry dams over active faults owing to their brittleness. For embankment dams it is advised to use zoned earth and rock fill dams with thick impervious clay cores protected by well proportioned filter and transition zones to prevent piping through cracks which might be opened by fault breaks.

PROBLEM OF WEAK SEAMS IN ROCK FOUNDATION

Firm rock foundations can sustain safely against strong earthquake waves, but weak and soft seams, especially low dip angle mud bands or water softening rocks, are troublesome to stability and deformation of concrete dams and locks because of their low strength and low frictional angle. Their behavior under dynamic earthquake action is even not well understood. Special research for this problem seems necessary.

Another problem which should be cautioned is the possibility of breakage of watertight membrane either of natural impervious strata or of man-made cut-off diaphragm wall or grouting curtain in pervious foundation by strong earthquake action. When this occurs, not only the water will leak through the breakage, but also the pore water pressure distribution in foundation will become worse to cause instability of the structure.

PROBLEM OF SOIL LIQUEFACTION

Practical consideration

Saturated cohesionless and less cohesive silty soils, if not densely compacted, are vulnerable to liquefaction during earthquakes because of increase of pore water pressure and decrease of internal shear resistance in the soil mass. However, the foundation may lose its service ability or fail when the pore water pressure becomes high enough and the internal shear resistance is reduced to be equal to or less than the driving shear stress before commencement of soil liquefaction. Therefore, in aseismic design of hydraulic structures it would be safer to keep the foundation always within the margin of stability without permission for liquefaction.

to actually occur.

Main category of liquefiable soil

Based on field data obtained from various earthquake damaged areas in China, it is found that saturated soils containing less than 15% (with maximum of 21%) of clay sized particles ($d < 0.005$ mm) by weight are liquefiable (Fig. 2). The plasticity index I_p of these soils are mostly less than around 10, but could go up to 14 (Fig. 3). Soils with plasticity index $I_p < 3$ are typical cohesionless soils while those with $I_p > 3$ may be called less cohesive silty soils. Among them saturated sands and silts are most vulnerable to liquefaction.

Some coarser grained soils, such as gravelly sands and sandy gravels, have also shown to be liquefiable. Sand volcanos, formed by bleeding of liquefied underlying strata over the bank of Manggou River near epicentrum, Gushan Hill, after 1975 Haicheng earthquake, contains about 25% of gravel sized particles ($d > 2$ mm). The submerged portion of sand gravel upstream protection layer with stone facing of Baihe main dam of Miyun Reservoir slid just as flow slide into bottom to the reservoir during 1976 Tangshan earthquake. The maximum ground acceleration recorded at dam site was around $0.05 g$ ($g = 9.8 \text{ m/s}^2$). It has been found that the liquefaction characteristics of saturated sand gravels is governed by its finer portion ($d < 5$ mm), when its coarser portion ($d > 5$ mm) is less than about 60% by weight.

Criteria for preliminary evaluation

1. For saturated sand foundations

(1) By standard penetration test (SPT)

The method given in the Aseismic Design Code of Industrial and Domestic Buildings (Tentative, 1974, China) is employed, which states that, if the SPT blow counts $N_{63.5}$ in a saturated sand layer at depth d_s (< 5 m) is less than N' computed by following equation (Eq. 1), then the saturated sand at depth d_s is considered to be liquefiable:

$$N' = \bar{N}' \left[1 + 0.125(d_s - 3) - 0.05(d_w - 2) \right] \quad (1)$$

where d_w is depth of ground water level below ground surface; \bar{N}' is critical SPT blow counts for $d_s = 3$ and $d_w = 2$, which equals 6, 10 or 16 for earthquake intensity VII, VIII or IX respectively.

However, two modifications have been made by the author when Eq. 1 is being used:

a. For shallow saturated sand layer of depth less than 5 m, N' is to be computed by setting $d_s = 5$ m in Eq. 1 instead of true depth, because it has been felt that the value N' given by Eq. 1 in this range of depth ($d_s < 5$ m) might be too low and on the unsafe side as compared with other criteria (Table 2).

b. If the ground surface and ground water levels before and after the construction of hydraulic structures are not same, the SPT blow counts $N'_{63.5}$ obtained before construction will be corrected to $N_{63.5}$ for conditions when structures are in normal operation by the following approximate relationship:

$$N_{63.5} = N'_{63.5} (d_s + d_w + 7.8) / (d'_s + d'_w + 7.8) \quad (2)$$

where the apostrophe " ' " denotes quantities measured at the time when SPT were performed before construction, while those without apostrophe " ' " are for conditions when the structures have been under normal operation.

(2) By relative density

Based on scattering data obtained both in China and from abroad, saturated sands possessing following ranges of relative density are supposed to be liquefiable under the vibratory action of earthquakes:

Earthquake intensity	Range of relative density
I_s (MM)	D_r (%)
VI	< 65
VII	< 70
VIII	< 75
IX	< 80-85

2. For saturated less cohesive silty soil foundations

Based on data of liquefied and nonliquefied silty soils obtained from various earthquake damaged areas in China during past two decades (Fig. 4 and 5), it is noticed that, when the water content w_s of the saturated less cohesive silty soil is equal to or greater than 90 - 100% of its liquid limit w_L or when its liquidity Index I_L is equal to or greater than 0.75-1, liquefaction of this soil is likely to occur during strong earthquakes.

The above mentioned correlation has been proposed as a criterion for preliminary evaluation which can be written as:

$$w_s \gg (0.9 - 1.0) w_L \quad (3)$$

and

$$I_L \gg 0.75 - 1 \quad (4)$$

where $I_L = (w_s - w_p) / I_p$, in which w_p is plastic limit.

Engineering remedies

Any potentially liquefiable soil layers should be avoided, otherwise they should be replaced or improved to fulfill the requirement of foundations for hydraulic structures. The fundamental improvement is to densify the soil layer by various techniques such as vibroflotation, deep compaction, compacting piles, deep brasting, vibro-compaction, etc. Other engineering measures such as use of pile foundation, sheet piling or underground wall enclosure, sand and gravel drains, superficial loading or dewatering are also effective to reduce damage of foundation which contains liquefiable soil layers. The main object of improvement is to eliminate factors which might bring about high pore water pressure rise in the soil and to strengthen the foundation.

PROBLEM OF SOFT CLAYS

There have been many cases in which foundation failures during strong earthquakes are due to instability and deformation of soft clay strata. Some examples which have occurred in China are given in Table 3. As another examples reported by Mitchell and Houston (1969), many landslides which developed during the 1964 earthquake in Anchorage, Alaska, involved, at least in part, failures in the sensitive Bootlegger Cove clay (Fig. 6).

In the Aseismic Design Code of Industrial and Domestic Buildings, soft clay foundations with bearing capacities less than 8, 10 and 12 t/m² are considered to be unsafe against strong earthquakes of intensities VII, VIII and XI respectively.

Based on the above mentioned data, the author has proposed the following index properties as criteria for soft clays which should be taken caution in the aseismic design of hydraulic structures:

Liquidity Index: $I_L \geq 0.75$

Unconfined compressive strength: $q_u \leq 0.5 - 0.7 \text{ kg/cm}^2$

SPT blow counts: $N \leq 4$

Sensitivity: $S_t > 4$

The peculiar behavior of soft clays is their low strength, high sensitivity and high compressibility. Special experimental and analytical studies of their dynamic behavior are required for aseismic design.

Soft clay strata, if being not avoidable, should be replaced or improved for foundations of hydraulic structures. Preloading, sand drains, pile foundation, sheet piling or underground wall enclosure, etc. are methods usually employed to strengthen soft clay foundations for different types of structures. Reduction of base pressure by broadening the base size, readjustment of load distribution by counter weights, increase of integrity and rigidity of foundation structure by adequate design, etc. are also ways of improvement. It is advised not to build concrete, stone masonry and rockfill dams on soft clay foundations.

PROBLEM OF SEEPAGE CONTROL SYSTEM

Seepage control system is important for water retaining structures such as dams, locks, etc.. It is not unusual that after strong earthquakes many water retaining structures have shown leakage through their foundations and abutments. In some severe cases, piping has developed, structure has collapsed and downstream area has been flooded. Therefore, how to maintain safety of seepage control system against strong earthquake is a very important problem.

Seepage control system is composed of both seepage prevention elements such as grouting curtain, cut-off wall or trench, upstream impervious blanket, etc. and seepage protection elements (for prevention of internal erosion) such as inverted filter, drainage system, etc.. Any breakage of the above mentioned elements will alter the pattern of seepage flow and reduce the seepage control ability of the foundation. Engineering measures have to be taken to provide a sound seepage control system for the foundation and at contact faces between structure and ground wherever breakage and leakage are likely to occur under earthquake action.

Instrumentation for measuring pore water pressures and seepage flow should be provided in order to detect seepage condition in the foundation and abutments during earthquake.

PROBLEM OF ERRATIC GROUND

If the characteristics of ground material, either rock or soil, change abruptly in lateral direction within extent of the foundation of hydraulic structure, nonuniform settlement of the foundation and its superstructure is likely to occur during strong earthquakes. This may also bring about breakage of seepage control elements and cause damage to the structure.

Remedies could be taken to eliminate heterogeneity of the foundation by strengthening the soft parts of the ground and to provide extra seepage control elements at places where leakages are likely to occur. The configuration of base and load distribution condition could also be regulated to fit the heterogeneity of the foundation.

ACKNOWLEDGMENTS

This paper is a contraction of part of the background material in relation to foundations prepared by the author for the Aseismic Design Code of Hydraulic Structures. The material has been discussed by many co-workers of the Code.

REFERENCES

- Houston, W. B. and Mitchell, J. K., 1969, Property Interrelationships in Sensitive Clays, JSMFD, ASCE, Vol. 95, No. SM4, pp 1037 - 1062.
- Kishida, H., 1966, Damage to Reinforced Concrete Buildings in Niigata City with Special Reference to Foundation Engineering, Soil and Foundation, Vol. 4, No. 1, pp 71 - 88.
- Mitchell, J. K. and Houston, W. N., 1969, Causes of Clay Sensitivity, JSMFD, ASCE, Vol. 95, No. SM3, pp 845 - 871.
- Nishigawa, H., Yakagi, K., Nakagawa, S. and Wada, K., 1977, Practical Method of Predicting Sand Liquefaction, Proc. 9th ICSMFE, Vol 2, pp 305 - 308.
- Seed, H. B. and Idriss, I. M., 1967, Analysis of Soil Liquefaction: Niigata Earthquake, JSMFD, ASCE, Vol. 93, No. SM3, pp 83 - 110.

- Sherard, J. L., Cluff, L. S. and Allen, C. R., 1974, Potentially Active Faults in Dam Foundations, Geotechnique, Vol. 24, No. 3, pp 367 - 428.
- Tsuchida, H., 1975, Current State and Problems of Aseismic Design for Liquefiable Foundations, Soil and Foundation (In Japanese), Vol. 23, No. 6, pp 5 - 6.

Table 1 Historic fault breaks

Maximum displacement, m	Number of fault breaks		
	In China (incomplete)	By Bonilla	By Ambrasseys
0.01 - 1.00	5	15	18
1.01 - 2.00	2	16	13
2.01 - 3.00	5	8	4
3.01 - 4.00	1	8	7
4.01 - 5.00	0	4	5
5.01 - 6.00	0	4	2
6.01 - 7.00	0	4	2
7.01 - 8.00	0	1	1
8.01 - 9.00	0	1	1
9.01 - 10.00	0	1	0
10.01 - 11.00	0	1	0
11.01 - 12.00	0	0	0
12.01 - 13.00	0	0	1
Total	13	63	54

Table 2 Comparison of critical SPT blow counts N_{cr} from different sources

	$N_{cr} = N'$ computed by Eq. 1					Japanese Harbour Standard	1964 Niigata earthquake	R. C. Buildings	Nishigawa, etc.
d_s, m	0	3	5	5	2 - 3	2 - 3		0 - 5 (at base)	0 5
d_w, m	0	3	0	5	2 - 3			1	
Earthquake intensity						Max. acc., g	Max. acc., g	N_{cr} at base Kishida etc.	
VII	4.4	6.6	5.7	8.1	6.6	0.1	7		
VIII	7.3	11.0	9.5	13.5	11.0	0.2	12	15	10-16 10-21.5
IX	11.6	17.6	15.2	21.6	19.2	0.4	21		

Table 3 Soft clay foundations of hydraulic structures affected by earthquakes

Foundations	Fuyanghe levee	North Shahe levee	Shagouju pumping sta.	Shuangtaizihe lock	Douhe earth dam
Earthquake intensity	VIII	VIII	VIII	VII	IX
location	Xingtai	Xingtai	Tonghai	Haicheng	Tangshan
Year	1966	1966	1966	1975	1976
Dry unite weight, g/cm^3	1.31-1.72	1.55-1.59	0.47-1.29	1.16	1.13-1.60
Void ratio, e_0	0.59-1.06	0.70-0.74	1.16-3.75	1.32	0.68-1.42
Liquidity index, I_L		1.08	0.46-1.73	0.96-1.31	0.61-1.95
Unconfined compressive strength, q_u , kg/cm^2			0.15-0.58	0.15-0.21	
Quick direct shear test					
ϕ	0-10	0-12		4-5	2-12
c	0.02-0.24	0.05-0.21		0.11-0.17	0.12-0.34
Undrained triaxial test					
ϕ				4-5	
c				0.23-0.28	
Vane test, c , kg/cm^2				0.24-0.40	
SPT blow counts, N				2-5	
	Heavy slope slide	Slope slide	Preloaded, Heavy settlement	Pile foundation, No damage	Heavy settlement

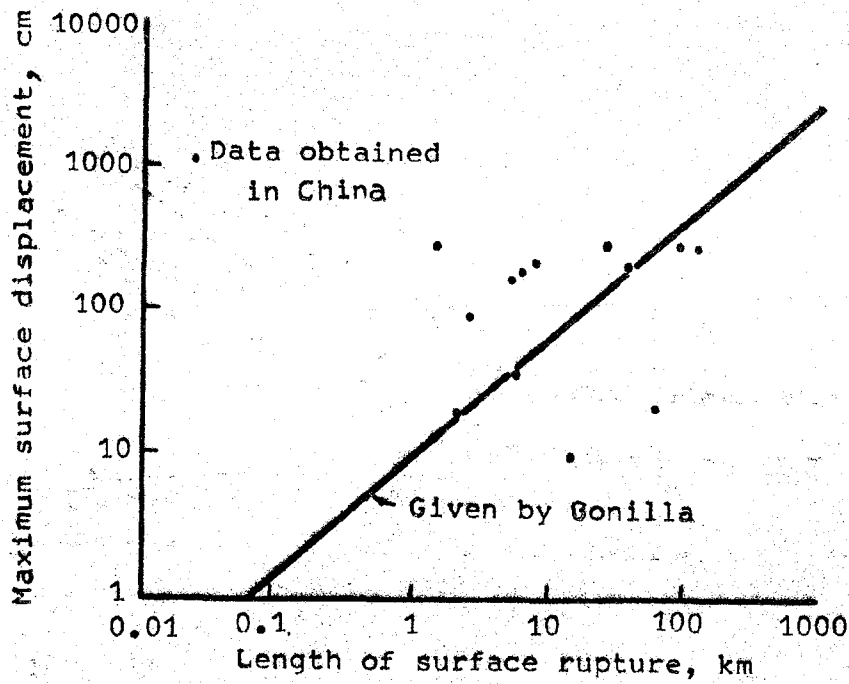


Fig. 1 Rough correlation between length of break and maximum relative displacement of ground on opposite sides

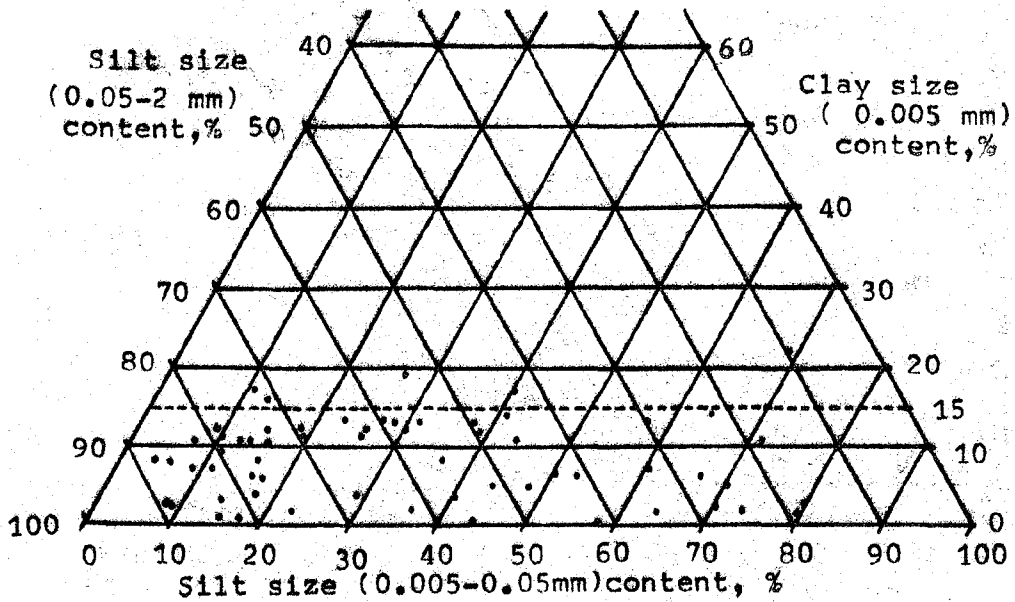


Fig. 2 Range of grain size of liquefied soils at various sites in China during strong earthquakes (VII-IX MM).

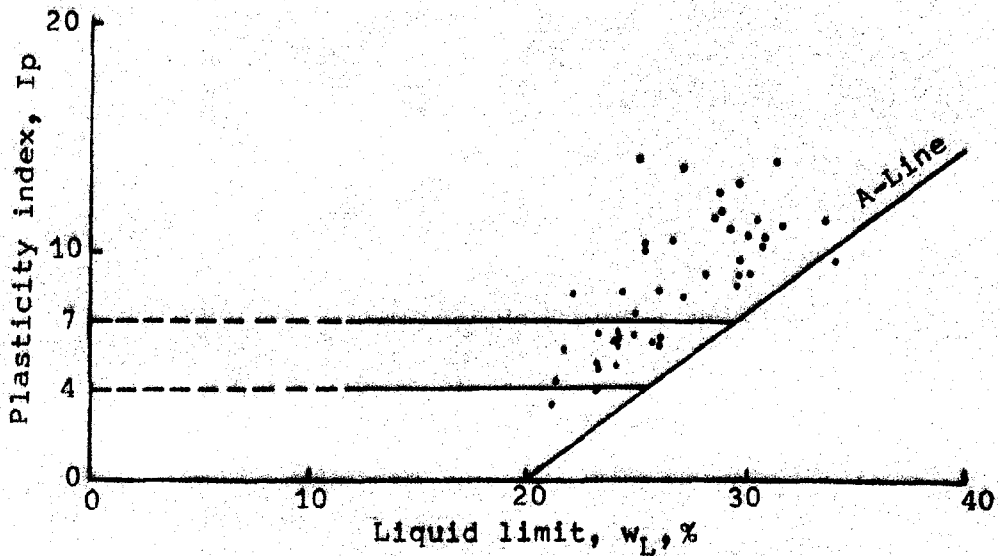


Fig. 3 Plasticity chart for liquefied less cohesive silty soils at various sites in China during strong earthquakes (VII-IX MM)

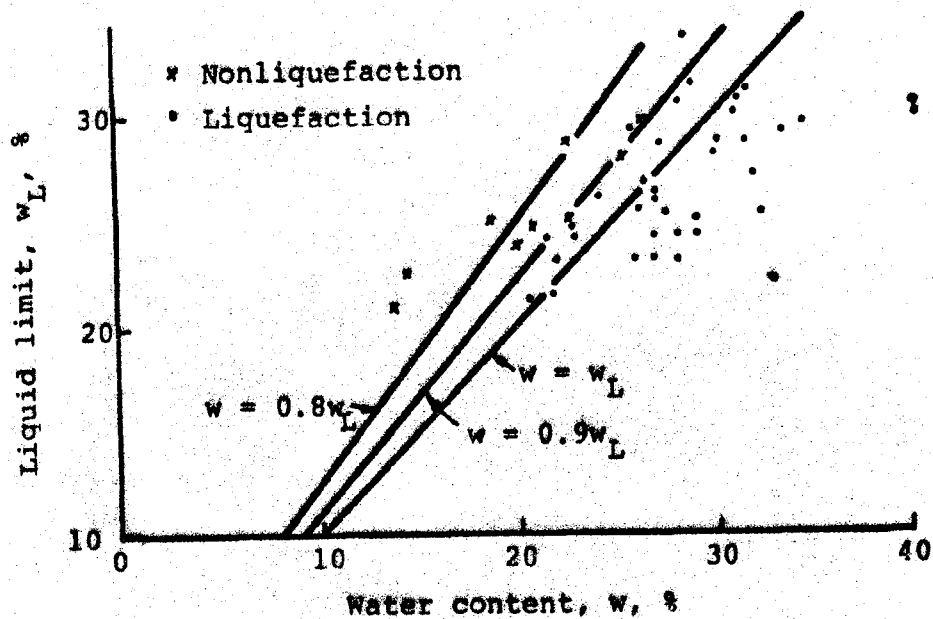


Fig. 4 Water content versus liquid limit of liquefied and nonliquefied less cohesive silty soils at various sites in China during strong earthquakes (VII-IX MM)

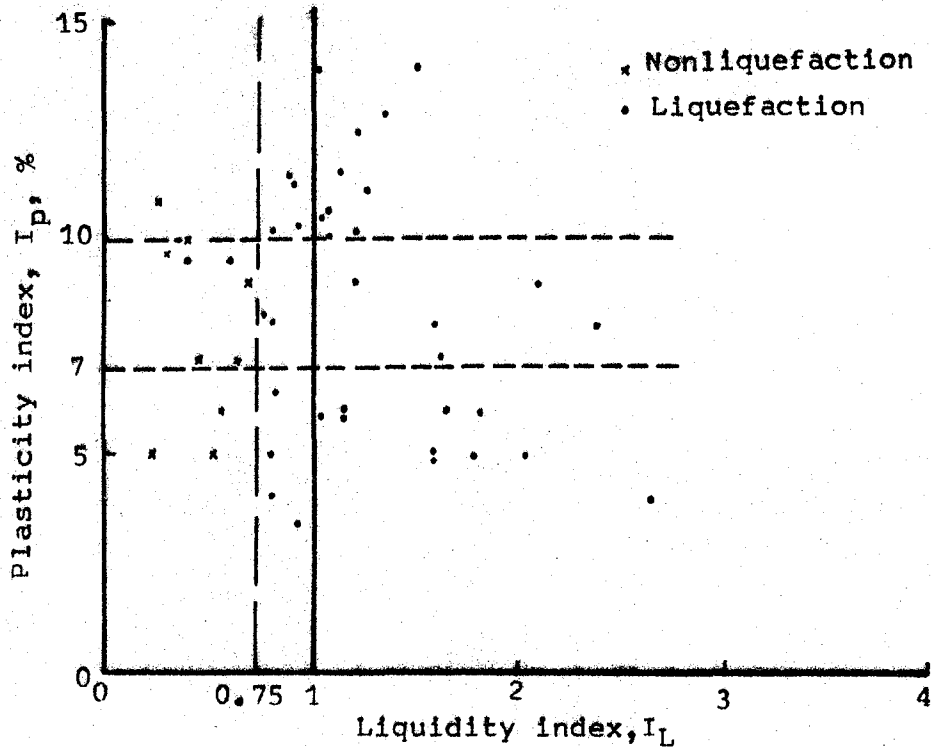


Fig. 5 Liquidity index and plasticity index of liquefied and nonliquefied less cohesive silty soils at various sites in China during strong earthquakes (VII-IX MM)

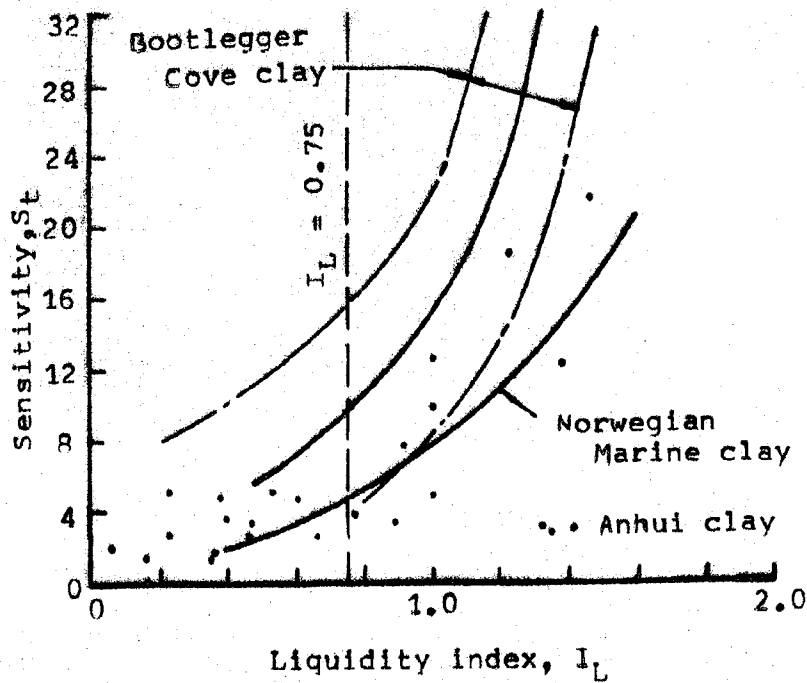
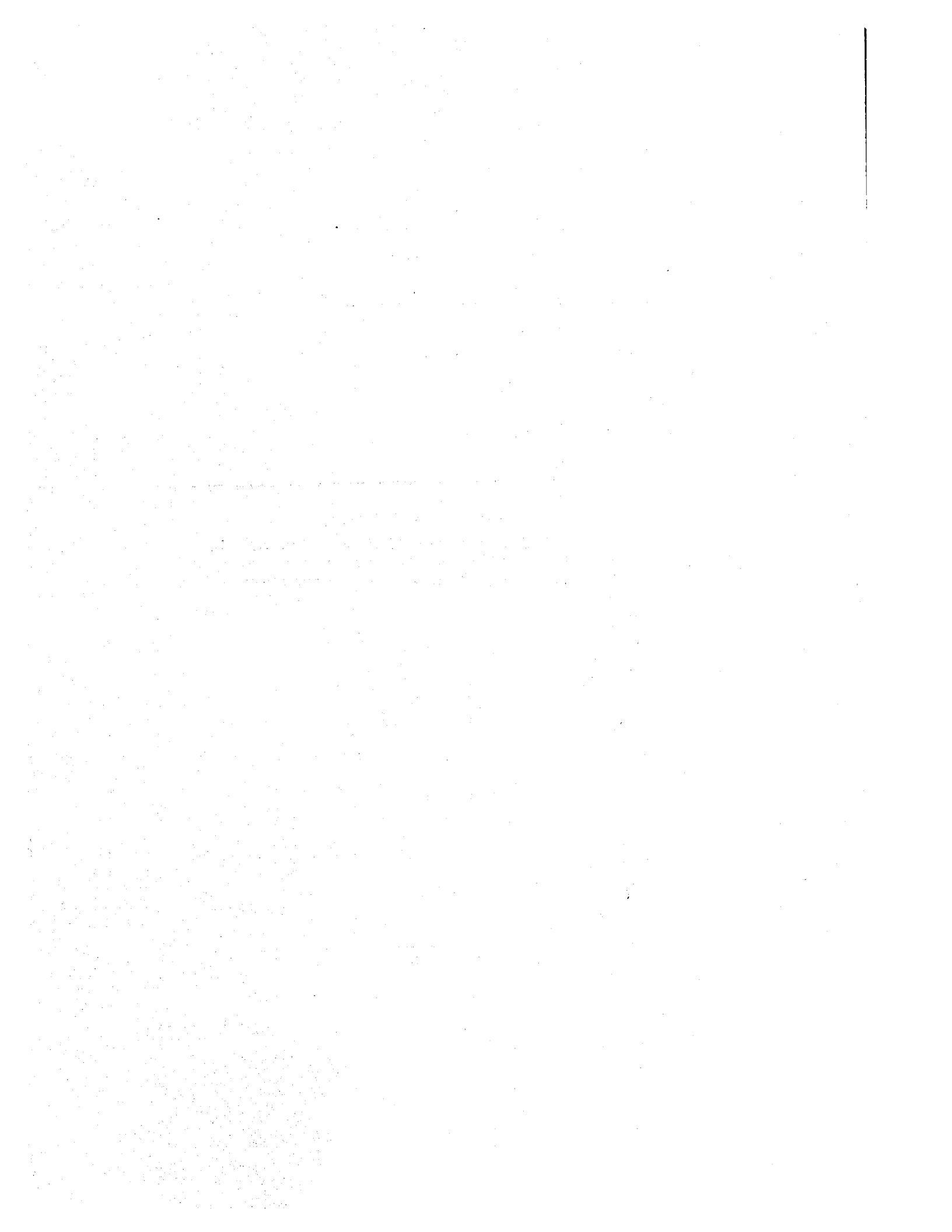


Fig. 6 Relation between sensitivity and liquidity index of soft clays



DYNAMIC SOIL PROPERTIES

by Isao Ishibashi¹

INTRODUCTION

Techniques for analyzing ground response and soil-structure interaction problems during earthquake vibrations (such as the lumped mass method, wave propagation technique, and finite element method) have been rapidly developed in recent years due to a marked improvement in large-capacity digital computation systems. However, successful application of these techniques requires the insertion of realistic and accurate dynamic soil properties into the computer programs. In this paper, the author aims to gather and clarify the information currently available regarding the dynamic soil properties: dynamic shear modulus and damping ratios.

ANALYTICAL MODELS

When either cohesive or noncohesive soils are subjected to cyclic shear loadings, their stress-strain relationships are usually nonlinear and form hysteresis loops, as illustrated in Fig. 1, even for very low cyclic shear strain levels. The path OAA'A" or ODD'D" in the figure, which connects the peak values of the stress-strain loops for different cyclic shear strain levels, is called a backbone curve. The backbone curve coincides with a loading curve for the first cycle and is usually nonlinear. The bulge of the loop also increases with increasing cyclic strain levels. The backbone curve characterizes the shear stiffness of the soil, while the bulge of the loop is attributed to the damping characteristic of the soil, which could include both hysteresis damping and viscous damping, depending on the type of dynamic tests performed.

A. Equivalent Linear Model

If the series of stress-strain loops obtained from laboratory cyclic tests have frequencies similar to those of earthquake vibrations such as 1 - 3 Hz, these loops themselves can be fitted by mathematical equations such as bilinear models or others discussed later and used for response analysis. Most conveniently, however, the stress-strain relationships obtained can be replaced by an equivalent linear model as follows. As shown in Fig. 2, a real stress-strain loop in (a) is approximately equal to a linear spring with spring constant G_{eq} in (b) and equivalent damping ratio D_{eq} in (c). D_{eq} is defined as

$$D_{eq} = \frac{1}{4\pi} \cdot \frac{\Delta W}{W} \quad (1)$$

where ΔW is the area inside a stress-strain loop or total energy dissipated in a complete reversed cycle, and W is the area of the triangle OAB in Fig. 2(a) or the maximum energy input in an equivalent linear system.

¹ Associate Professor, School of Civil and Environmental Engineering, Cornell University, Ithaca, New York, 14853.

Once the equivalent shear modulus G_{eq} and equivalent damping ratio D_{eq} are determined, the linear vibration equation shown below is applicable:

$$\ddot{u} + 2D\dot{u} + \omega^2 u = -a \quad (2)$$

where $D = D_{eq}$, $\omega^2 = K$ (stiffness)/ m (mass) and "a" is the earthquake acceleration. The stiffness K is related to the equivalent dynamic shear modulus G_{eq} , dynamic Poisson's ratio, and geometry of the elements, and is equal to $(G_{eq}/h)A$ in the lumped mass model, where h is the thickness of the subdivided soil layer and A is the area of the soil column.

The damping ratio D in Eq. 2 should be modified by Eq. 3 only when the dynamic stress-strain relationship is obtained from a slow (compared with earthquake frequency) cyclic testing during which the viscous response of the soil is eliminated, as suggested by Idriss and Seed (1968).

$$D = D_{eq} + D_{vis} \quad (3)$$

where D_{vis} is the viscous damping ratio. Parmelee et al. (1964) determined D_{vis} values from the logarithmic decrement (Eq. 4) of free vibrations and obtained an average value of 9.4% for various cohesive soils. Idriss and Seed (1968) used $D_{vis} = 6\%$ for their response analysis:

$$D_{vis} = \frac{1}{2\pi} \log \frac{a_i}{a_{i+1}} \quad (4)$$

where a_i and a_{i+1} are the peak accelerations measured during the i^{th} and $(i+1)^{th}$ cycles in free vibration. It should be noted, however, that if the real stress-strain loops are obtained from laboratory cyclic tests with earthquake frequencies, no viscous damping modification, as was made in Eq. 3, is necessary, since the loops already include the effect of viscous damping, as well as hysteresis damping, for that frequency level.

B. Linear Visco-elastic Model (Kelvin Model)

The first and simplest simulation of the soil model may be a Kelvin model, which consists of a linear spring and a linear dashpot, as seen in Fig. 3. The dynamic response of this model is first analyzed in order to demonstrate the nonlinear behavior of soils. When the total shear stress τ is developed upon the application of shear deformation γ , the equation is

$$\tau = G\gamma + C \frac{d\gamma}{dt} \quad (5)$$

where G and C are considered constants for the linear visco-elastic model.

For sinusoidal cyclic strain application, Eq. 5 becomes

$$\gamma = \gamma_0 \sin \omega t \quad (6)$$

$$\frac{d\gamma}{dt} = \omega \gamma_0 \cos \omega t \quad (7)$$

Therefore, substituting Eqs. 6 and 7 into Eq. 5, Eq. 8 is obtained:

$$\tau = \gamma_0 G \sqrt{1 + \frac{c^2 \omega^2}{G^2}} \cdot \sin(\omega t + \delta) \quad (8)$$

where γ_0 and ω are the amplitude and frequency of the applied cyclic shear strain, respectively, and δ is a phase angle.

Eq. 8 can be plotted in the τ - γ domain, and it shows an ellipse for a given ω , as seen in Fig. 4. When the frequency ω is varied, the shape of the ellipse changes while keeping G and γ_0 as constants, as seen in Fig. 5. Fig. 5 demonstrates that the visco-elastic material behaves as a function of the frequency of the applied cyclic strain and that the area inside the loop (energy loss) depends greatly on the frequency ω , and becomes zero at $\omega = 0$. Although this simple model demonstrates the frequency-dependent nature of soils, it does not adequately represent the nonlinearity of spring and dashpot.

C. Bilinear Model

Real cyclic stress-strain relationships can be approximately replaced by a parallelogram, as shown in Fig. 6. The straight lines 1-2 and 4-3 are extended and intersect at 5. Lines 4-6 and 1-6, with tangents G_1 and G_2 , are parallel to lines 1-5 and 4-5 respectively. In the bilinear model, a yielding shear strain γ_y is defined, as seen in Fig. 6. The stress-strain relationship follows path 0-7 with G_1 until the shear strain exceeds γ_y , and path 7-1 with G_2 thereafter until γ reaches γ_{\max} . Therefore, in this model, G_1 , G_2 , and γ_y values should be determined as a function of γ_{\max} . Idriss and Seed (1968) showed that the response values determined by the equivalent linear model and the bilinear model are in good agreement.

A bilinear model can be replaced by an equivalent linear model by using the following equations:

$$G_{eq} = \text{slope of 0-1} = G_2 \left(1 - \frac{\gamma_y}{\gamma_{\max}} \right) + G_1 \frac{\gamma_y}{\gamma_{\max}} \quad (9)$$

and

$$D_{eq} = \frac{1}{4\pi} \cdot \frac{\Delta W}{W} = \frac{2}{\pi} \cdot \frac{\left(1 - \frac{G_2}{G_1} \right) \left(\frac{\gamma_{\max}}{\gamma_y} - 1 \right)}{\frac{G_2}{G_1} \left(\frac{\gamma_{\max}}{\gamma_y} - 1 \right) + 1} \cdot \frac{\gamma_y}{\gamma_{\max}} \quad (10)$$

P. Ramberg-Osgood Model

In this model, the backbone curve is linear up to the yielding strain γ_y and becomes nonlinear thereafter, as shown in Fig. 7.

$$\tau = G_1 \gamma \quad \text{for } 0 \leq \gamma \leq \gamma_y \quad (\text{path 0-1}) \quad (11)$$

$$\tau = G_1 \gamma - \alpha \frac{\tau^r}{(G_1 \gamma_y)^{r-1}} \quad \text{for } \gamma_y \leq \gamma \leq \gamma_{\max} \quad (\text{path 1-2}) \quad (12)$$

where α and r are modification constants. The value r should be equal to or greater than 1.

The curve 5-6-7-2 has the same shape as the one through 1-2, but it is enlarged to fit points 1 to 5 and 2 to 2 (Masing criterion), as

$$\tau + \tau_{\max} = G_1(\gamma + \gamma_{\max}) - \alpha \frac{(\tau + \tau_{\max})^r}{(2G_1 \gamma_y)^{r-1}} \quad (13)$$

The path 2-3-4-5 is obtained by rotating the curve 5-6-7-2 180 degrees:

$$\tau - \tau_{\max} = G_1(\gamma - \gamma_{\max}) - \alpha \frac{(\tau - \tau_{\max})^r}{(2G_1 \gamma_y)^{r-1}} \quad (14)$$

In the Ramberg-Osgood model, the values of G_1 , γ_y , α , and r should be determined as a function of γ_{\max} . The equivalent linear model corresponding to the Ramberg-Osgood model is

$$G_{eq} = \frac{G_{\max}}{1 + \alpha \left(\frac{\tau_{\max}}{G_{\max} \gamma_y} \right)^{r-1}} \quad (15)$$

$$D_{eq} = \frac{2}{\pi} \cdot \alpha \frac{r-1}{r+1} \left(1 - \frac{G_{eq}}{G_1} \right) \quad (16)$$

Idriss et al. (1978) recently reported the values of $R = 3.5$ and $\alpha = 0.5$ in the Ramberg-Osgood model to characterize the dynamic behavior of San Francisco Bay mud. It is also interesting to note that the same authors showed experimentally that the backbone curve could be determined approximately by the results of one fast monotonic undrained test with a strain rate such as 8%/sec.

E. Hardin-Drnevich Model

Hardin and Drnevich (1972) assumed that the backbone curve is defined by a hyperbolic curve and that the curve approaches the τ_{\max} value (static shear strength value) at γ (dynamic shear strain) $= \infty$ and has its maximum slope G_{\max} (maximum shear modulus) at $\gamma = 0$, as seen in Fig. 8 and expressed in Eq. 17:

$$\tau = \frac{G_{\max} \gamma}{1 + \frac{\gamma}{\gamma_r}} \quad (17)$$

or

$$G_{eq} = \frac{\tau}{\gamma} = \frac{G_{\max}}{1 + \frac{\gamma}{\gamma_r}} \quad (18)$$

where $\gamma_r = \tau_{\max}/G_{\max}$ is called the reference strain.

Instead of defining any equations for the loop, they assumed that the area of the loop A_L was a constant percentage of the area of the triangle $abc, A(abc)$, as seen in Fig. 9:

$$\frac{A_L}{2} = K_1 A(abc) \quad (19)$$

where K_1 is constant.

Therefore, the equivalent damping ratio, D_{eq} , in the model is

$$D_{eq} = \frac{1}{4\pi} \cdot \frac{\Delta W}{W} = \frac{2K_1}{\pi} \left(1 - \frac{G_{eq}}{G_{\max}} \right) \quad (20)$$

When γ approaches infinity (or $G_{eq} \rightarrow 0$),

$$D_{eq, \max} = \frac{2K_1}{\pi} \quad (21)$$

Therefore,

$$D_{eq} = D_{eq, \max} \left(1 - \frac{G_{eq}}{G_{\max}} \right) = D_{eq, \max} \frac{\gamma/\gamma_r}{1 + \gamma/\gamma_r} \quad (22)$$

In summary, the Hardin-Drnevich model uses Eq. 18 for equivalent shear moduli and Eq. 22 for equivalent damping ratios, but it is slightly modified by substituting the modified γ/γ_r values expressed in Eq. 23 into the original γ/γ_r in Eqs. 18 and 22 in order to fit their resonant column test results.

$$\frac{\gamma}{\gamma_r} = \frac{\gamma}{\gamma_r} \left(1 + a \cdot e^{-b(\gamma/\gamma_r)} \right) \quad (23)$$

where a and b are experimental constants and given in Table 1 as functions of the number of applied cycles, N , cyclic frequency f , and the mean principal effective stress $\bar{\sigma}_0$. The maximum shear modulus G_{max} is also given, which was determined from their earlier resonant column experiments:

$$G_{max} = 1,230 \frac{(2.973 - e)^2}{1 + e} (OCR)^K \bar{\sigma}_0^{0.5} \quad (24)$$

where G_{max} and $\bar{\sigma}_0$ are in psi, e is the void ratio, OCR is the overconsolidation ratio, and K is the plasticity index-dependent constant, as shown in Table 2.

τ_{max} values are determined geometrically by using a static failure envelope as demonstrated in Fig. 10:

$$\tau_{max} = \left\{ \left[\frac{1 + K_0}{2} \bar{\sigma}_v \sin \bar{\phi} + \bar{c} \cos \bar{\phi} \right]^2 - \left[\frac{1 - K_0}{2} \bar{\sigma}_v \right]^2 \right\}^{1/2} \quad (25)$$

where $\bar{\sigma}_v$ is effective vertical stress, \bar{c} and $\bar{\phi}$ are the cohesion and angle of internal friction of soil in effective failure envelope, and K_0 is the coefficient of lateral earth pressure at rest.

The last undetermined value in the model, $D_{eq,max}$, is also given in Table 3.

EXPERIMENTAL RESULTS

Sands

Sherif and Ishibashi (1976) and Sherif et al. (1977) conducted dynamic testing in the torsional simple shear device in order to determine the dynamic shear moduli and damping ratios for various sands, ranging from fine to coarse grains. The equivalent shear modulus G_{eq} is summarized in the following two equations:

$$G_{eq} = 112 \phi (\bar{\sigma}_0)^{11.67\gamma + 0.5} \cdot (0.205)^{\gamma/0.03} \quad \text{for } 0 \leq \gamma \leq 0.03\% \quad (26)$$

$$G_{eq} = 2.8 \phi (\bar{\sigma}_0)^{0.85} \cdot \gamma^{-0.6} \quad \text{for } 0.03\% \leq \gamma \leq 1\% \quad (27)$$

where G_{eq} and the mean effective confining pressure $\bar{\sigma}_0$ are in psi, the soil's angle of internal friction ϕ is in degrees, and the dynamic shear strain γ is in percent. All of the experimental data, including various soil types and confining pressures, are plotted in Figs. 11 and 12, which show a reasonable agreement.

The equivalent damping ratio D_{eq} is also found as follows:

$$D_{eq} = \frac{50 - 0.6\bar{\sigma}_0}{38} (73.3F - 53.3)\gamma^{0.3} \quad (28)$$

where D_{eq} and γ are expressed in percent and $\bar{\sigma}_0$ is in psi. F is called the soil gradation and sphericity factor and is defined as

$$F = \frac{1}{\psi^2 C_g} \quad (29)$$

where ψ (soil sphericity) = S'/S (S' and S refer respectively to the surface area of a sphere of the same volume as the soil particle and the actual surface area of the soil), and C_g (coefficient of gradation) = $D_{30}^2/D_{10} \times D_{60}$ (D_{10} , D_{30} , and D_{60} are the soil diameters than which 10, 30, and 60% of the soil by weight is finer, respectively.) Fig. 13 shows a plot of all of the experimental data.

The importance of soil angularity (or sphericity) is emphasized in determining ratios (or soil liquefaction (Sherif and Ishibashi, 1981)) for sands. The approximate soil sphericity can be determined visually as suggested by Rittenhouse (1943). This method involves the microscopic classification of 100 arbitrarily picked sand grains into several representative groups, shown in Fig. 14, and averaging them to determine sphericity.

Iwasaki et al. (1978) and Tatsuoka et al. (1978) determined the G_{eq} and D_{eq} values for sands from resonant column tests for a small shear strain ($\gamma = 10^{-4} - 10^{-2}\%$) and from the torsional shear test for a large strain ($\gamma = 10^{-2} - 1\%$) and proposed the following relationships:

$$\frac{G_{eq}}{G_{eq,max}} = K(\gamma) \cdot \bar{\sigma}_0^{-m(\gamma)} \quad (30)$$

$$\frac{D_{eq}}{D_{eq,max}} = g \left(\frac{G_{eq}}{G_{eq,max}} \right) \quad (31)$$

where $G_{eq,max}$ is the maximum shear modulus (or G_{eq} values at $\gamma = 10^{-4}\%$), $D_{eq,max}$ is the maximum damping ratio at $G_{eq} = 0$, $\bar{\sigma}_0$ is the mean effective confining pressure, and $K(\gamma)$, $m(\gamma)$, and $g(G_{eq}/G_{eq,max})$ are unique functions irrespective of the kind of sands but functions of only γ , γ , and $G_{eq}/G_{eq,max}$ respectively. $K(\gamma)$ and $m(\gamma)$ are shown in Figs. 15 and 16, respectively, with other researchers' results.

In Fig. 17, this author plotted the $g(G_{eq}/G_{eq,max})$ function as determined by several researchers. In Figs. 15, 16, and 17, the variations among these researchers' results are relatively small; therefore, the above simple equations could be used in determining approximate shear moduli and damping ratios for sands. In order to utilize the above convenient relationships, $G_{eq,max}$ and $D_{eq,max}$ values should first be determined. These values are summarized below:

Hardin and Drnevich (from Eq. 24):

$$G_{eq,max} = 1,230 \frac{(2.973 - e)^2}{1 + e} (OCR)^K \bar{\sigma}_0^{0.5} \quad (32)$$

$$D_{eq,max} = 33 - 1.5(\log_{10}N) \quad \text{for clean dry sand} \quad (33)$$

$$= 28 - 1.5(\log_{10}N) \quad \text{for clean saturated sand} \quad (34)$$

where N is the number of applied cycles.

Sherif and Ishibashi (from Eqs. 26 and 28):

$$G_{eq,max} = 118 \bar{\sigma}_0^{0.5} \quad (35)$$

$$D_{eq,max} = \frac{50 - 0.6 \bar{\sigma}_0}{38} (73.3F - 53.3) \quad (36)$$

Iwasaki et al. for Toyoura sand:

$$G_{eq,max} = 4,426 \frac{(2.17 - e)^2}{1 + e} \bar{\sigma}_0^{0.4} \quad (37)$$

$$D_{eq,max} = 33\% \quad \text{for non-clean sand} \quad (38)$$

$$D_{eq,max} = 42\% \quad \text{for clean sand} \quad (39)$$

where $G_{eq,max}$ and $\bar{\sigma}_0$ are expressed in psi, ϕ is in degrees, and $D_{eq,max}$ is in percent.

More realistic and accurate values of $G_{eq,max}$ for individual sands can best be determined by resonant column tests or field shear velocity measurements, both of which are nondestructive and suited for low shear strain applications.

Clays

Dynamic shear moduli for clays are affected by many factors: shear strain amplitude, confining pressure, void ratio, degree of saturation, overconsolidation ratio, number of stress cycles, time effects, etc.

Efforts to normalize G_{eq} values by undrained shear strength S_u and $G_{eq,max}$ values are not always successful in the case of clays (for example, Kovacs et al., 1971; Anderson and Richart, 1976; Koutsoftas and Fischer, 1980; etc.).

It is apparent that no general relationship for the determination of shear moduli and damping for clays has yet been found. One of the important but overlooked parameters which affect the dynamic properties of clays is the generation of pore pressure due to cyclic loadings. There is a definite need for future research and data accumulation in this important area.

SUMMARY AND CONCLUSIONS

Models and empirical equations of dynamic shear moduli and damping for soils are summarized in this paper. Experimental laboratory or in-situ test results could be fitted by the equivalent linear model, bilinear model, Ramberg-Osgood model, or Hardin-Drnevich model and then used further for dynamic analysis. In the case of sandy soils, however, dynamic properties are approximated by the empirical results summarized in Eqs. 30 through 39 and Figs. 15, 16, and 17, without conducting any dynamic tests.

More realistic and accurate results could be obtained by determining $G_{eq,max}$ values by the resonant column technique and field shear velocity measurements for low levels of cyclic strain, and still using the average curves shown in Figs. 15, 16, and 17 for high strain levels.

For soils other than sands, no general and comprehensive relationships among dynamic soil properties and other soil parameters have yet been established. Further research and data accumulation in this area are needed.

REFERENCES

- Anderson, D.G., and Richart, F.E., Jr. (1976), "Effects of Straining on Shear Modulus of Clays," *Journal of Geotechnical Engineering Division, ASCE*, Vol. 102, No. GT9.
- Hardin, B.O., and Drnevich, V.P. (1972), "Shear Modulus and Damping in Soils: Design Equations and Curves," *Journal of Soil Mechanics and Foundations Division, ASCE*, Vol. 98, No. SM7.
- Idriss, I.M., and Seed, H.B. (1968), "Seismic Response of Horizontal Soil Layers," *Journal of Soil Mechanics and Foundations Division, ASCE*, Vol. 94, No. SM4.
- Idriss, I.M., Dobry, R., and Singh, R.D. (1978), "Nonlinear Behavior of Soft Clays during Cyclic Loading," *Journal of Geotechnical Engineering Division, ASCE*, Vol. 104, No. GT12.
- Iwasaki, T., Tatsuoka, F., and Takagi, Y. (1978), "Shear Moduli of Sands under Cyclic Torsional Shear Loading," *Soils and Foundations, Japanese Society of Soil Mechanics and Foundation Engineering*, Vol. 18, No. 1.
- Koutsoftas, D.C., and Fischer, J.A. (1980), "Dynamic Properties of Two Marine Clays," *Journal of Geotechnical Engineering Division, ASCE*, Vol. 106, No. GT6.
- Kokusho, T. (1980), "Cyclic Triaxial Test of Dynamic Soil Properties for Wide Strain Range," *Soils and Foundations, Japanese Society of Soil Mechanics and Foundation Engineering*, Vol. 20, No. 2.
- Kovacs, S.D., Seed, H.B., and Chan, C.C. (1971), "Dynamic Moduli and Damping Ratios for a Soft Clay," *Journal of Soil Mechanics and Foundations Division, ASCE*, Vol. 97, No. SM1.
- Parmelee, R., Penzien, J., Scheffey, C.E., Seed, H.B., and Thiers, G.R. (1964), "Seismic Effects on Structures Supported on Piles Extending through Deep Sensitive Clays," Report No. 64-2, Institute of Engineering Research, University of California, Berkeley.
- Rittenhouse, G. (1943), "A Visual Method of Estimating Two-Dimensional Sphericity," *Journal of Sedimentary Petrology*, Vol. 13.
- Seed, H.B., and Idriss, I.M. (1970), "Shear Moduli and Damping Factors for Dynamic Response Analysis," *Earthquake Engineering Research Center, University of California, Berkeley*, No. EERC 70-10.
- Sherif, M.A., and Ishibashi, I. (1976), "Dynamic Shear Moduli for Dry Sands," *Journal of Geotechnical Engineering Division, ASCE*, Vol. 102, No. GT11.
- Sherif, M.A., Ishibashi, I., and Gaddah, A.H. (1977), "Damping Ratio for Dry Sands," *Journal of Geotechnical Engineering Division, ASCE*, Vol. 103, No. GT7.

References (Continued)

Sherif, M.A., and Ishibashi, I. (1981), "A Rational Theory for Predicting Soil Liquefaction," *Journal of Earthquake Engineering and Soil Dynamics* (in press).

Tatsuoka, F., Iwasaki, T., and Takagi, Y. (1978), "Hysteretic Damping of Sands under Cyclic Loading and its Relation to Shear Modulus," *Soils and Foundations, Journal of Japanese Society of Soil Mechanics and Foundation Engineering*, Vol. 18, No. 2.

TABLE 1. VALUES OF a AND b^a

Soil type (1)	Modulus or damping (2)	Value of a (3)	Value of b (4)
Clean dry sands	Modulus	$a = -0.5$	$b = 0.16$
	Damping ^b	$a = 0.6(N^{-1/6}) - 1$	$b = 1 - N^{-1/12}$
Clean saturated sands	Modulus ^b	$a = -0.2 \log N$	$b = 0.16$
	Damping ^b	$a = 0.54(N^{-1/6}) - 0.9$	$b = 0.65 - 0.65N^{-1/12}$
Saturated cohesive soils	Modulus	$a = 1 + 0.25 (\log N)$	$b = 1.3$
	Damping	$a = 1 + 0.2(f^{1/2})$	$b = 0.2f \left(\frac{-\bar{\sigma}_v}{e_x \bar{p}_v} \right) + 2.25\bar{\sigma}_v + 0.3 (\log N)$

^a f is in cycles per second and $\bar{\sigma}_v$ is in kilograms per square centimeter.

^b These values for modulus and damping of clean sands are for less than 50,000 cycles of loading. Beyond 50,000 cycles the damping begins to increase with number of cycles, possibly due to fatigue effects (2). The behavior of modulus for saturated sands beyond 50,000 cycles is not yet established.

TABLE 2. VALUES OF K

PI (1)	K (2)
0	0
20	0.18
40	0.30
60	0.41
80	0.48
≥100	0.50

TABLE 3. VALUES OF D_{max} ^a

Soil type (1)	Value of D_{max} as a percentage (2)
Clean dry sands	$D_{max} = 33 - 1.5 (\log N)$
Clean saturated sands	$D_{max} = 28 - 1.5 (\log N)$
Saturated Lick Creek silt	$D_{max} = 26 - 4\bar{\sigma}_v^{1/2} + 0.7f^{1/2} - 1.5 (\log N)$
Various saturated cohesive soils including Rhodes Creek Clay	$D_{max} = 31 - (3 + 0.03f)\bar{\sigma}_v^{1/2} + 1.5f^{1/2} - 1.5 (\log N)$

^a f is in cycles per second and $\bar{\sigma}_v$ is in kilograms per square centimeter.

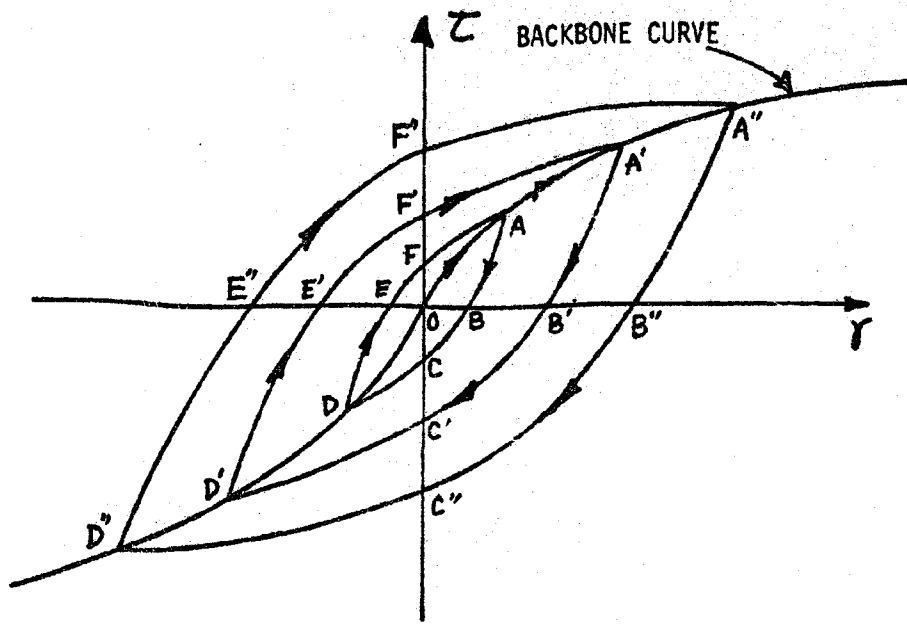


Fig. 1. Nonlinear cyclic stress-strain relationship

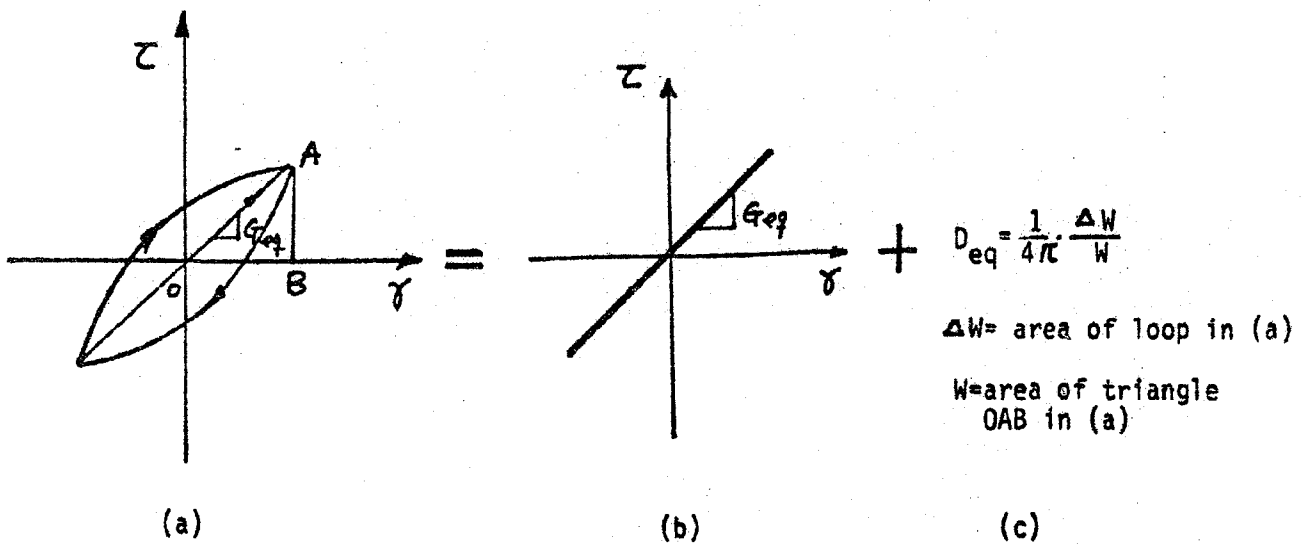


Fig. 2. Equivalent linear model

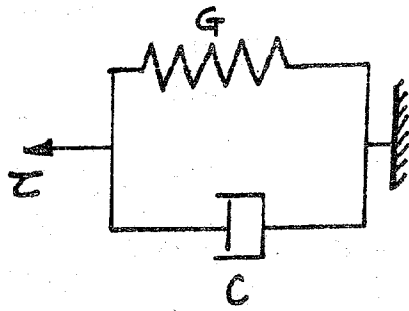


Fig. 3. Visco-elastic model (Kelvin model)

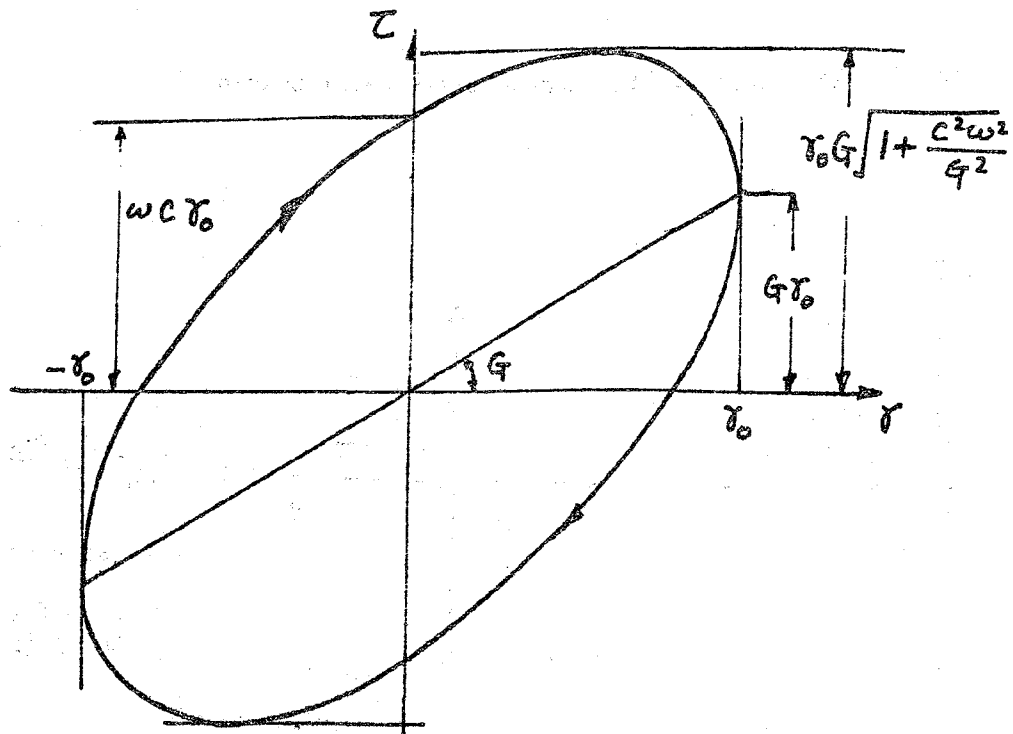


Fig. 4. Stress-strain relationship of Kelvin model

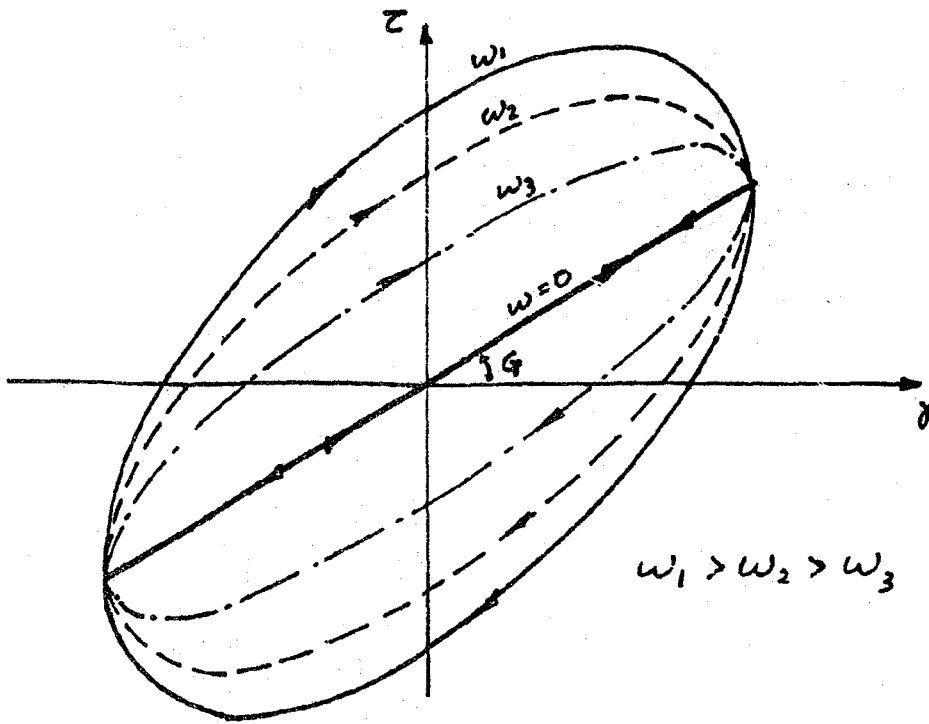


Fig. 5. Stress-strain relationship of Kelvin model with various frequencies

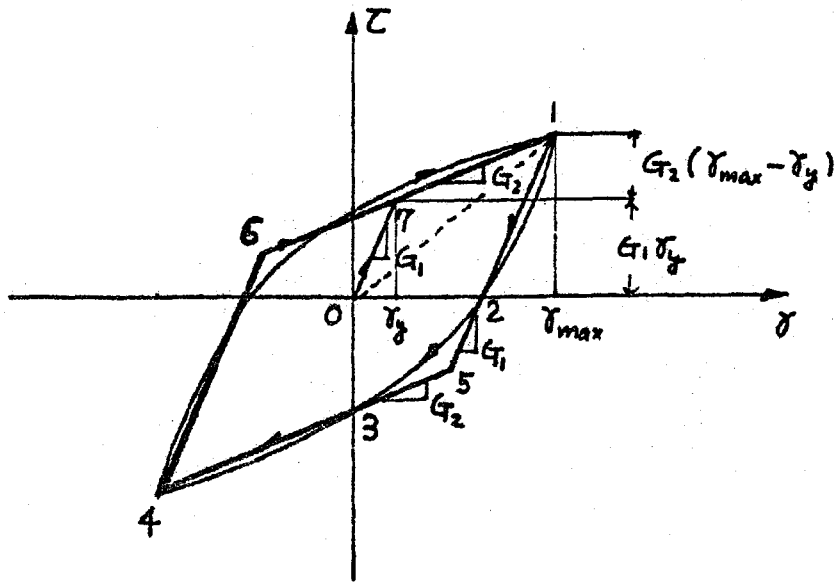


Fig. 6. Bilinear model

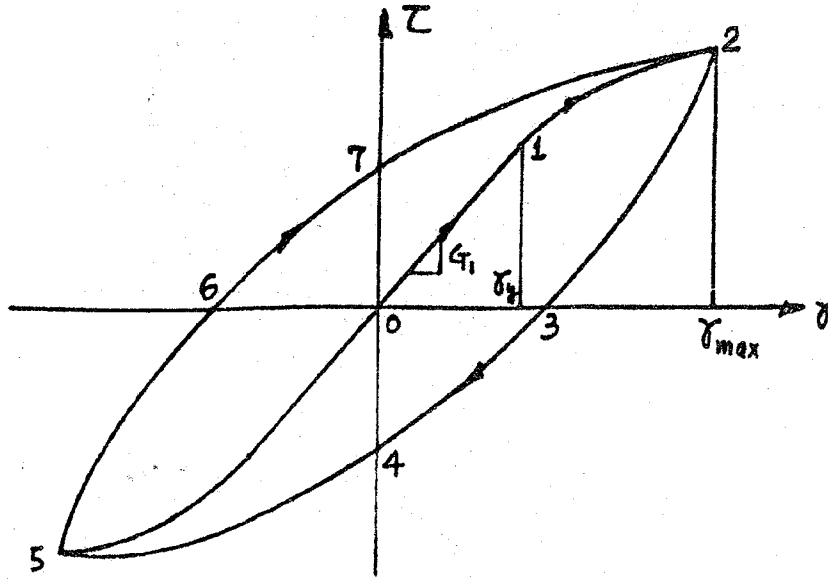


Fig. 7. Ramberg-Osgood model

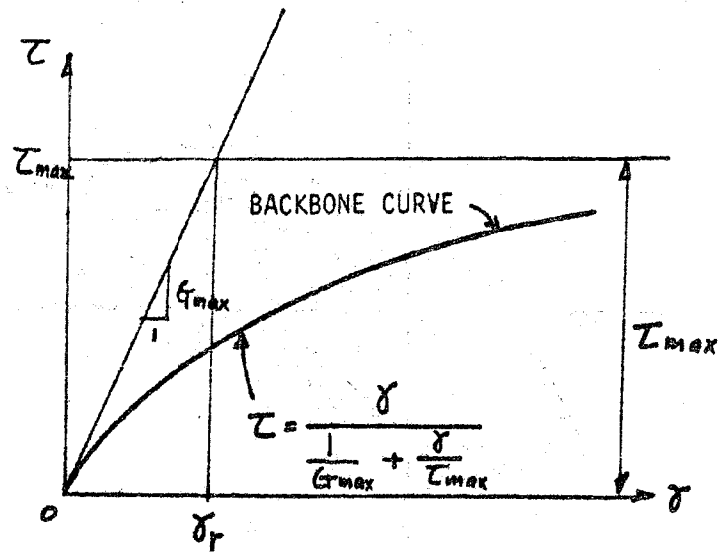


Fig. 8. Hardin-Drnevich model (backbone curve)

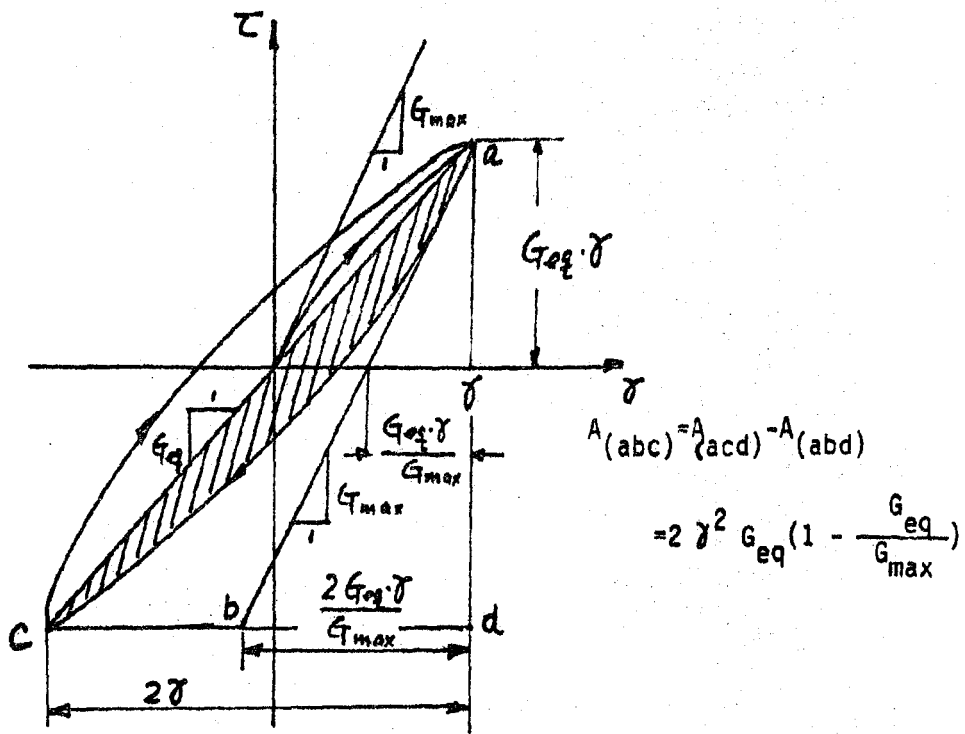


Fig. 9. Hardin-Drnevich model (loss of energy)

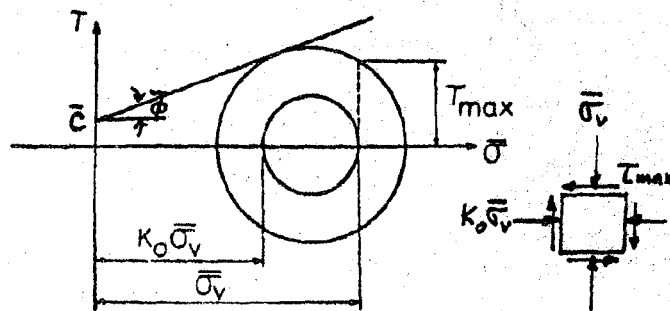


Fig. 10. Hardin-Drnevich model (τ_{max} determination)

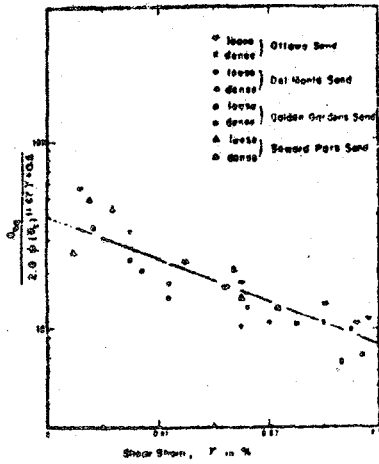


Fig. 11. Analytical and experimental G_{eq} values for $0 < \gamma < 0.03\%$ (Sherif & Ishibashi, 1976)

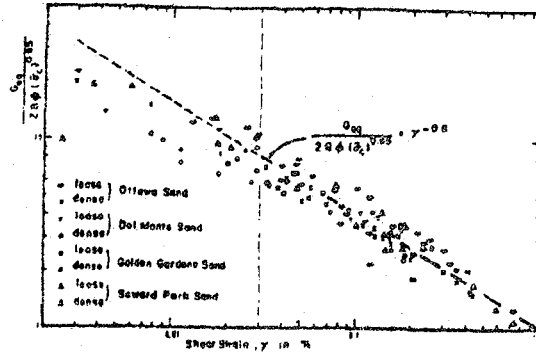


Fig. 12. Analytical and experimental G_{eq} values for $0.03 \leq \gamma \leq 1.0\%$ (Sherif & Ishibashi, 1976)

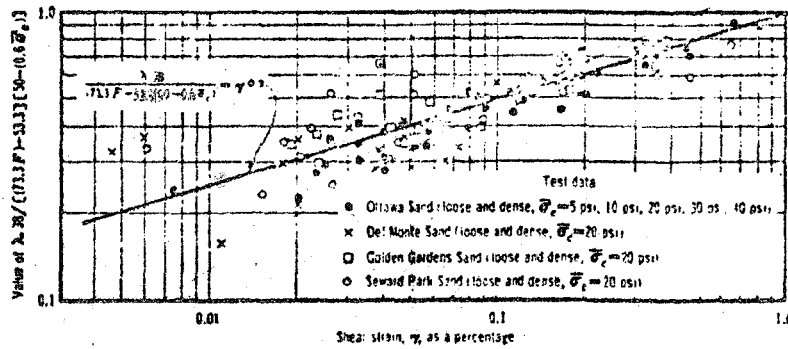


FIG. 13 $\text{Log} \lambda 38 / \{ (73.3F) - 53.3 \} (50 - 0.6\bar{\sigma}_c)$ versus $\text{Log} \gamma$ for Four Types of Sand ($1 \text{ psi} = 6.89 \text{ kN/m}^2$) (Sherif et al., 1977)

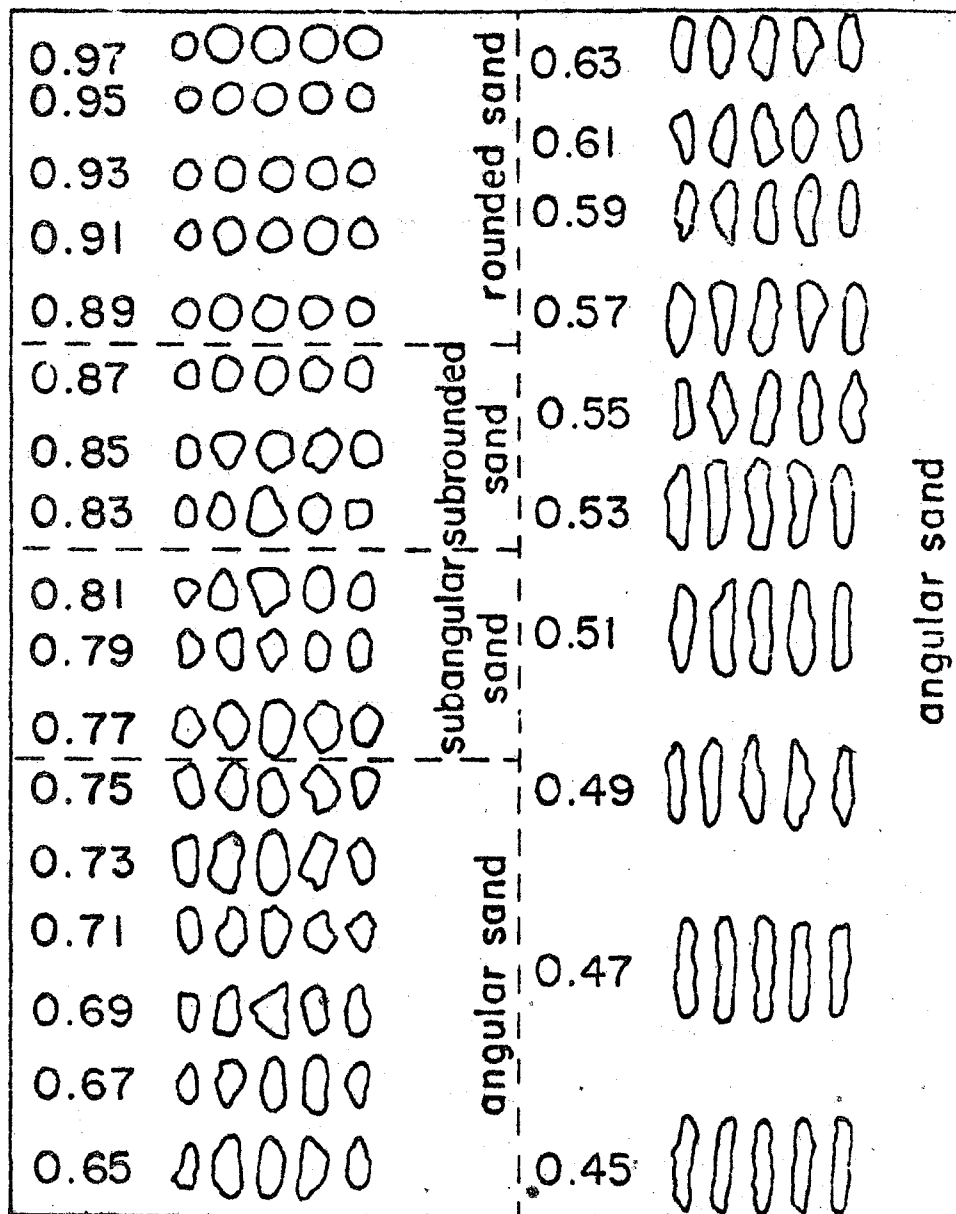


Fig. 14.--Chart for determination of sphericity by visual method

(after Rittenhouse, 1943).

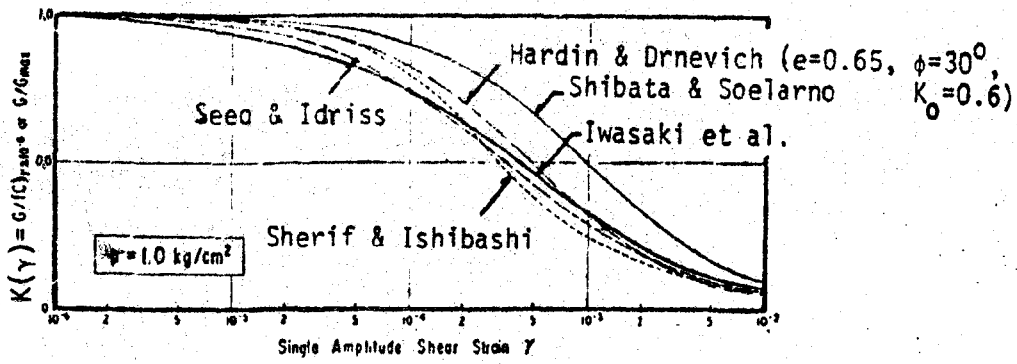


FIG. 15 Comparison among G/G_{max} versus γ Relationships (Iwasaki et al., 1978)

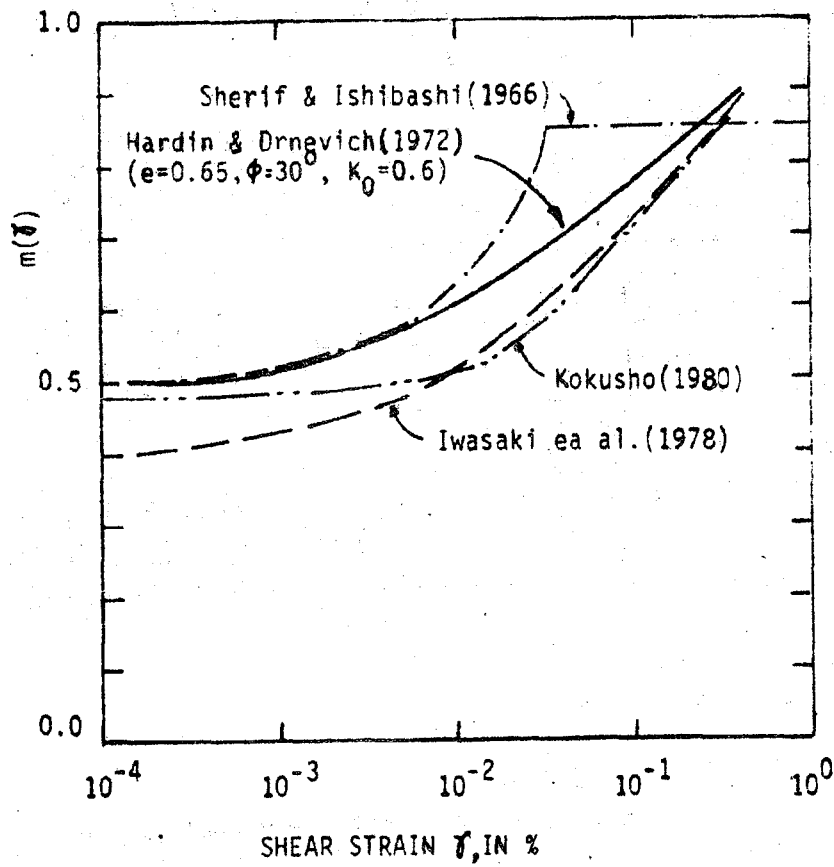


FIG. 16. Function $m(\gamma)$ versus shear strain γ
16-20

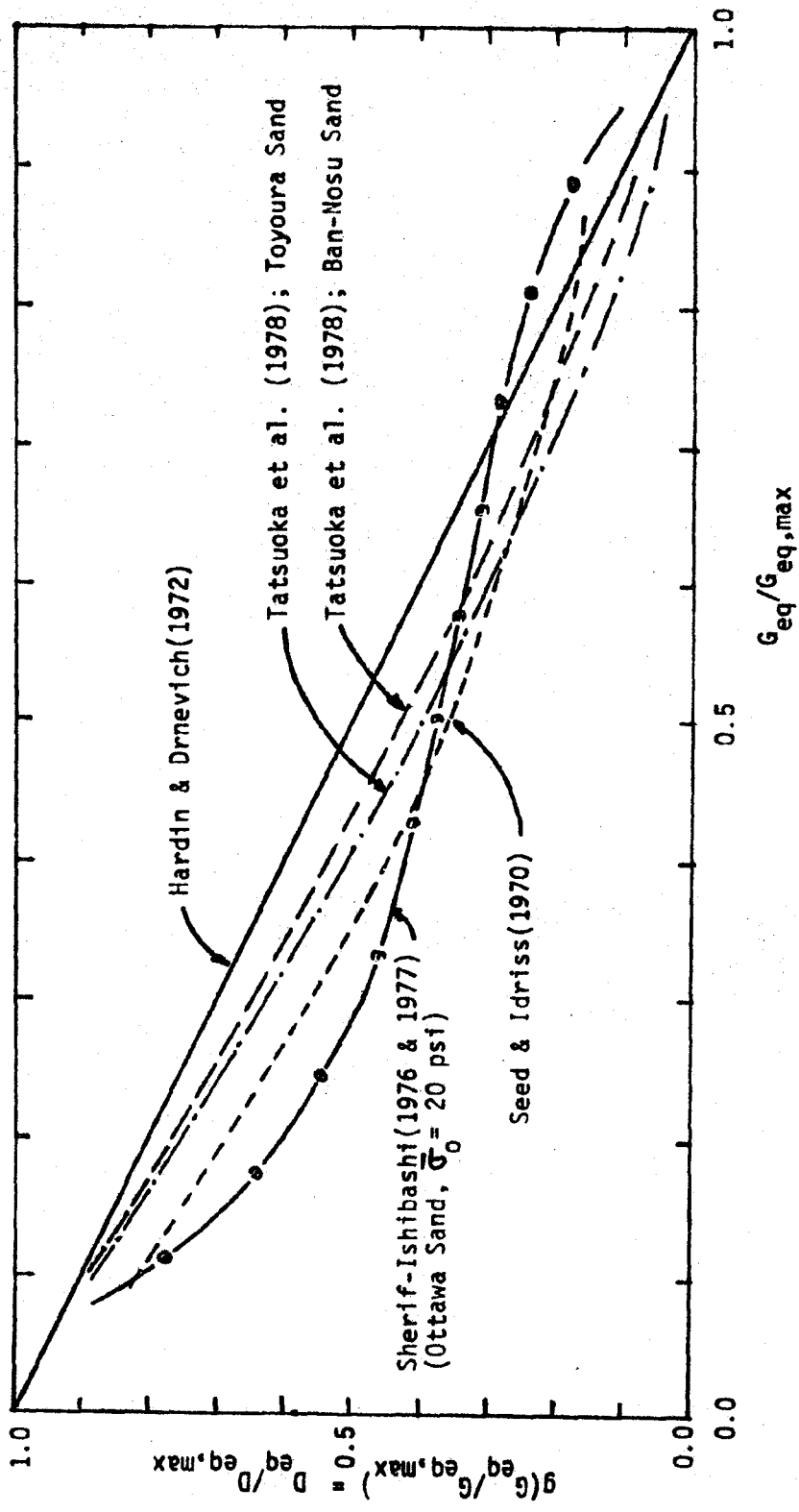
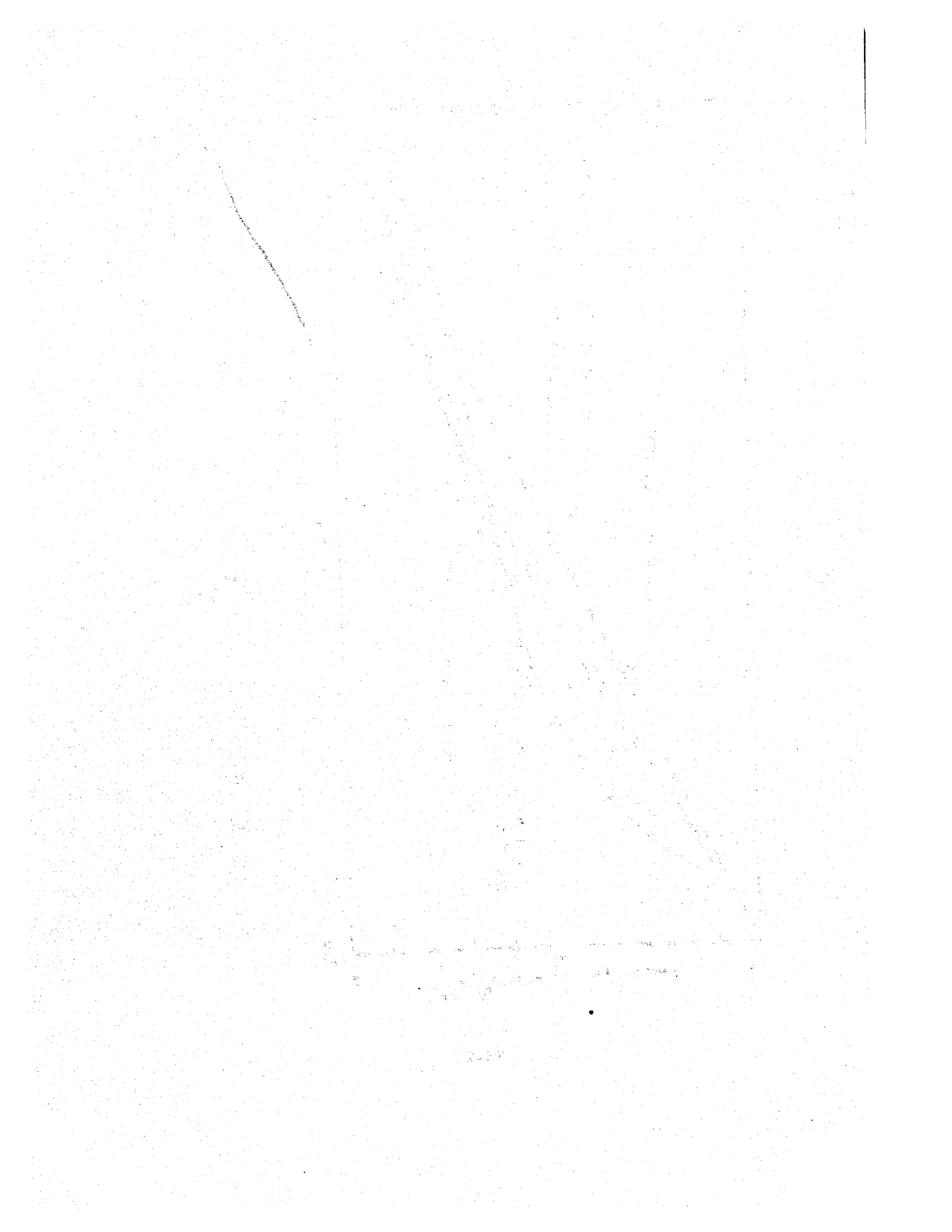


FIG. 17. Relationship between $D_{eq}/D_{eq,max}$ and $G_{eq}/G_{eq,max}$



LIQUEFACTION FAILURE OF SATURATED SANDY SOILS UNDER CYCLIC LOADING

Liu Ying¹, Tong Jun², Qi Xin³

ABSTRACT

The limit equilibrium condition and liquefaction failure process of saturated sandy soil under cyclic loading are discussed in the paper. As a result, a generalized coulomb's equation used to analyze seismic stability of saturated sand layer is proposed.

This paper suggests an approach for determining the dynamic shear strength of effective stress in saturated sandy soil, based on a single sand liquefaction testing record only. For practical engineering purposes, the liquefaction failure process of saturated sandy soil under cyclic loading is separated into two stages and the pore water pressure in the beginning of these two stages are proposed to be used as the failure criteria of sandy soil.

INTRODUCTION

In order to study the limit equilibrium condition and the liquefaction failure process of saturated sandy soil under cyclic loading. Cyclic triaxial test and data analysis were carried out. First of all, specimens of sandy soil were consolidated under consolidation ratio $K_c=2$, and then uniform cyclic load was applied in axial direction of the specimen with a frequency of one circle per second. The sand tested have an average diameter of 0.053mm, with uniform coefficient of 4, void ratio of 0.815 and minimum void ratio of 0.503.

LIMIT EQUILIBRIUM CONDITION

Assuming that under undrained cyclic loading condition, the shear strength of saturated sand consists of two parts, namely, viscous resistance and frictional resistance, the former being directly proportional to the dynamic deformation rate, while the latter being directly proportional to the normal stress. Therefore, the limit equilibrium condition can be written as follows,

$$\tau_{dN} = C_{dN} + \sigma_{dN} \tan \phi_{dN} \quad (1)$$

in which τ_{dN} = shear stress on the failure plane in the Nth

-
1. Associate Professor, Institute of Engineering Mechanics (IEM), Chinese Academy of Sciences, Harbin.
 2. Technician, IEM, Chinese Academy of Sciences, Harbin.
 3. Technician, IEM, Chinese Academy of Sciences, Harbin.

cycle (including static shear stress too); C_{VN} = viscous resistance in the Nth cycle; $\bar{\sigma}'_{dN}$ = effective normal stress on the failure plane in the Nth cycle (including static normal stress too); ϕ'_d = dynamic friction angle.

Referring to fig. 1, the following equations can be deduced based on our assumption

$$C_{VN} = \xi \frac{\Delta h}{\Delta t} = \frac{1}{2 \cos \phi'_d} \{ (\sigma'_1 - \sigma'_3) - (\sigma'_1 + \sigma'_3) \sin \phi'_d \} \quad (2)$$

$$\bar{\sigma}'_{dN} = \bar{\sigma}_{dN} - U_N = \frac{1}{2} \{ (\sigma'_1 + \sigma'_3) - (\sigma'_1 - \sigma'_3) \sin \phi'_d \} \quad (3)$$

in which ξ = apparent coefficient of viscosity; $\frac{\Delta h}{\Delta t}$ = average dynamic deformation rate in the Nth cycle; $\bar{\sigma}_{dN}$ = total normal stress on the failure plane in the Nth cycle; U_N = pore pressure in the Nth cycle (see equation (6)).

ϕ'_d in equations (2) and (3) is still unknown at present. On the assumption that, after reaching the limit equilibrium state, the apparent coefficient of viscosity and the dynamic friction angle both remain constant an expression for ϕ'_d can be established by solving the equations in the two successive cycles. Therefore, from fig. 1, the following equations can be obtained.

$$\begin{aligned} \tan \phi'_d &= \frac{\frac{1}{2}(\sigma'_1 - \sigma'_3) \cos \phi'_d - C_{VN}}{\frac{1}{2}(\sigma'_1 + \sigma'_3) - \frac{1}{2}(\sigma'_1 - \sigma'_3) \sin \phi'_d} \\ \frac{1}{2}(\sigma'_1 - \sigma'_3) \cos \phi'_d &= \xi \frac{\Delta h}{\Delta t} + \frac{1}{2} \{ (\sigma'_1 + \sigma'_3) - (\sigma'_1 - \sigma'_3) \sin \phi'_d \} \frac{\sin \phi'_d}{\cos \phi'_d} \end{aligned}$$

According to the assumption, the following equations both hold true

$$\begin{aligned} \frac{1}{2}(\sigma'_1 - \sigma'_3)_1 \cos \phi'_d &= \xi \frac{\Delta h_1}{\Delta t} + \frac{1}{2} \{ (\sigma'_1 + \sigma'_3)_1 - (\sigma'_1 - \sigma'_3)_1 \sin \phi'_d \} \frac{\sin \phi'_d}{\cos \phi'_d} \\ \frac{1}{2}(\sigma'_1 - \sigma'_3)_2 \cos \phi'_d &= \xi \frac{\Delta h_2}{\Delta t} + \frac{1}{2} \{ (\sigma'_1 + \sigma'_3)_2 - (\sigma'_1 - \sigma'_3)_2 \sin \phi'_d \} \frac{\sin \phi'_d}{\cos \phi'_d} \end{aligned}$$

in which the subscript 1 or 2 indicates the given variable belonging to the previous cycle or the later cycle. Solve simultaneously the above two equations about ϕ'_d , the following expression will be obtained

$$\phi'_d = \sin^{-1} \frac{\frac{\Delta h_2}{\Delta t} (\sigma'_1 - \sigma'_3)_1 - \frac{\Delta h_1}{\Delta t} (\sigma'_1 - \sigma'_3)_2}{\frac{\Delta h_2}{\Delta t} (\sigma'_1 + \sigma'_3)_1 - \frac{\Delta h_1}{\Delta t} (\sigma'_1 + \sigma'_3)_2} \quad (4)$$

substituting the value of ϕ'_d obtained from equation (4) into equations (2), (3) and (6), C_{VN} and $\bar{\sigma}'_{dN}$ can be determined and hence, the limit equilibrium condition of the saturated sandy soil in this particular case can be obtained.

PROCESS OF LIQUEFACTION FAILURE

A liquefaction test record for the given dense saturated sand specimen is shown in fig. 2. After consolidating under $\sigma_{vc} = 1.0 \text{ kg/cm}^2$ and $\sigma_{ic} = 2.0 \text{ kg/cm}^2$, cyclic load of 1.07 kg/cm^2 was applied to the specimen axially with frequency of one circle per second. Under this anisotropic consolidation condition, liquefaction failure can take place only in the half compression cycle. In this case $U_N = U_{cN}$, $\sigma'_1 = \sigma'_{ic} + \sigma_{ad} - U_{cN}$, and $\sigma'_3 = \sigma'_{3c} - U_{cN}$. Substituting these values into equation (4) the following expression will result

$$\phi'_d = \sin^{-1} \frac{\frac{\Delta h_2}{\Delta t} (\sigma_{1c} - \sigma_{3c} + \sigma_{ad})_1 - \frac{\Delta h_1}{\Delta t} (\sigma_{1c} - \sigma_{3c} + \sigma_{ad})_2}{\frac{\Delta h_2}{\Delta t} (\sigma_{1c} + \sigma_{3c} + \sigma_{ad} - 2U_{cn}) - \frac{\Delta h_1}{\Delta t} (\sigma_{1c} + \sigma_{3c} + \sigma_{ad} - 2U_{cn})} \quad (5)$$

The liquefaction test record shown in fig. 2 is analyzed using equation (5) with results shown in Table 1 and in Figs. 3 and 4.

Table 1 computed and measured values of friction angle
($K_c = 2$)

Number of cycles	ϕ'_d values		C_{uv}
	Computed	Measured	
36	43° 36'	43° 39'	0.043
38	44° 58'	44° 51'	0.028
40	46° 0'	45° 52'	0.024
42	45° 56'	45° 57'	0.053
44	47° 35'	47° 33'	0.050
46	45° 54'	45° 54'	0.113
48	48° 50'		
50	46° 55'	46° 56'	0.158

According to the above mentioned results of test, the liquefaction failure process can be obviously separated into two stages dynamic instability stage and static instability stage.

(1) In the dynamic instability stage, it can be seen by Fig. 2 that, if the pore pressure in the Nth cycle has increased so that the saturated sand specimen begins to reach the limit equilibrium condition, then the expression for pore pressure at that time can be established as follows

$$U_{cn} = \frac{1}{2 \sin \phi'_d} [(\sigma_{1c} + \sigma_{3c} + \sigma_{ad}) \sin \phi'_d - (\sigma_{1c} + \sigma_{ad} - \sigma_{3c}) + 2C_{uv} \cos \phi'_d] \quad (6)$$

For practical purposes, the static friction angle may be used instead of dynamic friction angle in equation (6), and therefore it can be further simplified as follows,

$$U_{cn} = \frac{1}{2 \sin \phi'_s} [(K_c + K_d)(\sin \phi'_s - 1) + (\sin \phi'_s + 1)] \quad (7)$$

$$U_{cn} = \frac{U_{cn}}{\sigma_{3c}}, \quad K_c = \frac{\sigma_{1c}}{\sigma_{3c}}, \quad K_d = \frac{\sigma_{ad}}{\sigma_{3c}}$$

(2) In the static instability stage, it can be seen also that if the pore pressure in the Nth cycle has increased so that the saturated sand specimen begins to reach the static limit equilibrium condition, then the expression for pore pressure at that time can be established as follows

$$U_{cn} = \frac{1}{2 \sin \phi'_s} [K_c (\sin \phi'_s - 1) + (\sin \phi'_s + 1)] \quad (8)$$

It can be seen from fig. 5 and equation (8) that the pore pressure ratio $U_{cn} = 1$ i.e., the pore pressure is equal to the confining pressure, is true only when the static instability is attained under the case $K = 1$, noting that when $K_c > 1$, pore pressure U_{cn} hasn't attained the level of confining pressure

CONCLUSION

Coulomb's equation is the simplest and the most useful laws in soil mechanics, but it can not be used directly to analyze the stability of soil mass subjected to dynamic loading. In order to extend this law to dynamic cases, it is necessary to how to determine the viscous and frictional resistances and the pattern of pore pressure development of the saturated sandy soil. Equations (1), (2), (3), (4) and (6) given in this paper are used for an attempt to solve the above problems.

For practical engineering purposes, the liquefaction failure process of saturated sandy soils under cyclic loading can be separated into two stages and the pore pressure in the beginning of these two stages may be regarded as the failure criteria of the sandy soil.

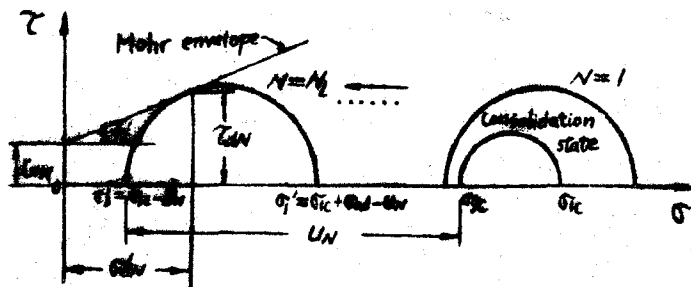


Fig. 1. Limit equilibrium condition in the Nth cycle

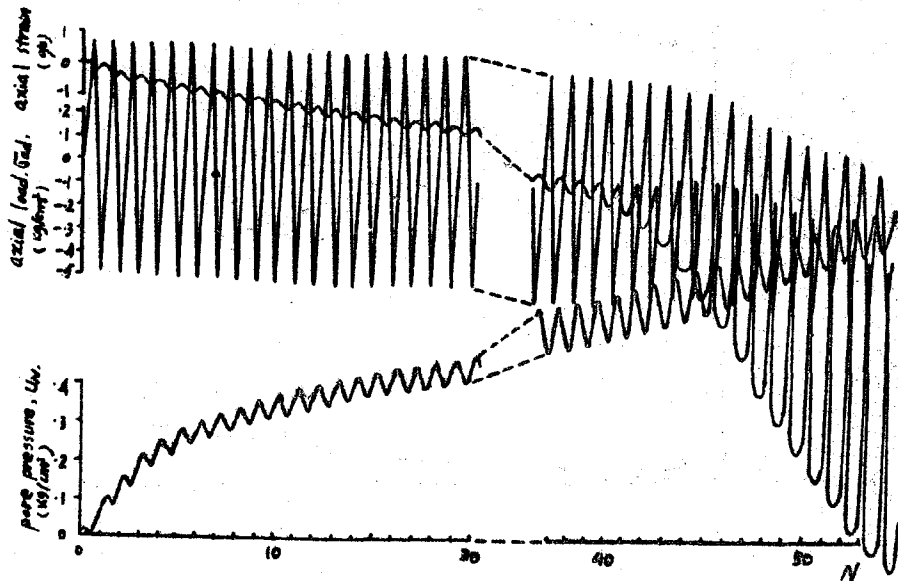


Fig. 2. Typical record of liquefaction test ($K_c=2$)

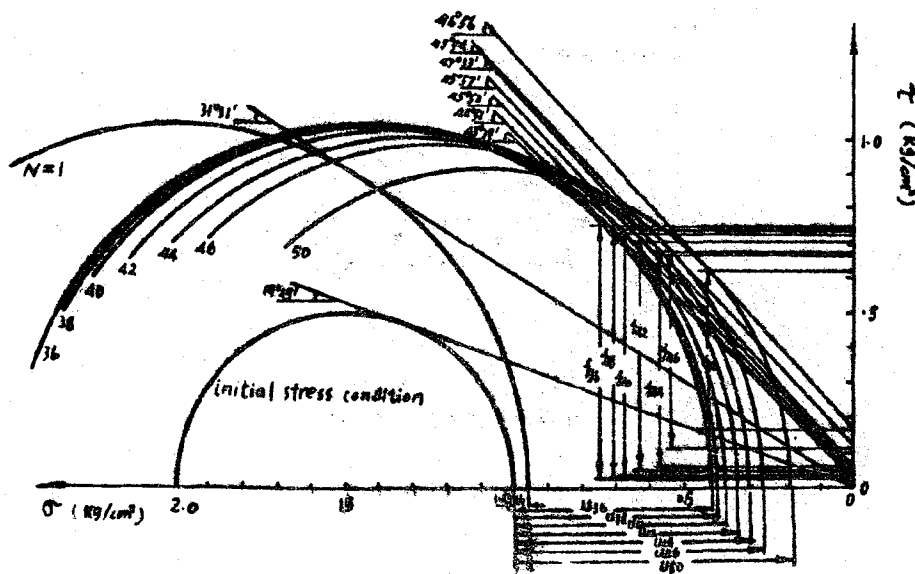


Fig. 3. Mohr's circle under cyclic loading ($K_c=2$)

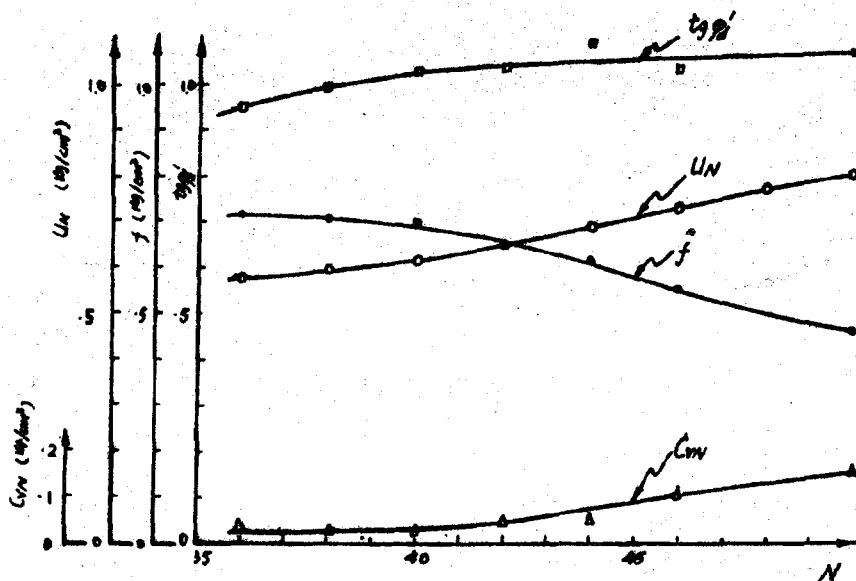


Fig. 4. Change of t_{90} , f , U_w and C_{wv} with number of cycles

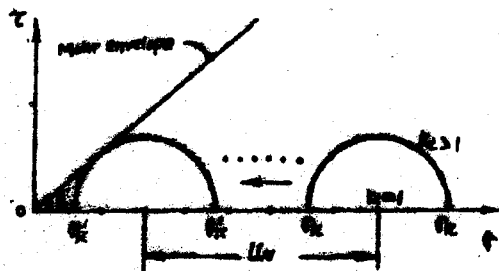


Fig. 5. Static instability condition ($K_c=2$)

ARCHITECTURAL PLANNING & DESIGN CONSIDERATIONS OF MICROZONATION

by

Henry J. Lagorio^I

Marcy Wang^{II}

ABSTRACT

This paper is written from the viewpoint of the environmental designer's interest in seismic zonation. An overview of the interdisciplinary network of those professionals directly and indirectly involved in seismic hazard mitigation is necessary to emphasize the relative roles of the environmental planner and designer in microzonation and land management. The fundamental types of knowledge that the architectural planner and designer needs and should be familiar with must be clearly delineated before attempts to feasibly bridge the interdisciplinary information gaps are made. Critical items in this overview include:

- (a) Identification and clarification of the roles of the environmental planner and designer in all large and small scale activities of microzonation efforts.
- (b) Architectural planning and design components in earthquake hazards reduction.
- (c) Differences between and relative uses of general seismic zonation and microzonation in environmental planning and design.
- (d) Examples and case studies where seismic-zonation of various scales has been successfully implemented in environmental planning and design, as well as where it has not but its need clearly indicated.
- (e) Current difficulties and limitations of accurate zonation for earthquake hazards in practical applications of architecture.

I Associate Dean for Research, and Director, Center for Planning and Development Research (CPDR), College of Environmental Design, UC Berkeley.

II Assistant Professor, Department of Architecture, UC Berkeley.

INTRODUCTION

The increasing vulnerability of high-density, metropolitan areas throughout the world, magnifies the necessity of input by the architectural, planning and design professions in seismic hazards reduction programs focusing on the urban environment. Considering the formidable economic investment in built structures, the potentially horrendous risks of critical facilities like nuclear power plants sited in an actively seismic area, it is not surprising that some of the most extensive and advanced research work on all aspects of seismic hazard mitigation has been taking place in countries such as the U.S.A., Japan and the U.S.S.R. For the purposes of investigating both zonation and structural engineering issues of earthquake hazard problems, these countries have invested intense efforts to develop widespread strong motion networks, laboratory experiments, equipment, and numerical methods to analyze data.

Although less developed and third world countries do not have equivalent research resources or major economic investments to protect, their need for hazard mitigation is equally if not more urgent. Comparison of the following mortality figures from recent earthquakes demonstrate the disparity of number of lives lost between those countries which are highly developed and those less technologically experienced.

<u>Date</u>	<u>Place</u>	<u>Richter Magnitude</u>	<u>Deaths</u>
March 27, 1964	"Good Friday E.Q." of Prince Wm. Sound, Alaska	M = 6.5	131
Feb. 9, 1971	San Fernando, Calif.	M = 6.5	65
July 27, 1976	Tangshan, China	M = 7.6	262,000
Oct. 10, 1980	El Asnam, Algeria	M = 7.2	20,000

Existing technology and knowledge about earthquakes and seismic zonation could significantly reduce the human vulnerability that these statistics portray. It is a question of feasibility and economically implementing hazard reduction programs in the latter countries. It is here where state-of-the-art knowledge in seismic zonation could make the greatest contribution to alleviate the human exposure to an earthquake disaster.

THE ROLE OF ARCHITECTURE IN SEISMIC ZONATION AND MICROZONATION AND ENVIRONMENTAL DESIGN

Design of a relatively safe human-built environment in a region of high seismicity requires the expertise and cooperation of numerous scientific, planning, and political entities. The environmental designer, particularly urban planners and architects, have the unique position of being the professionals who are most responsible for decision making for the final built products of our cities and towns, yet most removed from the raw data and state-of-the-art research in the basic seismic investigations of the earth sciences and engineering. (Figure 1) Since seismic safety is only one of a multitude of crucial issues an environmental designer might be concerned with, the presentation of geologic and engineering material must be distilled to a form that both is comprehensible to and includes the most essential, important information for the environmental design professionals and other persons involved with construction and land use planning. The quantity and importance of engineering or geoscience information which is conveyed to the environmental designer is much greater than those environmental design issues which an earth scientist or engineer must be familiar with, in the making of cogent environmental design decisions based on seismic zonation.

The architect should possess a basic understanding of and take an active role in both primary categories of strategies for earthquake hazard mitigation, namely, 1) Structural design for seismically resistant buildings, and 2) Zonation of land use based on risk and hazard.¹ The importance of the first category of hazard mitigation has long been recognized and most widely used aseismic approach in the building professions. The second category has more recently been explored as a major method of mitigating earthquake hazard. Research in this area, and recognition of its validity as an additional line of defense against earthquakes, is increasing.

On a larger scale, the architect as an urban planner and designer must give similar consideration to the growth and form of a city or regional metropolitan area when dealing with seismic safety concerns. This is particularly important today as urban areas expand into places which are more difficult to develop safely. When prime locations in an urban setting are exhausted by development, it is often necessary to move to less desirable areas to accommodate increases in population, urban sprawl, and services demanded by the public. As any culture becomes more complex it becomes more reliant on critical facilities which are extremely vital to the continued function of its urban centers.⁵

¹There is an important distinction in meaning between the words 'risk' and 'hazard' when used in the context of earthquake engineering. H. Shah provides the following definitions: seismic hazard is "expected occurrence of a future adverse seismic event,"; seismic risk is "expected consequences of a future seismic event." (Mortgat, C. and Shah, H., June 1978.) (Ref. 3)

Recent earthquakes in California, southern Italy, and Algeria represent specific examples in which losses to certain critical facilities exacerbated what already was a major disaster. Two cities lost services of their hospitals during the 1980 earthquake in southern Italy. The San Fernando earthquake of 1971 clearly indicated the vulnerability of major, acute hospitals and their importance as a critical facility in the immediate post-earthquake recovery period experienced by a metropolitan area. Following the earthquake, architects participated in the development of new performance standards promulgated to insure, insofar as practicable, that hospitals would remain operable and functional during and after a seismic event. To assure compliance in the planning and design of all new hospitals the State legislature passed the California Hospital Act of 1972 into law in which a building safety board in the Office of Statewide Health Planning and Development acts as a review body for questions relating to the seismic safety of hospitals.⁶

Finally, another area in which the architectural planning and design practitioner plays an important role deals with the existing hazardous, older building problem. Architects have participated in the rehabilitation of existing buildings, and their strengthening, for many years, and it is only recently that this critical aspect of urban seismic safety has been realized. Whether it is called "redesign, retrofitting, renovation, rehabilitation, renewal, recycling, remodeling, restoration, preservation, conservation, revitalization, reuse" or by any other name, the reconstruction of the existing building stock in the United States has become a very important part of an architect's responsibilities.⁷ In 1979, in the United States alone, more than forty billion dollars was spent nationally on the renovation of existing buildings for a myriad of reasons, one of which is seismic safety. Reconstruction expenditures for non-residential buildings have nearly doubled in the past five years, from \$19.4 billion in 1975 to nearly \$35.6 billion in 1980, while "in another five years such reconstruction is expected to amount to half of all the building activity in the nation".⁷ The existing, older building problem will receive more attention in our urban areas in the future. Research activity in the seismic performance of older, existing hazardous buildings is included among the top priorities of the National Science Foundation through its Earthquake Hazards Mitigation Program.

THE ARCHITECTURAL PLANNING & DESIGN COMPONENTS OF EARTHQUAKE HAZARDS REDUCTION

Although a newly designed, high-valued, engineered structure may not suffer total collapse in a severe earthquake, there is sufficient evidence available from past major earthquakes that damage to non-structural components and systems in a building can result in losses equal to 60 to 75 percent of replacements costs and lead to significant life loss. Elevators and other electrical mechanical systems in multi-story buildings have proven to be particularly sensitive. In the aftermath of the San Fernando earthquake in 1971, about 90 percent of all elevators in the Los Angeles area adjacent to the San Fernando Valley were inoperable. The more recent Imperial Valley earthquake (6.6 M, October 15, 1979) resulted in an estimated damage of \$1,000,000 to the non-structural components and systems in the slightly and moderately damaged buildings, excluding residential damage, and an additional estimated \$112,800 loss to mobile homes.⁴ Although the extent

of non-structural, architectural losses to the severely damaged buildings in the City of El Centro has not been accurately estimated, a total dollar loss to buildings in this category has been indicated as being in the \$6.6 million range. If past experience from previous earthquakes are reliable, this total can be translated into a dollar loss of about \$3.9 to \$4.9 million for architectural, non-structural systems and components.

Other architectural planning and design considerations which are related to the seismic safety of an urban area deal with site planning and the location of buildings on a given plat of property. It is in this category that geologic hazards must be given appropriate consideration. Potential hazards such as structurally poor ground, geologically active fault systems, earthquake induced landslides, and coastal zone inundation areas represent site location conditions which directly influence building placement. As each hazard will affect the building in a different manner, all must be given consideration in terms of public safety when the architectural planning and design professional initiates the schematic phases of building design and configuration.

THE CONCEPTUAL BASES OF ZONATION IN THE CONTEXT OF ARCHITECTURE AND ENVIRONMENTAL DESIGN

To the architectural planning and design professional, the seismic-zonation of land requires earth science information in contrast to the structural design of buildings which utilizes concepts of structural mechanics, analysis and design. Similarly, the translation of geologic and structural data into a form which environmental planners and designers can use is also quite different. Products of structural engineering research that aid in building design such as, for example, design response spectra and performance standards in building codes, are simplified, somewhat subjective interpretations of real data which design engineers use, hopefully, in early collaboration with architects. The analogous products of earth science studies in the context of various scales of seismic-zonation, including microzonation, are maps which generally are intended to correlate geologic, demographic, economic and/or probabilistic risk information to seismic hazard. Such maps can indicate specific information related to probable peak ground acceleration, velocity or displacement; areas of potential liquefaction, landslide, tsunami inundation, population downstream from dams and reservoirs, and other extraordinary hazards; soil type, alluvium depth, shear wave velocity, and so forth. It is a matter of scale and amount of detail which delineates general seismicity maps, or general seismic-zonation maps, into various categories such as those developed by microzonation objectives. For the architectural planner and designer, prevalent usage of the term "seismic zoning" takes into account "the distribution of earthquake hazard over . . . an entire region",¹ whereas "microzoning defines the detailed distribution of earthquake risk within each seismic zone".² In this context a "zone" can be inferred to represent a "seismogenetic source region which can be assumed to be governed by the same earthquake generating process",² and whose boundaries largely depend on subjective translations of data based on past experience.

MACROZONATION

The architectural planning and design professional must understand that analysis of geological and seismological data provides much of the basis for regional seismic zonation. Information regarding location of active faults, recent history of tectonic movements, regional crustal structure, in addition to data gathered from strong motion records, are useful in defining earthquake zones. Much earthquake engineering research has concentrated on the creation of empirical formulas which correlate various parameters of a) ground motion acceleration, velocity or displacement, or b) probable intensity of damage, and/or c) sources and size of earthquake energy. The typical relations most often investigated include acceleration - intensity¹, magnitude - frequency, and attenuation² functions based on strong motion recorded data and geophysical information in conjunction with statistical methods. A plethora of such formulas attest to their equivocality. They are nevertheless convenient and useful in the construction of zoning maps.

The acceleration - intensity relation has been extensively studied because scientific data is often in the form of strong motion records, (such as time histories of earthquake ground acceleration) and intensity is a quantity that is both comprehensible and of interest to environmental designers as well as engineers. It is therefore an extremely common quantity in zoning maps (see intensity map of Figure 2) despite the failure of researchers to prove a simple and certain relationship between acceleration and intensity.

There are also many contradictory results of research in attenuation studies which attempt to correlate earthquake effects to epicentral distance from the earthquake source. The great number of attending features one must consider in attenuation effects precludes the possibility of arriving at a very simple model. Soil type, alluvial depth, surface topography, magnitude of earthquake, earthquake mechanism and source are just a few of the factors which complicate this issue.

Seismic zoning of land at the large "macro" scale is useful to the architectural planner and designer when it not only uses geologic and

¹Macroseismic intensity describes a subjective evaluation of seismic event size by observation of degree of damage after an earthquake. The Modified Mercalli Scale, which has degrees ranging from I through XII to indicate increasing damage effects, on the built environment and the surface of the earth, is a commonly used intensity scale in the U.S.A.

²Attenuation describes the lessening of certain parameters (in seismic context, ground acceleration, for example) as a function of distance from the epicenter of an earthquake.

other earth science data, but also incorporates information from the risk analysis and probabilistic approach. An earthquake recurrence model which is developed to indicate measures of seismicity of a zone can be most useful to the urban designer when it utilizes data from historic records of earthquakes of a region, in conjunction with statistical methods, probabilistic treatment of attenuation relationships, and identification of earthquake sources. This method of evaluating regional seismicity can prove to be of great, potential value to the environmental planner and designer where, for example, a seismic risk analysis had pinpointed an area to be most vulnerable in a country as was the case in the recent earthquake at El Asnam, Algeria (7.2 M, October 10, 1980).³ Figure 3, the zonation map with isoseismals showing peak acceleration (cm/sec²) for a recurrence period of one hundred years, indicates this conclusion in H. Shah's seismic hazard analysis.

The limitations of solely using historic data, which earth scientists and risk analysts themselves warn of, however, must also be kept in mind by the architect. Historic records, with few exceptions, are neither extensive, nor accurate in most parts of the world, thus the data upon which historic risk analysis is based is rarely extremely reliable. In comparison to the scale of geologic time, that of human history and records is quite brief, thus the recurrence period of an area may well be 'visible' only from geologic studies. Finally, the concept of a 'seismic gap' whereby the greatest strain, thus the greatest seismic energy release potential, in the earth's crust exists where a fault is locked, and has not been active for a long time, poses a direct contradiction to basing prediction of seismicity on historic records, which directly correlates recurrence period to frequency of past events. In these quiescent areas, geophysical investigations are necessary to better determine the probability of future earthquake activity.

As long as their respective limitations are kept in perspective, all methods of zonation can be of value in providing useful information at a macro level to architects, urban planners and public policy makers. The type of zonation study that is most practical to execute for one region may not be the best for another especially if there is a limitation of economic or technologic constraints. Two industrialized areas of the world in seismic regions, California, U.S.A., and northern Algeria, provide a comparison between the situations of a technologically sophisticated and a technologically developing country. (California has a slightly higher level of seismicity than Algeria, on the whole.) To the environmental designer, some of the most advanced work in the area of geologic zonation based on data gathered from extensive strong motion instrumentation networks has been taking place in California. The coincidence of major academic (Cal Tech in Pasadena, Stanford University, University of California, Berkeley) or governmental (USGS, Menlo Park) agencies in areas of significant population densities in seismic regions, create both a public awareness of the earthquake problem and a research sector that is extremely active. Original research executed in the U.S. and other technically developed countries, such as the USSR and Japan, yields results which not only these countries, but other countries as well, depend upon for seismic zonation and other hazard reduction programs. An interesting example of a developing country in a seismic area is Algeria which suffered a major earthquake in 1980. Algeria, in contrast to the United States, although a rapidly developing industrialized nation, does not have the research capabilities nor the technology to carry out strong motion

instrumentation programs, nor any other earth science/seismic engineering research programs, essential for seismic hazard investigations of this nature. Furthermore, since winning independence from the French in 1963, the Algerians have understandably tended to avoid a dependence upon foreign technology to the point of rejecting the use of their only seismic code because of its French origins. In the seventies, the political sensitivity to eliciting Western technological aid had been reduced to the point that it was possible, with the help of Stanford University's department of engineering, for a seismic hazard map specific for Algeria to be developed as a basis for a future lateral force code. Probably, for economic reasons, the use of existing data for a risk analysis was the most feasible path, although it should be emphasized that researchers strongly recommended a more thorough instrument program and geologic survey.¹⁰ Unfortunately, the few strong motion instruments that had been installed in Algeria, were inoperable when the 7.2 shock of 1980 hit El Asnam. As a result of this tragic earthquake, the Algerians are more aware than ever of the long range value (both economically and in terms of public safety) of investing in a strong motion system and a complete geologic understanding of their country.

MICROZONATION

Traditionally, microzonation has implied the study of the effect of local, varying soil conditions on ground motion in an earthquake. Soil conditions include such aspects as soil type, alluvium depth to bedrock, shear wave velocity, areas of special liquefaction or landslide potential, etc., which can be the basis of microzoning maps covering areas more local and in greater detail than macrozonation maps.

Two aspects of microzonation concerns, which include soil instability such as liquifaction and landslides triggered by earthquake, and variations in ground shaking itself, are particularly important to the architect. These major concerns must be separately considered due to the very different natures of their causes.

The environmental designer should realize that microzonation considerations are not limited specifically to soil studies. Other studies and aspects that provide useful geologic, seismologic and geotechnical information that could be incorporated into a microzonation map include:

- 1) Identifying seismic faults by location and type.
- 2) Studying the records of recurrence rate, spatial distribution, magnitude of earthquake for an area.
- 3) Analyzing the soil dynamics of a region for ground response prediction.

The gathering of information provided by each of these three points of investigation is not always ideally accessible or reliable as the environmental designer would hope. Although microzonation would be less likely to miss important geological features such as faults, it is still very possible that latently active faults are camouflaged after long inactivity.

Secondly, the problems of historic seismicity records which have been discussed, exist at the micro as well as macro level of zonation. To the architect, the last category of predicted ground response is the research area that contains contradictory research results and is still very much in the infancy of development. Research concerning the rigidity or period of soil, depth of overburden, and attenuation functions in relation to earthquake hazard, have yielded contradictory results indicating that there are many more factors affecting a situation than have been included in the models analyzed. D. Hudson of the California Institute of Technology in Pasadena, found from his analysis of instrumentation data recorded during the 1971 San Fernando earthquake, that contrary to previous studies by other researchers, maximum ground response tended to be on rock sites rather than alluvium sites. B. Gutenberg's studies of the Pasadena area strong motion records of smaller ground motions in the 1950's, indicated that "motion on the alluvium would be expected to be considerably greater than on the rock."¹⁴

Often extensive microzonation techniques are conducted based upon unconfirmed hypotheses, perhaps because there do not exist more proven or simple methods. Micro tremor analysis in Japan, the USSR and other countries is based upon the concept that soils and thus damage potential can be classified according to analysis of small, chronic vibrations, or microtremors of the earth. Despite a certain degree of success in ground microzonation with this method, many scientists question this method because it does not consider inelastic behavior of soil under the unusually large strains in the ground during a major tremor. The enormous expense, and uncertainties which emerge out of new research in a field as complicated as microzonation is a necessary phase of progress.

The architectural planning and design professional perceives microzonation as a special research area in itself since "most studies of the distribution of damage caused by earthquakes indicates that the areas of severe damage are highly localized and that the degree of damage may change abruptly over distances as short as .5 to 1.0 km."² Examples of this observed phenomenon are confirmed by extensive descriptive reports from the 1906 San Francisco Earthquake, and more recently, a detailed study of instrument records of the 1971 San Fernando Earthquake.¹⁴ In the 7.2 earthquake of North Algeria this past October 1980, a high intensity but quite localized radius of damage occurred in the city of El Asnam, which was the closest urban area to the epicenter. As a member of a joint EERI/NAS investigative team for this event, one of the authors observed the pattern of building damage as shown in Figure 4a which is of interest to the architect and urban planner. The most severe damage in the downtown area occurred in pockets or more linear concentrations. An attempt to correlate these areas of most severe damage to some structural factor was inconclusive; apparently the factor was connected possibly to local anomalous and intense ground motion, which in turn may have been caused by soil conditions in the immediate region. Unfortunately, no soils or geological information was available yet to confirm or contradict this thesis. One pocket of extremely severe damage was on the north side of the downtown region, in the vicinity of building 14, (See Figure 4b) which was the Cite an Nasr Market and Housing Complex on a large block measuring 492 feet square. This particular building complex completely collapsed except for one corner, (Figure 5) and is estimated

to have killed about three thousand people (unconfirmed). Other major buildings in this particular pocket of damage include the town hall, police station, and a mosque. It must be remembered that since El Asnam had been destroyed by a 1954 earthquake, all buildings are fairly modern if not new. Although structurally, in terms of design concept, materials, detailing and so forth, the EERI/NAS team observed many substandard conditions in the buildings, this does not explain the pattern of damage (Figure 4) wherein other areas had buildings equally old or deficient that did not completely collapse. This suggests that were it not for particularly bad local soil and geologic conditions, even inferior structures might well have survived this earthquake at least to the point of not collapsing and killing or injuring many people. In terms of urban planning, there is an unconfirmed possibility that the Cite An Nasr may have been sited on an old creek bed parallel to the River Cheliff, in which uncompacted fill had been placed¹; this provides one explanation for the dramatic and tragic collapse of the complex. The River Cheliff most likely was associated with the northern region of very severe damage on the north side of town, either in terms of slope instability, soil type, water saturation of soil, or old drainage patterns to the river.

Numerous dramatic examples of local soil failures occurred on the outskirts of El Asnam, and it can be considered relatively fortunate for the city that the urban areas did not suffer similar extreme ground failures. This avoidance of the worst ground failure being coincident with the town's location, is of course fortuitous since no microzonation studies had preceded the rebuilding of El Asnam in the 1950's. A rare phenomenon occurred where a lake was completely created as a result of the earthquake, because of subsidence due to liquefaction and the proximity of the River Cheliff whose water drained into the new depression. Within three weeks, the lake covered 10,000 acres and was still growing. Had such a phenomenon occurred in an urban area, losses in a city would be critical. (See Figure 6)

In the rural areas, displaced faults exhibited massive vertical and/or horizontal motion. (See Figure 7) Again, it is fortunate and fortuitous that from the urban design point of view, none of these faults went directly through El Asnam itself. The wisdom of avoiding the placement of a structure directly on a fault is self evident to the environmental designer and even people without any training in earthquake engineering. The hazard of active faults, curiously enough, in terms of total risk is overrated by many people in the building professions, including architects, environmental planners, policy makers, and engineers. First of all, since faults are generally quite linear, the amount of actual area that they themselves occupy is quite small. Secondly, contrary to many popular beliefs, experience indicates there is not necessarily a consistent direct increase of hazard or risk, with proximity to an active fault. There are several theories, details of which are beyond the scope of this paper, that attempt to explain why it appears that in some cases there is a drop in damage to buildings sometimes only tens of feet away from a fault, as compared to structures at a more distant location. In Figure 8, the fault can be seen in the background of the photograph. One would expect that any structure in the vicinity of such great vertical displacement would suffer total collapse, however, the rural Algerian structures in the foreground appear to be relatively intact. It was observed that houses of similar

construction and farther from the fault, either collapsed or had much damage. Evidently, the highest ground shaking is not necessarily adjacent to the fault in some instances. Accordingly, the architectural planning and design professional must be aware of the multitude of issues which govern seismic safety concerns.

Clearly, architectural decisions could affect the chances of a building's survival in an earthquake, especially when microzonation factors are recognized. In the question of soil-structure interaction, engineering judgement has more bases on which to be made if microzonation data is provided. In general, soil-structure interaction particularly tends to be a problem when tall, flexible buildings are set upon soft, deep alluvium, which has a very high period. By avoiding the combination of certain building or structure periods with certain corresponding soil periods, the hazard of soil structure interaction can be somewhat reduced. The natural period of a structure is the result of its scale, configuration, massing, and structural system; all these factors are inextricably related to architectural and engineering decisions.

SEISMIC ZONATION AND MICROZONATION MAPS

The representation of zonation and microzonation information is often conveyed by cartographic means. Graphic representation of data is particularly comprehensible to environmental designers and planners although the maps should be accompanied by explanation of their use and degree of reliability. There is a great variety of the types of zonation maps used. This is due to the type of information on which it is based, the scale of the zonation being attempted, and the audience for whom it is intended.

From a cost-benefit perspective, it is critical that the methods and data used for the preparation of microzonation maps be developed on a standardized basis so that all design professionals can abstract the same results for site planning and building design purposes. This is particularly true for multidisciplinary design teams operating at international levels in other countries. Currently, this is not the case as many methods are being utilized to derive microzonation models. To be useful to the architectural planning and design professional, it is essential that all maps present reliable information derived from a common base-line. When promulgated by different methods, representation of microzonation data to design professionals can only lead to questionable interpretation. As a result, there is a tendency for some design professionals to request substantial amounts of additional research, including clarification and/or standardization of criteria, before making final planning and design decisions based solely on some methods currently used in microzonation mapping.

In the United States of America, perhaps the zoning map most widely familiar to architects and engineers in western regions of the country, is the UBC (Uniform Building Code) map of seismic zones. This type of map can be classified in the general category of "engineering" zoning maps. Typical of such maps, the UBC 1979 edition, map, (See Figure 9) scales zones of increasing intensity from '0' to '4'.

Another type of macrozonation map which is commonly used for showing more specific information of a region is a maximum acceleration

(or velocity, or displacement) for different return periods. H. Shah's map (Figure 3) based on historic seismicity is an example of this variety. This type of map could also be based on geological information. In such a case, epicenter maps and earthquake source maps, strong motion records, are interesting supplementary documents to have as reference. These maps, which show isoseismals of peak ground motion parameters, are most useful to engineers.

A third family of commonly used zonation maps shows maximum expected seismic intensity for various zones. Only some of these maps give a return period of time on which they are based. This type of map can be based on geological information or historic seismicity data and probability methods. Despite the disadvantages of using as subjective a measure as intensity, as a zoning determinant, it is popularly used in the USA as well as the USSR, Japan and other countries. In California, this form of zonation is widely employed for developers, architects, planners, and other persons dealing with issues of environmental design, because the amount of interpretation that the user must make is minimal. For use by the environmental designer, microzonation maps differ from macrozonation maps not only because the former examines a smaller region and in closer detail, but also because the type of information represented is usually different. Often these maps concentrate on a particular type of hazard such as ground liquefaction or land slide potential. (See Figure 10) If the map indicates that a planned structure is in the vicinity of such a serious hazard, the architect is warned that a more detailed geology and solid analysis may be necessary for the site, especially in the case of a large or critically important facility.

RECOMMENDATIONS ON ARCHITECTURAL PLANNING & DESIGN CONSIDERATIONS IN MICROZONATION

While much earthquake engineering research has emphasized specific elements abstracted from the urban environment, very little work has focused on a balanced approach to comprehensive urban planning and design as a means by which the seismic vulnerability of major metropolitan areas may be addressed. The respective design professions have responded in a variety of ways to the constraints induced on site planning and building design. Until the results of the ATC-3 Project (Tentative Provisions for the Development of Seismic Regulations for Buildings) were released in the United States, architectural planners and designers in the country did not have a common base-line for approaching seismic resistant design in all areas throughout the nation. Consequently for those who were interested, it was found that their preparedness and capacity to address hazard reduction design were blunted by local custom when performance criteria varied from region to region with no basis of a common base-line visible for deviation. Under such a system, many communities could only ignore the potential hazards of earthquakes until forced to do so by realities of the situation. Clearly, a similar balanced approach as that achieved by ATC-3 for building design is recommended for the development of microzonation models.

As people and facilities become concentrated in areas of seismic vulnerability, it becomes proportionally imperative for the architectural planning and design profession to have access to relevant microzonation

data. This is particularly true for those urban centers located in areas of high seismic activity in the United States such as California, Utah, Washington, Alaska, Tennessee, Nevada, Missouri, and others, although the scale of seismicity of the latter three is way below that of California earthquakes because of an anomalous history. For an example of an area with high seismic exposure due to high-density population concentrations, urban planners and designers in the United States cite data in California that by the year 2075 more than 20 million people will be located in the corridor area stretching from the San Francisco Bay Area (population approximately 5.1 million) in the northern part of the State to Tijuana (population approximately 1.0 million) on the Mexican border to the south, along a zone known to be one of the greatest seismic hazards in the country. This implies that by the year 2000, nearly one out of every fifteen persons in the United States will live in this potential megalopolis stretching from San Diego to just north of San Francisco. A severe earthquake in this area could cause a major disaster by disrupting transportation lines, resource distribution, communication systems, and other critical services in addition to causing dramatic life losses and economic dislocations. A clear cut recommendation can be made that such an area is a logical candidate for more detailed microzonation mapping of critical urban centers located along the vulnerable corridor. Such a project could be a welcome effort by planning and design practitioners who foresee a professional commitment to the area in the years ahead. In such areas the development of microzonation data useful to the pattern of urban location, design of buildings, selection of structural systems, choice of appropriate construction materials, and the planning of suitable egress systems would be most helpful to the architectural planning and design professional. Building planning and design concepts could then be carefully classified by the design professional in consideration of potential hazards revealed relative to the intensity of ground shaking, ground rupture and displacement, structurally poor ground, induced landslides, soil-structure interaction, and tsunami inundation.⁹

On a long term basis, urban planning and design objectives could be correlated to microzonation techniques in order to provide the basis for identifying potential areas for urban renewal or revitalization in metropolitan centers which have a particularly high hazard. In these areas are typically found the older, existing buildings which in many instances are unreinforced masonry structures that represent a potentially hazardous situation. In the City of Los Angeles alone, the number of older buildings which do not meet current code standards for earthquake resistance has been estimated as high as 20,000 to 50,000. Of these, approximately 8,000 are pre-1933, earthquake hazardous, unreinforced masonry buildings located mostly in the city's congested downtown area and in the Hollywood, Wilshire, and Westlake districts. In these areas it is critical for the architectural planning and design professional to understand what the implications are for building construction by first reviewing microzonation data when available. Accordingly it is recommended that in order to place the design professional and public in a better position to make informed decisions relative to areas of potential urban renewal and/or revitalization, public officials consider developing microzonation maps for such areas.

By reviewing microzonation data, the design professional can achieve a better approach to seismic safety in building design by

considering options regarding building location and size, configuration, height, materials of construction, structural systems, and corridors for egress. A careful consideration of each architectural planning and design component indicated above will have a direct influence on the seismic performance of a building, while, correspondingly, disregard for the correlation of design strategies with microzonation data could easily reduce building's capacity to resist earthquake forces. The foundation soil failure of the four story, reinforced concrete apartment building complex due to soils liquefaction during the much studied Niigata, Japan, earthquake in 1964 remains the classic example of siting buildings on newly deposited or reclaimed land areas without taking geologic hazards into consideration during the building planning and design phases.¹⁰ The availability of a comprehensive microzonation map, as an additional architectural planning tool, for this area in the city of Niigata could alleviate the negative situation by pinpointing the fact that appropriate soil tests and site investigations would be necessary before the architect started any site plan or building design preliminaries. Liquefaction susceptibility maps currently being developed on a small scale for areas of downtown Tokyo represent one model for flagging sites which require detailed investigation before major buildings are placed on them. (See Figure 11)

The environmental planner and designer must consider microzonation data and risk analysis models in the planning and design of buildings which are critical to the continued functioning of an urban area and those structures regarded as emergency service facilities which assume vital roles in immediate post-earthquake response. Structures which are crucial in providing emergency services to a community require special design review and assessment. New critical facility buildings should be constructed to conform to the best design standards including levels of seismic resistance appropriate to earthquake hazards revealed by microzonation models which can serve as design guidelines influencing the type and siting of structures. Such buildings and facilities include the following types:

- | | |
|-------------------------|--------------------------------------|
| (a) Hospitals | (e) Police and Fire Stations |
| (b) Ambulance Services | (f) Emergency Communications Systems |
| (c) Nuclear Facilities | (g) Reservoirs and Dams |
| (d) Strategic Utilities | |

It is most cost-efficient to deal with the safety and seismic resistance of buildings in the preliminary design stage rather than discovering it necessary to recycle former design decisions by returning to the drawing board to strengthen or repair existing facilities. Some of the latter have been found to have potential hazards too costly to correct.⁶ However, by constructive use of microzonation mapping as an additional preliminary tool in the design process, future problems can be avoided by the design professional.

Existing hazardous, older building areas in urban environments can be identified and targeted for attention when located in districts having questionable site conditions and underlying geologic deficiencies. The problem posed by existing, unreinforced masonry structures is critical in itself, but when coupled with geologically hazardous sites, the problem may surpass the possibility of taking corrective measures to ensure public safety. This is particularly true for buildings with

high density populations as opposed to unoccupied structures used for the storage of expendable supplies and less critical equipment. In such cases, when coupled with microzonation data and risk analysis results which indicate extreme hazard exposure, abatement programs may be considered as part of a community's projected general plan. The alternative could mean facing severe social dislocation and economic forfeiture which could seriously test a community's survival as was the case in some of the small agricultural communities after the Imperial County earthquake of 1979 in California. In the small community of Imperial, about a dozen old brick buildings housing thirteen businesses and local government offices were condemned and demolished after the earthquake, leaving the downtown area "looking like an unpaved parking lot".¹² Eighty percent of the buildings in the downtown area of Imperial were declared post-earthquake hazards due to the damage sustained by these older masonry buildings during a brief period of intense ground shaking and were all dismantled. For all practical purposes the downtown area of Imperial has disappeared, and its loss reinforced the tendency of its residents to take their business to the City of El Centro located only about five miles to the south. The community of Imperial was located approximately three miles from the Imperial Fault trace displacement of the 1979 earthquake.¹³ (See Figure 12)

SUMMARY

For utilization by architectural planning and design professionals, it is important that microzonation maps and techniques be developed from a common base-line to facilitate the interpretation of data as a preliminary design tool. By reviewing microzonation data and other risk analysis models, the design professional can achieve a better approach to seismic safety in building siting and design by reviewing design options while in a flexible position to do so during the preliminary planning and design stages of building construction.

Microzonation mapping can be of assistance to urban designers and public officials dealing with the existing, older hazardous building problem in urban environments located in areas of extreme seismic risk. Such areas can be targeted for future renewal and revitalization projects in districts of high-density population concentrations in order to insure their continued viability.

A clear cut benefit of microzonation for environmental design is the identification of sites where there is great potential for seismically induced ground failures, such as liquefaction and land slides, sites which are directly astride active faults, and sites which may have some anomalous condition such as uncompacted fill or dried creek bed below grade. Work in these aspects of microzonation have been done to a successful and practical extent in the San Francisco Bay Area, by researchers in government organizations, private practice, and universities. Ground shaking prediction in both micro and macrozonation is valuable though difficult because of the innumerable variables both in the local geography and soil conditions, and in the characteristics of the earthquake source. Particular caution must be taken by those interpreting information presented in zonation maps, lest overdependence upon this aspect of seismic hazard mitigation result. At all times, architects and planners must realize that zonation is only one aspect of the earthquake resistant design procedure.

If as the bounds of zonation's reliability are recognized, the additional information provided by micro and macrozonation can decrease uncertainty and excessive conservatism in the structural design of structures; both economical cost and risk are reduced.

As research in zonation and microzonation becomes more prolific and sophisticated in the earth science and engineering fields, its application to environmental design decisions in planning and architecture becomes increasingly justified. In the United States, where much seismic hazard mitigation research is ongoing, the current trend of this consciousness among environmental design professionals has been encouraging. In the future, it is hoped that applications of zonation considerations in environmental design will remain commensurate to the state-of-the-art of engineering and geology research knowledge in this specific field.

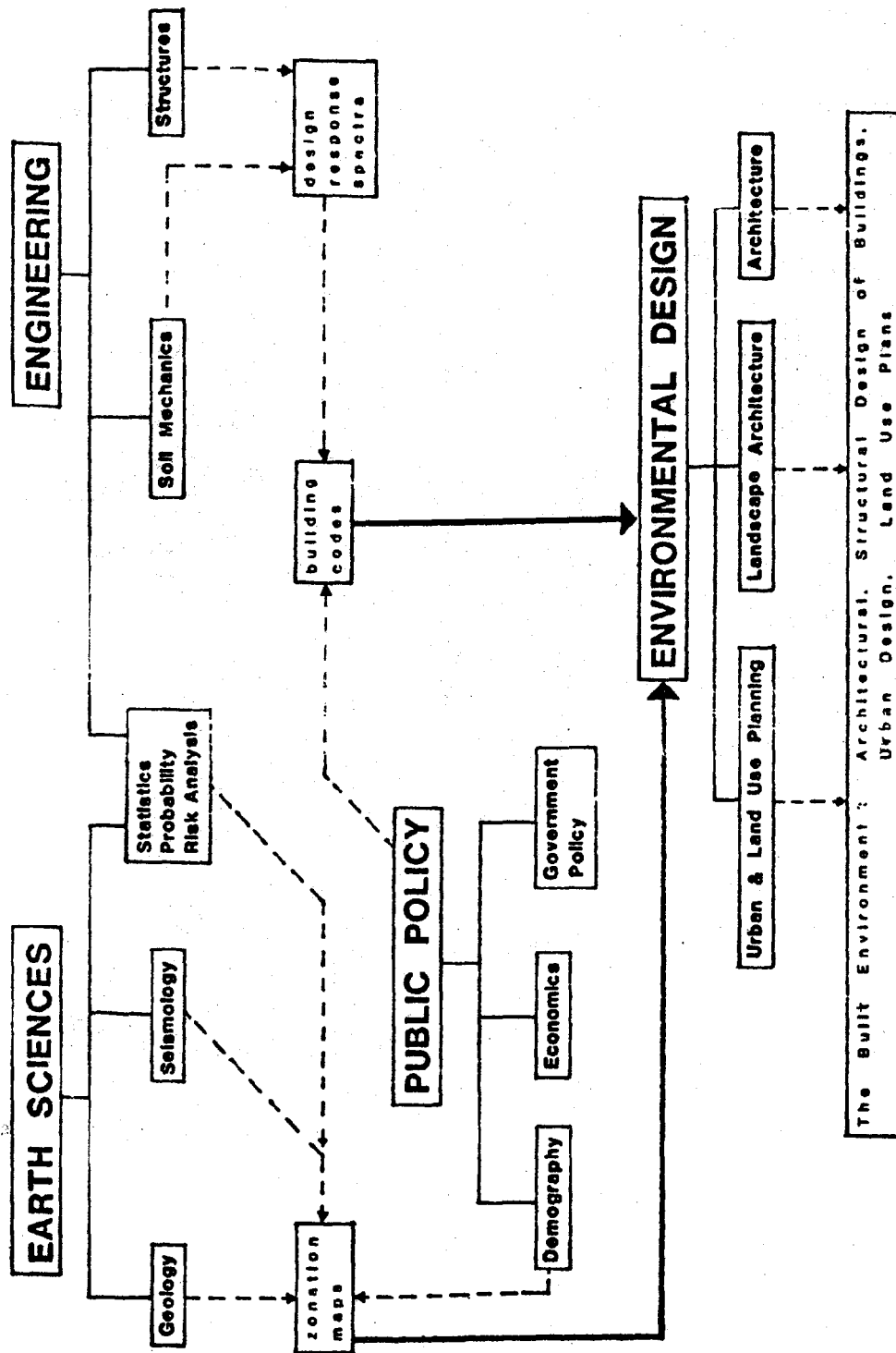


Figure 1. Flowchart of interdisciplinary relations in seismic hazard mitigation for the built environment.

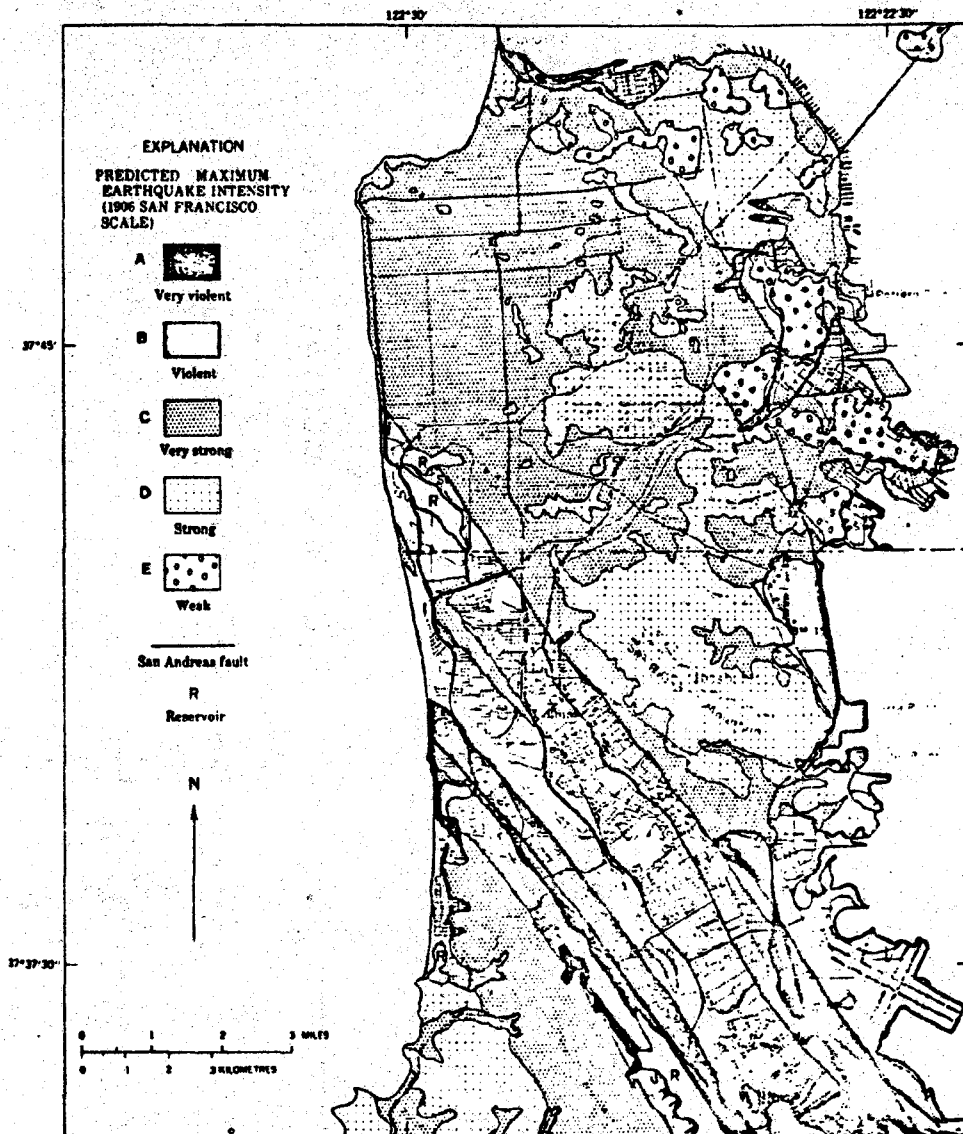


Figure 2. Maximum earthquake intensities predicted for San Francisco (map is excerpt from Borchardt, Gibbs, and Lajoie, 4).

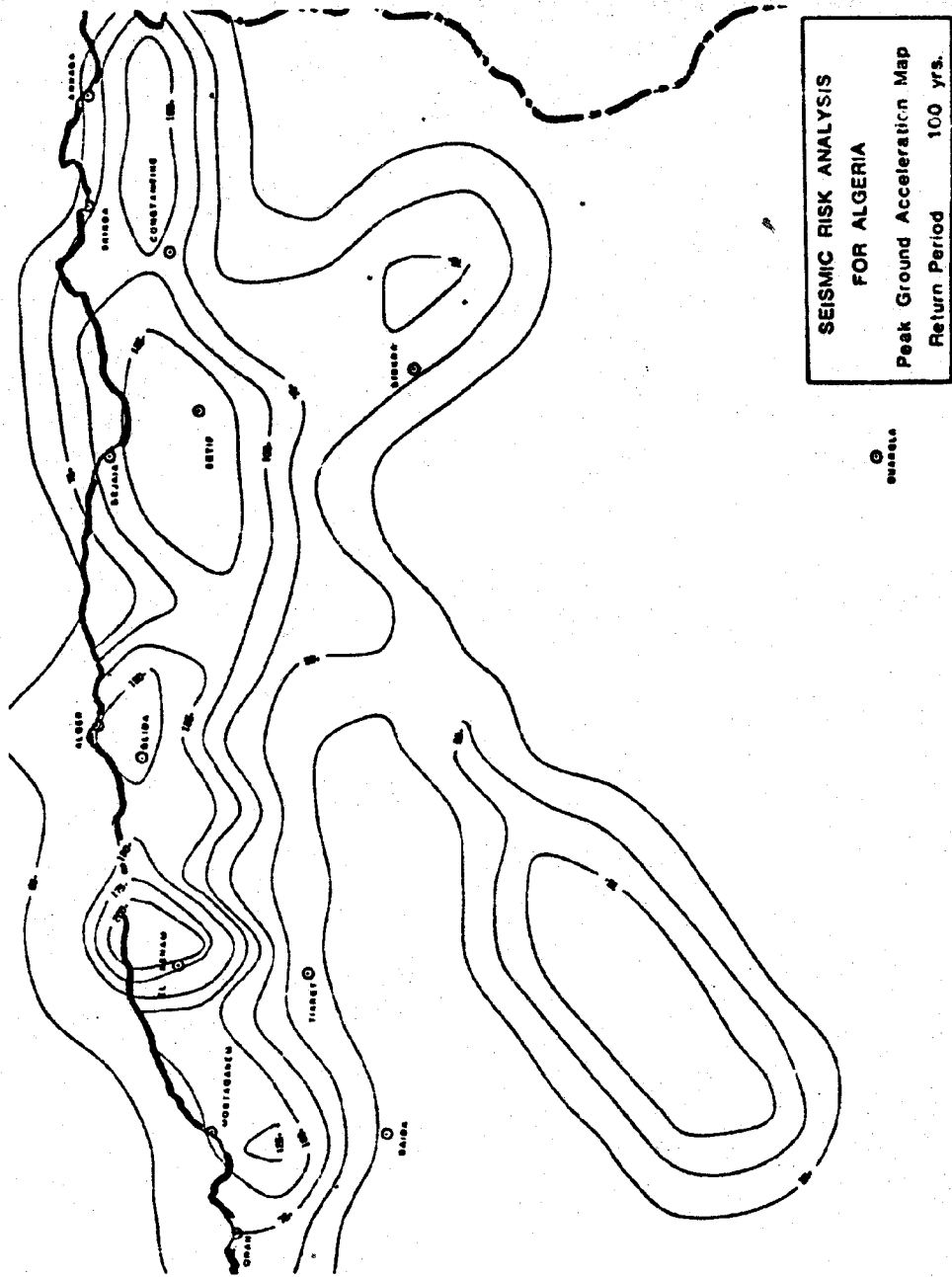


Figure 3. From Shah and Mortgat. (Ref. 3)

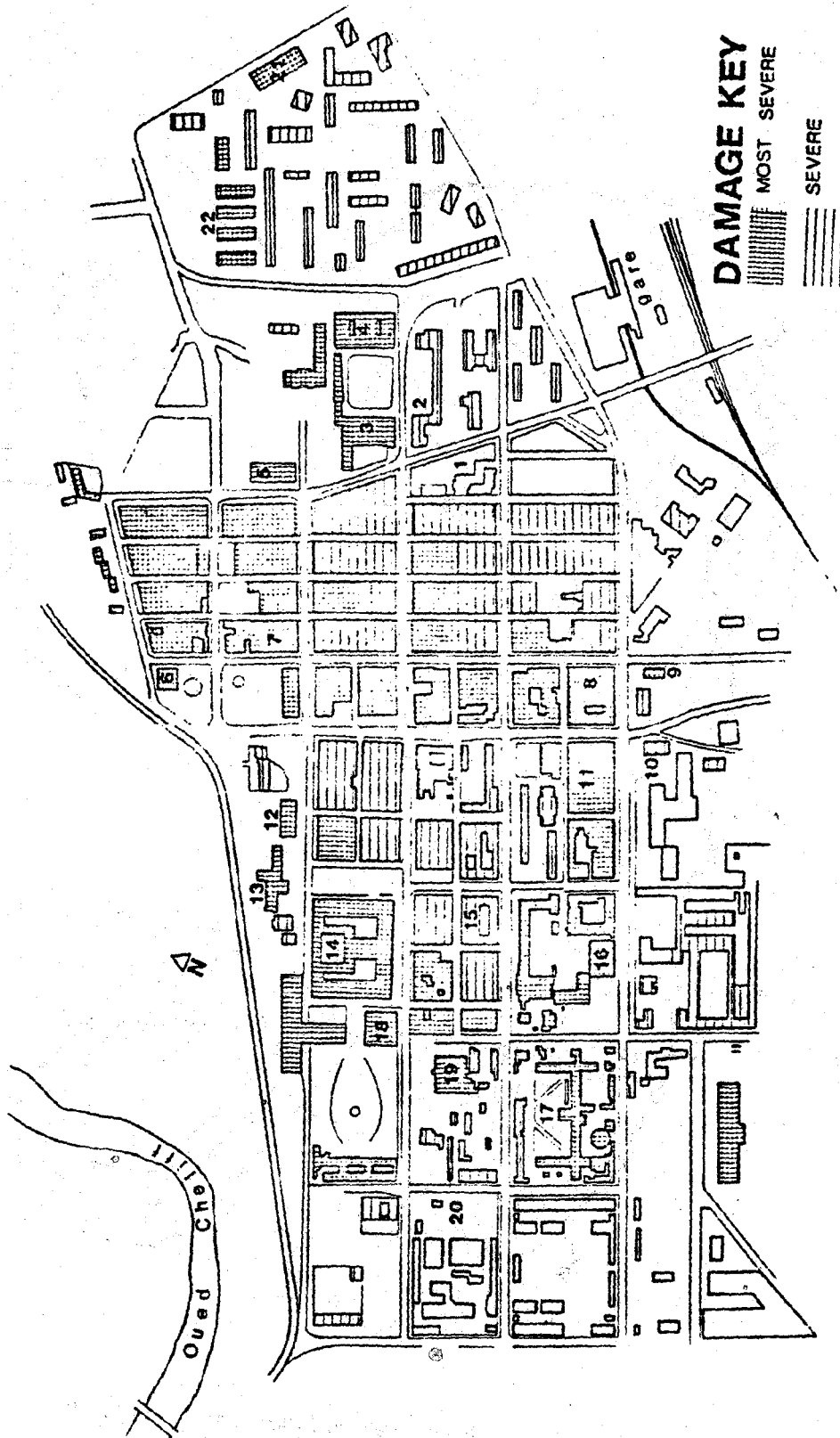


Fig. 4a. El Asnam 1980 E.Q., building damage distribution.
18-20

KEY FOR BUILDINGS IN DOWNTOWN EL ASNAM

<u>BUILDING NUMBER</u>	<u>BUILDING NAME</u>
1	C.T.C. Headquarters
2	Bridge Construction Design Office
3	Hotel Cheliff
4	Palais du Justice
5	Sonacome
6	Commissariat National du Parti FLN
7	Centre Medico Social
8	Nouvelles Galeries Algeriennes
9	Telephone Building
10	High School
11	L'Hôtel des Finances
12	Police Station
13	Town Hall
14	Cité an Nasr
15	Bureau de Poste
16	Maison de la Culture
17	Hospital
18	Mosque
19	Mosque
20	Military Headquarters
21	Clinic
22	Apartment Buildings

Figure 4b. Key to Figure 4a.

Reproduced from
best available copy.

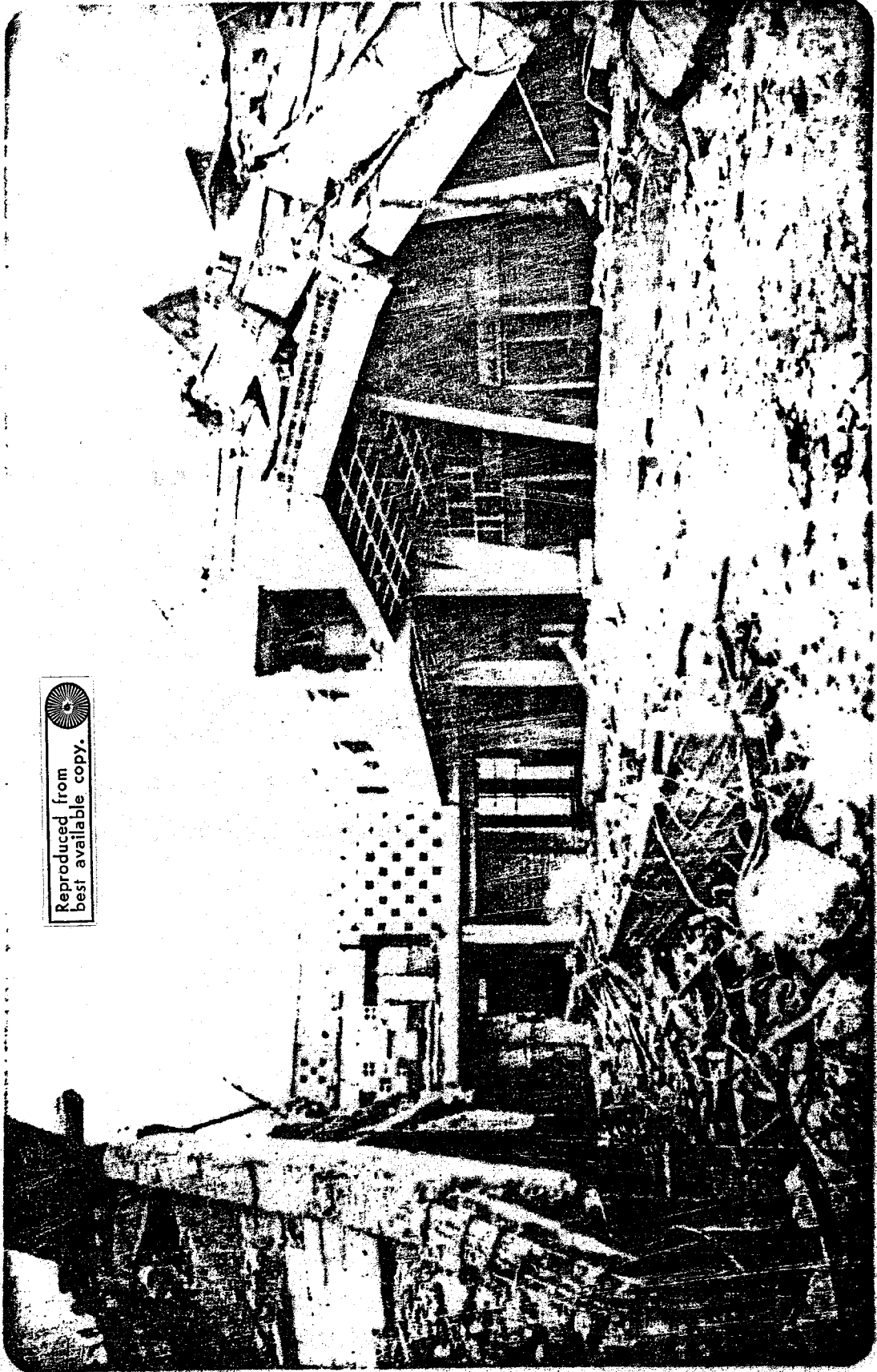


Figure 3. Remaining corner of Cite An Nasr, El Asnam, Algeria, 1980. (M. Wang)

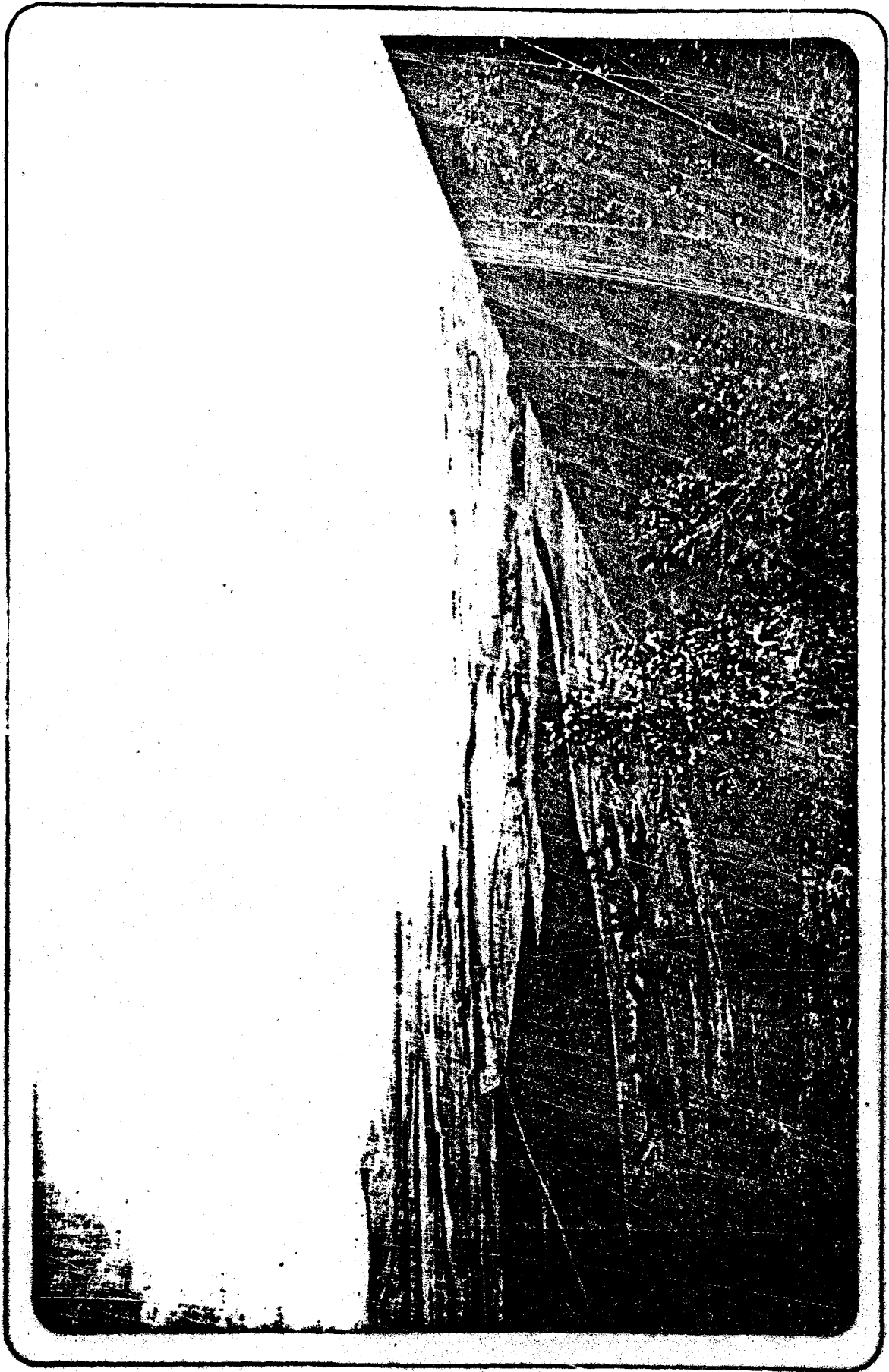


Figure 6. River Cheliffe and new tectonic lake (Tor). (M. Wang)

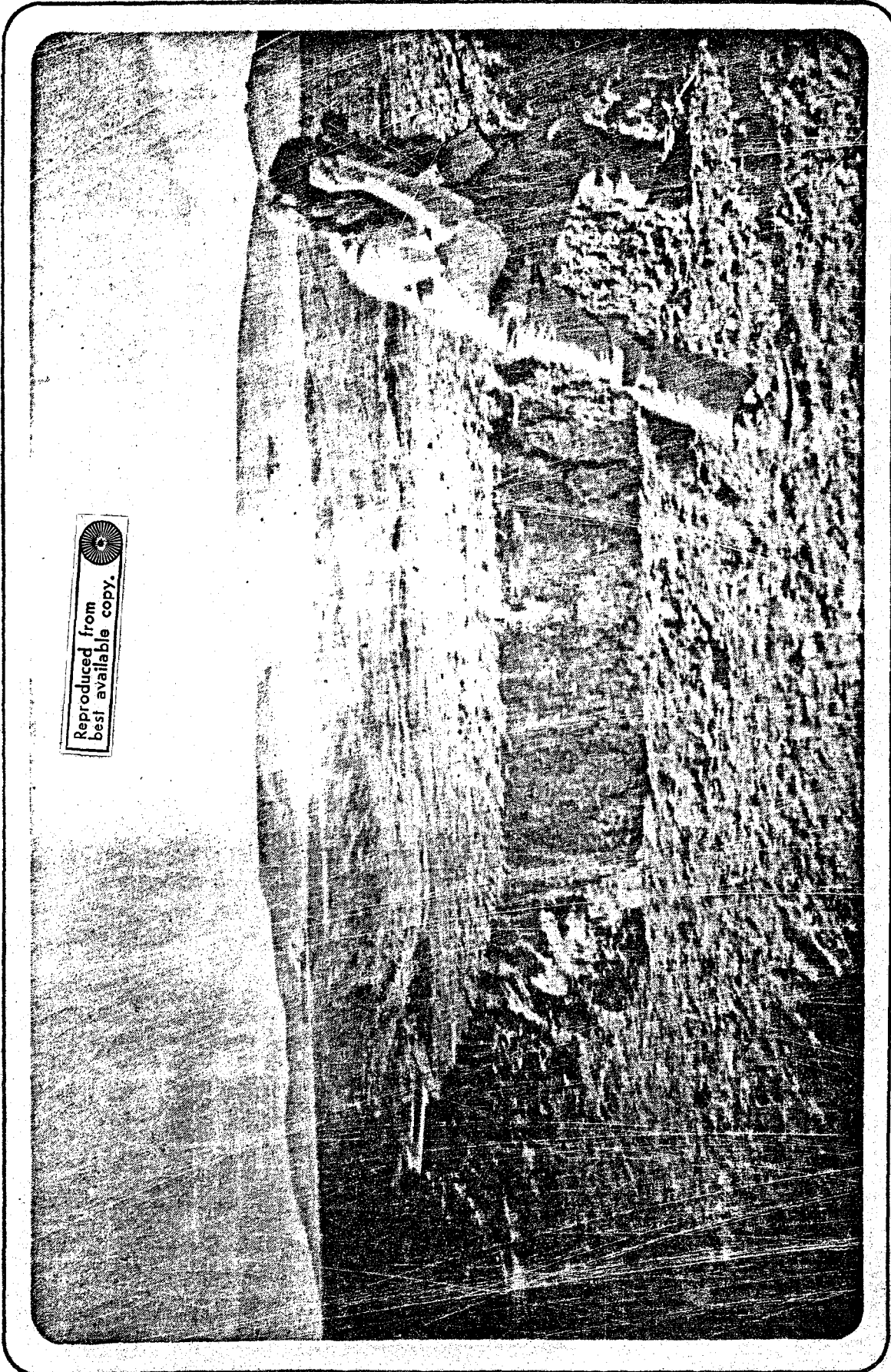


Figure 7. Fault near El Asnam, 1980. (M. Wang)

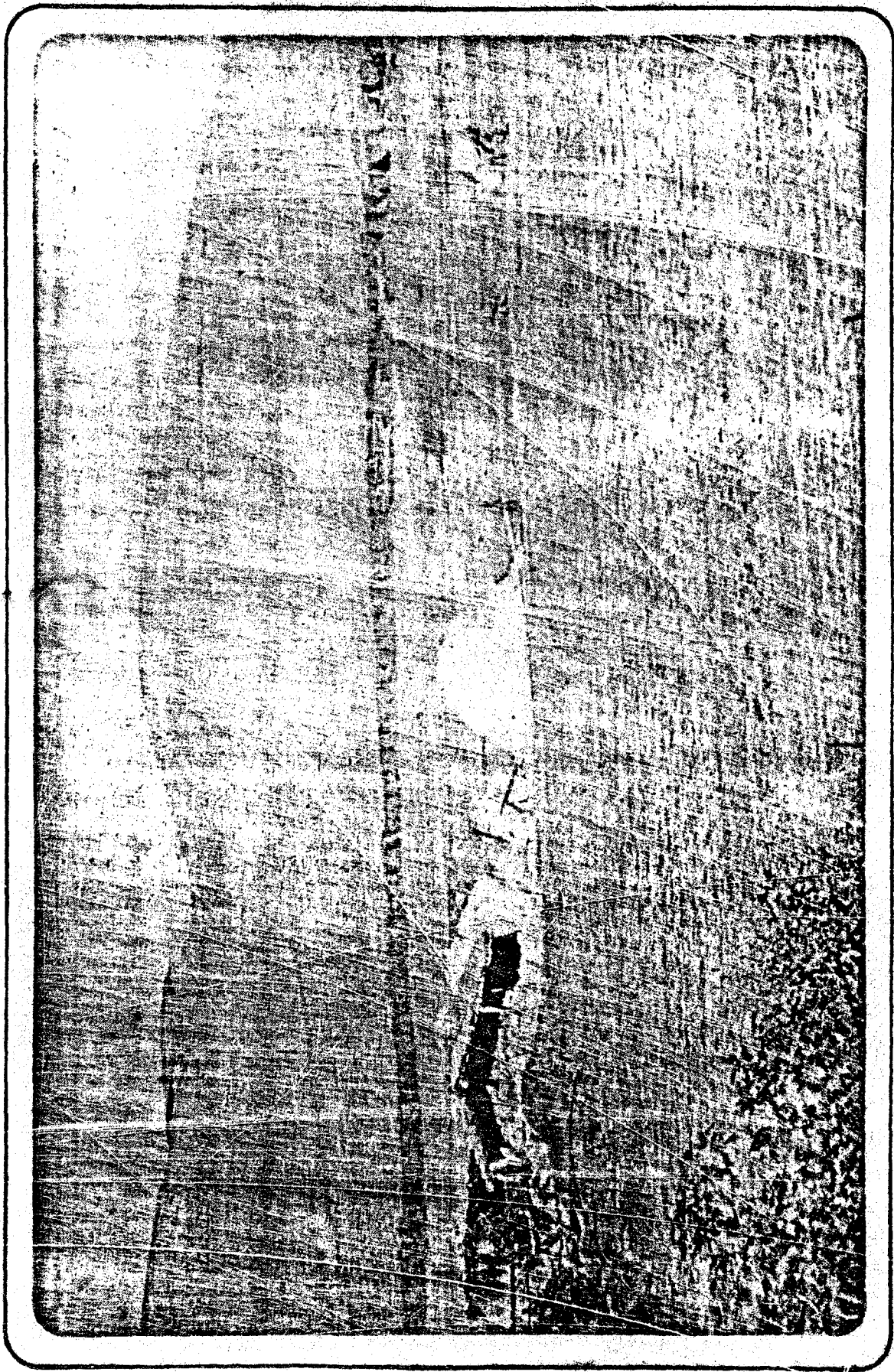


Figure 8. Fault in countryside near El Asnam. Note standing structures in foreground. (M. Wang)

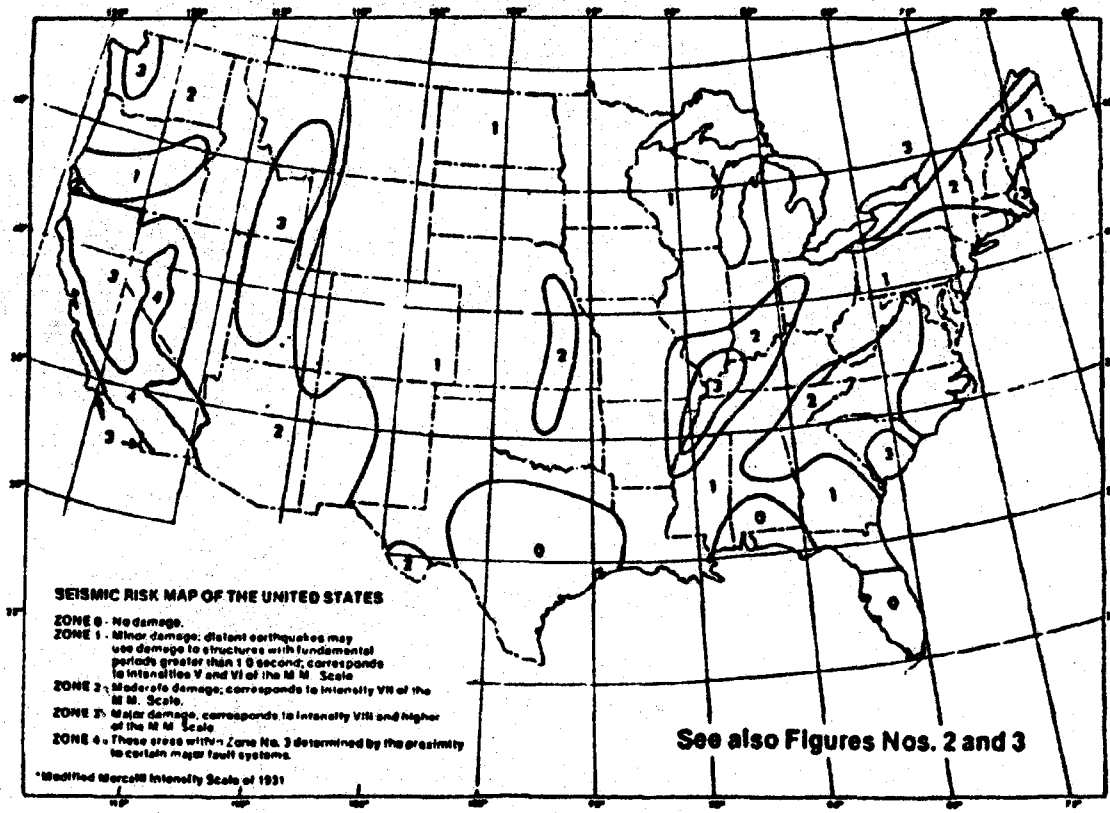


Figure 9. Seismic zone map of the United States. For areas outside of the United States, see Appendix Chapter 23. Source: UCB 1979.



ZONES OF HIGH SUSCEPTIBILITY TO SEISMICALLY INDUCED LANDSLIDES




<u>SYMBOL</u>	<u>POSSIBLE LANDSLIDE TYPES</u>	<u>MAPPING CRITERIA</u>
	SOIL AVALANCHES; FALLS, SLUMPS, BLOCK SLIDES AND SHALLOW DISINTEGRATING SLIDES IN SOIL AND/OR ROCK	SLOPES STEEPER THAN 35°
	LATERAL SPREADS AND WET FLOWS	UNDERLAIN BY SATURATED SANDY AND SILTY HOLOCENE ALLUVIUM
	SLUMPS AND BLOCK SLIDES IN SOIL AND/OR ROCK	ACTIVE AND RECENTLY ACTIVE LANDSLIDES

Figure 10. Preliminary seismically induced landslide susceptibility map of the La Honda area. (Rev. 18)

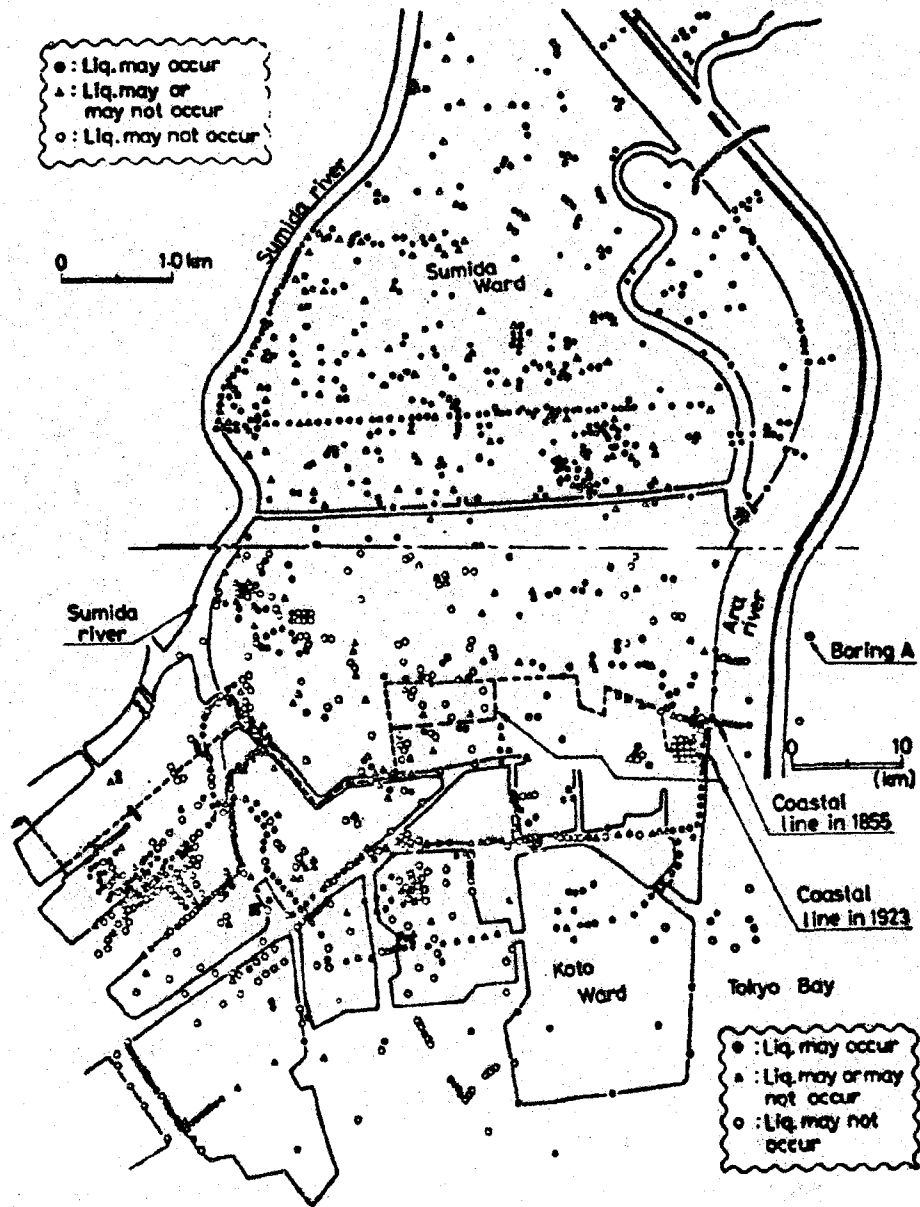
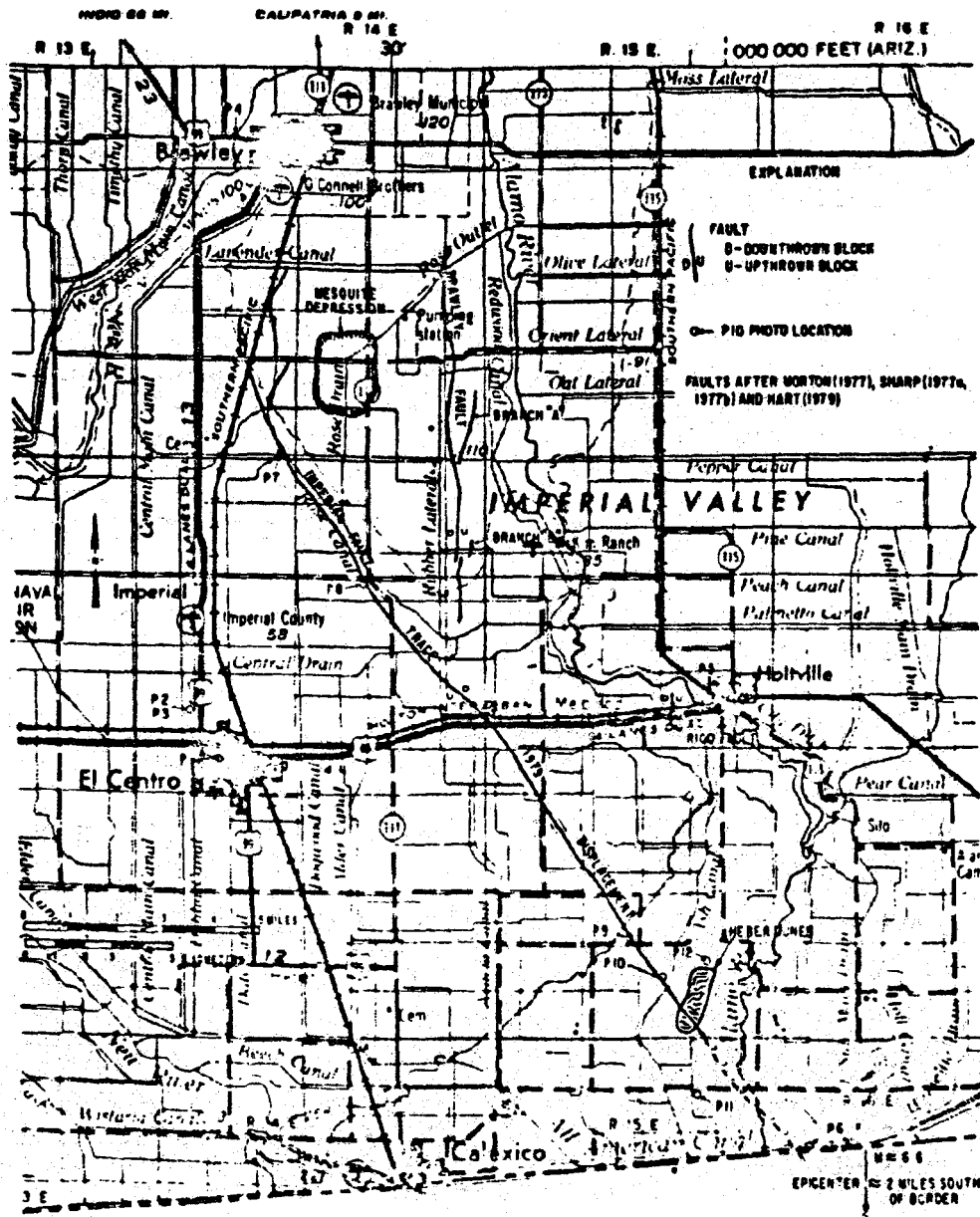


Figure 11. Likelihood of liquefaction occurrence in the downtown area of Tokyo. (Ref. 11)



Reproduced from
best available copy.

Figure 12. Area of surface faulting, Imperial Valley earthquake, October 15, 1979. For a more detailed delineation of surface rupture, see Hart (1979). (Ref. 13)

REFERENCES

- ¹ Karnik, V. and Algermissen, S.T., "Seismic Zoning" The Assessment and Mitigation of Earthquake Risk, UNESCO, 1978.
- ² Petrovski, J., "Seismic Microzonation and Related Problems" - The Assessment and Mitigation of Earthquake Risk, UNESCO, 1978.
- ³ Mortgat, C. and Shah, H., "Seismic Hazard Analysis of Algeria", John Blume Earthquake Engineering Center, Stanford University, June 1978.
- ⁴ Arnold, C., "Architectural Implications", Reconnaissance Report, Imperial County, California, Earthquake - October 15, 1979, EERI, February 1980.
- ⁵ Allen, C. R., Testimony in U.S. Senate, 92nd Congress, 1st Session, 1971, Governmental Response to the California Earthquake Disaster of February 1971.
- ⁶ Scott, S., "Policies for Seismic Safety: Elements of a State Governmental Program", Institute of Governmental Studies, University of California, Berkeley, 1979.
- ⁷ Green, K. W., "Energy Conscious Redesign", Research & Design, AIA Research Corporation, Washington, D.C., Summer 1980.
- ⁸ Bertero, V., Gergely, P. Shah, H., Wang, M., et al, "Preliminary Report, El Asnam Earthquake of October 10, 1980", EERI, December 1980.
- ⁹ Lagorio, H. J. and Botsai, E., "Urban Design and Earthquakes", Proceedings of Second International Conference on Microzonation, University of Washington, Seattle, 1978.
- ¹⁰ Bolt, B., Horn, W. L., et al, "Geological Hazards", 2nd Edition, Springer-Verlag, New York, 1977.
- ¹¹ Ishihara, I., and Ogawa, N., "Liquefaction Susceptibility Map of Downtown Tokyo", Proceedings of the Second International Conference on Microzonation, University of Washington, Seattle, 1978.
- ¹² Seiler, M., "Downtown After the Quake", San Francisco Chronicle, November 30, 1980.
- ¹³ Leivas, E., Hart, E. W., et al, "Geological Setting, Historical Seismicity and Surface Effects of the Imperial Valley Earthquake", Reconnaissance Report, Imperial County, California, Earthquake - October 15, 1979, EERI, February 1980.
- ¹⁴ Hudson, D. E., "Local Distribution of Strong Earthquake Ground Motions", Bull. of Seismological Society of America, December 1972.

REFERENCES (continued)

- 15 1979 Uniform Building Code.
- 16 Borchert et al, "Prediction of Maximum Earthquake Intensity in the San Francisco Bay Region, California", USGS MF 709, 1975
- 17 Keefer, D. K., et al, "Preliminary Assessment of Seismically Induced Landslide Susceptibility", USGS Circular 807.

THE PREDICTION AND ZONATION OF EARTHQUAKES
GROUND MOTION IN THE BEIJING PLAIN

JIANG PU*, XU FENG* and WANG QIMING*

ABSTRACT

On the basis of seismogeological studies in the Beijing area the sketch of distribution of potential bedrock motion are determined. In this map are shown potential maximum acceleration contour, predominant periods and duration as well as two average response spectra with damping 0.05 and 0.2.

According to the horizontal zonation and vertical changes of unconsolidated deposits in the Beijing plain and their depositional characteristics, the delineation of three depositional regions and 61 geologic units is made. The analysis of earthquake response for each geological unit is made by means of one-dimensional linear elastic lumped-mass method. Basing upon the characteristics of earthquake response spectra for each geological body, the bedrock motion response is comprehensively delineated and each region is marked with acceleration spectra, velocity spectra and displacement spectra.

I. The general seismogeological features of the Beijing plain

The Beijing plain is a part of the North China plain and geologically can be regarded as a northern part of the North-China subsidence seismic belt in the North China fault block region (1). Since Cenozoic time the study plain has been subjected to a strong subsidence. There developed four sets of faults, from them the NE and NNE-trending ones being predominant and constituting the main outline of this plain (2). These faults in the direction stated above show a clear activity; under their control in the study region are developed a lot of uprisings and fault basins in the same direction as the faults. The EW-running faults are the relatively old structural lines being active in Cenozoic. As a result, the NW-trending uprising and depression are superimposed by the NE and NNE uprising and fault depression. As to the NW fault, it extends intermittently and shows a higher activity. The intersection of the four sets of faults, especially the NE and NNE faults with the NW faults, as well as the reversed overlapping of NE and NNE uprising and fault depression, are just right the places where most of shocks in study region would be probably occurred. For example, the Mafang earthquake of September 2, 1679 just took place at the intersection of a fault at the northern end of Dachang fault depression and newly activated Ershilichangshan fault (1). Since Cenozoic the study region was controlled by the

*Research Associate, Institute of Geology, State Seismological Bureau

regional stress field with the NEE trending principal compression stress that is leading to the right-lateral strike slip of NNE and NE faults and the left-lateral strike slip of NW and nearly EW faults. Besides, the vertical additional stress field caused by the upper mantle upwarping also gives a certain influence on the fault basin region. Just on this tectonic mechanical background proceed the current tectonic activities and seismicities in the study region (2). The Beijing plain has a tectonic framework of so-called "two uprisings and one depression", namely this plain is cut by a NE fault into the West-Beijing uprising, the Beijing depression and the Daxing uprising. And the Xiadian fault together with the Huangzhuang fault formed the Dachang depression giving a structural scheme of "two uprisings and two depressions". Furthermore, the West-Beijing uprising is cut by NW Nankou-Tongxian fault into the Changping-Huairou uprising and the Shahe depression and the Beijing depression into the Fanshan uprising and Shunyi depression; while the Ershilichangshan fault separates the Daxing uprising from the Pinggu depression.

During the last thousand years in the Beijing plain have recorded 8 destructive events and 5 events with magnitude more than 6 (Table 1) or 8 in maximum. In the North China fault block region the destructive earthquakes in the Beijing plain were chiefly concentrated with in 250 years, i.e. From 1500 to 1750 A.D., the third seismic period for the North China region(3).

There are three active seismotectonic belts in the Beijing plain, the Pinggu-Xianghe belt, the Nankou-Tongxian belt, and the Fangshan-Huarou belt. There can be mainly distinguished two earthquake risk areas (Fig.1): Xianghe-Sanhe area and Qinghe-Tongxian area.

The former is located at the intersection (near Xianghe) of the NE Pinggu-Sanhe seismic belt with the nearly EW Baodi-Laishui active fault, i.e. at the southern end of the Dachang depression. There exist three active faults, the Chenggezhuang-Xiadian fault, Baodi-Laishui fault and Huangzhuang fault. The levelling and fault displacement observation also indicate their recent activity(4). It is assumed that the study area has a risk level of 7-7½ in magnitude.

The Qinghe-Tongxian earthquake risk area falls between the NW Nankou-Tongxian active belt, the Fangshan-Huairou active belt and the Nanyuan-Tongxian active belt. Within this area can be found the Huang-Gaoliying active fault, the Nanyuan-Tongxian fault and Nankou-Sunhe active fault, of which the recent activity (4) has been testified by the levelling and fault displacement measurements. It is estimated that this area has a risk level of 6-6½ in magnitude.

II. The bedrock motion in the Beijing region

To predict and zone the bedrock motion for a certain region usually has two steps, the first is to predict the bedrock motion, the second to make the earthquake response

analysis of unconsolidated soil layer on the basis of bedrock motion(5,6,7,).

The prediction of bedrock motion in the Beijing region covers the following steps.

1. The estimation of the main risk area

The two earthquake risk areas determined above according to the essential seismogeological characteristics of the Beijing plain are; Xianghe-Sanhe area with magnitude of 7-7½ and Qinghe-Tongxian area with magnitude of 6-6½. For the purpose of making zonation and from the angle of earthquake resistant engineering we focus our attention on the maximum earthquake risk. The position of both the risk areas is plotted on the Fig.1. Taking 20-25km as the depth of occurrence of earthquake in the study area the faulting slip mode can be left out of consideration. But due to the influence of the directions of regional structures and earthquake faults on the distribution of bedrock motion and structure failure it is appropriate to evaluate the action of NE and NW structures in sketching the amplitude contour of bedrock motion.

2. The main potential bedrock motion

It includes amplitude value, predominant or main period and duration. In coincidence with the "Code of Earthquake

Resistant Construction of China"(8,9,)the bedrock accelerations are used as basic parameters, while the relationship between the earthquake magnitude, the peak bedrock acceleration and fault distance and the relationship between the predominant period for maximum acceleration in rock, earthquake magnitude and fault distance are studied in the light of Seed's work (10). As to the duration we take 15-20 sec. for 6½ M and 25-30 sec. for 7½ M.

3. The average earthquake response spectra

The study region has little records of bedrock motion excepting a bedrock record obtained in a Beijing suburb during the Tangshan earthquake. In studying the general features of bedrock motion we have chosen the strong motion recorded not from rocks to change the maximum amplitude period It is found that the basic shape and feature of response spectra (=5 and =20%) vary with the maximum amplitude period(6).Some results gained have been shown in Fig 2-5. The comparison of the response spectra given in case of the shorter maximum amplitude period (Figs. in 2-5) with that recorded from bedrock motion (shown in Fig.6) indicates their close similarity(11). With regard to this the maximum amplitude period can be approximately applied to reedominant period of bedrock motion.

It can be seen from Figs.2-5 that for the spectra with 5% damping the maximum response coefficient is about of 3; in case of 20% damping it would be less than 2. Furthermore, the res-

ponse spectra on opposing sides of main peak are decreasing inversely in proportion with the structural period to form a bicurve. Thus, on this background the practical records are utilized to calculate the response spectra of various maximum amplitude periods and the average response spectra can be gained for some region on the basis of the mean value of response spectra the maximum amplitude period is the same. The Fig.7 gives the distribution of the potential bedrock motion in Beijing area, the application of which would provide the engineers with the potential bedrock motion including the parameters calculated from basic intensity scale.

III. The zonation of deposit-facies units in the Beijing plain and the earthquake response of geologic units

1. Delineation of the deposit-facies units

Along the western and northern Beijing plain runs the Yanshan range, and its southern and eastern parts gently go down toward the North China plain. Since the quaternary due to the relative uplift of Yanshan range and subsidence of this plain the abundant clastic materials have been driven by rivers running through the mountain area of NW Yanshan and plain and deposited at the piedment in different geological times. As a result, the broad alluvial foreland plain, Beijing plain, was progressively formed. In correspondence with the characteristic relief the underground current in the Beijing plain shows a regular change. In general, it flows from NW to SN and the groundwater table also becomes more shallow in the same direction leading its slow flow. And in the low-lying land located between the foreland alluvial fans the ground water level has a less depth. On the alluvial fan margin the deposit-facies change always makes the groundwater flowing on surface resulting in formation of a series of lakes and marsh lands, such as Kunming Lake, Lianhua Lake and so on(12).

The unconsolidated deposits in the Beijing plain are characterized by the gradual change in the spatial distribution from the forland to plain. From the Fig.8 showing the distribution of unconsolidated deposits, can be seen that in the western plain the coarse-grained clastic deposits are predominated and constitute the top of alluvial fan. This kind of deposits consists of pebbles, gravel and boulder in part. To the east they become gradually more fine in grain size consisting of sand and clay and substituting the horizons with coarse-grained deposits. That is to say, it is a result of gravitational sorting of depositional materials. In the Beijing plain, which was one of the places where the Early man lived, the original distribution of these deposits have been changed to a certain extent. According to the features of unconsolidated deposits from the boreholes at a depth of more 50 M and of depositfacies the Beijing plain can be divided into three depositional regions that are: A-region of the upper alluvial fan, B-region of marginal alluvial fan, and C-region of alluvial plain.

A. The depositional region of the upper alluvial fan

In addition to the deluvial and eluvial deposits in small amount, such as eluvial loess, weathered debris, boulder and clay, there appear mostly diluvial and alluvial deposits of coarse-grain materials, such as gravel, coarse sand and etc., cropping out on the surface in one place and covered by a clayey soil layer in other place. It is generally believed that the study region is a favorable site for the engineering construction due to the greater underground water level.

From the geographical position of alluvial fan and the main drainage running through this fan, the depositional region of the upper alluvial fan can be subdivided into six subregions: A₁-Yongdinghe subregion, A₂-Shanhe subregion, A₃-Chaobaihe subregion, A₄-Chaobaihe subregion, A₅-Jumahe subregion and A₆-Dashihe subregion.

According to the changes of depositional facies in the time profile in each depositional region, the composite features of deposit-facies vary with the different regions. Therefore we further distinguished geologic units on the basis of the features of deposits found in boreholes at a depth of 50 M and their composite characteristics. In the study region there exist five depositional constitutions: a-the gravel and boulder, b-the sandy gravel-clayey soil, c-the sandy gravel-silt, d-the interbanding of sandy gravel with clayey soil, e-the clayey soil with gravel.

B. The region of the marginal alluvial fan

This region denotes the transitional area from the upper alluvial fan to alluvial plain. There can be found the alternation of coarse-grained deposits by the fine ones. As a result, the ground water flows out on the surface wherein. In many lowlands and logged lands deposited mud and silt layer rich in organic matter. They can be categorized as the localities with the ground base unsuitable for the engineering geologic purpose. Each of the six alluvial fans stated above has a corresponding marginal depositional region, under which the subregions are signed by B₁ B₂ B₃ B₄ B₅ and B₆, comparable with the above-mentioned subregions of the upper alluvial fan. In the marginal depositional region there are following five kinds of depositional constitutions: f-interbanding of sand with mud, g-interbanding of clayey soil-mud with silt, h-sandy gravel-silt constitution, i-interbanding of sandy gravel with clayey soil, j-intercalated constitution of clayey soil with sandy gravel.

C. The depositional region of the alluvial plain

From the geomorphological features this alluvial plain region is a rather flat and broad plain with fine-grained deposits being predominant. The alteration of the drainage

system in the plain during geological periods resulted in the formation of aquifers with coarse sand and gravel in the historical channel and old stream and in the deposition of fine-grained silt and mud layers in the old and historical lakes. These layers occurred in the form of band and lens at a different depth.

In the study region can be found following six kinds of depositional constitutions: k-interbanding of clayey soil with the median-fine grained sand, l-intercalating of clayey soil with median-fine grained sand, m-clayey soil-silt bed, n-intercalating of clayey soil layer with mud, o-clayey soil-mud layer, p-interbanding of clayey soil with silt and mud.

2. The response of geologic units to earthquakes

The three depositional regions in the Beijing plain are of 16 types of constitutions and 61 geologic units(6). According to the physio-mechanical properties of each geologic unit the one-dimensional linear elastic lumped-mass method is used to response of each geologic unit to earthquakes. The structural period is with damping $=0.05$ and $=0.20$ and the acceleration response spectra S_a , velocity response spectra S_v and displacement response spectra S_d are calculated. Therefore, we obtained 366 response curves belonging to various types for 61 geologic units.

Basing upon morphological features and the peak numbers of various kinds of response spectra, they are categorized as three types(See Table 2 and Fig.9).

The zoning map of earthquake response in the Beijing plain(Fig.11) was compiled in the light of average response curves stated above and shown in Fig.10. It is proved to be effective during the Tangshan earthquake which caused failure in the Beijing plain(5).

Generalizing the above-mentioned facts in connection with the studies of engineering seismics effect,(6, 13), the main steps to make microseismic zoning are as follows:

1. To give a sketch showing the distribution of potential bedrock motion on the basis of the characteristics of focus of earthquake and the propagation of seismic waves.
2. To separate the effect of shock failure from that of ground failure and to make the corresponding zoning maps on account of the possible types of earthquakes effect in the unconsolidated deposits of some region(6).
3. To delineate the deposits into the different depositional regions and geologic units according to their origin, features and the constitution changes shown in the vertical profile. Then, to make an analysis of the earthquake response for each geologic units, and at last to work out a synthetic zonation based on the characteristics of response spectra and to mark the earthquake response spectra in order to satisfy the earth-

quake resistant requirement for each region at present.

IV. ACKNOWLEDGEMENT

The authors wish to thank Prof. Hu Lu-xian, Chief engineer Chen Dehe, Chief engineer Wang Zhongqi and Associate Scientist Chen Dasheng for their supporting this work. Our thanks also due to the Engineering Institute of Mechanics, Academia Sinica for providing the records of strong earthquakes, the Topographic-Geological Survey Office of Beijing Municipality for providing the geological data on the Beijing plain.

REFERENCES

- (1) Institute of Geology, Academia Sinica (1974), an introduction to seismogeology in China, Science Press.
- (2) Jiang Pu and Deng Qiding (1980), the development of precursory field and the tectonomechanical condition in the Haicheng-Tangshan earthquake series, Seismology and Geology, V.2, 31-41.
- (3) Institute of Geology, Academia Sinica and Institute of Geology, State Seismological Bureau (1980), Formation and development of the North China fault block region, pp. 192-205, Science Press.
- (4) Ibid, pp. 281-286.
- (5) Jiang Pu et al. (1979), Discussion on the anomalous areas of high intensity nearby Beijing caused by the Tangshan earthquake, Seimology and Geology, V.1, 90-80.
- (6) Jiang Pu et al. (1980), The study and zonation of seismic effect in engineering field (in press).
- (7) Borcherdy R.O. (1975), Studies for seismic zonation of the San Francisco Bay region, U.S. Government Printing Office, Washington, P.A 88-96.
- (8) Chinese Academy of Architectural Sciences, State Construction Commission and Sichuan Academy of Architectual Sciences (1974), Code of Earthquake Resistant Construction for Civil Engineering TJ.11-74, Architectural Engineering Publishing House of china.
- (9) Ministry of Water Conservancy and Electric Power (1978), Code of Earthquake Resistant for Hydraulic Buildings SDJ 10-78(trial), Hydroelectric Press.
- (10) Seed N.B. (1969), characteristics of rock motion during earthquakes, Am.Soc. Civil Engineers Proc., J. Soil Mechanics and Found.Div., V.95, p.1199-1218.
- (11) Chen Dasheng (1965), Some data for maximum acceleration response spectra to ground motion, Collected papers of studies of Seismic Engineering, No.2, Science Press.
- (12) Zhou Mulin (1956), the geological problems in construction of the Capital, Geological knowledge, No.7.
- (13) Jiang Pu and Gao Weian (1976), on the effect of the ground failure by strong earthquakes and the geological conditions required for its production, Scientia Geological Sinica, No.1, p.64-73.

Table1.

Date	Long.lat.		Reference locality	Magnitude
	N	E		
1076.2	39° 58'	116° 30'	Beijing city	5-5.9
1484.1.29	40° 24'	116° 10'	Juyongguan	7
1536.10.22	39° 48'	116° 48'	S.Tongxian	6
1586.5.26	40° 01'	116° 10'	W.Beijing	5
1665.4.16	39° 54'	116° 42'	Tonxian	6½
1679.9.2	40° 00'	117° 00'	Mafang	8
1730.9.30	40° 00'	116° 00'	W.suburb,Beijing	6½
1746.7.29	40° 17'	116° 15'	Changping	5

Table2. Types of response spectra

Types	Acceleration response spectra	Velocity response spectra	Displacement response spectra
I	Type of main peak	Type of main peak	Type of polypeak
II	Type of double peak	Type of double peak	Type of double step
III	Type of smooth peak	Type of smooth peak	Type of single step

Table 3 Amplitude value division type I of spectra

Order	Acceleration response spectra in m/sec		Velocity response spectra, in m/sec		Displacement response spectra, in cm	
	$\lambda = 5\%$	$\lambda = 20\%$	$\lambda = 5\%$	$\lambda = 20\%$	$\lambda = 5\%$	$\lambda = 20\%$
strong	> 0.8	> 0.5	> 40	> 20	> 4	> 3
intermediate	0.4-0.7	0.2-0.4	25-40	10-20	3-4	2-3
weak	< 0.4	< 0.2	< 25	< 10	< 3	< 2

Table 4. Statistics of types of response spectra for individual depositional region

Depositional region	Total of geol. units	Types of response spectra					
		Type I		Type II		Type III	
		amount	%	amount	%	amount	%
A	21	19	90	2	10	0	0
B	14	0	0	6	42	8	58
C	26	10	38	10	38	6	24

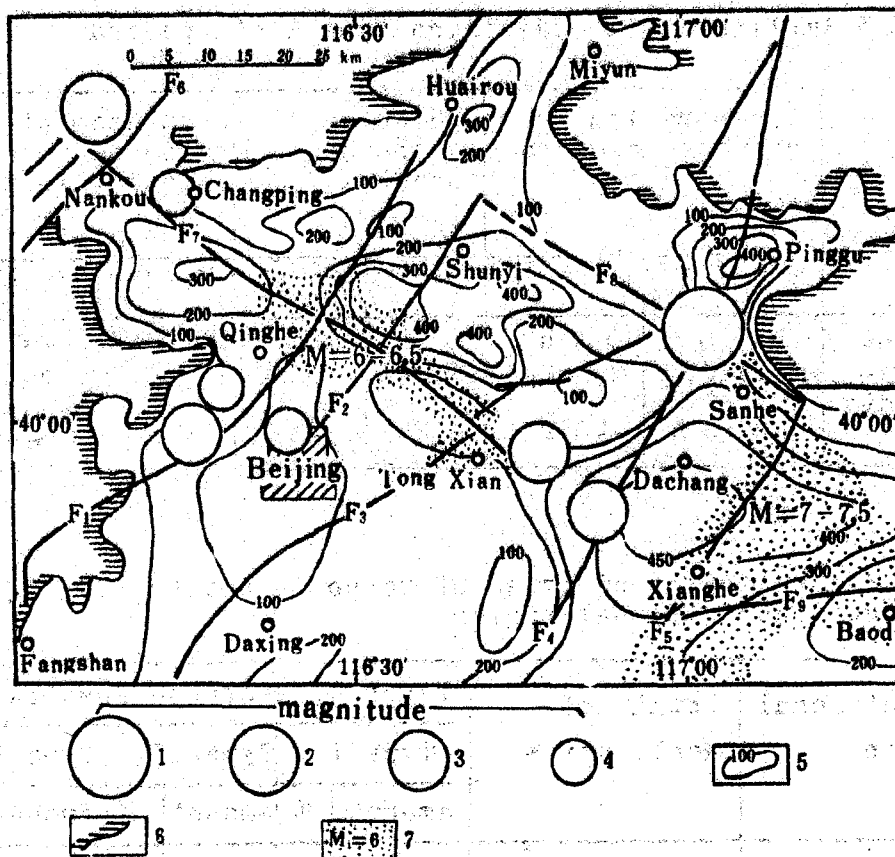


Fig.1 Seismogeological map of Beijing plain

1-4, Earthquake: 1, M=8; 2, M=6.6-7.0; 3, M=6.0-6.5; 4, M=5.0-5.9; 5, Isopach of Quaternary deposits(m); 6, Mountain area; 7, Potential earthquake risk region, numbers show the potential magnitude of future earthquake; F1, Fangshan-Huairou fault; F2, Qianmen-Liangxiang fault; F3, Nanyuan-Tongxian fault; F4, Chengu-Zhuang-Xiadian fault; F5, Huangzhuang fault; F6, Pred-mountain Nankou fault; F7 Nankou-Tongxian fault; F8, Ershilichangshan fault; F9, Baodi-Shui fault.

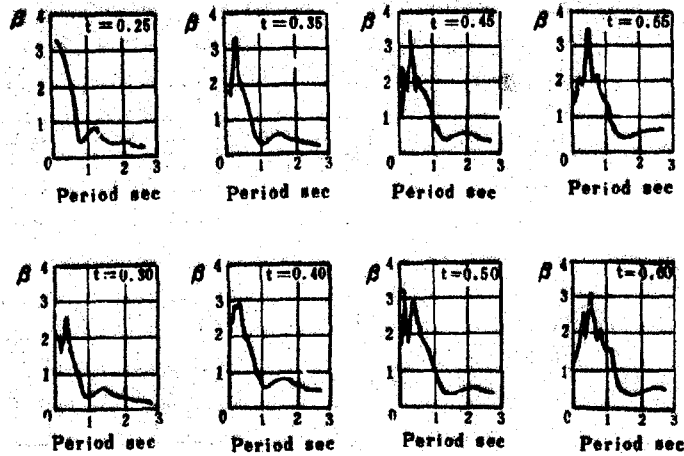


Fig.2 Sketch showing the influence of given maximum amplitude period on the response spectra for 5% damping. β , factor of amplification; t , given maximum amplitude (calculated after El Centro, Cal. earthquake of 18 May 1940, NS component)

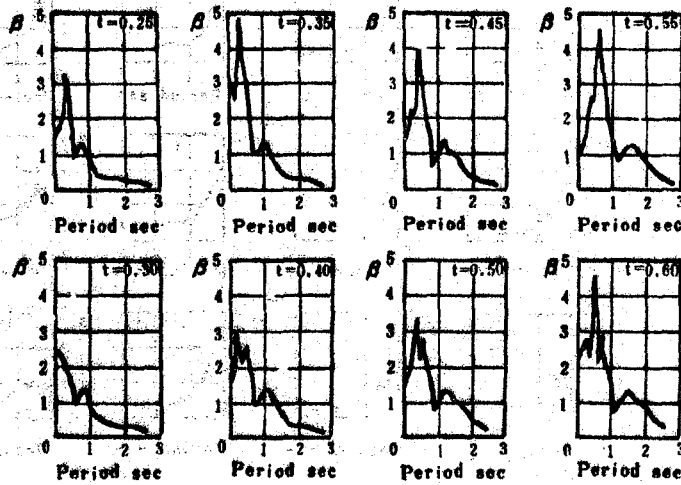


Fig.3 Sketch showing the influence of given maximum amplitude period on the response spectra for 5% damping. β , factor of amplification; t , given maximum amplitude period (calculated after Haicheng after-shocks of 15 Feb. 1975 at bedrock site)

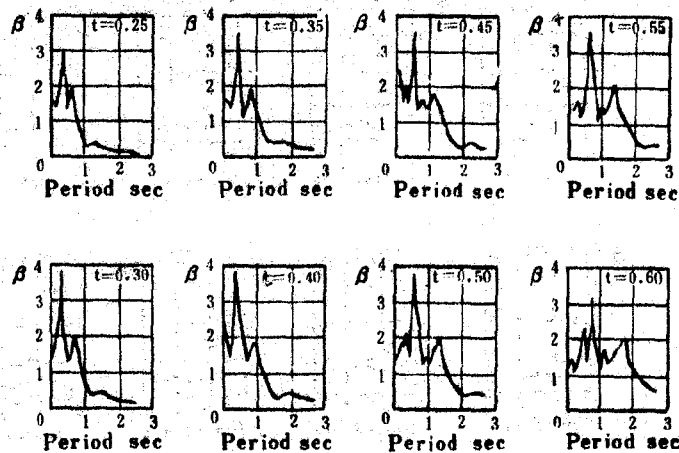


Fig.4 Sketch showing the influence of given maximum amplitude period on the response spectra for 5% damping. β , factor of amplification; t , given maximum amplitude period (calculated after Xingtai aftershocks of 3 Dec. 1967, NS component)

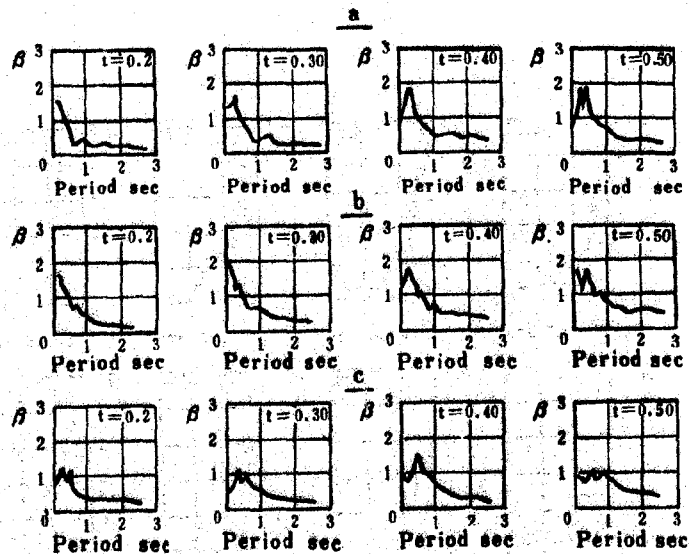


Fig.5 Sketch showing the influence of given maximum amplitude period on the response spectra for 20% damping. a, data from Fig.2; b, data from Fig.3; c, data from Fig.4.

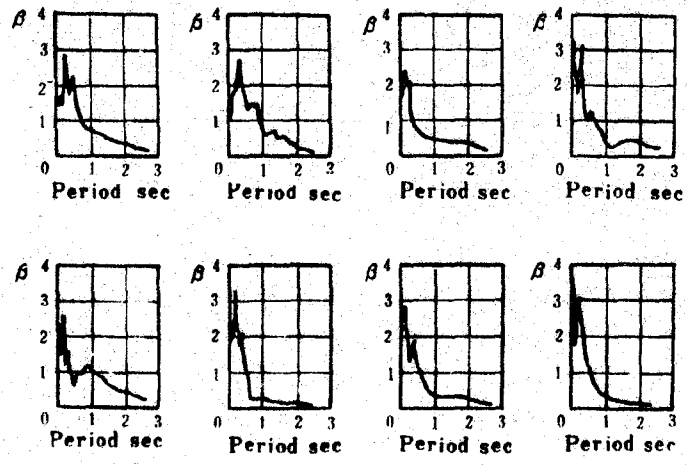


Fig.6 Response spectra at bedrock sites (after Chen Da-heng)

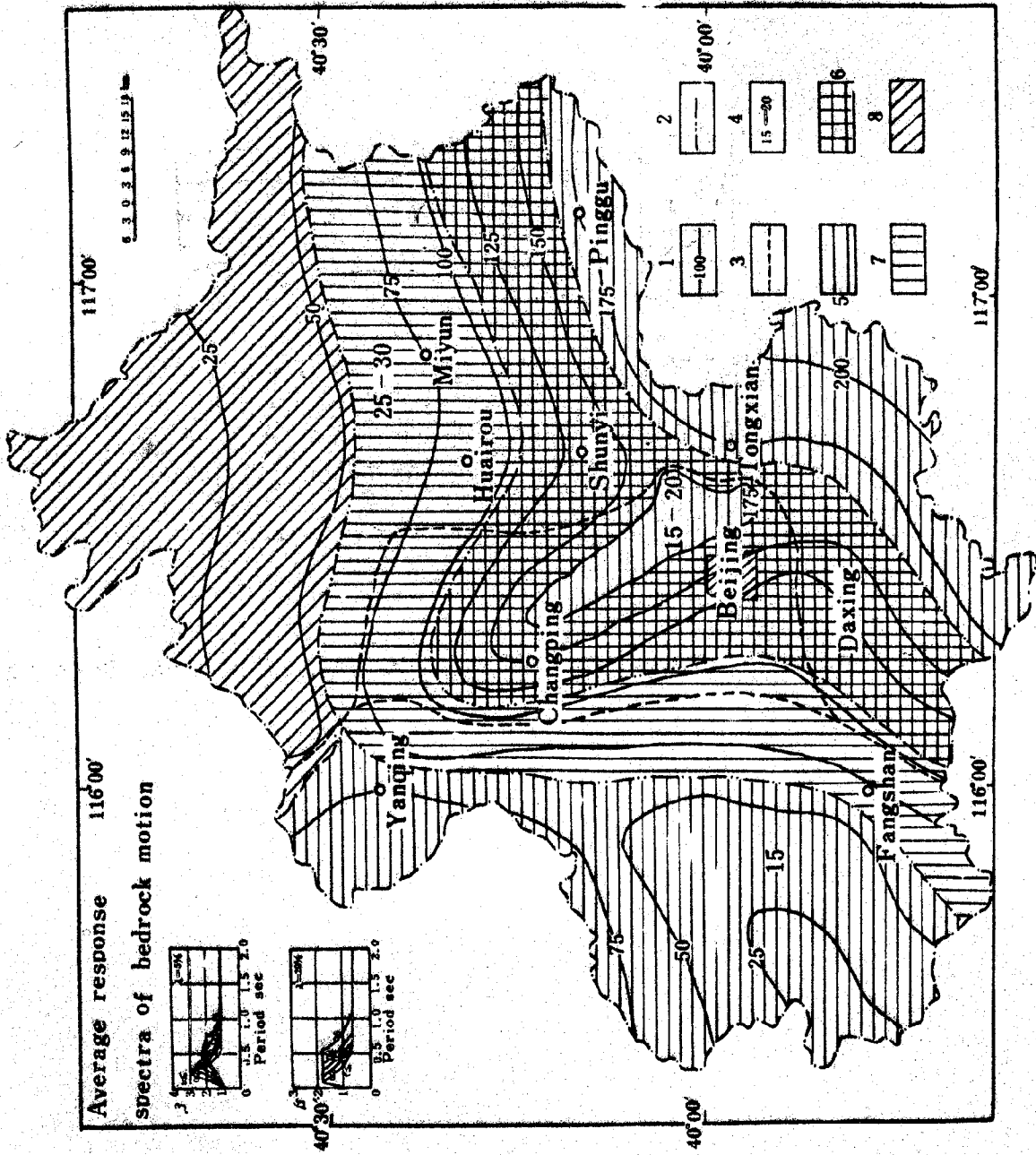


Fig. 7 Map showing the distribution of potential bedrock motion in Beijing area. 1, Isoline of maximum acceleration (gal); 2, Boundary of maximum amplitude period; 3, Boundary of duration; 4, Duration (sec.) Zone of maximum amplitude period: 5, 0.3 sec.; 6, 0.3-0.4 sec.; 7, 0.4 sec.; 8, 0.5 sec.; λ , damping; β , factor of amplification; t , maximum amplitude period.

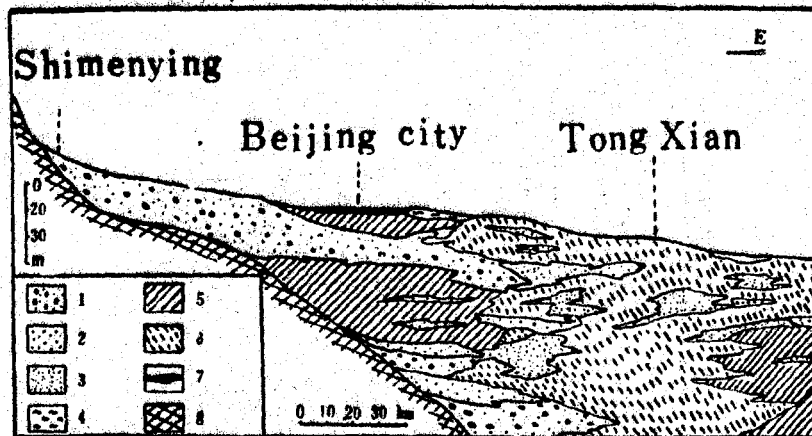


Fig.8 Section of the unconsolidated deposits from piedmont to plain.
 1, Layer of gravel with sand; 2, Middle-coarser sand layer; 3, Silt layer; 4, Mud layer; 5, Clay layer; 6, Sandy-soil and clay soil layer; 7, Artificially accumulated layer.

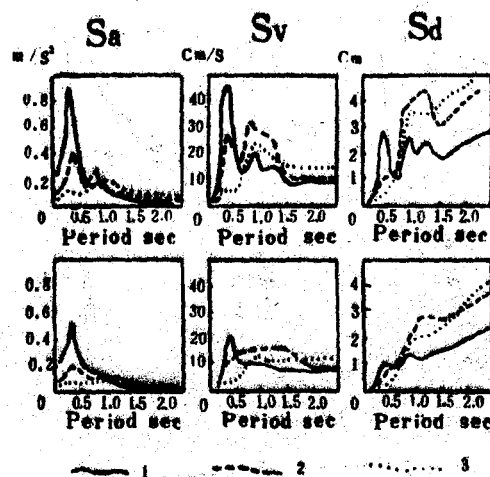


Fig.9 Main types of response spectra
 1, Type I; 2, Type II;
 3, Type III.

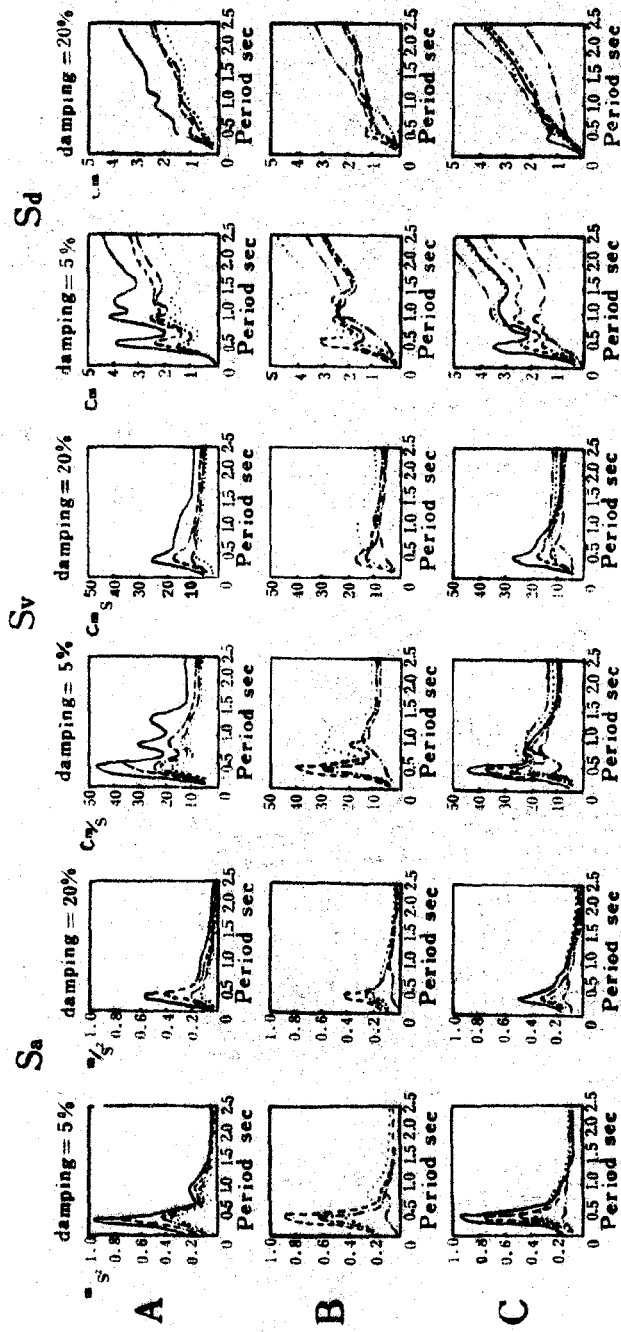
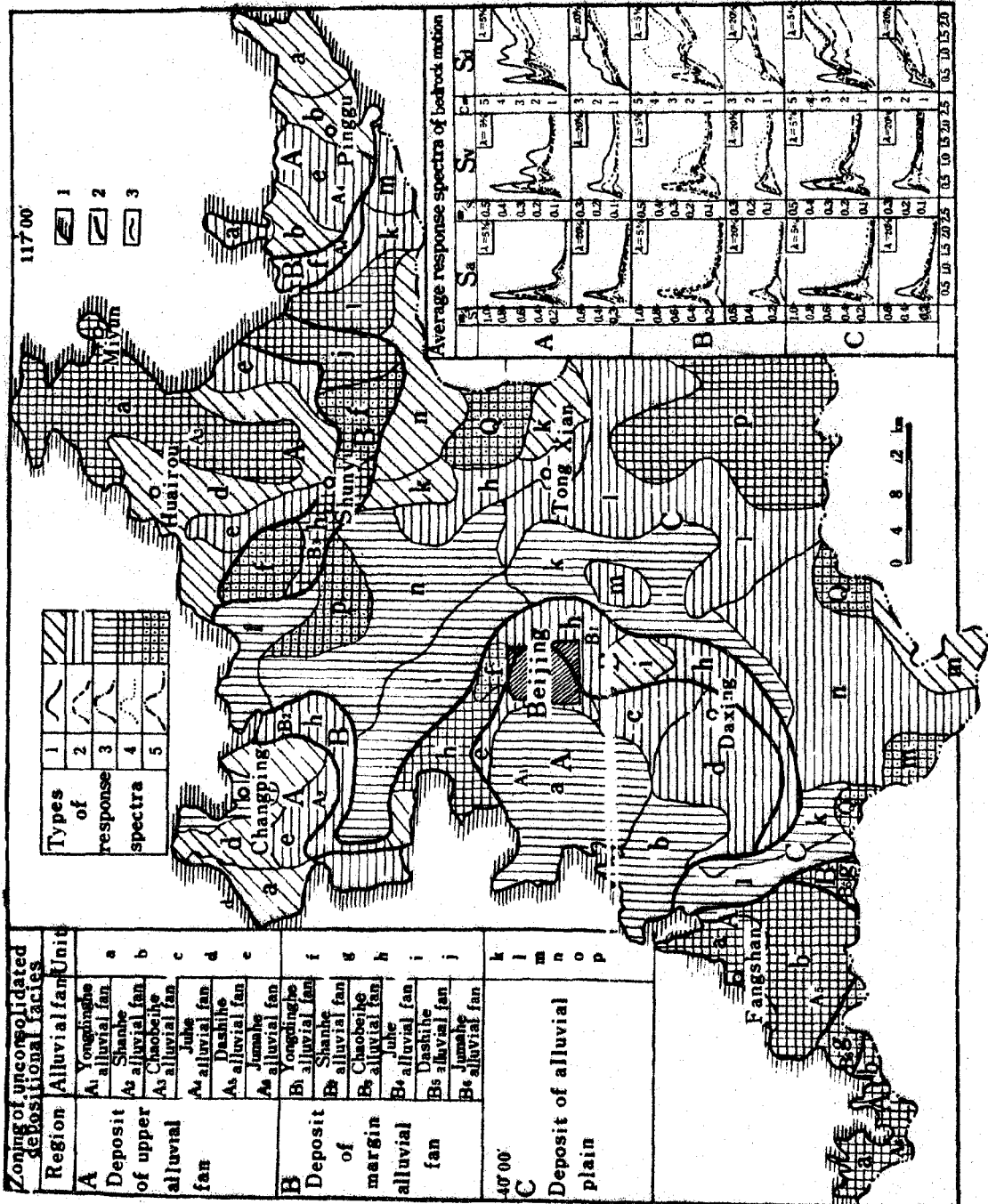


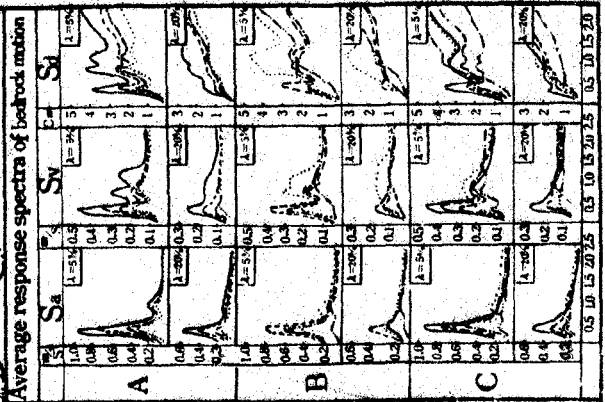
Fig. 10 Average response spectra for three unconsolidated depositional regions

Fig. 11
 Zoning map of earthquake response in Beijing plain and Mountain area;
 2, Boundary of unconsolidated depositional regions of geological units;
 3, Boundary of types of spectra:
 I Type
 1, strong;
 2, moderate;
 3, weak;
 4, II Type;
 5, III Type;



Region	Zoning of unconsolidated depositional facies	Unit
A	Deposit of upper alluvial fan	a
		b
		c
		d
		e
B	Deposit of margin alluvial fan	f
		g
		h
		i
		j
C	Deposit of alluvial plain	k
		l
		m
		n
		o
		p

Types of response spectra	1	2	3	4	5





1917

EARTHQUAKE HAZARDS AND VULNERABILITY ANALYSIS

Zhu Haizhi^I, Wang Ligong^{II}

Abstract

The characteristics of earthquake hazards caused by historical and recent great earthquakes obviously show that various earthquake hazards had appeared in different geological and geomorphological areas, such as on high mountains, plateau (especially loess plateau), hills, plains (including littoral plain) etc. Analysis of geological conditions for these characteristics and research on destruction mechanism by earthquake are importance for scientific prediction of earthquake hazards.

In this paper a method of vulnerability analysis and estimation of earthquake hazard is used in the Tangshan urban, Hebei Province and Liyan area, Jiangsu Province, where occurred destructive earthquakes in recent time. The factors for this analysis are the indexes of basic ground response component (i), Loose sand layer (liquefaction potential) component (s), resonance (R), faults (f), relief (m), depth of ground water (h). From these factors we can obtain a general index (I) of seismic vulnerability in each given unit.

According to the results of this analysis a given seismic area may be divided into sections with different seismic vulnerability.

Finally a discussion is given about the vulnerability analysis in different locations with different effects during earthquake.

I. Associate research professor, II. Research Associate,
Institute of Geology, State Seismological Bureau.

Introduction

Geological research on earthquake hazards includes studies of the earthquake-generated effect of the fault rupture, ground shaking, failure of unstable ground surface, such as the failure of slopes, avalanches, landslides, rockfalls, collapses etc. and ground failure in the plain areas such as sand liquefaction and mud softening during earthquakes.

These geological hazards caused by earthquakes have appeared at different geomorphological sites, and have different characteristics of their destruction.

I, The main characteristics of Earthquakes Hazards in China.

China is one of the earthquake-prone countries and has undergone relatively serious earthquake disasters in historical time. According to statistics of incomplete data on 91 historic earthquakes, the number of population death killed by earthquakes in China is larger in the world (Fig 1). It depends on the characteristics of geological background on which the earthquake hazards had occurred.

Making a generalizing analysis of geologic and geomorphologic conditions along a profile from Mt. Altun shan in west along the latitude $N38^{\circ}$ to Bohai Bay in east (Fig 2), we can obviously find high mountainous region in western part, loess plateau in middle part, the sedimentary plain in eastern part, and the Bohai Bay further in east.

The strong earthquake hazards had appeared in all these different geomorphological settings.

1. Earthquake hazards in high mountainous region. There was plenty of earthquakes on high mountains in the western Sichuan Province and Yunnan Province. The strong earthquakes caused disasters to various extent. There can be distinguished three categories of earthquake hazards i.e. earthquake-gravitational, earthquake-tectonic and earthquake-gravitational -

tectonic disrptures. The earthquake-gravitational disrpture usually ocured in large scale in neotectonically uplifted areas, in which the relief is precipitous and the earthquakes caused avalanches, sometimes river stopping and rockfalls. For example, there were numerous avalanches and rockfalls led to from the piles more than 160 metres above the warter table of Minjian River during Diexi earthquake (Aug. 25, 1933, M=7½) in Sichuan Province. The Minjian River was stopped up and three barrier lakes were formed. After forty days the seismic dam was failured, consequently great secondary disaster had been caused by the water. The Zhaotong earthquake in Yunnar province caused avelanches and landslides everywhere in Zhaotong mountainous seismic area. The remarkable ohrecteristic appears to be the destructed cliff slopes, precipitous in topography, at an angle of slope more 30 degrees⁽¹⁾. The destructure by earthquake was planary in this area. The earthquake-tectonic disrpture in high mountainous area represented the direct effect controlled by seismic fractures, and appeared along the seismogenic faults. For instance, during the Luhuo earthquake (Feb.6, 1973, M=7.9) in western Sichuan Province, the seismogenic fault extented up to 80-90 km along the Xianshuihe River. Along the fault trace the slope surface was collapsed and fractured, the alluvial terrace has subsided, and the river bed has risen and deformed. All buildings on the fault were distroied. Along this left-handed NW-SE fault belt the ground surface was characterized by linear or zonal deformation and destruction, the earthquake-tectonic-gravitational disrpture is a complex result of both tectonic and gravitional actions during strong earthquake.

2. Earthquake hazards in plateau region (mainly on loess plateau)

Seismic hazards were serious on loess plateau. Frequency of population death killed by earthquakes was more concentrated on Chinese loess plateau. Two strong earthquakes ocured

in Huaxian County, Shanxi Province (Jan. 23, 1556, M=8) and in Haiyuan County, Ningxia Autonomous Region (Dec. 16, 1920, M=8½) had killed total population death 1,060,000⁽²⁾ ⁽³⁾.

The cause of the great hazards was related directly to arid climate, tectonic conditions and lithologic composition and structure on loess plateau. The arid plateau was scarcely covered by plants and the antiseismic buildings were few and almost absent. More population lived in cave dwellings in loess deposits. The loess consists of silt. It is loose in lithology and large in thickness (30-100 metres). In loess deposits numerous joints and fissures are developed. The slope of loess mountains was unstable, especially the loess cliffs and ravines between loess ridges are easily destroyed during earthquake. As a result the avalanches, collapses and landslides in large area have occurred. And the cave dwellings were collapsed, so that the population deaths had taken place, moreover, the seismic barrier lakes and group of collapses and landslides generated by Haiyuan earthquake (Dec. 16, 1920, M=8½) are still preserved in Xiji County now.

3. Earthquake hazards in sedimentary plains.

The sedimentary plains in East China are densely populated. Along the long coast line the littoral plain extends. In the delta plains of Changjiang River and Huanghe River the thick Quaternary sediments have deposited, and the buried river beds have developed. Different kinds of earthquake hazards take place in these plains, such as ground cracks, landslides, sand liquefaction, collapses etc. Basing on the analysis of dynastic records of historic earthquakes, liquefaction areas occurred in eastern plain. Tangshan (Jul. 28, 1976, M=7.8) and Haichong earthquakes (Feb. 4, 1975, M=7.3) caused to prodigious disaster⁽⁴⁾. The different kinds of earthquake hazards had appeared along the seismogenic fault. Sand liquefaction, ground cracks, ground collapses and landslides had widely distributed in the plains. Along the whole profile from the high mountainous to the loose sedimentary plain the earthquake

hazards were different in relation to the geological conditions, which must be considered in seismic micro-zoning or vulnerability analysis of a given area.

II. Application of the method of earthquake vulnerability analysis in predication of earthquake hazards.

There are three categories of direct effects by an earthquake in nature: a. Earthquake Magnitude and amplitude of fault displacement under the action of seismic force and ground shaking; b. Amplification and reduction of ground motions by local geological conditions including ground failure (sand liquefaction) and loss of slope stability; c. The reaction of man-made constructions to the earthquake forces. From these we can obtain a relationship between earthquake force, Ground medium, and upper constructions. The earthquake vulnerability-analysis of constructions has well described in other papers. Nevertheless, the problem on reaction of ground medium to earthquake force is a main subject for this discussion, and is one comprehensive research work for prediction of geological hazards.

1. Method

Recently the office of the united Nations Disaster Relief Coordination (UNDRO) proposed a method of seismic vulnerability analysis for urban planning and estimation of earthquake hazards. They gave an example on the analysis in the Metro Manila Area. This analysis involves: a. Basic ground response component (i) b. loose sand layers (liquefaction potential) (s) component c. Faults (f) component. d. Total ground response index I.e. Resonance $R^{(5)}$.

The earthquake vulnerability analysis can be made in combination with the concrete conditions in our country, geomorphological units and geological sitting of earthquake hazards.

2. Examples

Two examples of analysis of eastern plain are given here.

(1) Example one: Earthquake vulnerability analysis of Tangshan urban area, Hebei Province. Tangshan earthquake (M=7.9 Jul. 28, 1976) had led the whole city to destroy. Earthquake intensity in epicentral area is XI. total Lose of population is 243,000. The obvious liquefaction had occurred on sides of Douhe River and southern part of Tangshan city where earthquake intensity is IX, VIII, VII.

The analyzed zone locates in tilt plain at the front of Yanshan mountains. The northwestern section of the zone is higher and the southeastern section is lower in topography, the altitude hight ranges from 33 to 13 metres. In this zone there are some isolated hills (such as Dachangshan hill, Fenghangshan hill, Jiajiashan hill etc.) with bedrocks exposed in area 1.5 km². Douhe River flows cross this zone (Fig.3). By the river locate two alluvial terraces. Coal layers occur in the southeastern part of this zone and occupies 1/3 area of the zone. The exploited coal layers leave some empty cavities.

Tectonically Tangshan area is an confluent part of Yangshan Folded Belt with Cangdong Fault. There is a system of NE trending faults and folds across this zone. Tongshan Fault and Douhe Fault are the main normal faults trending to N30°-50°E with steep dip angle 70°-80°. Nearby these faults there is a series of anticlines and synclines. The derrection of fold axis is also NE. Between the Tangshan Fault and Douhe Fault there exists a NE trending horst, expressed some residual hills on geomorphologic surface (such as Dachangshan, Fanghuangshan etc.)

For the earthquake vulnerability analysis one must consider the soil composition and volume of sedimentary layers, depth of underground water, potational sand liquefaction, the presence of faults. The catagories of soil composition and depth of Quaternary sediments may mainly determine the

ground motion during earthquake. In one unit for analysis these factors have large proportion in estimation of total ground response index (I), but effects of underground water, potational sand liquefaction, fault and topography are secondary factors.

(I) Basic ground response component (i) (Index of soil's vulnerability analysis)

Accoding to genetic clasifioation of sediments, lithological chracteristics and structure, physico-machanical properties, the soils are devidid into 6 catagories (Table 1)

Standard composition of soils in Tongshan Tab. 1

Categories of Soils	Geomorphological site	Lithology and structure	Main physico-machanical index
a	Isolated danuded hills	Thick limistone and thin sandy shales	R > 50
b	Proluvial group and second terrace of Douhe R.	Rigid-plastic and plastic eluvial-deluvial: clay and proluvial, aluvial sand, gravel with filled clay sediments.	Clay: $\rho = 1.90-2.02$ $= 0.016-0.019$ R=23 Sand: R=20-22
c	The second terrace and tilt plain of Douhe R.	Plastic-Soft plastic aluv.: clay and silt, fine sand and mid-sand interbeds	Clay: $\rho = 2.00-2.08$ $= 0.014-0.024$ R=16-20 Sand: $\rho = 2.00-2.06$ $= 0.010-0.012$ R=20-25
d	First terrace of Dauhe R.	Soft plastic aluv.: clay and silt, fine sand interbeds	Clay: $\rho = 1.93-2.03$ $= 0.019-0.054$ R=10-15 Sand: $\rho = 1.72$ $\epsilon = 0.01$ R=10-15 Upper 10m. N=10-20 Lower 10m. N > 20

e	Buried river bed in first terrace, old bayou (lake)	Soft plastic aluv.: Clay with filled mud layer	Mud clay: $\rho < 1.57$ $\epsilon = 0.132$ $R < 7$ with thexotropy
f	Depression or pit and pond	Loose filled gangue and other deposits	

Notes: R — Loading pressure T/M^2
 ρ — Density of mass $T \text{ sec}^2/M^2$
 ϵ — Coefficient of compression
N — $N_{63.5}$ Number of shots in standard penetration test

Practically, earthquake hazards have obvious different effects. Earthquake hazards are lightest on bed rocks, somewhat intensive on eluvial-deluvial clay soil and proluvial-alluvial, sand gravel layers more intensive on high terrace consisted of thick clay soil and silt, mud, fine sand interbeds, highly intensive on first terrace consisted of clay soil and silt, fine sand interbeds and, at last, the sediments on recent valley flat and puddly soil can be most intensively affected by earthquake. But earthquake hazards on filled soil are the same as on soil of I, II terraces. This situation had presented for the effects of Tangshan earthquake $M=7.8$.

Index of earthquake hazards had not significant change in same intensity area by Tangshan earthquake when thickness of soil more than 20 metres. Seismic effect is highest on the soil with thickness of 0-5 metres.

According to the conditions resistant to earthquake the earthquake vulnerability index of soil (1) is estimated as follows:

Thickness of soil layer (m)	Categories of soils (see Tab. 1)					
	a	b	c	d	e	f
	Vulnerability index of 1					
0-5	0.5	1	3	5	6	3
5-10	0	2	5	7	8	5

10-20	0	3	6	9	10	7
20	0	4	6	9	10	7

(II) Other earthquake vulnerability index of geological factors

1. Depth of ground water (h)

When the depth of ground water varies in different sites, the level of earthquake hazards is also different. The shallow depth of ground water (2-4m) is in northeastern part of studied zone, the depth of ground water is 6-8 m or more than in middle part of this zone. The soil layer in northeastern and southeastern parts was saturated by underground water, so the soil became softer and weaker in resistance to earthquake.

According to the hydrological record in 1979 this zone has been divided into four microzone with depth of ground water 2-4, 4-6, 6-8. and more than 8 meters respectively. So the corresponding indexes (h) are 3, 2, 1, 0.

ii. Sand liquefaction (s), Data on some great earthquakes occurred in plain show that in the lower seismic intensity areas (I-VI, VII, VIII) liquefied sand ground was failed, and earthquake hazards were greater.

If sand liquefaction appeared in area of higher seismic intensity and adjacent unliquefied area where the earthquake disaster were reduced. The construction slower destroyed by earthquake. Duration of process shock-liquefaction-destroy was longer, so the people could quickly left the danger constructions when the shock begins. This is named "slower shaking" effect. According to results of analysis of geological conditions the potential liquefaction vulnerability is as follows: Index S=2, 1, 0.

iii. Fault (f): Tangshan fault is seismogenic fault for Tangshan earthquake. The length of ground crack along the Tangshan fault is about 8-10 km. Nearby the fault had appeared serious hazards, as the index f=3.

iv. Relief (m): The earthquake hazards have same different at different microreliefs, such as isolated hills,

slope of band, cliff slope, highland, lowland etc., all these have direct affect on the earthquake hazards.

Isolated hills and subsided places due to the excavated coal layer below and the main river bed have this index $m=1$.

The dense soil surface and the higher land (such as Tangshan airport), $m=-1$.

(III) Map for earthquake vulnerability analysis:

1. Index of earthquake vulnerability analysis consists of many grids of seismic vulnerability. Total ground response index is a sum of indexes from seismic analysis expressed by a formula:

$$I=i+n+s+m+f+\dots$$

To obtain the index i , it is necessary to know the standard soil composition (G) at first. There are all six soil categories (a to f) presented in Tangshan city. In general each unit has no more than four categories, so the standard soil composition (G) may expressed as follows:

$$G=\frac{1}{4}a+\frac{1}{4}b+\frac{1}{4}c+\frac{1}{4}d$$

or
$$G=\frac{1}{4}b+\frac{0.5}{4}e+\frac{0.5}{4}f$$

or
$$G=\frac{2}{4}c \dots$$

From the average thickness of Quarternary sediments in each unit for vulnerability analysis we can obtain value i . If the average thickness is more than 20 metres, the standard composition will be $G=\frac{2}{4}c+\frac{1}{4}d+\frac{1}{4}e$.

For this range of thickness, $C=6$, $d=9$, $e=10$. For simplicity the original fractions for these proportions are kept. By this way $G=1$:

$$i=6 \times \frac{2}{4} + 9 \times \frac{1}{4} + 10 \times \frac{1}{4} = 7.75$$

For each unit we can obtain values n , s , f , m .

11. Map for seismic vulnerability analysis.

This map consists of 130 units (Fig.4, in this map only shown units in central part of Tangshan city) maximum $I=18$, minimum $I=2$.

Seismic ground-response: According to value I four areas of seismic ground-response can be divided:

Area A: Weakest seismic ground response (I=2-5)

Area B: Weaker seismic ground response (I=6-9)

Area C: Stronger seismic ground-response (I=10-14)

Area D: Strongest seismic ground-response (I=15-18)

(2) Example 2: For Liyan Area, Jiangsu Province.

Seismic vulnerability analysis is following: Liyan area locates to the west of Taihu Lake plain. In this area the hills, highlands, lower paddy fields and lowlands are distributed. Liyan area had suffered seismic hazards by M=5.5 earthquake on Apr. 22, 1974. and M=6.0 earthquake on Jul. 9, 1979. (Fig. 5,6). Although their magnitudes were not large. There was death 41, and injured more than 3,000 persons.

The epicenters of these two earthquakes are located east side of Maoshan fault. The topographic surface appeared lower from west to east. In this direction the age of soil and sedimentary deposits represents from older to younger, the lithologic structure of soil from denser to looser, so the earthquake hazards showed the same trend: weaker in the western part of hills area, and stronger in the eastern part. Index of destroyed buildings correspondingly changes along this direction (Fig 7).

For Liyan area twice earthquake repeatedly occurred at the same location interval between them is only five years. Therefore, to find the regularity of destruction by earthquakes is of significance for prediction of earthquake hazards in future in the plain south of Changjiang River.

The method of vulnerability analysis is the same as in example one.

(I) Basic ground response component (1) (Index of soil's vulnerability analysis)

1. Standard composition of soils can be distinguished as five categories: a, Bedrocks (Paleozoic and Mesozoic sand-shales, limestones, volcanic rocks) b, Xishu clay layer (Upper Pleistocene) c, loess-like deposits (Holocene)

d, Soft clay (Holocene). f, Saturated sands, silt and clay interbeds:

Thickness of soil layer (m)	Categories of soils				
	a	b	c	d	e
	Vulnerability index I				
0-10	0.5	1	2	2	3
10-30	0.5	1	3	3	4
30-50	0.5	1	4	4	5
50	0.5	2	5	5	5

$$I = n_1 a_t + n_2 b_t + n_3 c_t + n_4 d_t$$

where $n_1+n_2+n_3+n_4$ indicates proportions of soil categories a, b, c, d. but t represents the soil thickness.

(II) Other earthquakes vulnerability index of geological factors

1. Sand liquefaction (s): Sand liquefaction appeared in east part of Liyan area during two earthquakes. The sand liquefaction may occur in the same areas by future great earthquake, the sand liquefaction (s) ≤ 2 in Wandu and Daxi velleges.

11. Soil thickness (R): To thickness of soft soil is closely related ground resonance.

111. Fault (f). The two earthquakes gave evidence that no seismogenic faults appeared on ground surface in seismic area. But the seismic hazards in NNE-SSW direction on the front of Maoshan hill had increased (Fig 8). It shows the approximate orientation of a fault in depth along this belt. The index of vulnerability ≤ 2 .

(III) Map for earthquake vulnerability analysis: The map consists of 168 units of vulnerability analysis (Fig 9), their index I varies from 2 to 21. According to the value I the mapped area is divided into four sections A.B.C.D. as follows;

Section A: Weakest seismic ground-response ($I=2-5$)

Section B: Weaker seismic ground-response (I=6-9)

Section C: Stronger seismic ground-response (I=10-14)

Section D: Strongest seismic ground-response (I=15-22)

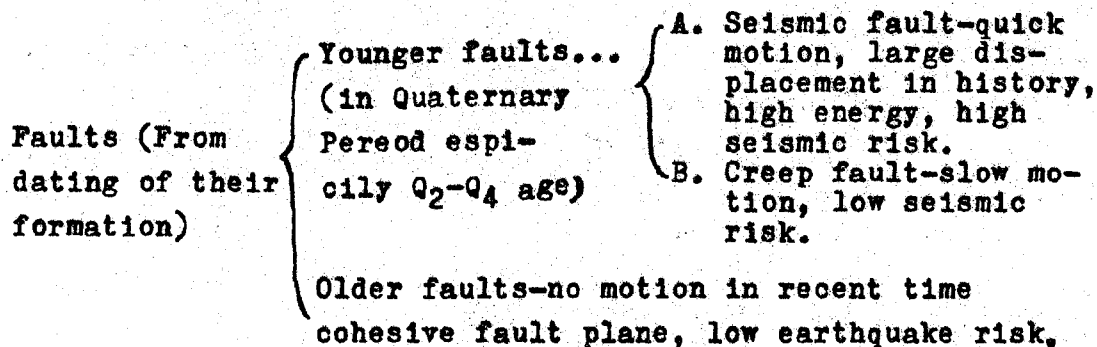
The soil thickness is divided into three categories: 0-5 metres, 5-30 metres, >30 meters, and the corresponding resonance (R) is also divided into 3 intervals in relation to different ranges of amplitudes.

III. A discussion of the problem:

The method of vulnerability analysis can be used in land-use, urban design and planning.

1. Estimation of faults by vulnerability analysis:

The fault is very important factor for the vulnerability analysis, what kind of fault does affect the earthquake hazards? and what doesn't affect? this question still now unanswerable. Preliminary analysis can distinguish the following faults:



When we make the earthquake vulnerability analysis of a given area, we must pay attention to fault of A and B kinds.

2. Estimation of potential liquefaction (s) by seismic vulnerability analysis. Geological conditions of potential liquefaction are in general as follows:

- (1) The littoral plain or an buried river bed.
- (2) Saturated silts, fine sandy deposit in Holocene period.
- (3) Appreciable thickness and area of distribution of liquefied sand layer.

- (4) Single grains are the main structural from of silts. Amount of easy liquefied sands (diameter 0.01-0.25mm) was more than 80%.
- (5) The thickness of clay and sand clay layers covered the liquefaction sand layer no more than 6 metres.
- (6) The area where sand liquefaction occurred in history.

3. Estimation of potential avalanches and landslides in high mountainous area and loess plateau

(1) In high mountainous area

The main earthquake destruction in high mountainous area is of earthquake-gravitational pattern. The geological and geomorphological conditions under which the area of earthquake-gravitational destruction can easily appear as follows:

(I) In the neotectonically violently uplifted area the rivers deeply cut the relief. The cliffs and canyons occur everywhere. The mountains are higher, the slopes are steeper (more than 30°).

(II) The rocks have been fractured and the joints in rocks are developed, especially on the slope of the stratified plane.

(III) The more precipitation and the more ground water.

(IV) The areas where avalanches, collapses and landslides have easily occurred in historical time.

(2) On loess plateau

The locations on loess plateau where the avalanches and landslides easily appear as follows;

(I) The walls of loess scarps and the ravines between loess ridges.

(II) The thick (more than 5 m. loess layers and Upper Pleistocene "Malan loess" in which dense buried soil layers are absent.

(III) The locations where the joints and cracks are developed and loess was cut.

(IV) The locations where the avalanches and landslides had occurred in historical time.

4. Other aspects concerned to earthquake hazards;

In areas where limestones and marbles are distributed, if seismic subsidence and ground fissures have appeared during earthquake and characteristics of ground shaking are distinct, it is necessary to take account the seismic vulnerability analysis.

References

1. Zhu Haizhi, Wang Kelu, Zao Qingina: A Discussion on the Seismic Ground Failure in Mountainous Region as from the Zhao Tong Earthquake Damage. *Scientia Geologica Sinica* No.3, Jul. 1975.
2. Group of historic earthquakes, committee of seismic work, Chinese Academy of Sciences: *Chronological Materials on Earthquakes in China*. Scientific Publication House, 1956.
3. Lancho Earthquake Research Institute State Seismological Bureau, and State Seismological Bureau Ningxia Autonomous: *The Great Haiyuan (China) earthquake of 1920*. Seismic Publication House 1980.
4. Zhu Haizhi, Wang Ligong et, al., *The Geological Aspect of Earthquake Hazards caused by Liquefaction of Sands in the Lower Liaohe river Region*, *Seismology and Geology*, Vol.1, No.2, Jun. 1979.
5. Office of the United Nation Disaster Relief Co-ordinator, *Composite Vulnerability Analysis (Revised Technical Report)*, Geneva.

Fig. 1

**A Comparison of population Deaths in Various Zones by 91 Great Earthquakes
(856-1976 A.D.) in the World**

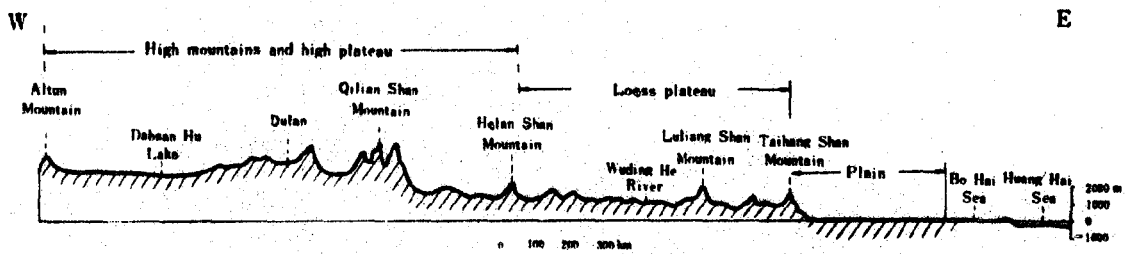
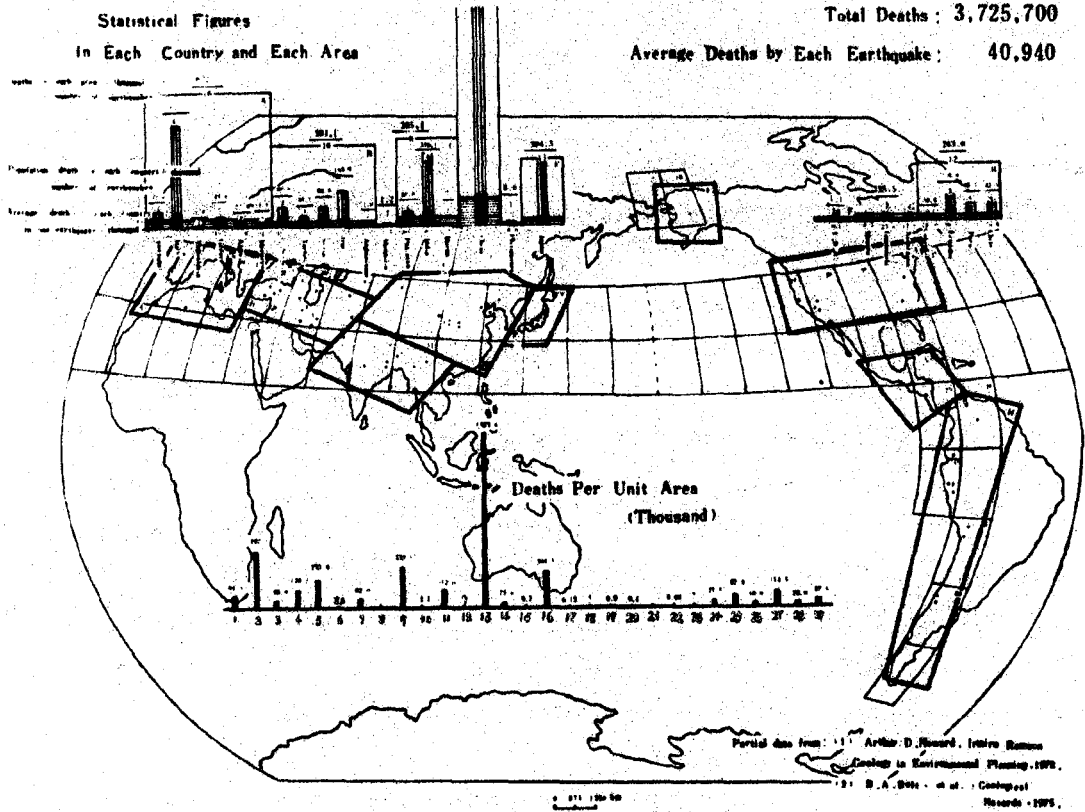


Fig. 2 A Latitudinal Profile from Altun Mountain to Bohai Bay

Fig.3 Map of Geological Factors of Tangshan Area

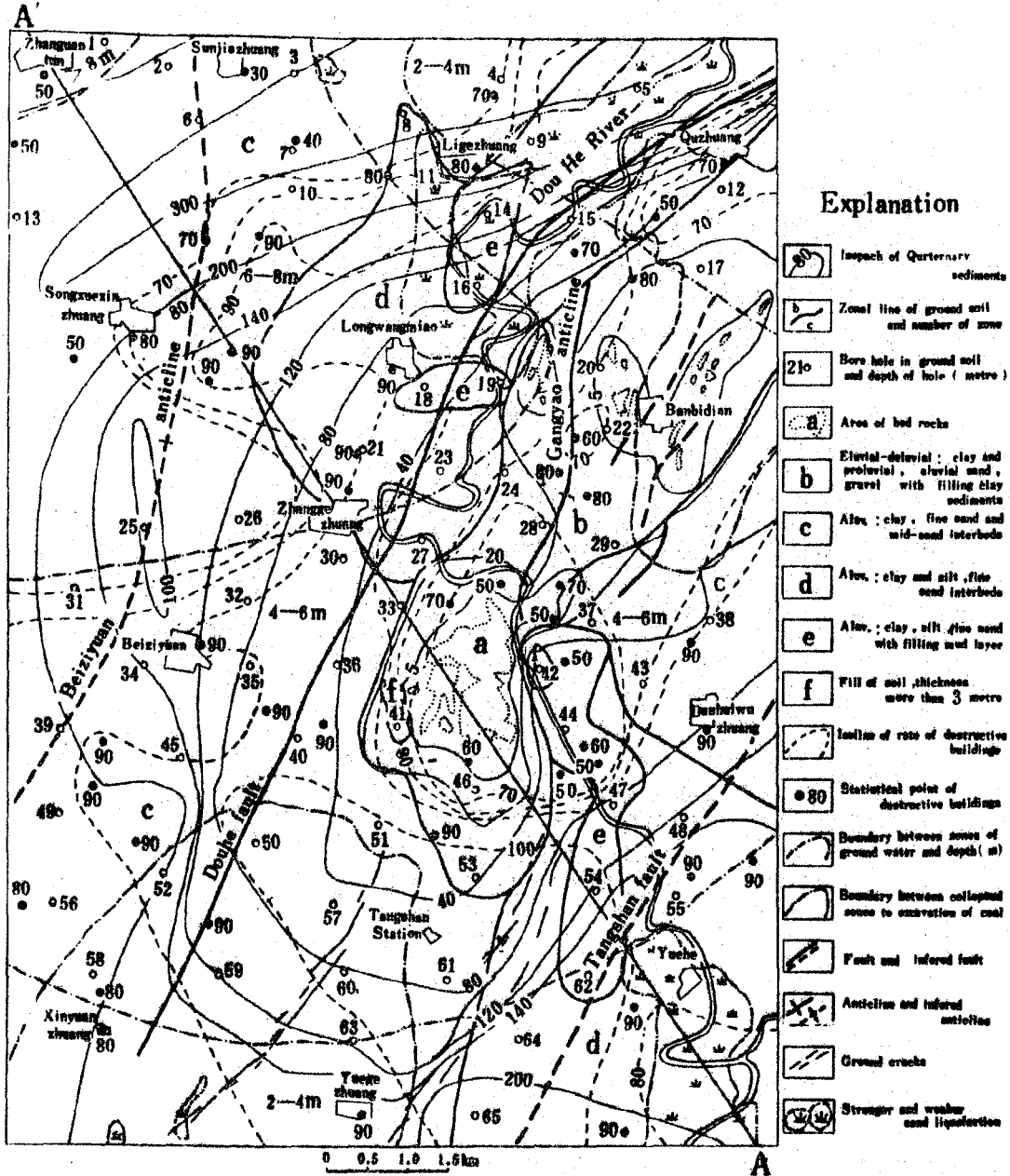
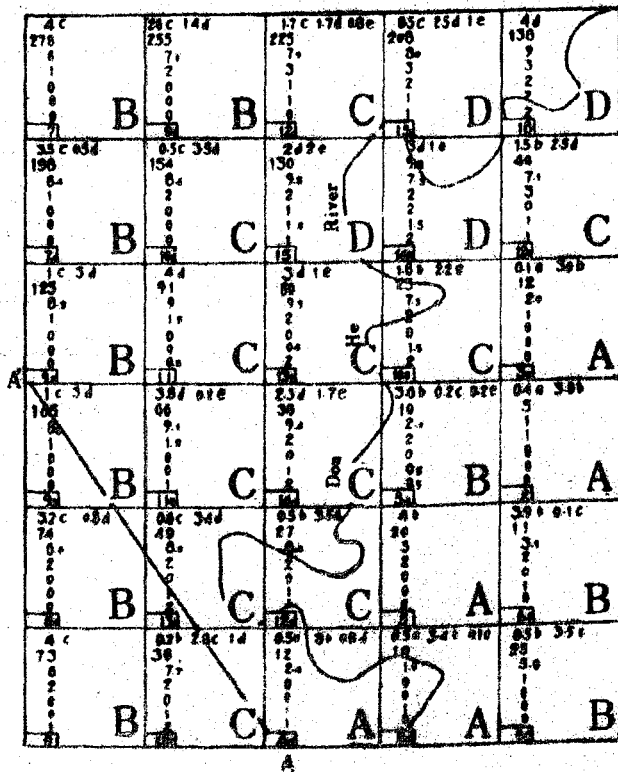
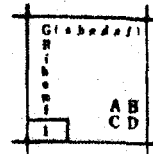


Fig. 4 Map for Vulnerability Analysis
in One Part of Tangshan Area

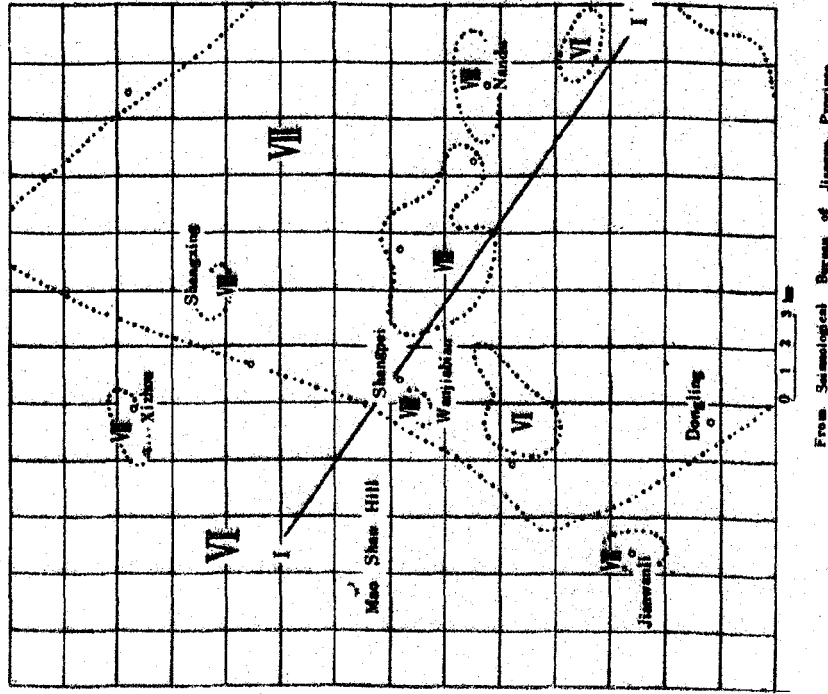
0 0.5 1.0 1.5 km



The units of vulnerability analysis

- G : Ground soil component
(a,b,c,d,e,f : Categories of soil)
- R : Thickness of Quarternary
sediments (metre)
- i : Index of seismic vulnerability
analysis of soil
- h : Index of seismic vulnerability
analysis of ground water
- s : Index of seismic vulnerability
analysis of sand liquefaction
- m : Index of seismic vulnerability
analysis of relief
- f : Index of seismic vulnerability
analysis of fault
- I : Total ground response index
- A : Section A seismic ground
- response weakest
- B : Section B seismic ground
- response weaker
- C : Section C seismic ground
- response stronger
- D : Section D seismic ground
- response strongest

Fig. 6 Map of Intensity
of Liyang Earthquake (Jul. 9, 1979, $M = 6.0$)
in Jiangsu Province



From Seismological Bureau of Jiangsu Province

Fig. 5 Map of Intensity
of Liyang Earthquake (Apl. 22, 1974, $M = 5.5$)
in Jiangsu Province

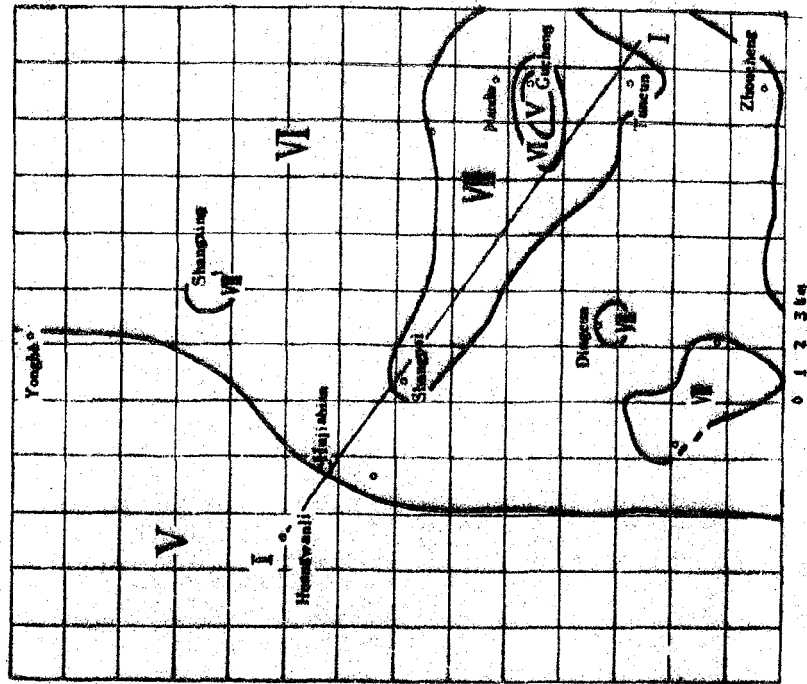


Fig. 7
A Comparative Map of Geological Conditions,
Index of Destructive Building and Index of Vulnerability Analysis

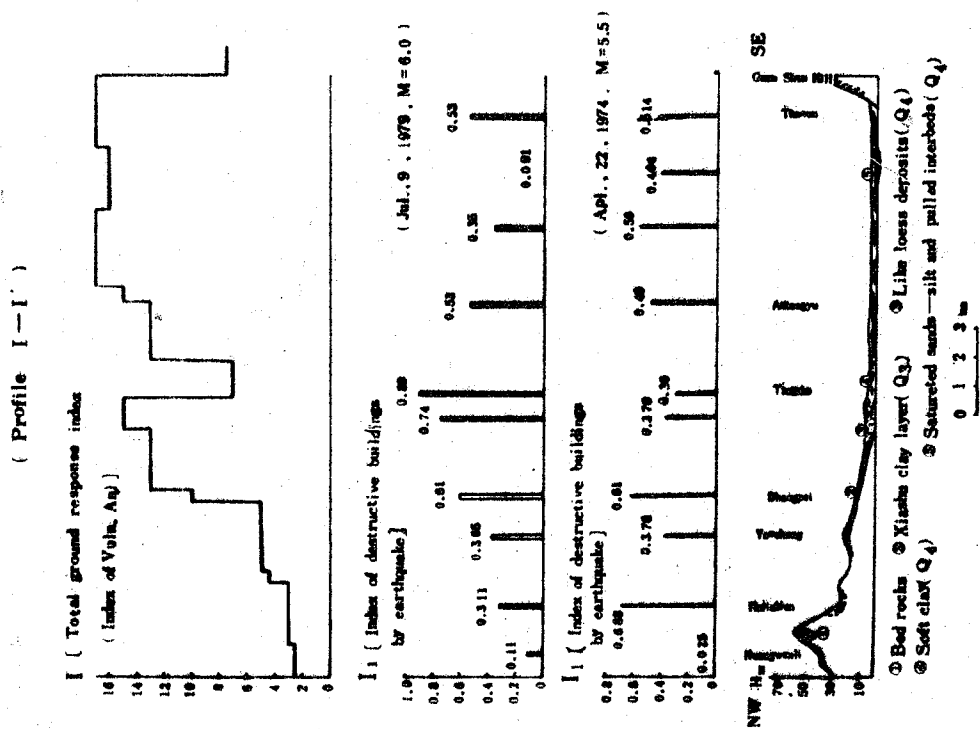
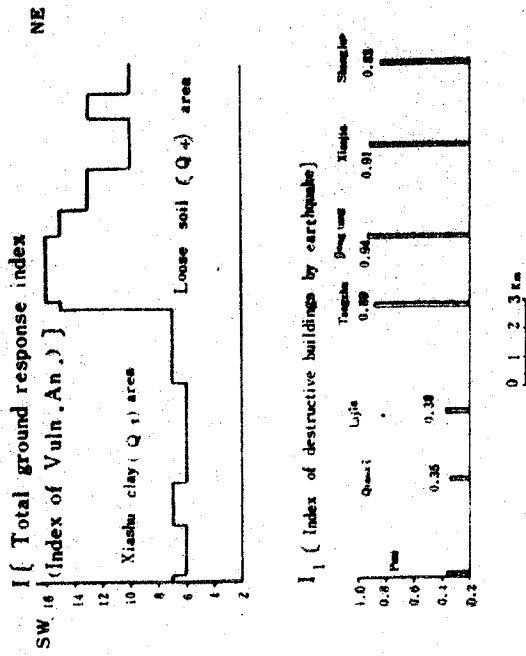
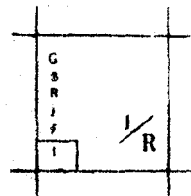
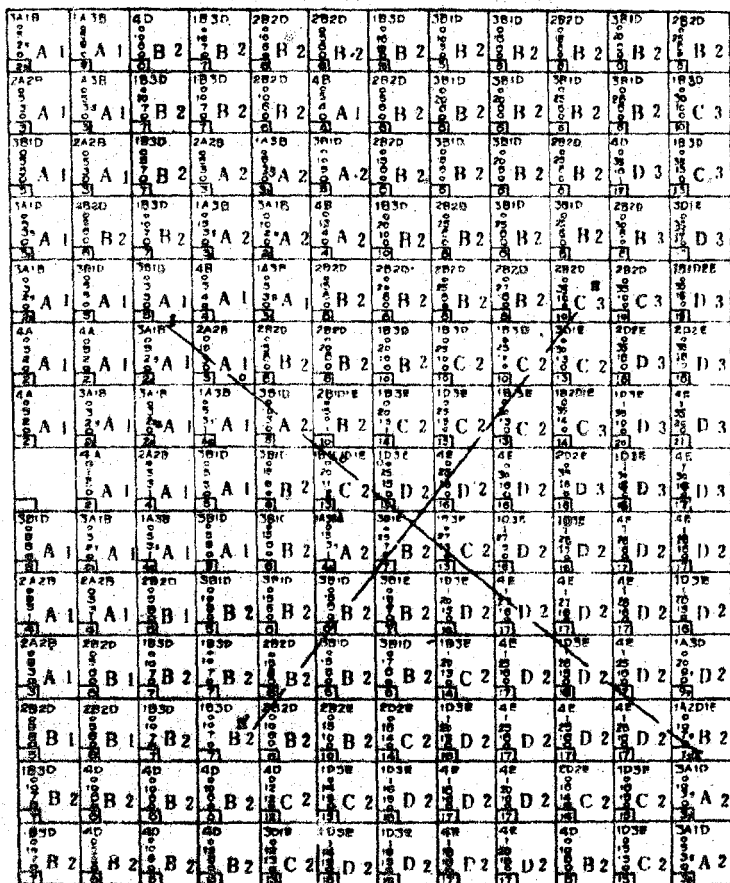


Fig. 8
A Comparative Map of Geological Condition,
Index of Destructive Buildings and Index of Vulnerability Analysis
by Liyang Earthquake (Jul. 9, 1979, M = 6.0)
(Profile II—II')



A Map for Vulnerability Analysis of Liyang Area, Jiangsu Province

Fig. 9 0 1 2 3 km



The units of vulnerability analysis

- G : Standard soil composition
- s : Loose sand layers
- R : Resonance
- i : Basic ground response
- f : Faults
- I : Total ground response
- A : Section A weakest seismic ground response
- B : Section B weaker seismic ground response
- C : Section C stronger seismic ground response
- D : Section D strongest seismic ground response

Reproduced from best available copy.

THE SEISMIC MICROZONING OF LANZHOU

Sun Chongshao^I and Chen Bingwu^{II}

Summary

The seismic microzoning of Lanzhou was carried out both by geological and theoretical analyses. The geological investigation was based on geological and engineering geological comparison and correlation. It determined the stability of the site and the potential eternal deformation, i.e., the failure, of foundation soil. The theoretical method is the two-dimensional finite element analyses, by which the response spectra for seismic design was obtained. The results of the seismic microzoning are shown in The Seismic Microzoning Map of Lanzhou (I) & (II).

Introduction

Lanzhou is a new industrial city of Northwest China and is also the political, economical and cultural center of Gansu Province. It is considered as one of the most earthquake prone city in China. Since 138 A.D., historical records have shown that 8 strong earthquake hit this city. Among them the most devastating was the earthquake in 1125 A.D.. The general intensity of earthquake, according to The Map of Seismic Regionation of China (1976) were 8 degree. For the purpose of urban planning, seismic design and the strengthening, the seismic microzoning of Lanzhou has been carried out since 1977.

There has not been any "definite" principles and methods for the seismic microzoning and, therefore, whatever microzoning carries with itself strongly regional and investigative characteristics. On the other hand, there are many varieties and types of the building in a modern city. Its vibration character requirement for the site and the method for calculating seismic load are not identical with each other. It is very difficult to make a "uniform utilized" seismic microzoning. At first in Lanzhou area, it is usually considered with the factor that there are wide-spread industrial and civil buildings.

In this paper the investigation was carried out with two method of microzoning. One of them was the geological comparison method, i.e., at first, it is necessary to have a profound grasp of the geological, tectonical, topographical, geomorphological, engineering geological, quaternal geological and other natural conditions. Beside detailed investigation of all the above-mentioned natural conditions, the dynamic data of loess and loessial soil have been determined in the laboratory, the velocity of the elastic wave have been measured

I, II Lanzhou Seismology Institute, State Seismological Bureau.

in the site, the microtremor characteristics have been studied, in detail and the hazards from the earthquakes, especially the earthquake of Dec. 16, 1920, has been analysed.

The other method is the theoretical analysis. Considering the requirement of present «The Seismic Design Code for Industrial and Civil Buildings (TJ11-78)»⁽²⁾ and the concrete conditions of Lanzhou, the two-dimensional finite element analysis was used to calculate the characteristics of ground motion from the strong earthquakes and response spectra.

So, the methods used in the microzoning are as follows: (1) the geological and engineering geological comparison and correlation and (2) the theoretical analyses. With the first method, the potential eternal deformation and its character, caused by earthquakes were determined, and «The Seismic Microzoning Map of Lanzhou (I)» was made, with which seismic engineers can adopt the necessary resistant measures against the hitting of earthquake, with the second method the acceleration response spectra were obtained for every location of Lanzhou and «The Seismic Microzoning Map of Lanzhou (II)» was made, the use of which is to determine the dynamic load from ground shaking. All the procedure of microzoning is shown in Fig. 1.

The Geological Structure and the Other Natural Conditions of Lanzhou and Its Surrounding Area

Lanzhou is located near the zone of geomorphological gradient in the eastern margin of Qing-Zhang Plateau. Fig. 2 shows the major active faults in the vicinity of this city. The potential source of strong ground motion will be caused along these active faults. Among them the nearest is the Maxian-Xinglong Mountain fault, which is only about 20 km from Lanzhou.

But within the urban area, there are not any major active faults. Only two secondary faults are developed: one of them is named as Jinchengguan Fault, whereas the other consists the northern boundary of the Qilihe Block Basin, which extends for about 15 km in the west part of Lanzhou Basin. Both Jinchengguan and Qilihe Faults are not-causative in the point of seismological view, i.e., they will not cause strong earthquakes.

The urban area and the surrounding areas of Lanzhou are located in the valley of the Yellow River. The whole valley is separated by Jinchengguan into two secondary basins—the western Lanzhou Basin and the eastern Lanzhou Basin.

Both of the Lanzhou Basins are covered by loess and loessial soil. Besides, the brownish-red sandstone and argillaceous rock of Neogene, and, more or less, Cretaceous sandstone, Precambrian metamorphic rock and Paleozoic granite appear on the ground surface, too. Among these soils and rocks the predominant on the ground surface is loess and loessial soil, property of which can strongly influence the ability of seismic resistance of the site.

Within this microzoning area, six terraces of the Yellow

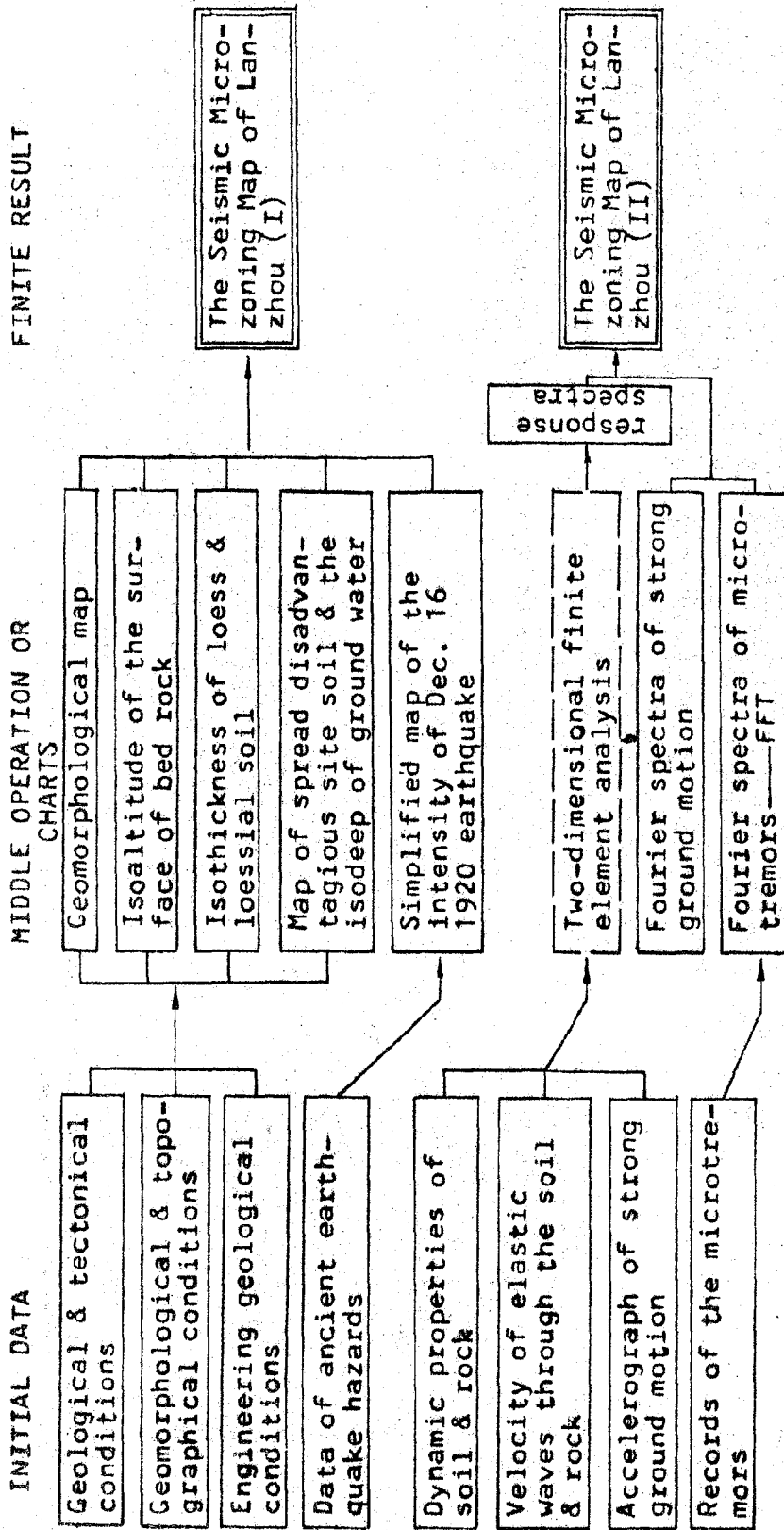


Fig 1 The procedure schema of seismic microzonation of Lanzhou

River are developed. Fig. 3 shows all these terraces and their extents. All these terraces consist of two strata: the lower is gravel stratum and the upper— the stratum of loess or loessial soil with different genesis and different properties. Lanzhou is mainly located on the I and II terraces of the Yellow River.

Geomorphological conditions are very important for seismic microzoning, because every terrace consists of the soils with their own properties, which more or less, are different from those, consisting other terraces.

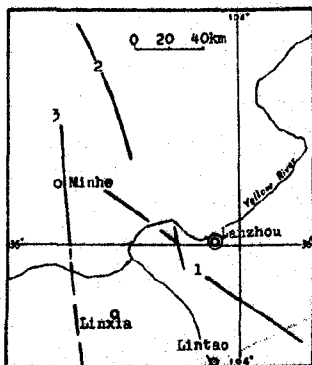


Fig. 2 The active faults in the vicinity of Lanzhou
1—Maxianshan fault, 2—Zuoglonghe fault, 3—Minhe—linxia fault

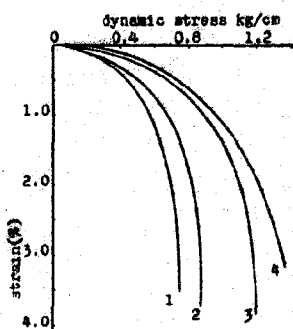
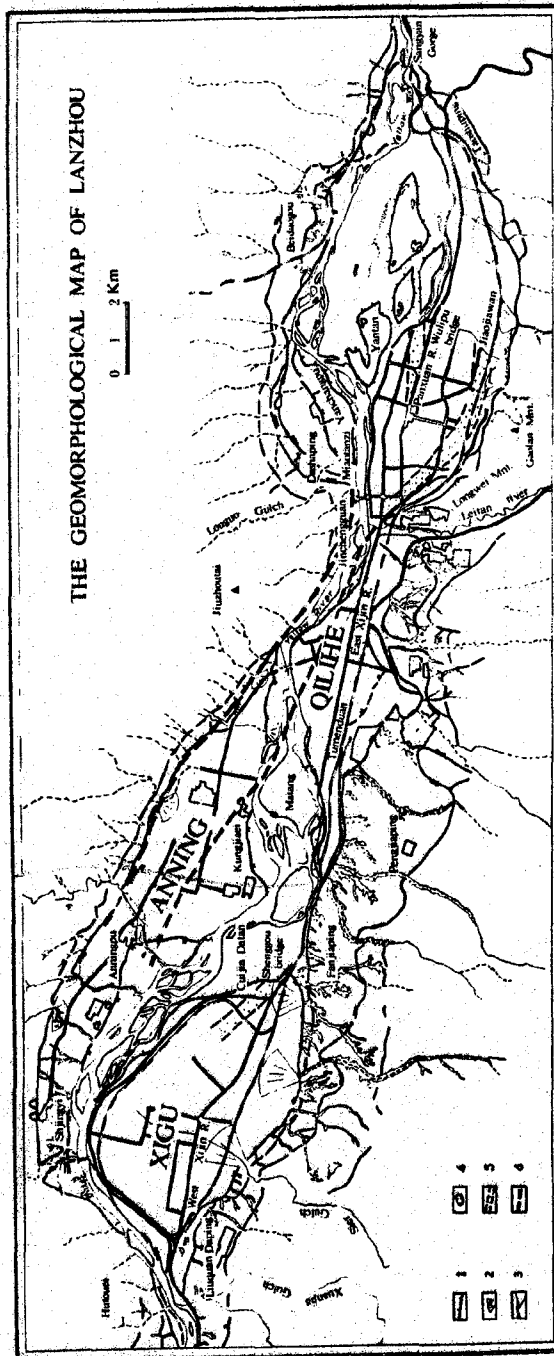


Fig. 4 The stress-strain curve for loessial soil of Lanzhou

Fig. 3



1. terrace ridge (Number of the north shows sequence of terraces) 2. fan 3. recent gash 4. landslide 5. ancient river bed 6. fault

The Method of Geological Correlation in Microzoning

The method of geological correlation was used for estimating the possible deformation of the soil foundation from strong motion. Considering the concrete circumstances of Lanzhou, it must be dealt with the follow 4 important problems.

(1) The stability of Jinchengquan and Qilihe Faults

As we have mentioned above, both of the faults are not active in the point of seismological view. But near them the depth of the bed rock surface is strongly changed in a short distance. According to the experience of past strong earthquakes the damage near such a belt is greater than that far away from this belt*. So, the influenced belt of the steep bed rock surface were thus divided. They included the south-west boundary of Qilihe Block Basin, although there the fault is absent.

On this belt it does not appear that any kind of buildings are not to be built, only those buildings which are very important or being easily to cause secondary damage, must be tried the best to avoid themselves from these belts. For the common constructions attention must be paid to solitify the soil foundation or adopt other measures against the earthquake motion.

(2) The Stability of Mountain Slopes

Based on the distribution of ancient landslides, engineering geological and topographical conditions of the slopes, it is concluded that the mountain slopes in Lanzhou are generally stable.

On the majority of the slopes, only the dry loess or loessial soil are developed and the strata are generally horizontal. In the history of geomorphological development, the landslides occurred rarely, although strong earthquakes often caused them so.

As we can see from the spreading of landslides on the loessial plateau,¹⁾ caused during strong ground motion from earthquakes in the past strong earthquake regions, the landslides were widely spread only there, where the intensity of ground motion was equal or more than 9 degree, and only there where the natural conditions were advantageous to the landslides. But all these conditions are absent in the main area of Lanzhou, so it is suggested that in this city during future earthquakes only a few landslides will occur and their size will be small.

But in a few localities the potential risk of landslides exists, especially, in the area of ancient landslides, for example, the landslide of Gaolan Mountain (Fig. 3), the soil on

* Liu Shoukuan, Cha Xiogang: The Earthquake Damage Anomaly of 1976 Tangshan Earthquake in Heigher Intensity Region, Lanzhou Seismologi Institute of State Seismologi Bureau, 1980.

the slope may creep down again during future earthquake. Moreover, the banks of the recent gulches, developed on the flats are unstable, too.

The landslides with a major size may cause heavy damages to constructions, so the area near the unstable slopes must be considered as dangerous zones, i.e., the sites are impossible to build anything on.

(3) The Problem of Failure of the Foundation Soil.

On the lower terraces in Lanzhou there are several zones where the saturated silver sands and puddly soil exist. They are expected to be liquefied and subsided during strong ground motion. The thickness of this disadvantageous site soil, is generally not more than 3m, and the depth of its apical plate is 4 - 12m.

According to the experience from the past earthquakes,^[4] such soil must be considered as possible failure foundation soil, except where its thickness is less than 0.5m and where the depth of the apical plate is more than 7m. Thus, the disadvantageous zone is small and easy to deal with. Such microzoning is both safe and inexpensive.

(4) The subsidence of macropore soil during earthquakes

The macropore soil in Lanzhou is generally loess and loessial soils. Their possibility of subsidence was determined in laboratory with triaxial dynamic press equipment. The result is shown in Fig. 4.^[5]

As we can see from Fig. 4, the subsidence of loess from strong ground motion increased with increase of the dynamic normal stress. According to Schroder^[6], the dynamic normal stress within the stratum during an earthquake of 8 degree is about 0.5 kg/cm². Under such dynamic normal stress, the subsidence of the loess is not more than 0.5%, it will not be dangerous to construction.

Through the study of geological and engineering geological conditions we divided the Lanzhou area into 6 microzones with a belt of steep bed rock surface at Jinchengguan and Qilihe Faults. The result is shown in «The Seismic Microzoning Map of Lanzhou (I)».

Theoretical Analysis in Microzoning

Theoretical analysis was carried out by the two-dimensional finite element calculation, because of the complicated topographical conditions in the urban area of Lanzhou. The method we adopted is based on solution of the equilibrium equations of elastic system without damping. The solution was put into practice by mode superposition. At first, it is necessary to solve the period of vibration and mode vector, then the response of the system to seismic motion of bed rock can be obtained by mode superposition.

The basic equation of elastic system under seismic motion

is

$$[M][\Delta_0]\{\ddot{Z}\} + [C][\Delta_0]\{\dot{Z}\} + [K][\Delta_0]\{Z\} = -[M](\{A_x\}\ddot{X}_0 + \{A_y\}\ddot{Y}_0) \quad (1)$$

where $[M]$, $[C]$, $[K]$ are respectively the mass, damping and stiffness matrix, while $[\Delta_0]$ is the matrix composed of the vectors, $\{Z\}$, $\{\dot{Z}\}$, $\{\ddot{Z}\}$ are the displacement, velocity and acceleration vectors of degree of freedom system. \ddot{X}_0 and \ddot{Y}_0 are the process of the horizontal and vertical accelerations of the bed rock surface, whereas $[C]$ is regarded as the linear composition of $[M]$ and $[K]$.

Premultiplying the both sides of the Eq. 1 with the transformed matrix $[\Delta_0]^T$, according to the orthonormalization of modes we obtained:

$$\left. \begin{aligned} [\Delta_0]^T[M][\Delta_0] &= [I] \text{ (identity matrix)} \\ [\Delta_0]^T[C][\Delta_0] &= \begin{bmatrix} \omega_1^2 & & 0 \\ & \omega_2^2 & \\ 0 & & \omega_n^2 \end{bmatrix} \\ [\Delta_0]^T[K][\Delta_0] &= \begin{bmatrix} 2\lambda_1\omega_1 & & 0 \\ & 2\lambda_2\omega_2 & \\ 0 & & 2\lambda_n\omega_n \end{bmatrix} \end{aligned} \right\} \quad (2)$$

Here the λ_i , ω_i are the modal damping parameters and the frequencies of i th mode. Putting Eq. 2 into Eq. 1, we obtained:

$$\ddot{Z}_i + 2\omega_i\lambda_i\dot{Z}_i + \omega_i^2 Z_i = -\{\delta\}_i^T [M] (\{A_x\}\ddot{X}_0 + \{A_y\}\ddot{Y}_0) \quad (3)$$

($i = 1, 2, 3, \dots, n$)

If we define Z_i^X , Z_i^Y as the horizontal and vertical response of i th mode, occurred by seismic ground motion X and Y , and η as the participation coefficient of mode shape of the horizontal and vertical seismic loads, so, Eq. 3 may be written as

$$\left. \begin{aligned} \ddot{Z}_{ix} + 2\omega_i\lambda_i\dot{Z}_{ix} + \omega_i^2 Z_{ix} &= \eta_{ix}\ddot{X}_0 \\ \ddot{Z}_{iy} + 2\omega_i\lambda_i\dot{Z}_{iy} + \omega_i^2 Z_{iy} &= \eta_{iy}\ddot{Y}_0 \end{aligned} \right\} \quad (i=1, 2, 3, \dots, n) \quad (4)$$

Then, $Z_{ix} = \eta_{ix}Z_i^X$, $Z_{iy} = \eta_{iy}Z_i^Y$, the following series of equilibrium equation will be established as

$$\left. \begin{aligned} \ddot{Z}_i^X + 2\omega_i\lambda_i\dot{Z}_i^X + \omega_i^2 Z_i^X &= -\ddot{X}_0 \\ \ddot{Z}_i^Y + 2\omega_i\lambda_i\dot{Z}_i^Y + \omega_i^2 Z_i^Y &= -\ddot{Y}_0 \end{aligned} \right\} \quad (i=1, 2, 3, \dots, n) \quad (5)$$

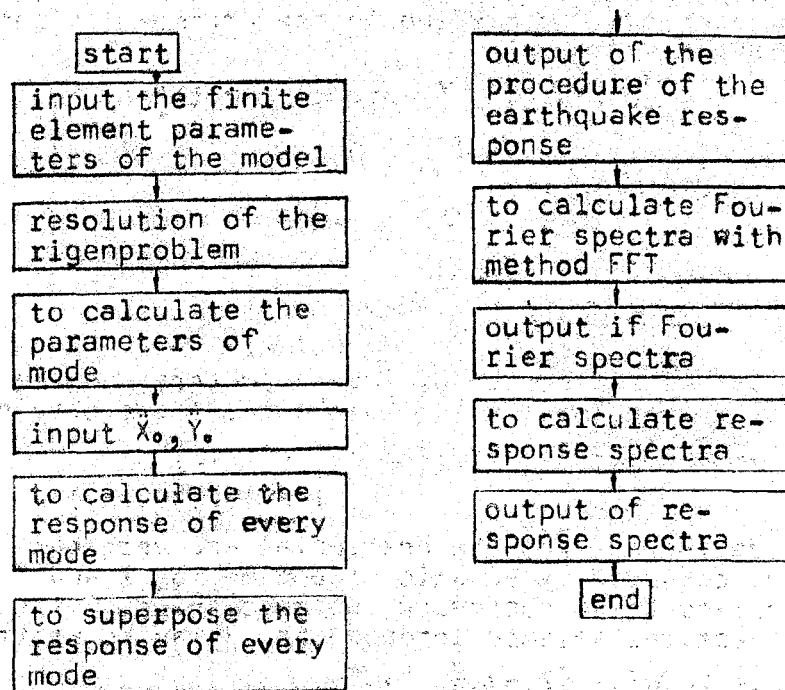
To resolve Eq. 5, $Z_i^X(t)$, $Z_i^Y(t)$ is obtained. The total displacement response may be obtained by mode superposition the response at horizontal and vertical directions. In fact, in the calculation, only the m_j modes are considered, displacement, velocity and acceleration responses may be expressed as

$$\left. \begin{aligned} \delta_x(t) &= \sum_{i=1}^{m_j} \eta_{ix} \delta_{oi}(\kappa) Z_i^X + \sum_{i=1}^{m_j} \eta_{iy} \delta_{oi}(\kappa) Z_i^Y \\ \dot{\delta}_x(t) &= \sum_{i=1}^{m_j} \eta_{ix} \delta_{oi}(\kappa) \dot{Z}_i^X + \sum_{i=1}^{m_j} \eta_{iy} \delta_{oi}(\kappa) \dot{Z}_i^Y \\ \ddot{\delta}_x(t) &= \sum_{i=1}^{m_j} \eta_{ix} \delta_{oi}(\kappa) \ddot{Z}_i^X + \sum_{i=1}^{m_j} \eta_{iy} \delta_{oi}(\kappa) \ddot{Z}_i^Y \end{aligned} \right\} \quad (6)$$

where $\delta_k(t)$, $\dot{\delta}_k(t)$ and $\ddot{\delta}_k(t)$ are the displacement, velocity and acceleration of k th degree of freedom, caused by horizontal and vertical seismic loads, $\delta_{0i}(k)$ is the general coordination.

When using the Wilson θ method of unconditional stability to resolve Eq. 6 the absolute maximum response in every nodal point of ground surface, it is possible to analyse the response procedure, Fourier and response spectra in the typical nodal points.

The calculation was made in 108 computer and the flow of the program are described as follows:



Records of the M7.2 Shongpan-Pingwu earthquake of Aug. 16th, 1976 was selected as an input seismic motion. The accelerometer was recorded in Wenxian, Gansu Province, and it was slightly remoulded as thus, the maximum acceleration was 0.2g, which is in correspondence with the intensity of 8 degree. The several rest models were calculated with Taft accelerometer of 1952 of the U.S.

Every parameter for calculation were strictly chosen, for example, the elastic module of soil and rock was defined both by velocity of acoustic wave, measured in situ and by dynamic triaxial press test in the laboratory. Then, the damping was chosen, cooresponding with 10^{-5} deformation degree.

Results of Calculation

The maximum acceleration, velocity and displacement of 312 nodal points from 20 sections were calculated. Fig. 4 shows an example of calculation.

The horizontal acceleration is immediately connected

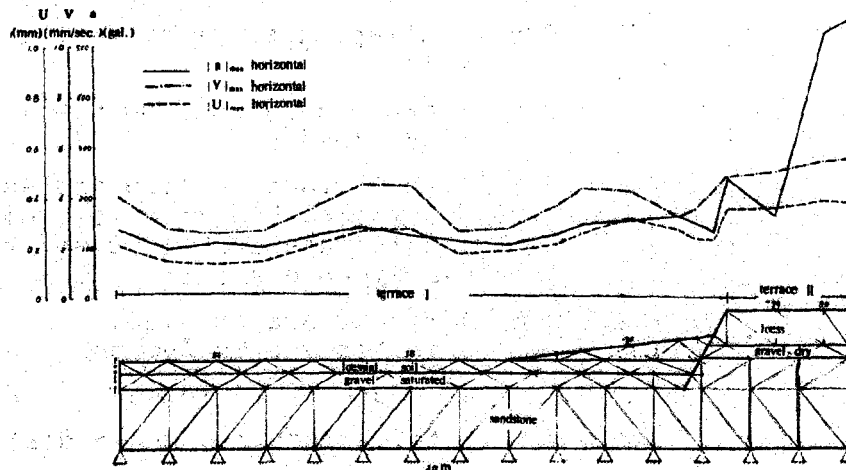
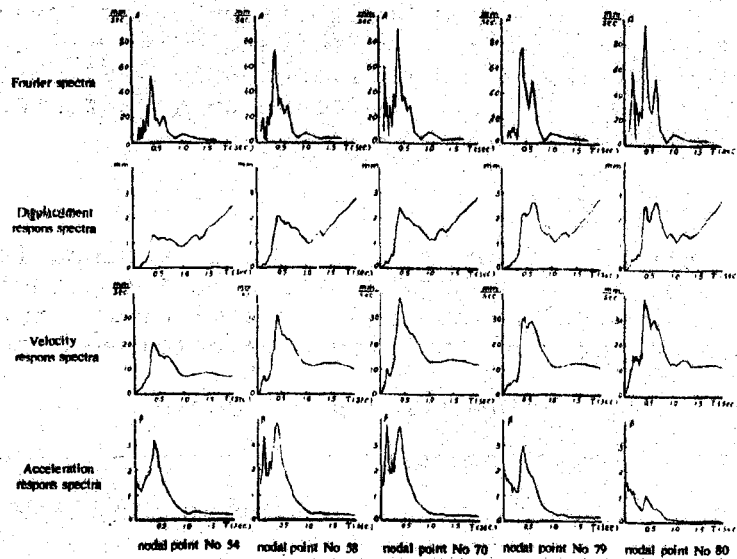


Fig 3 A example of the calculate results—Miektarzi-Dashaping model

with the geomorphological unit of Lanzhou, i.e., with the property of the site soils. While as the influence of the partial topographic effect only shows partial meaning. For instance, the average horizontal acceleration in some areas are shown as follows:

IIth terrace, in Yanchangpu,	240 gal.
IVth terrace,	200 gal.
I & IIth terrace in Xigu & Anning district (The bed rock is of argillite)	168 gal.
IIth terrace in Ahning & Qilihe district (The bed rock is of Q gravel) and,	133 gal.
Ith terrace from Qilihe to Pan-xuan Road,	
Ith terrace to the east of Wulipu Bridge,	100 gal.

Altogether we calculated 156 curves of acceleration re-

sponses $\beta-T$ (Among them horizontal—84, vertical—72). The form of these $\beta-T$ curves are similar to the $\beta-T$ curves of other places, informed in published articles,^[7] that is, the value β has a peak (β_{max}, T), over which β decreased according to the following formula:

$$\frac{\beta}{\beta_{max}} = \left(\frac{T}{T_0}\right)^n \quad (T \geq T_0) .$$

The form of different districts in Lanzhou is greatly identified each from other. According to the principles used in the Code TJ11-78, by putting the similar $\beta-T$ curves together, 7 idealized $\beta-T$ function were obtained (see tab. 1).

Idealized $\beta-T$ curves

Tab. 1

No	β_{max}	T_0	T_1	β_{min}	zone, appropriate
1	4	0.2	1	0.8	Fanjiaping, slope of Lonwei Mountain
2	4	0.4	2	0.8	Panxuan Rd., Yanchangpu, all the flood land
3	3	0.4	2	0.6	IIth terrace in Xigu and Anning districts (bed rock is argillite, Ith terrace in Qilihe and the Old Urban district
4	3	0.5	2.5	0.6	IVth terrace in Xigu, IIth terrace in Tumenduen
5	2.5	0.4	2.5	0.5	at south of Xijin Road of Xigu
6	2.5	0.5	2.5	0.5	IIth terrace, in Anning district
7	1.6	0.5	2.5	0.32	IIth terrace (bed rock is of Q gravel)

But in project practise, the response spectra with unit of acceleration of gravity often used, i.e., $\alpha = k\beta$ (where $k = \frac{a_{0max}}{g}$, the seismic coefficient). After idealization 6 $\alpha-T$ response spectra were obtained (Table 2). By these 6 $\alpha-T$ response spectra the whole Lanzhou city was microzoned as « The Seismic Microzoning Map of Lanzhou (II) », it shows

(1) The loess and loessial soil in Lanzhou generally correspond to the soil of II-III category in the Code TJ11-78, they approximate the soil of II category more than that of III category.

(2) The period and value of the peak are related with the stiffness of the site soil, the looser the site soil, the longer the period of spectrum peak; the thicker the loose soil, the greater the value of the peak.

(3) In the flood land of the Yellow river, in spite of the high level of ground water, the period of the peak does not tend to long period, because there is a gravel stratum underlying immediately below the loose surface ground.

(4) Difference of the dynamic load from ground motion in different districts of Lanzhou may be more than twice in the meaning of "intensity", which corresponds to 7.5—8.5 degrees.

(5) The results of calculation in many aspects agree with the experience from the past strong earthquakes. A part of calculated results was established taking the truth of the Haiyuan earthquake in 1920.

Conclusion

1 The compiling of The Seismic Microzoning Map of Lanzhou is considered as a research object rather than a productive one all the method used may be divided into two parts—geological correlation and the analytical calculation.

2 Seismic Microzoning must be appropriate according to the concrete circumstances of the district. For instance, in Lanzhou the greatest problems are the subsidence of the loess, the stability of faults, the stability of slopes and the dangers of failure of soil foundation.

3 The calculation shows that the appearance of the response spectra in Lanzhou can be divided into six. By the acceleration response spectra, the difference of the dynamic load from ground motion may reach more than two times, corresponding to 7.5—8.5 degree of the intensity.

4 The appearance of the acceleration response spectra is strongly dependent upon the thickness and properties of the surface soil.

5 In general, the part of the calculation was established taking the truth of Haiyuan earthquake in 1920.

Acknowledgement

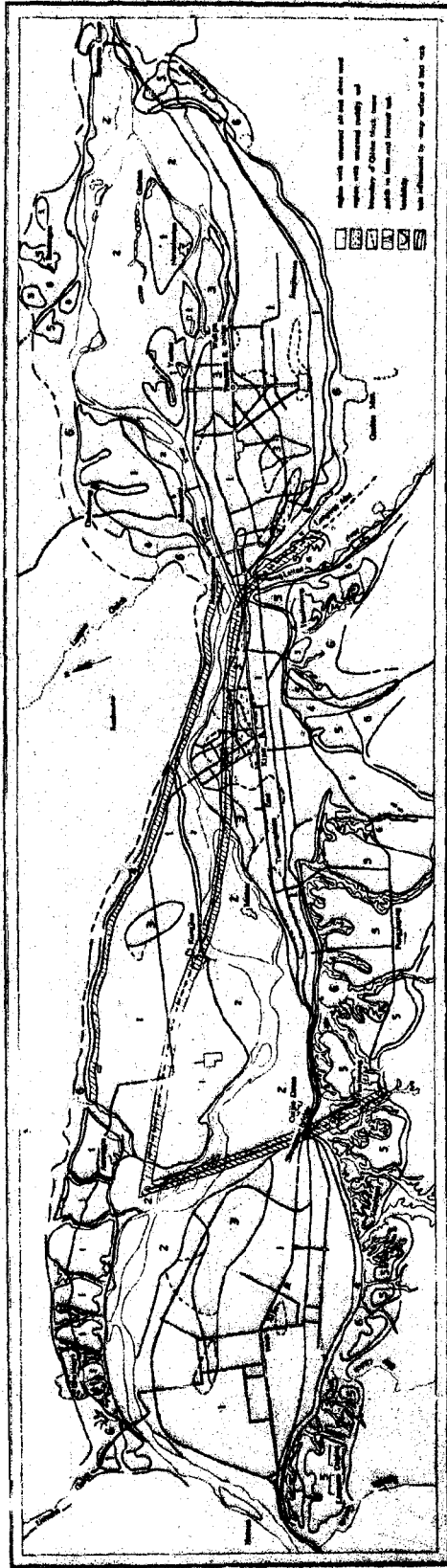
Appreciation is expressed to Mr. Huang Zupeng and Mrs. Duan Ruwen for their studying the geomorphology and dynamic mechanical property of loess for this seismic microzoning. The experimental work and data reduction were carried out by Messrs. Zheng Tiesheng, Zhang Shuqing, Zuo Baolin and Li Fanwen. The authors would like to thank Mrs. Ai Zhilian and Feng Aimin for their drawing all the figures.

Reference

- 1 Medvedev S.V. et al.: Seismic microzoning, Science Press, Moscow, 1977 (in Russian).
- 2 The Seismic Design Code for Industrial and Civil Buildings (TJ11-78), Architectural Industry Press of China, 1978 (in Chinese).

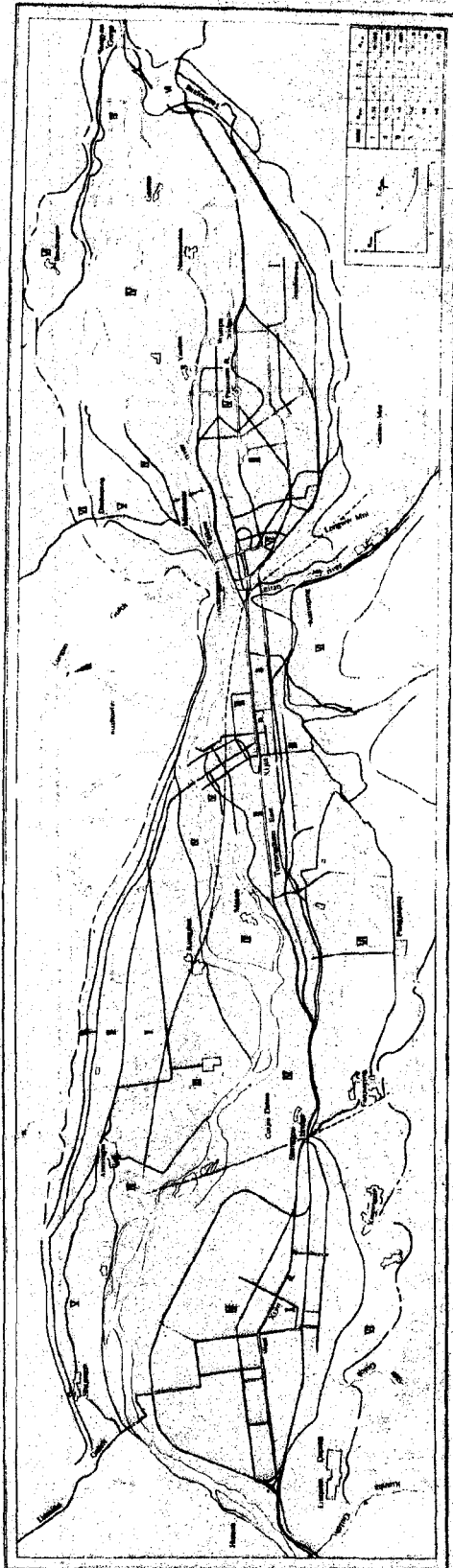
- 3 Lanzhou Seismology Institute, Seismology Bureau of Ningxia Hui-Autonomous Region, The great Haiyuan Earthquake on Dec. 16, 1920, Seismology Press of China, 1980 (in Chinese).
- 4 Institute of Engineering mechanics, Ac. Sinica: Earthquake Damage of Haicheng Earthquake, Seismology Press of China, 1980 (in Chinese).
- 5 Duan Ruwen: Experimental study on dynamic characteristics of Lanzhou loessial soils, Northwestern Seismological Journal vol.1 No2, 1979(in Chinese).
- 6 Editorial Group: Introduction to earthquake engineering, Science Press of China, 1977. (in Chinese).
- 7 Chen Dasheng et al.: The response spectra for earthquake resistant design, Collected Research Reports on Earthquake Engineering, Institute of Engineering Mechanics, Ac. Sinica vol. 3, 1977 (in Chinese).

THE SEISMIC MICROZONING MAP OF LANZHOU(I)



1 district, generally without any disadvantageous engineering geological phenomena during earthquake; 2 district with ground water level less than 3m or with recent made land; 3 district with saturated silver sand or puddly soil; 4 district possible to cause small landslide or collapse during earthquake; 5 district covered by loose macropore loessial soil, easily subsiding during earthquake; 6 district possible to cause landslide with great size during earthquake or where the site is so bad that in fact cannot be built anything on

THE SEISMIC MICROZONING MAP OF LANZHOU(II)



ON THE SEISMIC ACTIVITY AND MICROZONATION
OF THE BEIJING AREA

Zhou Xiyuan, Fu Shengcong and Wang Guangjiun¹

ABSTRACT

The paper first of all laconically reviews the history of the seismic microzonation in the Beijing area. Based on the historical seismic records and monitoring by instruments and meters, it attempts to discuss the seismic activity in the Beijing-Tienjin-Tangshan-Zhangjiakou area. With the simple probability model, the paper has analyzed the seismic hazard and calculated the probabilities of the peak acceleration over different value levels in any locality in the Beijing area. The paper gives an account of the basic method to locate the seismic microzonation and its result. It finally discusses the uncertainty of the seismic microzonation in the Beijing area.

INTRODUCTION

Historically there had been many violent earthquakes in Beijing and its surrounding areas, the earliest record being in the year of 274. Ever since 1057, there had been fairly detailed records of earthquakes. However, due to late development of monitoring instruments and meters, China started the work in real earnest only after 1949. Not long after the founding of new China, the Geo-physics Institute of Academia Sinica established seismologic

¹ Engineer, Institute of Building Earthquake Engineering,
Chinese Academy of Building Research

observation stations to proceed with seismic hazard and intensity regionization of the Beijing area. After the earthquake in Xingtai in 1966, the Engineering Mechanics Institute of Academia Sinica and the Chinese Academy of Hydro-electric Power and Water Conservancy set up strong earthquake observation stations in the Beijing area. Of late, our institute is carrying out a program to develop a strong motion network in the area, which was jointly signed by the Chinese government and the UNDP. The establishment of such a network with great density will undoubtedly promote and stimulate the research into seismic activity and the work of microzonation in the area.

The work to locate the microzonation in the Beijing area has been mainly through the following three stages:

(1) In the mid-1950's, the basic intensity in the urban area was determined in accordance with regional seismic activity and geological structure, and then it was readjusted in accordance with local engineering geology and hydrogeological conditions. As a result, the intensities of various sites were determined and the seismic microzonation of the urban area of Beijing were made [1].

(2) In the mid-1960's, the Engineering Mechanics Institute of Academia Sinica, in accordance with the research results and strong earthquake acceleration records available at that time, put forward a draft of aseismatic design code [2], that is, the designs should be done, in accordance with four kinds of site, with different response spectra [3] and the conception of site intensity be discard. The Engineering Mechanics Institute and the Geology Institute of Academia Sinica, the department of geological exploration Beijing Municipality and other units, in accordance with earthquake damage experiences

under different site conditions and with the requirements as set by the draft of the code, made microzonation of the urban area. The above work was all conducted by summarizing the macroseismic experience and lacked in quantitative mechanic analysis.

(3) The possible epicentre and seismic magnitude are first evaluated in accordance with the seismic activity and seismogeological data in Beijing and its surrounding areas, the incident motion of base rock is estimated, the dynamic response of soil is analyzed, and then the microzoning under the influence of the earthquake are made in light of the regional variation of the parameters of ground motion and response spectra [4]. This is the practice since the 1970's. This paper first discusses the seismic activity in the Beijing area with a simple statistic method, then proceeds to analyze the seismic damages in Beijing's surrounding areas and some of the results about the microzoning work. It will also make a comparative study of the seismic environment in Beijing and in California and has a general discussion relation to the uncertainty of microzonation in the Beijing area.

The work has won support by the Beijing Geological Bureau and the major results of our work were achieved in collaboration with Dong Jincheng, Zhang Zaimin, Yang Delin and Tang Haishan of the Beijing Municipal Geological Surveying and prospecting Team.

THE STATISTIC ANALYSIS OF SEISMIC ACTIVITY IN BEIJING AREA

What we mean by the Beijing area there is the area 38.5-41 degrees north latitude and 114 -- 120 degrees east longitude embracing Beijing, Tianjin, Tangshan and Zhangjiakou, which is

part of North China's seismic region. There has been fairly complete records of earthquakes in the area ever since 1057. According to statistics, there had been 661 earthquakes over than Richter magnitude 4 in the Beijing area in the period of 1057-1977. The statistic result of the relations between magnitude and frequency of earthquakes is shown with sold dots in Fig. 1, the line A is the statistic regressive line of these dots of data. Fig. 2 shows the sequence of the Occurrence of earthquake in the Beijing area since 1000. From the chart people may see a seemingly abvious increase of the frequency of earthquake in the area since 1484. We think that it is mainly because many of the earthquakes in the early period were not recorded, especially those of minor magnitude. From the chart, people may also see that another obvious feature is that there is a given cycle in the occurence of earthquake. Fig. 2 shows the active period when the intensity of earthquakes is great and their frequency is high and also relatively quiet period when the situation is just vice versa. From Fig. 2, people will see that now the area is still in the active period. However, it is difficult to judge the development of earthquakes only with this chart. As we have stated above, the Beijing area is part of North China's seismic region. In the Fig. 2 we show the four seismic active periods 5 over the last 1,000 years in the North China area. From this it may be concluded that the seismic activity in the Beijing area is identical with that in entire North China. The periodic variation of seismic activity in California U.S.A. is not as outstanding as one in North China [16].

Construction on the seismoscopic station in the Beijing area started in 1957. However, we got fairly systematic monitoring records only after 1959. We made a statistic analysis of these records and obtained the data as shown in the dots in Fig. 1, line B is the statistic regressive line based on these data. By comparing the A and B lines in Fig. 1, it can

be noted that the level of seismic activity in the last 20 years is much higher than the average level in the last 1,000 years. Theoretically, line B should represent the level of seismic activity in the recent active period, however, due to a fairly short monitoring period including some large earthquakes like Tangshan earthquake, the frequency of strong earthquakes is estimated too high in the statistic results.

We may just as well discuss the seismic activity in the Beijing area with extreme value statistic method [6]. For the purpose, we suppose the times of earthquake in a year is a Poisson stochastic process, the average value is α , magnitude M is a stochastic variable and its accumulated distribution function is $P(M) = 1 - e^{-\beta M}$, Then the accumulated probability of the maximum magnitude M will correspond with extreme value I type distribution:

$$G(M) = \exp(-\alpha e^{-\beta M}) \quad (1)$$

In order to appraise the values of α and β from the annual maximum magnitude value of M_1, M_2, \dots, M_n of n years, we put into order from small to large magnitude earthquakes, for instance, $M(1) \leq M(2) \leq \dots \leq M(n)$, in which $M(j)$ is the j -th annual maximum magnitude. Each $M(j)$ is given the value of $G(M(j)) = \frac{j}{n+1}$. From Eq. 1 we obtain:

$$\ln[-\ln G(M)] = \ln \alpha - \beta M \quad (2)$$

The maximum magnitude of earthquake of each year in the last 23 year in the Beijing area follow:

Year	57	58	59	60	61	62	63	64	65	66	67	68
Mmax	5.4	3.5*	3.8	4.5	4.2	4.9	4.0	4.5	4.7	4.5	6.7	3.9
Year	69	70	71	72	73	74	75	76	77	78	79	
Mmax	4.5	4.8	5.0	5.1	5.6	4.9	4.2	7.9	5.5	5.1	5.4	

*We adopt a smaller value as the monitoring record of the year is missing in the seismic data provided by the State Seismological Bureau.

By using the least square method we obtain the coefficients in formula (2), $\text{Ln}\alpha=4.91$, $\beta=1.11$. If the above results are drawn on the extrem value probability diagram we obtain an approximate line representing Eq. 2 (see Fig. 3). It is not difficult to note that $\alpha e^{-\beta M}$ is the number N_M of the earthquakes, expected in a year, that surpasses magnitude M. However, we usually employ the following magnitude-frequency formula:

$$\log N_M = a - bM \quad (3)$$

Parameters a, b and α , β have the following simple relations:

$$\begin{aligned} a &= \alpha / \text{Ln } 10 \\ b &= \beta / \text{Ln } 10 \end{aligned} \quad (4)$$

Based on the above relations, we get the annual number of Earthquakes with magnitude M:

$$\log N_M = 2.13 - 0.428 M \quad (5)$$

For the purpose of comparison, we integrate line B in Fig. 1, indicative of the relations between magnitude and frequency, with Eq.5 in Fig. 4. From Fig. 4, we can see that though the results obtained by using the extrem value method and the results got with calculating the magnitude-frequency relations are

not totally identical, however, they are quite close to each other with only the a value of the latter a little higher.

We have discussed the seismic activity in the Beijing area with historical and instrumental data and obtained line A and B in Fig. 1. We think that both types of data have their limitations. In fact, though historical records cover a fairly long time, yet, are incomplete; especially it is quite possible to overlook earthquakes of minor magnitude because their damage are light and non-existent. No doubt, the instrumental data collected over the last 20-odd years is quite valuable inspite of the short duration because of the Tangshan earthquake people tended to overestimate the frequency of the occurrences of earthquakes. However, we do not think that such earthquakes as over a magnitude 6.5 should have been overlooked by historical records. Owing to the high frequency of the occurrences of small earthquakes with magnitude lower than 4 the data monitored over the last 20-odd years are quite representative. So, the line C in Fig. 1, made from the dots based on both of the historical and the instrumental data may well represent the average seismic activity in the area in the last 1,000 years. For comparison, we draw line C of Fig. 1 together with the lines representing the magnitude-frequency relations [7] we can see that the seismic activity in the Beijing area is approximately lower by an order of magnitude than in the California area in the United States. It is worthy of noting that the active level of earthquakes in the last ten-odd years obviously in higher than the average level in history.

THE SEISMIC ENVIRONMENT IN THE BEIJING AREA

Historically, there had been many large earthquakes in Beijing and its surrounding areas. Fig. 6 shows the distribution of epicentres. The short lines connected with the circles indicate the isoseismal directions. From the chart, we can see that the epicentres in the area in history were quite

scattered. Further analysis shows that the large earthquakes in history were all controlled by the northeastward, northward, eastward and northwestward faults. Nevertheless, the relations of large earthquakes in the Beijing area to the trunk fault belt are not so concentrated and obvious as in California [8] and some parts of West China region, and long axes of the isoseismic are not all so obviously controlled by the direction of the faults. This shows the complexity of the area's geological structure and that it is a very difficult work to study the relations of seismic activity to faults. More data and deeper research are desired.

According to the existing seismic-geological data [9], the Beijing Plain is at the intersection of the Yan Mountain Range fault fold belt, the Shanxi fault swells and the Hebei-Shandong seg and its geological structure is very complicated. There is a tremendous growth of faults in the area and there exist at least three groups of faults: the northeastward (northern northward), northwestward and near east-west. The northeastward, eastward) fault is the trunk fault in the plains, mainly Bapaoshan-Gaoliying, Liangxiang-Shunyi, Nanyuan-Tongxien and the Xiadian fault from west to east. They separate rock mass in the plains into a series of swells and segs with the same directions as the trunk fault: Jingxi swell, Beijing seg, Daxing swell and Dachang seg. After analyzing the characteristics of the surface structure and deep structure and their relations, the conventional idea is concluded that there had existed a very strong, NWW-SEE-oriented horizontal pressure stress in the earth's crust in the area, which had caused the basic structural units of swells and segs in the area (Fig. 7). The stress field of the regional structure in the Beijing area is identical with that in the entire North China region with the position of the axis of the major pressure stress running north east eastward [10]. According to Deng Qidong and other researchers [11], the structural stress field in the North China region, taken as a whole, controlled by the joint action of the Pacific and Indian plates.

However, the analysis of the data of the geodetic survey over the last 20 years [12] shows that the modern structural form in the Beijing plains does not correspond with the mixed shape of swells and segs formed in the Tertiary Period. Compared with the northeastward faults in the area, it seems that the various sections on northwestward Nankou-Sunhe fault and the east-west Paodi fault show strong activity. It is worth while nothing that a modern depression has come into being with Shahe as the center on the northeast outskirts of Beijing southwest to the Nankou-Sunhe fault (Fig. 8). It seems that it could be taken as a signal to indicate the growing activity of the northwestward fault. Geological, morphological and archaeological research shows that the north-northeastward structure played a dominant role from 475 to 221 B.C. and the northwestward structure reigned supreme from 907 to 1125. The last view is in conformity with the data of modern morphological survey. It is estimated that the growing activity of the northwestward fault will possibly lead to the disintegration of the seg structure in the Beijing plains. It needs further study to decide whether such a background of the geological structure will show that the process of a medium-intensity earthquake is under way.

The Institute of Geology under the State Seismological Bureau has drawn a seismic and geological map to indicate the earthquake hazard zones in the Beijing-Tianjin area and its vicinity [13]. According to their map, there are two hazard zones, one on the northeastern corner and the other on the southeastern outskirts of Beijing. We show a simplified map here in Fig. 8.

We usually take 100 years as a period for seismic macrozoning. This period shows our requirements for general buildings. How to make a correct appraisal of the maximum seismic exposure in a locality on the basis of as detailed as possible investigation and study of the seismic environment seems to be the key question in carving out seismic macrozoning and microzoning. There have been various kinds of appraisals of the seismic

activity in the North China region, including Beijing, after the Tangshan earthquake. After analyzing all recorded earthquakes at magnitude 8 since ancient times, Xu Shaoxi and other researchers [14] discovered that there would be a M = 8 or 7.5 earthquakes in a given distance from its epicenter after or before each 8 magnitude earthquake. The distance span has two predominant distributions, one at a distance of about 480-550 kilometres and another at a distance of about 1.100 kilometres. Beijing is 180 kilometres from Tangshan. In their view, there is little possibility for another strong earthquake over 7 magnitude in a short time. Song Liangyu and other seismologists [15], based on the seismic records of the North China region over the last 500 years, separately made extension predictions in the light of the stochastic model and the autoregressive model of the steady stochastic process and concluded that the North China seismic peak which began with the Haicheng earthquake would decline after 1980 and would resume activity around 2001. Nevertheless, Li Ziqiang and others [5] think that the peak of the North China seismic activity is still under way now. After the Tangshan earthquake, the seismo-geological Team of the State Seismological Bureau predicts that the intensity of the earthquake in the Beijing area will be at 8 magnitude and the basic intensity in Langfang, Dachang and other areas on the southeastern outskirts of Beijing at as high as 9 degrees.

Based on the data already obtained and the research results achieved by various institutions, we maintain that the inferable seismic focus with magnitude 6 lying 15 Km. north-east of downtown Beijing and the magnitude one lying 45 kilometres southeast to the city can be made as the basis for the microzoning of the urban area and the peak acceleration of the baserock motion is taken as around 100 gals.

ESTIMATION OF THE MAXIMUM ACCELERATION IN BEIJING

Proceeding from the seismic environment in Beijing and its surrounding area, we have in the above chapters discussed the seismic hazard in the urban area. But, it is very difficult to pinpoint the position of the epicenter of each earthquake and the highest magnitude of each locality for a fairly long duration of time as the geological structure in the Beijing area is very complicated and many of the research projects have just started. Another means [7] is to suppose that the time for the occurrence of earthquake in the Beijing area and the space distribution are all stochastic. Then, the different degrees of seismic activity in each part will not be taken into consideration. With this method, we can estimate the average level of seismic activity in the Beijing-Tianjin-Tangshan-Zhangjiakou area. When we have not studied well the seismo-geological conditions in a given area and lack reliable data, the latter means should be something we have to use. As a complement to the discussion in the last chapter, we used the simple method employed by Housner in California [7] to calculate the probability of the different peak accelerations which a given locality in the Beijing area would have in the coming 10 to 100 years. In the calculation, we considered the average magnitude-frequency relations in the last 1000 years represented by line A of Fig. 1 and the magnitude-frequency relations, in Fig. 4, obtained with the extrem value statistic method based on the maximum magnitude in the last 23 years. The latter approximately represents the seismic activity in the Beijing area in the high-tide period. Using the ideal intensity distribution law, given by Housner[7], we obtained the percentage probabilities of the given seismic accelerations in a certain locality in the Beijing area in about the last 1,000 years, see Table 1, The numbers in brackets in the Table represent the corresponding probabilities in the high-tide period. For the purpose of comparison, we also give the corresponding acceleration probabilities in California.

From Table 1, we can see that according to the average seismic activity in the last 1,000 years, the seismic risks in the Beijing area are obviously much lower than in California; however, in terms of the high-tide period in the last 23 years, they are higher than in California. In comparison, we have to note that the area of California is four times the Beijing area but the population in both areas is almost the same. Generally speaking, the seismic activity of the Beijing area and California is comparable. With 100 years taken as a period, in the terms of the average, normal level of seismic activity in the area, the probability of the ground motion acceleration that is bigger than 0.1 g is 74 per cent, that is, the possibility of the occurrence of seismic impacts higher than intensity 7 is fairly great; and in terms of the high-tide period the probability of the acceleration that is bigger than 0.2 g is 69 per cent, that is, the possibility of such an occurrence is great likewise. So, with the Beijing-Tianjin-Tangshan-Zhangjiakou area taken as a whole on an average level, the possibility of the occurrence of a seismic impact that is at intensity 7 to 8 is fairly great.

THE EARTHQUAKE EFFECT IN THE URBAN AREA

In literature [4], we considered mainly the impacts upon the urban area of an earthquake at magnitude 7 about 40 kilometres southeast of Beijing and, on the basis of it, made microzoning of earthquake effect of late, in collaboration with Dong Jincheng and others of the Department of Geological Exploration of Beijing we supposed that a 6.5-magnitude earthquake would occur in the settlement district with Shahe as its center northeast of Beijing, conducted the analysis of seismic response of soil layers in accordance with the method as expounded in the literature[4] and obtained the distribution of the isorithms of the various parameters of ground motion. Finally, we on the basis of comprehensive studies of the effect of the possible epicentres on the urban areas, made predictions of the parameters of ground motion.

If the effect of a number of hypocenter in a given area have to considered as whole, generally speaking, the following formula may be adopted to assess the comprehensive affect of these hypocenters:

$$E [S] = \sum E [S_I / I] P [I]$$

In the formula, $E [S]$ is the expected value of the parameter S of ground motion in a given area, $E [S_I / I]$ is the expected value of parameter of ground motion under the condition of I -th hypocenter and $P [I]$ is the probability of occurrence of I -th hypocenter, that is, the distribution of probability of all the possible hypocenter, namely, $\sum P (I) = 1$. In the Beijing area, we suppose for the time being the possibility of the occurrence of the two hypocenters northeast and southeast to Beijing is similar, then, we may adopt the average value of the seismic response corresponding with the two hypocenter for the parameter of the ground motion in a given locality. We have given the isorithms of the ground peak acceleration in the urban area in Fig. 9. From it, we may see that the expected ground motion acceleration in the urban area approximately varies within 100-200 gals, only that in the southwestern part a little more than 200 gals. The parameters of the ground motion in other parts of the area can be obtained with the same method. We will not elaborate here.

DISCUSSION

We have in the above chapters discussed the seismic activity and the microzonation of the urban area of Beijing and conducted a comparative study of Beijing and California in some aspects. Generally speaking, though the historical seismic data of the Beijing area are richer than in California, yet, its instrumental records are far less than the latter. As the geological structure in the area is quite complex and the seismic-

geological work has started not long ago, the work to make microzonation of the area has met with many difficulties.

In making the seismic microzoning in the past, we had mainly considered the effect of the side conditions on ground motion. We aim to forecast the effect of a possible earthquake on various kinds of buildings. Of course, there are many uncertain factors in the forecast. The greatest problem is that it is very hard to make correct predictions of the hypocenter location and magnitudes. Though the paper, based on data of various kinds, has studied the effect of the possible hypocenter on the ground motion in the urban area, nevertheless, it can not surely pinpoint the locality. Take the Haicheng and Tangshan earthquakes in North China for example, before the occurrences, seismological departments had come to understand that there would possibly occur fairly large earthquakes, however, they could not pinpoint the locality of the epicentre. From past experience, we think that it is more difficult to make macrozoning in North China than in other parts of the country. As a matter of fact, a fairly long time before the occurrences of Xingtai, Haicheng and Tangshan earthquakes, the seismic risks had not been fully understood. Under such circumstances, to make rational seismic microzonation, it is first of all imperative to take note of the average tendency of seismic activity in the area, then, in accordance with the seismic environment round the site, to determine the parameters of ground motion. If necessary, it is also imperative to make proper evaluation of the uncertainty of the data in use and the reliability of the microzonation. Based on such considerations, we have of late conducted initial research into the average seismic activity in the Beijing area. At present it might be a better method.

REFERENCES

- (1) Li Ziqiang (1957). Earthquakes in Beijing, Geo-physical

Journal, Vol. 16, No. 2 (Chinese).

- (2) Liu Huixian, (1965). Some Views and Proposals on the Calculation Methods of Seismic Loads in Aseismic Design code, Collection of Research Reports on Seismic Engineering, Vol. 2, Science Press (Chinese).
- (3) Zhou Xiyuan, (1965). Effect of Soil Conditions on Seismic Loads Acting on Buildings, Ibid.
- (4) Zhou Xiyuan, Tung Jingzheng, Fu Shengcong, Zhang Zaimin, (1980). The Seismo-geological Background and the Earthquake Response of Typical Structures in Beijing, VII WCEE, Vol. 2, p.507.
- (5) Li Ziqiang, Li Yiming, He Jingmei, Tian Kangyuan, (1980). A Preliminary Study of the Process of Development and Occurrences of A Series of Recent Strong Earthquakes in North China, Acta Seismologica Sinica, (Chinese).
- (6) M.Caputo, (1974). Analysis of Seismic Risk, Engineering Seismology and Earthquake Engineering, edited by Julius Solnes, Noordhoff-Leiden.
- (7) Robert L. Wiegel, (1970). Earthquake Engineering, Prentice-Hall.
- (8) Allen, C.R., St. Amand, P., Richter, C.F., and Nordquist, J.M., (1965). Relationship Between Seismicity and Geologic Structure in the Southern California Region, BSSA, Vol.55, No. 4, pp753-797.
- (9) Shao Xuezhong, Zhang Jiaru: Experiments on the Depth Cross-section of Kanghzhang-Dachang in the Beijing Area with Seismic Transformed Waves, Acta Seismological Sinica, No. No. 1, p.51.
- (10) Xu Zhongzhun, Liu Yufeng, Zhang Chengchen: Characteristics of the Seismic Field of Stress and Direction in the Beijing-Tianjin-Tangshan-Zhangjiakou Area, Acta Seismological Sinica Vol. 1, No. 2, p. 121.
- (11) Deng Qidong, Zhang Yuming, Xu Guilin, Fan Futian, (1979). On the Tectonic Stress Field in China its Relation to plate Movement, Seismology And Geology, Vol. 1, No. 1 (Chinese).
- (12) Zhang Cunde, Xiang Jiacui, (1979). On the Recent Tectonic

Movement and Strain Field in Beijing plain Area by the Geodetic Data, Seismology and Geology, Vol. 1, No.3, p.57 (Chinese).

- (13) Xiao Yiyue, Li Ping, (1979). Employment of Pattern Recognition for Locating Strong Earthquake Zones in Beijing-Tianjin Area and its Adjacent Regions, Seismology and Geology, Vol. 1, No.1, p.66 (Chinese).
- (14) Xu Shaoxi, Shen Peiwen, (1980). Some Features of Earthquakes Distribution Around Beijing and Crustal Buckling, Acta Seismologica Sinica, and Vol.2, p.153, (Chinese).
- (15) Song Liangyu and others, (1980). Stochastic Models For Earthquake Occurrence, Acta Seismologica Sinica, Vol. 2, No.3, p.281 (Chinese).
- (16) B.K. McGuire, T.P. Barnhard, (1965). Non-stationary Estimates of Seismic Hazard Using the Chinese Earthquake Catalog, 3WCBE, Vol. 1, p.347.

Table 1

cycle in term of years								
Acc. % g	10		25		50		100	
	Bei.	Cal.	Bei.	Cal.	Bei.	Cal.	Bei.	Cal.
≥5	28 (56)	65	56 (87)	92	81 (98)	99	93 (99)	99
≥10	13 (33)	37	29 (64)	70	49 (87)	88	74 (97)	98
≥15	6 (20)	19	14 (42)	41	25 (66)	64	44 (88)	87
≥20	3 (11)	10	7 (39)	23	13 (45)	40	24 (69)	63
≥25	1.3 (6.5)	5	3.2 (15)	12	6.3 (28)	22	12 (49)	37
≥30	0.6 (3.3)	2.5	1.5 (8)	5.5	3 (15)	10	6 (28)	19
≥35	0.15 (1.6)	1.0	0.4 (4)	2.5	0.7 (7.6)	4.4	1.4 (15)	8.7

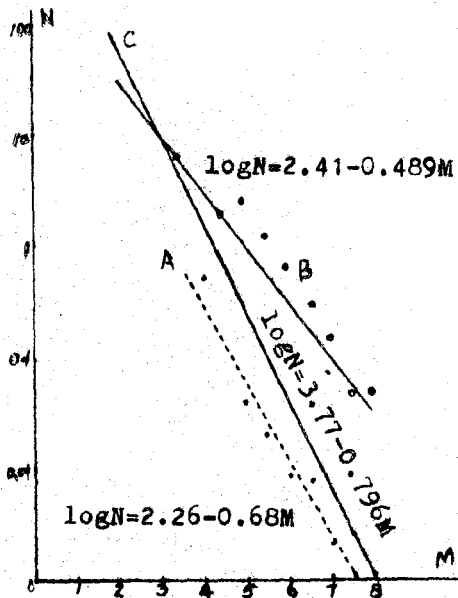


Fig. 1 The relations between magnitude and frequency in Beijing area

Note: 1. The black dots indicate the magnitude-frequency relations calculated according to the historical seismic records between 1057-1977, the small hollow circles connote that relations calculated according to the instrumental data between 1959-1979.
 2. The data from Geo-physics Institute of the State Seismological Bureau.

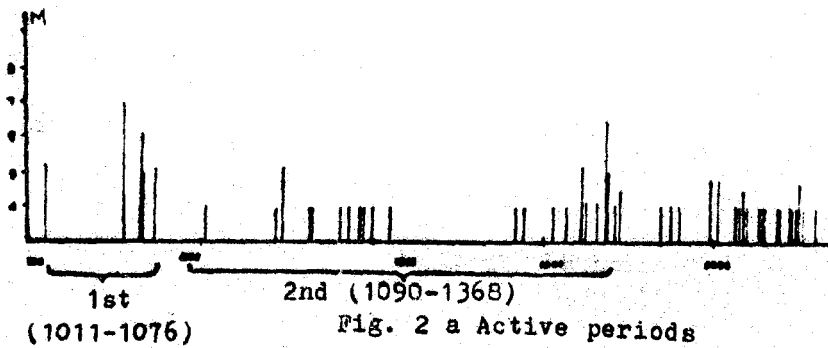


Fig. 2 a Active periods

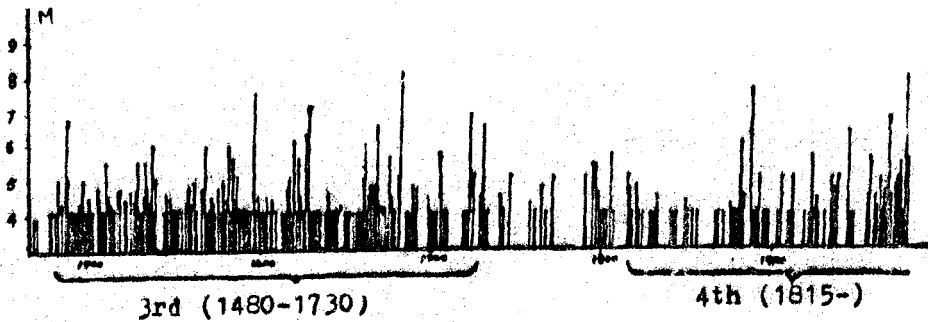


Fig. 2 b Active periods

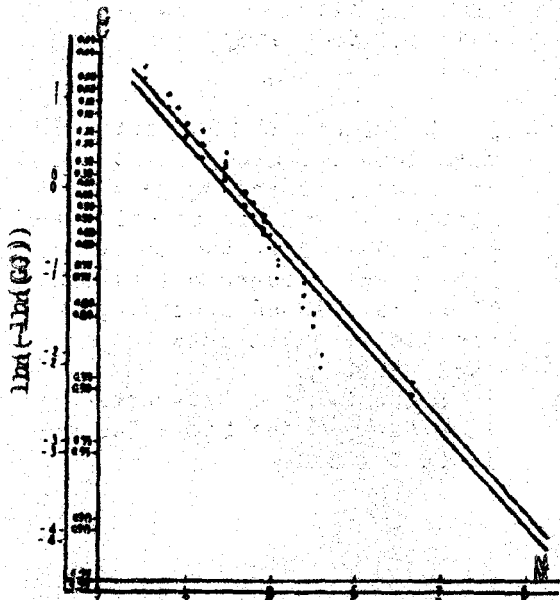


Fig. 3 Results of the extrem value statistics over the last 23 years

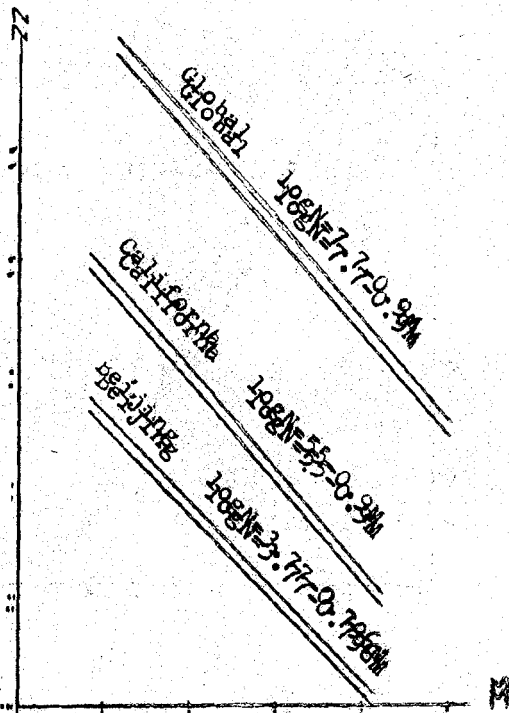


Fig. 5 The annual average rate of occurrence in the world; California U.S.A.; and Beijing Area

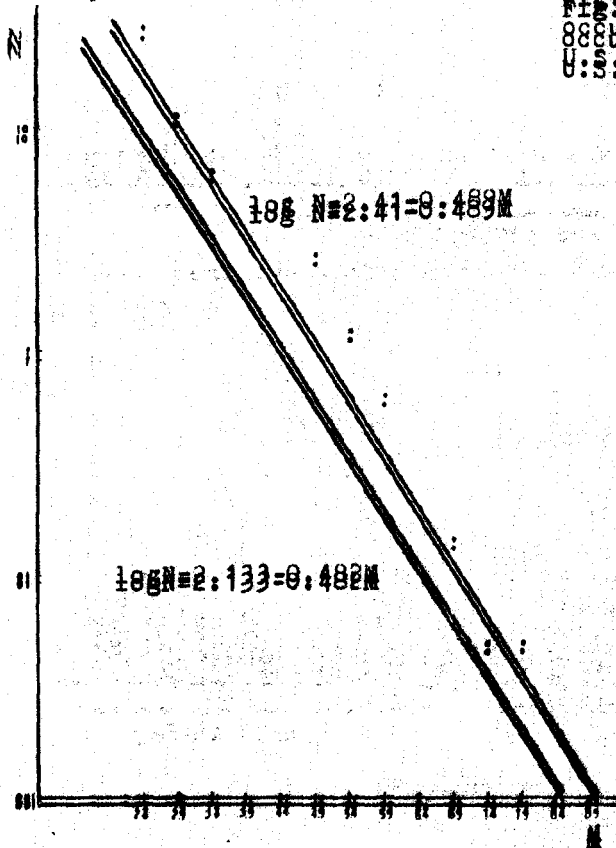


Fig. 4 The Magnitude-frequency statistics relations of Beijing and its surrounding area (Gutenberg Method for 1959-1979; the extrem value method for 1957-1979)

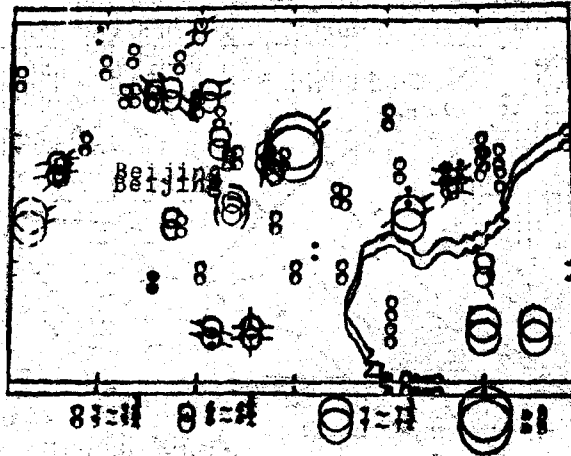


Fig: 6 Map of distribution of large earthquake epicentres in the Beijing area

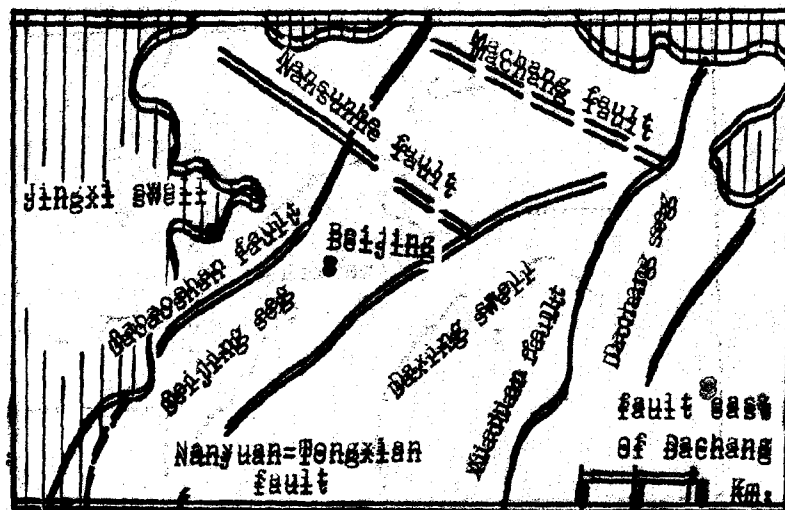


Fig: 7 Map of geological structures in the Beijing Area

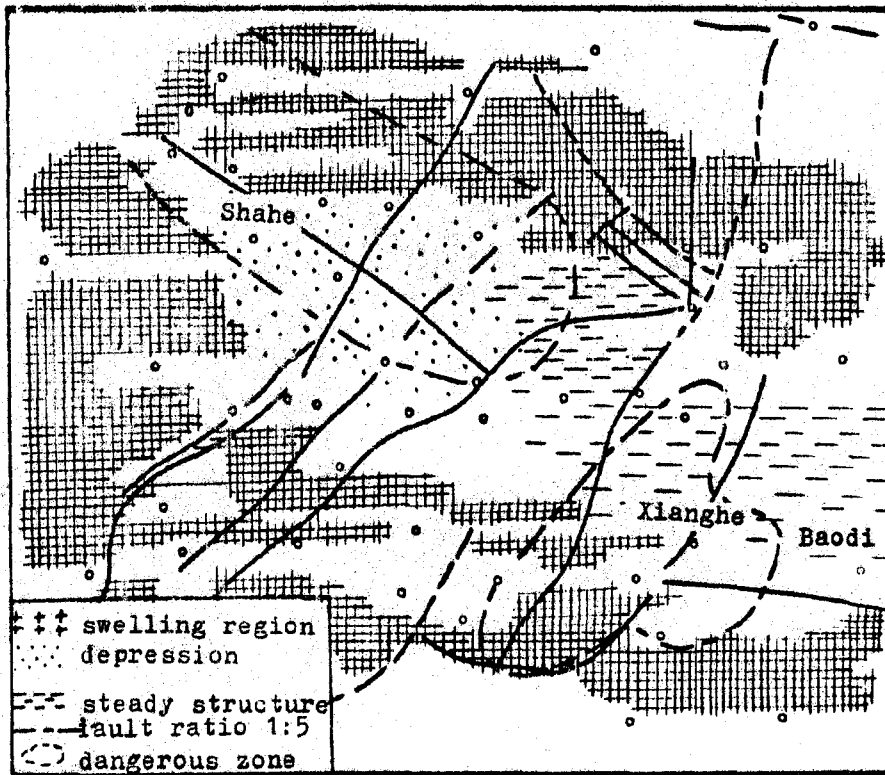
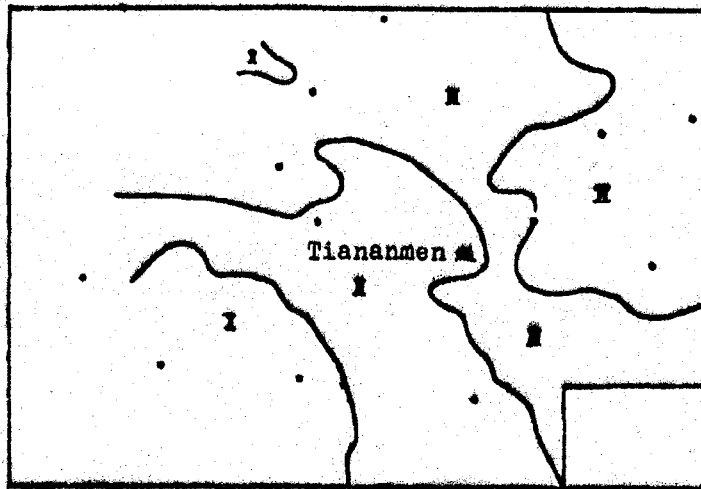


Fig. 8 Modern swells and depression and risk zones in Beijing Plains



Note: I zone: Max. acc. > 200 gals; II zone: Max. acc. = 150-200 gals; III zone: Max. acc. = 100-150 gals

Fig. 9 Map of zones of different maximum accelerations of ground motion

SITE RESPONSE AND INTERACTION ANALYSIS

by John Lysmer¹

ABSTRACT

The significance of the spatial and temporal variation of seismic free-field motions on soil-structure interaction is discussed. It is concluded that the only free-field motions which influence the seismic response of structures are those within the volume excavated for the structure and that the proper determination of the variation of the free-field motions within this volume is the most important part of any soil-structure interaction analysis. This variation cannot be chosen arbitrarily but must satisfy certain criteria imposed by the laws of physics.

It is the aim of this paper to establish what the above criteria are and what they tell us about how to specify the seismic environment for a seismic soil-structure interaction analysis. The discussion will show that for most cases it can be assumed that the seismic environment consists of vertically propagating waves and that the most appropriate point at which to specify the control motion is at a free ground surface.

¹Professor of Civil Engineering
University of California, Berkeley, California, U.S.A.

INTRODUCTION

In order to perform a seismic soil-structure interaction analysis of a structure on a given site it is necessary to define the seismic environment on the site prior to construction. Thus, it is important to identify exactly what must be known about the seismic environment in order to proceed with the interaction analysis, and also, to identify which part of this information can realistically be obtained from our data base of seismic records.

The latter exercise will show that our ability to obtain the required data is very limited and that for a foreseeable future much of this data must be estimated. Such estimates must depend on many factors such as earthquake magnitude, source mechanism, propagation path and local site conditions. Furthermore, and this is the major point to be discussed in this paper, the spatial and temporal variations of seismic motions must, at least locally, satisfy the laws of mechanics. These laws impose severe restrictions on which types of motions can exist on a given site. The restrictions can be determined by local site response analyses and must be considered when specifying the seismic environment.

A good theoretical understanding of the nature of the above restrictions can be of tremendous help in defining appropriate seismic environments for soil-structure interaction analysis and may in many cases lead to simplification of such analyses. On the other hand, a poor understanding of the physical requirements may lead to completely unrealistic design motions. It is the aim of this paper to illustrate the above points.

THE INTERACTION PROBLEM

The basic problem of soil-structure interaction is illustrated in Fig. 1. It involves the determination of the motions of one or more structures at a given site from a knowledge of a given motion (the control motion) at a specified point (the control point) of the site prior to construction (the free field).

A complete soil-structure interaction analysis for any structure must necessarily consist of two distinct parts; a site response analysis and an interaction analysis. Unless the nature of the seismic wave field into which the structure is being placed is known with a reasonable degree of accuracy, there is no way in which the resulting interaction of the structure with the soil deposit and the wave field can be determined.

The site response analysis involves the determination of the temporal and spatial variations of the free-field motions. The interaction analysis involves the determination of the motions of a structure placed in the above seismic environment. These are different types of problems but each needs to be addressed to determine a solution to the soil-structure interaction problem.

Each of the above problem types can in principle be formulated in terms of continuum models or discretized models, and it is not possible here to describe all of the possible forms of equations of motion which have been proposed. It is, however, useful for a better understanding of the nature of and the connection between the two problem types to consider

the equations of motion for the three linear models shown in Fig. 2. The models are identical in the sense that all are of the finite element type and all are spanned by the same finite element mesh. Also, all masses and stiffnesses are the same, except that the structural part of the model shown in Fig. 2(b) has no stiffness and mass, and that for this model the structural nodes above ground level are assumed to be fixed in space (actually these points can be given any specified motion without loss of generality).

Since the fixed nodes have no influence on the motion of the ground Fig. 2(b) represents a free-field site response problem. It has the equation of motion

$$[M_f]\{\ddot{u}_f\} + [C_f]\{\dot{u}_f\} + [K_f]\{u_f\} = \{Q_f\} \quad (1)$$

where $[M_f]$, $[C_f]$, $[K_f]$ are the mass, damping, and stiffness matrix, respectively, for the free field, and $\{u_f\}$ is a vector containing the nodal point displacements. Since the source of excitation is outside the model the load vector $\{Q_f\}$ has non-zero elements on the external boundary only. Particular solutions to the equation of motion, Eq. (1), can be obtained by site response analysis as described below and it will here be assumed that a free-field solution is available. Thus $\{u_f\}$ and $\{Q_f\}$ are known.

Figure 2(a) represents the corresponding interaction problem. The total displacements can be written

$$\{u\} = \{u_f\} + \{u_i\} \quad (2)$$

where $\{u_f\}$ are the known free-field displacements and $\{u_i\}$ are the interaction displacements. Assuming that the external boundary is very far away from the structure the equation of motion for the interaction problem is

$$[M]\{\ddot{u}\} + [C]\{\dot{u}\} + [K]\{u\} = \{Q_f\} \quad (3)$$

where $\{Q_f\}$ is the same load vector as in Eq. (1) and $[M]$, $[C]$, and $[K]$ are the total mass, damping, and stiffness matrices, respectively. Substitution of Eqs. (1) and (2) into Eq. (3) yields

$$[M]\{\ddot{u}_i\} + [C]\{\dot{u}_i\} + [K]\{u_i\} = \{Q_i\} \quad (4)$$

where

$$\{Q_i\} = ([M_f] - [M])\{\ddot{u}_f\} + ([C_f] - [C])\{\dot{u}_f\} + ([K_f] - [K])\{u_f\} \quad (5)$$

The load vector, $\{Q_i\}$, in Eq. (5), can be computed from the known free-field displacements. It depends only on the difference in properties between the structure and the excavated soil. Thus $\{Q_i\}$ has non-zero elements only at the structure and Eq. (4) is the equation of motion for the problem illustrated by Fig. 2(c). This problem is well-posed and can

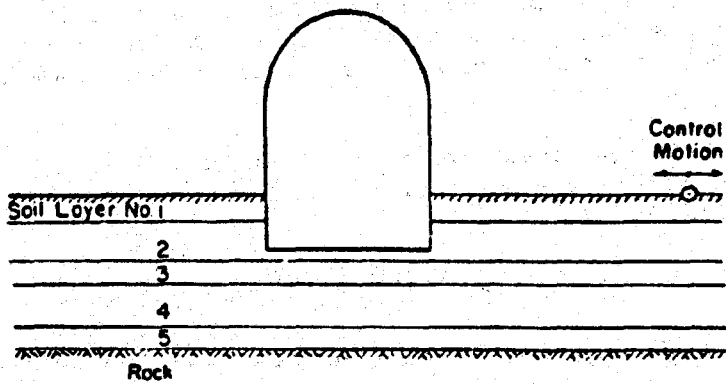
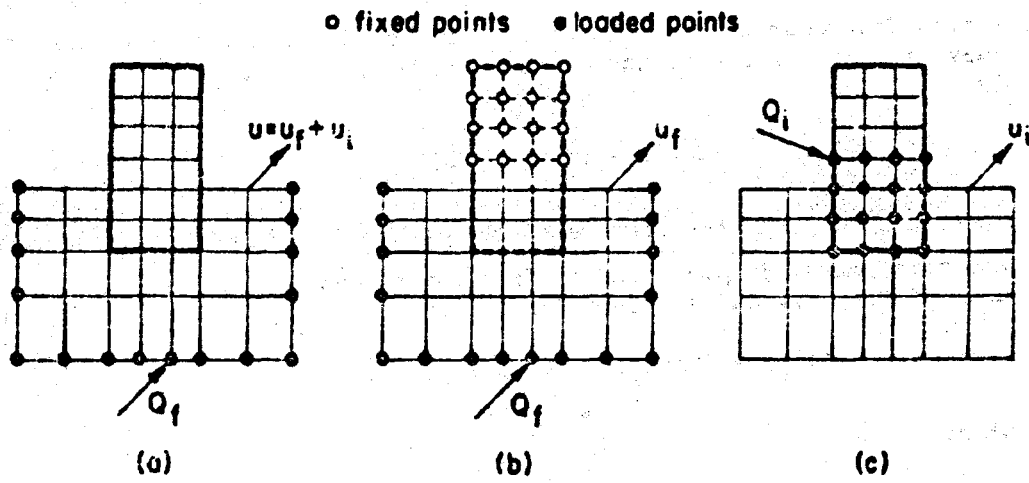


Fig. 1 SOIL STRUCTURE INTERACTION PROBLEM



Interaction Problem = Site Response Problem + Source Problem

Fig. 2 SUPERPOSITION THEOREM FOR INTERACTION PROBLEMS

be solved for the interaction displacements, $\{u_i\}$. The total displacements for the soil-structure interaction problem can be found by superposition as indicated by Eq. (2).

Equations (2) and (4) remain valid even as the distance to the boundary goes to infinity and the mesh size shrinks to infinitesimal dimensions. Hence, the above formulation can be extended to continuum mechanics and three dimensions.

The above formulations reveal three important characteristics of the soil-structure interaction phenomenon:

1. The only free field ground motions which are of importance for the interaction phenomena are those within the volume to be excavated for the embedded part of the structure.
2. For the embedded structures the amount of interaction depends on the difference in mass and stiffness between the structure and the volume of excavated soil, see Eqs. (4) and (5). This implies that embedment of structures will usually lead to smaller interaction effects.
3. Soil-structure interaction analysis implies the use of superposition, see Eq. (2). Thus true nonlinear analyses may not be possible.

The first observation has far reaching consequences; especially for embedded structures on relatively soft sites since, for such sites, both theory and observation indicate that the free-field motions vary significantly with depth. This implies that the site response analysis is an important, and in the opinion of the writer perhaps the most important, part of a soil-structure interaction analysis.

THE SITE RESPONSE PROBLEM

Site response problems involve the determination of the temporal and spatial variation of motions within a site. In principle, these motions can be determined from a large model which includes the source of the earthquake. However, in practice the source parameters and the regional geology cannot be determined in sufficient detail to solve this problem with a high degree of accuracy in the frequency range of interest for design. Thus, current methods of site response analysis attempt to predict the above variation of motions locally from a single specified control motion at some control point within the site. This problem is mathematically ill-posed and unique solutions can be obtained only by the introduction of assumptions regarding the geometry of the site and the nature of the wave field causing the control motion. In practice, consistent solutions can be obtained only for horizontally layered sites. Possible wave patterns include: vertically propagating or inclined plane body waves, and horizontally propagating surface waves. Only the case of vertically propagating shear waves can currently be solved by truly nonlinear methods.

Control Motion and Control Point

The inherent problem in site response analysis is the choice of wave field to be used in the analysis and it is therefore natural to classify and discuss the different available methods according to the type of wave field assumed. However, before doing so it should be mentioned that the choice of an appropriate control motion and control point is just as, and in most cases, more important than the choice of wave field.

The control motion should be chosen with due respect to observed relations between earthquake magnitude, epicentral distance, maximum acceleration, duration, frequency content, see Idriss (1978) and Ref. 1, and the site-dependent characteristics established by Hayashi et al., (1971), Seed et al. (1976a, 1976b), Faccioli (1978), and Ref. 1.

Except for the obvious case in which the control motion is an observed record at the control point, the preferable control point is a point either at the ground surface or, as discussed below, at an assumed rock outcrop at the depth of which the motion is specified. This is so because most of our data base of strong motion earthquake records from which the control motion has to be estimated was obtained at surface stations and, even more important, because the frequency content of motions at points below the ground surface is strongly influenced by reflections at the free surface, the major effect being the suppression of certain frequencies by wave interference. Thus the specification that the control motion at depth should be a broad-band spectrum or a motion recorded at another site or depth may result in completely unrealistic computed motions for the site.

Choice of Wave Type

With the control motion and control point fixed, the solution to the site response problem depends entirely on the nature of the wave field producing the ground surface motions. This wave field may consist of many components including:

- (1) some Rayleigh waves
- (2) some Love waves
- (3) some plane vertically propagating waves
- (4) some plane body waves inclined at an angle to the vertical
- and (5) some other wave types such as spherical and cylindrical waves which are usually not considered.

At the present time seismologists cannot advise engineers in sufficient detail on the relative contents of the different possible wave forms which make up the surface motion. Thus, even though soil-structure interaction analyses can be performed for an arbitrary wave field, in practice, such analyses cannot be made due to lack of data on the characteristics of the wave field involved.

Under these conditions, a typical engineering approach is to make analyses for extreme cases of possible wave fields, e.g., for a motion

represented by all Rayleigh waves or for a motion represented entirely by a system of body waves, and to determine the influence of the motion specification on the results of the analysis. If the differences are small, then precise specification of the components of the wave field is considered unnecessary. If the differences are large, then increasing efforts must be made to determine even a crude assessment of the relative components of different wave types, or alternatively, conservative choices of wave components may have to be made for different parts of the analysis. It is important therefore to examine the characteristics of the different wave forms which might contribute to the surface control motion.

Horizontally Propagating Waves

For horizontally layered sites it is relatively easy to set up linear methods of analysis for horizontally propagating waves. However, many possible choices of wave patterns exist (inclined body waves at different angles of incidence, different modes of surface waves, etc.) and it is currently impossible to determine from available seismological data the exact contributions of each wave type to earthquake motions near the surface in the frequency range of interest to earthquake engineers. However, some estimates have been made (Trifunac and Brune, 1970; Randall, 1971; Chandra, 1972; Nair and Emery, 1975; Liang and Duke, 1977; and Toki, 1977). These estimates involve considerable uncertainties however; in view of these uncertainties analysis of site response for motions represented only by horizontally propagating waves is mainly an academic exercise based on assumed data. Nevertheless, as will be discussed below, some practical conclusions can be drawn from such analyses.

The free-field motions caused by horizontally propagating waves will be discussed in three parts: Surface waves are discussed immediately below, inclined body waves are discussed after the section on vertically propagating waves and, finally, the three wave types are discussed together in a section on motions at shallow depths.

Surface Waves

Rayleigh waves in a perfect elastic half-space are well-known and the theory for these are given in standard textbooks, e.g., Richart et al., (1970). However, for obvious reasons soil dynamics analysts are much more interested in surface waves in multi-layered systems, Thomson (1950), Haskell (1953), Ewing et al. (1957). Two types of waves may occur in such systems: Love waves, in which the motions are horizontal and perpendicular to the direction, x , of wave propagation, and Rayleigh waves which involve both vertical and horizontal motions in the vertical xz -plane. For plane harmonic waves the displacement fields are of the form:

$$\text{Love waves: } u_y = \sum_{s=1}^{\infty} L_s \cdot h_s(z) \cdot e^{i(\omega t - c_s x)} \quad (6)$$

$$\text{Rayleigh waves: } \left\{ \begin{array}{l} u_x = \sum_{s=1}^{\infty} R_s \cdot f_s(z) \cdot e^{i(\omega t - k_s x)} \\ u_z = \sum_{s=1}^{\infty} R_s \cdot g_s(z) \cdot e^{i(\omega t - k_s x)} \end{array} \right\} \quad (7)$$

where ω and t are the frequency and time, respectively, and L_s and R_s are unknown mode participation factors. The infinite sets of wave numbers, c_s and k_s , and mode shapes, $h_s(z)$, $f_s(z)$, and $g_s(z)$, may in principle be determined by methods developed by Thompson (1950) and Haskell (1953). The wave numbers are directly related to the phase velocities of the different wave modes through $V_L = \omega/c$ and $V_R = \omega/k$. Thus the fundamental problem of site response analysis with surface waves is to determine the infinite set of factors L_s and R_s from a single given amplitude of the control point. This is clearly an ill-posed problem and solutions can only be obtained by further assumptions, the most common of which is to assume that only the fundamental Rayleigh or Love mode, corresponding to $s = 1$, exists. For undamped systems the frequency-dependent phase velocity and mode shape can be found by the Thomson-Haskell method and the amplitude L_1 or R_1 may be determined from the control motion.

Continuum analyses are possible for the case of viscoelastic layers over an undamped half-space (Ewing et al. (1957), Boncheva (1977)). However, for this case it is more practical to first discretize the semi-finite system by the use of finite elements as proposed by Lysmer (1970) and Waas (1972) for Rayleigh waves and Waas (1972), Lysmer and Waas (1972) for Love waves. Only Rayleigh waves will be discussed here. The theoretical model is shown in Fig. 3. It involves the assumption of a linear variation of displacements between layer interfaces and the existence of a stationary rigid base at some finite depth. If this depth is chosen to be considerably larger than the wave length of the Rayleigh waves of interest, a half-space is simulated by this model.

For an N-layer system these assumptions reduce the equation of motion for the layered system to a quadratic eigenvalue problem:

$$([A]k^2 + [B]k + [C] - \omega^2[M])\{v\} = \{0\} \quad (8)$$

where $[A]$, $[B]$, $[C]$ and $[M]$ are simple $2N \times 2N$ matrices which can be formed from the stiffnesses, damping ratios and mass densities of the layered system, and $\{v\}$ is an eigenvector (mode shape) which contains the $2N$ displacement amplitudes of the layer interfaces. The mode shape represents the functions $f_s(z)$ and $g_s(z)$ in Eq. (7). For a given frequency, ω ,

Eq. (3) can be solved by methods developed by Waas (1972). The solution consists of $2N$ possible wave numbers, k_s , and associated mode shapes $\{v\}_s$ and, in analogy with Eq. (7), the general solution to the equation of motion may be expressed in the form:

$$\{u\} = \sum_{s=1}^{2N} R_s \{v\}_s \cdot e^{i(\omega t - k_s x)} \quad (9)$$

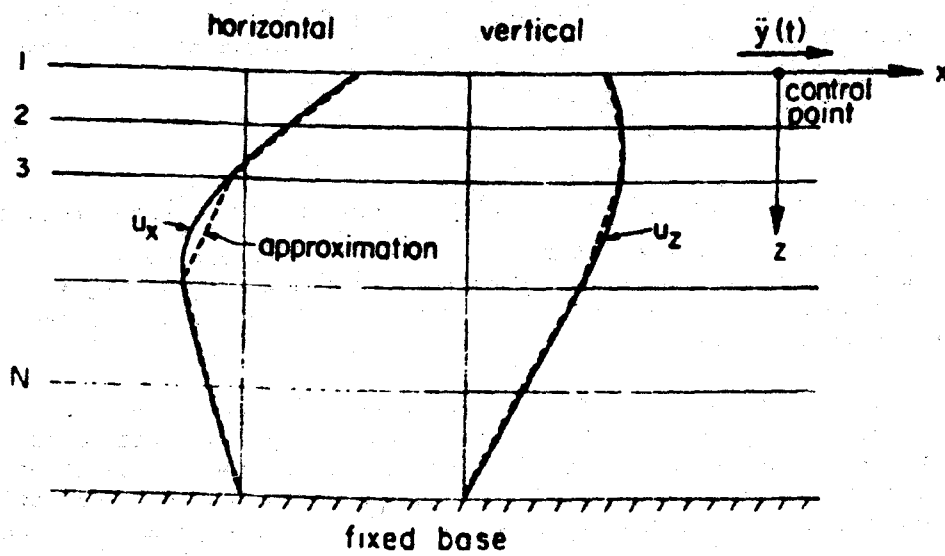


Fig. 3 TYPICAL SOIL PROFILE AND RAYLEIGH WAVE MODE SHAPE

For a damped system all the wave numbers will be complex with negative imaginary parts. Hence, Eq. (9) can also be written

$$\{u\} = \sum_{s=1}^{2N} e^{i\text{Im}(k_s)x} \cdot R_s \{v\}_s \cdot e^{i(\omega t - \text{Re}(s_s)x)} \quad (10)$$

which represents a system of generalized Rayleigh waves (modes) which propagate in the positive x-direction, each with its own mode shape, $\{v\}_s$, phase velocity, $\omega/\text{Re}(k_s)$, and decay factor, $\exp[2\pi\text{Im}(k_s)/\text{Re}(k_s)]$, per wave length, $\lambda = 2\pi/\text{Re}(k_s)$. Experience with the method has shown that most of the Rayleigh modes decay extremely rapidly in the frequency range of interest to earthquake engineers and only a few terms of Eq. (9) need therefore be considered. If it is assumed that only the fundamental mode (defined as the mode with the largest value of $\text{Re}(k_s)$) is present, Eq. (9) reduces to

$$\{u\} = R_1 \cdot \{v\} e^{i(\omega t - k_1 x)} \quad (11)$$

and the mode participation factor, R_1 , can be determined at each frequency from the amplitude of the control motion at say the surface at $x = 0$. Transient motions can be handled by Fast Fourier Transform techniques. This requires that the eigenvalue problem in Eq. (8) be solved for each frequency of the transform.

The above method has been used by Chen et al. (1981) to determine possible Rayleigh wave motions in several sites. A typical example of these computations is shown in Fig. 4. The site consisted of 128 ft of medium dense sand overlying a rock formation. A horizontal control motion with the maximum acceleration 0.25 g was specified at the ground surface (distance 0). The response spectrum of the control motion is shown in Fig. 4 (top curve in upper left graph). The computational model consisted of 18 layers in the sand plus 10 thicker layers in the rock.

The equivalent linear method was used to simulate nonlinear effects, i.e. the stiffness and damping ratio in each sand layer were adjusted iteratively to be compatible with the shear stress amplitude developed in the layer. As a result of these iterations the shear wave velocities in the sand profile varied from 621 fps near the surface to 786 fps at the rock interface. Since the average low strain (microseismic) shear wave velocity was about 1150 fps this indicates quite strong nonlinear effects at the excitation level specified. The damping ratio converged to an average value of about 10% with slightly lower values near the ground surface.

Figure 4 shows surface response spectra for a Rayleigh wave field propagating from left to right. It is readily apparent from these spectra that the high frequency components of the wave field are rapidly damped out as a result of the relatively high damping ratio in the sand and in fact, at a distance of a few hundred feet, virtually all motions with frequencies higher than 2 Hz have decayed to insignificant values. Similar results have been obtained for other soil profiles. Since most soil

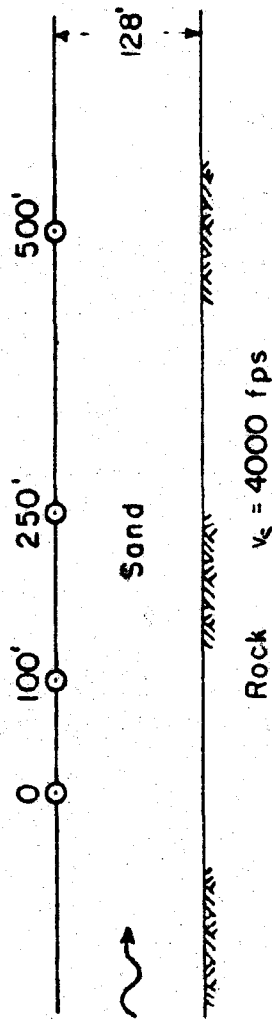
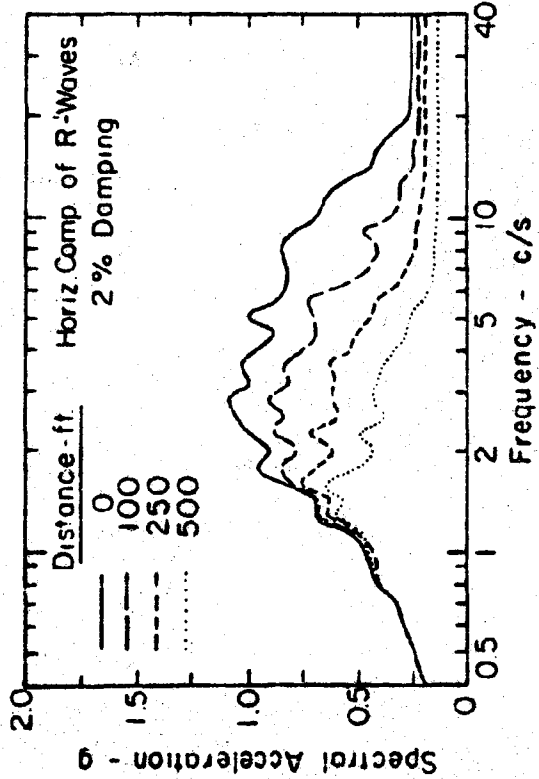
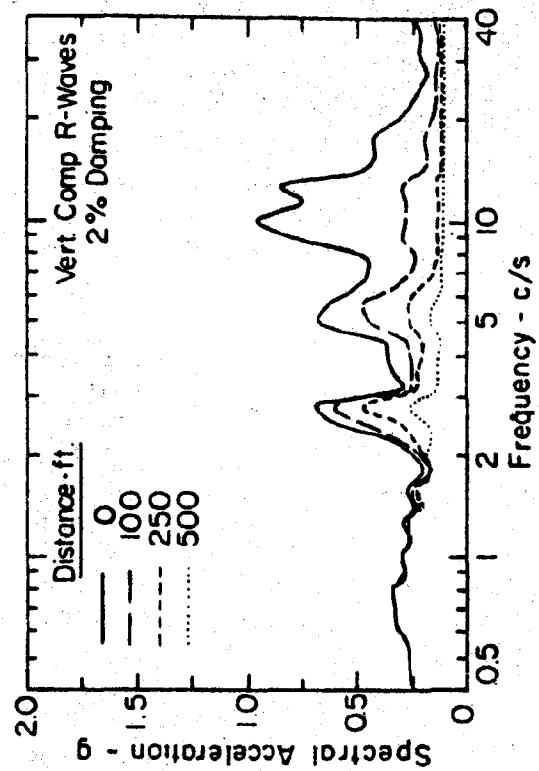


Fig. 4 ATTENUATION OF RAYLEIGH WAVE CHARACTERISTICS WITH DISTANCE TRAVELLED THROUGH SOIL DEPOSIT

deposits extend horizontally for thousands of feet, it is thus unrealistic to expect that a significant part of the high frequency components of strong motions in such deposits could result from horizontal propagation of fundamental Rayleigh waves. Similar results have been obtained for Love waves in soil sites.

The above theoretical observation is confirmed by the fact that, as far as the writer can ascertain, the seismological literature contains no reports of observation of strong Rayleigh waves at frequencies higher than 2 Hz.

The only practical conclusion which can be reached from the above observations is that fundamental surface waves need not be considered in the seismic design of relatively stiff structures of small lateral extent on soil sites.

Such motions may be important for structures with very low natural frequencies, say below 1 Hz, and for structures on rock where the much lower damping and higher wave velocities could lead to lower rates of attenuation of high frequency surface waves in the horizontal direction. However, even in rock surface waves have not been observed in the frequency range above 2 Hz. Furthermore, soil-structure interaction effects are likely to be small for structures built on rock sites.

In summary, fundamental surface waves are not likely to be of significance for the design of relatively stiff structures of small lateral extent, say nuclear power plants.

Higher-order Surface Waves

The fundamental Rayleigh mode defined above is, as shown by Lysmer (1970), identical to the fundamental mode considered by seismologists in layered systems overlying a deformable half space. The rest of the terms of Eq. (10) represent higher-order Rayleigh modes (in the terminology of seismologists) and body waves. These modes will have longer wavelength and will propagate faster than the fundamental mode which by definition has the shortest wavelength and thus the lowest phase velocity. While most of these higher modes can be neglected, since they decay rapidly in the direction of wave propagation, others may decay less rapidly than the fundamental mode. This phenomenon occurs only at relatively high frequencies on sites with a marked increase in stiffness with depth; say a sand profile over rock. These low-decay modes could conceivably contribute significantly to the motion at a surface control point. However, studies by Chen et al. (1981) have shown that such modes, when they occur, cause near surface motions which are similar to those caused by vertical or slightly inclined body waves. That this is so is not surprising when one considers the propagation mechanism of these modes. The very facts that the waves travel at high velocities and decay slowly indicate that the major part of the energy propagation occurs in deeper layers with high body wave velocities and low damping. This immediately implies that insignificant amounts of energy are propagated horizontally in the softer surface layers or, in other words, that the higher frequency motions in the surface layers are maintained through nearly vertical energy propagation through a mechanism similar to that of slightly inclined body waves. The result is that the upper parts of mode shapes, i.e. the variation of displacements

with depth, are virtually identical to those found in analyzing vertically propagating or slightly inclined body waves.

Thus, in practical calculations the effects of higher-order surface wave components can be considered by assuming a certain content of slightly inclined or vertical body waves in the control motion.

Vertically Propagating Waves

The great majority of methods for site response analysis use Kanai's (1952) assumption of vertically propagating shear waves. This assumption leads to simple one-dimensional mathematical models for horizontally layered systems and has, partly because of the similarity between motions caused by different wave fields, led to remarkable success in predicting the major features of site response during earthquakes, especially since the analytical procedure was modified by introduction of the equivalent linear method by Seed and Idriss (1969).

Linear site response problems with vertically propagating waves can be solved by a multitude of numerical techniques which are described in texts on soil dynamics, e.g., Desai and Christian (1976). The most efficient method for computing free-field motions from a specified surface control motion appears to be the complex response method used in the program SHAKE, Schnabel et al. (1972). With these methods it is currently possible to analyze any layered viscoelastic soil system overlaying a viscoelastic half-space. The control motion can be specified at the ground surface, at any depth in the soil deposit or as an outcrop motion. Non-linear effects can be approximated by the equivalent linear method.

Recent efforts have been directed towards the development of true non-linear methods of analysis. Several methods have been proposed for performing nonlinear total stress analysis of site response problems with vertically propagating shear waves. The most important of these are: The method of characteristics, Streeter et al. (1974), Idriss et al. (1976), Taylor and Larkin (1978); the finite difference method, Joyner (1977); and implicit integration schemes, Martin (1975). In addition several methods of effective stress analysis have been proposed, Ghaboussi and Dikmen (1978), Zienkiewicz et al. (1978), Finn et al. (1977), Liou et al. (1977), and Martin and Seed (1979), which can predict the pore pressure build-up in saturated sands during seismic excitation.

Comparative studies of ground motion characteristics computed by the equivalent linear method and non-linear methods show relatively small differences except where motions are very strong and soils relatively weak. Thus the development of non-linear analysis techniques has further confirmed the fact that equivalent linear methods are sufficiently accurate for virtually all practical purposes in evaluating site response for soil-structure interaction analyses.

A major problem of current methods of nonlinear site response analysis is a limitation on the location of the control point. It is not currently possible to specify the control motion at the surface, and specification at a deeper point within the profile is, for reasons to be discussed in the following section, not desirable. However, the motion may be specified at a deep outcrop. This problem has been solved by Joyner and Chen (1975) for the special case of a layered nonlinear system overlying a uniform linearly

elastic half-space, see Fig. 5(a). Joyner and Chen specify the outcrop control motion, $y(t)$, at the surface of the elastic half-space shown in Fig. 5(b). The horizontal motions in the half-space, Fig. 5(b), are by simple wave theory

$$u_b(z,t) = \frac{1}{2} y(t + z/V_s) + \frac{1}{2} y(t - z/V_s) \quad (12)$$

where V_s is the shear wave velocity for the half-space. In the combined system, Fig. 5(a), an additional downward propagating wave occurs due to reflections from the upper soil layer. Hence the motions in that system are:

$$u_a(z,t) = \frac{1}{2} y(t + z/V_s) + u(t - z/V_s) \quad (13)$$

The function $u(t)$ must be such that: $u_a(0,t) = u_o(t)$, where $u_o(t)$ is the actual motion of $z = 0$. Hence, $u(t) = u_o(t) - 1/2 y(t)$ and

$$u_z(z,t) = \frac{1}{2} y(t + z/V_s) - \frac{1}{2} y(t - z/V_s) + u_o(t - z/V_s) \quad (14)$$

This leads to the following shear stress at $z = 0$

$$\tau_o(t) = \rho V_s \dot{y}(t) - \rho V_s \dot{u}_o(t) \quad (15)$$

where ρ is the mass density of the half-space. Joyner and Chen apply this stress boundary condition at the base of the upper soil column and thus achieve a system which can be analyzed by nonlinear methods and which correctly accounts for the effects of the underlying half-space.

The boundary condition expressed by Eq. (15) may be achieved by the physical model shown in Fig. 5(c). In this model the upper soil column is supported on a Lysmer-Kuhlemeyer (1969) dashpot and excited by a horizontal force at the base proportional to the known outcrop velocity time history.

Inclined Body Waves

Some energy may be arriving at the control point in the form of non-vertically propagating body waves. This includes the effect of the high-order surface wave modes discussed in a previous section.

The response of horizontally layered sites to plane harmonic body waves arriving at a specified incident angle through an underlying elastic half-space has been investigated by several researchers. The fundamental work was done by Thomson (1950) and Haskell (1960, 1962) who developed an efficient matrix method for computing the frequency-dependent transmission coefficients in a layered continuum for incident SH, SV and P-waves. Efficient computer codes for the Thomson-Haskell method were developed by Hannon (1964) and Teng (1967). Silva (1976) extended the Thomson-Haskell method to include damping in the soil layers. With this method it is possible to solve linear or equivalent linear site response problems with inclined body waves for systems consisting of viscoelastic soil layers overlying a uniform undamped half-space, provided the incident angle in the half-space is known. Since no damping is included in the half-space

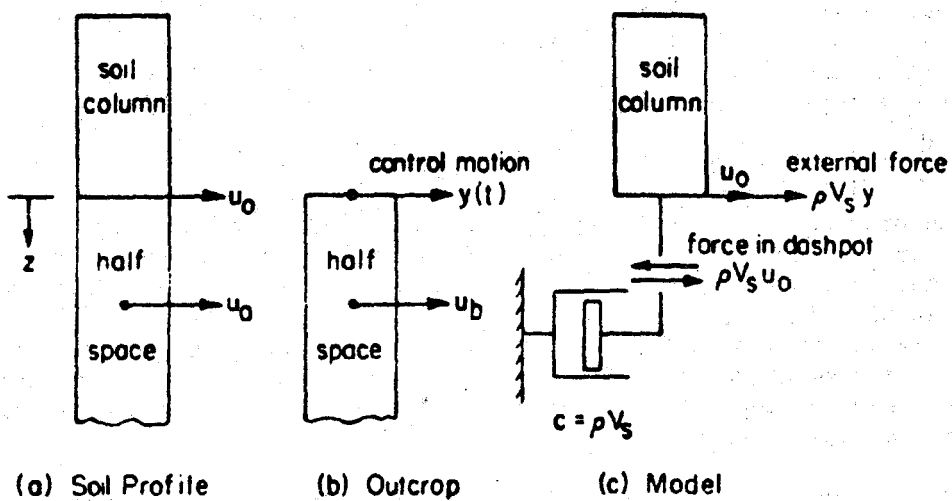


Fig. 5 CONTROL MOTION AT OUTCROP

the resulting surface motions do not decay in the horizontal direction. More recently, Chen et al. (1981) have developed a method which includes damping in the underlying half-space.

Analyses of surface response to inclined body waves have also been made by Joyner et al. (1976), who determined the transfer functions from bedrock to the soil surface for a soil deposit 186 m in depth for shear waves propagating at various angles to the vertical. The results of this study are shown in Fig. 6, and it is apparent that for angles of incidence up to 60°, there is a negligible difference between the motions computed for inclined waves and for vertically propagating waves.

It is reasonable to conclude therefore that the variation of horizontal motions with depth within a soil deposit are for all practical purposes the same, whether they are computed for vertical or inclined directions of propagation within the depth range of interest to engineers. On this basis it is appropriate to use analyses for vertically propagating waves because of their greater simplicity and availability of solutions.

Motions of Shallow Depth

As discussed earlier, only the motions within a relatively shallow depth (the projected depth of embedment) of the free-field will influence the motions of structures. The same discussion also indicates that both the spatial and temporal variation of the free-field motions within this depth are of importance in evaluating soil-structure interaction effects. It is therefore appropriate to discuss in more detail how the amplitude and frequency content of free-field motions vary with depth and in particular how they vary near the free ground surface.

As will be shown in the following, the presence of the strong discontinuity represented by the free ground surface imposes predictable and observable limitations on how horizontal amplitudes and the frequency content of motions vary with depth near the ground surface.

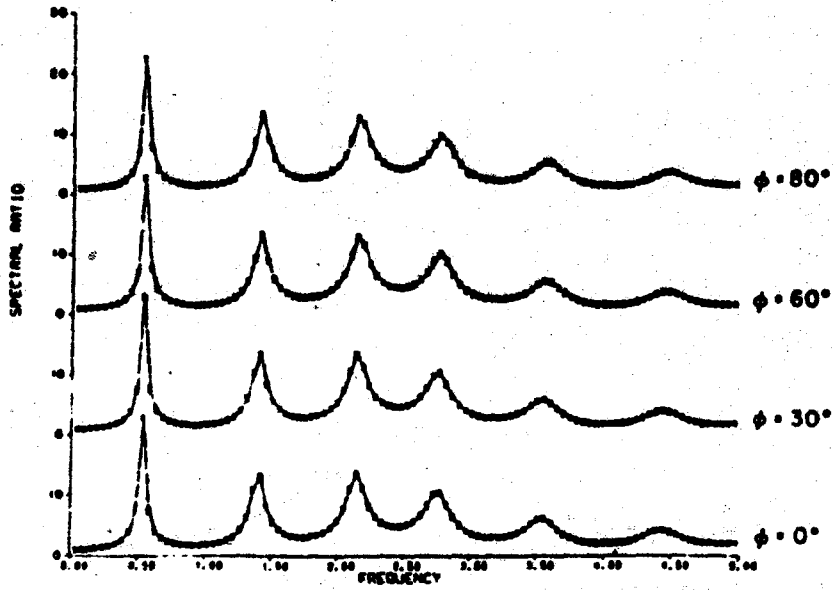
The potential effects of the free ground surface on the amplitude and frequency content of waves at various depths in a uniform deposit is shown in Figs. 7 and 8. Both figures show the variation of amplitude with the dimensionless depth z/λ_s in a perfect half-space, where $\lambda_s = V_s/f$ is the wavelength of shear waves at the frequency, f [Hz], considered.

Figure 7 corresponds to the case of vertically propagating shear waves for which the horizontal amplitude is

$$U = U_0 \cos 2\pi \frac{z}{\lambda_s} \quad (16)$$

and Fig. 8 corresponds to the case of horizontally propagating Rayleigh waves.

The two types of wave fields are obviously quite different. It is remarkable, however, that both the shear wave field and the Rayleigh wave



(c) Computed Horizontal Spectral Ratios Between Surface and 186 m

Fig. 6 INFLUENCE OF ANGLE OF SHEAR WAVE INCIDENCE ON COMPUTED SURFACE RESPONSE

(after Joyner et al., 1976)

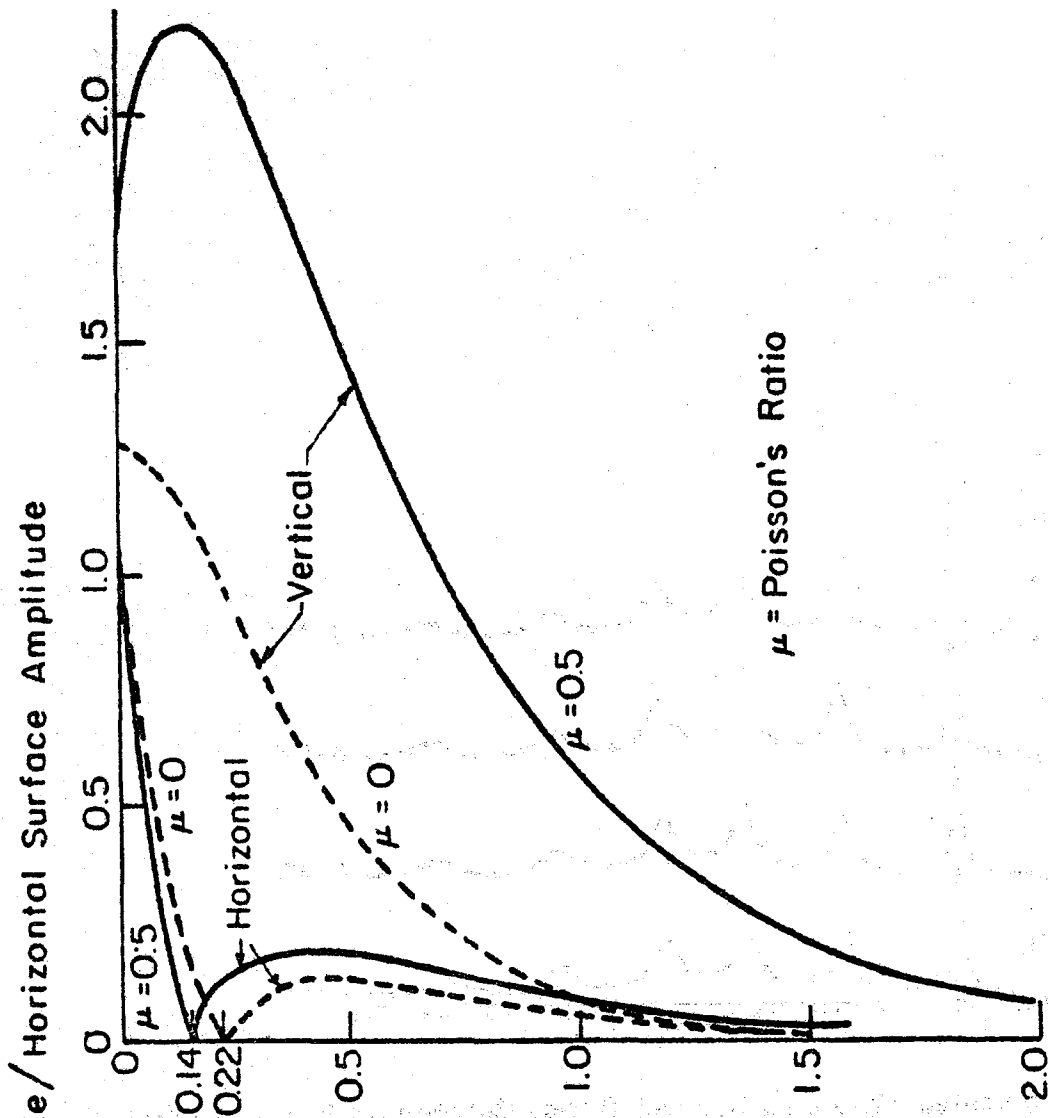


Fig. 8 RAYLEIGH WAVES

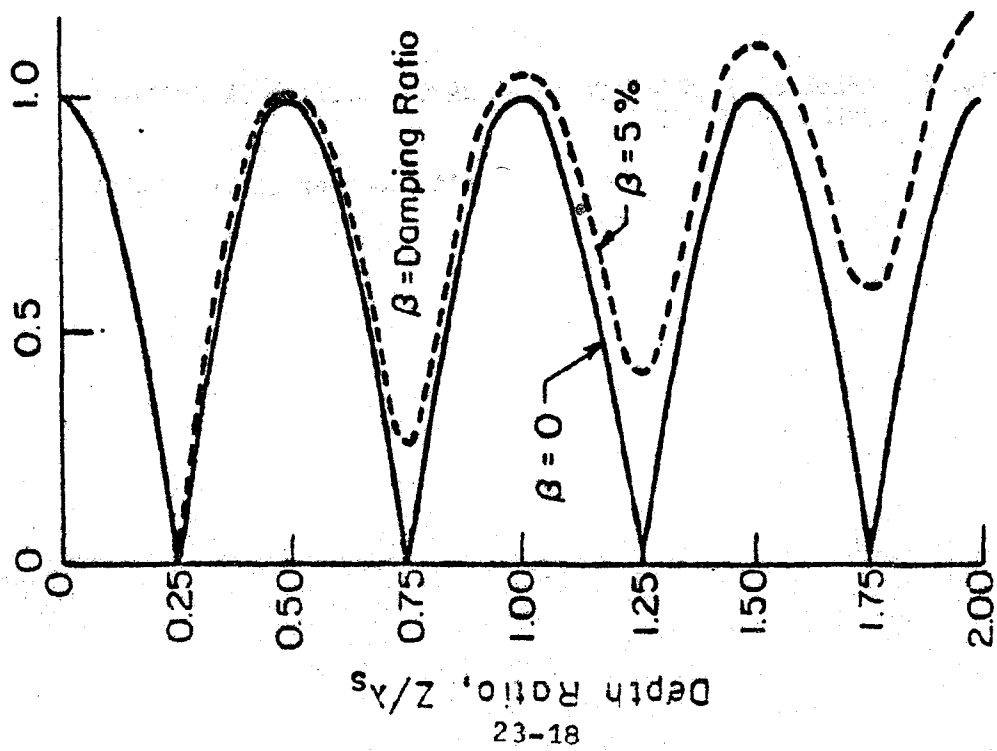


Fig. 7 SHEAR WAVES

field produce monotonically decreasing horizontal displacements within the approximate depth

$$z \approx \frac{1}{4} \lambda_s \quad \text{to} \quad \frac{1}{5} \lambda_s$$

$$\approx \frac{\bar{V}_s}{4f} \quad \text{to} \quad \frac{\bar{V}_s}{5f}$$
(17)

and that all horizontal displacements vanish at this depth. A similar phenomenon occurs for inclined shear waves and for layered soil systems where V_s in Eq. (17) can be replaced by the average shear wave velocity, \bar{V}_s above the depth z . As can be seen from the dotted curve shown in Fig. the existence of material damping does not change the substance of these observations.

Two important conclusions can be drawn from these analyses:

- (1) Any horizontal motion computed (or observed) at the depth z must be deficient of components of the frequency

$$f \approx \frac{\bar{V}_s}{4z} \quad \text{to} \quad \frac{\bar{V}_s}{5z}$$
(18)

i.e., its response spectrum will have a dip at the approximate frequency f , which incidentally is equal to the fixed base natural frequency of the soil column above the depth z . Thus, the only level at which a smooth spectrum can exist is at a free surface, and specifying a control motion with a smooth spectrum at any other depth will, as experience has shown, lead to completely unrealistic results. This free surface can be the actual ground surface or a real or imaginary outcrop; however a smooth spectrum cannot exist within a soil deposit, whether the motions be due to near-vertically propagating body waves or to horizontally propagating Rayleigh waves.

- (2) In a deposit with uniform properties, seismic motions will decrease with depth below the ground surface at least down to the depth

$$z \approx \frac{\bar{V}_s}{4f_{\max}} \quad \text{to} \quad \frac{\bar{V}_s}{5f_{\max}}$$
(19)

where f_{\max} is the highest frequency present in the motion.

This follows directly from Eq. (16) which shows that all components decrease in amplitude within the above depth. Because of variations in soil characteristics with depth this predicted reduction will often extend to depths greater than those indicated by Eq. (19). For a typical soil site, with say $\bar{V}_s = 1000$ fps, and a seismic environment, with say

$f_{\max} \approx 20$ Hz, the above formula shows that a significant reduction in the free field motion may occur within the upper 10 ft (or deeper if the

predominant frequency of the control motion is lower) of the site. Thus in view of the discussion in connection with Eq. (4), even relatively shallow embedment may significantly influence the seismic response of structures on soft sites and both the embedment and the reduction in the amplitude of the seismic environment with depth should be considered in a rational interaction analysis.

Substitution of realistic values of V_s and f into Eq. (17) will show that z is typically larger than 20 ft for soil sites and 60 ft for rock sites. Thus typical structures experience only the upper part ($z/\lambda_s < 0.2$) of the motions shown in Figs. 7 and 8. In this "shallow" depth range horizontal motions produced by any seismic environment with the same horizontal surface control motion are quite similar. It is therefore to be expected that the horizontal motions produced at points below the ground surface during earthquakes will be relatively independent of the type of wave field producing the motion.

The above observations were made for motions in a uniform half-space. For layered systems, the stiffness of which usually increases with depth, calculations have shown that the similarity between motions produced at shallow depth by different types of wave fields is even more pronounced. This is so because, just as for the higher-order surface waves discussed above, the upper parts of the mode shapes of fundamental surface waves in layered systems tend toward the mode shapes produced by vertically propagating or slightly inclined body waves.

An interesting example of these effects in a 600 feet deep soil deposit overlying a rigid half-space is shown by the analytical results presented in Figs. 9, 10, and 11. To study the response at different depths in this deposit, analyses were made using vertically propagating shear wave theory for 15 different excitation records. In eight of the analyses, existing records obtained on deep soil deposits were scaled to have a peak acceleration of 0.20 g and considered to be developed at the ground surface. The distribution of acceleration with depth and the frequency characteristics of the motions developed at depths of 40 and 76 ft were then determined by deconvolution analyses.

For the same soil deposit, a second study was made in which seven records representative of rock motions were used as base excitation and the base motions were scaled in each case to produce a peak acceleration of 0.20 g at the ground surface. In spite of the fact that specification of control motions at depth is not recommended, see above; for this case there was surprisingly little difference in the computed distribution of motions whether the excitation was applied at the ground surface or whether it was applied at the base of the soil deposit. The results of the two sets of studies were analyzed statistically to determine the mean acceleration distribution separately for the deconvolution analyses and for the base input analyses. The results of this analysis are shown in Fig. 9. On the whole the results are remarkably similar, all showing a marked drop in peak acceleration within the upper 100 ft.

The response spectra for the motions developed at depths of 40 and 76 ft were also computed and analyzed statistically for the two different groups. The 84 percentile spectra for surface motions, motions at 40 ft depth and motions at 76 ft depth for the deconvolution analyses are shown

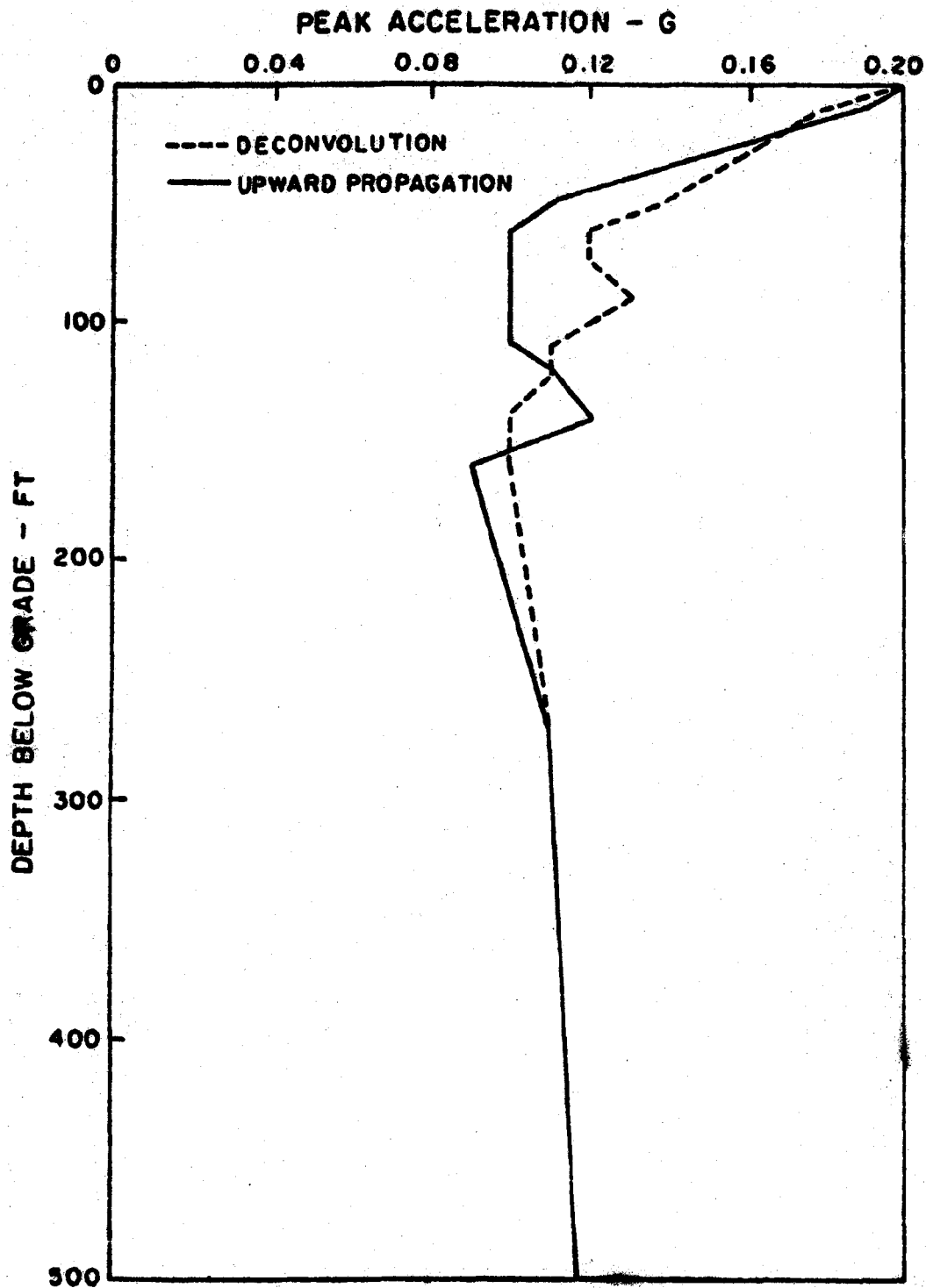


Fig. 9 VARIATION OF MEAN PEAK ACCELERATION WITH DEPTH OF DECONVOLUTION AND UPWARD PROPAGATION ANALYSES

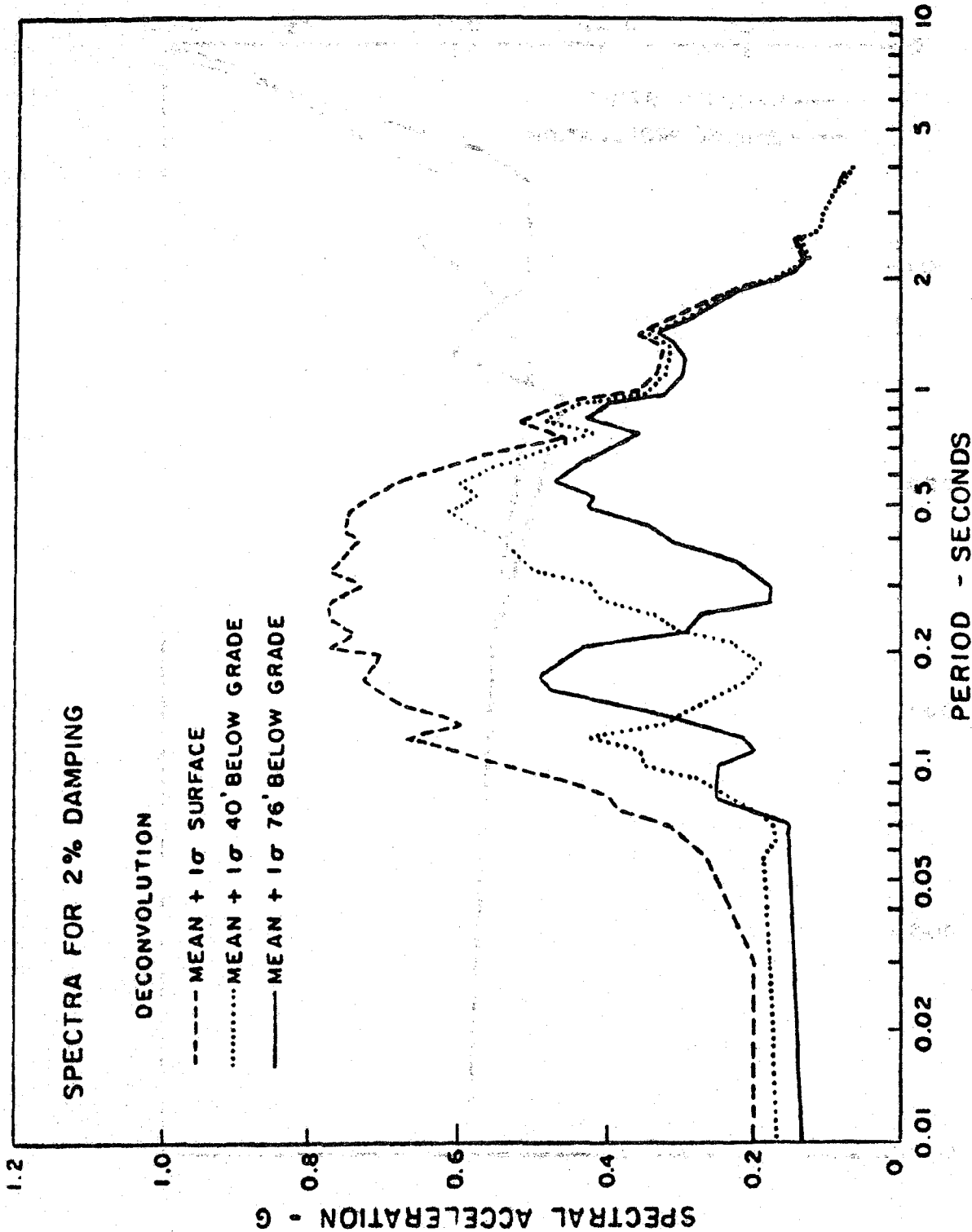


Fig. 10 STATISTICAL ANALYSIS OF COMPUTED SPECTRAL SHAPES AT DIFFERENT DEPTHS IN SOIL DEPOSIT

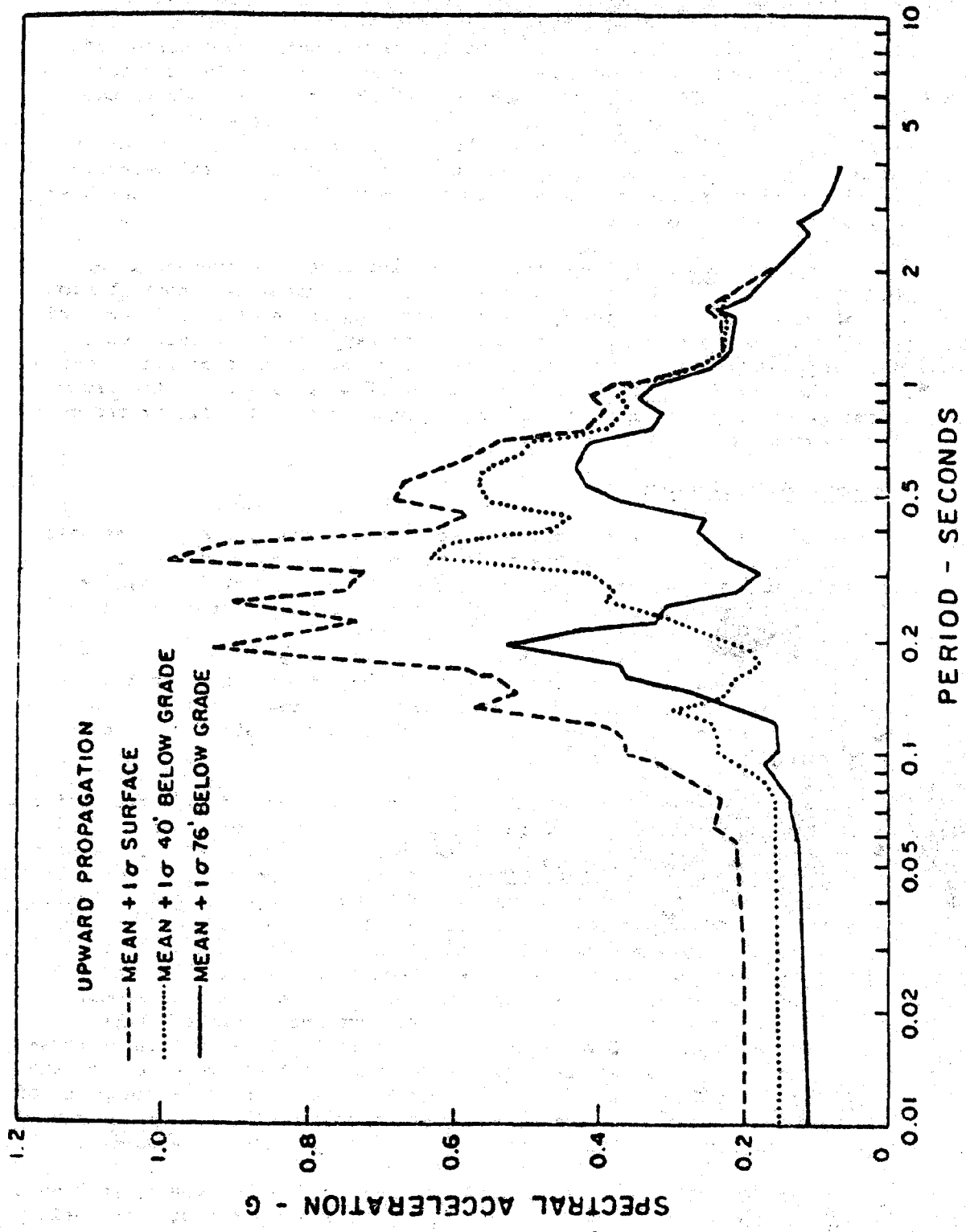


Fig. 11 STATISTICAL ANALYSIS OF SPECTRAL SHAPES AT DIFFERENT DEPTHS IN SOIL DEPOSIT

in Fig. 10. It may be seen that while the spectrum for the surface motions is of the broad band type, the spectrum for motions at a depth of 40 ft contains a marked suppression of frequencies corresponding to a period of about 0.18 second while that for motions at a depth of 76 ft shows a marked suppression of frequencies corresponding to a period of about 0.3 second. The fixed base natural periods of this deposit for 40 ft of soil and 76 ft of soil were about 0.18 and 0.3 seconds respectively. Similar results are shown in Fig. 11 for the base excitation analyses. Thus it may be seen that the frequency suppression effect, as predicted by Eq. (18), is mainly a feature of the geometry and material characteristics of the deposit and depends only slightly on the time history of the motion involved.

In a deposit 600 ft deep extending to substantial distances in all directions there would not be expected to be any substantial contribution of surface waves to the motions in the frequency range of 1 to 20 Hz, and thus the use of vertically propagating shear waves as the primary wave field is appropriate. Nevertheless the effect of the discontinuity provided by the ground surface on the amplitudes of motions and the frequency characteristics of motions at different depths is clearly illustrated by this example.

Summary and Conclusions

At the outset of this section it was shown that any analyses of soil-structure interaction must necessarily be based on a knowledge of the seismic environment to which the structure will be subjected. This requires an understanding of the spatial distribution of motions in the ground surrounding and underlying the structure.

In the light of the discussion of this subject presented in the preceding pages it seems reasonable to draw the following conclusions concerning the role of the seismic environment in soil-structure interaction analyses.

1. On rock sites structures are likely to be founded near the surface. For such sites, earthquake motions may consist of an unknown mixture of Rayleigh waves, Love waves and near-vertically propagating body waves. Because of the low damping in the rock, attenuation of Rayleigh and Love waves will be small within the general area of the site but the contribution of these types of waves to the total ground motion, within the frequencies of interest for nuclear power plants, will nevertheless be small. The presence of such waves will tend to increase the rocking and torsional excitation on the base of the structure due to out of phase effects as the waves pass across the base. Thus structures located on rock should be analyzed for these motions to determine the potential severity of their contributions to the total response of the structure. However, the greater part of the response can be considered to result from vertically propagating body waves.

In analyses using vertically propagating waves, however, it should be noted that because of the fact that these waves will in reality be inclined at different angles to the vertical and will be out-of-phase at different points on the base of the structure due to non-homogeneities in the rock through which they must travel, some

allowance could be made for the "base-slab averaging effect" which will cause the average motions developed in a stiff base slab to be somewhat less than those developed at individual points on the rock surface.

2. For soil sites, structures are likely to be embedded at some depth (say 20 to 80 ft) below the ground surface. The effects of fundamental Rayleigh and Love waves need not be considered at such sites in most designs because the high frequency components of these waves (greater than 1 Hz) will have been damped out by the soil if it extends to any significant distance (say 1000 ft) around the location of the structure. Higher order Rayleigh modes can be simulated by inclined body waves. Thus the main source of excitation will be inclined body waves and for all practical purposes, these can be analyzed as if they propagated in a vertical direction. However in soil deposits there will be an important variation in motion characteristics with depth and this should be considered in the analysis if meaningful results are to be obtained. The assumption of uniform motions in the upper layers of a soil deposit is inconsistent with the physical nature of wave mechanics and observations in the field and can only lead to misleading results unless the specified control motion is intended to take the natural variations in motion characteristics into account in some way. Without knowing something about the variations in motion it is difficult to see how this can be done realistically without introducing an unwarranted degree of conservatism into the soil-structure analysis procedure.

It should not be construed from the above statements that the assumption of vertically propagating waves at soil sites is appropriate for all types of structures. The long-period components of horizontally propagating waves may be extremely important for the design of buried pipelines, tunnel linings and earth retaining structures. However, except for increased stresses in the walls of buried or embedded structures the change in the stress field due to these waves appear to have little effect on the overall horizontal motions of such structures.

The propagating nature of the displacement field may also induce additional displacements and stresses in long above-ground structures such as bridges, Bogdanoff et al. (1965), Johnson and Galletly (1972), Abdel-Ghaffar and Trifunac (1976); and rocking and torsional motions in long period single structures, Wong (1975), Scanlan (1976) and Wong and Luco (1976).

Finally, and perhaps most important, control motions should be chosen with due respect to site conditions and, if a broad band design spectrum is used the control point should be located at the ground surface or, alternatively, at an imaginary outcrop, where it could conceivably exist, and not at some arbitrary depth below the ground surface where the boundary conditions resulting simply from the existence of a ground surface preclude this possibility.

The above conclusions have been drawn mainly on theoretical grounds. However, despite the fact that no concerted effort has been made to date to obtain field data to confirm the above conclusion, a substantial body of field data does in fact exist. Thus, observations by, e.g. Joyner et

al. (1976) and Ohsaki and Higawara (1970) confirm that near surface seismic motions do in fact decrease with depth and Hays et al. (1979) and Gazetas and Bianchini (1979) have presented data which confirms the depth dependent frequency suppression.

REFERENCES

1. "Statistical Analysis of Earthquake Ground Motion Parameters," Report No. NUREG/CR-1175 prepared for the U. S. Nuclear Regulatory Commission by Shannon & Wilson, Inc. and Agabian Associates, December, 1979.
2. Abdel-Ghaffar, A. M. and Trifunac, M. D. (1976) "Antiplane Drafting Soil-Bridge Interaction for Incident Plane SH-Waves (draft)," California Institute of Technology, Pasadena, California, 1976.
3. Bogdanoff, J. L., Goldberg, J. E. and Schiff, A. J. (1965) "The Effect of Ground Transmission Time on the Response of Long Structures," Bull. Seis. Soc. Am., Vol. 55, pp. 627-640, June, 1965.
4. Boncheva, H. (1977) "Soil Amplification Factor of Surface Waves," Proc. 6th World Conf. Earthq. Engrg., Vol. 6, pp. 6-189, New Delhi, 1977.
5. Chandra, U. (1972) "Angles of Incidence of S-Waves," Bull. Seis. Soc. Am., Vol. 62, No. 4, pp. 903-915, 1972.
6. Chen, J.-C., Lysmer, J. and Seed, H. B. (1981) "Analysis of Local Variations in Free Field Seismic Ground Motion," Report No. EERC 81/03, Earthquake Engineering Research Center, University of California, Berkeley, January, 1981.
7. Desai, C. S. and Christian, J. T. (1976) "Numerical Methods in Geotechnical Engineering," McGraw-Hill Book Company, 783 pp., 1976.
8. Ewing, W. M., Jardetzky, W. S. and Press, F. (1957) "Elastic Waves in Layered Media," McGraw-Hill Book Company, 1957.
9. Faccioli, E. (1978) "Response Spectra for Soft Soil Site," Proc. ASCE Specialty Conference, Earthquake Engineering and Soil Dynamics, Vol. 1, pp. 441-456, Pasadena, California, June, 1978.
10. Finn, W. D. L., Lee, K. W. and Martin, G. R. (1977) "An Effective Stress Model for Liquefaction," Journal Geotech. Engrg. Div., ASCE, Vol. 103, No. GT6, pp. 517-533, June, 1977.
11. Gazetas, G. and Bianchini, G. (1979) "Field Evaluation of Body and Surface-Wave Soil-Amplification Theories," Proc. 2nd U. S. Nat. Conf. on Earthq. Engrg., August, 1979.
12. Ghaboussi, J. and Dikmen, S. U. (1978) "Liquefaction Analysis of Horizontally Layered Sands," Journal Geotech. Engrg. Div., ASCE, Vol. 104, No. GT3, pp. 341-356, March, 1978.
13. Hannon, W. J. (1964) "An Application of the Haskell-Thomson Matrix Method to the Synthesis of the Surface Motion due to Dilatational Waves," Bull. Seis. Soc. Am., Vol. 54, pp. 2067-2079, December, 1964.
14. Haskell, N. A. (1953) "The Dispersion of Surface Waves in Multi-Layered Media," Bull. Seis. Soc. Am., Vol. 43, No. 1, pp. 17-34, February, 1953.

15. Haskell, N. A. (1960) "Crustal Reflection of Plane SH Waves," *Journal Geophysical Research*, Vol. 65, No. 13, pp. 4147-4150, December, 1960.
16. Haskell, N. A. (1962) "Crustal Reflection of Plane P and SV Waves," *Journal Geophysical Research*, Vol. 67, No. 12, pp. 4751-4767, November, 1962.
17. Hayashi, S., Tsuchida, H. and Kurata, E. (1971) "Average Response Spectra for Various Subsoil Conditions," Third Joint Meeting, U. S. - Japan Panel on Wind and Seismic Effects, UJNR, Tokyo, May 10-12, 1971.
18. Hays, W. W., Rogers, A. M. and King, K. W. (1979) "Empirical Data About Local Ground Response," Proc. 2nd U. S. Nat. Conf. on Earthq. Engrg., Earthq. Engrg. Res. Inst., Stanford University, August, 1979.
19. Idriss, I. M. (1978) "Characteristics of Earthquake Motions--A State-of-the-Art Review," Proc. ASCE Geotechnical Engineering Division Specialty Conference on Earthquake Engineering and Soil Dynamics, Vol. III, Pasadena, California, June, 1978.
20. Idriss, I. M., Dobry, R., Doyle, E. H. and Singh, R. D. (1976) "Behavior of Soft Clays Under Earthquake Loading Conditions," Proc. Offshore Technology Conference, Paper No. OTC 2671, Dallas, May, 1976.
21. Johnson, N. E. and Galletley, R. D. (1972) "The Comparison of Response of a Highway Bridge to Uniform and Moving Ground Excitation," *Shock and Vibration Bulletin*, Vol. 42, p. 2, January, 1972.
22. Joyner, W. B. (1975) "A Method for Calculating Nonlinear Seismic Response in Two Dimensions," *Bull. Seis. Soc. Am.*, Vol. 65, No. 5, pp. 1337-1357, October, 1975.
23. Joyner, W. B. (1977) "A FORTRAN Program for Calculating Nonlinear Seismic Ground Response," Open File Report No. 77-671, U. S. Geological Survey, Menlo Park, California, 1977.
24. Joyner, W. B. and Chen, A. T. F. (1975) "Calculation of Nonlinear Ground Response in Earthquakes," *Bull. Seis. Soc. Am.*, Vol. 65, No. 5, pp. 1315-1336, October, 1975.
25. Joyner, W. B., Warrick, R. E. and Oliver, A. A. (1976) "Analysis of Seismograms from a Downhole Array in Sediments Near San Francisco Bay," *Bull. Seis. Soc. Am.*, Vol. 66, No. 3, pp. 937-958, June, 1976.
26. Kanai, K. (1952) "Relation Between the Nature of Surface Layer and the Amplitudes of Earthquake Motions," *Bull. Earthquake Research Institute*, Vol. 30, pp. 31-37, Tokyo, 1952.
27. Liang, G. C. and Duke, C. M. (1977) "Separation of Body and Surface Waves in Strong Motion Records," Proc. 6th World Conference on Earthquake Engineering, Vol. 2, pp. 215-220, New Delhi, India, January, 1977.

28. Lion, C. P., Streeter, V. L. and Richart, F. E., Jr. (1977) "Numerical Model for Liquefaction," Journal Geotech. Engrg. Div., ASCE, Vol. 103, No. GT6, pp. 589-606, June, 1977.
29. Lysmer, J. and Kuhlemeyer, R. L. (1969) "Finite Dynamic Model for Infinite Media," Journal Engrg. Mech. Div., ASCE, Vol. 95, No. EM4, pp. 859-877, August, 1969.
30. Lysmer, J. and Waas, G. (1972) "Shear Waves in Plane Infinite Structures," Journal Engrg. Mech. Div., ASCE, Vol. 98, No. EM1, pp. 85-105, February, 1972.
31. Martin, P. P. (1975) "Non-Linear Methods for Dynamic Analysis of Ground Response," Ph.D. Thesis, University of California, Berkeley, June, 1975.
32. Martin, P. P. and Seed, H. B. (1979) "Simplified Procedure for Effective Stress Analysis of Ground Response," Journal Geotech. Engrg. Div., ASCE, Vol. 105, No. GT6, pp. 739-758, June, 1979.
33. Nair, G. P. and Emery, J. J. (1975) "Spatial Variations in Seismic Motions," Second Canadian Conference on Earthquake Engineering, Preprint No. 5, Hamilton, Ontario, June, 1975.
34. Ohsaki, Y. and Hagiwara, T. (1970) "On Effects of Soils and Foundations upon Earthquake Inputs to Buildings," Research Paper No. 41, Building Research Institute, Ministry of Construction, Japan.
35. Randall, M. J. (1971) "Revised Travel Time Table for S," Geophys. J., Vol. 22, pp. 229-234, 1971.
36. Richart, F. E., Jr., Hall, J. R., Jr. and Woods, R. D. (1970) "Vibrations of Soils and Foundations," Prentice-Hall, Inc., 1970.
37. Scanlan, R. H. (1976) "Seismic Wave Effects on Soil-Structure Interaction," Earthquake Engineering and Structural Dynamics, Vol. 4, pp. 379-388, June, 1976.
38. Schnabel, P. B., Lysmer, J. and Seed, H. B. (1972) "SHAKE - A Computer Program for Earthquake Response Analysis of Horizontally Layered Sites," Report No. EERC 72-12, Earthquake Engineering Research Center, University of California, Berkeley, December, 1972.
39. Seed, H. B. and Idriss, I. M. (1969) "The Influence of Soil Conditions on Ground Motions During Earthquakes," Journal Soil Mech. Found. Div., ASCE, Vol. 94, No. SM1, pp. 99-137, January, 1969.
40. Seed, H. B., Murarka, R., Lysmer, J. and Idriss, I. M. (1976b) "Relationships Between Maximum Acceleration, Maximum Velocity, Distance from Source and Local Site Conditions for Moderately Strong Earthquakes," Bull. Seis. Soc. Am., Vol. 66, No. 4, pp. 1323-1342, August, 1976.
41. Seed, H. B., Ugas, C. and Lysmer, J. (1976a) "Site Dependent Spectra For Earthquake Resistant Design," Bull. Seis. Soc. Am., Vol. 66, No. 1, pp. 221-243, February 1976.

42. Silva, W. (1976) "Body Waves in a Layered Anelastic Solid," Bull. Seis. Soc. Am., Vol. 66, No. 5, pp. 1539-1554, October, 1976.
43. Streeter, V. L., Wylie, E. B. and Richart, F. E., Jr. (1974) "Soil Motion Computations by Characteristics Method," Journal Geotech. Engrg. Div., ASCE, Vol. 100, No. GT3, pp. 247-263, March, 1974.
44. Taylor, P. W. and Larkin, T. J. (1978) "Seismic Site Response of Non-linear Soil Media," Journal Geotech. Engrg. Div., ASCE, Vol. 104, No. GT3, pp. 369-383, March, 1978.
45. Teng, T.-L. (1967) "Reflection and Transmission from a Plane Layered Core-Mantle Boundary," Bull. Seis. Soc. Am., Vol. 57, No. 3, pp. 477-499, June, 1967.
46. Thomson, W. T. (1950) "Transmission of Elastic Waves through a Stratified Soil Medium," Journal Appl. Physics, Vol. 21, February, 1950.
47. Toki, K. (1977) "Disintegration of Accelerograms into Surface and Body Waves," Proc. 6th World Conference on Earthquake Engineering, Vol. 2, pp. 209-214, New Delhi, India, January, 1977.
48. Trifunac, M. D. and Brune, J. N. (1970) "Complexity of Energy Release During the Imperial Valley, California Earthquake of 1940," Bull. Seis. Soc. Am., Vol. 60, No. 1, pp. 137-160, 1970.
49. Waas, G. (1972) "Analysis Method for Footing Vibrations through Layered Media," Ph.D. Dissertation, University of California, Berkeley, December, 1972; also published under the title "Earth Vibration Effects and Abatement for Military Facilities," Report 3, U. S. Army Engineer WES, Vicksburg, Miss., September, 1972.
50. Wong, H. L. (1975) "Dynamic Soil/Structure Interaction," Report No. EERC 75-01, Ph.D. Dissertation, California Institute of Technology, Pasadena, California, May 1975.
51. Wong, H. L. and Luco, J. E. (1976) "Dynamic Response of Rigid Foundations of Arbitrary Shape," Earthquake Engineering and Structural Dynamics, Vol. 4, pp. 579-587, 1976.
52. Zienkiewicz, O. C., Chang, C. T. and Hinton, E. (1978) "Nonlinear Seismic Response and Liquefaction," Submitted for publication in the Int. J. Numerical and Analytical Methods in Geomechanics, 1978.

THE REGIONAL CHARACTERISTICS OF SEISMIC INTENSITY
ATTENUATION IN CHINA

Chen Pei-shan, Jin Yan, and Li Wen-xiang

Institute of Geophysics, State Seismological
Bureau, Beijing, China

ABSTRACT

The coefficient of seismic intensity attenuation depends on the properties of the medium through which seismic waves propagate. Its variations may mean that the structures and/or properties of the crust and upper mantle are different for different regions. We have adopted a linear seismic source model suggested by J.F. Evernden to analyze the data of isoseismal lines of 107 earthquakes occurred in China, using the Marquardt's method for least-squares estimation of nonlinear parameters to get the coefficients of seismic intensity attenuation K , and equivalent focal depth C and earthquake fault length $2L$. The value K appears to show some regional characteristics: the K value is highest in southwestern China and gradually decreases towards the north-east. These results indicate that there exist some differences in the structure and/or property of the crust and upper mantle for various parts of China.

INTRODUCTION

Attenuation of seismic intensity with distance, apparently, has direct and practical significance to engineering constructions. At the same time, it is also a geophysical factor related to crustal and upper mantle

structures, involving therefore also academic value.

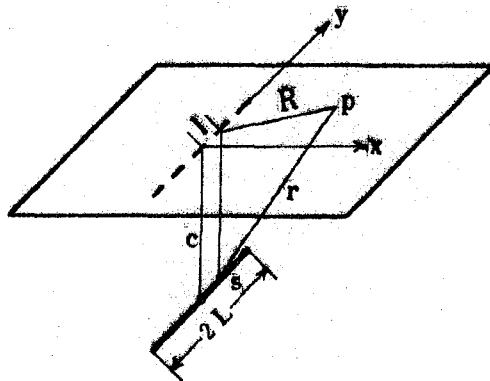


Fig.1 Adopted model

MODEL, DATA AND COMPUTATIONAL METHOD

We have adopted a linear seismic source model suggested by J.P. Evernden.^[1,2] He regards the earthquake fault as a linear source which radiates uniformly seismic waves and is buried at a depth C , its length is $2L$, the distance from each point S of the linear source to a observation point P on the ground is r (see Fig.1)

$$r = (R^2 + C^2)^{1/2}, \quad R^2 = x^2 + (y-l)^2$$

The seismic waves radiated from every point of the linear source attenuate as $1/r^{4K}$, K is the seismic intensity attenuation coefficient. Thus, the formula for the intensity value of every point on the ground can be deduced as

$$I(x, y) = 14.37 + \frac{3}{4} \log \left[L^{11} \int_L^L \frac{1}{(R^2 + C^2)^{2K}} dl \right] \quad (1)$$

The constants in the formula (1) obviously depend on the seismic intensity scale: they have been determined on the basis of the seismic intensity distribution in U.S.^[1,2] However, the intensity I in the formula(1) is not in the modified Mercalli Scale of 12 used in U.S. now, but in the Rossi-Forel Scale of 10. The new intensity scale used in China is closer to the M-M Scale.^[3] Therefore, it is necessary to transform the intensity values in using the

formula(1), (see Fig.2).^[7]

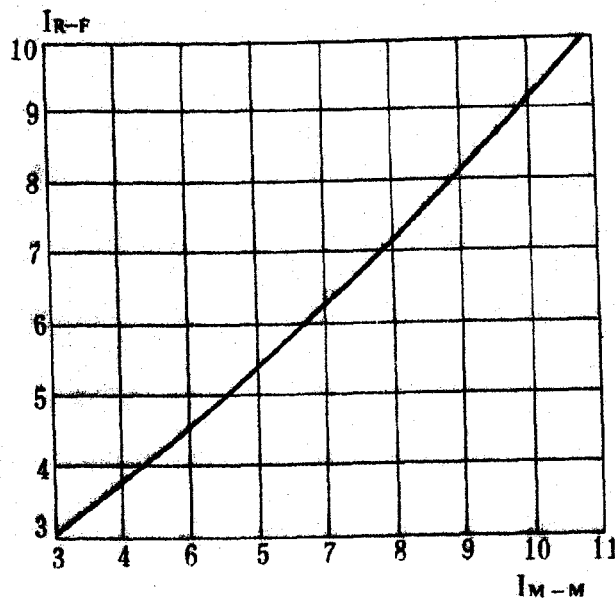


Fig.2 Transformation of intensity scales

From the "Collection of Isoseismal Maps of China" we take the data of isoseismal lines of 107 earthquakes.^[4] A coordinate system must at first be set up on each of the isoseismal maps, taking the epicenters as the origin and the direction of earthquake fault as the y axis. Take the x,y coordinates values of 8 points from every isoseismal line and their intensity values, at uniform azimuthal angles(see Fig.3). If an isoseismal is not closed, take the I and x,y values only at the point investigated. After a large number of groups of (x,y,I) values have been sampled the Marquardt's method for least-squares estimation of nonlinear parameters is used to get the parameters K,C,L by iteration several times.^[3] The parameter K tends to be stable after iteration 2-4 times, but L and C are not as stable. Therefore the K values in the result are comparatively reliable, and the L and C values can only be taken

TABLE 1. The Intensity Attenuation Coefficients K and Seismic Source Parameters

No	Date	Location	Lat(^o N)	Long(^o E)	Ms	L	U	K	Q	V
2	Jan. 19, 1501	Chaoyi	34.8	110.1	7.0	20.2	17.4	2.2	7.7	.70
4	Jan. 23, 1556	Huaxian	34.5	109.7	8.0	.8	16.5	1.2	32.4	.98
7	Dec. 29, 1604	Qianzhong	25.0	119.5	8.0	83.8	71.4	1.7	2.0	.38
10	July 25, 1668	Tancheng	35.3	118.6	8.5	85.5	42.8	1.4	3.9	.36
17	July 01, 1879	Wudu	33.2	104.7	7.5	19.7	36.3	1.6	4.7	.47
18	Mar. 17, 1906	Jiayi	23.5	120.5	6.8	15.0	16.2	2.0	5.5	.51
19	Apr. 21, 1935	Taizhong	24.8	120.8	7.0	46.1	29.4	2.0	6.7	.63
21	Aug. 22, 1902	Atushen	39.9	76.2	8.3	71.1	37.4	1.6	5.0	.47
22	Dec. 23, 1906	Manasi	44.1	85.8	8.0	.9	17.7	1.4	4.8	.47
24	Dec. 17, 1941	Jiayi	23.6	120.6	7.0	27.8	33.4	1.7	4.7	.47
26	Dec. 21, 1913	Eshan	24.2	102.5	6.5	21.8	21.2	2.2	7.6	.53
27	Aug. 05, 1914	Belikun	43.8	93.6	7.5	.8	89.7	1.3	1.3	.30
28	July 31, 1917	Deguan	28.0	104.0	6.5	10.6	18.4	2.1	1.6	.28
29	Feb. 13, 1918	Nanao	23.5	117.2	7.5	57.6	105.0	1.6	.4	.20
31	Dec. 16, 1920	Haiyuan	36.7	105.9	8.3	27.2	29.4	1.5	7.2	.45
32	Mar. 24, 1923	Daofu	31.5	101.0	7.3	27.7	9.8	2.5	3.5	.33
33	Mar. 16, 1925	Dali	25.7	100.2	7.0	51.3	19.4	2.3	4.0	.44
34	May 23, 1927	Gulang	37.8	102.8	8.0	.3	13.1	1.1	9.4	.64
35	Aug. 25, 1927	Tainan	23.2	120.7	6.8	5.1	12.6	2.0	1.2	.27
36	Apr. 21, 1935	Xinzhong	24.9	121.1	6.0	20.0	9.7	2.6	4.7	.56
37	Oct. 22, 1951	Huelian	24.0	121.9	7.3	64.4	28.1	2.0	3.2	.49
40	June 11, 1931	Fuyun	47.0	90.1	8.0	4.8	38.0	1.3	2.2	.35
41	Apr. 06, 1932	Macheng	31.4	115.1	6.0	391.6	-13.3	3.2	3.6	.38
42	Dec. 25, 1932	Changma	39.8	97.1	7.5	132.5	66.9	1.9	3.8	.54
43	Aug. 25, 1933	Dixi	32.0	103.7	7.5	11.0	13.6	1.9	2.8	.30
44	Feb. 07, 1936	Kangle	35.2	103.4	6.8	26.7	16.8	2.5	1.1	.24
45	Apr. 01, 1936	Lingshan	22.9	109.8	6.8	.0	11.8	1.0	4.3	.34
46	Aug. 01, 1936	Tianshui	34.8	106.2	6.0	2.3	20.8	2.1	5.4	.47
48	Aug. 01, 1937	Heze	35.2	115.3	7.0	.2	35.0	1.3	10.1	.56
50	May 05, 1941	Suifeng	46.7	127.1	6.0	237.4	10.0	3.3	1.9	.28
51	May 16, 1941	Gengma	23.7	99.4	7.0	9.7	15.0	2.2	.5	.17
53	Dec. 26, 1941	Mengzhe	22.2	100.1	7.0	65.2	17.6	2.7	5.0	.51
55	Sep. 23, 1945	Luanxian	39.7	118.7	6.3	1.8	24.6	1.9	4.0	.48
56	May 25, 1948	Litang	29.7	100.3	7.3	6.1	23.7	1.6	4.2	.51

TABLE 1. Continued

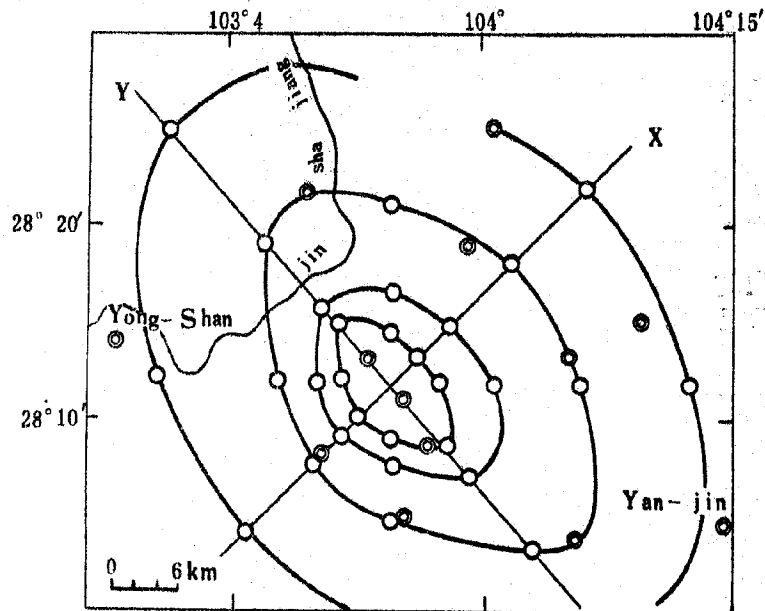
No	Date	Location	Lat(^o N)	Long(^o E)	Ms	L	C	K	Q	V
57	Oct. 09, 1948	Shimenkan	27.4	103.9	5.8	17.2	17.2	2.5	2.6	.33
59	Aug. 15, 1950	Chayu	28.5	96.0	8.5	38.3	48.7	1.4	3.2	.50
60	Dec. 21, 1951	Jianchuan	26.7	100.0	6.3	17.2	15.3	2.2	4.5	.47
61	Sep. 30, 1952	Mianning	28.4	102.2	6.8	.3	58.4	1.3	4.3	.49
62	Oct. 08, 1952	Guoxian	38.9	112.8	5.5	.1	13.8	1.7	.9	.20
63	Feb. 11, 1954	Shandan	39.0	101.3	7.3	10.2	18.0	2.0	.5	.17
64	Apr. 15, 1955	Wuqia	39.8	74.5	7.0	.9	29.1	1.4	2.6	.39
65	June 07, 1955	Huaping	26.5	101.1	6.0	3.0	18.8	2.3	1.4	.30
66	Sep. 23, 1955	Yuzha	26.4	101.9	6.8	24.6	26.2	2.1	4.9	.46
70	Nov. 09, 1960	Zhangla	32.8	103.7	6.8	3.8	9.3	2.5	3.1	.45
72	Jan. 18, 1964	Taidong	23.2	120.6	7.0	.2	9.9	1.3	.7	.19
74	Apr. 13, 1960	Yushu	45.3	127.6	5.8	1.9	38.9	1.9	1.7	.31
75	Mar. 08, 1961	Yidu	30.3	111.2	5.2	.3	25.8	1.8	1.4	.27
76	June 12, 1961	Tengchong	25.2	98.5	5.8	155.2	10.1	3.5	1.3	.35
77	Apr. 14, 1961	Bachu	39.9	77.8	6.8	.3	14.9	1.5	4.1	.35
78	June 27, 1961	Zhongdian	27.8	99.7	6.6	28.3	35.1	2.1	1.8	.32
79	Oct. 01, 1961	Minxian	34.3	104.8	5.7	1.0	64.8	1.6	2.9	.39
81	Mar. 19, 1962	Heyuan	23.7	114.7	6.1	29.8	47.1	1.5	240.9	2.52
82	June 24, 1962	Nanhua	25.9	101.8	6.2	.2	41.9	1.5	1.9	.28
83	Aug. 20, 1962	Sailimuhu	44.3	81.7	6.4	68.8	78.9	2.0	1.0	.24
84	Dec. 07, 1962	Lingwu	38.1	106.3	5.4	1.1	47.0	1.8	7.7	.58
85	Dec. 11, 1962	Gangu	34.8	105.1	5.0	2.7	27.7	2.2	.8	.20
86	Dec. 18, 1962	Lingwu	38.0	105.2	5.5	9.2	68.1	1.8	5.5	.55
87	Jan. 11, 1963	Meiyuan	37.5	101.9	4.8	3.6	48.6	1.9	3.1	.41
88	Apr. 19, 1963	Lanhu	35.7	97.8	7.0	12.0	39.0	1.9	.1	.10
89	Apr. 23, 1963	Kunlong	26.0	99.7	6.0	3.4	43.0	2.1	.6	.17
90	Feb. 13, 1964	Binchuan	25.9	100.9	5.4	1.6	63.5	1.8	1.0	.21
91	May 08, 1964	Zhuanghe	39.8	123.3	4.3	59.1	64.8	2.2	.5	.21
92	Sept 05, 1964	Yunxi	33.1	110.7	4.6	.1	21.2	1.7	2.8	.28
93	Jan. 13, 1965	Yuanqu	35.1	111.6	5.5	.2	22.6	1.7	.7	.19
94	May 07, 1965	Shacheng	42.4	115.4	4.3	7.6	13.7	3.0	3.1	.30
95	May 24, 1965	Eshan	24.6	102.8	5.2	.6	49.3	1.8	1.6	.27
96	July 03, 1965	Jiangcheng	22.9	101.8	6.1	35.5	31.3	2.4	1.5	.25
97	Nov. 13, 1965	Wulumuqi	44.0	88.1	6.6	.4	59.0	1.3	.9	.25
98	Jan. 31, 1966	Zhongdian	27.9	99.7	5.1	15.8	14.0	3.0	5.3	.47

TABLE 1. Continued

No	Date	Location	Lat(^o N)	Long(^o E)	Ms	L	C	K	Q	V
99	Feb. 05, 1966	Dungchuan	26.2	103.2	6.5	.3	20.9	1.6	8.2	.48
100	Mar. 06, 1966	Ningjin	37.5	115.0	5.2	34.9	25.1	2.6	2.5	.34
101	Mar. 08, 1966	Longyao	37.4	114.9	6.8	.1	19.2	1.3	20.2	.63
102	Mar. 22, 1966	Dongwang	37.5	115.1	7.2	.6	26.1	1.3	12.8	.49
105	Sept 23, 1966	Xuanwei	26.3	104.5	5.0	.2	-7.8	2.9	.8	.23
107	Oct. 02, 1966	Hualde	43.8	125.8	5.2	3.4	40.4	2.0	4.7	.36
108	Mar. 27, 1967	Hejian	38.5	116.5	6.3	.4	71.3	1.4	3.4	.32
109	June 21, 1967	Bateraqi	48.4	122.2	4.8	.7	79.5	2.0	1.1	.26
110	July 28, 1967	Huailai	40.7	115.8	5.5	13.7	44.2	1.8	1.1	.22
111	Aug. 20, 1967	Nanzheng	33.7	107.5	4.8	31.3	22.8	2.8	1.3	.28
112	Aug. 30, 1967	Luhuo	31.6	100.3	6.8	6.8	17.2	2.2	5.1	.49
117	Jan. 02, 1969	Baokang	31.5	111.4	4.7	16.5	25.2	2.6	3.9	.41
118	Dec. 12, 1969	Wushen	41.5	79.4	6.5	9.7	-9.9	3.0	2.9	.41
120	July 18, 1969	Bohai	38.6	119.8	7.4	36.1	200.0	1.6	.2	.13
121	July 26, 1969	Yangjiang	21.8	111.8	6.4	25.1	21.8	2.4	3.1	.41
122	Dec. 03, 1970	Xiiji	35.9	105.6	5.5	.2	28.0	1.6	2.8	.31
123	Jan. 05, 1970	Tonghai	24.6	103.3	7.7	35.1	15.5	2.2	6.3	.46
124	Feb. 24, 1970	Dayi	31.2	103.8	6.3	.5	39.3	1.7	3.3	.45
125	Nov. 10, 1970	Baotou	41.4	110.0	4.8	1.0	49.2	1.9	1.4	.28
127	Mar. 23, 1971	Wushen	41.5	79.3	6.0	.0	12.2	1.5	4.5	.43
128	Mar. 24, 1971	Tuosuohu	35.5	98.5	6.8	.9	31.2	1.7	4.0	.37
131	June 16, 1971	Wushen	41.5	79.4	5.8	18.6	16.6	2.8	2.2	.35
132	July 26, 1971	Xikeer	39.9	77.3	5.6	1.5	50.6	1.7	.5	.19
133	Aug. 01, 1971	Wusu	43.9	84.4	4.8	22.0	37.4	2.4	1.8	.30
134	Jan. 16, 1972	Keping	40.6	79.3	6.2	1.2	20.7	2.2	4.5	.43
135	Aug. 16, 1971	Mabian	28.9	103.6	5.8	9.4	16.1	2.6	2.7	.33
136	Apr. 09, 1972	Luntai	42.2	84.6	5.6	4.8	58.2	1.8	5.4	.45
138	Feb. 06, 1973	Luhuo	32.1	101.0	7.9	27.2	16.9	2.1	13.3	.69
141	June 03, 1973	Jinghe	44.4	83.5	6.0	.5	72.1	1.5	3.9	.39
143	Aug. 11, 1973	Songpan	32.9	104.9	6.5	14.0	15.8	2.8	1.1	.21
144	Apr. 22, 1974	Liyang	31.5	119.2	5.5	6.7	22.3	2.4	6.3	.51
145	May 11, 1974	Yongshan	28.4	104.1	7.1	.0	3.8	1.3	3.7	.34
147	Feb. 04, 1975	Haicheng	40.7	122.8	7.3	.5	28.1	1.4	6.3	.50

TABLE 1. Continued

No	Date	Location	Lat(^o N)	Long(^o E)	Ms	L	C	K	Q	V
148	Apr. 06, 1976	Helingeer	40.9	112.9	6.1	51.4	59.3	2.1	3.8	.38
150	July 28, 1976	Tangshan	39.5	118.2	7.8	.2	9.7	1.2	5.1	.33
151	Aug. 16, 1976	Songpan	33.0	104.3	7.2	5.4	32.3	1.9	18.1	.73
152	Aug. 23, 1976	Songpan	32.7	104.5	7.2	21.2	-9.8	2.9	.6	.16
153	Aug. 18, 1952	Dangxung	30.6	91.5	7.5	11.5	14.9	1.9	3.2	.32



No 145 May 11, 1974 Yongshan Earthquake
 Epi: 28.2° N, 103.9° E M:7.1 I₀:IX h: 14

Fig. 3 A sampling example

as a reference.

RESULTS

We have calculated almost all the data of earthquakes given by the "Collection of Isoseismal Maps of China" except only a few earthquakes of which the data are not reliable. The results of the calculations are listed in table I.

We can see from the table that the K values lie in the range 1.1-3.5 and also the values of the residual squares Q and variance V. Some values of L and C are certainly not appropriate. The reasons may be: 1. The intensity scale used is not adequate. 2. The isoseismal lines are too irregular in shape. 3. The directions of the major axis of the inner and outer isoseismal lines are different. It is believed that good results can give us information about attenuation, while poor results might make us think in order

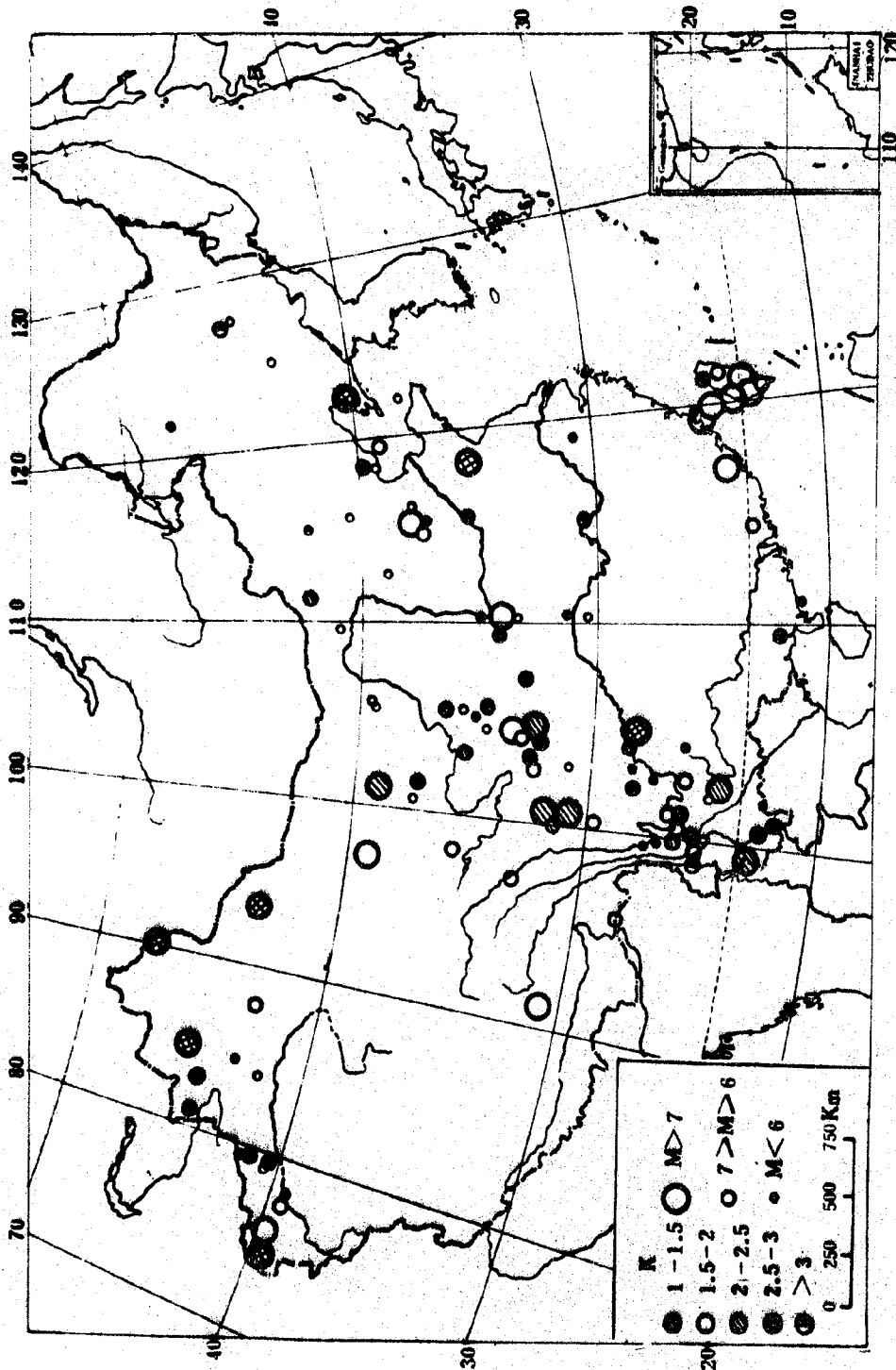


Fig.4 The distribution of the coefficient K of seismic intensity attenuation

to find out the defects.

By representing the K values in Fig.4, their distribution appears to have some regional characteristics. It is highest in southwestern China, where the attenuation of seismic intensity is greatest. On the north China plain K values are generally lower and attenuation becomes less. This may indicate that the absorption by the crustal and upper mantle of seismic waves in southwestern China is stronger.

DISCUSSION

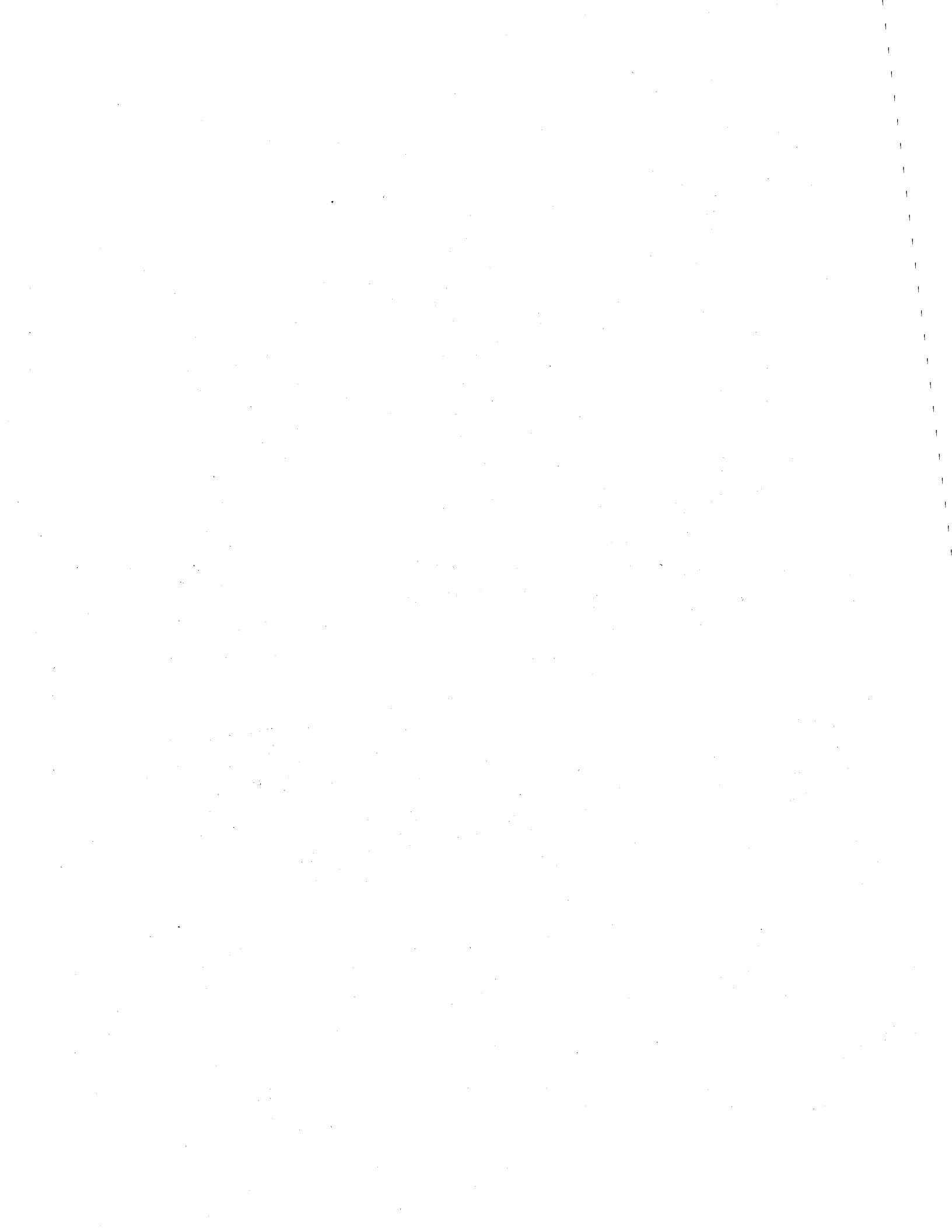
Evernden has been determining by inversion of the data of distribution of seismic intensity, the attenuation coefficients and source parameters of earthquakes at the same time quantitatively. He opens up a new direction in the utilization of isoseismal data. Before, only the intensity attenuations in the direction of the major and minor axes of the isoseismals were considered respectively, thus two different attenuation coefficients were found. This is unreasonable from physical point of view, because it means that there exists anisotropy in the crustal medium. Obviously, we have not made such an assumption and it is not in accord with facts. Besides, the source parameters of earthquakes are not obtainable at the same time.

However, there are some shortcomings in the linear source model mentioned above. Some factors influencing the seismic intensity distribution have not been considered such as 1. the azimuthal distribution of radiation energy, 2. the direction and speed of earthquake rupture. The seismic wave radiation will be enhanced in the front and weakened at the back of the rupture, due to Doppler's effect. 3. the dip of the earthquake fault. Chen Pei-shan et al have considered some of these effects, but obtained no analytic formula for intensity distribution, so that their results are still not applicable.^[5,6] If one should make use of the more rational points of Evernden and Chen to get an analytic ex-

pression closer to reality, it would be beneficial to the work of seismic micro-zonation and seismic intensity prediction.

REFERENCES

1. J.F.Evernden, Seismic intensity, "Size" of earthquake and related parameters. Bull. Seism. Soc. Am., 65, 5, 1287-1313 (1975)
2. J.F.Evernden, RR. Hibbard, and J.F.Schneider, Interpretation of seismic intensity data, B.S.S.A., 63, 2, 399-422 (1973)
3. Statistic computation of probability, Computational Center, Academia Sinica. (in Chinese)
4. Collection of Isoseismal maps of China, a set of seismic intensity regionalization maps, State Seismological Bureau. .
5. Chen Pei-shan, Yen Shou-min, Relation between the seismic source mechanism and intensity distribution, Acta Geophysica Sinica, 18, 1, (1975)
6. Chen Pei-shan, Relation between the seismic source mechanism and intensity distribution (continued), ACTA Geophysica Sinica, 20, 1, (1977)
7. M. Bath, Introduction to seismology. John Wiley & Sons. New York (1973)
8. Hsieh Yu-shou, A New Scale of Seismic Intensity Adapted to the Conditions in Chinese Territories, Acta Geophysica Sinica, Vol. 6, No. 1, 35-47, (1957).



EFFECTS OF IRREGULAR TOPOGRAPHY AND NON-UNIFORM SOIL PROFILES ON EARTHQUAKE MOTION AND EARTHQUAKE DAMAGE

CHEN BINGWU^I

Summary

This paper presents a short summary of the results obtained by the author in recent years.

In the study of the effects of irregular topography on earthquake damage, an isolated-protruding spur is considered. The author presents a double shear deformation finite element model which reduces a three-dimensional problem into a two-dimensional one and evidently simplifies the process.

The dynamic characteristics of the one-dimensional non-uniform soil profile are studied through a vertical shear beam model with variable stiffness. A mathematical expression containing three parameters for the distribution of stiffness has been presented. It is easy to fit the distribution of stiffness of actual soil profiles by changing the value of these parameters.

The two-dimensional non-uniform soil profiles are studied with the finite element method. As an example, the calculated results of the profile with a sloping rock boundary are discussed. In this case the main conclusion is that at the side on the thicker soft soil layer near the slope, the heavier ground motion in vertical component is evident.

Comparison between the calculated results and the earthquake damage distribution has also been made, and both are in good agreement.

1 Effects of Irregular Topography on Earthquake Motion and Earthquake Damage

1.1 Introduction

In the investigations^[1, 2, 3] of destructive earthquake in China in recent years, it was found that the earthquake damage at the top of an isolated-protruding spur or isolated hill was generally much more serious than that at the adjacent flat sites. The present "The Seismic Design Code for Industrial and Civil Buildings (TJ11-78)"^[4] has pointed out: "generally the disadvantageous district for building to eqk. resistance are the third soil, long-protruding spur, high-isolated hill

^I Deputy Head of Seismozoning and Earthquake Resistant Division, Lanzhou Seismology Institute, State Seismological Bureau.

and non-rock (including bad-cemented Tertiary sedimentary rock) scarp slope district etc." The Code⁽⁴⁾ has recommended that the above mentioned disadvantageous districts should be as far as possible avoided in choosing a constructive site. In practice for some cases because of varied reasons such sites cannot really be avoided, but the Code has not presented any methods of quantitative evaluating for such sites. Although the harmful effect of the local isolated-protruding topography condition on earthquake damage was found early, up to now, the quantitative study about this problem has been far not enough. A lot of construction works will be made in the mountain region in China so the problem about effect of topography on earthquake motion and earthquake damage constitutes an important and considerable interesting research object.

Since it has been recognized that the effect of local topography on earthquake damage is an important aspect in earthquake engineering, a number of analytical works have been presented in the world in recent years. Especially, the strong motion record, the peak acceleration of which was the very large value of 1.25g had obtained in San Fernando Earthquake at Pacoima Dam during 1971. Part of this enormous surface acceleration may be explained by the magnification of base bedrock motion arising from the location of the recording instrument on a steep ridge of the valley. This example causes a lot of theoretical works^(5,6,7,8) studying on this problem. In the USSR, in order to solve the task of seismomicrozoning of the towns in mountain region, some theoretical studies were carried out.

The most of the above mentioned theoretical studies adopted analytical methods and assumed that the topography was a simple geometric figure. At present, the accurate study for the complex irregular topography can be realized only by means of the three-dimensional finite element method. For example, in the reference⁽⁹⁾ this method had been adopted. In this way, the amount of the computing work was very heavy, it usually required a faster and bigger computer, which was very expensive. In this paper we present a double shear deformation finite element model, which reduces the three-dimensional problem into the two-dimensional one, thus it can greatly simplify the computing process.

1.2 Examples of the investigation of some heavy earthquakes

In 1970 a severe earthquake hit Tonghai, Yunnan Province of China. The earthquake was of 7.7 magnitude and the epicentral intensity was over X grade. Because it occurred in the mountain region, where a lot of villages were located at the top of an isolated hill or at the ridge of an isolated small mountain. Some of these hills were formed of New Tertiary rocks, and others were formed of bedrocks. The harmful effect of the former on the earthquake damage was more notable. Yet latter, if the height of the hills were less than 30m, the harmful effect was generally not very obvious. According to the statistics of the earthquake damage of 67 villages which were located at the top of an isolated hill or on the ridge of the

spur, compared with the villages at the flat site under the same site soil condition, the damage of theirs was 0.5--1 grade higher than that of the latter.

In the 1975 Haicheng and 1976 Tangshan earthquakes it was discovered that the destruction of the villages or buildings at the top of an isolated hill was far more serious.

The effect of the height difference of the topography on earthquake intensity was very obvious in the loessial plateau region. Tianshui, Gansu Province of China, was of such a typical region, the experience of the earthquakes in the past decades indicated that the villages about 100m above the riverbed compared with the villages at the river banks, their earthquake intensity was one grade higher than that of the latter.

In 1974 a destructive earthquake hit Yongshan-Daguan, Yunnan Province of China, The earthquake was of 7.2 magnitude, and the epicentral intensity was IX grade, the isoseismol map of which is shown in Fig.1.1. Because this earthquake occurred in the mountain area, there were a lot of examples which can illustrate the harmful effect of an isolated topography on earthquake damage. We choose the most typical of them as an example described as follows.

In this earthquake, there was a VIII grade anomalous region, Huilongwan, which located in the VII grade region (Fig.1.1). In this anomalous region there was a village of Lujiawan. The epicentral distance of the village was about 18 km. The whole village was located at the ridge of a saddle isolated-protruding spur. The topographical map of Lujiawan is shown in Fig.1.2. The strike of the spur was in the near N-S direction, the head part of the spur changed in the N-E direction. The spur was about 150m long and 50m high. The width of the ridge, generally was 10m the most was 15m and the least about 5m. The thickness of the surface soil layer at the ridge was very thin, generally it was only 20--30cm at the saddle it was a little thicker, about 50cm. The surface soil was of residual deposit, there was a flag marl appeared at the locality. There were altogether 14 buildings (29 bays) in the village. These buildings were located respectively at the three different parts of the spur. At the front top of which isolated feature was the most outstanding, the earthquake intensity was IX grade. At the saddle which had the least isolated feature, the intensity was only VII grade. At the back part of the spur, because of its altitude being higher it adjoined the back big mountain, so its isolated feature was between those of the top and the saddle, its earthquake intensity was VIII grade.

Generally speaking, the earthquake damage relates with a lot of factors. In order to study the effect of a factor, one has to clear up all the effects of other factors. We describe these factors one after another as follows.

All the buildings of the village were built with the similar materials, the structure type and construction quality of the buildings were also all the same. So, their capacity for earthquake resistance was more or less alike.

The dimension of the spur compared with the epicentral distance was very small. So we can consider that the conditions about the source mechanism, epicentral distance, transmission-path characteristics etc. at the different parts of the village were also all the same.

Investigation indicated that the local non-causative faults, local subsoil, underground water level etc. all were not the very factors which can cause the earthquake intensity difference at different parts of the village.

In addition, there were not any harmful physical geology phenomena occurring in these sites. Thus, we can firmly believe that except for the local topography condition, all other factors were not the reason which caused the intensity difference at the different parts of the village.

1.3 Theoretical analysis

1.3.1 Assumptions and analytical model

As previously mentioned, in the example that has been analysed the geologic structure and rock characteristic are quite homogeneous. Under such magnitude and epicentral distance conditions, we can then consider that the earthquake response of the spur was basically in the linear elastic stage. Because the dimensions of the spur are small, we can consider that the earthquake motion at the bottom-face and conjunctive-face between the spur and back big mountain are in the same phase.

In analysis we only consider the pure shear deformations of the spur. The effects of spur on the earthquake intensity in different direction will be not alike. Considering the direction of the seismic wave propagation and the strike of the spur are roughly parallel, the SH wave will cause the transverse vibration of the spur. Thinking over the characteristic of the spur itself and the direction of the seismic wave propagation, we come to know that the influence of the spur on the intensity should be much more evident in the cross direction.

In order to consider the binding effect of the back mountain on the earthquake response to the spur and to make the theoretical calculation as far as possible reflect the influence of the complex feature of it, we present the double shear deformation finite element model to carry out the earthquake response analysis. The theoretical model is shown in Fig.1.3.

1.3.2 Characteristics of the element

The double shear deformation finite element is shown in Fig.1.4.

There are 8 nodal points per element. Under general deformation state, each point will have 3 displacement components, in this case, there are 24 unknown nodal point displacements for each element. Assuming pure shear deformation condition, for all nodal points, we have

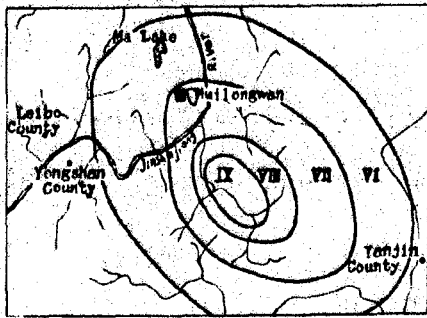


Fig 1.1 Isoseismal map of 1974 Yongshan-Daguan earthquake

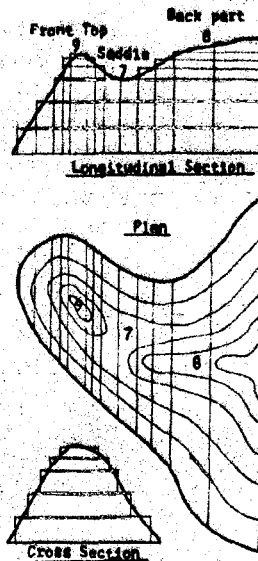


Fig.1.2 Schematic topographical map of Lujiawan

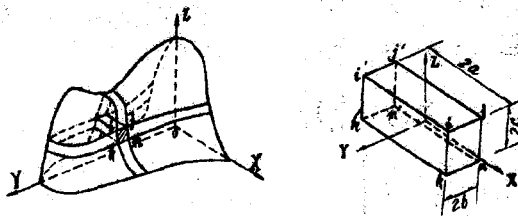


Fig.1.3 Theoretical model

Fig.1.4 Double shear deformation finite element

$$W_i = V_i = 0, \quad U_i = U_i(Y, Z) \quad (1.1)$$

where U_i, V_i, W_i are respectively displacement components in the X, Y, Z directions of the point i .

Because of the same reason as shown above, we also have

$$U_i = U_i, \quad U_j = U_j, \quad U_k = U_k, \quad U_m = U_m,$$

in this case, there are only 4 independent displacements, which can completely define the deformation state of the whole element. Defining

$$\{U\}^e = (U_i \quad U_j \quad U_m \quad U_k)^T \quad (1.2)$$

so as to express the displacement of any point of the element, through the nodal displacements $\{U\}^e$, we assume that the local element displacement U is given in the form of polynomials in the local coordinate variables Y and Z ;

$$U(Y, Z) = a_1 + a_2 Y + a_3 Z + a_4 YZ. \quad (1.3)$$

Under the previous assumption about deformation conditions every element has got only two stress components τ_{xy}, τ_{zx} , and strain components γ_{yx}, γ_{zx} .

By means of the Eq.1.3, the displacements of any points of

the element are expressed by its nodal displacements that follows:

$$U(Y,Z) = [N] \{U\}^e \quad (1.4)$$

where N is the shape function,

$$[N] = \frac{1}{4bc} \begin{bmatrix} (b+Y)(c+Z) & (b-Y)(c+Z) & (b-Y)(c-Z) & (b+Y)(c-Z) \end{bmatrix}.$$

The strains of the element are expressed by the nodal displacements as the following

$$\xi(Y,Z) = [B] \{U\}^e \quad (1.5)$$

where

$$[B] = \frac{1}{4bc} \begin{bmatrix} (b+Y) & (b-Y) & (b-Y) & (b+Y) \\ (c+Z) & (c+Z) & (c-Z) & (c-Z) \end{bmatrix}$$

According to the above Eqs., we can obtain the element stiffness matrix which are as follows

$$\begin{aligned} [k]^e &= 2a \int_0^b \int_0^c [B]^T [D] [B] dY dZ \\ &= \frac{aG}{3} \begin{bmatrix} 2\left(\frac{b+c}{c}\right)\left(\frac{b+c}{b}\right) & 2\left(\frac{b+c}{c}\right)\left(\frac{b+c}{b}\right) & 2\left(\frac{b+c}{c}\right)\left(\frac{b+c}{b}\right) & 2\left(\frac{b+c}{c}\right)\left(\frac{b+c}{b}\right) \\ 2\left(\frac{b+c}{c}\right)\left(\frac{b+c}{b}\right) & 2\left(\frac{b+c}{c}\right)\left(\frac{b+c}{b}\right) & \left(\frac{b+c}{c}\right)\left(\frac{b+c}{b}\right) & \left(\frac{b+c}{c}\right)\left(\frac{b+c}{b}\right) \\ \text{symmetric} & & 2\left(\frac{b+c}{c}\right)\left(\frac{b+c}{b}\right) & 2\left(\frac{b+c}{c}\right)\left(\frac{b+c}{b}\right) \end{bmatrix} \end{aligned} \quad (1.6)$$

where

$$D = \frac{E}{2(1+\mu)} \begin{bmatrix} 1 & 0 \\ 0 & 1 \end{bmatrix} = G \begin{bmatrix} 1 & 0 \\ 0 & 1 \end{bmatrix}$$

and E, G , and μ are material constants i.e., E is Young's modulus, G is shearing modulus and μ is Poisson's ratio.

We can also obtain the element mass matrix as the following

$$\begin{aligned} [m]^e &= 2a\rho \int_0^b \int_0^c [N]^T [N] dY dZ \\ &= \frac{2abc\rho}{9} \begin{bmatrix} 4 & 2 & 1 & 2 \\ 2 & 4 & 2 & 1 \\ \text{symmetric} & & 4 & 2 \\ & & & 4 \end{bmatrix} \end{aligned} \quad (1.7)$$

where ρ is the mass density of the material.

In order to obtain the damping matrix, the Rayleigh damping can be assumed, which is of the form as

$$[c]^e = \alpha [m]^e + \beta [k]^e$$

where α and β are constants to be determined from two given damping ratios that correspond to two unequal frequencies of vibration.

1.3.3 Analysis of response to earthquake

Concerning the response of the spur to earthquake ground motion, we have the dynamic equilibrium equations:

$$[M] \{\ddot{U}\} + [C] \{\dot{U}\} + [K] \{U\} = -[M] \ddot{U}_g(t) \quad (1.8)$$

in which $[M]$, $[C]$, and $[K]$, are mass, damping and stiffness matrices of the whole spur. They assemblage from the matrices $[m]^e$, $[c]^e$

and $[k]^e$ of the elements respectively. $\ddot{U}_0(t)$ is the earthquake motion input at the bottom of the spur.

In this research, we have not been interested in the stresses of the spur, and only the displacement, velocity, and acceleration response processes at the different parts of the spur are mainly interested. By using the step-by-step integration procedure, we direct integrate the Eq.1.8.

Assuming the response accelerations appeared linear variation each time within interval Δt , we have

$$\{\ddot{U}\}_t = \{\ddot{U}\}_{t-\Delta t} + (\{\ddot{U}\}_t - \{\ddot{U}\}_{t-\Delta t}) \tau / \Delta t \quad (1.9)$$

$$(0 \leq \tau \leq \Delta t)$$

Integrating Eq.1.9 twice, we obtain

$$\{\dot{U}\}_t = \{\dot{U}\}_{t-\Delta t} + \frac{\Delta t}{2} \{\ddot{U}\}_{t-\Delta t} + \frac{\Delta t}{2} \{\ddot{U}\}_t \quad (1.10)$$

$$\{U\}_t = \{U\}_{t-\Delta t} + \Delta t \{\dot{U}\}_{t-\Delta t} + \frac{\Delta t^2}{3} \{\ddot{U}\}_{t-\Delta t} + \frac{\Delta t^2}{6} \{\ddot{U}\}_t \quad (1.11)$$

By using Eq. 1.8., we have, at time t ;

$$[K] \{U\}_t + [C] \{\dot{U}\}_t + [M] \{\ddot{U}\}_t = -[M] \ddot{U}_0(t) \quad (1.12)$$

Substituting Eqs. 1.10 and 1.11 into Eq.1.12, we obtain

$$[Q] \{U\}_t = -[M] \ddot{U}_0(t) - [C] \{A\}_{t-\Delta t} - [K] \{B\}_{t-\Delta t}$$

where

$$[Q] = [M] + \frac{\Delta t}{2} [C] + \frac{\Delta t^2}{6} [K]$$

$$\{A\} = \{\dot{U}\}_{t-\Delta t} + \frac{\Delta t}{2} \{\ddot{U}\}_{t-\Delta t}$$

$$\{B\} = \{U\}_{t-\Delta t} + \Delta t \{\dot{U}\}_{t-\Delta t} + \frac{\Delta t^2}{3} \{\ddot{U}\}_{t-\Delta t}$$

Triangularizing the matrix $[Q]$, $[Q] = [L] [L_0] [L]^T$, then for each step, using the above Eqs. we can obtain the displacements, velocities and accelerations of the different points at the spur surface. The results are expressed in the form of the distributions of the relative maximum displacements and velocities, as well as the absolute accelerations along the surface of the spur. We can take further steps to calculate the Fourier spectra and response spectra of these acceleration response processes, and study the characteristics of the earthquake motion at different parts of the spur.

1.4 Numerical results

The example mentioned in the section 1.2, the earthquake response analysis is carried out at Lujiawan village. The finite element idealization of the spur of Lujiawan, is shown in Fig.1.2. According to the material properties of the spur, we adopt the values of the material constants as follows. $E = 0.756 \cdot 10^9 \text{ kg/m}^2$, $\rho = 0.25 \cdot 10^3 \text{ kg} \cdot \text{sec}^2 / \text{m}^4$, $\mu = 0.25$, and the value of damping ratio, $\xi = 0.05$.

May 18, 1940 El Centro California, accelerogram N-S component, is adopted as the earthquake input for this analysis.

In order to coincide with the basic intensity of the region where Lujiawan locats, according to the statistical relationship between the magnitudes, epicentral distance and the maximum acceleration in bedrock, which was presented by Seed at al., we scale down the amplitudes of the El Centro accelerogram into 0.6 times, so the peak acceleration of the input becomes 0.224g. According to the relationship between the magnitudes, epicentral distances and the predominant periods as maximum accelerations in bedrock, which was presented by Seed at al. too, we do not change the scale of time variable to the accelerogram.

When using step-by-step integration method, considering the stability condition, we adopt the time step equal to 0.005 sec., we calculate altogether 1024 time steps, the total duration is 5.12 seconds.

The calculated results are shown in Fig. 1.5. It indicates that the distribution of the calculated peak accelerations and the distribution of the actual earthquake damage are quite in agreement.

The analyses of the Fourier spectra and the response of the calculated acceleration response processes are carried out. The acceleration response spectra of the three typical positions are shown in Fig. 1.5. These spectra are very similar, it indicates that the intensity difference of the different parts of the village, as concerns this exampl, are mainly caused from their differential peak accelerations, and the influence of the spectra of the earthquake motion are not obvious. But, generally speaking, concerning the effects of the earthquake motion on the earthquake damage, both the peak acceleration and the spectra of the ground motion must be considered.

2. Dynamic Characteristics of One-Dimensional Non-Uniform Soil Profiles

2.1 Introduction

The experience of the past heavy earthquakes in the world indicated that the effect of local site soil condition

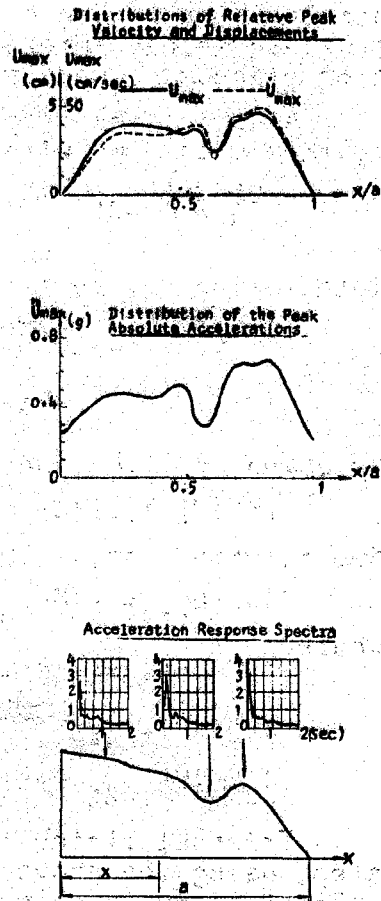


Fig. 1.5 Calculated Results

on earthquake damage was considerable. Generally speaking, the actual constructive site which is made up of a uniform single-layer soil profile is usually very few. Thus, the study of the dynamic characteristics of the non-uniform soil profiles and taking future steps to study the influence of them on earthquake damage, constitutes a very important and interesting research problem.

In several cases, the stiffness of the profile is not varied in horizontal directions, but in the vertical it is continuously varied with depth. In this case, one can use a vertical shear beam model to carry out the study of the problem.

Several works treating this question have presented, some cases having been studied are shown in Fig.2.1.

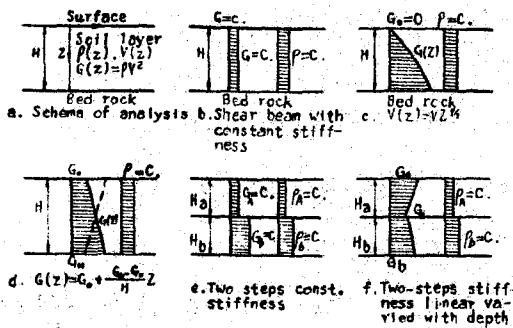


Fig.2.1 Schematic diagram of one-dimensional soil profiles

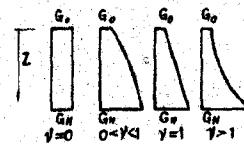


Fig.2.2 Stiffness and value of ν

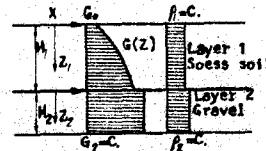


Fig.2.3 Scheme of two-layers soil profile

As the Fig. 2.1 shows that all the authors have assumed that the mass of the soil layer is uniformly distributed along the depth. We think that this assumption is available, because the difference of the unit weight of the soil, generally, is not too big, in the calculation we can use the average value of its unit weight.

Actual informations indicated that the seismic wave of the soil are possibly varied very notable. Under the pressure of its self-weight the consolidated state of the soil becomes better with the increase of depth, thus for the most actual single-layer soil profile, its stiffness increases with depth too.

Considering the information acquired from the observation and better coinciding with the stiffness variation of some actual sites, in this paper referring to the reference (1), a mathematical expression for distribution of stiffness of soil profile is presented as follows

$$G(z) = G_0 \left(1 + \mu \frac{z}{H}\right)^\nu \quad (2.1)$$

where G_0 is the stiffness at the surface, H is the thickness of the soil layer, μ and ν are no-dimensional parameters. G_0 , μ

and ν all are constants, considering their physical meaning they must be $G_0 > 0$, $\mu > 0$, $\nu \geq 0$. properly selecting the value of these parameters, we can easily obtain the stiffness distribution in good agreement with the situation of the actual soil profile. Correspond to different values of ν the stiffness distributions are shown in Fig 2.2.

2.2 Dynamic characteristics of the single-layer soil profile

The equation of free vibration for a variable stiffness shear beam is

$$\frac{\partial}{\partial Z} \left[G(Z) \frac{\partial X(Z,t)}{\partial Z} \right] - \rho(Z) \frac{\partial^2 X(Z,t)}{\partial t^2} = 0 \quad (2.2)$$

considering the solution of Eq.2.2 as the following form

$$X(Z,t) = X(Z) \sin \omega t \quad (2.3)$$

substituting Eq.2.3. into Eq.2.2., we obtain

$$\frac{d}{dZ} \left[G(Z) \frac{dX(Z)}{dZ} \right] + \rho(Z) \omega^2 X(Z) = 0 \quad (2.4)$$

the boundary conditions are

$$\frac{dX}{dZ} = 0, \text{ when } Z=0 \text{ and } X=0, \text{ when } Z=H.$$

Substituting Eq.2.1. into Eq.2.4, we obtain

$$\left(1 + M \frac{Z}{H}\right)^\nu \frac{d^2 X}{dZ^2} + \nu \frac{M}{H} \left(1 + M \frac{Z}{H}\right)^{\nu-1} \frac{dX}{dZ} + \frac{\omega^2}{V_0^2} X = 0 \quad (2.5)$$

where V_0 is shear wave velocity at the surface, $V_0 = \sqrt{\frac{G_0}{\rho}}$ and ρ is the average mass density of the soil.

When $0 < \nu < 2$, introducing the following variable transformation

$$U = \xi \left(1 + \frac{Z}{H}\right)^{1-\frac{\nu}{2}} \quad (2.6)$$

then Eq.2.5. transforms into

$$\frac{d^2 X}{dU^2} + \frac{1-\nu}{U} \frac{dX}{dU} + \frac{4H^2 \omega^2}{M^2 \xi^2 (2-\nu)^2} X = 0 \quad (2.7)$$

defining

$$\xi = \frac{2H\omega}{M(2-\nu)V_0} \quad (2.8)$$

we can rewrite the Eq.2.7 into

$$\frac{d^2 X}{dU^2} + \frac{\nu}{1-\nu} \frac{1}{U} \frac{dX}{dU} + X = 0 \quad (2.9)$$

we take further steps to transform function X into function W

$$W = U^n X, \quad n = \frac{1-\nu}{2-\nu}$$

then Eq.2.8 transforms into the standard Bessel differential equation of n scale

$$\frac{d^2 W}{dU^2} + \frac{1}{U} \frac{dW}{dU} + \left(1 + \frac{n^2}{U^2}\right) W = 0 \quad (2.10)$$

When n is an integer, the solution of Eq.2.10 is

$$X = U^n \left[A J_n(U) + B Y_n(U) \right]. \quad (2.11)$$

When n is not integer, the solution of Eq.2.10 may be written as

$$x = U^n [A J_n(U) + B Y_n(U)] \quad (2.12)$$
 where $J_n(U)$ and $Y_n(U)$ respectively are Bessel function of the first and the second kind of n th order, and A, B are the integral constants which can be determined by the boundary conditions.

When n is integer according the Eq. 2.11, if $Z=0, \frac{dx}{dz}=0$, we obtain

$$AJ_{n-1}(\xi) + BY_{n-1}(\xi) = 0 \quad (2.13)$$

when $Z=H, X=0$, we obtain

$$AJ_n(\alpha\xi) + BY_n(\alpha\xi) = 0 \quad (2.14)$$

where $\alpha = (1 + \mu)^{-1/2}$

From Eqs. 2.13 and 2.14 we obtain the frequency equation as follows

$$J_{n-1}(\xi)Y_n(\alpha\xi) - Y_{n-1}(\xi)J_n(\alpha\xi) = 0 \quad (2.15)$$

Difining constant $A=1$, corresponding to Eq. 2.13 we obtain

$$B = \frac{-J_{n-1}(\xi)}{Y_{n-1}(\xi)}$$

the mode shape of vibration is

$$x(Z) = U^n [J_n(U) + BY_n(U)] \quad (2.16)$$

When n is not integer, corresponding with Eq. 2.12, and following boundary conditions, when $Z=0, \frac{dx}{dz}=0$, we obtain

$$AJ_{n-1}(\xi) - BJ_{n-1}(\xi) = 0 \quad (2.17)$$

and when $Z=H, X=0$ we obtain

$$AJ_n(\alpha\xi) + BJ_n(\alpha\xi) = 0 \quad (2.18)$$

According Eqs. 2.17 and 2.18 we can obtain the frequency equation will be as follows

$$J_{n-1}(\xi)J_n(\alpha\xi) + J_{(n-1)}(\xi)J_n(\alpha\xi) = 0 \quad (2.19)$$

Difining constant $A=1$, corresponding to Eq. 2.18, we obtain

$$B = -\frac{J_n(\alpha\xi)}{J_n(\alpha\xi)}$$

the model shape of vibration is

$$x(Z) = U^n [J_n(U) + BJ_n(U)] \quad (2.20)$$

By solving the frequency equations 2.15 or 2.19 we can obtain its roots, then by using Eq. 2.8 we can obtain frequency for every order

$$\omega_j = \frac{(2-\nu)M V_0}{2H} \xi_j \quad (2.12)$$

Substituting ξ_j into Eq. 2.16 or 2.20 we can obtain model shape of vibration corresponding to each order frequency.

2.3 Dynamic characteristics of two-layers non-uniform soil profile

The previous calculating method for single-layer soil profile, can be easily extended to the case of two-layers non-uniform soil profile. Combining the seismomicrozoning work of Lanzhou and considering the typical site condition of it, we analyse a two-layer soil profile, its calculated model is shown in Fig. 2.3. The first is a soil layer of loess, in which stiffness distribution goes along the depth in the manner as $G_1(Z) = G_0(1 + M_1 Z/H_1)^{n_1}$. The second layer is a gravel in which stiffness is

a constant. The mass density of the two layers are different in constants.

The equations of the profile free vibration are

$$\left\{ \begin{aligned} \frac{\partial}{\partial Z_1} \left[G_1(Z_1) \frac{\partial X_1(Z_1, t)}{\partial Z_1} \right] - \rho_1 \frac{\partial^2 X_1(Z_1, t)}{\partial t^2} &= 0 \end{aligned} \right. \quad (2.21)_a$$

$$\left\{ \begin{aligned} G_2 \frac{\partial^2 X_2(Z_2, t)}{\partial Z_2^2} - \rho_2 \frac{\partial^2 X_2(Z_2, t)}{\partial t^2} &= 0 \end{aligned} \right. \quad (2.21)_b$$

Assuming that the Eqs. 2.21 have the solutions in following forms

$$\left\{ \begin{aligned} X_1(Z_1, t) &= X_1(Z_1) \sin \omega t \end{aligned} \right. \quad (2.22)_a$$

$$\left\{ \begin{aligned} X_2(Z_2, t) &= X_2(Z_2) \sin \omega t \end{aligned} \right. \quad (2.22)_b$$

Substituting the Eqs. 2.22 into Eqs. 2.21, we obtain

$$\left\{ \begin{aligned} \frac{d}{dZ_1} \left(G_1(Z_1) \frac{dX_1(Z_1)}{dZ_1} \right) + \rho_1 \omega^2 X_1(Z_1) &= 0 \end{aligned} \right. \quad (2.23)_a$$

$$\left\{ \begin{aligned} G_2 \frac{d^2 X_2(Z_2)}{dZ_2^2} + \rho_2 \omega^2 X_2(Z_2) &= 0 \end{aligned} \right. \quad (2.23)_b$$

Substituting the relationship $G_1(Z) = G_0 \left(1 + \mu_1 \frac{Z_1^{\nu_1}}{H_1^{\nu_1}} \right)$ into Eq. 2.21 we obtain

$$\left(1 + \mu_1 \frac{Z_1^{\nu_1}}{H_1^{\nu_1}} \right) \frac{d^2 X_1}{dZ_1^2} + \nu_1 \frac{\mu_1}{H_1} \left(1 + \mu_1 \frac{Z_1^{\nu_1}}{H_1^{\nu_1}} \right)^{\nu_1 - 1} \frac{dX_1}{dZ_1} + \frac{\omega^2}{V_0^2} X_1 = 0 \quad (2.24)$$

where $V_0 = \sqrt{G_0/\rho_1}$ is the shear wave velocity at the surface. Introducing the variable transformations which are similar to the above in the case of a single-layer. Defining

$U_1 = \xi_1 \left(1 + \mu_1 \frac{Z_1^{\nu_1}}{H_1^{\nu_1}} \right)^{1-\nu_1/2}$, $\xi_1 = \frac{2\omega H_1}{(2-\nu_1)\mu_1 V_0}$, $W_1 = U_1^{-\nu_1} X_1$, $n_1 = \frac{1-\nu_1/2}{2-\nu_1}$, we can obtain the equations as follows

$$\left\{ \begin{aligned} \frac{dW_1}{dU_1^2} + \frac{1}{U_1} \frac{dW_1}{dU_1} \left(1 - \frac{n_1^2}{U_1^2} \right) W_1 &= 0 \end{aligned} \right. \quad (2.25)_a$$

$$\left\{ \begin{aligned} \frac{d^2 X_2}{dZ_2^2} + \frac{\omega^2}{V_2^2} X_2 &= 0 \end{aligned} \right. \quad (2.25)_b$$

where V_2 is the shear wave velocity of the second soil layer

When $0 < \nu_1 < 2$ and n is an integer, the solutions of Eq. 2.29 can be

$$\left\{ \begin{aligned} X_1 &= A_1 U_1^{n_1} \left(J_{n_1}(U_1) + B_1 Y_{n_1}(U_1) \right) \end{aligned} \right. \quad (2.26)_a$$

$$\left\{ \begin{aligned} X_2 &= A_2 \left(\sin \frac{\omega Z_2}{V_2} + B_2 \cos \frac{\omega Z_2}{V_2} \right) \end{aligned} \right. \quad (2.26)_b$$

the integral constants A_1, B_1, A_2, B_2 are determined by the boundary and continuous conditions which are as follows. When $Z_1 = 0$,

$$\frac{dX_1}{dZ_1} = 0, \text{ we obtain } B_1 = -\frac{J_{n_1-1}(\xi_1)}{Y_{n_1-1}(\xi_1)} \quad (2.27)$$

$$\text{and when } Z_2 = H_2, x_2 = 0, \text{ we obtain } B_2 = -\text{tg} \frac{\omega H_2}{V_2} \quad (2.28)$$

When $Z_1 = H_1$ the displacement Δ_1 and the shear stress τ_1 at the bottom-face of the first layer, are respectively

$$\Delta_1 = |X_1|_{Z_1=H_1} = A_1 (\alpha_1 \xi_1)^{n_1} \left(J_{n_1}(\alpha_1 \xi_1) + B_1 Y_{n_1}(\alpha_1 \xi_1) \right) \quad (2.29)$$

$$\tau_1 = \left| G_1 \left(1 + \mu_1 \frac{Z_1^{\nu_1}}{H_1^{\nu_1}} \right)^{\nu_1} \frac{dX_1}{dZ_1} \right|_{Z_1=H_1} = A_1 (\alpha_1 \xi_1)^{n_1} G_0 \left(1 + \mu_1 \right)^{\nu_1/2} \frac{\omega}{V_1} \left(J_{n_1-1}(\alpha_1 \xi_1) + B_1 Y_{n_1-1}(\alpha_1 \xi_1) \right) \quad (2.30)$$

When $Z_2 = 0$, the displacement Δ_2 and the shear stress τ_2 at the top-face of the second layer are respectively

$$\Delta_2 = |X_2|_{Z_2=0} = A_2 B_2 \quad (2.31)$$

$$\tau_2 = \left| G_2 \frac{dX_2}{dz} \right|_{z=0} = G_2 A_2 \frac{\omega}{V_2}$$

according to the continuous conditions of the displacements and the shear stresses at the interface between the first and the second layers, i.e., $\Delta_1 = \Delta_2$ and $\tau_1 = \tau_2$, we can obtain the frequency equation as follows

$$\frac{J_{n_1}(\alpha_1 \xi_1) + B_1 Y_{n_1}(\alpha_1 \xi_1)}{J_{n_1-1}(\alpha_1 \xi_1) + B_1 Y_{n_1-1}(\alpha_1 \xi_1)} = B_2 \frac{G_2 V_2 (1 + \mu_1)^{1/2}}{G_1 V_1} \quad (2.33)$$

where $\alpha_1 = (1 + \mu_1)^{1/2}$

When $0 < \nu < 2$ and n is not an integer, the solutions of Eq. 2.25 are

$$X_1 = A_1 U_1^n [J_{n_1}(U_1) + B_1 J_{-n_1}(U_1)] \quad (2.34)$$

$$X_2 = A_2 \left[\sin \frac{\omega Z_2}{V_2} + B \cos \frac{\omega Z_2}{V_2} \right] \quad (2.34)$$

By using a quite similar deriving process to the previous, we can obtain the equations corresponding to those as the above. They are

$$B_1 = \frac{J_{n_1-1}(\xi_1)}{J_{n_1}(\xi_1)}, \quad B_2 = -\text{tg} \frac{\omega H_2}{V_2}, \quad \Delta_1 = A_1 (\alpha_1 \xi_1)^{n_1} [J_{n_1}(\alpha_1 \xi_1) + B_1 J_{-n_1}(\alpha_1 \xi_1)],$$

$$\tau_1 = A_1 (\alpha_1 \xi_1)^{n_1} G_1 (1 + \mu_1)^{1/2} \frac{\omega}{V_1} [J_{n_1-1}(\alpha_1 \xi_1) - B_1 J_{-n_1-1}(\alpha_1 \xi_1)], \quad \Delta_2 = A_2 B_2, \quad \tau_2 = A_2 G_2 \frac{\omega}{V_2},$$

and the frequency equation is

$$\frac{J_{n_1}(\alpha_1 \xi_1) + B_1 Y_{n_1}(\alpha_1 \xi_1)}{J_{n_1-1}(\alpha_1 \xi_1) - B_1 Y_{n_1-1}(\alpha_1 \xi_1)} = B_2 \frac{G_2 V_2 (1 + \mu_1)^{1/2}}{G_1 V_1} \quad (2.35)$$

According to the Eqs. 2.33 or 2.35, we obtain their roots and further we calculate then substitute the value of ξ_j into Eq. 2.26 or 2.34 obtaining the mode shapes of vibration corresponding to each n th order frequencies.

3. Analysis of Response of Two-Dimensional Soil Profile to Earthquake

3.1 Introduction

In practice we often have to treat the sites in which the soil property is variable not only with depth, but also in one horizontal direction, merely in other horizontal direction it is uniform. For in this case, the two-dimensional model must be employed in analysis. For example, some sites locate on the valley terrace, if taking a cross perpendicular to the valley, evidently, to such profile the one-dimensional model will not be the proper way to handle the case.

Carrying out the seismomicrozoning work of Lanzhou and Tianshui, which located on the valley terrace, in analysis of response of the sites to earthquakes, we have employed two-dimensional finite element models.

In this analysis, actually, the effects of both topography

* Sun Chongshao, Chen Bingwu: The Seismic Microzoning of Lanzhou, Lanzhou Seismology Institute of State Seismology Bureau, 1981.

and soil conditions on the earthquake intensity are considered.

In this paper, as an example, the calculated results of the profile with sloping rock boundaries are briefly discussed.

3.2 Method of analysis

The schematic diagram of the analysis is shown in Fig. 3.1. The slope of the bedrock is caused from various possible reasons of tectonism or deposition. The slope will give greater influence on the earthquake damage.

In analyses, two acceleration histories are used as the input earthquake motion, they are El Centro (1940) and Wenxian (1976, Songpan-Pingwu earthquakes) strong motion records. The mode superposition method is employed, the first lower-frequency 5 modes are taken in the calculation. Analysing the response of each mode to the earthquake, the Wilson θ method is used.

The boundary conditions have been chosen as follows. At the bottom-face of profile the fixed boundary is employed. For the two lateral end-face, corresponding with the input motion, vertical or horizontal, we use the vertical or horizontal slide boundary conditions respectively. The practical calculated experience indicates that such boundary conditions will reduce the influence of boundaries on the calculated results.

3.3 Discussion of calculated results

On these calculated results we can arrive at the following conclusions.

(1) As shown in Fig. 3.1, when the soil profile is only subjected to the vertical input motion, the vertical surface motion will be strongly induced on the thicker soft soil layer adjacent to the slope, due to the underground topographical feature. When the soil profile is subjected to both vertical and horizontal input motions, at that position the vertical surface motion will be evidently intensified. We consider that this is the reason which causes the earthquake damage exacerbation at such position. This result was found in 1976 Tangshan* earthquake. As a conclusion, some characteristics of the damage distribution in this earthquake can be explained by the underground topographical feature.

(2) The distribution of the peak acceleration response along the surface relates to the earthquake input. At the time when it is subjected to the lower frequency acceleration history (El Centro record) the bigger peak acceleration will distribute at the side of thicker soft soil. As opposed to the above mentioned, when the higher frequency acceleration histories (Wenxian records of Shongpan-Pingwu earthquake) are used

*Liu Shoukuan, Cha Xigang: The Earthquake Damage Anomaly of 1976 Tangshan Earthquake in Higher Intensity Region, Lanzhou Seismology Institute of State Seismology Bureau, 1980.

as the input motion, the bigger peak acceleration will distribute at the site of thin soft soil.

(3) As might be expected, the Fig. 3.1 shows that considering the site conditions on earthquake damage, we should count both the peak acceleration and the frequency spectra of ground motion. As concerning this calculated example, under the condition for dynamic characteristics of ordinary building, the thicker soft soil layer is always disadvantageous for most of the ordinary buildings to earthquake resistance.

(4) For this kind of soil profile as shown in Fig. 3.1, generally speaking, the one-dimensional model is not a suitable model for approximate analysis. Once the one-dimensional model is used in the analysis, the results of vertical motion being intensified would not be obtained.

The above results are strongly supported by the motion observation data. The strong motion records of the main shock and the series of stronger after-shocks have been obtained during the day in 1976 Shongpan-Pingwu earthquake at the station of Wenxian. As to these records the ratios of the acceleration vertical components to the horizontal components are evidently bigger. The Fig. 3.2 shows the comparison of the data of Wenxian records and the statistical informations which were taken from the reference.

The strong motion station of Wenxian was located at the first step valley terrace of Beishuijiang River, the profile of which is shown in Fig. 3.3. Because the observation instruments were just located near the slope of bedrock, as having shown above at such position the ground motion vertical components will be strongly intensified. Thus it will make the ratios of acceleration vertical components become evidently bigger to horizontal components.

The problems discussed in this paper are all related to the effects of site condition on earthquake damage and necessary to solving the problem of seismomicrozoning of the sites. The main results of this paper have been applied in the work of seismomicrozoning at Lanzhou and Tianshui (in Gansu Province of China).

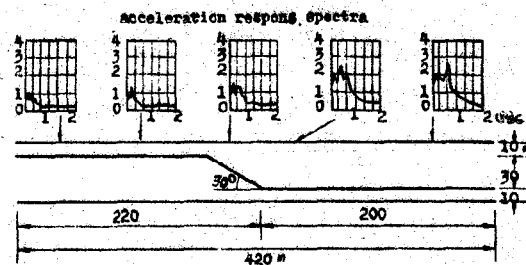
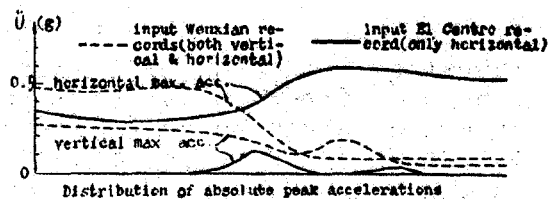


Fig. 3.1 Schema of profile with sloping rock boundary

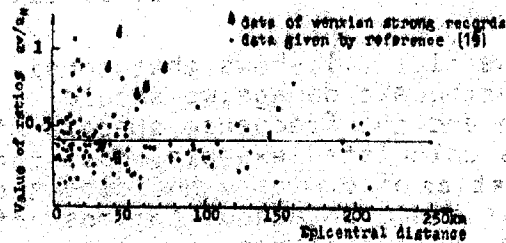


Fig. 3.2 Variety of a_v/a_h with epicentral distance

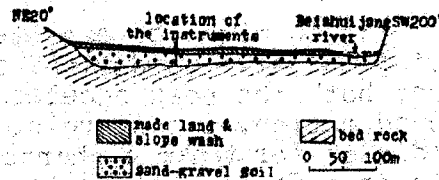


Fig. 3.3 Profile of the site of Wenxian Station

Acknowledgements

The author would like to thank Mr. Lin xuwen for his co-operation on the earthquake damage investigation of Yongshan-Daguan Earthquake, and to thank Ms. Zhong Tingjiao for her help in writing the computer program.

Numerical calculations were carried out through the DJS-108 computer in the earthquake observation department of Lanzhou Seismology Institute. The author is also grateful to Ms. Lin Jinying, for her help in numerical computation.

References

- [1] Investigative Group of Tonghai Earthquake: Intensity distribution and effects of site conditions in TONGhai Earthquake, Research report on earthquake engineering, Institute of Engineering Mechanics, Ac. Sinica, 1973 (in Chinese).
- [2] Earthquake Resistant Research Group of Lanzhou Seism. Insti: Investigation report on 1974 Yongshan-Daguan Earthquake, 1974 (no published, in Chinese).
- [3] Institute of Engineering Mechanics, Ac. Sinica: The relationship between distribution of earthquake damage and site conditions in 1975 Maicheng Earthquake, Earthquake Damage of Maicheng Earthquake, Seismology Press of China, 1980 (in Chinese).
- [4] The Seismic Design Code for Industrial and Civil Buildings (TJ11-78), Architectural Industry Press of China, 1978 (in Chinese).
- [5] Boore D.M., The effect of simple topography on seismic waves, Implication for the acceleration recorded at Pacoima Dam, San Fernando Valley, California, BSSA, vol. 63 No 5, 1973.
- [6] Bouchon M.: Effect of topography on surface motion, BSSA, vol. 63 No 5, 1973.
- [7] Trifunac M.D.: Scattering of plane SH waves by a semi-cylindrical canyon, EESD, vol. 1, 1973.
- [8] Reimer R.B.; Clough R.W., Raphael J.M.: Evaluation of the

- Pacoima Dam accelerogram, Proc. 5th WCEE, 1973.
- [9] Dobry R.D., Oweis I. and Urzua A.: Simplified procedures for estimating the fundamental period of a soil profile, BSSA, vol. 66, 1976.
 - [10] Duke C.M.: Effects of ground on destructiveness of large earthquakes, SMFD, vol 84, 1958.
 - [11] Wang Guangyuan: Calculating methods for free vibration of Multi-story buildings, Bulletin of Harbin Architectural Industry Institute, vol. 3 1963 (in Chinese).
 - [12] Idriss I.M., Seed H.B.: Seismic response of horizontal soil layer, SMFD vol. 94, 1968.
 - [13] Yuzo Sasaki et al.: Effects of topographical features on earthquake-induced damage — A numerical study — Bulletin of the Earthquake Research Institute, University of Tokyo vol. 53, part 1, 1978 (in Japanese).
 - [14] He Yinru, Shao Shiqin et al.: The spectrum analyses of strong motion records of Shongpan-Pingwu Earthquake, Seismology Press of China, 1979 (in Chinese).
 - [15] Chen Dasheng: Several data about peak accelerations and acceleration response spectra of strong motion records, Collected Research Reports on Earthquake Engineering, Institute of Engineering mechanics, Ac. Sinica, vol. 2 1965 (in Chinese).

A PROBABILISTIC ESTIMATE OF MAXIMUM ACCELERATION IN ROCK IN NORTH CHINA

Song Liang yu

Wei Gong yi

Summary

Preliminary map of maximum acceleration (expressed as 1 percent of gravity) in rock with 90 percent probability of not being exceeded in 50 years in North China was made using the seismic data of the period 1448-1980, some attenuation models and the law of magnitude and frequency of earthquakes.

The maximum acceleration within the 100 percent contour along the Fen Wei graben and Tan Lu fracture zone reaches to 115% of g (using the attenuation curve of McGuire.R.K , 1974).

1. Introduction

It is needless to say that making a thorough study of the earthquake prediction is indispensable. However, from the standpoint of reducing earthquake hazards, it is not sufficient only to predict hypocenter, magnitude and origin time of a forthcoming earthquake. It is also important to estimate ground motion produced by the future earthquake, damages followed and the countermeasures, corresponding counterplans as well.

The method used in this study is to define the expectation of the maximum ground motions by using the seismic data within the past about 500 years, attenuation models and some statistical method. However, there are two points which must be put forward clearly, (1) the maximum ground motion are given instead of defining concretely the ground motions, (2) it is meaningless to define the expectations because of great errors due to the very short data period.

2. Seismic data

The seismic data of the period 1448-1980, from the North China seismically active region have been used in this study. During these 532 years, about 76 earthquakes of magnitude greater than or equal to 6, and about 274 earthquakes of magnitude greater than or equal to $4\frac{3}{4}$ occurred in the region. Fig 1 representing

Institute of Geophysics, State Seismological Bureau. Beijing.

the distribution of the epicenters of the earthquakes covers the very region we chose for study. The circles in the figure indicate the earthquakes used for analysis, and also show the approximate range of the well known seismically active region of the North China plate including the Liaodong and Shandon peninsulas.

Fig 2. show the distribution of the faults compiled from various publications. We assumed that in areas with similar geological conditions, the seismicity may be same. Thus by comparing the characters of various geological areas we have divided the North China region into seven seismic zones in line with the similar geological conditions for seismicity. (See Table 1.)

3. Method

The method used in the present study was applied to the Continental United States by S.T. Algermissen and David M. Perkins (1976). Preparation of a probabilistic maximum acceleration map involves three main steps: (1) delineation of seismic source areas; (2) analysis of the statistical characteristics of historical earthquakes in each seismic source area; and (3) calculation and mapping of the extreme cumulative probability $F_{\max, t}(a)$ of acceleration for some time, t . These steps are shown schematically in figure (A) (B) (C) (D). (A) Area of typical source zones and grid points at which the hazards are to be computed. (B) Statistical analysis of seismicity data and typical attenuation curves. (C) Cumulative conditional probability distribution function of acceleration. (D) The extreme probability $F_{\max, t}(a)$ for various accelerations in different time intervals (T).

4. Practical treatment

(1) Delineation of seismic source areas

The seismic source areas of the North China region are shown in Figure 2. as shown by the solids, by which the acceleration map has been computed. These source areas are delineated on the basis of historical seismicity together with the available geological data related to earthquake activity.

(2) Analysis of the statistical characteristics

After the zones are delineated, relationships between the various magnitudes as shown by the following expression

$$\text{Log } N_1 = a - bM_1$$

are determined for each source area. N_1 is the number of earthquakes occurring with magnitudes $M_1 \pm 0.25$. a and b are constants to be determined (namely, the law of magnitude and frequency of earthquake). The fitting has been done by the linear least square regression to $\text{Log } N_1$ on M_1 . The b value and maximum magnitude (the known maximum magnitude or statistically estimated), for seven zone are given in table 1. Once the distribution function of earthquakes with various magnitudes likely to occur in each seismic zone is determined the effects at each gridpoints due to the future earthquakes in each source region can be computed using suitable acceleration attenuation model.

(3) Attenuation models

Some of the attenuation models which have been proposed are tabulated in Table 2. Besides these models there are still many proposed, and recently, some models based on the dislocation theory of earthquake faults have also been suggested. In this study the attenuation model (2) has been used (McGuire, R.K., 1974) which is closer to the mean value of others.

(4) The hazard map

Analysis of the acceleration has been made at every 0.2° in latitude and longitude, North China. Let the peak acceleration be a , then

$$F(a) = P(A \leq a \mid M > M_{\min})$$

the observed acceleration A is less than or equal to the value a , given that an earthquake with magnitude M , greater than some minimum magnitude of interest, has occurred. The calculation at a given gridpoint is performed for every acceleration a of interest using:

$$F(a) = \frac{\text{expected number of occurrences with } A \leq a \text{ and } M > M_{\min}}{\text{total expected number of occurrences (} M > M_{\min} \text{)}}$$

In fact, the distribution of acceleration is computed for a large number of sites on a grid pattern. The earthquake source areas are, ofcourse, also included in the grid pattern.

Now if $\lambda = \phi t$, where ϕ is mean number of earthquakes $M \geq M_{\min}$ per year and t is number of years in a period of interest, then

$$F_{\max, t}(a) = e^{-\phi t} [1 - F(a)]$$

For $t=50$, then $F_{\max, t}(a)$ is calculated, and the value of a for a given extreme probability, say $F_{\max, t}(a)=90$, is obtained by interpolation.

The space distribution of acceleration (given in percent of the acceleration of gravity) in bed rocks beneath the North China region with 90 percent probability of not being exceeded in 50 years is shown in figure 3. That is, there are only 10 percent probability of these values in future 50 years. From Fig 3. an outline of the seismic risk in this region can be studied.

The maximum acceleration within the 100 percent contour along the Fen Wei graben and Tan Lu fracture zone is 115 percent of g .

In Fig 3. the recurrence period for the accelerations is about 475 years.

References

- (1) Algermissen, S.T: and Perkins, D. M., A Probabilistic Estimate of Maximum Acceleration in rock in the Contiguous United States.
- (2) Sadaiku Hattori, Seismic Risk Maps in the World (Maximum Acceleration and Maximum Particle Velocity) (1)*-China and its Vicinity
- (3) Academia Sinica, Institute of Geophysics (1970 a), Catalog of Chinese Earthquake, Academia Sinica, Peking, 361 pp.
(in Chinese)

Table 1 Earthquake parameters for source areas of seven seismic zones

No.	Name of the seismic zones	b	Maximum M_1
1	Fen he - Wei he seismic zone	-0.41	$8\frac{1}{2}$
2	Hua Bei seismic zone	-0.48	$7\frac{1}{2}$
3	Qin Ling--Da Bie Shan seismic zone	-0.67	$6\frac{1}{2}$
4	Yin Shan seismic zone	-0.39	$8\frac{1}{4}$
5	Tan Chen-Lu Jiang seismic zone	-0.33	$8\frac{1}{2}$
6	Yang Zhou-Tong Ling seismic zone	-0.49	$7\frac{1}{2}$
7	Ning Xia-Yin Chuan seismic zone	-0.37	8

Table 2 Attenuation models

NO	Researcher	Formula
1	Oliveira, C. (gal)	$y = b_1 e^{b_2 m} (R+25)^{-b_3}$ $b_1 = 1230 \quad b_2 = 0.8 \quad b_3 = 2$
2	McGuire, R.K. (gal)	$y = b_1 10^{b_2 m} (R+25)^{-b_3}$ $b_1 = 472.3 \quad b_2 = 0.278 \quad b_3 = 1.301$
3	Esteva, L. Rosenblueth, E. (gal)	$a_D = 110 e^{0.8 m} R^{-1.6}$
4	Kawasumi, H. (gal)	$a = 0.253 \cdot 10^{1/2} I \text{ (gal)}$ $I = M_k + I'$ $I' = \begin{cases} 2.1 \ln\left(\frac{100}{\Delta}\right) - 0.00183(\Delta - 100) & \Delta \geq 100 \\ 2 \log\left(\frac{r}{r_0}\right) - \frac{2L}{1.1n10}(r - r_0) & \Delta < 100 \end{cases}$ $L = 0.0192 / \kappa m, \quad r_0^2 = 100^2 + 18^2$
5	Katayama, T.	$\log A = 0.982 - 1.290 \log \Delta + 0.466 M$
6	Katayama, T. (gal)	$\log A = 2.308 - 1.637 \log(R+30) + 0.411 M$
7	Watabe, M. (gal)	$A \text{ (gal)} = 10^{0.472 M - (1.97 - 1.8/X) \log X + (2.2 - 11.1/X)}$

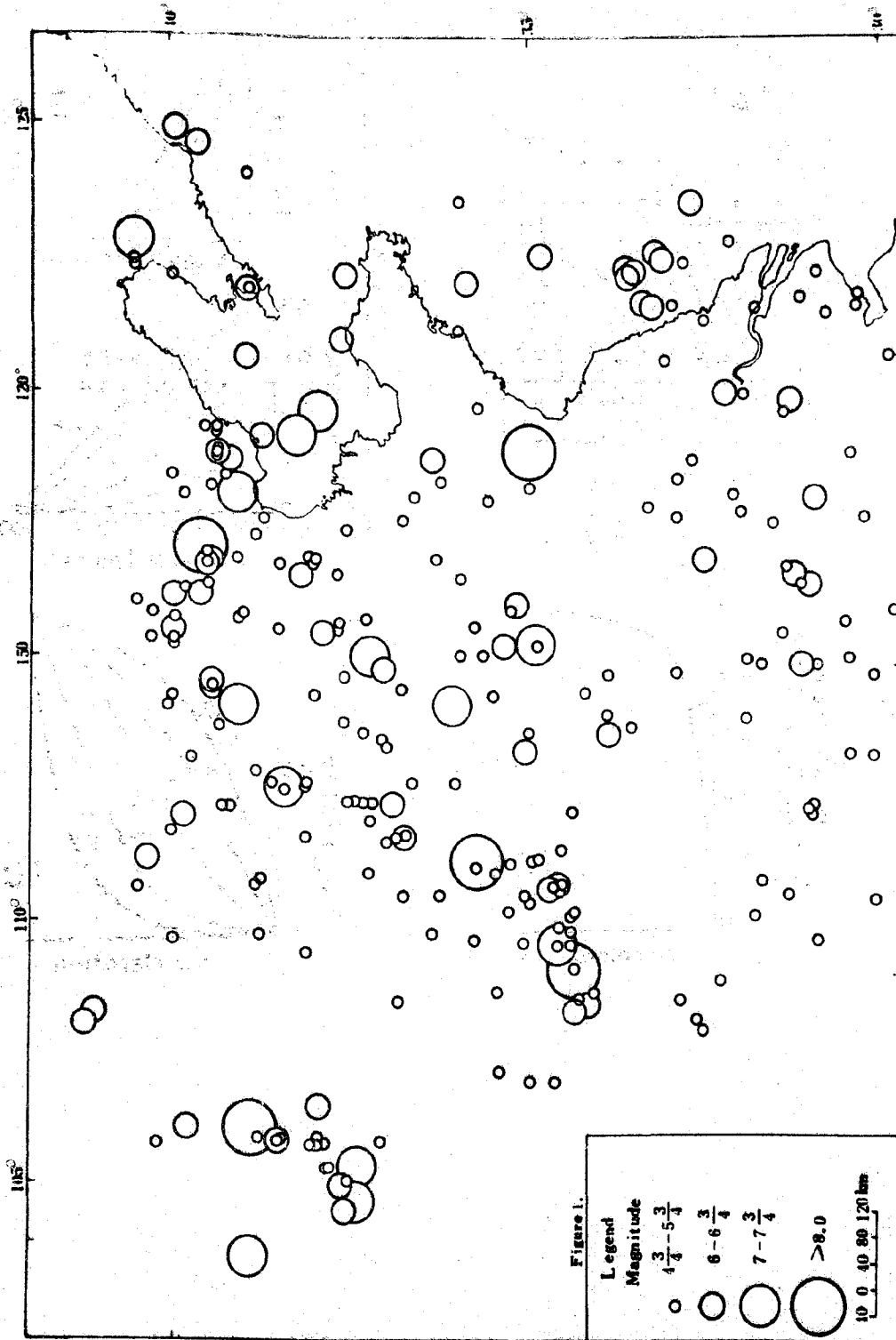
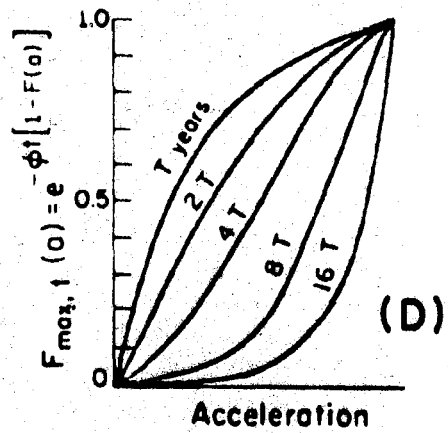
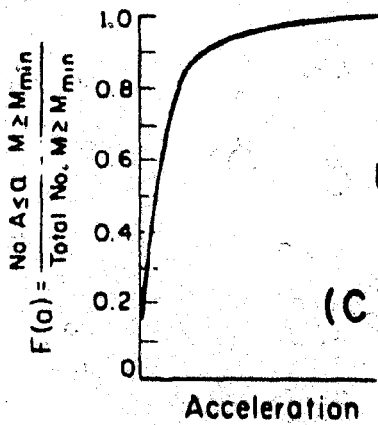
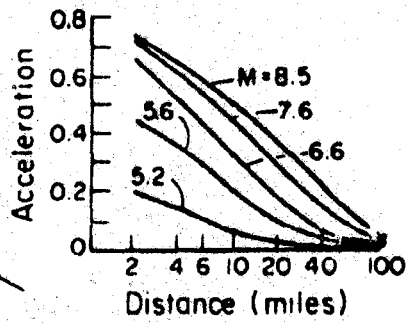
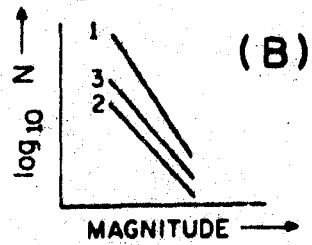
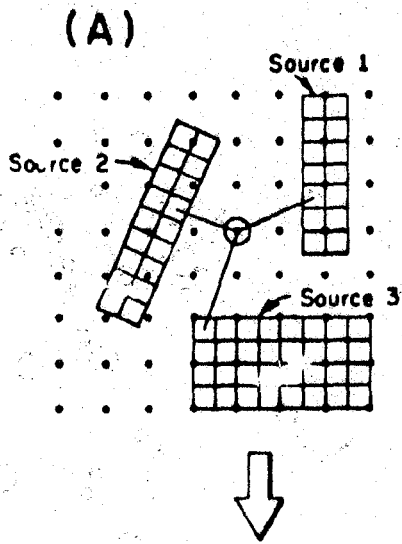
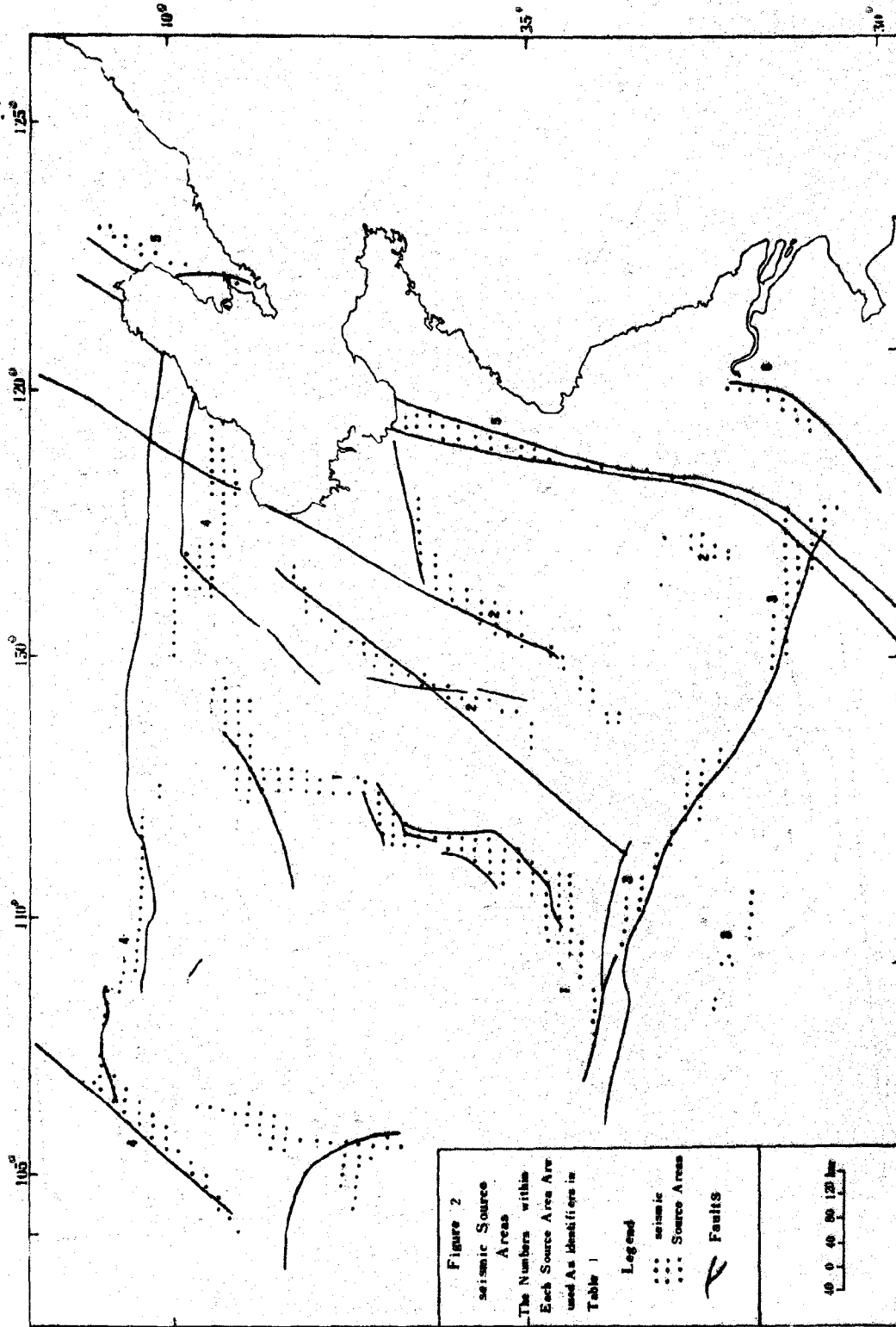
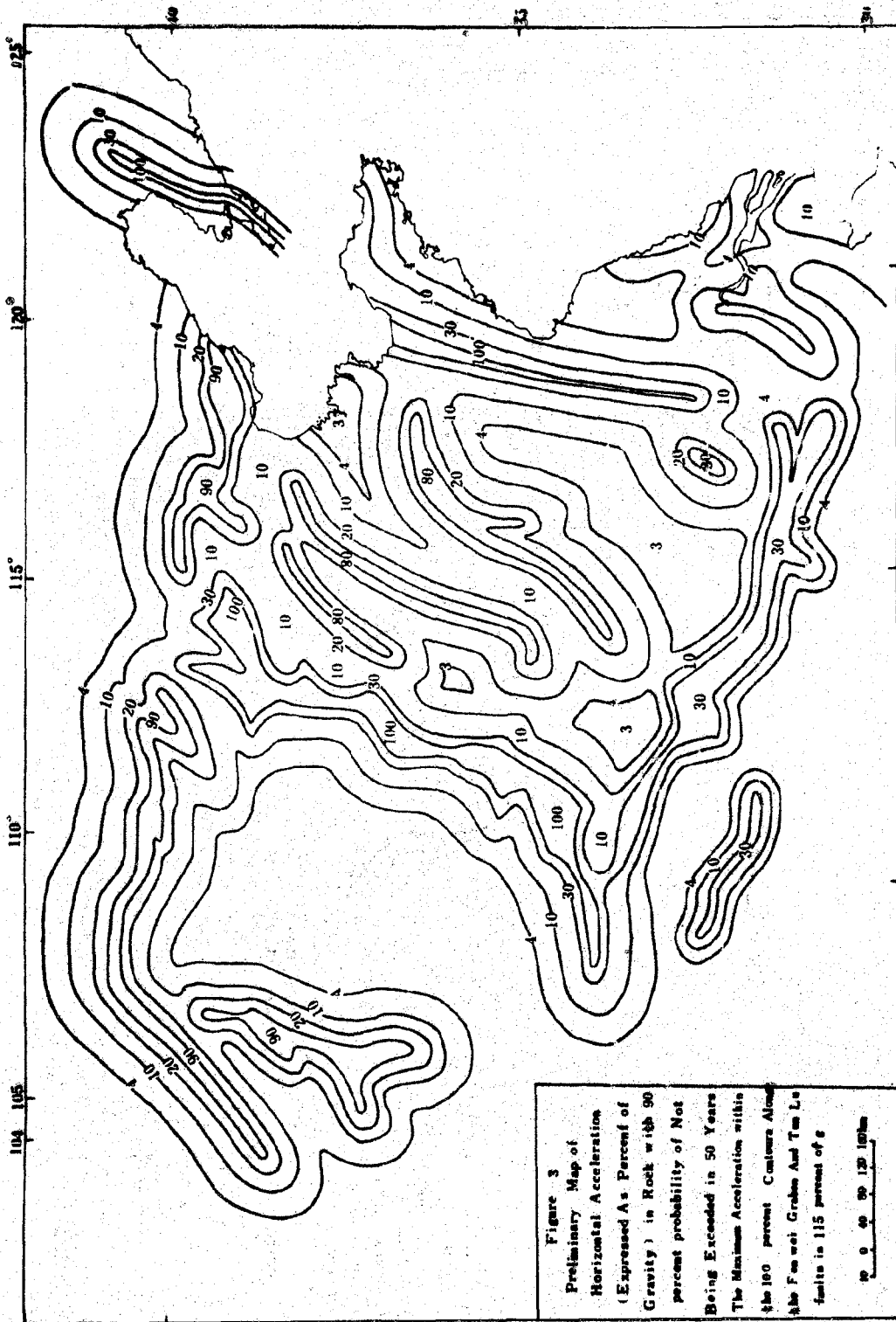


Fig. 1 Map of distribution of epicenters of earthquake in North China M \geq 4 $\frac{3}{4}$ 1418-1980







SEISMIC HAZARD AND UNCERTAINTY
ANALYSIS FOR MICROZONATION

ANNE S. KIREMIDJIAN*

ABSTRACT

The state-of-the-art seismic hazard analysis methods widely used in earthquake resistant structural design and for microzonation are reviewed. Model and parameter uncertainties are identified and their effect on the hazard forecasts are discussed. A simple approach is developed for estimating upper and lower limits on the parameters of the different relationships used in seismic hazard analysis. Upper and lower limits on the forecasted ground motion intensities are obtained as functions of the uncertainties in the parameters. Propagated error from model parameters to hazard forecasts are computed from estimates on the variance of the ground motion intensities. The effect of errors of individual parameters as well as cumulative errors can be examined on the basis of the techniques developed in this paper.

*Assistant Professor, Department of Civil Engineering,
Stanford University, Stanford, California 94305

INTRODUCTION

Evaluation of seismic hazard is an essential step in seismic microzonation for design of structures. The seismic hazard is determined on the basis of probabilistic exposure models which provide information on the severity of ground motion for a specified probability or risk level at various geographical locations. Most of the models for seismic hazard analysis currently in use in the United States and elsewhere in the world assume that earthquake events follow the Poisson probability law (e.g., Cornell, 1968; Cornell and Vanmarcke, 1969; Der Kiureghian and Ang, 1977; Kiremidjian, 1976). Bayesian statistical techniques have been employed (Esteva, 1969; Mortgat and Shah, 1978) to represent the distributions on some of the model parameters and to incorporate subjective information. In addition, several earthquake hazard formulations have been developed to represent specific phenomena such as seismic gaps (Patwardhan et al., 1980), foreshock and aftershock sequences (Knopoff and Kagan, 1977) and clustering of seismic events (Shlien and Toksoz, 1970; and Esteva, 1976). Many of these models, however, are not easily amenable to the diverse geological and geophysical situations in the world. For some, the problem is further complicated by insufficient data or altogether unavailable information for parameter estimation. The validity of forecasts obtained by hazard analysis techniques is often questioned because many parameters are based on scarce and biased

data. The importance of understanding and evaluating the uncertainties in the model parameters is continuously stressed but the reasons are poorly understood and studied only to a limited extent.

The objectives of this paper is to review the state-of-the-art seismic hazard analysis procedures widely used in earthquake-resistant design of structures and to present simple techniques for obtaining upper and lower limits on the seismic hazard forecasts as measures of their variabilities. The uncertain parameters in the various empirical or probabilistic formulas are identified in the review of seismic hazard analysis procedure. The approach for obtaining the upper and lower bounds on the ground motion forecasts is based on simple mathematical estimates utilizing the $(1-\alpha) \times 100$ percent confidence bands on each uncertain parameter of the model. The effect of individual parameter uncertainties can be determined by the approach presented in this paper. Upper and lower bound estimates are particularly useful in seismic code formulations when safety factors are to be established. They are also important for identifying features in the models which are sensitive to parameter uncertainties thus requiring further investigation or improvement of data.

SEISMIC HAZARD FORECASTING

Seismic hazard analysis involves the development of probabilities of ground motion intensity curves at a given site. For microzonation purposes, such seismic hazard curves are computed for all nodal points on a grid which covers the study region. Nodal ground motion intensity values are obtained by specifying the hazard level on these curves. Lines of equal ground motion (or iso-intensity lines) are drawn by interpolation between nodal values. The resulting hazard map is particularly useful in zonation for disaster mitigation and seismic code formulation. Such maps have been developed for California (Kiremidjian and Shah, 1975, 1978), the contiguous United States (Algermissen and Perkins, 1976; ATC, 1978), and other countries in the world including Nicaragua (Shah et al., 1975), Guatemala (Kiremidjian and Shah, 1977), Honduras (Kiremidjian et al., 1979) and Algeria (Mortgat et al., 1979). As an example, the iso-acceleration map for California (Kiremidjian and Shah, 1978) is shown in Figure 1.

The available methods for evaluating the seismic hazard exposure at a site have several basic steps common to all procedures. These include:

1. Study of the geotectonic regime and seismicity of the region;
2. Model the seismic features as point line and area sources, dipping planes or diffused areas of activity;
3. Determine frequency of earthquakes for each seismic sources;
4. Develop a site-specific or utilize an existing ground motion intensity attenuation relationship;
5. Determine a fault rupture or area rupture relationship or use existing ones;

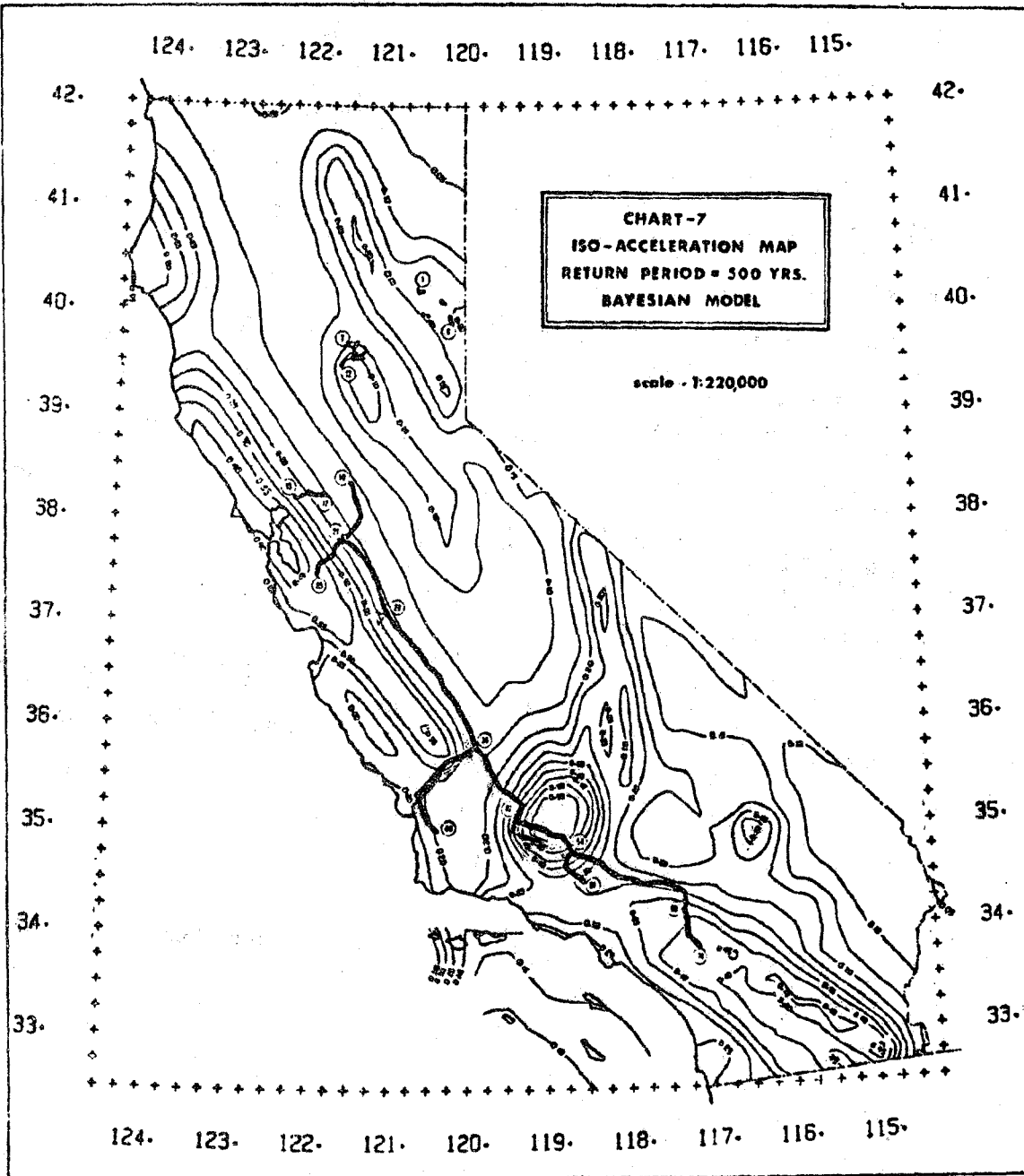


Figure 1. Seismic Hazard Map for California (from Kiremidjian and Shah, 1978).

6. Employ basic probability laws to combine the information from steps 1 to 5 to compute probabilities of seismic hazard exposure.

Seismicity Modeling

Figure 2 shows these steps schematically. In step 1, major geotectonic features such as location of tectonic plates, grabens and dipping planes are reviewed and all known active and potentially active faults are identified. Past earthquake occurrence data is collected and plotted in order to correlate tectonic features with seismic activity. Faults and tectonic provinces are represented geometrically as either line or area sources. Faults are usually modeled as line sources and dipping planes are modeled as closely as possible to their original geometry. Often, the geologic features are not well known or the fault structure is too complex to model each fault-line individually. In such cases, diffused area sources are used to describe the seismicity of the region assuming homogeneous activity throughout the source.

Magnitude-Frequency

The frequency of occurrence of earthquakes for each seismic source is represented by the well known Gutenberg and Richter relationship:

$$\log_{10} N(M) = a + bM \quad (1)$$

where M = Richter magnitude

$N(M)$ = number of events of magnitude greater than M

a, b = constants

Seismic Hazard Model

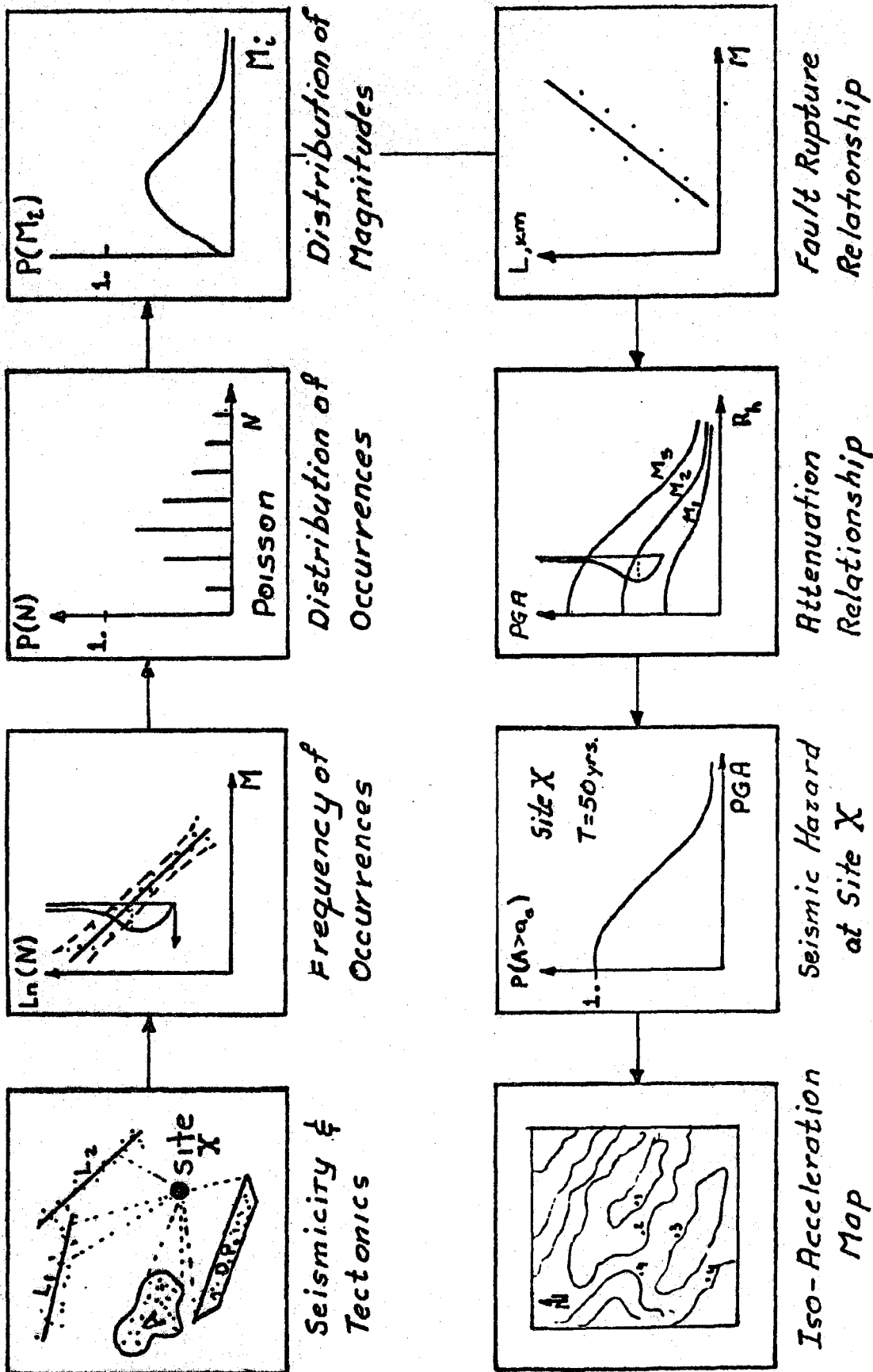


Figure 2. Steps in Seismic Hazard Analysis.

The values of the constants a and b will vary for each region. They are determined by either the least squares or maximum likelihood methods of analysis of earthquake occurrence data. For example, the frequency curve for the northern part of the San Andreas fault in California is shown in Figure 3. A problem common to most areas in the world is the lack of sufficient data. Instrumental data are available only for the last century. Historical accounts of earlier events are incomplete and biased towards the larger events. Deviations from the straight line behavior of the frequency of earthquakes is caused primarily by missing small magnitude data. In the effort to reliably represent the frequency of earthquakes of various magnitudes, bilinear frequencies (Mortgat et al., 1977; Kiremidjian et al., 1979), second order polynomial (Merz and Cornell, 1973), and higher order polynomial (Ferraes, 1967) have been employed. The use of these relationships, however, is recommended only after a careful examination of all available data. For all frequency laws, an upper bound magnitude, M_{max} , is assigned to represent the maximum capacity of the seismic source. The value of M_{max} is obtained by the tectonic features of the seismic source, such as its length or total area, and by the size of the largest event ever recorded. Recently, carbon dating techniques have been utilized to determine the occurrence of large events for which no historical records are available or to reconfirm reported large earthquake events. This information is particularly useful in obtaining the proper upper bound magnitude and in modifying the earthquake frequency law.

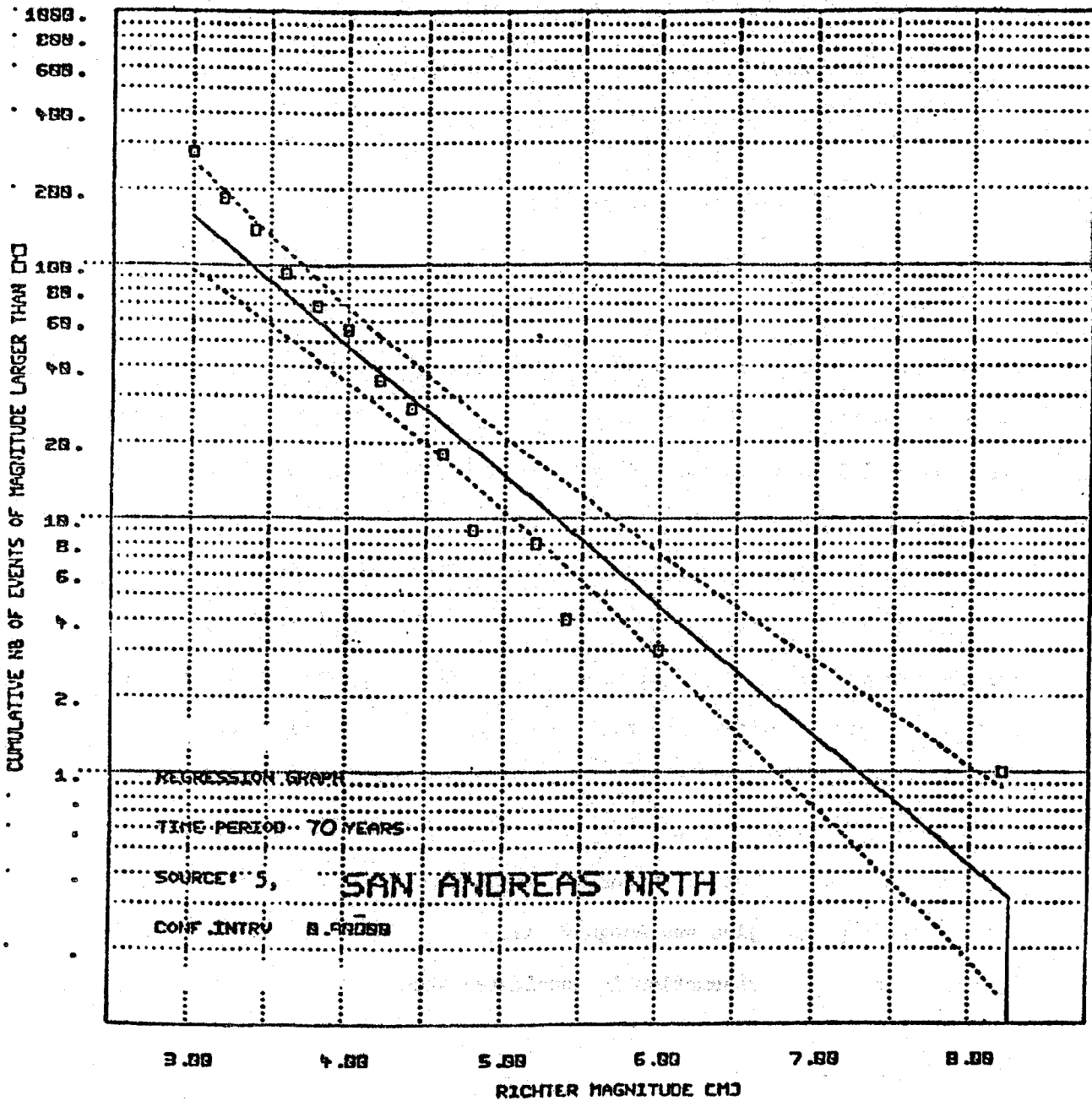


Figure 3. Frequency of Earthquake Occurrences Along the Northern San Andreas Fault (from Kiremidjian and Shah, 1978).

Poisson Occurrences

As already stated in the introduction, most probabilistic models assume that earthquake events are independent in time and space and thus follow the Poisson probability law of Equation 2.

$$P[n, \lambda(m)] = \frac{[\lambda(m)t]^n \exp[-\lambda(m)t]}{n!} \quad (2)$$

for $n=0,1,2,3 \dots$

where $\lambda(m) = N(M)$; t is the duration of forecast; n is the number of events of magnitude greater or equal to M , and $P[n, \lambda(m)]$ is the probability that there will be n events of magnitude M or greater in some future time window of length t .

The assumptions on spatial and temporal independence have been challenged (e.g., Ferraes, 1973, Knopoff, 1964; Lomnitz, 1966). In order for the process to remain homogeneous, the rate λ has to remain constant in time. However, variations of λ with time have been obtained for data in the Eastern Mediterranean and China, where seismological records span 2,000 to 3,000 years. Current research is concentrated on developing time and space dependent earthquake occurrence models (e.g., Patwardhan et al., 1980; Kiremidjian and Anagnos, 1980). For most practical purposes, however, the Poisson assumption is considered acceptable.

Attenuation Laws

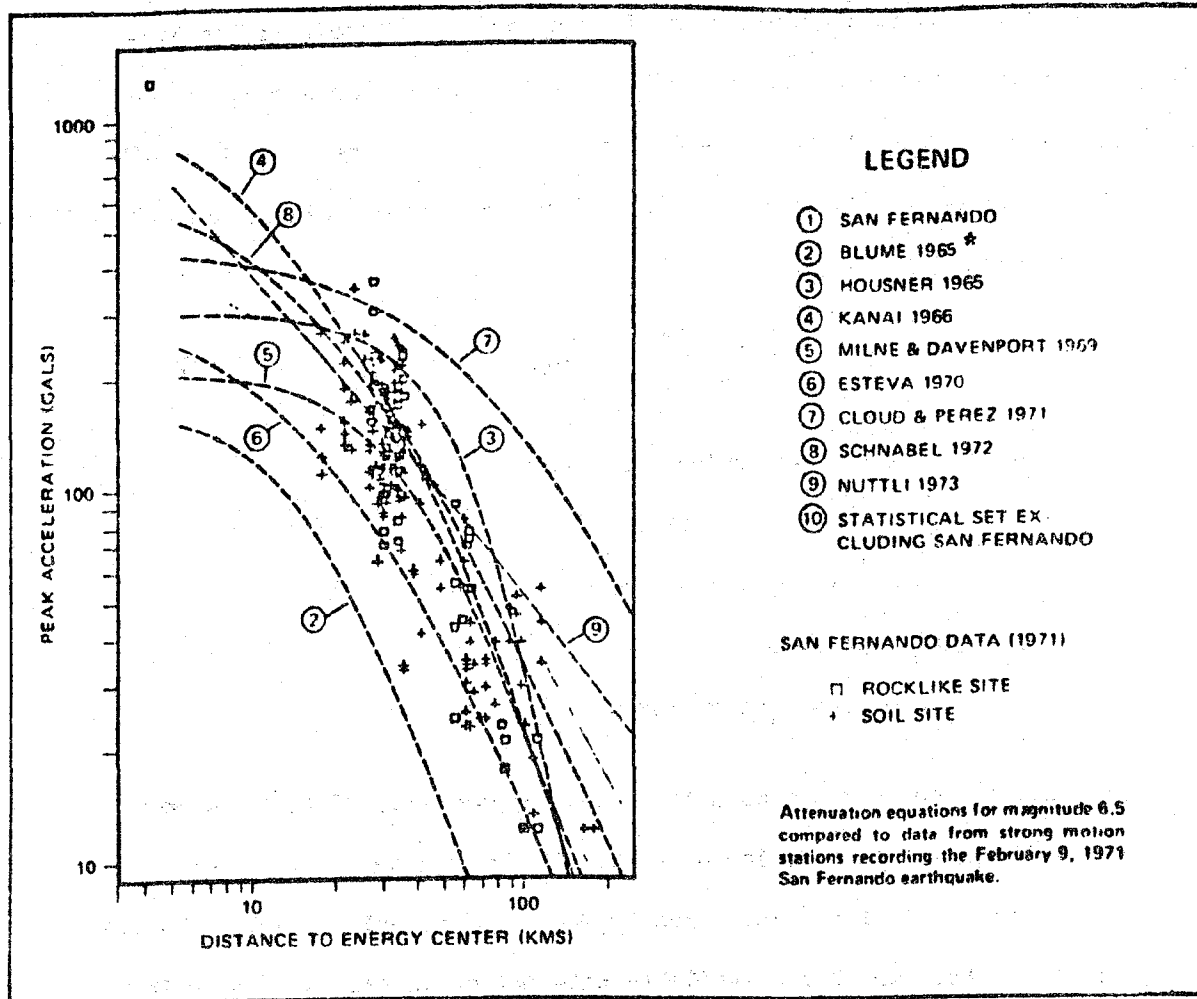
Numerous attenuation laws are available for many regions in the world. The parameters most widely used in these relationships are the peak ground acceleration and the Modified Mercally Intensity (MMI), although, in recent years attenuation functions for spectral accelerations,

velocities and displacements and Fourier spectral accelerations have also been reported (McGuire, 1977). Yegian (1979) has summarized most of the available attenuations developed for various parts of the United States and North and South America. The most common form of the attenuation is given in Equation 3.

$$y = b_1 e^{b_2 m} (R + b_4)^{-b_3} \cdot \epsilon \quad (3)$$

where y = ground motion parameter
 m = Richter magnitude
 R = hypocentral distance
 b_1, b_2, b_3, b_4 = constants
 ϵ = random error term.

The random error term is such that it is lognormally distributed with median 1 and standard deviation of $\sigma_{\ln \epsilon}$. The random error term was first used by Blume in 1965, then by Merz and Cornell in 1973. Donovan (1974) plotted ten of the available attenuation functions to describe the large variations in ground motion prediction from the different curves. This graph is shown in Figure 4. The large variations in attenuation laws is due to differences in the earthquake energy release mechanism, variations in transmission paths, and different local soil conditions at recording sites. Coefficients of variations of peak ground acceleration for specified distance and magnitude have been reported to be as large as 0.7 (OASES, 1978). Seismic hazard forecasts are very sensitive to the attenuation relationship and predicted values can vary by as much as one order of magnitude. The random error term, however, provides the means for



* This relation can provide results which are very close to mean data behavior if the soil characteristics for the region are recognized. The soil characteristics input was not used in the preparation of this figure from Donovan (1974).

Figure 4. Attenuation Relationships as Summarized by Donovan (1974).

incorporating the uncertainty on the ground motion parameter by weighting the possible values with their corresponding probabilities.

Fault Rupture

Earthquake events of magnitudes larger than 5 are often the result of ruptures along major faults or tectonic structures. The rupture can propagate in one or two directions, releasing the energy along its path. Thus, for a site located near a fault the energy transmission path may be shortened considerably than the distance from the epicenter to the site. In such cases, it is the distance between the site and the point on the rupture length which is nearest to the site that is the actual energy transmission path. In order to incorporate this feature into the seismic hazard modeling, fault rupture relationships as functions of magnitudes have been developed (e.g., Mark and Bonilla, 1977; Patwardhan et al., 1975; Slemmons, 1978). Several such relationships are shown in Figure 5. The general form of the fault rupture relationship is given by Equation 4.

$$\ln l = sm + q \quad (4)$$

where l = fault rupture length

m = Richter magnitude

s, q = constants

Der Kiureghian and Ang (1977) and Blume and Kiremidjian (1980) utilized this function in earthquake hazard models for linear seismic sources. The data used in determining the constants s and q are very sparse and non-homogeneous thus further contributing to the errors in the hazard forecast.

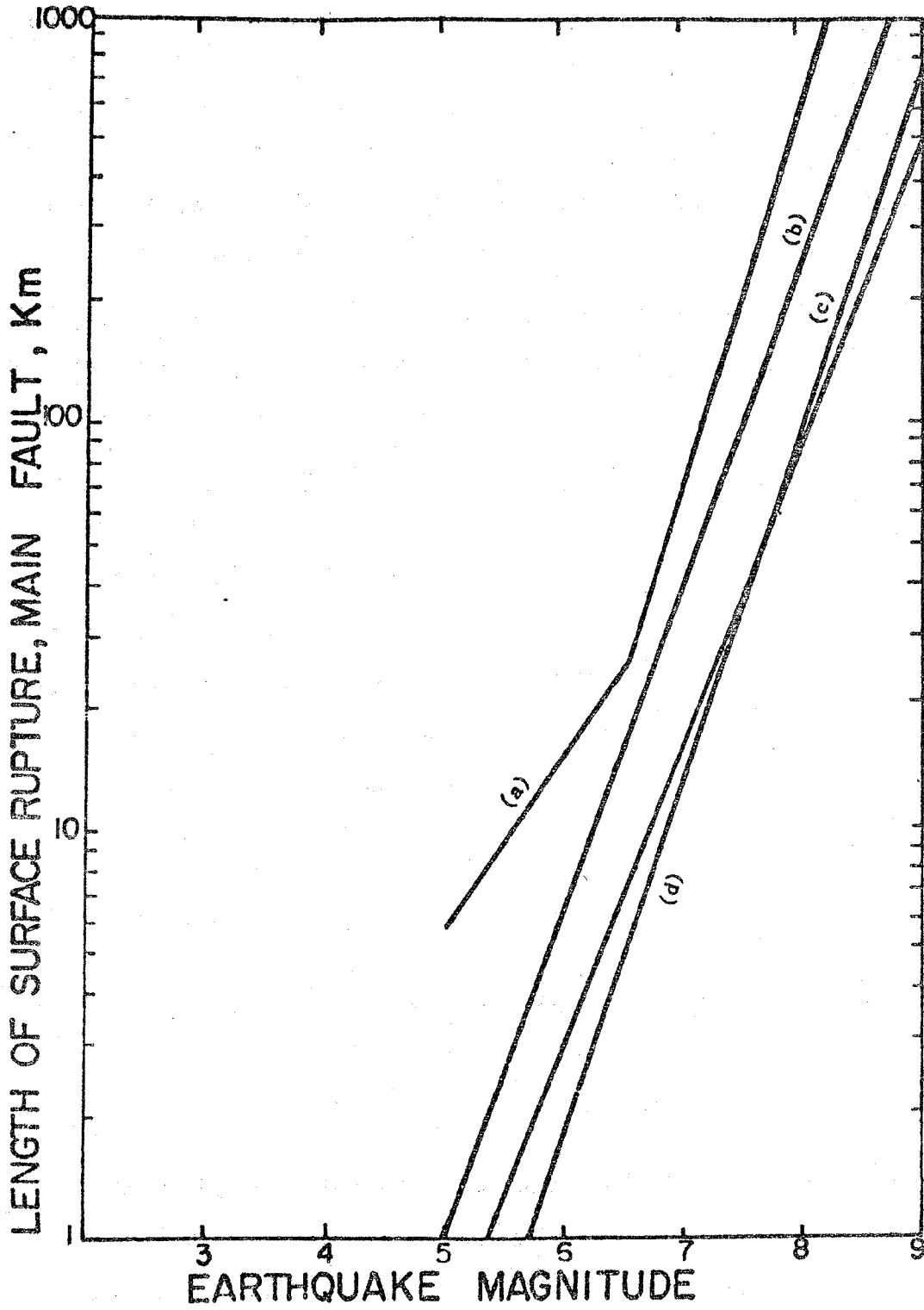


Figure 5. Fault Rupture Relationships; (a) Patwardhan et al. (1975), (b) Mark and Bonilla (1977); (c) and (d) Siemmons (1978).

Site Seismic Hazard

The seismic hazard at a site due to all earthquake sources around that site is found by integration over all relationships defined by Equations 1 to 4. Of the many available hazard functions two are reproduced in this paper for the purposes of uncertainty analysis of model parameters. For the case of linear seismic source, the hazard function developed by Kiremidjian (1976) is given in Equation 5.

$$P[Y \geq y, t] = 1. - \exp[-\gamma \left(\frac{y}{b_1}\right)^\delta t \int_{l_1}^{l_2} [(d^2 + l^2 + h^2)^{1/2} + b_4]^\rho dl] \quad (5)$$

where $\gamma = e^\alpha$

$$\delta = \beta/b_1$$

$$\rho = \beta b_3/b_2$$

y = ground motion parameter,

d, l, h, l_1, l_2 = line source parameters as shown in Figure 6,

and

$$\alpha = a \ln 10$$

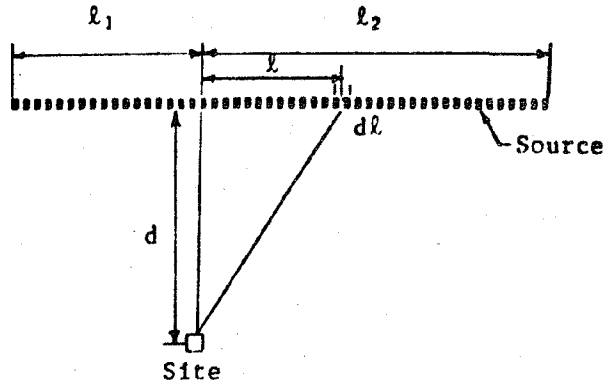
$$\beta = b \ln 10,$$

a, b are as defined by Equation 1

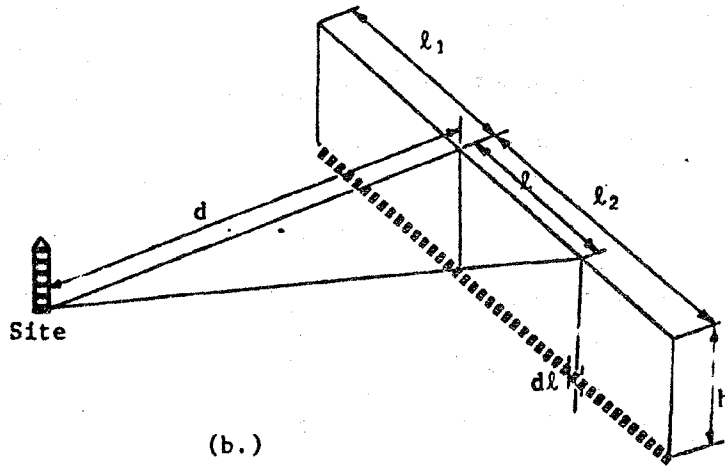
b_1, b_2, b_3, b_4 are as defined by Equation 3

The hazard function which also includes the fault rupture mechanism as obtained by Blume and Kiremidjian (1980) is reproduced in Equation 6.

$$P[Y \geq y] = \sum_{ijk > y} P[M_i] P[R_j/M_i] P[\epsilon_k/M_i, R_j] \quad (6)$$



(a.)



(b.)

Figure 6. Line Source Model.

where

y = ground motion parameter

M = Richter magnitude

R = distance from the site to the nearest point on the
fault rupture

ϵ = standard error term in Equation 3.

Probabilities of M_1 are computed from Equation 1 and probabilities of R_j for a given M_1 are expressed in terms of the fault rupture relationship (Equation 4). The standard error term is lognormally distributed with median of 1 and standard deviation of $\sigma_{\ln \epsilon}$.

Similar relationships are also obtained for other types of seismic sources, however they are not included in this paper. The reader is referred to the studies listed in the introduction for more detailed developments.

The results from the application of Equation 6 to a site in San Francisco due to all earthquake faults in the area is shown in Figure 7. The seismic hazard is expressed as probabilities of exceeding the various levels of peak ground acceleration per year.

Return period of events is a hazard measure often used in engineering design and is directly related to the probabilities of exceedence of ground motion intensities. The return period of a ground motion intensity level is defined as the reciprocal of the annual probability of exceedence of that ground motion intensity. Figure 7 shows the values of return period for each peak ground acceleration for the San Francisco site. From this graph the design ground motion level is selected depending on

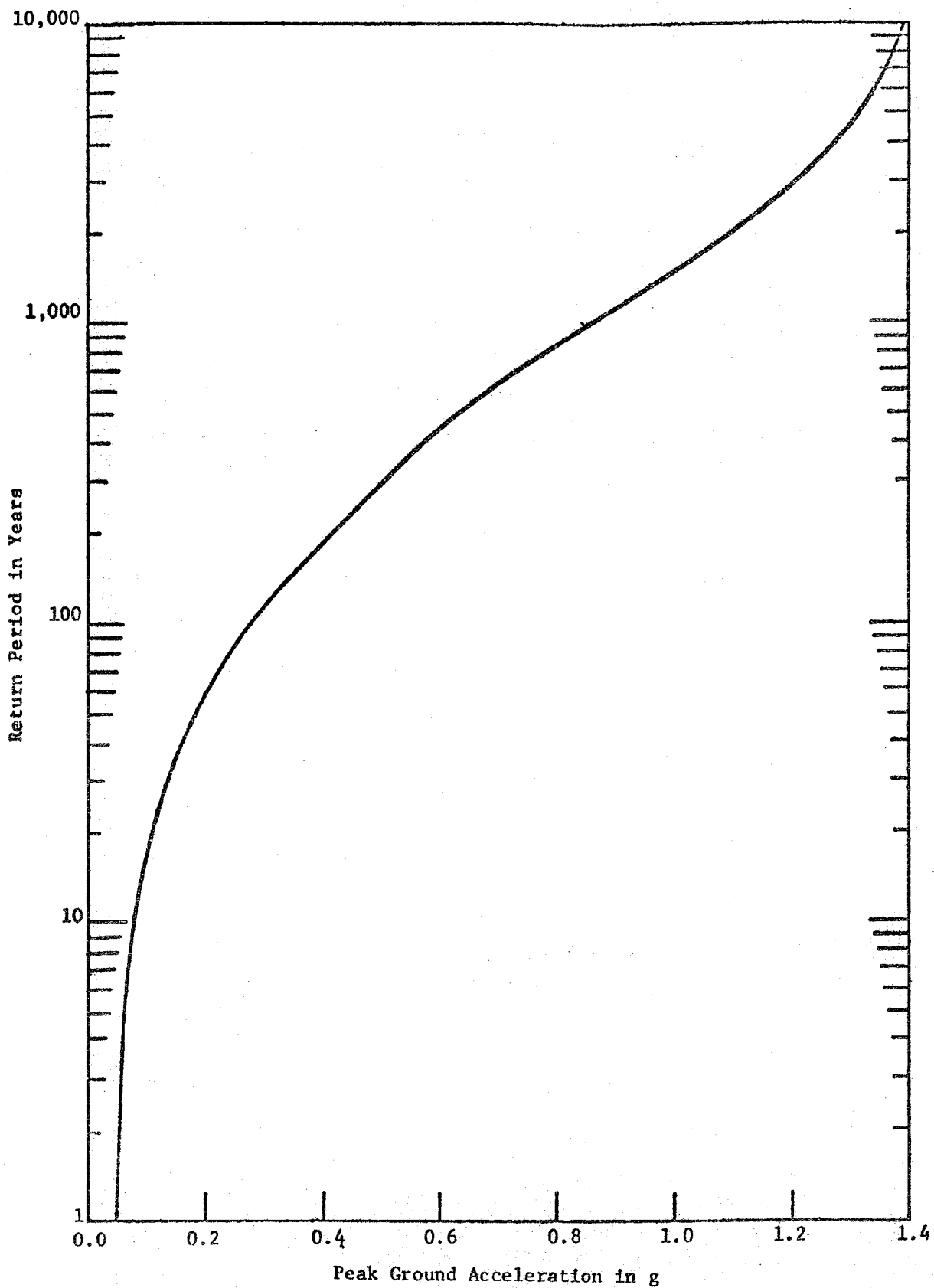


Figure 7. Hazard Function for San Francisco.

the type and use of the structure. Different hazard levels or return periods of events will be selected for structures whose failures can have serious consequences than for conventional dwellings. Thus the design is said to be consistent with the risk level of the structure.

UNCERTAINTY ESTIMATES OF FORECASTS

Application of seismic hazard analysis requires the evaluation of model parameters which are specific to the region under study. Parameter estimates are obtained from earthquake occurrence data, fault rupture data or strong ground motion data. Since these data are insufficient, the computed values for each parameter have errors. In addition to the errors in estimation, there are modeling uncertainties which result from the selection of one functional relationship over another. For example, there are many attenuation relationships none of which truly represents the physical behavior of a given region. Bayesian methods of statistical analysis provide the means for incorporating some of the parameter and model uncertainties. Esteva (1976) and Mortgat and Shah (1979) have used Bayesian methods to describe the error in model parameters by treating them as random variables with corresponding probability distributions. Cornell and Merz (1975) have employed Bayesian methods to assign subjective weights to alternative model relationships. Seismic hazard forecasts are then obtained as a weighted average from the forecasts of all the alternatives. In both applications of Bayesian statistical methods, overconservative estimates of the hazard from ground motion intensities may result.

In this paper, it is proposed that a best estimate of all parameters be used in the seismic hazard model and then upper and lower bounds be obtained as measures of the uncertainty in the forecasts. These upper and lower bounds are important for the determination of safety factors which can be made to vary with the type of structure. Simple mathematical tools are employed to evaluate the upper and lower bounds on the best estimates of forecasts.

The seismic hazard equation for a given site is a function of the parameters of the earthquake frequency, attenuation, and fault rupture relationships and of the variables describing the local geometry of the tectonic structure. In Equation 5 the parameters α , β , b_1 , b_2 , b_3 , ℓ_1 and ℓ_2 are estimated from data or geometry of faults. Each of these parameters is treated as a random variable with a corresponding probability distribution. For totally random samples, the parameters can be assumed to be normally distributed and estimates on the $(1-\alpha) \times 100$ percent confidence bounds are obtained from the Student t-distribution. These $(1-\alpha) \times 100$ percent confidence bands provide the upper and lower limit on the estimated mean. For most purposes either 95% or 99% confidence bands are sufficient to include even large errors in the estimated mean. Some of the parameters can be further bound by geophysical or seismological conditions. For example, from analysis of data it can be shown that the values of $|\beta|$ range from 1 to 3. Thus, $(1-\alpha) \times 100$ percent confidence bands larger than the 1 to 3 range will not be meaningful.

The general formulation for computing the upper and lower limits on the parameters can be summarized as follows:

$$\text{Let } F_y(y, a) = 1 - P\{Y \geq y\} \quad (7)$$

where $\underline{a} = \{a_1, a_2, \dots, a_n\}$ is the vector of all parameters of the seismic hazard function. For Equation 5 the vector $\underline{a} = \{\alpha, \beta, b_1, b_2, b_3, b_4, k_1, k_2\}$. Each a_i has a probability density function $f_{A_i}(a_i)$. From data, the best estimate of a_i , or the sample mean \bar{a}_i , and the sample standard deviations S_{a_i} are computed for all $i = 1, 2, 3, \dots, n$. It is assumed that the samples are completely random and the distributions of $(\bar{a}_i - a_i)/s_{a_i}/\sqrt{n}$ can be approximated by the Student's t-distribution. (Of course, if the population is normal then the distribution is exact.) The following probability statement can be written.

$$P\left[-t_{\alpha/2, n-1} \leq \frac{\bar{a}_i - a_i}{S_{a_i}/\sqrt{n}} \leq t_{\alpha/2, n-1}\right] = 1 - \alpha \quad (8)$$

where $t_{\alpha/2, n-1}$ denotes the value of the t-distribution variable at the cumulative probability of $1 - \alpha/2$ as shown in Figure 8. The upper and lower limits on a_i are then given by

$$\langle a_i^1, a_i^2 \rangle = \left[\bar{a}_i - t_{\alpha/2, n-1} \frac{S_{a_i}}{\sqrt{n}} ; \bar{a}_i + t_{\alpha/2, n-1} \frac{S_{a_i}}{\sqrt{n}} \right] \quad (9)$$

This procedure is repeated for all parameters a_i , $i=1, 2, 3, \dots, n$. Let \underline{a}^1 and \underline{a}^2 denote respectively the vectors of all lower bound and upper bound parameters. Then with each of them a corresponding $F_Y(y, \underline{a}^1)$ and $F_Y(y, \underline{a}^2)$ is obtained. Figure 9 shows three hypothetical curves corresponding to $(1 - F_Y(\underline{a}^1))$, $(1 - F_Y(y, \underline{a}_i^1))$, $(1 - F_Y(y, \underline{a}_i^2))$. Two types of limits can be evaluated from these curves. First, if the hazard level, or probability of exceedence of ground motion intensity is fixed at some value p_0 , then the upper and lower limit on the estimated mean ground motion

intensity are computed from the $(1-F_Y(y, \underline{a}^1))$ and $(1-F_Y(y, \underline{a}^2))$. Since there is a one-to-one correspondence between the various functions, the bounds (y_1, y_2) on the estimated mean y will be also at the same confidence level as the vector \underline{a} .

The second type of limits that can be obtained from the curves in Figure 9 are the bounds on the hazard level for a specified ground motion intensity y . This statement can be read as the "reliability of the reliability", and should be interpreted as the change in the hazard level with variations in data. The limits, p_1, p_2 are particularly useful for existing structures which have already been designed for some specified level of ground motion intensity. If the variations in hazard level are very large, i.e., the (p_1, p_2) bounds are very wide, then the reevaluation of the original design may be conducted and strengthening may be recommended.

For safety factor estimations and code formulation purposes, it is often of interest to obtain an estimate in the variance or standard deviation of the forecasted ground motion intensity. First order approximations of the variance of \bar{y} can be computed by Equation 10.

$$\text{Var}[Y] \approx \sum_{i=1}^n c_i^2 \text{Var}(a_i) \quad (10)$$

where $\text{Var}(a_i)$, $i=1,2,3 \dots n$, are the variances of all the parameters; and c_i 's are defined in terms of the inverse of $(1-F_Y(y, \underline{a}))$ as

$$c_i = \frac{\partial \phi(p, \underline{a})}{\partial a_i} \quad (11)$$

Equation 11 is evaluated at the mean values of the parameters \underline{a} . The function $\phi(p, \underline{a})$ is obtained as follows:

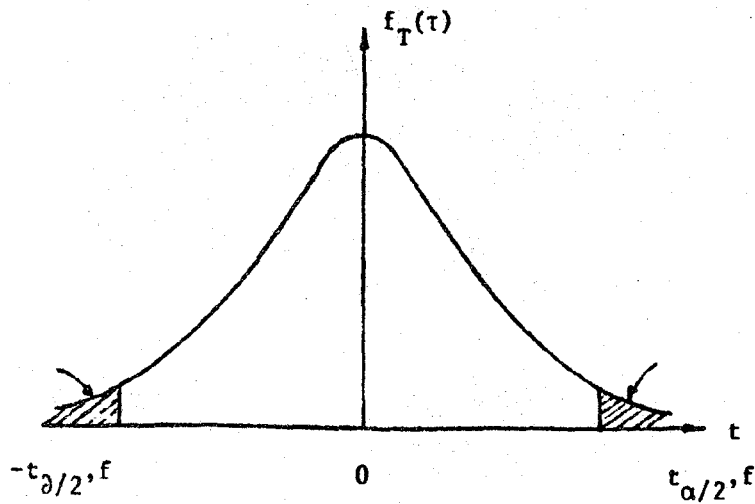


Figure 8. Student's t-distribution with $(1-\alpha)$ Confidence Bands.

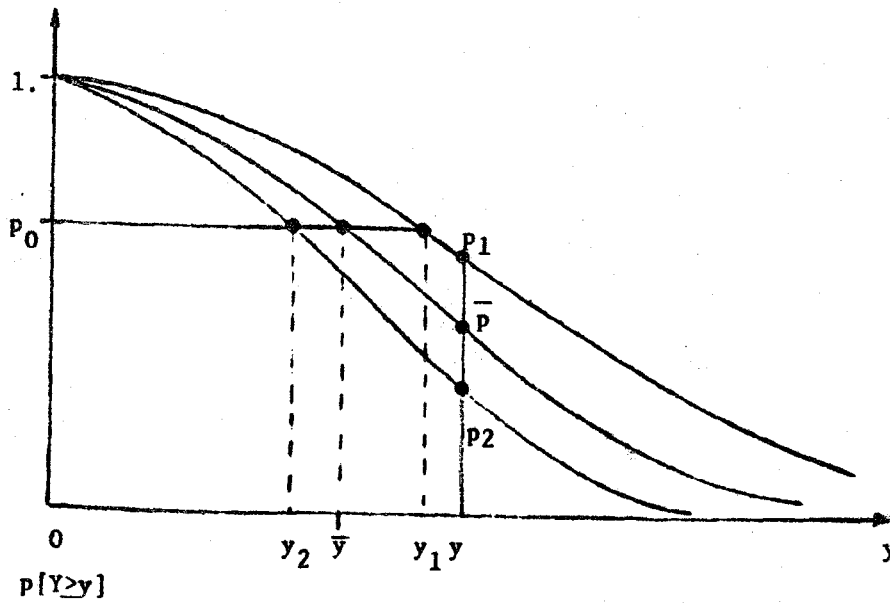


Figure 9. Probabilities of exceedence of ground motion intensities; (a) curves obtained from upper band values of model parameters; (b) curves obtained from mean value estimates of the model parameters; (c) curves obtained from lower bands of the model parameters.

$$\text{Let } p = 1 - F_Y(y, \underline{a}) \quad (12)$$

then, since p is monotonic, there exists a function of ϕ such that

$$y = \phi(p, \underline{a}) \quad (13)$$

For some hazard functions, the computation of c_i 's may prove to be rather tedious and numerical techniques may be necessary. However, the estimate of the variance of y may be more useful than the absolute upper bound which may be unnecessarily overconservative. The estimate of $\text{Var}[Y]$ is also representative of the error accumulation of all the parameters.

CONCLUSIONS

The important results in this paper include the methods of estimation of upper and lower limits on the model parameters and on the ground motion intensity obtained from the seismic hazard analysis. The approach is simple but innovative and promising. Most importantly, it provides for variations in risk level estimations with different types of structures. A method for evaluation of propagated error from the uncertainties in model parameters is presented in the form of variance of ground motion intensity forecast. The effect of individual parameter uncertainties on the hazard values, as well as the cumulative error can be determined by this approach. For microzonation and seismic design purposes, it is recommended that the best estimates, i.e., the sample mean values of parameters be used in computation of the potential ground motion intensities at different sites. Then cumulative error values should be incorporated in safety factors for seismic loads.

Variations in the probability values at specified ground motion intensity are useful for rehabilitation and upgrading of existing structures. The level of improvement will be dictated by the upper and lower limit range of probabilities and the degree of conservatism necessary for the specific structure.

REFERENCES

- Algermissen, S. T. and Perkins, D. M. (1976). "A Probabilistic Estimate of Maximum Acceleration in Rock in the Contiguous United States," U.S. Department of the Interior, Geological Survey, Open File Report 76-416.
- Applied Technology Council (1978). "Tentative Provisions for the Development of Seismic Regulations for Buildings," National Science Foundation, Publication 510, June.
- Blume, J. A. (1965). "Earthquake Ground Motion and Engineering Procedures for Important Installations Near Active Faults," Proceedings of the Third World Conference on Earthquake Engineering, Vol. III.
- Blume, J. A. and Kiremidjian, A. S. (1979). "Probabilistic Procedures for Peak Ground Motions," Journal of the Structural Division, ASCE, Vol. 105, No. ST11, pp. 2293-2311.
- Cornell, C. A. (1968). "Engineering Seismic Risk Analysis," BSSA, Vol. 58, No. 5-6, pp. 1583-1606.
- Cornell, C. A. and Vanmarcke, E. H. (1969). "The Major Influences on Seismic Risk," Proceedings of the 4th World Conference on Earthquake Engineering, Santiago, Chile.
- Cornell, C. A. and Merz, H. A. (1975). "Seismic Risk Analysis of Boston," Journal of the Structural Division, ASCE, Vol. 101, No. ST10, pp. 2027-2043.
- Der Kiureghian, A. and Ang, A. H-S. (1977). "A Fault-Rupture Model for Seismic Risk Analysis," BSSA, Vol. 67, No. 4, pp. 1173-1194.
- Donovan, N. (1974). "Earthquake Hazard for Buildings," Dames & Moore Engineering Bulletin 46, Dames & Moore, Los Angeles, California.
- Esteva, L. (1969). "Seismicity Prediction: A Bayesian Approach," Proceedings of the 4th World Conference on Earthquake Engineering, Santiago, Chile.
- Esteva, L. (1976). "Seismic Risk and Seismic Design Decisions," Seismic Design for Nuclear Power Plants, Ed. R. J. Hansen, MIT Technology Press.

- Ferraes, S. G. (1973). "Earthquake Magnitude Probabilities and Statistical Independence for Mexico City Earthquakes," BSSA, Vol. 63, No. 6, pp. 1913-1919.
- Kiremidjian, A. S. and Shah, H. C. (1975). "Seismic Hazard Mapping of California," The John A. Blume Earthquake Engineering Center, Department of Civil Engineering, Technical Report 21, Stanford University, Stanford, CA.
- Kiremidjian, A. S. (1976). "Seismic Hazard Mapping and Probabilistic Site-Dependent Response Spectra," Ph.D. Dissertation, Dept. of Civil Engineering, Stanford University, Stanford, CA.
- Kiremidjian, A. S. and Shah, H. C. (1977). "Seismic Hazard Mapping for Guatemala," The John A. Blume Earthquake Engineering Center Report No. 26, Dept. of Civil Engineering, Stanford University, Stanford, CA.
- Kiremidjian, A. S. and Shah, H. C. (1978). "Seismic Risk Analysis for the California Water Project," The John A. Blume Earthquake Engineering Center, Report No. 33, Dept. of Civil Engineering, Stanford University, Stanford, CA.
- Kiremidjian, A. S., Shah, H. C. and Sutch, P. L. (1979). "Seismic Hazard Analysis of Honduras," The John A. Blume Earthquake Engineering Center, Report No. 38, Dept. of Civil Engineering, Stanford University, Stanford, CA.
- Kiremidjian, A. S. and Anagnos, T. S. (1980). "A Homogeneous Alternating Markov Model for Earthquake Occurrences," Proceedings of the 7th World Conference on Earthquake Engineering, Istanbul, Turkey, pp. 355-363.
- Knopoff, L. (1964). "The Statistics of Earthquakes in Southern California," BSSA, Vol. 54, pp. 1871-1873.
- Lomnitz, C. (1966). "Statistical Prediction of Earthquakes," Review of Geophysics, Vol. 4, pp. 377-393.
- Knopoff, L. and Kagan, V. (1977). "Analysis of the Theory of Extremes as Applied to Earthquake Problems," Journal of Geophysical Research, Vol. 82, No. 36.
- Mark, R. K. and Bonilla, M. G. (1977). "Regression Analysis of Earthquake Magnitude and Surface Fault Length Using the 1970 Data of Bonilla and Buchanan," U.S.G.S Open Report 77-614, Menlo Park, CA.
- McGuire, R. K. (1977). "A Simple Model for Estimating Fourier Amplitude Spectra," Submitted to the Seismological Society of America Bulletin.

- Merz, H. A. and Cornell, C. A. (1973). "Seismic Risk Analysis Based on Quadratic Magnitude - Frequency Law," BSSA, Vol. 63, pp. 1999-2006.
- Mortgat, C. P. et al. (1977). "A Study of Seismic Risk for Costa Rica," The John A. Blume Earthquake Engineering Center, Report No. 25, Dept. of Civil Engineering, Stanford University, Stanford, CA.
- Mortgat, C. P. and Shah, H. C. (1979). "A Bayesian Model for Seismic Hazard Mapping," BSSA, Vol. 69, No. 4, pp. 1253-1266.
- Mortgat, C. P. et al. (1979). "Seismic Hazard Analysis of Algeria," The John A. Blume Earthquake Engineering Center, Dept. of Civil Engineering, Stanford University, Stanford, CA.
- Patwardhan, A. S., Tocher, D. and Savage, E. D. (1975). "Relationship Between Earthquake Magnitude and Length of Rupture Surface Based on Aftershock Zones," Earthquake Notes, Eastern Sec. Seism. Soc. of America, Vol. 46.
- Patwardhan, A. S., Kulkarni, R. B. and Tocher, D. (1980). "A Semi-Markov Model for Characterizing Recurrence of Great Earthquakes," BSSA, Vol. 70, No. 1, pp. 325-347.
- Shah, H. C. et al. (1975). "A Study of Seismic Risk for Nicaragua," Parts I and II, The John A. Blume Earthquake Engineering Center, Technical Report Nos. 11 and 12, Dept. of Civil Engineering, Stanford University, Stanford, CA.
- Shlien, S. and Toksoz, M. (1970). "A Clustering Model for Earthquake Occurrences," BSSA, Vol. 60, No. 6, pp. 1765-1787.
- Slemmons, D. B. (1978). "Seismological Environment," Lecture given at the EERI Seminar on Seismic Risk Analysis, Los Angeles, CA.
- Yegian, M. K. (1979). "State-of-the-Art for Assessing Earthquake Hazard in the United States," U.S. Army Engineer Waterways Experiment Station, Technical Report No. 13, Vicksburg, Mississippi.



ERRATUM

Page	Line	Original	Corrected
2-3	21	Eq.1	Eq.3
2-4	formula(7)	$C_R = (C_{NS}^2 + C_{EW}^2 + V_{vt}^2)$	$C_R^2 = (C_{NS}^2 + C_{EW}^2 + V_{vt}^2)$
2-8	formula(10)	$\psi = \frac{\psi \sum N_i}{\sum N_i}$	$\psi = \frac{\sum \psi_i N_i}{\sum N_i}$
2-9	formula(11)	$\left[\frac{10.66}{C_u - 2.07 C_u + 1.1} + 74 \right]$	$\left[\frac{10.66}{C_u^2 - 2.07 C_u + 1.1} + 74 \right]$
2-26	Fig.16	THICKNESS > 10FT THICKNESS > 10FT	THICKNESS > 10FT THICKNESS > 10FT
10-3	6	(m/sec)	(m/sec ²)
10-3	13	=1.7	$\alpha = 1.7$
10-3	14	=1.67	$\alpha = 1.67$
10-3	15	=1.6	$\alpha = 1.6$
10-4	30	(equivalent to grade...)	(equivalent to 7 grade...)
10-5	2	1/2.25	1/5.3
10-8	14-15	(0.5-80HZ \pm 10%)	(0.5-80HZ \pm 15%)
10-14	Fig.2right	(KG ³ /M)	(KG ^{1/3} /M)
11-2	11	result [2]	result [1]
11-2	21	survey	survey [2]
11-2	24	1:25000	1:2500
11-2	33	descendants"	descendants" [3]
11-4	11	photographic geodesy	photogrammetry
11-12	26	Intensity Scale	Isoseismal map
11-13	1	secod	second
14-3	12	esists	exists
14-3	14	Fig.	Fig.6
14-3	37	values of there	values of these
14-6	39	same as the	same as

14-6	53	VII or IX,	VII or IX.
14-7	13	substituting in	substituting in formula
14-7	30	min. normal	min. principal
19-1	1	PREDICTON	PREDICTION
19-1	15	liner	linear
19-1	17	bedrock	ground
19-2	20	last thousand years	last more thousand year
19-2	21-22	and 5 events with magnitude more than 6	and 5 events with magnitude more than 6 among them and one with magnitude 8 in maximum
19-2	29	two earthquake risk arers(Fig.);	two earthquake risk areas:
19-2	30	area.	area(Fig.1)
19-2	35	Huangzhuang fanlt	Huangzhuang fault
19-2	39-40	falls between the NW Nankou-Tongxian active belt	involves the intersection of the NW Nankou-Tongxian active belt with
19-2	42	Huang-Gaoliying	Huangzhuang-Gaoliying
19-2	44	(4) has	has
19-2	45	measurements	measurements(4).
19-3	21 & 26	predominant	predominant
19-3	25	acceleation	acceleration
19-3	36	It	it
19-3	37	(-5 and -20%)	(damping 5% and damping 20%)
19-3	38	maximumamplitude	maximum amplitude
19-3	44	reoredominant	predominant
19-3	46	coeffcientis	coefficients
19-4	1	on oppoing	on two
19-4	21	pliedment	pliedment and plain
19-4	25	SN	SE
19-4	35	forland	foreland

19-5	6	end	and
19-5	12	subdided	subdivided
19-5	14	A ⁴ Chaobaihe	A ₄ Juhe
21-1	20-21	general intensity	basic intensity
21-1	31	diffecult	difficult
21-2	1	in the site	in situ
21-2	7	two-dimentional	two-dimensional
21-2	35	not-causative	non-causative
21-6	45	victor	vector
21-7	3	victor	vector
21-7	4-5	victor	vector
21-7	30	may be obtain	may be obtained
21-8	11	Shongpan-Pingwu	Songpan-Pingwu
21-8	25	Fig.4	Fig.5
21-9	13	Q gravel	Q ₁ gravel
21-11	14	aresearch	a research
22-5	16	$G(M)=\exp(-\alpha e^{-\beta M})$ (1)	$G(M)=\exp(-\alpha e^{-\beta M})$ ($M \geq 0$) (1)
22-5	17	values of and from	values of α and β from
22-5	18	of M, M, ...M of n	of M ₁ , M ₂ , ...M _n of n
22-12	25	effect of late, in	effect. Of late, in
22-16	14	(1965)	(1980)
22-16	16	3WCEE	7WCEE
26-3	36	building	buildings
26-3	48	ofter	after
26-5	7	difine	define
26-12	18	Difining	Defining
26-14	9	tectonism	tectonics



